



## TABLE OF CONTENTS

### MINERAL INDUSTRY

<i>Yukon Mining, Development and Exploration Overview 2004</i>	
M. Burke.....	2
Appendix 1: 2004 exploration projects .....	30
Appendix 2: 2004 drilling statistics .....	33
<i>Yukon Placer Mining and Exploration Overview 2004</i>	
W. LeBarge .....	35

### GOVERNMENT

<i>Yukon Geological Survey</i>	
G. Abbott and staff.....	43
<i>La Commission géologique du Yukon</i>	
G. Abbott et M. Colpron.....	57
<i>Robert E. Leckie Awards for Outstanding Reclamation Practices</i>	
J. St. Amand.....	61

### GEOLOGICAL FIELDWORK

<i>Late Wisconsinan McConnell ice-flow and sediment distribution patterns in the Pelly Mountains, Yukon</i>	
J.D. Bond and K.E. Kennedy .....	65
<i>Quaternary, structural and engineering geology of the Aishihik River landslide, Cracker Creek area (NTS115A/15), Yukon</i>	
M-A. Brideau, D. Stead, C. Huscroft and K. Fecova.....	83
<i>Preliminary investigation of the bedrock geology of the Livingstone Creek area (NTS 105E/8), south-central Yukon</i>	
M. Colpron .....	95
<i>Flood basalts of the Wrangellia Terrane, southwest Yukon: Implications for the formation of oceanic plateaus, continental crust and Ni-Cu-PGE mineralization</i>	
A.R. Greene, J.S. Scoates, D. Weis and S. Israel.....	109
<i>Lead isotope signatures of Tintina Gold Province intrusions and associated mineral deposits from southeastern Yukon and southwestern Northwest Territories: Implications for exploration in the southeastern Tintina Gold Province</i>	
R.S. Heffernan, J.K. Mortensen, J.E. Gabites and V. Sterenberg.....	121
<i>Preliminary geology of the Quill Creek map area, southwest Yukon parts of NTS 115G/5, 6 and 12</i>	
S. Israel and D.P. Van Zeyl .....	129
<i>Character and metallogeny of Permian, Jurassic and Cretaceous plutons in the southern Yukon-Tanana Terrane</i>	
T. Liverton, J.K. Mortensen and C.F. Roots .....	147

*continued*

<i>Sedimentology and hydrocarbon potential of fluvial strata in the Tantalus and Aksala formations, northern Whitehorse Trough, Yukon</i> D.G.F. Long.....	167
<i>Sedimentology, stratigraphy and source rock potential of the Richthofen formation (Jurassic), northern Whitehorse Trough, Yukon</i> G.W. Lowey.....	177
<i>Landslide processes in discontinuous permafrost, Little Salmon Lake (NTS 105L/1 and 2), south-central Yukon</i> R.R. Lyle, D.J. Hutchinson and Y. Preston .....	193
<i>Application of placer and lode gold geochemistry to gold exploration in western Yukon</i> J.K. Mortensen, R. Chapman, W. LeBarge and L. Jackson.....	205
<i>Reconnaissance geological and geochemical studies of the Joe Mountain Formation, Joe Mountain region (NTS 105D/15), Yukon</i> S.J. Piercey .....	213
<i>The isotopic sulphur composition of two barite samples from Rose Mountain area near Faro, Yukon</i> L.C. Pigage .....	227
<i>Structural evolution of the Tally Ho shear zone (NTS 105D), southern Yukon</i> A. Tizzard and S. Johnston.....	237
<i>Case study of Donjek debris flow, southwest Yukon</i> D.P. Van Zeyl and J.G. Cogley.....	247

## PROPERTY DESCRIPTIONS

<i>The Tsa da Glisza (Regal Ridge) emerald occurrence, Finlayson Lake district (NTS 105G/7), Yukon: New results and implications for continued regional exploration</i> H.L.D. Neufeld, J.K. Mortensen and L.A. Groat .....	261
<i>Mineralogical and geochemical study of the True Blue aquamarine showing, Shark property, southern Yukon</i> D. Turner, L.A. Groat and W. Wengzynowski.....	275



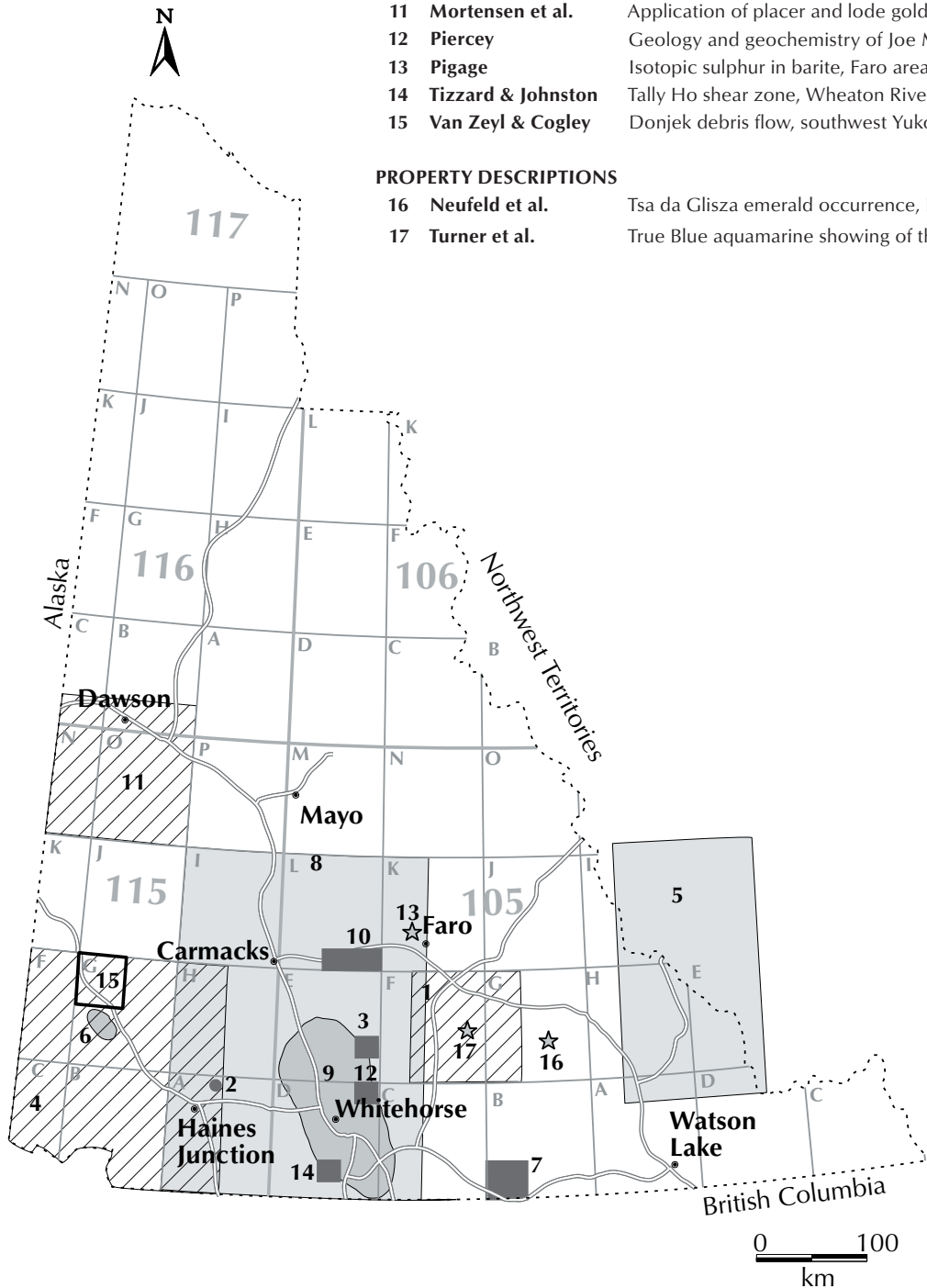
# YUKON EXPLORATION AND GEOLOGY 2004

## GEOLOGICAL FIELDWORK

- |  |   |
|--|---|
| <ul style="list-style-type: none"> <li>1 Bond &amp; Kennedy</li> <li>2 Brideau et al.</li> <li>3 Colpron</li> <li>4 Greene et al.</li> <li>5 Heffernan et al.</li> <li>6 Israel &amp; Van Zeyl</li> <li>7 Liverton et al.</li> <li>8 Long</li> <li>9 Lowey</li> <li>10 Lyle et al.</li> <li>11 Mortensen et al.</li> <li>12 Piercey</li> <li>13 Pigage</li> <li>14 Tizzard &amp; Johnston</li> <li>15 Van Zeyl &amp; Cogley</li> </ul> | <ul style="list-style-type: none"> <li>Glacial history, Pelly Mountains</li> <li>Aishihik River landslide, Cracker Creek area</li> <li>Bedrock geology, Livingstone Creek area</li> <li>Flood basalts of Wrangellia, southwestern Yukon</li> <li>Lead isotope signatures of Tintina Gold Province intrusions</li> <li>Geology, Quill Creek</li> <li>Plutons in southern Yukon-Tanana Terrane</li> <li>Hydrocarbon potential, Tantalus and Aksala formations</li> <li>Richthofen formation, northern Whitehorse Trough</li> <li>Landslide processes, Little Salmon Lake</li> <li>Application of placer and lode gold geochemistry, Klondike area</li> <li>Geology and geochemistry of Joe Mountain formation</li> <li>Isotopic sulphur in barite, Faro area</li> <li>Tally Ho shear zone, Wheaton River area</li> <li>Donjek debris flow, southwest Yukon</li> </ul> |
|--|---|

## PROPERTY DESCRIPTIONS

- |   |   |
|---|---|
| <ul style="list-style-type: none"> <li>16 Neufeld et al.</li> <li>17 Turner et al.</li> </ul> | <ul style="list-style-type: none"> <li>Tsa da Glisza emerald occurrence, Finlayson Lake area</li> <li>True Blue aquamarine showing of the Shark property</li> </ul> |
|---|---|





# MINERAL INDUSTRY

## Yukon Mining, Development and Exploration Overview 2004

*Mike Burke*  
Yukon Geological Survey

Yukon map.....	2
Abstract .....	3
Résumé.....	3
Introduction .....	4
Precious metals .....	6
Porphyry/sheeted-vein associated .....	6
Skarn/replacement associated.....	10
Vein/breccia associated .....	12
Sediment associated.....	17
Base metals .....	18
Volcanic associated.....	18
Wernecke Breccia.....	22
Porphyry/sheeted-vein associated .....	24
Gemstones .....	25
Acknowledgements.....	28
References.....	29
Appendix 1: 2004 exploration projects.....	30
Appendix 2: 2004 drilling statistics .....	33

## Yukon Placer Mining and Exploration Overview 2004

*William LeBarge*  
Yukon Geological Survey

Summary.....	35
Aperçu.....	40

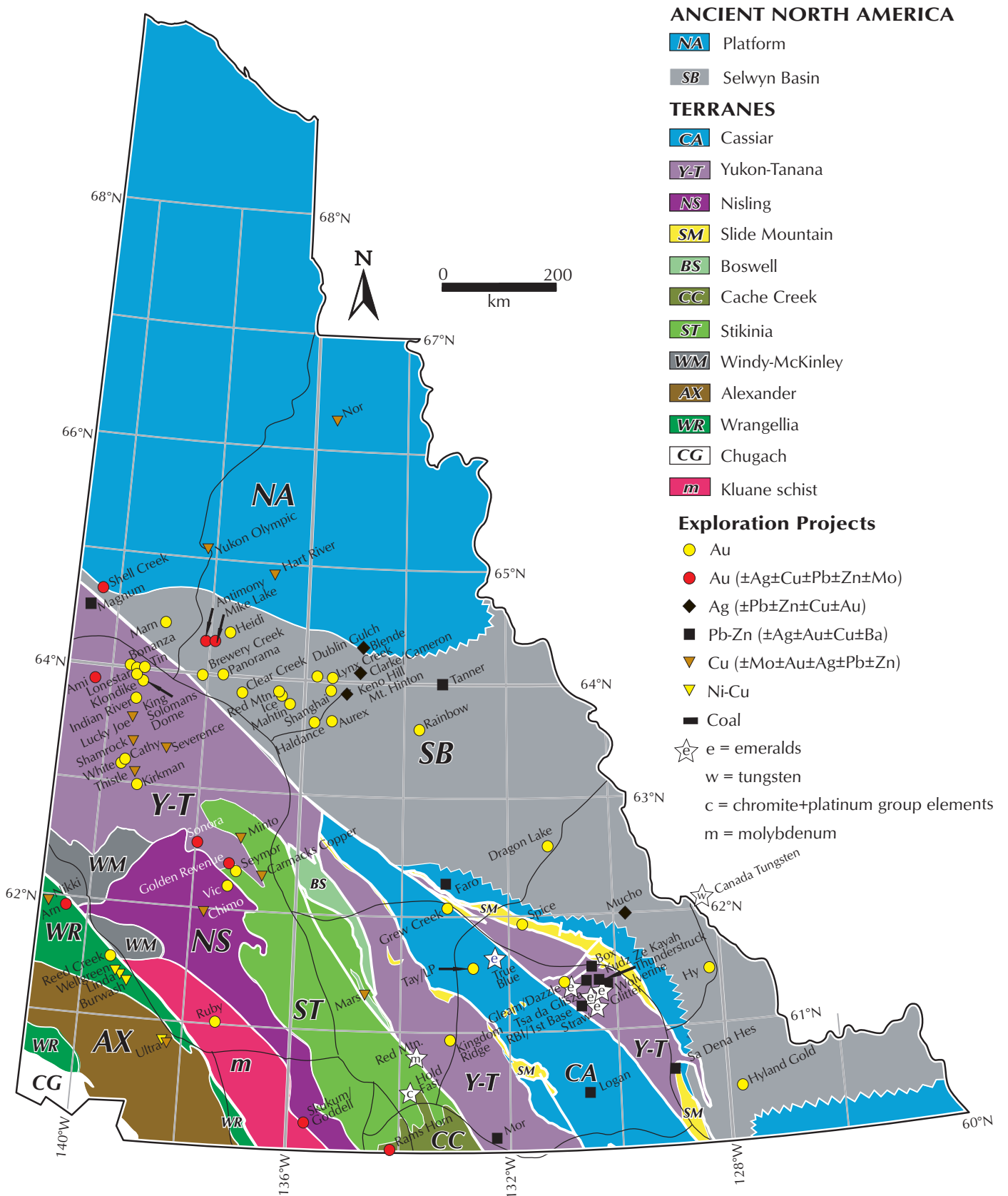


Figure 2. Location of Yukon exploration projects in 2004.

# Yukon Mining, Development and Exploration Overview 2004

*Mike Burke<sup>1</sup>*

*Yukon Geological Survey*

Burke, M., 2005. Yukon Mining, Development and Exploration Overview 2004. In: Yukon Exploration and Geology 2004, D.S. Emond, L.L. Lewis and G.D. Bradshaw (eds.), Yukon Geological Survey, p. 2-33.

## **ABSTRACT**

Mineral exploration in Yukon increased dramatically in 2004 with estimated total expenditures of \$22 million, compared to \$13 million spent in 2003. Most was spent on gold exploration, with less spent on base metals and gemstones. The exploration industry in Yukon continues to be dominated by junior mining companies although several major mining companies are also involved in exploration projects. The number of new mineral claims staked also rose substantially in 2004, as did the claims in good standing. Current or anticipated mining development projects in Yukon include: the Wolverine (Zn-Cu-Pb-Ag-Au) project, the Carmacks Copper (Cu-Au) project and the Minto (Cu-Au-Ag) and Keno Hill (Ag-Pb) projects.

## **RÉSUMÉ**

En 2004, l'exploration minière au Yukon a énormément augmenté : les dépenses estimées ont atteint 22 millions de dollars cette année, par rapport à 13 millions de dollars en 2003. Environ 60 % des dépenses ont été consacrées à la prospection d'or, 25 % à la prospection de métaux communs (surtout le Zn, le Cu et le Pb), et 15 % à la recherche de pierres précieuses. L'exploration minière au Yukon continue d'être dominée par de petites sociétés, qui sont responsables de 90 % des dépenses totales de prospection. Toutefois, plusieurs grandes sociétés minières, notamment Kennecott, Newmont, Northgate et Teck-Cominco participent aussi à des projets d'exploration. Le nombre de nouveaux claims miniers jalonnés a aussi considérablement augmenté en 2004, atteignant 9061 claims à la fin d'octobre, soit presque 3 000 de plus qu'en 2003. Le nombre total de claims en règle est passé à 49 772. Les projets miniers actuels ou prévus au Yukon comprennent le projet Wolverine (Zn-Cu-Pb-Ag-Au), pour lequel le processus d'émission de permis est en cours, le projet Carmacks Copper (Cu-Au), qui devrait faire l'objet d'une demande de permis, et les projets Minto (Cu-Au-Ag) et Keno Hill (Ag-Pb), qui sont à vendre.

<sup>1</sup>mike.burke@gov.yk.ca

## INTRODUCTION

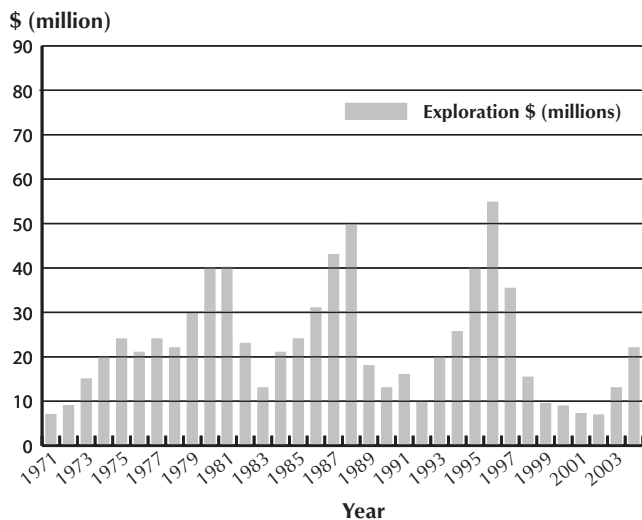
Mineral exploration in Yukon increased dramatically in 2004 with estimated total expenditures of \$22 million (Fig. 1), compared to \$13 million spent in 2003. Approximately 60% of expenditures were spent on gold exploration, 25% on base metal (mainly zinc, copper and lead) exploration and 15% on the search for gemstones. The locations for most 2004 Yukon exploration projects are shown in Figure 2 (page 2). The exploration industry in Yukon continues to be dominated by junior mining companies, who accounted for 90% of total exploration expenditures. Several major mining companies, however, including Kennecott, Newmont, Northgate and Teck-Cominco are also involved in exploration projects. The number of new mineral claims staked also rose substantially in 2004 (Fig. 3); the 9061 claims staked in 2004 is nearly a three-fold increase over the 3571 claims staked in 2003. The total number of claims in good standing increased to 49 442 (Fig. 4). Current or anticipated mining development projects in Yukon include: the Wolverine zinc-copper-lead-silver-gold project, for which mine permitting is underway; the Carmacks Copper copper-gold project, for which an application for a mining permit is expected; and the Minto copper-gold-silver and Keno Hill silver-lead projects, which are for sale.

On April 1, 2003, responsibility for managing the Territory's public lands, water, mineral resources, forests and environment was devolved from the federal to the Yukon government. This transfer of authority has had a positive impact on the mineral industry. The Yukon government offers a 25% direct tax credit on mineral exploration expenditures, which is in place until March 31, 2007. The Yukon Mining Incentive Program is another Yukon government initiative, which provides a portion of the risk capital required to explore for mineral deposits. In 2004, the Yukon Mining Incentive Program offered over \$1 million to individuals and companies active in Yukon.

Gold exploration continued to be led by the search for intrusion-related gold deposits, mainly related to mid-Cretaceous plutons in the Tombstone Gold Belt portion of the Tintina Gold Province. Although this belt of gold occurrences as a whole is perceived to be at an advanced stage of exploration, the reality is quite the opposite. There are advanced projects within the belt, but only six properties have received over 5000 m of drilling. Some of the more advanced projects include the

Brewery Creek mine and the Red Mountain project, where exploration has been ongoing since the early 1990s. StrataGold Corporation recently acquired the Dublin Gulch deposit and the Clear Creek property, two advanced properties within the belt that have numerous high-quality exploration targets and potential for resource expansion; however, each property has remained dormant since 1996 and 2000, respectively. The belt also has many properties such as the Mahtin and Heidi properties that have excellent drill targets yet have never had a single drill hole. New targets that have just received their first drilling are highlighted by the program at Antimony Mountain, where porphyry-style mineralization with very little alteration in a Cretaceous Tombstone intrusion was tested.

**Figure 1.** Exploration expenditures 1971 to 2004 (estimated).



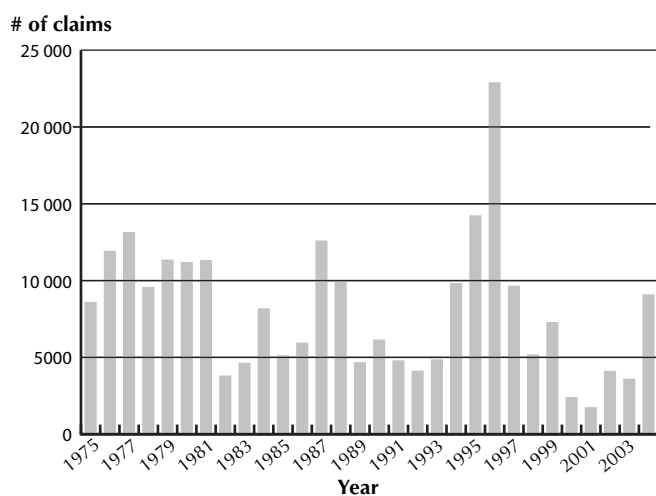


**Figure 3.** Claims staked 1975 to 2004.

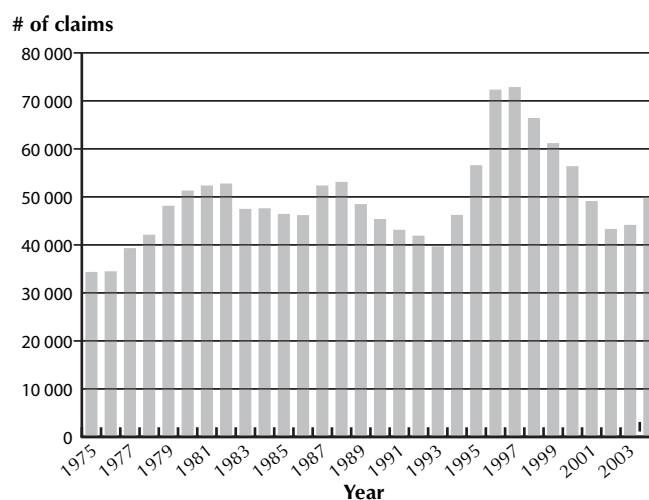


**Figure 4.** Claims in good standing 1975 to 2004.

Companies and prospectors have expanded the search for gold in Yukon, looking for various deposit types, such as gold-rich porphyry targets in the Stewart River area south of Dawson and in the Dawson Range Mineral Belt; orogenic gold veins in the White River and surrounding areas and in the Klondike; and epithermal gold-silver mineralization at the Grew Creek deposit near Ross River.

Base-metal exploration also mounted a significant comeback in 2004. The Finlayson Lake Volcanogenic Massive Sulphide District was the focus of renewed exploration after a lull of several years. The largest program in the district was conducted by Expatriate Resources on their Wolverine deposit. Early in the year, Expatriate purchased joint venture partner Atna Resources' interest in the Wolverine joint venture to own 100% of the project; the company is advancing the project to a bankable feasibility and production decision in 2004-2005. Teck-Cominco renewed their exploration efforts in the Finlayson Lake District by optioning a block of land known as R-15 from the Kaska Mineral Development Corporation (KMDC). The KMDC was able to obtain a 5-year lease on the land, with the permission of the Ross River Dena Council (RRDC), from the Yukon government. The block was interim-protected since 1983 as part of the RRDC land claim; thus, this agreement could not have been completed before devolution. Iron-oxide-copper-gold deposits were also a favoured target for base metal exploration this year, with several programs examining occurrences within Proterozoic inliers in north-central Yukon.

Exploration for coloured gemstones, mainly emeralds, continued at significant levels in 2004. True North Gems completed a large program of bulk sampling, core drilling and prospecting on the Tsa da Glisza project (formerly called Regal Ridge) in the Finlayson Lake District. Several companies were also active in the area, continuing the search for additional emerald deposits (Appendix 1).



## PRECIOUS METALS

### PORPHYRY/SHEETED-VEIN ASSOCIATED

**Figure 5.** Geologists and students examining drill core at Brewery Creek as part of a field trip during the first Dawson Rocks conference.



NovaGold Resources conducted a four-hole (769-m) diamond drilling program, which was stopped due to encroaching forest fires on the **Brewery Creek** mine property (Yukon MINFILE 2004, 116B 160, Deklerk and Traynor, 2004). Drilling followed a program of geophysics consisting of an induced polarization survey over a 2-km square grid. Brewery Creek produced approximately 280,000 ounces (8 700 000 g) of gold from a heap leach operation that operated from 1998 to

2002. Previous exploration focused on the search for additional oxide resources. NovaGold is exploring Brewery Creek based on similarities with their 25-million-ounce (780-million-g) Donlin Creek deposit in Alaska. NovaGold tested several targets, which included a higher grade and deeper structural sulphide zone. It successfully intersected a massive stibnite-arsenopyrite-pyrite mineralized vein within sheared argillite, however, results of the drilling have not been released (Fig. 5).

ASC Industries optioned the **Red Mountain** property (Yukon MINFILE 2004, 115P 006, Deklerk and Traynor, 2004) from Regent Ventures and merged it with their wholly owned and adjoining Ice claims. Drilling on the Ice claims was directed at the Jethro structure which was discovered in 2003, with an intersection of 102 m grading 0.88 g/t Au in DD03-12. Drilling in 2004 was again directed at the

**Table 1.** Drill highlights from the Jethro structure of the Red Mountain property.

Drill hole	Depth		Width (m)	Au (g/t)
	From (m)	To (m)		
DDH04-13	33.0	48.0	15.0	1.10
DDH04-14	3.8	120.0	116.2	1.07
DDH04-16	2.0	112.8	110.8	0.485
including	12.60	16.2	3.60	5.57
DDH04-17	11.00	12.0	1.00	2.00
	19.00	21.0	2.00	1.10
	34.00	35.0	1.00	9.24
	52.00	53.0	1.00	10.20
DDH04-18	17.00	191.00	174.00	0.95
including	17.00	142.00	125.00	1.14
or	45.00	113.00	68.00	1.49
or	74.00	113.00	39.00	1.97
DDH04-19	67	113	46	0.86
	98	118	20	1.01
	128	167	39	0.90

1.2 km strike-length of the structure (Fig. 6). Six of the holes that were drilled intersected significant gold mineralization within Cretaceous quartz monzonite of the Tombstone Plutonic Suite and hornfelsed siltstone of the Neoproterozoic to Lower Cambrian Hyland Group. The zone remains open along strike to the northeast and southwest and at depth. Highlights from drilling on the Jethro structure are presented in Table 1. Drilling also tested the Treadwell structure with four holes following up on the discovery hole of 2003. Results have been released from one hole (Table 2) with additional results pending.

**Table 2.** Drill highlights from the Treadwell structure of the Red Mountain property.

Drill hole	Depth		Width (m)	Au (g/t)
	From (m)	To (m)		
DDH04-41	34.60	35.60	1.00	1.15
	62.00	68.00	6.00	1.05
	154.50	157.50	3.00	1.85
	164.50	165.50	1.00	1.24
	172.60	173.60	1.00	1.24





**Figure 6.** Drill operating on the Jethro structure at the Red Mountain property.



**Figure 7.** Julianne Madsen examines evidence of historical gold exploration, an old flume located on a ridgecrest within the Jethro structure, Red Mountain.

StrataGold Corporation conducted induced-polarization surveys followed by diamond drilling on their **Lynx Creek** property (Yukon MINFILE 2004, 106D 020, Deklerk and Traynor, 2004). The property has not been explored since 1997 when previous operators drilled a shear-hosted quartz-sulphide mineral vein zone within a small Cretaceous Tombstone Plutonic Suite plug over a 500-m strike length that assayed up to 7.37 g/t Au over 3.4 m. Drilling in 2004 mainly tested geochemical anomalies proximal to the intrusive body and intersected gold-bearing sheeted and cross-cutting quartz and quartz/calcite veins. Higher grades were generally associated with arsenopyrite, pyrite, stibnite and sphalerite in veinlets within metasedimentary rocks of the Neoproterozoic to Lower Cambrian Hyland Group proximal to the granodiorite intrusion (Fig. 8). Five of the fourteen drill holes (2070 m) intersected significant mineralization:

- LX04-20: 17.1 m averaging 1.50 g/t Au;
- LX04-18: 7.6 m averaging 1.09 g/t Au;
- LX04-11: 27.5 m averaging 0.62 g/t Au;
- LX04-08: 8.1 m averaging 0.48 g/t Au;
- LX04-13: 4.5 m averaging 0.89 g/t Au.

Lynx Creek is located ~6 km east of the **Dublin Gulch** deposit (Yukon MINFILE 2004, 106D 025, Deklerk and Traynor, 2004). Dublin Gulch is a plutonic-related gold deposit hosted by sheeted quartz veins in Cretaceous granodiorite of the Tombstone Plutonic Suite. StrataGold Corporation entered into a binding agreement in October to purchase the Dublin Gulch deposit and the **Clear Creek** property (Yukon MINFILE 2004, 115P 011,012,013, Deklerk and Traynor, 2004) from Sterlite

**Figure 8.** Quartz-carbonate mineral vein with pyrite-arsenopyrite from drilling at the Lynx Creek property.



Gold Ltd. The occurrence at Clear Creek consists of a number of plutonic-associated gold occurrences related to several Cretaceous granodiorite intrusions of the Tombstone Plutonic Suite. Snowden Mining Industry Consultants has reviewed and confirmed the resource estimates for the Eagle zone located on StrataGold's Dublin Gulch property. Snowden confirms that, at a cut-off grade of 0.5 g/t Au, the Eagle zone contains 55.2 million tonnes of indicated resources at a grade of 0.934 g/t Au (1,658,000 ounces, 51 570 000 g) and 17.3 million tonnes of inferred resources grading 0.734 g/t Au (412,000 ounces, 12 800 000 g). Subsequent to the purchase, StrataGold conducted airborne magnetic and electromagnetic surveys of Dublin Gulch and their surrounding claims. In conjunction with this acquisition, on December 1, 2004, StrataGold closed an \$18.4-million special warrant and flow-through share private-placement financing. Additionally, Newmont Mining Corporation invested \$3.25-million in a subscription receipt private-placement financing which closed on November 16, 2004. Newmont also participated in the December 1, 2004, special warrant financing as to 1 million special warrants. StrataGold now holds over 740 km<sup>2</sup> of mineral claims in the Mayo Mining District, which include the Dublin Gulch, Clear Creek, Lynx Creek and **Aurex** properties.

Strategic Metals staked claims to cover a portion of the Antimony Mountain pluton which it subsequently optioned to War Eagle Mining. Previous exploration at the **Antimony Mountain** property (Yukon MINFILE 2004, 116B 094, Deklerk and Traynor, 2004) targeted high-grade gold-bearing quartz-sulphide mineral veins proximal to the main intrusive body. In 2004, the companies focused on porphyry-style mineralization within the syenite to monzonite intrusive rock of the Cretaceous Tombstone Plutonic Suite. An area of anomalous copper, gold and silver in stream sediments, soils and rocks was tested with four diamond drill holes (832 m; Fig. 9). The drilling intersected arsenopyrite and chalcopyrite occurring on hairline fractures, in 0.2- to 2-cm-wide quartz veinlets, or in narrow alteration envelopes surrounding the mineralized fractures and veinlets. The drilling returned values in the range of 200-300 ppb Au over 20 to 40 m in three of the four holes.

**Figure 9.** (left) Mike Phillips of Archer, Cathro and Associates with Craig Hart and Lara Lewis from the Yukon Geological Survey, viewing core at Antimony Mountain.



Yale Resources and Atac Resources completed a 13-hole core drilling program (Fig. 10) on their **Golden Revenue** property (Yukon MINFILE 2004, 115I 107, Deklerk and Traynor, 2004) located within the Dawson Range Mineral Belt. This belt includes several Late Cretaceous copper-gold and gold porphyry deposits and targets (including the Casino deposit of Lumina Copper, 964 million tonnes grading 0.22% Cu, 0.24 g/t Au and 0.02% Mo) in central Yukon. Drilling was directed at a 1000-m by 400-m area within the Nucleus zone which had returned gold intersections from previous drilling. Disseminated sulphide minerals and quartz-sulphide mineral veins and stockwork are hosted within quartz-feldspar dykes



and adjacent metavolcanic and metasedimentary schists. Holes drilled late in the program intersected more copper-rich mineralized rock indicating drilling was approaching the porphyry centre, which was previously thought to be a deeper system. Table 3 contains highlights from the 2004 drilling.

Firestone Ventures optioned the **Sonora Gulch** property (Yukon MINFILE 2004, 115J 008, Deklerk and Traynor, 2004) which is also located within the Dawson Range Mineral Belt. The company explored the property with a small program of geochemistry, prospecting and geological mapping. At Sonora Gulch, high-grade gold-tetradymite veins are hosted within structural zones, and copper and gold occur in quartz-chalcopyrite stockwork and disseminated pyrite-chalcopyrite within a quartz-feldspar porphyritic intrusion. The company focused their attention on the newly discovered K-467 zone, where quartz-pyrite-chalcopyrite stockwork within intrusive rocks returned values up to 0.232 g/t Au, 8.4 g/t Ag and 0.168% Cu from a 1.4-m chip sample (Fig. 11). Composite grab samples of quartz-arsenopyrite veins returned values up to 0.95 g/t Au and 10.6 g/t Ag. Silt sampling and reconnaissance-scale geochemical sampling returned values suggesting the new zone may be quite extensive.

Other companies active in the belt included Atac Resources, who trenched on the **Seymour** property (Yukon MINFILE 2004, 115I 051, Deklerk and Traynor, 2004).



**Figure 10.** Drilling at the Golden Revenue property in early October.



**Figure 11.** Dennis Ouellette examining outcrop in the K-467 zone at Sonora Gulch.

**Table 3.** Highlights from 2004 drilling on Golden Revenue property.

Drill hole	Depth		Width (m)	Au (g/t)
	From (m)	To (m)		
DN04-01	8.84	115.5	106.66	0.57
DN04-02	8.38	65.53	57.15	0.71
DN04-03	16.0	126.0	110.0	0.76
DN04-04	14.63	37.0	22.37	0.66
DN04-06	95.40	110.30	14.90	0.92
including	99.84	110.30	10.19	1.13
DN04-07	32.63	53.07	20.44	0.62
including	43.28	53.07	9.79	0.88
including	43.28	50.60	7.32	1.07
DN04-08	6.25	117.06	110.81	1.35
including	6.25	84.6	78.35	1.69

Drill hole	Depth		Width (m)	Au (g/t)
	From (m)	To (m)		
DN04-09	109.27	127.73	18.46	0.64
including	109.27	115.76	6.49	1.04
and	138.94	148.74	9.80	0.51
and	170.84	172.98	2.14	3.70
DN04-12	141.55	157.35	15.80	0.572
including	147.22	151.79	4.57	1.112
and	227.09	238.66	11.57	0.619
DN04-13	105.36	112.7	7.34	6.78
and	123.15	127.94	4.79	1.87
DN04-14	17.37	23.65	6.28	1.18
and	37.80	41.15	3.35	1.150
and	147.10	151.53	4.43	0.613



## SKARN/REPLACEMENT ASSOCIATED



**Figure 12.** Dig here! Callum Ryan exposing skarn rock in a blast trench at the Mahtin property.

International Gold Ventures optioned the **Mahtin** property (Yukon MINFILE 2004, 115P 007, Deklerk and Traynor, 2004) and performed a program of geological mapping, geochemistry, geophysics (magnetics) and trenching (Fig. 12). The Mahtin property covers the Cretaceous Sprague Creek stock, which intrudes Upper Cambrian-Ordovician limestone of the Rabbitkettle Formation. The property is host to several styles of intrusive-related gold occurrences, including sheeted quartz-arsenopyrite veins within the intrusion, and skarn and calc-silicate rock within the Rabbitkettle Formation.

Logan Resources completed a program of geophysics (magnetics, induced polarization (IP) and electromagnetics) on the **Heidi** property (Yukon MINFILE 2004, 116A 037, Deklerk and Traynor, 2004). The magnetometer survey covered an area of 3.2 km<sup>2</sup>,

whereas the IP covered a smaller 0.5-km<sup>2</sup> grid. Four short lines of horizontal-loop electromagnetics were also completed. The surveys outlined geophysical anomalies (magnetic and chargeability) that coincide with areas of anomalous geochemistry (up to 1100 ppb Au and 12 000 ppm As) defined by Homestake, who held the property in the mid-1990s. Sphide minerals on the property replaced limestone and calcareous grit of the NeoProterozoic to Lower Cambrian Hyland Group. The area is likely distal to an unexposed intrusion as indicated by regional geophysics, the presence of porphyry dykes and hornfelsing of the sedimentary rocks. No drilling has ever been done on the property.

**Figure 13.** Diamond drilling on the Hyland Gold property.



Northgate Exploration and StrataGold Corporation conducted a program of geophysics (IP) and diamond drilling (Fig. 13) of eight holes (1800 m) on the **Hyland** property (Yukon MINFILE 2004, 095D 011, Deklerk and Traynor, 2004) in

southeastern Yukon. A historical oxide resource of 3.2 million tonnes grading 1.1 g/t Au exists on the property. The claims are underlain by the Neoproterozoic to Lower Cambrian Hyland Group phyllite and quartzite, which in the main area of exploration are interpreted to form an east-verging overturned anticline. A large magnetic-low feature is located just to the north of the Main zone. There is intense silica and sulphide mineral replacement of the phyllite and quartzite in the core of the anticline. Three drill holes tested an area along strike from the Main zone, where drilling in 2003 intersected significant gold-silver mineralization which assayed up to 1.38 g/t Au and 3.54 g/t Ag over 53.2 m, and 2.02 g/t Au and 64.87 g/t Ag over

6.5 m. Drilling in 2004 returned significant results, but grades were generally lower than in the core of the Main zone. An additional two holes tested quartz-sulphide veins in the hanging wall of the Main zone and also intersected gold mineralized rock (Table 4).

Three regional targets up to 2.7 km from the Main zone were each drilled with a single drill hole based on geophysics, geochemistry and structural interpretations. No significant results were reported from these holes.

In the Mayo area, John Peter Ross staked the **Haldane** property (Yukon MINFILE 2004, 105M 056, Deklerk and Traynor, 2004) on Mt. Haldane, based on a similar geologic setting to the McQuesten and Aurex properties located 10 km to the east. The properties are located along the Robert Service Thrust fault in hangwall rocks of the Neoproterozoic to Lower Cambrian Hyland Group. Klondike Gold Corporation optioned the property from Ross and performed a small program of geochemistry on the claims.

Yankee Hat Exploration conducted a program of geochemistry and geological mapping on the **Shanghai Creek** property (Yukon MINFILE 2004, 105M 028, Deklerk and Traynor, 2004) near Mayo. Shanghai Creek is located on the north limb of the McQuesten anticline. The claims cover a portion of the Robert Service Thrust, are underlain by the Neoproterozoic to Lower Cambrian Hyland Group rocks, and are intruded by a small plug. This is the same geologic setting as the McQuesten and Aurex properties located 10 km to the south. The program outlined several areas anomalous in gold, arsenic and antimony (Fig. 14). The claims were staked based on data from geochemical and heavy-mineral sampling done by the Geological Survey of Canada as part of Operation Keno in the 1960s (Boyle and Gleeson, 1971).

Eagle Plains Resources conducted a geophysical program consisting of IP and horizontal-loop electromagnetics on their **Dragon Lake** property (Yukon MINFILE 2004, 105J 007, Deklerk and Traynor, 2004) located approximately 85 km northeast of Ross River. Previous work by the company,

**Table 4.** Significant drill intersections from the Hyland property.

Drill hole	Depth		Width (m)	Au (g/t)
	From (m)	To (m)		
<b>Main Zone</b>				
Hy04-13	111.48	113.48	2.00	0.79
including	147.83	153.39	5.56	0.47
including	186.46	218.22	31.76	0.63
	194.00	198.06	4.06	0.99
	201.71	204.42	2.71	1.24
HY04-14	65.25	79.80	14.55	0.54
including	74.58	78.03	3.45	0.97
including	85.64	88.68	3.04	0.70
	166.66	168.17	1.51	0.87
	210.47	237.45	26.98	0.61
	210.47	216.69	6.22	0.93
HY04-15	68.32	77.42	9.10	0.45
including	69.76	71.48	1.72	0.89
including	166.30	173.30	7.00	0.48
including	167.60	169.16	1.56	0.92
	226.50	245.31	18.81	0.75
	241.78	245.31	3.53	1.06
<b>Hanging wall veins</b>				
HY04-16	99.81	101.51	1.70	0.62
	109.62	112.31	2.69	0.56
	115.14	116.05	0.91	0.60
HY04-17	92.02	94.84	2.82	0.56



**Figure 14.** Demobilizing from the Shanghai Creek property near Mayo.





**Figure 15.** Helicopter-portable drill on the Arn property.

**Table 5.** Significant drill intersections from the Arn property.

Drill hole	Interval (m)	Au (g/t)	Ag (g/t)	Copper (%)
Arn-05	5.28	2.17	9.4	1.27
	5.19	3.17	18.9	2.50
Arn-06	1.39	0.53	5.1	0.92
Arn-09	0.99	15.55	2.1	0.48
Arn-10	2.32	18.10	0.5	nil
	3.05	3.05	26.9	3.18
Arn 11	1.85	1.57	nil	0.03
	1.34	1.98	17.1	3.95
Arn-12	1.38	1.38	20.4	3.24
	8.59	8.59	10.4	1.30
Arn-14	0.6	1.72	3.1	0.63
Arn-16 including	6.34	8.60	2.7	0.50
	0.75	66.30	12.2	0.92
Arn-20	1.83	0.9	0.10	3.63

including diamond drilling in 1999 (3.7 g/t Au over 1.2 m), outlined extensive metalliferous calc-silicate rock within calcareous sedimentary rocks of the Neoproterozoic to Lower Cambrian Hyland Group, which were intruded by a small mid-Cretaceous stock.

Cash Minerals Ltd. conducted a five-hole (671 m) diamond drill program on their wholly owned **Mucho** property (Yukon MINFILE 2004, 105I 004, Deklerk and Traynor, 2004) in southeastern Yukon. The property hosts numerous intrusion-related mineralization styles, including skarn, veins and shears associated with the Cretaceous Nar pluton. Cash Minerals targeted silver-zinc-copper-lead-gold mineralized rock with the drilling that

was conducted late in the season. Results from the drilling had not been released by year's end.

Klondike Gold optioned the **Arn** property (Yukon MINFILE 2004, 115F 048, Deklerk and Traynor, 2004), a copper-gold skarn occurrence, from Atac Resources. The Arn property is located only 6 km from the Alaska Highway in southwestern Yukon. Skarn is developed in Upper Jurassic to Lower Cretaceous volcanic and sedimentary rocks that have been intruded by a swarm of late Early Cretaceous porphyritic to non-porphyritic andesite, diorite and latite dykes. Drilling (Fig. 15) targeted a zone where drilling in 2003 intersected skarn that assayed 11.92 g/t Au over 12.67 m, including 64.40 g/t Au over 1.98 m. This year's drilling intersected numerous skarn units, but abundant post-mineralization dykes disrupted many of the zones. Despite that, many significant pyrrhotite-magnetite-pyrite-chalcopyrite-rich zones were drilled (Table 5). Numerous other skarn zones have been discovered on the property by prospecting and trenching, and remain to be further tested.

**VEIN/BRECCIA ASSOCIATED**

Ross River Minerals digitally compiled all previous drilling on their **Tay-LP** property (Yukon MINFILE 2004, 105F 121, Deklerk and Traynor, 2004) and computer modeling of the data suggested a westerly dip to mineralized structures intersected in earlier drill programs. The earlier holes were oriented mostly parallel to the structurally hosted quartz-sulphide mineral veins, which are not exposed in the bottom of the till-

covered valley. The drilling was reoriented and the first target was a 1.6-km-long magnetic-electromagnetic anomaly intersected in hole TLP02-7 drilled in 2002, which assayed 8.99 g/t Au over 3.56 m. The drilling successfully intersected mineralized rock in all holes drilled at various spacings along the geophysical anomaly over a 1.3 km strike length. Quartz occurs in veins with pyrrhotite-pyrite (Fig. 16) and minor chalcopyrite and tourmaline, hosted within a Lower Cambrian

calcareous biotite schist and interbedded limestone. Gold-bearing sulphide replacement zones occur over significant thicknesses adjacent to the veins. Table 6 summarizes drilling highlights from this year's program.

There is a new exploration revival in the Klondike, with several companies focusing on gold mineralization in this large, and still active, placer gold district. Klondike Star optioned a number of properties from Klondike Gold Corporation and constructed a pilot mill (Fig. 17) on the **Lone Star** property (Yukon MINFILE 2004, 115O 072, Deklerk and Traynor, 2004). This was in preparation for a bulk sampling program which will test rock from this occurrence and other properties in the region. In addition to the mill construction, Klondike Gold conducted geological mapping, prospecting, geochemical surveys and mechanized trenching on their extensive claim groups in the area. Prospecting resulted in the discovery of an old shaft approximately 1300 m along strike from the historic Lone Star adit. Grab samples of quartz vein material from the newly discovered shaft assayed up to 13.68 g/t Au. Soil sampling along the trend of the Lone Star vein returned anomalous gold values for an additional 900 m beyond the new discovery. This zone will be a high priority target for bulk sampling in 2005.

Klondike Source Limited, an Australian-based exploration company, conducted an exploration program on their **Klondike** property (Yukon MINFILE 2004, 115O 079, etc., Deklerk and Traynor, 2004), which included diamond drilling (Fig. 18) of six holes (1437 m). Klondike Source has been working on their holdings which consist of 490 wholly owned claims and an additional 443 claims optioned from PacRim Resources. The company has performed geochemical surveys, structural interpretation from landsat and airphotos, and geological mapping on the claims. The drilling was designed to test the theory that the source of the abundant placer gold in the Klondike District was from flat-lying zones similar to the Pogo deposit in Alaska. Drilling was concentrated in the area above Victoria Gulch and Bear Creek. Drill hole 04-01 intersected 0.018 g/t Au and 1070 g/t Ag over 2.88 m and hole 04-06 intersected 1.2 m of 0.951 g/t Au associated with a narrow arsenopyrite vein.

J.A.E. Resources conducted a geological sampling and prospecting program on their claims, which cover the east and north flanks of **King Solomon Dome** (Yukon MINFILE 2004, 115O 068, Deklerk and Traynor, 2004) in the heart of the Klondike District. The program was following up on significant results generated by

**Table 6.** Significant drill intersections from the Tay-LP property.

Drill hole	Interval (m)	Au (g/t)
TLP04-01	19.6	1.33
including	3.4	5.13
TLP04-02	10.5	3.96
including	6.1	6.5
TLP02-03	5.5	0.7
TLP04-04	11.0	3.0
including	1.08	12.5
TLP04-05	3.2	1.85
and	10.52	2.0
TLP04-07	8.02	0.91
TLP04-08	1.08	1.68



**Figure 16.** Jeff Bond of the Yukon Geological Survey with a cored section of quartz-pyrrhotite-pyrite vein from the Tay-LP property.



**Figure 17.** Pilot-scale mill on the Lone Star property in the Klondike.



**Figure 18.** Drill set-up on Klondike Source's Klondike property. The headwaters of Victoria Gulch are in the background.



Barramundi Gold who optioned the property during 1996-97. Work by Barramundi generated 72 chip and grab samples grading from 0.1 to 32.0 g/t Au. In 2004, values up to 3.72 g/t Au were obtained from pyritic chlorite-muscovite schist adjacent to gold-quartz veins. Chip sampling across a zone of narrow mesothermal quartz veins (>15 cm) hosted in pyritized dark green schist (quartz porphyry?) returned values of 0.633 g/t Au over 4.13 m and 1.162 g/t Au over 3.1 m. Elsewhere on the property, limonitic and pyritized schist adjacent to quartz-pyrite-galena veins returned up to 40.7 g/t Au over 0.7 m, with the vein assaying 3.4 g/t Au over 2.2 m.

Hinterland Metals Inc. explored the **Helen** gold vein (Yukon MINFILE 2004, 105G 030, Deklerk and Traynor, 2004), with prospecting, geochemical sampling and a horizontal-loop electromagnetic (HLEM) survey. The Helen vein was discovered in 2003 while conducting gemstone exploration adjacent to a Cretaceous intrusion in the Finlayson Lake District. The vein contains quartz, arsenopyrite and pyrite. The HLEM survey outlined a weak conductor over 300 m long that encompasses the newly discovered vein showing. Prospecting along the conductor discovered poorly exposed mineralized rock that assayed 3.41 g/t Au and 2.9 g/t Au approximately 50 m from the original showing. Rusty quartz float in talus that assayed 59.6 g/t Ag was found a further 80 m from the newly discovered mineralization.

Freegold Ventures Limited optioned the Eocene **Grew Creek** low sulphidation epithermal gold-silver deposit (Yukon MINFILE 2004, 105K 009, Deklerk and Traynor, 2004) from Whitehorse prospector Al Carlos. Drill-indicated reserves (non-compliant with the National Instrument 43-101) of 773 020 tonnes grading 8.92 g/t Au and 33.6 g/t Ag exist in the Main zone. The property is midway between Ross River and Faro and is located 1 km from the Robert Campbell Highway on the main Yukon power grid. The deposit is hosted in Eocene volcanic rocks within a graben formed by the Tintina fault system. A new interpretation of the dominant vein direction in the deposit is being tested by Freegold. Initial results support their hypothesis that the veins have a northerly strike and that previous drilling was conducted subparallel to the veins (Fig. 19). The new interpretation indicates additional potential for expanding the Main zone 200 m to the south and to depth. Quartz-adularia veins and stockwork are hosted within pyroclastic felsic tuffs. Based on the immediate success of the drilling, Freegold expanded their exploration budget (12 holes, 2077 m) and mobilized a second drill to the property. Drilling continued through December. Several other zones exist on the property that remain to be drill tested. Results available by year end are highlighted in Table 8.



**Figure 19.** Narrow quartz-adularia vein from drilling at Grew Creek.

Tagish Lake Gold conducted a two-hole (900 m) drill program on the **Goddell** shear zone (Yukon MINFILE 2004, 105D 025, Deklerk and Traynor, 2004). The drilling was used to train diamond drill helpers and was funded by the Yukon government's Department of Energy, Mines and Resources, and administered by the Yukon Mining Training Trust Fund. The drilling was directed along strike from the zone which

**Table 8.** Drill intersections from the Grew Creek property.

Drill hole	Width (m)	Au (g/t)	Au (g/t)
GC-04-225	118.0	1.81	2.6
including	90.5	2.25	3.2
including	17.5	6.79	8.8
including	2.0	14.38	8.5
and	2.3	17.77	30.2
GC-04-226	128.0	0.38	0.70
including	90.0	0.46	0.65
including	57.5	0.53	0.65
including	7.5	1.56	0.80
GC-04-227	6.25	22.12	44.7
and	1.55	60.50	149.0





**Figure 20.** Participants in a Mining Analyst Tour sponsored by the Yukon government, viewing Goddell core.

contains indicated mineral resources of 320 000 tonnes grading 11.2 g/t Au and inferred mineral resources of 280 000 tonnes grading 9.21 g/t Au. Last year, Tagish Lake Gold drilled two holes 225 m along strike from the resource, with the best hole intersecting 26.9 m grading 2.5 g/t Au, including 9.0 m grading 5.9 g/t Au. This year's drilling was a further 200 m stepout along strike from last year's intersections. Drill hole GG04-03 intersected intensely sheared Cretaceous quartz monzonite cut by dark mylonitic shear fabrics that contain fine pyrite and arsenopyrite. The quartz monzonite is also cut by rhyolite and andesite dykes. Intervals in this zone assayed 0.99 g/t Au over 0.35 m and 1.03 g/t Au over 1.21 m. The drilling indicates the zone is still present but is less mineralized in this area. The second hole, drilled 40 m along strike from the first, intersected a 49-m-wide barren rhyolite dyke within the shear zone. A 1.5-m section of sheared quartz monzonite and mylonite graded 1.03 g/t Au (Fig. 20).

The **Shell Creek** property (Yukon MINFILE 2004, 116C 029, Deklerk and Traynor, 2004) was explored by Logan Resources with silt sampling, geochemistry, geological mapping and excavator trenching in 2004. The property covers a Precambrian or Cambrian Algoma-type banded iron formation (BIF) consisting of a magnetite-chert unit that has been subjected to several phases of folding. In 2002, prospector Shawn Ryan discovered a visible gold- and copper-mineralized quartz-carbonate zone hosted by chloritic schists and phyllites in the hanging wall of the iron formation. Mapping in 2004 suggests the quartz-carbonate veins formed in the noses of folds, similar to saddle reef-type veins (Fig. 21). Mapping and prospecting concentrated on the northern portion of the BIF, where four, or possibly five, gold-copper-mineralized quartz saddle reef structures were identified over a 6-km

**Figure 21.** Massive quartz saddle reef vein on the Shell Creek property.







**Figure 22.** *Cheyenne Ryan learning to trench at the White property.*

**Figure 23.** *Shawn Ryan stands on a massive gold-bearing quartz vein exposed by trenching on the White property.*



strike length. Quartz reefs along the northern belt of BIF form shallow southwest-plunging, upright, openly folded, anticlinal structures that are from 50 to 75 m wide across the region of the fold closure. Individual reefs consist of a number of stacked quartz veins that range from less than half a metre to several metres in thickness, separated by intervals of variably chloritized, host sedimentary rock. Quartz reefs are thickest at the hinge zone and progressively thin out and dissipate as the veins roll into the steeper fold limbs. In addition to the

gold in quartz veins, clastic metasedimentary rocks proximal to zones with late-stage vein development are typically pervasively chloritized and contain elevated copper. This copper occurs as disseminated chalcocite developed along schistosity surfaces. Grab samples of chalcocite-bearing, chloritized sedimentary rocks returned assays up to 1.8% copper. One trench was excavated on the property and uncovered veins and extensive quartz-carbonate mineral float where predicted by mapping. The morphology of the veins was not well exposed by the trench. Assay results of sampling from this year's program are not yet available. Results from last year's exploration on the property returned up to 9.08 g/t Au in quartz-carbonate.

Madalena Ventures optioned the **White** property (Yukon MINFILE 2004, 115O 012, Deklerk and Traynor, 2004) which is located on the Yukon River across from the mouth of the White River. In 2003, prospector Shawn Ryan discovered quartz float on the property that contained traces of galena, tetrahedrite and chalcopyrite and assayed 50 g/t Au. A return visit to the site resulted in the discovery of an old hand trench approximately 25 m from the location of the float. The company performed a program of geological mapping, line-cutting, geochemistry, geophysics

(magnetics) and trenching (Fig. 22) in 2004. Trenching at the location of the original hand trench exposed two parallel quartz veins with trace galena, chalcopyrite and visible gold. The veins vary from 1 to 5 m in width and are each exposed over a 12-m length. The veins dip steeply, and are hosted in Devonian to Mississippian quartz-sericite schist with a shallow foliation, which is in turn intruded by a large mid(?) to late Paleozoic gabbroic body (Fig. 23).

Cordilleran Minerals Limited, a private Whitehorse-based exploration company, staked the **Kingdom Ridge** property (Yukon MINFILE 2004, 105C 022, 027, Deklerk and Traynor,



2004) south of Quiet Lake in 2003. Gold-bearing quartz veins are hosted in Devonian to Mississippian rocks of the Yukon-Tanana Terrane which are intruded by the mid-Cretaceous Quiet Lake Batholith. In the area of quartz veining, host rocks are described as orange-weathering carbonates intercalated with a light green to dark green amphibolite(?). Grab samples of quartz vein material assayed up to 15.2 g/t Au, 4.3 g/t Ag and 912 ppm As. In 2004, the company completed a 700 line-km airborne magnetic, electromagnetic and radiometric survey over the property, as well as stream sediment sampling.

Aurchem Exploration, a private company, explored the **Vic** claims (Yukon MINFILE 2004, 115I 068, Deklerk and Traynor, 2004) which are approximately 10 km to the north of the former producing Mt. Nansen gold-silver mine. The company conducted diamond drilling of the “28 zone,” a quartz vein that varies from 1 to 3 m over an approximately 200-m strike length. The quartz vein contains no sulphide minerals and cuts a Jurassic porphyritic syenite. The company reported drilling intersected values up to 40.02 g/t Au over 1.34 m.

### SEDIMENT ASSOCIATED

Boulder Mining conducted an extensive program of roto-sonic drilling, bulk sampling and trenching on two large bench deposits of White Channel gravels on the **Indian River** project, south of the Klondike Goldfields on claims optioned from the Western Prospector Group. This is one of the first large-scale, methodical exploration programs conducted by a publicly traded company on this type of placer deposit in Yukon. Results from the program have been very encouraging and indicate that a large economic placer deposit may be contained in the benches. Results of the program are outlined in the Placer Mining Overview section of this publication (LeBarge, this report). Boulder Mining also staked over 1000 quartz claims covering exposures of the Cretaceous **McKinnon Creek** conglomerate (Yukon MINFILE 2004, 115O 054, Deklerk and Traynor, 2004; Fig 24). These conglomerates were first explored in the early 1900s and have seen sporadic exploration since the 1960s. Past work has identified gold in the matrix of the conglomerate suggesting paleoplacer potential. Additional potential for epithermal



**Figure 24.** Cretaceous gold-bearing McKinnon Creek conglomerate from the Indian River area.

mineralization, related to the coeval Cretaceous Carmacks flows, sills and dykes, is indicated by anomalous silver, arsenic, barium, mercury, lead and antimony (c.f., Lowey, 1983). Boulder has confirmed the gold-bearing potential of the conglomerates in several areas, and through their drilling and trenching program has identified areas of higher placer-gold potential that are underlain by conglomerates.

## BASE METALS

Base metal exploration made a healthy comeback in 2004. Volcanogenic massive sulphide (VMS) deposits in the Devonian to Mississippian Yukon-Tanana Terrane with high zinc and precious metal values were the main target of companies. The Finlayson Lake VMS District experienced renewed exploration after a lull of several years. Exploration in other areas of Yukon-Tanana Terrane was successful, with the discovery of zinc-copper-lead-gold-silver-bearing massive sulphide in drill core on the Mor property near Teslin in southern Yukon. Strong copper prices resulted in an increase in exploration for porphyry and iron-oxide-copper-gold deposits throughout many areas of Yukon. Very little attention was given to the potential of sedimentary-exhalative (SEDEX) zinc-lead deposits in the Selwyn Basin, with the exception of a small program conducted by Expatriate Resources on their HP/Nod claims near Howard's Pass. With strengthening of the zinc price, it is anticipated that exploration for SEDEX deposits in Yukon will be renewed after a hiatus of nearly twenty years.

## VOLCANIC ASSOCIATED

The largest program in the Finlayson Lake VMS District was conducted by Expatriate Resources on their **Wolverine** deposit (Yukon MINFILE 2004, 105G 072, Deklerk and Traynor, 2004). Early in the year, Expatriate purchased Atna Resources' interest in the Wolverine joint venture to own 100% of the project. Expatriate has submitted its project description report to the Yukon Ministry of Energy, Mines and Resources for the development of the Wolverine deposit as a 1250-tonne-per-day underground mine. The report is in support of an application to the Yukon Water Board for a Class A water licence for development of a mine. The application was made in conjunction with a quartz-mining licence application that has also been filed with the Yukon government.

The Wolverine deposit resource in all categories is 6 237 000 tonnes grading 12.66% Zn, 1.55% Pb, 1.33% Cu, 371 g/t Ag and 1.76 g/t Au. Currently, the probable diluted mining reserve, determined by Hatch Associates in a November, 2000 prefeasibility study, is 3 470 000 tonnes grading 336.6 g/t Ag, 1.59 g/t Au, 12.43% Zn, 1.44% Pb and 1.37% Cu (using a 4-m minimum thickness of the sulphide deposit) and will provide an eight-year mine life. Expatriate conducted heavy media separation studies in 2004 that were very successful in separating lighter hanging-wall and footwall argillite from massive sulphide. Initial testwork recovered 98% of base metals and 95% of precious metals. Further heavy media studies and test-mining in 2005 will determine the ability to mine and process thinner parts of the ore-body and increase the projected mine-life.



Recent geological mapping by Murphy et al. (2001), shows that the Wolverine deposit is hosted within a Lower Mississippian package of felsic metavolcanic and metasedimentary rocks of lower greenschist metamorphic rank, referred to as the Wolverine Succession. In 2004, Expatriate drilled the Wolverine deposit (9 holes – 1758 m) to provide metallurgical samples and to infill (Fig. 25) the area proposed for test mining as part of their feasibility study. The drilling confirmed the high-grade nature and continuity of mineralized rock within the deposit as highlighted by hole WV04-124, which intersected 5.3 m of massive sulphide grading 4.29 g/t Au, 669.8 g/t Ag, 0.65% Cu, 1.73% Pb and 8.25% Zn and included a spectacular 2.6 m of 7.37 g/t Au, 1136.8 g/t Ag, 0.67% Cu, 3.01% Pb and 11.48% Zn. Expatriate continued with their drilling program into the fall and winter on the **Fisher** zone (Yukon MINFILE 2004, 105G 040, Deklerk and Traynor, 2004) of the Wolverine property. Previous wide-spaced drilling on the Fisher zone intersected base- and precious-metal-bearing sulphide mineralized rock in all drill holes. The most significant hole to date was WV95-06, which intersected 2.4 m of semi-massive sulphide rock that graded 0.14 g/t Au, 66.3 g/t Ag, 0.12% Cu, 1.41% Pb and 2.84% Zn. Drilling of the Fisher zone continued in December and results were not available at year end.

At Wolverine Lake, the company expanded their camp facilities with the addition of a mine dry, kitchen enlargement, recreation hall and additional sleeping facilities (Fig. 26). They also lengthened the airstrip and began site preparation of the mine portal (Fig 27). Expatriate closed a \$13 626 840 brokered private placement in the fall of 2004, \$11 million of which is earmarked for the exploration, feasibility study and test mining of the Wolverine deposit. Expatriate immediately initiated their program in late 2004, and after a Christmas break will renew work in January, 2005.

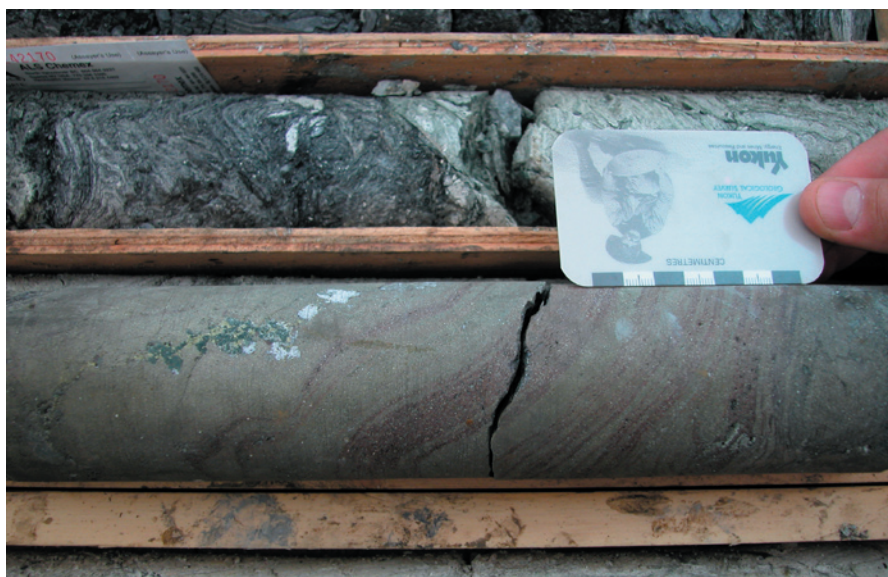


**Figure 25.** High-grade Zn-Ag-Cu-Pb-Au core from infill drilling on the Wolverine deposit.



**Figure 26.** Expanded kitchen facility at the Wolverine camp.



**Figure 27.** Portal site on the Wolverine property.

Late in 2004, Expatriate completed a company reorganization; Expatriate will change its name to Yukon Zinc Corp. which will retain the Wolverine deposit and Finlayson assets. A new exploration company, Pacifica Resources Ltd., will be formed and will hold Expatriate's non-Finlayson assets.

Expatriate conducted regional mapping, sampling and prospecting on some of their 640 km<sup>2</sup> claim holdings in the Finlayson district. This work resulted in the discovery of outcropping mineralized rock dubbed the Thunderstruck showing (Fig. 28). The Thunderstruck is located on the southern portion of the **Goal-Net** property (Yukon MINFILE 2004, 105G 121, Deklerk and Traynor, 2004), which has had previous exploration programs that included diamond drilling, but only reconnaissance-scale work in the area of the discovery. The discovery outcrop contains pyrrhotite, sphalerite, galena and chalcopyrite, and assayed 13.4% Zn, 5.07% Pb, 0.3% Cu, 40.7 g/t Ag and 0.04 g/t Au over 0.3 m. The Thunderstruck showing is hosted in the lower portion of the Devonian to Mississippian Kudz Ze Kayah felsic metavolcanic unit (unit DK; Murphy and Piercey, 2001). This is at the same stratigraphic level interpreted to host Teck-Cominco's **GP4F** deposit (Yukon MINFILE 2004, 105G 143, Deklerk and Traynor, 2004) located approximately 15 km to the north. Expatriate conducted a winter drilling program of three widely spaced holes on Thunderstruck, with results from that program pending.

Teck-Cominco conducted an exploration program on a 44 km<sup>2</sup> parcel of land known as **R-15** optioned from the Kaska Mineral Development Corporation (KMDC), as mentioned in the introduction. Teck-Cominco conducted a University of Toronto electromagnetic (UTEM) geophysical survey on the property in the spring of 2004. The survey outlined geophysical targets in the lower portion of the Devonian to Mississippian **Kudz Ze Kayah** felsic metavolcanic unit (unit DK; Murphy et al., 2001) that hosts their adjoining Kudz Ze Kayah (Yukon MINFILE 2004, 105G 117, Deklerk and Traynor, 2004) and GP4F deposits (11.3 Mt @ 5.9% Zn, 1.5% Pb, 0.9% Cu, 133 g/t Ag, 1.3 g/t Au and 1.5 Mt @ 6.4% Zn, 3.1% Pb, 0.1% Cu, 90 g/t Ag, 2.0 g/t Au, respectively). Teck-Cominco drilled eight holes (1727 m; Fig. 29) and intersected mineralized rock in several of the holes, however, detailed results have not been released.



**Figure 28.** Jason Dunning and Phu van Bui of Expatriate Resources at the Thunderstruck discovery outcrop.





**Figure 29.** Drill on the R-15 land claim block optioned by Teck-Cominco from the Kaska Mineral Development Corporation.



**Figure 30.** Chuck Downie (Bootleg Exploration) and Maurice Colpron (Yukon Geological Survey) examine massive sulphide in the discovery hole at the Mor property.

In southern Yukon, Kobex Resources optioned the **Mor** property (Yukon MINFILE 2004, 105C 061, Deklerk and Traynor, 2004) from Almaden Resources. Exploration interest in the region has recently risen as most of the rocks are similar in age (Devonian-Mississippian) and lithology to those hosting VMS occurrences in the Finlayson Lake District. The Mor property is located within the Big Salmon Complex, a sequence of Late Devonian to late Mississippian deformed and metamorphosed rocks considered to be part of the Yukon-Tanana Terrane. Kobex, following up on previous exploration work, conducted an IP geophysical survey in the area of the Discovery showing. The survey generated an 800-m-long IP chargeability anomaly. The company subsequently conducted a two-hole (185 m) drilling program (Table 9). The two holes, spaced 100 m apart, intersected VMS mineralized rock in a package of mixed felsic and mafic volcanic rocks. The drill holes intersected significant but low-grade mineralization massive pyrite with sphalerite, chalcopyrite and galena (Fig. 30).

**Table 9.** Drill intersections from the Mor property.

Drill hole	From m	To m	Interval m	Cu %	Zn %	Ag g/t	Au g/t	Pb %
MO04-01	18.0	22.9	4.9	0.69	1.31	39.70	0.82	0.15
including	19.3	21.7	2.4	0.83	1.43	40.71	0.83	0.14
	19.3	19.9	0.6	1.06	1.27	25.28	0.63	0.06
	41.9	42.6	0.9	0.69	0.18	11.80	0.50	0.05
MO04-02	23.30	27.05	3.75	0.17	0.76	12.95	0.17	0.11
including	24.50	24.85	0.35	0.44	2.17	26.20	0.41	0.27
including	66.12	68.00	1.88	0.97	0.21	19.78	0.35	0.05
	67.30	68.00	0.70	1.23	0.37	37.65	0.50	0.12

## WERNECKE BRECCIA

The other main target of base metal explorationists was the iron-oxide-copper-gold (IOCG) targets hosted in Proterozoic Wernecke Breccias. At least 65 bodies of Wernecke Breccia are known throughout Yukon, and all contain iron-oxide copper ( $\pm$  gold, uranium, cobalt) mineralized rock. Janina Resources conducted magnetic and gravity surveys and outlined significant anomalies on the **Yukon Olympic** property (Yukon MINFILE 2004, 116G 082, Deklerk and Traynor, 2004), optioned from Copper Ridge Exploration. The early 2004 winter exploration program included detailed gravity, magnetic and IP surveys on 31 km of line grid at the eastern end of the previously defined, 12-km-long gravity and magnetic trend. The survey successfully defined a strong, roughly circular magnetic anomaly with a partially fringing gravity anomaly locally in excess of 2 mGal. The southeastern portion of the gravity anomaly correlates with known copper-bearing hematite (iron oxide) breccia in Spectacular Creek. The source of the combined magnetic and gravity feature is mostly hidden under younger cover rocks.

Copper Ridge conducted geological mapping, prospecting, soil, rock and silt geochemical sampling, and a helicopter-supported gravity survey on the **Hart River** property (NTS 116A/15), a new IOCG breccia discovery made in 2002. The 2004 program focused on six showings of iron oxide breccias and gabbro stocks with associated copper and locally gold. The mineralized gabbro and breccias are developed within the 6- by 10-km area of a large magnetic anomaly and on the margins of three newly defined gravity anomalies. A partially defined, 5-mGal gravity anomaly coincides with a new copper-bearing hematite breccia occurrence (Fig. 31), known as the Ironman. At the Ironman showing, one day of prospecting discovered a body of hematite breccia occurring over at least a 200- by 50-m area. Grab samples of the breccia contained up to 5373 ppm copper. The Ironman showing, which occurs near an unconformity separating underlying Proterozoic sedimentary rocks from overlying Paleozoic carbonate rocks, was discovered on the last day of the 2004 field program. A porous iron- and manganese-oxide

**Figure 31.** Hematite breccia from the Ironman showing on the Hart River IOCG property.



cemented breccia, that occurs over at least a 200- by 100-m area, contains up to 1151 ppm Cu. At the Smokey showing, copper is hosted in a strongly silicified and pyrite-rich fine-grained sandstone, and is spatially related to a prominent northwest-trending structure. Chip sampling in 2004 in this area returned copper values up to 0.74% over 1.5 m and 0.70% over 3 m. The Copper Slope showing is associated with the same structure that hosts the Smokey showing. Anomalous copper is hosted in a sericite-, tourmaline- and albite-altered dolomitic siltstone. Copper values in scarce outcrop are highly anomalous and a 30-cm piece of angular float returned a value of 6.7% Cu. The Copper Slope showing occurs on the eastern side of



a newly defined gravity anomaly. A large area of hematite breccia occurs on the western side of this anomaly. At the Copper Top showing, copper, and local gold were discovered over a 100-by 300-m area in dolomitic siltstones within the contact halo of a gabbro stock. Grab samples returned values up to 2.0% Cu and 509 ppb Au from outcrop (Fig. 32). At the AA Petite showing, massive chalcopyrite and magnetite with anomalous gold and uranium occur in a dolomitic siltstone adjacent to a gabbro stock. Outcrop samples returned values up to 2.1% Cu over 1.1 m, while float grab samples returned values of up to 15.0% Cu and 148 ppb Au.

International KRL Resources staked the **NOR** breccia occurrence (Yukon MINFILE 2004, 106L 061, Deklerk and Traynor, 2004) late in the season. The claims are underlain by an 800- by 1800-m heterolithic, diatreme breccia body (Fig. 33) intruded into a fault-bounded outlier of Middle Proterozoic limy siltstone and argillite. This Proterozoic rock is exposed through Cambrian limestone, which unconformably overlies it. Previous sampling of brannerite-bearing boulders assayed as high as 4%  $U_3O_8$ . The copper and gold potential of the breccia body was reconfirmed by sampling that was conducted in 2004.

### PORPHYRY/SHEETED-VEIN ASSOCIATED

Copper Ridge Exploration continued to be active in the Stewart River area south of Dawson (Fig. 34), exploring for occurrences similar to that discovered on their **Lucky Joe** property (Yukon MINFILE 2004, 115O 051, Deklerk and Traynor, 2004), which is currently optioned to Kennecott Exploration. Kennecott has outlined a large area of alteration and mineralized rock on the Lucky Joe that they have interpreted as a metamorphosed porphyry copper-gold deposit. Copper Ridge conducted a program of geochemical sampling, mapping and prospecting on the **Shamrock** and **Thistle** properties (Yukon MINFILE 2004, 115O 007,008,009, Deklerk and Traynor, 2004), which lie immediately to the south of the Lucky Joe property. The claim groups are on



**Figure 32.** Massive chalcopyrite from the Copper Top showing from the Hart River IOCG property.

**Figure 33.** Hematite breccia from the Nor property, North Yukon.



**Figure 34.** Fires consumed much of the area south of Dawson. Outcrop exposure should be enhanced in 2005.



trend, and have similar linear magnetic anomalies to those that define the Lucky Joe property. On the Thistle property, the company outlined a 7.5-km-long soil anomaly defined by copper values in the range of 120 to 400 ppm, with anomalous gold (up to 650 ppb) and molybdenum (up to 20 ppm). Zinc and lead values are also locally anomalous adjacent to the copper zone. This is a similar geological, geophysical and geochemical setting to Lucky Joe. The anomalous copper and gold values follow the edge of a linear magnetic anomaly within a sequence of Paleozoic metamorphic rocks. Reconnaissance-scale geochemistry was performed on the Shamrock property, which identified two areas with copper anomalies (from 200 to 850 ppm) in a similar geological and geophysical setting as the Lucky Joe.

Approximately 65 km northeast of Whitehorse, Saturn Ventures explored the **Mars** property (Yukon MINFILE 2004, 105E 002, Deklerk and Traynor, 2004) with a 7-hole (827-m) diamond drilling program. The Mars property covers the Jurassic alkalic Teslin Crossing pluton. Several drill targets have been identified within a 1.5- by 3-km area of alteration with an associated copper-gold-silver-molybdenum showing. The drilling failed to intersect significant mineralized rock, and Saturn relinquished its option on the claims.

Copper Ridge Exploration explored the **Chimo** property (Yukon MINFILE 2004, 115I 070, Deklerk and Traynor, 2004) in the Dawson Range Mineral Belt with a program of geochemistry, geological mapping and IP geophysics. The IP survey succeeded in defining a moderate to strong, 300- to 400-m-wide chargeability anomaly that trends eastward for at least 1200 m. The chargeability anomaly borders a copper-molybdenum anomaly to the south, and is coincident with the central part of a linear gold-in-soil anomaly. Outcrop on the property is rare, but mapping showed the copper-molybdenum anomaly to be underlain by mid-Cretaceous andesitic volcanic rocks and quartz-diorite intrusive rocks. The company is refining drill targets based on the data acquired in the 2004 and 2003 exploration programs.



## GEMSTONES

Coloured gemstone exploration in Yukon continued to be led by True North Gems, mainly in the Finlayson Lake District focusing on similar geologic settings to the **Tsa da Glisza** project (Yukon MINFILE 2004, 105G 147, Deklerk and Traynor, 2004; Neufeld, this volume). At Tsa da Glisza, emeralds occur where quartz-tourmaline veins cut mafic-rich layers in a shallowly dipping mica-chlorite schist of the Upper Devonian Fire Lake mafic metavolcanic unit (unit DF, Murphy and et al., 2001). The quartz-tourmaline veins are genetically linked to a body of mid-Cretaceous granite exposed approximately 1 km to the east. Other companies that continued to look for emeralds in the district stood to benefit from recent 1:50 000-scale mapping conducted by the Yukon Geological Survey.

True North Gems' main focus was on the Tsa da Glisza project (formerly Regal Ridge). The company renamed the project in recognition of the renewal of the memorandum of understanding signed in 2003 with the Ross River Dena Council. The program included geological mapping and sampling, prospecting, trenching, bulk sampling, diamond drilling and upgrading of the processing plant (Fig. 35). The company also conducted testwork comparing mechanized faceting versus hand-cutting of gem and near-gem rough material, and dense media separation for mechanized recovery of emeralds as opposed to manual collection at the wash plant. Hand cutting of gemstones resulted in an average 5 to 15% yield with nominal yields on select splits as high as 20% for cabochons and 30% for beads as opposed to the 5% yield for the mechanized cutting. Dense media separation produced positive results, and the company will continue to test this recovery process, which would result in improved security and potentially higher gemstone recoveries.

Mini-bulk sampling in 2003 and 2004 from the Mattscar, Far West and Southwest veins of the Summit zone, including material from underground exploration in 2003,



**Figure 35.** Upgraded processing plant at the Tsa da Glisza emerald project.

resulted in the recovery of 38.8 kg of gem, near-gem and non-gem material from 2533 tonnes of material processed; 1 g is equal to 5 carats. Details of the mini-bulk sampling result are available at the company website<sup>1</sup>. Table 10 outlines the yields.

The 2004 exploration program included 46 core holes (3084 m) on the Summit zone, which encompasses most of the main showings on Regal Ridge. The drilling intersected numerous zones of multistage quartz-tourmaline-scheelite veins accompanied by tourmaline and rusty mica-rich alteration of the Fyre Lake chlorite schist. All these features are indicative of the known emerald mineralization, but in this case occur up to 100 m below the known surface showings. Emerald was intersected in eight diamond drill holes.

**Table 10.** Bulk sampling results from the Tsa da Glisza property.

	Emerald weight (grams)	Emerald grade (grams/tonne)
Gem	1502.53	0.59
Near-gem	14 334.24	5.66
Non-gem	23 026.33	9.09
<b>Total emerald</b>	<b>38 863.10</b>	<b>15.34</b>

Approximately 1 km southwest of the Summit zone, geologist Heather Neufeld, while mapping and prospecting soil geochemical anomalies on Howdy Ridge as part of the company’s regional exploration work at Tsa da Glisza, discovered a significant new zone of emerald-bearing quartz and tourmaline veins. The newly

discovered Shadow zone (Fig 36) crystals are described as coarse gem and near-gem quality emeralds, 2 mm to 3.5 cm long with excellent colour. The largest stone recovered was 10 cm in length. Access to the new discovery was constructed and an 8-hole (418-m) diamond drilling program was conducted. Drilling intersected the favourable Fyre Lake schist and quartz-tourmaline scheelite veins, the latter correlating with subvertical and shallow-dipping emerald-bearing veins exposed in the initial trenching program. Property-scale geological mapping has expanded the outcrop distribution of the Fyre Lake sequence, which hosts emeralds on Howdy Ridge (Shadow zone) and on the adjacent ridge exposed above the contact with the Cretaceous granite.

True North Gems also conducted regional exploration on other properties in the Finlayson area for emeralds. At the **True Blue** property (Yukon MINFILE 2004, 105F 081, Deklerk and Traynor, 2004; Turner, this volume), the company collected a mini-bulk sample of aquamarine hosted in a Mississippian syenite stock that

intruded Lower Paleozoic carbonate rocks. Diamond-impregnated chain saws (Fig. 37) were used to collect the samples. Results of the mini-bulk sample were not available by year-end.

Firestone Ventures conducted a program of hand-trenching on the **Straw** property (NTS 105G/8) located 5 km southeast of on the Tsa da Glisza property. A total of 165 hand pits were excavated (Fig. 38) to a depth of 1.0 to 1.5 m in areas highlighted by coincident beryllium and chromium soil geochemical anomalies in conjunction with



**Figure 36.** Greg Davison with the discovery boulder from the Shadow zone on Howdy Ridge at the Tsa da Glisza emerald project.

<sup>1</sup>www.truenorthgems.com





**Figure 37.** Diamond-impregnated chain saws were used for sampling at the True Blue property.

favourable geology, alteration and structure as defined by work conducted in 2003. Although no emeralds were found, a copper-cobalt geochemical anomaly was outlined. The property is located close to the Kona copper-gold-cobalt deposit on the adjoining Fyre Lake property (Sebert et al., 2004).

Entourage Mining Ltd. conducted a program of prospecting and helicopter-supported mechanized trenching on several zones identified in regional geochemical sampling conducted in 2003. The zones are distributed throughout the Finlayson Lake area on claims optioned for their gemstone potential from Expatriate Resources. Results from the program had not been released at year's end.

Arcturus Resources conducted a short program of geological mapping and geochemical sampling on their **Fife** property (Yukon MINFILE 2004, 105G 142, Deklerk and Traynor, 2004), which is located south and west of, and contiguous with, True North Gems' Tsa da Glisza property. The potential of the northern portion of the property has improved due to the newly discovered Shadow zone on True North Gems' Tsa da Glisza property.

Hinterland Metals conducted limited work on their **Gleam** and **Dazzle** properties (Yukon MINFILE 2004, 105G 030,031,120 Deklerk and Traynor, 2004) in the Finlayson Lake area. The



**Figure 38.** Hand-pitting at the Straw property.

**Figure 39.** Slinging a net load of chrysoprase from the Dazzle property.



properties were optioned from True North Gems in 2003, and were originally staked based on the similar geologic setting to the Tsa da Glisza property. No significant results were reported. The company collected a bulk sample of chrysoprase (Fig. 39), a gem quality, cryptocrystalline variety of chalcedony used to make beads, cabachons and carved figures. The company discovered the chrysoprase in 2003, and was successful in manufacturing some jewelery from their 2003 samples.

## ACKNOWLEDGEMENTS

This report is based on public information gathered from a variety of sources. It also includes information provided by companies through press releases, personal communications and property visits conducted during the 2004 field season. The cooperation of companies and individuals in providing information, as well as their hospitality, time and access to properties during field tours, is gratefully acknowledged. Safe, reliable helicopter transportation provided by Helidynamics, TransNorth and Fireweed helicopters during the field season is always appreciated. The editing skills of Diane Emond, Lara Lewis and Geoff Bradshaw are also appreciated.



## REFERENCES

- Deklerk and Traynor, 2004. Yukon MINFILE – A database of mineral occurrences. Yukon Geological Survey, CD-ROM.
- Boyle, R.W. and Gleeson, C.F., 1971. Gold in the Heavy Mineral Concentrates of Stream Sediments, Keno Hill Area, Yukon Territory. Geological Survey of Canada, Paper 71-51.
- LeBarge, W.P., 2005 (this volume). Yukon Placer Mining and Exploration Overview 2004. *In: Yukon Exploration and Geology 2004*, D.S. Emond, L.L. Lewis, G.D. Bradshaw (eds.), Yukon Geological Survey, p. 35-40.
- Lowey, G.W., 1983. Auriferous conglomerates at McKinnon Creek, west-central Yukon (115O/11). *In: Yukon Exploration and Geology 1983*, Exploration and Geological Services Division, Yukon Region, Indian and Northern Affairs Canada, p. 69-78.
- Murphy, D.C., Colpron, M., Gordey, S.P., Roots, C.F., Abbott, G. and Lipovsky, P.S., 2001. Preliminary bedrock geological map of northern Finlayson Lake area (NTS 105G), Yukon Territory (1:100 000 scale). Exploration and Geological Services Division, Yukon Region, Indian and Northern Affairs Canada, Open File 2001-33, 1:250 000 scale.
- Murphy, D.C. and Piercey, S.J., 1999. Finlayson project: Geological evolution of Yukon-Tanana Terrane and its relationship to Campbell Range belt, northern Wolverine Lake map area, southeastern Yukon. *In: Yukon Exploration and Geology 1998*, C.F. Roots and D.S. Emond (eds.), Exploration and Geological Services Division, Yukon Region, Indian and Northern Affairs Canada, p. 47-62.
- Neufeld, H.L.D., Mortensen, J.K. and Groat, L.A., 2005 (this volume). The Tsa da Glisza (Regal Ridge) emerald occurrence, Finlayson Lake district (NTS 105G/7), Yukon: New results, and implications for continued regional exploration. *In: Yukon Exploration and Geology 2004*, D.S. Emond, L.L. Lewis and G.D. Bradshaw (eds.), Yukon Geological Survey, p. 261-273.
- Sebert, C., Hunt, J.A. and Foreman, I.J., 2004. Geology and litho geochemistry of the Fyre Lake copper-cobalt-gold sulphide-magnetite deposit, southeastern Yukon. Yukon Geological Survey, Open File 2004-17, 46 p.
- Turner, D., Groat, L.A. and Wengzynowski, W., 2005 (this volume). Mineralogical and geochemical study of the True Blue aquamarine showing, Shark property, southern Yukon. *In: Yukon Exploration and Geology 2004*, D.S. Emond, L.L. Lewis and G.D. Bradshaw (eds.), Yukon Geological Survey, p. 275-285.

## APPENDIX 1: 2004 EXPLORATION PROJECTS

PROPERTY	COMPANY/OWNER	MINING DISTRICT	MINFILE # or (1:50 000 NTS)	WORK TYPE	COMMODITY
<b>Ami</b>	Grid Capital Corp.	Dawson	115N 39,40	reclamation	Cu-Mo, Ag-Pb-Au
<b>Antimony</b>	Strategic Metals Ltd./ War Eagle Mining Company Inc.	Dawson	116B 094	G,GC,DD	Au-Cu
<b>Arn</b>	Klondike Gold Corp./ Atac Resources Ltd.	Whitehorse	115F 048	G,GC,T,DD	Au-Cu
<b>Aurex</b>	StrataGold Corp.	Mayo	105M 060	G,GC	Au
<b>Brewery Creek</b>	NovaGold Resources	Dawson	116B 160	G,GP,DD	Au
<b>Blende</b>	Eagle Plains Resources/Shoshone Silver Mining Company	Mayo	106D 064	G,GC,P	Ag-Pb-Zn
<b>Bonanza</b>	International Gold Ventures	Dawson	115O 161	G,GC,P,GP	Au
<b>Box</b>	Expatriate Resources	Watson Lake	(105G/10)	G	Cu-Pb-Zn-Ag-Au
<b>Burwash</b>	Golden Chalice Resources/Strategic Metals Inc.	Whitehorse	115G 100	G,GC,T	Ni-Cu-PGE
<b>Cathy</b>	International Gold Ventures	Dawson	115O 010	G,GC,P	Au
<b>Chimo</b>	Copper Ridge Exploration	Whitehorse	115I 070	G,GP,GC,P	Cu-Au
<b>Clark/Cameron</b>	Klondike Gold Corp.	Mayo	106D 011,012	P,GC	Ag-Pb-Zn
<b>Clear Creek</b>	StrataGold Corp.	Dawson	115P 012,013	AGP	Au
<b>Dazzle/Gleam</b>	Hinterland Metals/ True North Gems	Watson Lake	105G 30,31,120	G,GC,P,GP	gemstones, Au
<b>Dragon Lake</b>	Eagle Plains Resources	Whitehorse	105J 007	G,GP	Au
<b>Dublin Gulch</b>	StrataGold Corp.	Mayo	106D 025	AGP	Au
<b>Fife</b>	Arcturus Ventures	Watson Lake	105G 102	G,GC,P	gemstones
<b>Finlayson emerald</b>	Entourage Mining/ Expatriate Resources	Watson Lake	105G various	G,GC,P,T	gemstones
<b>Fisher</b>	Expatriate Resources	Watson Lake	105G/08	G,DD	Zn-Pb-Cu-Au-Ag
<b>Grew Creek</b>	Freegold Resources	Whitehorse	105K 009	DD	Au-Ag
<b>Goddell Gully</b>	Tagish Lake Gold	Whitehorse	105D 025	DD	Au-Ag
<b>Golden Revenue</b>	Yale Resources Ltd/ Atac Resources	Whitehorse	115I 107	G,GC,DD	Au-Cu
<b>Haldane</b>	Klondike Gold Corp.	Mayo	105M 056	G,GC	Au
<b>Hart River IOCG</b>	Copper Ridge Exploration	Mayo	(116A/15)	G,GC,P,GP	Cu-Au
<b>Heidi</b>	Logan Resources	Dawson	116A 037	G,GC,GP,P	Au

**Abbreviations**

BS – bulk sample  
D – development  
DD – diamond drilling

ES – environmental studies  
F – feasibility  
G – geology  
GC – geochemistry

GP – geophysics  
IOCG – iron-oxide copper gold  
M – mining  
PD – percussion drilling

PF – prefeasibility  
R – reconnaissance  
T – trenching  
U/GD – underground development



## APPENDIX 1 (continued): 2004 EXPLORATION PROJECTS

PROPERTY	COMPANY/OWNER	MINING DISTRICT	MINFILE # or (1:50 000 NTS)	WORK TYPE	COMMODITY
<b>Helen</b>	Hinterland Metals Inc.	Watson Lake	105G 030	G,GP	Au
<b>Hold Fast</b>	Gordon McLeod	Whitehorse	105C 012	G,GC	Cr-PGE
<b>Hy/Fer</b>	Dentonia	Watson Lake	105H 102	G,GC	Au
<b>Hyland Gold</b>	Northgate Exploration Ltd./StrataGold Corp.	Watson Lake	95D 011	G,GC,GP,DD	Au
<b>Indian River</b>	Boulder Mining Corp./Western Prospector Group	Dawson	115O 054	G,GC,P	Au
<b>Kirkman</b>	International Gold Ventures	Dawson	115O 016	G,GC,P	Au
<b>Klondike</b>	Klondike Source	Dawson	115O 079	G,GC,DD	Au
<b>Kudz Ze Kayah (R-15A)</b>	Teck-Cominco/Kaska Development Corp.	Watson Lake	105G	GP,DD	Zn-Pb-Cu-Au-Ag
<b>Lonestar etc.</b>	Klondike Star Mineral Corp./Klondike Gold Corp.	Dawson	115O 072	G,GC,T	Au
<b>Lynx Creek</b>	StrataGold Resources	Mayo	106D 020	DD,GP	Au
<b>Mt. Hinton</b>	Yukon Gold Corp.	Mayo	105M 052	T	Au
<b>Mahtin</b>	International Gold Venture	Mayo	115P 007	G,GC,GP,P,T	Au
<b>Mars</b>	Saturn Ventures Inc.	Whitehorse	105E 002	G,GC,DD	Cu-Au
<b>Maverick</b>	Al Carlos	Whitehorse	105K 009	DD	Au-Ag
<b>Minto</b>	Minto Resources	Whitehorse	115I 021,022	D	Cu-Ag-Au
<b>Mike Lake</b>	Dynamite Resources	Dawson	116A 012	G,GC,P	Au-Cu
<b>Morley</b>	Kobex Resources Ltd./Almaden Minerals Ltd.	Whitehorse	105C 061	GP,DD	Cu-Zn-Pb-Au-Ag
<b>Mucho</b>	Cash Resources	Watson Lake	105I 004	DD	Pb-Zn-Cu-Ag
<b>Nikki</b>	Atac Resources	Whitehorse	115K 082	G,GC,P	Cu-Au
<b>Nor</b>	KRL Resources	Dawson	106L 061	GC,P	Cu-Au
<b>Panorama</b>	Atac Resources	Dawson	116A 031	G,GC,P	Au
<b>Rainbow</b>	Klondike Gold	Mayo	(105N/12)	G,GC,P	Au
<b>Rams Horn</b>	Oredorado Resources	Whitehorse	105D 002,003	G,GC	Au-Ag
<b>Red Mountain</b>	ASC Industries/Regent Ventures	Mayo	115P 006	G,GC,GP,DD	Au
<b>Red Mountain Mo</b>	Tintina Mines	Whitehorse	105C 009	G	Mo
<b>Reed Creek</b>	Cercom Electric	Whitehorse	115G 102	DD	Au
<b>Severence</b>	Eagle Plains Resources	Dawson	115J 003	G,GC,GP	Au

**Abbreviations**

BS – bulk sample  
D – development  
DD – diamond drilling

ES – environmental studies  
F – feasibility  
G – geology  
GC – geochemistry

GP – geophysics  
IOCG – iron-oxide copper gold  
M – mining  
PD – percussion drilling

PF – prefeasibility  
R – reconnaissance  
T – trenching  
U/GD – underground development

## APPENDIX 1 (continued): 2004 EXPLORATION PROJECTS

PROPERTY	COMPANY/OWNER	MINING DISTRICT	MINFILE # or (1:50 000 NTS)	WORK TYPE	COMMODITY
<b>Shamrock</b>	Copper Ridge Exploration	Dawson	(115O/6)	GC	Cu-Au
<b>Shanghai Creek</b>	Yankee Hat Resources	Mayo	105M 028	G,GC,P	Au
<b>Shell Creek</b>	Logan Resources	Dawson	116C 029	G,GC,P,T	Au-Cu
<b>Sonora Gulch</b>	Firestone Ventures Inc.	Whitehorse	115J 008	G,GC,P	Au-Cu
<b>Spice</b>	Klondike Gold Corp.	Whitehorse	105G 150	G,GC	Au-Ag
<b>Straw</b>	Firestone Ventures Inc./True North Gems	Watson Lake	(105G/2)	G,GC,P	gemstones
<b>Tanner</b>	Manson Creek Resources	Mayo	106C 091	G,GC	Zn-Pb-Ag
<b>Tay/LP</b>	Ross River Minerals	Whitehorse	105F 121	G,GC,DD	Au
<b>Tin</b>	Madelena Ventures	Dawson	116B 157	G,GC,GP	Au
<b>Thistle</b>	Copper Ridge Exploration	Dawson	(115O/6)	G,GC	Cu-Au
<b>Thunderstruck</b>	Expatriate Resources	Watson Lake	(105G/8)	G,GC,DD	Zn-Pb-Cu-Ag-Au
<b>True Blue</b>	True North Gems	Whitehorse	105F 081	G,P,T	gemstones
<b>Tsa da Glisza</b>	True North Gems	Watson Lake	105G 147	G,GC,T,DD,BS	emeralds
<b>Ultra</b>	Klondike Gold	Whitehorse	115B 008	G,GC,AGP	Ni-Cu-PGE; Zn-Cu-Au-Ag
<b>Wellgreen</b>	Northern Platinum Ltd.	Whitehorse	115G 024	G	Ni-Cu-PGE
<b>White</b>	Madalena Ventures	Whitehorse	115O 011,012	G,GC,P	Au, Cu
<b>Wolverine</b>	Expatriate Resources	Watson Lake	105G 073	G,DD,PF	Zn-Pb-Cu-Au-Ag
<b>Vic</b>	Aurchem Exploration	Whitehorse	115I 068	G,DD	Au-Ag
<b>Yukon Olympic</b>	Janina Resources Limited/Copper Ridge Exploration	Dawson	116G 082	G,GP	Cu-Au
<b>Yukon regional</b>	Rimfire Minerals Corp./Newmont Exploration		various		

**Abbreviations**

BS – bulk sample  
D – development  
DD – diamond drilling

ES – environmental studies  
F – feasibility  
G – geology  
GC – geochemistry

GP – geophysics  
IOCG – iron-oxide copper gold  
M – mining  
PD – percussion drilling

PF – prefeasibility  
R – reconnaissance  
T – trenching  
U/GD – underground development

## APPENDIX 2: 2004 DRILLING STATISTICS

PROPERTY	COMPANY	DIAMOND DRILL		RC/ PERCUSSION/ *ROTONIC	
		metres	# holes	metres	# holes
Antimony Mountain	Strategic/War Eagle	832	4		
Arn	Klondike Gold/Atac	900	18		
Brewery Creek	NovaGold Resources	769	4		
Goddell Gully	Tagish Lake Gold	900	2		
Golden Revenue	Yale Resources/ATAC	1832	14		
Grew Creek	FreeGold Resources	2077	12		
Hyland Gold	Northgate/StrataGold	1800	8		
Indian River	Boulder Mining/Western Prospector			*552	61
Klondike	Klondike Source	1537	6		
Kudz Ze Kayah (R-15A)	Teck Cominco/Kaska Development Corporation	1727	8		
Lynx Creek	StrataGold	2070	14		
Mars	Saturn Ventures	827	7		
Maverick	Al Carlos	220	5		
Mor	Kobex Resources	185.3	2		
Mucho	Cash Resources	671	5		
Red Mountain	ASC/Regent Ventures	1922	12		
Kelli (Reed Creek)	Cercom Electric/Reed Creek Placers	330	5		
Tay-Lp	Ross River Minerals	1002	9		
Thunderstruck (3 holes) Goal Net (1 hole)	Expatriate Resources	1034	4		
Tsa da Glisza	True North Gems	3504	54		
Vic	Aurchem	2535	26		
Wolverine	Expatriate Resources	1758.4	9		
Wolverine (Fisher zone)	Expatriate Resources	1150	2		
<b>TOTAL</b>		<b>29 582.7</b>		<b>552</b>	





# YUKON PLACER MINING AND EXPLORATION OVERVIEW 2004

*William LeBarge<sup>1</sup>*  
*Yukon Geological Survey*

LeBarge, W., 2005. Yukon Placer Mining and Exploration Overview 2004. *In: Yukon Exploration and Geology 2004*, D.S. Emond, L.L. Lewis, G.D. Bradshaw (eds.), Yukon Geological Survey, p. 35-40.

Even prior to the arrival of European explorers to the Yukon, placer mining had been conducted by First Nations people, who recovered native copper nuggets from the White River area in southwestern Yukon. Explorers from the Hudson Bay Company first reported fine gold on the banks of the Pelly River around 1850. In 1874, coarse gold was discovered on a tributary of the Liard River, and in 1885 significant quantities of gold were found on river bars of the Stewart. Gold was discovered in the Fortymile area on both sides of the border the following year, and by 1893, active mining was taking place on Miller and Glacier creeks in the Sixtymile district.

On August 17, 1896, the discovery of nugget gold on Rabbit Creek (renamed Bonanza) set off the Klondike gold rush. By 1900, over a million ounces (30 million grams) was being mined in a season, at that time completely by hand. Later years saw the arrival of large-scale mining with dredges and heavy equipment.

Today, over 100 years later, placer mining is still an important sector in the Yukon's economy. Over 16.5 million crude ounces (513 tonnes) of placer gold have been produced to date in the Yukon – at today's prices that would be worth more than \$7 billion.

## PLACER MINING

Approximately 500 people were directly employed at 163 placer mines in 2004 – and at least several hundred more were employed in businesses and industries that serve the placer mining industry. Most of the placer operations are small and family-run, with an average of three or four employees.

The majority of active placer mining operations were in the Dawson Mining District (116), followed by the Whitehorse Mining District (25), and the Mayo Mining District (21) (Fig. 1). One operation was reported as active in the Watson Lake Mining District.

The total Yukon placer gold production in 2004 was 101,108 crude ounces (3.1448 million g), compared to 50,888 crude ounces (1.5828 million g) in 2003 (Fig. 2). The value of this 2004 gold production was \$42.9 million, more than double the \$42.9 million mined in 2004. It should be noted that over 20,000 ounces (600 000 g) was reported as royalties in March; this probably reflects 2003 production and may have inflated the apparent production for 2004 for some areas.

Over 90% of the Yukon's placer gold was produced in the Dawson Mining District, which includes the unglaciated drainages of Klondike River, Indian River, West Yukon (Fortymile and Sixtymile rivers, and the Moosehorn Range) and lower Stewart River. The remaining gold came from the glaciated Mayo and Whitehorse mining districts, which include the placer areas of Clear Creek, Mayo, the Dawson Range, Kluane, Livingstone and Whitehorse South.

Reported placer gold production from Indian River drainages in 2004 increased compared to the previous year, from 16,126 crude ounces (501 580 g) to 36,279 crude ounces (1 128 400 g). Most of this increase came from operations in Dominion Creek.

<sup>1</sup>*bill.lebarge@gov.yk.ca*

In Klondike area drainages, production rose to 20,031 crude ounces (623 030 g), at least partly because of an increase in gold coming from operations on Last Chance Creek.

A large increase was seen in West Yukon placer gold production, mainly due to increased output from operations on Sixtymile River. Royalty totals for the 2004 season were more than triple the previous year, at 20,454 crude ounces (636 190 g).

Reported production from operations in the Lower Stewart drainages nearly quadrupled in 2004, to a total of 15,617 crude ounces (485 740 g). Most of the increase came from operations on Thistle and Black Hills creeks.

As usual, little gold was reported from Clear Creek drainages although several operations were active in 2004. The total reported gold from royalties increased slightly to 341 crude ounces (10 600 g).

In the Dawson Range, reported placer gold production dropped slightly to 1619 crude ounces (50 370 g).

In the Mayo area, gold production increased somewhat in 2004 to 2539 crude ounces (78 970 g). Significant increases were seen in Owl and Duncan creeks.

In the Kluane area, reported placer gold production rose slightly to 1670 crude ounces (51 940 g).

The Livingstone area remained inactive; however 17.2 crude ounces (535 g) of gold were reported in royalties.

Conversely, although some mining activity took place in the Whitehorse South area (which includes Moose Brook and Wolverine creek), no gold was reported in royalties.

## **PLACER EXPLORATION**

Although it is essentially unreported, exploration on placer mining properties has been a part of the process for many miners since they began to mine. Traditional methods of sampling and exploration include auger, reverse circulation and churn drilling, and geophysics including seismic surveys, ground-penetrating radar and magnetometer surveys. Trenching and bulk sampling also continue to be well used methods of testing placer ground.

An upsurge of placer exploration in 2004 was due, to a large extent, to activity by a single joint venture. Boulder Mining Corporation, a Vancouver-based company, began exploration of a prospect in the Indian River area south of Dawson City, along with Western Prospector Group. The property was discovered by long-time prospector and miner Pete Risby, and consists of a large-volume bench deposit which lies above the modern valley of Indian River. Generalized stratigraphy consists of a Tertiary, 'White Channel' gold-bearing gravel on a bedrock terrace, which is in part overlain by glaciofluvial and glaciolacustrine sediments deposited during the earliest pre-Reid glaciation. A total of 795 placer claims in 3 zones (Upstream, Downstream and Ruby benches) were staked on a 21-km stretch of Indian River, and cover an estimated 8300 hectares.



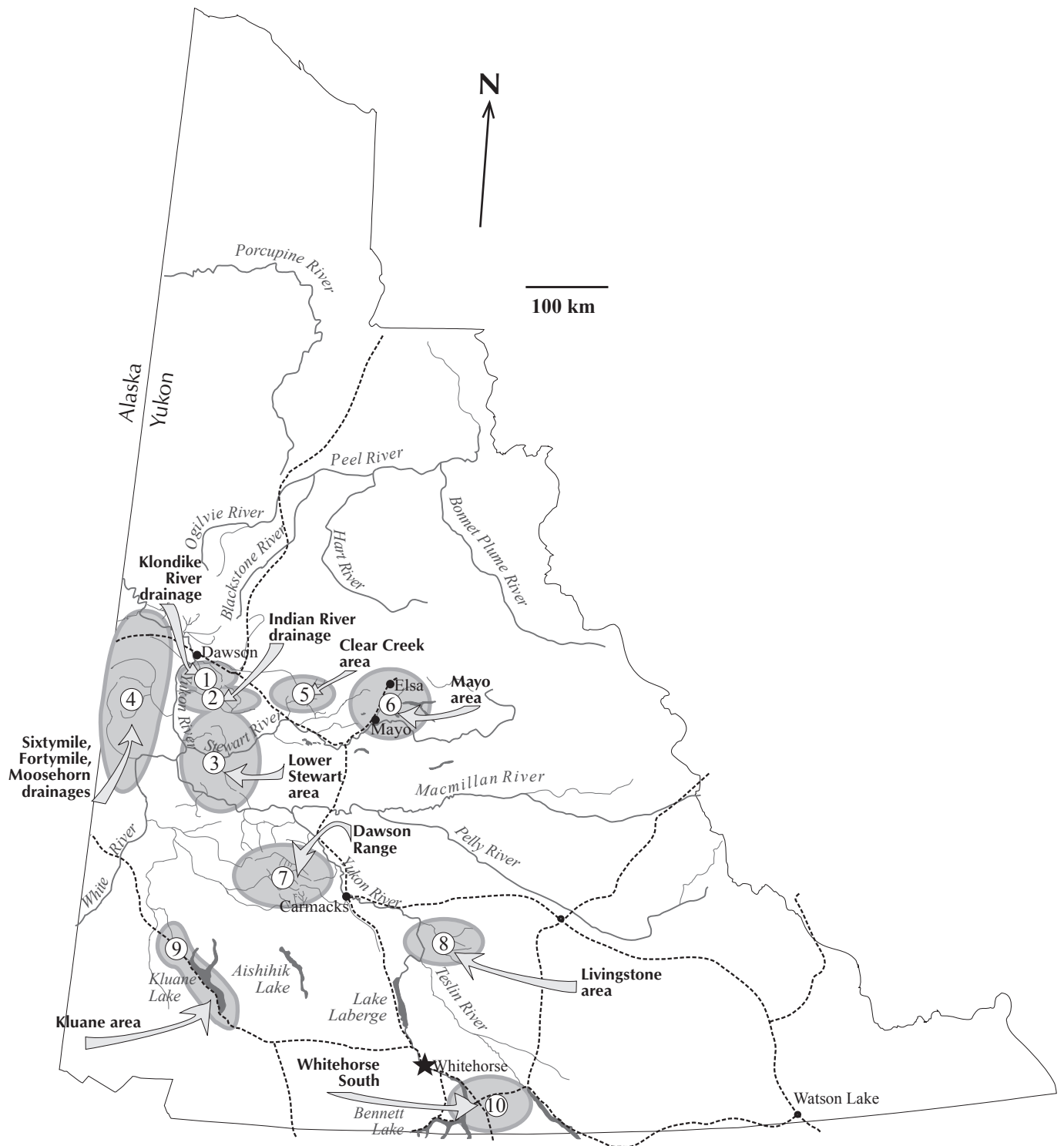


Figure 1. Yukon placer mining areas.

Exploration on this property consisted of an extensive program of auger drilling, rotonsonic drilling, ground-penetrating radar, bulk sampling and geological mapping. The total cost of this program was well over the initial projected expenditures of \$500 000 and represents the largest placer exploration program undertaken in recent history by a public company in Yukon. Agreements are to spend a further \$750 000 prior to December 31, 2005; \$1.25-million prior to December 31, 2006; and \$2.5-million prior to December 31, 2007.

Auger drilling on the Downstream bench early in the program resulted in a weighted average gold grade in five holes of 2.3 grams per tonne (g/t) gold over 6.1 m. On the Upstream bench, the weighted average gold grade of 10 holes along a 3500-m length and 750-m width was 0.58 g/t gold over 21.5 m.

Rotosonic drilling results included intersections of 3.16 g/t over 0.9 m, 1.08 g/t over 1.7 m, and 0.319 g/t over 2 m. Cut-off grades for the deposit are estimated to be 0.1 g/t.

Bulk sampling by excavator in test pits increased the gold grades compared to drilling, as well as recovering coarser gold, with several nuggets in the +1 gram range. Some typical gold grades in test pits were 0.411 g/t over 0.8 m, 0.586 g/t over 0.93 m, and 0.220 g/t over 1.12 m. Individual bulk sample weights were in the range of 12.3 to 34 tonnes.

In the fall, Boulder Mining Corp. staked hundreds of quartz claims over local sedimentary rocks, targeting a quartz-pebble conglomerate, which in sampling has proven to have disseminated grains of fine gold throughout. The possibility exists that this may be a paleoplacer deposit which was a source for both the bench deposits and the local placer gold in Indian River.

Similar geologic and geomorphic settings to that of Indian River exist in other unglaciated drainages in the Yukon, specifically in Fortymile and Sixtymile areas. Although limited placer exploration has taken place on alluvial terraces in these areas, they remain poorly understood. It is possible that significant quantities of gold lie in these bench deposits, which have yet to be methodically evaluated.

**Figure 2.** Yukon gold production figures and average US gold price, 1971-2004.

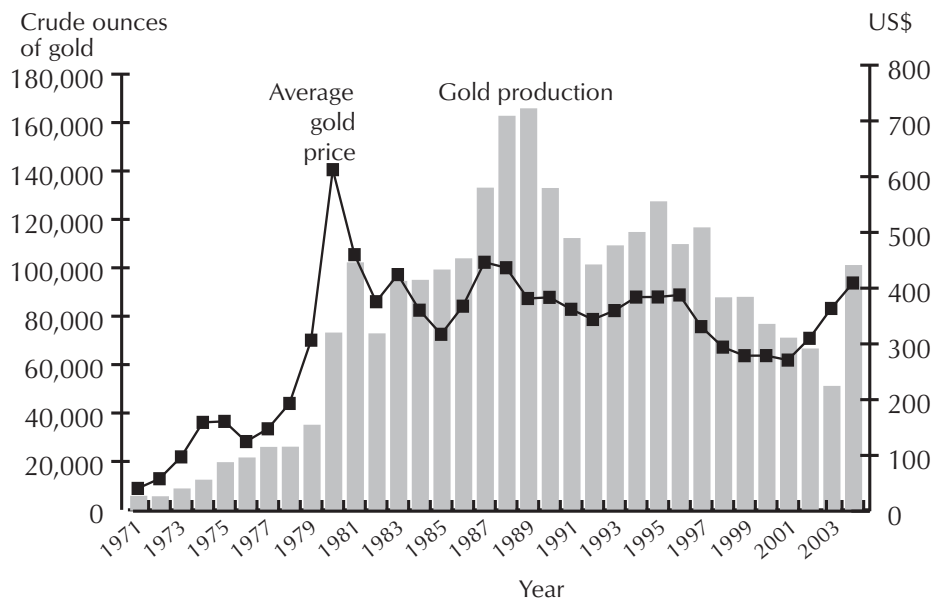




**Figure 3.** Boulder Mining Corporation's rotonomic drill in operation in the Indian River area in 2004. The drill was successful in recovering intact stratigraphic samples of gravel in core which was processed for heavy minerals and gold after detailed descriptions and documentation.

The long-term health of the Yukon's placer mining industry requires that new placer gold reserves be discovered as traditional mining areas become depleted. With the application of new placer exploration and research techniques and new ideas, additional placer gold reserves may be found in non-traditional, more complex geological settings.

The staff at the Yukon Geological Survey and the Client Services and Inspection Division (Department of Energy, Mines and Resources, Yukon government) can provide information and advice regarding placer mining in the Yukon. Publications on placer mining in the Yukon are available through the Yukon Geological Survey office at Room 102, Elijah Smith Building, 300 Main St. Whitehorse, Yukon. Many recent publications and maps can be downloaded for free from our website at [www.geology.gov.yk.ca](http://www.geology.gov.yk.ca).



## APERÇU

Même avant l'arrivée des explorateurs européens au Yukon, des autochtones exploitaient des placers, notamment dans la région de la rivière White, dans le sud-ouest du Yukon, où ils récoltaient des pépites de cuivre natif. Vers 1850, des explorateurs de la Compagnie de la Baie d'Hudson ont été les premiers à signaler la présence d'or fin sur les berges de la rivière Pelly. En 1874, on a découvert de l'or grossier dans un tributaire de la rivière Liard, et en 1885 on a trouvé d'importantes quantités d'or dans des bancs de la rivière Stewart. L'année suivante, on a découvert de l'or dans la région de Fortymile, de part et d'autre de la frontière, et en 1893 on exploitait des placers dans les ruisseaux Miller et Glacier, dans le district de Sixtymile.

Le 17 août 1896, la découverte d'or en pépites dans le ruisseau Rabbit (que l'on a renommé Bonanza) a lancé la ruée vers l'or du Klondike. En 1900, on récoltait manuellement plus d'un million d'onces par saison. Plus tard, on s'est mis à exploiter les placers à grande échelle au moyen de dragues et d'équipement lourd.

Aujourd'hui, plus de 100 ans plus tard, l'exploitation de placers est encore un secteur important de l'économie du Yukon. Jusqu'à maintenant, plus de 16,5 millions d'onces (513 tonnes) d'or placérien brut ont été produites au Yukon, ce qui vaudrait plus de sept milliards de dollars au prix actuel de l'or.

En 2004, 163 exploitations de placers employaient environ 500 personnes, et plusieurs centaines d'autres personnes travaillaient dans des commerces et des industries fournissant des services à l'industrie des placers. Les exploitations de placers sont pour la plupart de petites entreprises familiales et emploient en moyenne trois ou quatre employés.

La plupart des exploitations de placers se trouvaient dans les districts miniers de Dawson (116), de Whitehorse (25) et de Mayo (21) (Fig. 1). Il y avait une exploitation active dans le district minier de Watson Lake.

À la fin de novembre 2004, 98 185 onces (3 053 900 g) d'or placérien brut avait été produit depuis le début de l'année au Yukon, en hausse par rapport à la production de 2003 qui s'est chiffrée à 50 888 onces (1 582 800 g) (Fig. 2). La valeur de cette production d'or en 2004 a atteint 41,8 millions de dollars, soit plus du double des 20,7 millions que valait la production de 2003. Il faut mentionner que plus de 20 000 onces (600 000 g) ont été déclarées comme des redevances en mars : cela correspond sans doute à de l'or produit en 2003 et pourrait avoir exagéré la production apparente de 2004 dans certaines régions.

Plus de 90 % de l'or placérien du Yukon a été produit dans le district minier de Dawson, qui comprend les régions non glaciaires de la rivière Klondike, de la rivière Indian, de l'ouest du Yukon (rivières Fortymile et Sixtymile et la chaîne Moosehorn) et le cours inférieur de la rivière Stewart. Le reste de l'or a été produit dans les districts miniers glaciés de Mayo et de Whitehorse, qui comprennent les zones de placers de Clear Creek, de Mayo, de la chaîne Dawson, de Kluane, de Livingstone et de Whitehorse Sud.

Il est évident que les réserves d'or placérien dans les parties non glaciaires traditionnellement exploitées du Yukon ont commencé à baisser, tandis que la production d'or dans les parties glaciaires du Yukon augmente. L'application de nouvelles techniques d'exploration et de recherche de placers pourrait permettre de trouver d'autres réserves d'or dans des cadres géologiques non traditionnels plus complexes, ce qui est essentiel pour assurer la santé à long terme de l'industrie des placers du Yukon. En 2004, la compagnie Boulder Mining de Vancouver, en collaboration avec le Groupe Western Prospector, a entamé un programme d'exploration pour les placers dans la région de la rivière Indian, au sud de Dawson (Fig. 2).

# GOVERNMENT

## Yukon Geological Survey

Grant Abbott and staff  
*Yukon Geological Survey*

Overview .....	43
Projects .....	45
Liaison and support to industry, First Nations and the public.....	48
Information management and distribution .....	49
2004 publications and maps .....	51

## La Commission géologique du Yukon

Grant Abbott et Maurice Colpron  
*La Commission géologique du Yukon*

Aperçu .....	57
--------------	----

## Robert E. Leckie Awards for Outstanding Reclamation Practices

Judy St. Amand  
*Mining Lands, Energy, Mines and Resources*

Awards.....	61
-------------	----





# Yukon Geological Survey

*Grant Abbott<sup>1</sup> and staff*  
Yukon Geological Survey

Abbott, J.G. and staff, 2005. Yukon Geological Survey. *In: Yukon Exploration and Geology 2004*, D.S. Emond, L.L. Lewis and G.D. Bradshaw (eds.), Yukon Geological Survey, p. 43-56.

## OVERVIEW

The Yukon Geological Survey (YGS; Fig. 1) is in its second year as part of the Minerals Development Branch of the Department of Energy Mines and Resources. YGS is comanaged by Grant Abbott and Rod Hill and includes 24 staff (Fig. 2). The Geological Survey of Canada (GSC) also maintains an office with YGS.

Welcome to new staff members Steve Israel as project geologist and Olwyn Bruce as geological and spatial database administrator. Thanks and farewell to previous spatial database administrator Amy Stuart, to surficial geologist Crystal Huscroft and to Director Jesse Duke. Welcome back to Julie Hunt who has successfully completed a PhD thesis at James Cook University in Australia and congratulations to Craig Hart who has also completed his PhD thesis at the University of Western Australia.



**Figure 1.** Yukon Geological Survey staff, left to right: Amy Stuart, Craig Hart, Rod Hill, Robert Deklerk, Lee Pigage, Jeff Bond, Grant Lowey, Diane Emond, Karen Pelletier, Bill LeBarge, Monique Raitchey, Geoff Bradshaw, Steve Traynor, Maurice Colpron, Crystal Huscroft, Mike Burke, Lara Lewis, Steve Israel, Olwyn Bruce, Charlie Roots and Grant Abbott. Absent: Julie Hunt, Panya Lipovsky, Don Murphy and Ali Wagner.

Funding for YGS remains close to the same level it has been over the past few years. This year, in addition to our core budget, we obtained additional short-term funding from Department of Indian Affairs and Northern Development (DIAND) through the Northern Geoscience and Knowledge and Innovation Funds, and from NRCan through the Targeted Geoscience Initiative (TGI).

This year, YGS embarked on the third in a series of five-year planning exercises that have guided government geoscience in the Yukon over the last ten years. The documents from previous exercises (“Yukon Geoscience – A Blueprint for the Future” in 1995 and “Yukon Geoscience: Looking to the Next Millennium” in 1999) have been used to design and implement mapping and

research programs that meet the needs of the mineral industry and other clients such as land use planners. The effectiveness and utility of these documents is demonstrated by the large proportion of high-priority projects that have been completed during this time and by the continued support and satisfaction reported by client groups for the work of YGS. The new document is still under development and will be released shortly.

A Technical Liaison Committee to YGS reviews our program twice a year. We are grateful to Chair Gerry Carlson and members Al Doherty, Moira Smith, Jean Pautler, Forest Pearson, Bernie Kreft, Jim Mortensen and Jim Christie for their valuable support and constructive advice. We welcome Greg Lynch to the committee to

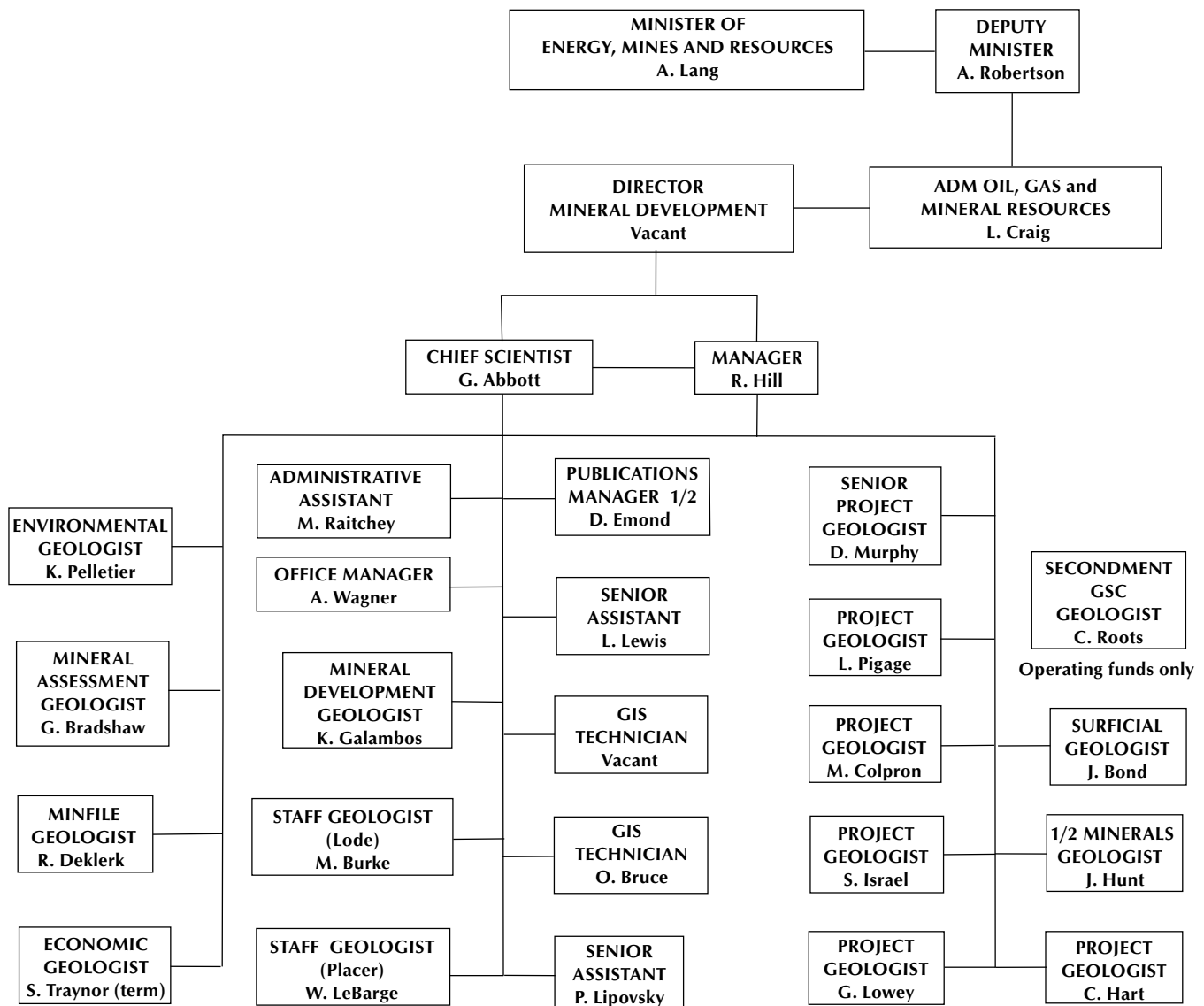


Figure 2. Yukon Geological Survey organization chart.

represent oil and gas interests. Greg has a long association with the Yukon and currently works as a project geologist with Shell Canada.

YGS has the responsibility “to build, maintain, and communicate the geoscience and technical information base required to enable stewardship and sustainable development of the Territory’s energy, mineral, and land resources.” Support for the mineral industry remains the primary focus of YGS, but this year we also took on the responsibility for geoscience studies to define petroleum potential. Effort is also going into environmental studies that have relevance to the extractive industries and land use issues. In recent years, interest and demand for geoscience information has increased substantially from regulators, First Nations, the general public and schools. In addition, the interests of resource industries are best served by informed decision-making and informed public opinion. As a result, the largest change is not in what we do, but in the increased diversity of our clients.

## PROJECTS

The Yukon Geological Survey completed a successful, but challenging, field season that saw widespread and prolonged forest fires interfere with several projects. This year included a greater diversity of work that reflected our new mandate to support hydrocarbon development and to meet increased demands for baseline data to address environmental and development issues, while continuing to support our primary client, the mineral industry. Projects included 1:50 000-scale bedrock mapping, mineral deposit studies, surficial studies and mapping, regional stream sediment geochemistry, topical geology studies and a regional seismic study. In addition, several office-based projects were undertaken to advance the Yukon Geoscience database.

### BEDROCK MAPPING

Three bedrock mapping projects were initiated this year. Near Livingstone Creek, Maurice Colpron continued his work on the Yukon-Tanana Terrane in an area where the source of historical placer deposits has not been defined. In southeastern Selwyn Basin near Toobally Lakes, Lee Pigage continued to map in areas that will help to define the potential for hydrocarbons and for sedimentary-exhalative deposits like those at Faro, Howard’s Pass and Macmillan Pass. In the Kluane Ranges, Steve Israel began a new project to better define the setting of magmatic nickel-copper-PGE deposits associated with Triassic

volcanic and related intrusive rocks of the Nicolai Greenstone.

### MINERAL DEPOSIT STUDIES

This year Craig Hart and Lara Lewis focused on beryl and emerald potential in the Yukon while continuing their work on the metallogeny of intrusion-related gold and tungsten. Julie Hunt continued her work on the Wernecke Breccias by focusing on summary reports and posters of their geology and mineral potential, with emphasis on uranium. Jim Mortensen at the University of British Columbia, in partnership with Bill LeBarge, is being supported to undertake a microprobe study to define the trace element characteristics of placer gold in order to identify distinct populations and potential lode sources.

### SURFICIAL GEOLOGY STUDIES

Surficial geology studies included ongoing work by Bill LeBarge and Mark Nowosad to characterize the grain size distribution in Yukon placer deposits, to estimate potential impact of sediment discharge from different types of gravel, and to study other sources of contamination in placer districts. Jeff Bond has several projects underway. His studies of the last glacial ice flow in the Pelly Mountains of southern Yukon show that the “Cassiar lobe” of the Cordilleran ice sheet flowed into and up the mountain valleys. These results have significant implications for mineral exploration projects that utilize soil and float geochemistry. He is also completing a surficial geology map of the greater Whitehorse Area. Panya Lipovsky is undertaking surficial geological mapping in southeast Yukon as part of a biophysical mapping project being led by the Department of Environment in support of land use planning initiatives. Panya and Crystal Huscroft have initiated monitoring studies of several land failures related to permafrost melting in central Yukon. These landslides are long-lived and may have a significant impact on water quality in salmon-bearing streams.

### GEOCHEMISTRY/MINERAL ASSESSMENTS

Our mineral assessment geologist Geoff Bradshaw has been mainly involved in the north Yukon land use planning initiative. In preparation for a mineral assessment of the area, the first phase of a regional stream geochemical survey was completed in partnership with the Geological Survey of Canada. Field visits to most mineral occurrences were also undertaken. Geoff has also been involved in other Yukon land use planning processes



and has given presentations to First Nations Groups on the mineral potential of their traditional territories.

### WHITEHORSE TROUGH PROJECT

The major initiative for YGS this year has been the Whitehorse Trough project which is largely aimed at better defining the hydrocarbon potential of this frontier basin. Late last winter, a seismic line was shot across the north end of the basin by the Geological Survey of

Canada in partnership with YGS. The bulk of the funding was provided by NRCan through their Targeted Geoscience initiative. Other components of the project include stratigraphic and sedimentological studies by Grant Lowey of YGS and Dr. Darrel Long from Laurentian University; igneous chemistry by Dr. Steve Piercey of Laurentian University; and structural studies by Amy Tizzard under the direction of Dr. Steven Johnston at the University of Victoria.

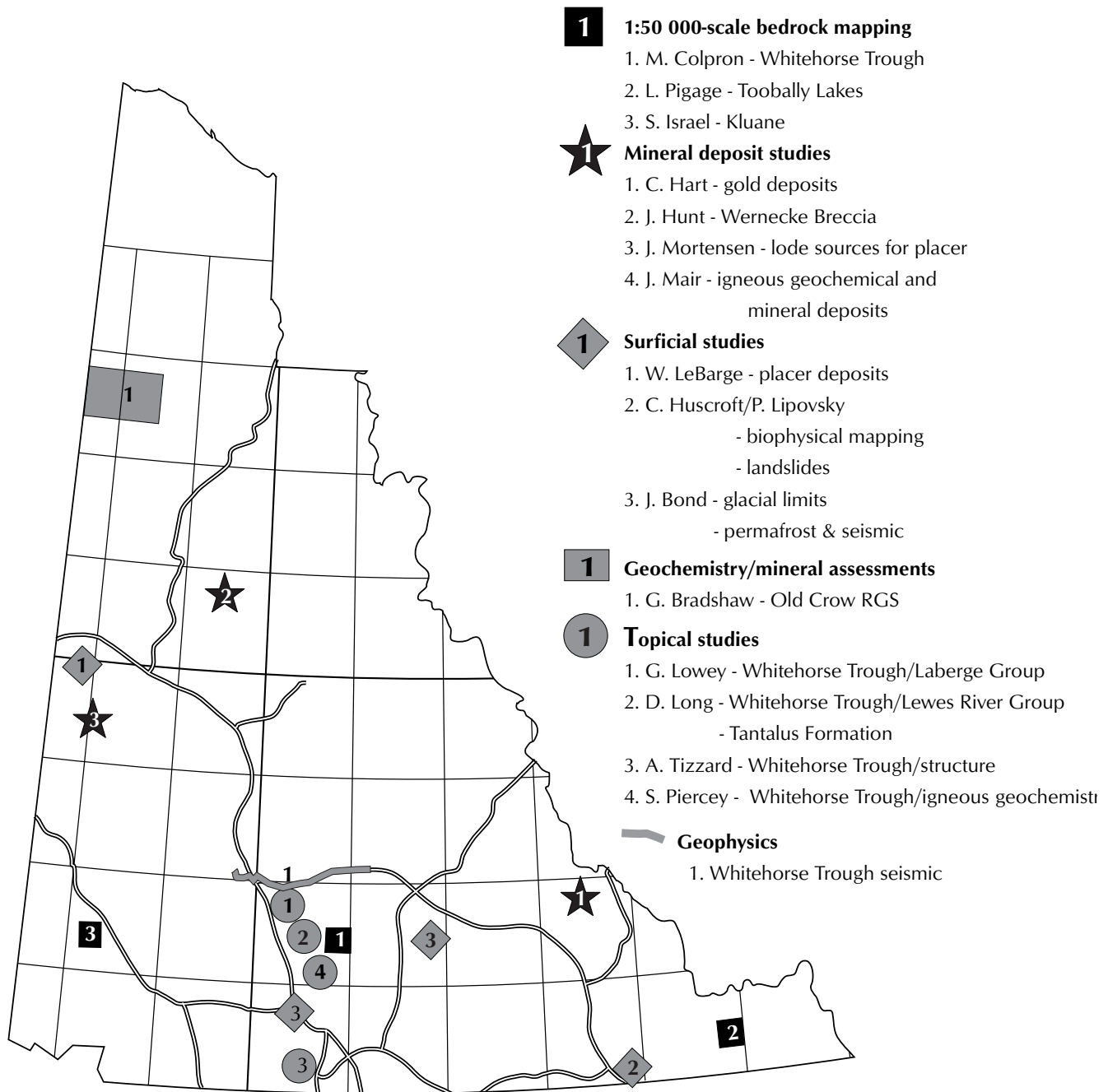


Figure 3. Field projects carried out or sponsored by the Yukon Geological Survey in 2004.

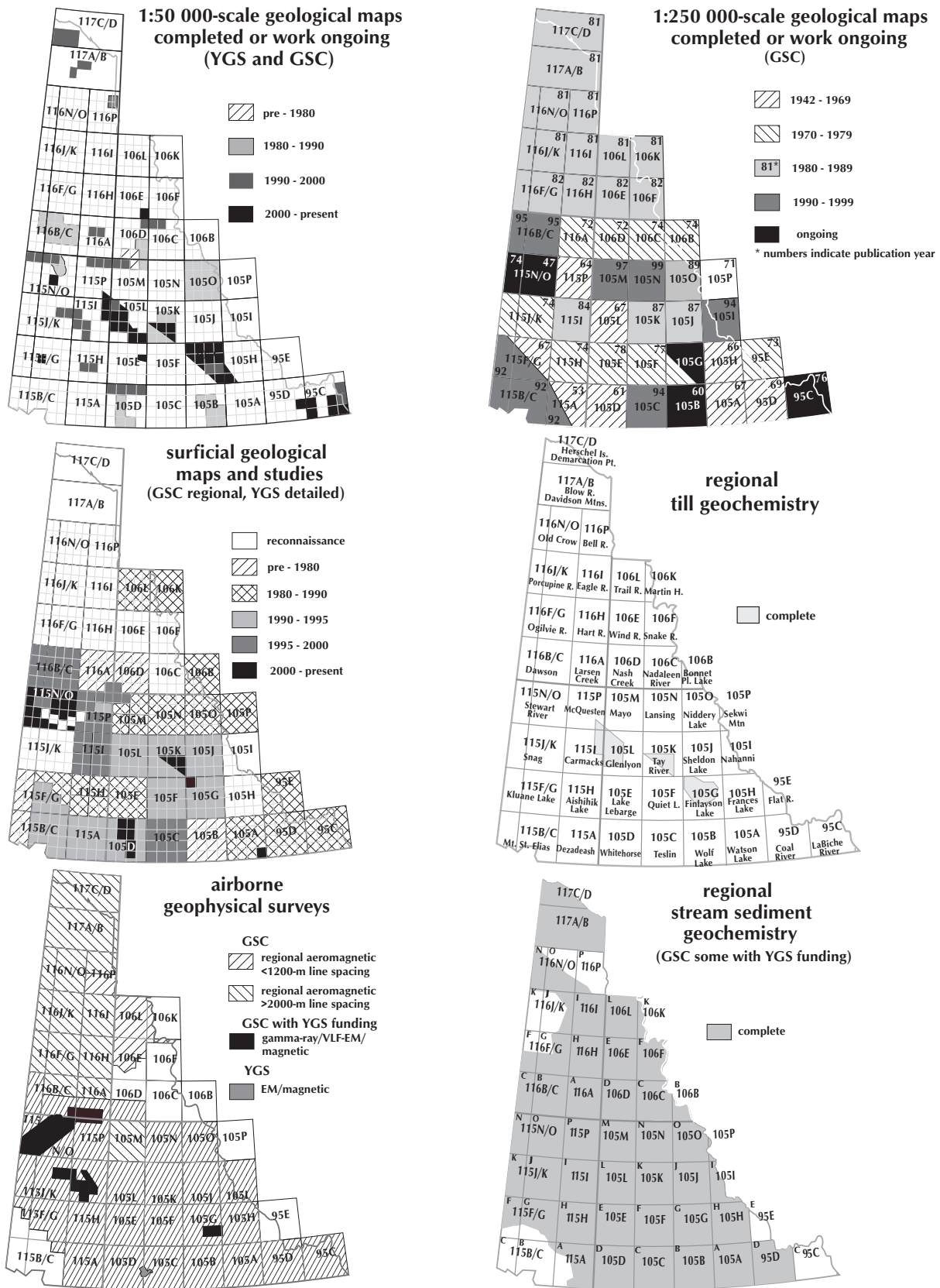


Figure 4. Summary of available geological maps, and regional geochemical and geophysical surveys in the Yukon.

## MINING ENVIRONMENT RESEARCH GROUP (MERG)

Karen Pelletier continued to administer the Mining and Environmental Research Group (MERG), YTC. Five projects were approved for funding in 2003/4. Baseline Selenium Studies by Laberge Environmental Services examined the fate and cycling of selenium in the natural environment at Earn Lake. The study is regarded as an initial step towards developing selenium water quality guidelines applicable to northern conditions, specifically for the Yukon. Final Repairs to Noname Bioengineering Structures by Laberge Environmental Services in the Carmacks area involved the completion of repairs using geo-textile to partially failed willow fences that were constructed to correct permafrost melt and extensive erosion on a north-facing slope. A Bio-Engineering Demonstration Project on the Klondike River at Germaine Creek was undertaken by M. Miles and Associates Ltd. and Polster Environmental Services. The aim of the project is to demonstrate how bioengineering can be used to stabilize various erosional environments at a site that is accessible and visible to the public. The project involved a large outreach component that included on-the-job training for interested participants and an information sign at the site. T. Hutchinson and Alison Clark from Trent University were funded for a second and final year of a MSc thesis project. The objective of the project, entitled "Creating a self-sustaining plant community in derelict mine sites in the YT using native colonizing vegetation by" is to create a long-term revegetation management solution for abandoned mine sites in the Yukon using local native plant species. Funding provided to the Metal Leaching and Acid Rock Drainage Prediction Methods project by Bill Price of NRCan will be put towards the completion of guidelines and recommended methods for the prediction of metal leaching. These methods and guidelines will be nationally applicable and will serve as a 'tool-kit' of current best-testing procedures, including northern considerations.

Karen continues to review Mining Land Use and Water License applications, and monitor reclaimed sites to document the effectiveness of mitigation practices. She represents the YGS on several committees that sponsor environmental research involving geology. Karen has also been involved in developing a best practices guide for reclamation of placer mines.

## YUKON MINING INCENTIVES PROGRAM (YMIP)

The Yukon Mining Incentives Program is administered by Ken Galambos. This year, funding was offered to 66 of 78 applications for a total of \$1 046 500. Nine of the successful applications were in the Grassroots-Prospecting, three in the Grassroots-Grubstake, 21 in the Focused Regional and 33 in the Target Evaluation modules. These applicants included 73% Yukon-based individuals or companies.

With the surge in the price of gold, there was a corresponding surge in precious metals exploration. In all, 70% of successful applicants were exploring for the yellow metal, including 20% who were exploring for alluvial gold; 27% proposed exploration programs for base metals (primarily copper); two applicants explored for gemstones or other commodities.

## LIAISON TO INDUSTRY, FIRST NATIONS AND THE PUBLIC

YGS recognizes the importance of effectively communicating information on the geology and mineral and energy resources of the Yukon to a broad audience that includes: industry, resource managers, First Nations and the general public. We are continuing to focus more attention on developing strategies and products that meet these needs.

Mike Burke and Bill LeBarge, our main links to the exploration industry, continued to monitor Yukon hard-rock and placer mining and mineral exploration activity, visit active properties, review reports for assessment credit, and maintain the assessment report library.

Karen Pelletier, Charlie Roots and other YGS staff continue to make presentations in the schools and conduct field trips in the communities. New products developed this year to increase public awareness of the geology and mineral resources of the Yukon include: an interpretive guide to the Whitehorse Copper Belt by Danièle Héon; a geological map and interpretive display of Tombstone Park by Charlie Roots; and a geological map of southwest Yukon with emphasis on the Kluane Ranges and Kluane Park in partnership with the Geological Survey of Canada.



## INFORMATION MANAGEMENT AND DISTRIBUTION

With the increasing volume of information generated by YGS and others, and rapidly evolving digital technology, the Survey has placed more effort and resources into making geological information more accessible. A large part of our effort has gone into developing and maintaining key databases and making all of our information internet-accessible. Ongoing activities include support for the H.S. Bostock Core Library and the Energy, Mines and Resources (EMR) library (Elijah Smith Building).

### DATABASES

With new reporting requirements to securities regulators, widely recognized mineral deposit models are becoming increasingly important. In cooperation with the British Columbia Geological Survey, Anna Fonseca and Geoff Bradshaw have adapted the British Columbia Geological Survey Mineral Deposit Models for the Yukon. These models are now incorporated into Yukon MINFILE and will be published in early 2005.

Yukon MINFILE, the Yukon's mineral occurrence database, is maintained by Robert Deklerk and Steve Traynor. An update was released in November, 2004. The database now contains 2606 records, of which more than 500 have been revised, and is complete to the end of 2003. All mineral occurrences are now assigned to a deposit model. Reserve tables have been completely revised and updated to match, as closely as possible, the Canadian Institute of Mining Standards for Reporting Mineral Resources and Reserves.

The Yukon Placer Database, compiled under the direction of Bill LeBarge, was updated in the spring of 2004. The database is in Microsoft Access 2000 format and is a comprehensive record of the geology and history of Yukon placer mining. The database contains descriptions of 440 streams and rivers, and 1356 associated placer occurrences of which about 200 were updated for this version. It also includes location maps in Portable Document Format (PDF).

The Yukon GEOPROCESS File, under the direction of Diane Emond, is an inventory of information on geological processes and terrain hazards. It includes 1:250 000-scale maps showing permafrost, landslides, recent volcanic rocks, structural geology and seismic events, and also includes references and summaries of bedrock and surficial geology. The GEOPROCESS File is intended as a

planning aid for development activities and is available for most areas south of 66° latitude. The maps are now standardized in colour, and available on a single compact disk. Maps with text are in AutoCAD 2000 and PDF formats.

The Yukon Digital Geology compilation was updated in 2003 by Steve Gordey and Andrew Makepeace of the Geological Survey of Canada with funding from YGS. It includes syntheses of bedrock geology and glacial limits, compilations of geochronology, paleontology and mineral occurrences, and a compendium of aeromagnetic images, as well as an oil and gas well database. All are now available on CD-ROM. Bedrock geology and glacial limit paper maps are also available at 1:1 000 000 scale.

The Yukon Regional Geochemical Database 2003, compiled by Danièle Héon, contains all of the available digital data for regional stream sediment surveys that have been gathered in the Yukon under the Geological Survey of Canada's National Geochemical Reconnaissance Program. It is available on CD-ROM in Microsoft Excel 2000 format and in ESRI ArcView Shapefile format. The database has been enhanced this year through a contract with Georeference Online. Multielement anomaly clusters were generated using Minematch software and matched with mineral deposit models. This exercise was essentially the same as one undertaken on the British Columbia stream geochemical database through the Rocks to Riches Program. Results are now available online through the YGS Map Gallery.

The YukonAge Database, compiled by Katrin Breitsprecher and Jim Mortensen at the University of British Columbia with funding from YGS, was updated in 2004. It can be viewed on the on-line YGS Map Gallery in a version modified by Mike Villeneuve and Linda Richard of the Geological Survey of Canada. The database now contains 1556 age determinations derived from 1166 rock samples from the Yukon Territory. It is available in both Microsoft Access 2000 format and as a flat file in Microsoft Excel 2000 format so that the data may be viewed without Microsoft Access.

The Yukon Geoscience Publications Database, 2003, compiled by Lara Lewis and Diane Emond, is current to 2003 and contains more than 5000 references to papers on Yukon geology and mineral deposits, including YGS publications. A completely up-to-date searchable version is now available on our website.

This year, YGS was fortunate to receive funding through the DIAND Northern Geoscience Program to continue

digitizing assessment reports. By April 2005, the entire collection of more than 5000 open reports will be in PDF format and accessible over the internet. In addition, we have acquired exploration records from the various companies that owned properties in the Faro District. This acquisition includes both records of the Faro District as well as outside projects; the records should be available for viewing by late winter of 2005.

### **H.S. BOSTOCK CORE LIBRARY**

Mike Burke and Ken Galambos maintain the H.S. Bostock Core Library. The facility contains about 128 000 m of diamond drill core from about 200 Yukon mineral occurrences. Confidentiality of material is determined on the same basis as mineral assessment reports. Confidential core can be viewed with a letter of release from the owner. Rock saws and other rock preparation equipment are available to the public.

### **EMR LIBRARY**

The EMR library in the Elijah Smith Building is an invaluable resource that is available to the public, but often overlooked. It is Yukon's largest scientific library and includes collections that, prior to devolution, belonged to Indian and Northern Affairs Canada and the Department of Energy, Mines and Resources, Yukon Government. The library houses Yukon assessment reports, maps (including geological, topographical and aeromagnetic), and aerial photographs. It contains most geological journals and a good selection of references on general geology, Yukon geology and economic geology. This year, the library\* has updated its online search capabilities, making search and retrieval of assessment reports and other documents easier and more efficient. The library will also be the point of contact for access to Faro exploration records. In addition to geological information, the library also has books, reports and journals for the following subjects: oil and gas, forestry, agriculture and energy.

### **INFORMATION DISTRIBUTION**

YGS distributes information in three formats: 1) paper maps and reports are sold and distributed through our Geoscience Information and Sales Office; 2) many recent publications and databases are available in digital format

on CD-ROM also from the same outlet; and, 3) most of our publications are available as free downloads on our website ([www.geology.gov.yk.ca](http://www.geology.gov.yk.ca)). A catalogue of assessment reports is also available online\*.

We are pleased to make spatial data available through our interactive map server – the Map Gallery; it can be accessed through the YGS website. We are continuing to improve the Map Gallery. This year a shaded relief map has been added and vector data can now be clipped and downloaded. Users are encouraged to provide feedback and suggest improvements (see website address below).

Hard copies of YGS publications are available at the following address.

Geoscience Information and Sales  
c/o Whitehorse Mining Recorder  
102-300 Main Street (Elijah Smith Building)  
P.O. Box 2703 (K102)  
Whitehorse Yukon Y1A 2C6  
Ph. (867) 667-5200  
Fax. (867) 667-5150  
E-mail: [geosales@gov.yk.ca](mailto:geosales@gov.yk.ca)

To access publications and to learn more about the Yukon Geological Survey, visit our website at <http://www.geology.gov.yk.ca>, or contact us directly.

Grant Abbott, Chief Geologist  
Yukon Geological Survey  
102-300 Main Street (Elijah Smith Building)  
P.O. Box 2703 (K102)  
Whitehorse, Yukon Y1A 2C6  
Phone (867) 667-3200  
E-mail: [grant.abbott@gov.yk.ca](mailto:grant.abbott@gov.yk.ca)

Rod Hill, Manager  
Yukon Geological Survey  
2099 Second Avenue  
P.O. Box 2703 (K10)  
Whitehorse, Yukon Y1A 2C6  
Phone (867) 667-5384  
E-mail: [rod.hill@gov.yk.ca](mailto:rod.hill@gov.yk.ca)

To access the EMR library website:  
[www.emr.gov.yk.ca/library](http://www.emr.gov.yk.ca/library)  
Phone: (867) 667-3111  
E-mail: [emrlibrary@gov.yk.ca](mailto:emrlibrary@gov.yk.ca)

\*[www.emr.gov.yk.ca/library](http://www.emr.gov.yk.ca/library)

## 2004 PUBLICATIONS AND MAPS

### YGS BULLETINS

Lowey, G.W., 2004. Placer Geology of the Stewart River (115N&O) and Dawson (116B&C) map areas, west-central Yukon, Canada. Yukon Geological Survey, Bulletin 14, report and two maps 1:250 000 scale, CD-ROM.

Pigage, L.C., 2004. Bedrock geology compilation of the Anvil District (parts of NTS 105K/2, 3, 5, 6 and 7), central Yukon. Yukon Geological Survey, Bulletin 15 (includes two 1:100 000- and fifteen 1:25 000-scale maps); also available on CD-ROM.

### YGS OPEN FILES

*(also see under Joint YGS/GSC Open Files)*

Héon, D. (compiler), 2004. The Whitehorse Copper Belt, Yukon – An annotated geology map. Yukon Geological Survey, Open File 2004-15, 2 sheets, 1:50 000 scale.

Huscroft, C.A., Lipovsky, P.S. and Bond, J.D., 2004. A regional characterization of landslides along the Alaska Highway Corridor, Yukon. Yukon Geological Survey, Open File 2004-18, report and CD-ROM, 65 p.

Israel, S. (comp), 2004. Geology of southwest Yukon. Yukon Geological Survey, Open File 2004-16, 1:250 000 scale.

Israel, S., 2004. Preliminary bedrock geology of the Quill Creek area (parts of NTS 115G/5, 6 and 12), southwest Yukon. Yukon Geological Survey, Open File 2004-20, 1:50 000 scale.

Kiss, F., Coyle, M., Forté, S. and Dumont, R., 2004. Aeromagnetic Total Field and Shaded Magnetic Vertical First Derivative 106F/NE-NW, 106K/NW-NE, 106L/NE-NW and 116P/SW-SE. Yukon Geological Survey, Open File 2004-4 to 9, 13 and 14; Geological Survey of Canada, Open Files 4503 to 4507, 4510, 4511 and 4514. 1:250 000 scale.

Lowey, G.W., Deforest, S. and Lipovsky, P.S., 2004. Stewart River Placer Project station location map, portions of NTS Sheets 116B & C and 115N & O. Yukon Geological Survey, Open File 2004-12; also Map 1 in Bulletin 14, 1:250 000 scale.

Murphy, D.C., Kennedy, R. and Tizzard, A., 2004. Geological map of parts of Waters Creek and Fire Lake map areas (NTS 105G/1, 2), southeastern Yukon. Yukon Geological Survey, Open File 2004-11, 1:50 000 scale.

Pigage, L.C., 2004. Preliminary geology of NTS 95D/8 (northern Toobally Lakes area), southeast Yukon. 1:50 000 scale. Yukon Geological Survey, Open File 2004-19.

Roots, C., Nelson, J. and Stevens, R., 2004. Geology of Seagull Creek (105B/3), Yukon Territory. Yukon Geological Survey, Open File 2004-1; Geological Survey of Canada, Open File 4632, 1:50 000 scale.

Roots, C., Nelson, J., Mihalynuk, M., Harms, T., de Keijzer, M. and Simard, R.L., 2004. Geology of Dorsey Lake (105B/4), Yukon Territory. Yukon Geological Survey, Open File 2004-2; Geological Survey of Canada, Open File 4630, 1:50 000 scale.

Roots, C., Nelson, J. and Stevens, R., 2004. Geology of Morris Lake (105B/5), Yukon Territory. Yukon Geological Survey, Open File 2004-3; Geological Survey of Canada, Open File 4631, 1:50 000 scale.

Sebert, C., Hunt, J.A. and Foreman, I.J., 2004. Geology and litho-geochemistry of the Fyre Lake copper-cobalt-gold sulphide-magnetite deposit, southeastern Yukon. Yukon Geological Survey, Open File 2004-17, 46 p.

Walton, L., 2004. Exploration criteria for coloured gemstone deposits in the Yukon. Yukon Geological Survey, Open-File 2004-10, 184 p.

### YGS GEOSCIENCE MAPS

Pigage, L.C., 2004. Intrusive suites and major stratigraphic-tectonic successions, Yukon (1:100 000 scale). Yukon Geological Survey, Geoscience Map 2004-1; also Plate 1 in YGS Bulletin 15.

Pigage, L.C., 2004. Geological map of Anvil District, Yukon (1:100 000 scale). Yukon Geological Survey, Geoscience Map 2004-2; also Plate 2 in YGS Bulletin 15.

Pigage, L.C., 2004. Geological map of Rose Mountain (NTS 105K/5 NW), Yukon (1:25 000 scale). Yukon Geological Survey, Geoscience Map 2004-3; also Plate 3 in YGS Bulletin 15.

Pigage, L.C., 2004. Geological map of Rose Mountain (NTS 105K/5 NE), Yukon (1:25 000 scale). Yukon Geological Survey, Geoscience Map 2004-4; also Plate 4 in YGS Bulletin 15.



- Pigage, L.C., 2004. Geological map of Rose Mountain (NTS 105K/5 SE), Yukon (1:25 000 scale). Yukon Geological Survey, Geoscience Map 2004-5; also Plate 5 in YGS Bulletin 15.
- Pigage, L.C., 2004. Geological map of Mount Mye (NTS 105K/6 NW), Yukon (1:25 000 scale). Yukon Geological Survey, Geoscience Map 2004-6; also Plate 6 in YGS Bulletin 15.
- Pigage, L.C., 2004. Geological map of Mount Mye (NTS 105K/6 W), Yukon (1:25 000 scale). Yukon Geological Survey, Geoscience Map 2004-7; also Plate 7 in YGS Bulletin 15.
- Pigage, L.C., 2004. Geological map of Faro (NTS 105K/3 NW) and Mount Mye (NTS 105K/6 SW), Yukon (1:25 000 scale). Yukon Geological Survey, Geoscience Map 2004-8; also Plate 8 in YGS Bulletin 15.
- Pigage, L.C., 2004. Geological map of Mount Mye (NTS 105K/6 NE) and Barwell Lake (NTS 105K/11 SE), Yukon (1:25 000 scale). Yukon Geological Survey, Geoscience Map 2004-9; also Plate 9 in YGS Bulletin 15.
- Pigage, L.C., 2004. Geological map of Mount Mye (NTS 105K/6 E), Yukon (1:25 000 scale). Yukon Geological Survey, Geoscience Map 2004-10; also Plate 10 in YGS Bulletin 15.
- Pigage, L.C., 2004. Geological map of Faro (NTS 105K/3 NE) and Mount Mye (NTS 105K/6 SE) (1:25 000 scale). Yukon Geological Survey, Geoscience Map 2004-11; also Plate 11 in YGS Bulletin 15.
- Pigage, L.C., 2004. Geological map of Blind Creek (NTS 105K/7 NW), Yukon (1:25 000 scale). Yukon Geological Survey, Geoscience Map 2004-12; also Plate 12 in YGS Bulletin 15.
- Pigage, L.C., 2004. Geological map of Blind Creek (NTS 105K/7 SW), Yukon (1:25 000 scale). Yukon Geological Survey, Geoscience Map 2004-13; also Plate 13 in YGS Bulletin 15.
- Pigage, L.C., 2004. Geological map of Swim Lakes (NTS 105K/2 W), Yukon (1:25 000 scale). Yukon Geological Survey, Geoscience Map 2004-14; also Plate 14 in YGS Bulletin 15.
- Pigage, L.C., 2004. Geological map of Blind Creek (NTS 105K/7 SE), Yukon (1:25 000 scale). Yukon Geological Survey, Geoscience Map 2004-15; also Plate 15 in YGS Bulletin 15.

Pigage, L.C., 2004. Geological map of Swim Lakes (NTS 105K/2 NE), Yukon (1:25 000 scale). Yukon Geological Survey, Geoscience Map 2004-16; also Plate 16 in YGS Bulletin 15.

Pigage, L.C., 2004. Geological map of Swim Lakes (NTS 105K/2 SE), Yukon (1:25 000 scale). Yukon Geological Survey, Geoscience Map 2004-17; also Plate 17 in YGS Bulletin 15.

## YGS DATABASES

Deklerk, R. and Traynor, S. (comps.), 2004. Yukon MINFILE 2004 – A database of mineral occurrences. Yukon Geological Survey, CD-ROM.

LeBarge, W.P. (comp), 2004. Yukon Placer Database 2004 – Geology and mining activity of placer occurrences. Yukon Geological Survey, CD-ROM.

Breitsprecher, K., Mortensen, J.K. and Villeneuve, M.E. (comps.), 2004. YukonAge 2004 – A database of isotopic age determinations for rock units from Yukon Territory. Yukon Geological Survey and Geological Survey of Canada, CD-ROM.

## JOINT YGS/GSC OPEN FILES AND GEOSCIENCE MAPS

Kiss, F., Coyle, M., Forté, S. and Dumont, R., 2004. Aeromagnetic Total Field and Shaded Magnetic Vertical First Derivative 106F/NE-NW, 106K/NW-NE, 106L/NE-NW and 116P/SW-SE. Yukon Geological Survey, Open File 2004-4 to 9, 13 and 14; Geological Survey of Canada, Open Files 4503 to 4507, 4510, 4511 and 4514, 1:100 000 scale.

## JOINT YGS/AGRICULTURE AND AGRI-FOOD CANADA PUBLICATION

Smith, C.A.S., Meikle, J.C. and Roots, C.F., 2004. Ecoregions of the Yukon Territory – Biophysical Properties of Yukon Landscapes. Agriculture and Agri-Food Canada, PARC Technical Bulletin 04-01, Summerland, British Columbia, 313 p., report and CD-ROM.

## YGS CONTRIBUTIONS

- Hart, C.J.R.**, Goldfarb, R.J., **Lewis, L.L.** and Mair, J.L., 2004. The Northern Cordillera Mid-Cretaceous Plutonic Province: Ilmenite/Magnetite-Series Granitoids and Intrusion-Related Mineralisation. *Resource Geology*, vol. 54, no. 3, p. 253-280.
- Huscroft, C.A.**, Ward B.C., Barendregt R.W., Jackson Jr. L.E. and Opdyke N.D., 2004. Pleistocene volcanic damming of Yukon River and the maximum age of the Reid Glaciation, west-central Yukon. *Canadian Journal of Earth Sciences*, vol. 41, p. 151-164.
- Marsh, E.E., Goldfarb, R.J., **Hart, C.J.R.** and Johnson, C.A., 2003. Geology and geochemistry of the Clear Creek intrusion-related gold occurrences, Tintina Gold Province, Yukon, Canada. *Canadian Journal of Earth Sciences*, vol. 40, p. 681-699.
- Marshall, D., Groat, L., Giuliani, G., **Murphy, D.**, Matthey, D., Ercit, T.S., Wise, M.A., Wengzynowski, W. and Eaton, W.D., 2003. Pressure, temperature and fluid conditions during emerald precipitation, southeastern Yukon, Canada: Fluid inclusion and stable isotope evidence. *Chemical Geology*, vol. 194, p. 187-199.
- Mueller, S.H., Goldfarb, R.J., **Hart, C.J.R.**, Mair, J.L., Marsh, E.E. and Rombach, C.S., 2004. The Tintina Gold Province, Alaska and Yukon – New World-Class Gold Resources and Their Sustainable Development. PACRIM 2004, Conference Proceedings, Australian Institute of Mining and Metallurgy, Adelaide, Australia, p. 189-198.
- Piercey, S.J., **Murphy, D.C.**, Mortensen, J.K. and Creaser, R.A., 2004. Mid-Paleozoic initiation of the northern Cordilleran marginal backarc basin: Geologic, geochemical, and neodymium isotope evidence from the oldest mafic magmatic rocks in the Yukon-Tanana terrane, Finlayson Lake district, southeast Yukon, Canada. *Geological Society of America Bulletin*, vol. 116, no. 9, p. 1087-1106.
- Pigage, L.C.** and Mortensen, J.K., 2004. Superimposed Neoproterozoic and Early Tertiary alkaline magmatism in the La Biche River area, southeast Yukon Territory. *In: Central Foreland NATMAP: Stratigraphic and Structural Evolution of the Cordilleran Foreland*, L.S. Lane (ed.), *Bulletin of Canadian Petroleum Geology*, vol. 52, p. 323-340.
- Schwab, D.L., Thorkelson, D.J., Mortensen, J.K., **Creaser, R.A.** and **Abbott, J.G.**, 2004. The Bear River Dykes (1265–1269 Ma): Westward Continuation of the Mackenzie Dyke Swarm into Yukon, Canada. *Precambrian Research*, vol. 133, p. 175-186.
- Selby, D., Creaser R.A., Heaman, L.M. and **Hart, C.J.R.**, 2004. Re-Os and U-Pb geochronology of the Clear Creek, Dublin Gulch, and Mactung deposits, Tombstone Gold Belt, Yukon, Canada: absolute timing relationships between plutonism and mineralization. *Canadian Journal of Earth Sciences*, vol. 40, p. 1839-1852.
- Simard, R.L., Dostal, J. and **Roots, C.F.**, 2003. Development of late Paleozoic volcanic arcs in the Canadian Cordillera: an example from the Klinkit Group, northern British Columbia and southern Yukon. *Canadian Journal of Earth Sciences*, vol. 40, p. 907-924.
- Stephens, J.R., Mair, J.L., Oliver, N.H.S., **Hart, C.J.R.** and Baker, T., 2004. Structural and Mechanical Controls on Intrusion-Related Deposits of the Tombstone Gold Belt, Yukon, Canada, with Comparisons to Other Vein-Hosted Ore-Deposit Types. *Journal of Structural Geology*, vol. 26, p. 1025-1041.
- Symons, D.T.A., **Hart, C.J.R.**, Harris, M.J. and McCausland, P.J.A., 2004. Paleomagnetism of the Eocene Flat Creek pluton, Yukon. Tectonics of the Intermontane terranes and Mackenzie Mountains. *In: Orogenic Curvature: Integrating Paleomagnetic and Structural Analyses*, A.J. Sussman and A.B. Weil (eds.), Geological Society of America, Special Paper 383, p. 187-204.
- Thorkelson, D.J., **Abbott, J.G.**, Mortensen, J.K., Creaser, R.A., Villeneuve, M.E., McNicoll, V.J. and Layer, P.W., 2004. Early and Middle Proterozoic evolution of Yukon, Canada. *Canadian Journal of Earth Sciences*, vol. 41.

## YGS ABSTRACTS

- Colpron, M.** and Nelson, J.L., 2004. Cordilleran terranes revisited: the dossier on some long-suspected relationships. *Geological Society of America, Abstracts with Programs*, vol. 36, no. 5, p. 271.

- Goldfarb, R.J., Groves, D.I. and **Hart, C.J.R.**, 2004. Overview on gold deposits in metamorphic belts – orogenic and intrusion-related deposits. *Ishihara Symposium Abstract Volume, Geological Survey of Japan, Tokyo.*

- Hart, C.J.R.**, Villeneuve, M.E., Mair, J.L., Goldfarb, R.J., Selby, D., Creaser R.A. and Wijns, C., 2004. Comparative U–Pb, Re–Os and Ar–Ar geochronology of mineralizing plutons in Yukon and Alaska. SEG 2004 Predictive Mineral Discovery Under Cover, Extended Abstract, J. Muhling et al. (eds.), Perth, Australia, p. 347-349
- Lewis, L.L., Hart, C.J.R.** and Garrett, R.G., 2004. Compatible behaviour of beryllium in fractionating granitic magmas, Selwyn Magmatic Province. Abstracts with Program, Geological Association of Canada, SS10-P08.
- Lipovsky, P.S., Huscroft, C.A.** and Lewkowitz, A.G., 2004. The Nines Creek Ice and Rock Avalanche: An Example of the Impact of Climate Change on Catastrophic Geomorphic Processes in the Kluane Ranges, Yukon Territory, Canada. Eos, Transactions, American Geophysical Union, 85(47), Fall Meeting Supplement, Abstract C13B-0281.
- MacNaughton, R.B., **Pigage, L.C.** and Fallas, K.M., 2004. Proterozoic to Devonian Stratigraphic Evolution of Southeasternmost Yukon Territory: New Insights From Surface Mapping. ICE 2004, CSPG-CHOA-CWLS Joint Conference, Calgary, Alberta, Abstracts CD-ROM, Abstract No. 082S0129.
- YUKON GEOLOGICAL PAPERS OF INTEREST**
- Cook, F.A., Clowes, R.M., Snyder, D.B., van der Velden, A.J., Hall, K.W., Erdmer, P. and Evenchick, C.A., 2004. Precambrian crust beneath the Mesozoic northern Canadian Cordillera discovered by Lithoprobe seismic reflection profiling. *Tectonics*, vol. 23,
- Dusel-Bacon, C., Wooden, J.L. and Hopkins, M.J., 2004. U–Pb zircon and geochemical evidence for bimodal mid-Paleozoic magmatism and syngenetic base-metal mineralization in the Yukon-Tanana terrane, Alaska. *Geological Society of America Bulletin*, vol. 116, no. 7, p. 989–1015.
- Gangloff, R.A., May, K.C. and Storer, J.E., 2004. An early late Cretaceous dinosaur tracksite in central Yukon Territory, Canada. *Ichnos*, vol. 11, p. 299-309.
- Jackson, D.E. and Norford, B.S., 2004. Biostratigraphical and ecostratigraphical significance of Tremadoc (Ordovician) graptolite faunas from the Misty Creek Embayment and Selwyn Basin in Yukon and Northwest Territories. *Canadian Journal of Earth Sciences*, vol. 41, p. 331-348.
- Mangan, M.T., Waythomas, C.F, Miller T.P. and Trusdell, F.A., 2003. Emmons Lake Volcanic Center, Alaska Peninsula: source of the Late Wisconsin Dawson tephra, Yukon Territory, Canada. *Canadian Journal of Earth Sciences*, vol. 40, p. 925-936.
- Morris, G.A. and Creaser R.A., 2003. Crustal recycling during subduction at the Eocene Cordilleran margin of North America: a petrogenetic study from the southwestern Yukon. *Canadian Journal of Earth Sciences*, vol. 40, p. 1805-1821.
- Pyle, L.J. and Barnes, C.R., 2003. Lower Paleozoic stratigraphic and biostratigraphic correlations in the Canadian Cordillera: implications for the tectonic evolution of the Laurentian margin. *Canadian Journal of Earth Sciences*, vol. 40, p. 1739-1753.
- Sack, R.O., Lynch, J.V.G. and Foit Jr., F., 2004. Fahlore as a petrogenetic indicator: Keno Hill Ag-Pb-Zn District, Yukon, Canada. *Mineralogical Magazine*, vol. 67, p. 1023-1038.
- Symons D.T.A., Erdmer, P. and McCausland, P.J.A., 2003. New 42 Ma cratonic North American paleomagnetic pole from the Yukon underscores another Cordilleran paleomagnetism-geology conundrum. *Canadian Journal of Earth Sciences*, vol. 40, p. 1321-1334.
- Simard R.-L., Dostal, J. and Roots, C.F., 2003. Development of late Paleozoic volcanic arcs in the Canadian Cordillera: an example from the Klinkit Group, northern British Columbia and southern Yukon. *Canadian Journal of Earth Sciences*, vol. 40, p. 907-924.
- YUKON THESES**
- Flück, P., 2003. Contributions to the geodynamics of Western Canada. PhD thesis, University of Victoria, Victoria, British Columbia, 326 p.
- Heffernan, R.S., 2004. Temporal, geochemical, isotopic, and metallogenic studies of mid-Cretaceous magmatism in the Tintina Gold Province, southeastern Yukon and southwestern Northwest Territories, Canada. MSc thesis, University of British Columbia, Vancouver, BC, 77 p.



- Heffernan, R.S., 2004. Temporal, geochemical, isotopic, and metallogenic studies of mid-Cretaceous magmatism in the Tintina Gold Province, southeastern Yukon and southwestern Northwest Territories, Canada. Unpublished MSc thesis, University of British Columbia, Vancouver, BC, 83 p.
- Kennedy, K., 2004. Surficial geology and Quaternary history of the Seagull Creek valley, Pelly Mountains, Yukon. Unpublished BSc (honours) thesis, Simon Fraser University, Vancouver, BC, 53 p.
- Ruhs, T.W., 2004. Petrology and tectonic significance of K-feldspar augen granitoids in the Yukon-Tanana terrane, Stewart River, Yukon Territory. Unpublished MSc thesis. Laurentian University, Sudbury, Ontario, 150 p.
- Stephens, J.R., 2003. Structural, mechanical and P-T evolution of intrusion-related gold mineralization at Clear Creek and Dublin Gulch, Yukon, Canada. PhD thesis, James Cook University of North Queensland, Australia, 210 p.
- YUKON GEOLOGICAL ABSTRACTS OF INTEREST**
- Fallas, K.M. and Lane, L.S., 2004. Comparative analysis of Stratigraphic influences on the Mechanics of Foreland deformation. ICE 2004, CSPG-CHOA-CWLS Joint Conference, Calgary, AB, Abstracts CD-ROM, Abstract No. 134S0130.
- Utting, J., Zonneveld, J-P., MacNaughton, R.B. and Fallas, K., 2004. Palynostratigraphy, organic matter and thermal maturity of the Lower Triassic of western Canada, and comparison with the Sverdrup Basin, Nunavut. XI International Palynological Congress. Pollen, vol. 14, p. 442.
- GSC CONTRIBUTIONS TO YUKON GEOLOGY**
- Dixon, J., 2004. Jurassic – Lower Cretaceous (Oxfordian to Lower Aptian) Strata, Yukon Territory – Northwest Territories (a contribution to the Geological Atlas of the Northern Canadian Mainland Sedimentary Basin). Geological Survey of Canada, Open File 4621, 39 p.
- Dixon, J., 2004. Lower Cretaceous (Albian) to Tertiary strata, Yukon Territory – Northwest Territories (a contribution to the Geological Atlas of the Northern Canadian Mainland Sedimentary Basin). Geological Survey of Canada, Open File 4633, 45 p.
- Fallas, K.M., Pigage, L.C. and MacNaughton, R.B. (comps.), 2004. Geology, southwest La Biche River (95C/SW), Yukon Territory and British Columbia. Geological Survey of Canada, Open File 4664, scale 1:100 000, 2 sheets.
- Kiss, F., Coyle, M. and Dumont, R., 2004. High resolution aeromagnetic total field map, Peel Plateau, Yukon (NTS 106F/NE-NW). Geological Survey of Canada, Open File 4503, 1 sheet; also YGS Open File 2004-4.
- Kiss, F., Coyle, M. and Dumont, R., 2004. High resolution aeromagnetic total field map, Peel Plateau, Yukon (NTS 106L/NE-NW). Geological Survey of Canada, Open File 4504, 1 sheet; also YGS Open File 2004-5.
- Kiss, F., Coyle, M. and Dumont, R., 2004. Shaded magnetic first vertical derivative map, Peel Plateau, Yukon (NTS 106F/NE-NW). Geological Survey of Canada, Open File 4505, 1 sheet; also YGS Open File 2004-6.
- Kiss, F., Coyle, M. and Dumont, R., 2004. Shaded magnetic first vertical derivative map, Peel Plateau, Yukon (NTS 106L/NE-NW). Geological Survey of Canada, Open File 4506, 1 sheet; also YGS Open File 2004-7.
- Kiss, F., Coyle, M., Potvin, J. and Dumont, R., 2004. Aeromagnetic total field, 106K/NW-NE, Yukon Territory/Northwest Territories (106K/NW-NE). Geological Survey of Canada, Open File 4507, 1 sheet; also YGS Open File 2004-13.
- Kiss, F., Coyle, M., Potvin, J. and Dumont, R., 2004. Aeromagnetic total field, 116P/SW-SE, Yukon Territory/Northwest Territories (116P/SW-SE). Geological Survey of Canada, Open File 4510, 1 sheet; also YGS Open File 2004-8.
- Kiss, F., Coyle, M., Potvin, J. and Dumont, R., 2004. Shaded magnetic first vertical derivative, 106K/NW-NE, Yukon Territory/Northwest Territories/Dérivée première verticale du champ magnétique (relief ombré), 106K/NW-NE, Territoire du Yukon / Territoires du Nord-Ouest. Geological Survey of Canada, Open File 4511, 1 sheet; also YGS Open File 2004-14.
- Kiss, F., Coyle, M., Potvin, J. and Dumont, R., 2004. Shaded magnetic first vertical derivative map, Peel Plateau, Yukon (NTS 116P/SW-SE). (106K/NW-NE). Geological Survey of Canada, Open File 4514, 1 sheet; also YGS Open File 2004-9.

- Lawrence, D.E., 2004. Survey of expert opinion on permafrost and geotechnical issues for northern pipelines. Geological Survey of Canada, Open File 4734, 24 p.
- Roots, C.F., Nelson, J.L., Mihalyuk, M.G., Harms, T.A., De Keijzer, M. and Simard, R.-L., 2004. Bedrock geology, Dorsey Lake, Yukon Territory. Geological Survey of Canada, Open File 4630, 1 sheet; also YGS Open File 2004-2, 1:50 000 scale
- Roots, C.F., Nelson, J.L. and Stevens, R.A., 2004. Bedrock geology, Morris Lake, Yukon Territory. Geological Survey of Canada, Open File 4631, 1 sheet; also YGS Open File 2004-3, 1:50 000 scale.
- Roots, C.F., Nelson, J.L. and Stevens, R.A., 2004. Bedrock geology, Seagull Creek, Yukon Territory. Geological Survey of Canada, Open File 4632, 1 sheet; also YGS Open File 2004-1, 1:50 000 scale.
- Ryan, J.J. and Gordey, S.P., 2004. Geology, Stewart River area (parts of 115 N/1, 2, 7, 8 and 115 O/2 - 12), Yukon Territory. Geological Survey of Canada, Open File 4641, 1 sheet.
- Smith, I.R., 2004. Surficial geology, La Biche River (southwest), Yukon Territory – British Columbia. Geological Survey of Canada, Open File 4680, 1 colour map, 1:100 000 scale.
- Smith, I.R., 2004. Surficial geology, Tika Creek (95 C/10), Yukon Territory – Northwest Territories. Geological Survey of Canada, Open File 4702, 1 colour map, scale 1:50 000.
- Smith, I.R., 2004 Surficial geology, Tika Creek, Yukon Territory – British Columbia. Geological Survey of Canada, Open File 4702, 1 sheet.

## **MERG REPORTS**

- EBA Engineering Consultants Ltd., 2004. Permafrost Considerations for Effective Mine Site Development in the Yukon Territory. MERG Report 2004-1, 24 p.
- EBA Engineering Consultants Ltd., 2004. Heavy Metals and Acid Rock Drainage: A Select Literature Review of Remediation and Recommendations for Applied Research. MERG Report 2004-2, 22 p.
- Laberge Environmental Services, 2004. Reconnaissance Survey of Erosion Site at Gold Run Creek. MERG Report 2004-3, 6 p.
- Access Consulting Group, 2004. Examination of Natural Attenuation of Metals in Aqueous Solution by Soils in Northern Environments. MERG Report 2004-4, 32 p.

# La Commission géologique du Yukon

*Grant Abbott et Maurice Colpron*  
*Le Service de géologie du Yukon*

Abbott, J.G. et Colpron, M., 2005. La Commission géologique du Yukon. Dans : Yukon Exploration and Geology 2004, D.S. Emond, L.L. Lewis et G.D. Bradshaw (réds.), la Commission géologique du Yukon, p. 57-59.

## APERÇU

La commission géologique du Yukon (CGY; Figure 1, p. 43) en est à sa deuxième année au sein de la Division de la mise en valeur des ressources minérales du ministère de l'Énergie, des Mines et de Ressources. La CGY est gérée conjointement par Grant Abbott et Rod Hill et comprend vingt-quatre employés (Figure 2, p. 44). La commission géologique du Canada (CGC) maintient aussi un bureau à la CGY.

Nous accueillons cette année Steve Israel à titre de géologue de projet et Olwyn Bruce comme gérante des données géologiques spatiales. Nous disons au revoir à Amy Stuart, gérante des données spatiales, Crystal Huscroft, géologue du Quaternaire, et à notre directeur, Jesse Duke. De plus, Craig Hart et Julie Hunt ont présenté leur thèse de doctorat, respectivement à l'Université d'Australie-occidentale (University of Western Australia) et à l'Université James Cook en Australie.

Le financement de la CGY demeure essentiellement au même niveau depuis quelques années. Cette année, en plus de notre financement de base, nous avons obtenu un financement additionnel à court terme du ministère des Affaires indiennes et du Nord canadien par l'entremise des Fonds pour le savoir et l'innovation, et du ministère canadien des Ressources naturelles dans le cadre de l'initiative géoscientifique ciblée.

Cette année, la CGY s'est embarquée dans le troisième d'une série d'exercices de planification quinquennal qui ont guidé les travaux géoscientifiques gouvernementaux au Yukon au cours de la dernière décennie. Les documents résultants des exercices précédants (« Yukon Geoscience – A Blueprint for the Future » en 1995, et « Yukon Geoscience : Looking to the Next Millenium » en 1999) furent à la base de la conception et de l'exécution de projets de cartographies et de recherches qui répondent aux besoins de nos clients dans l'industrie minérale et d'autres groupes tels que ceux préoccupés de la gestion des terres. L'usage et l'efficacité de ces documents est clairement indiquée par le nombre de projets de « haute priorités » complétés depuis leurs publication et par la satisfaction et le support continu de nos clients envers les travaux de la CGY.

Un Comité de liaison technique à la CGY examine nos programmes deux fois par année. Nous remercions le président, Gerry Carlson et les membres du comité Al Doherty, Moira Smith, Jean Pautler, Forest Pearson, Bernie Kreft, Jim Mortensen et Jim Christie pour leur précieux appui et les conseils constructifs qu'ils nous fournissent. Nous accueillons au comité Greg Lynch qui représentera les intérêts du secteur pétrolier. Greg a une longue association avec le Yukon et travaille présentement pour Shell Canada à titre de géologue de projet.

La CGY a la responsabilité « d'accumuler, de gérer et de communiquer la base d'information géoscientifique et technique nécessaire pour la gérance et le développement durable des ressources en énergie, en minéraux et en terres du territoire ». Le soutien à l'industrie minérale reste l'objectif premier de la CGY, mais cette année on a aussi assumée la responsabilité des études géoscientifiques ayant pour but l'évaluation du potentiel pétrolier du territoire. Des ressources sont



aussi consacrées aux études environnementales pertinentes aux industries d'extraction et à l'utilisation des terres. Au cours des dernières années, la demande d'information géoscientifique de la part des organismes de réglementation, des Premières nations, du grand public et des écoles a considérablement augmenté. De plus, les intérêts de l'industrie des ressources sont mieux servis par une prise de décision éclairée et un public bien informé. Le changement le plus important pour la CGY n'est donc pas dans la nature de nos activités, mais plutôt dans la diversité croissante de notre clientèle.

## TRAVAUX SUR LE TERRAIN

La CGY a connu cette année une campagne de travaux sur le terrain mouvementée en raison des conditions extrêmes d'incendies forestiers, mais néanmoins couronnée de succès. Nos travaux furent plus diversifiés en réponse à notre nouveau mandat de soutien à la mise en valeur des hydrocarbures et à la demande accrue pour les données de base à l'appui de la réglementation dans le domaine de l'environnement et de la gestion des terres, tout en continuant nos projets en support de l'industrie minière. Des projets ont été menés en cartographie géologique du substratum rocheux et en géochimie régionale des cours d'eau, en plus des études de gisements minéraux, d'études géologiques détaillées, d'études et de travaux de cartographie de formations superficielles, d'un levé sismique régional et de l'amélioration de plusieurs bases de données.

## CARTOGRAPHIE DU SUBSTRATUM ROCHEUX

Trois projets de cartographie du substratum rocheux ont été complétés dans les régions ci-après : ruisseau Livingstone par Maurice Colpron; lacs Toobally par Lee Pigage; et ruisseau Quill par Steve Israel. Ces régions avaient été choisies pour leur potentiel minéral.

## ÉTUDES DE GISEMENTS MINÉRAUX

Craig Hart et Lara Lewis ont poursuivi leurs travaux sur l'or associé aux roches intrusives, le tungstène et les pierres précieuses. Julie Hunt poursuit ses travaux sur la géologie et le potentiel minéral des brèches de Wernecke. Jim Mortensen de l'université de Colombie-Britannique a étudié en collaboration avec Bill LeBarge (CGY) les caractéristiques des éléments traces des gîtes d'or placériens afin d'identifier des populations distinctes et d'éventuelles sources d'or filonien.

## ÉTUDES DE FORMATIONS SUPERFICIELLES

Parmi les études des formations superficielles, mentionnons les travaux de Bill LeBarge et Mark Nowosad visant à caractériser la granulométrie des gîtes placériens au Yukon à des fins environnementales. Jeff Bond a étudié l'écoulement glaciaire de «haute vallée» pour le «lobe de Cassiar» au Yukon méridional et ses incidences pour l'exploration; il a complété une carte géologique des formations superficielles de la région de Whitehorse et plusieurs études de gîtes placériens. Panya Lipovsky a effectué des travaux de cartographie géologique de formations superficielles pour un projet de cartographie biophysique (ministère de l'Environnement du Yukon) dans le sud-est du Yukon et a travaillé avec Crystal Huscroft à la surveillance des effondrements de terrain liés à la fonte du pergélisol dans le centre du Yukon et à l'étude de leur incidence sur la qualité des cours d'eau à saumons.

## ÉVALUATIONS GÉOCHIMIQUES/MINIÈRES

Notre géologue évaluateur des ressources minérales, Geoff Bradshaw, a principalement travaillé dans le cadre de l'initiative de planification de l'utilisation des terres du nord du Yukon. Afin de préparer une évaluation minérale de la région, il a effectué un levé géochimique régional des cours d'eau en partenariat avec la CGC en plus d'examiner plusieurs indices de minéralisation. Geoff a en outre tenu à l'intention de groupes des Premières nations des présentations sur le potentiel minéral de leurs territoires traditionnels.

## PROJET DU BASSIN DE WHITEHORSE

Le Projet du bassin de Whitehorse fut l'initiative majeure de la CGY cette année; il vise à mieux définir le potentiel en hydrocarbures de ce bassin sous-exploré. Vers la fin l'hiver dernier, un relevé sismiques à l'extrémité nord du bassin fut exécutés par la CGC en partenariat avec la CGY. Des études stratigraphiques et sédimentologiques par Grant Lowey (CGY) et Darrel Long de l'Université Laurentienne, une étude de la chimie des roches ignées par Steve Piercey de l'Université Laurentienne et des études structurales par Amy Tizzard sous la direction de Steven Johnston de l'Université de Victoria constituent d'autres volets de ce projet.

## AUTRES INITIATIVES

Cette année la CGY a reçu un appui financier par l'entremise du fonds de développement économique du ministère des affaires indiennes et du Nord canadien pour la poursuite de la numérisation des rapports d'évaluation – toute la collection comptant plus de 5000 rapports sera convertie au format PDF et accessible par Internet avant la fin de l'année. Nous avons en outre acquis les dossier d'exploration des projets menés au fil des ans dans le district de Faro et à l'extérieur par les diverses sociétés qui en ont été propriétaires (disponibles vers le fin de l'hiver, 2005). Notre base de données géochimiques sur les cours d'eau a été analysée par la société Georeference Online afin d'y repérer des groupements d'anomalies multi-éléments (MineMatch). Les résultats sont maintenant disponibles en ligne.

## DIFFUSION DE L'INFORMATION

La Commission géologique du Yukon (CGY) produit maintenant une gamme complète de publications numériques. Toutes nouvelles cartes et rapports géologiques sont disponibles sur demande en format numérique, et toutes publications récentes sont aussi disponibles (sous format PDF) sans frais sur notre site internet (<http://www.geology.gov.yk.ca>). De plus, une gammes de rapports d'évaluation de propriété minières est maintenant disponible par l'entremise de notre site internet. Nous sommes aussi fier de notre service de carte interactive ('Map Gallery'). Ce service est disponible par l'entremise de notre site internet et permet la visualisation de la géologie régionale, des sites MINFILE, des levés régionaux de géochimie des sédiments de ruisseaux, de la topographie, des routes et des communautés du Yukon, et des sélections des terres des nations autochtones. Les données vectorielles peuvent maintenant être sélectionnées et téléchargées. Certaines des améliorations à venir incluent l'addition de données géophysiques, géochronologiques et paléontologiques. De plus, la couverture des concessions minières sera bientôt disponible.

Les publications de la Commission géologique du Yukon sont diffusées par le Bureau d'information et des ventes en géoscience. Elles sont disponible à l'adresse suivante :

Bureau d'information et des ventes en géosciences  
a/s Conservateur des registres miniers  
le ministère de l'Énergie, des Mines et des Ressources  
le gouvernement du Yukon  
300 rue Main-bur. 102  
C.P. 2703 (K102)  
Whitehorse (Yukon) Y1A 2C6  
Téléphone : (867) 667-5200  
Télécopieur : (867) 667-5150  
Courriel : [geosales@gov.yk.ca](mailto:geosales@gov.yk.ca)

Pour en savoir plus long sur le Commission géologique du Yukon, visitez notre page d'accueil à [www.geology.gov.yk.ca](http://www.geology.gov.yk.ca) ou communiquez directement avec :

Grant Abbott, Géologue principal  
le Commission géologique du Yukon  
300 rue Main-bur. 102  
C.P. 2703 (K102)  
Whitehorse (Yukon) Y1A 2C6  
Téléphone : (867) 667-3200  
Courriel : [grant.abbott@gov.yk.ca](mailto:grant.abbott@gov.yk.ca)

Rod Hill, Gestionnaire  
le Commission géologique du Yukon  
2099-2nd Ave  
C.P. 2703 (K10)  
Whitehorse (Yukon) Y1A 2C6  
Téléphone : (867) 667-5384  
Courriel : [rod.hill@gov.yk.ca](mailto:rod.hill@gov.yk.ca)





# Robert E. Leckie Award for Outstanding Reclamation Practices

*Judy St. Amand<sup>1</sup>*

*Mining Lands, Energy Mines and Resources*

St. Amand, J., 2005. Robert E. Leckie Awards for Outstanding Reclamation Practices. *In: Yukon Exploration and Geology 2004*, D.S. Emond, L.L. Lewis and G.D. Bradshaw (eds.), Yukon Geological Survey, p. 61-63.

The 2004 Robert E. Leckie Award for outstanding reclamation practices for quartz exploration and mining were presented to **NovaGold Resources Inc.** NovaGold is an international company with interests in Yukon, British Columbia and Alaska. Reclamation work at their McQuesten property in the Mayo mining district has been very commendable.

The company began their reclamation in November 2003. They performed most of the required reclamation, leaving a few outstanding issues that could not be addressed in winter. At that time, they surpassed government expectations in some areas.

In September 2004, they returned to complete the decommissioning of the property. They re-assessed the results of the previous work and felt that more could be done. At that time they put in water control bars and regroomed the whole area. Contouring, brush disposal and drag-bag of vegetative mat was undertaken again. Where there was a scarcity of vegetative mat, the company scarified the ground to enable entrapment of water and airborne seed. They also decommissioned the access roads (Fig. 1).

Redistribution of the organic material over access roads contributes largely to the revegetation success of a disturbed site by providing capture areas for moisture, shade for seedlings, and habitat for small animals. The practice also prevents access by small terrain vehicles and snow machines. It is anticipated that the area will be more pristine than when work began.

This company shows a dedication to reclamation that is exemplary. They are good corporate citizens and are very worthy of this award.



**Figure 1.** Reclaimed access road to the McQuesten property.

<sup>1</sup>[judy.stamand@gov.yk.ca](mailto:judy.stamand@gov.yk.ca)

**Figure 2.** Martin Knutson (left) and John Alton (right) of Henry Gulch Placer.

The 2004 Robert E. Leckie Award for outstanding reclamation practices in placer mining was presented to Henry Gulch Placers' **Martin Knutson** and **John Alton** (Fig. 2). They have been mining together for 22 years throughout the Klondike area and have consistently maintained high standards of reclamation.

They moved to Last Chance Creek in July, 2000. This site had been severely disturbed since 1896. White channel gravels had sloughed down to the creek and formed a fan up to 18 m deep in areas. These gravels are a poor host for revegetation. Previous mining on the right limit hillside resulted in a slump into Last Chance Creek. Old drains, still in place, posed a safety hazard. The creek was completely destabilized by the onslaught of all these effects, which then contributed to sedimentation of Hunker Creek.

Massive amounts of White Channel gravels were moved to the left limit to form low-relief rolling hills, and covered with overburden to ensure swift natural revegetation. Old mine pits were reclaimed and stabilized. A pond was built



**Figure 3.** Aerial photo of Henry Gulch property shows reclamation work recently completed on the site.



to catch material from ongoing degradation of old workings above the site, to further protect the creek. The drains have been removed and that area restored. The creek has been stabilized (Fig. 3). A new, safer road system is in place. All areas have been sloped and contoured, and materials conducive to revegetation have been spread. This represents an immense effort to restore old mine works that could not have successfully recovered without the dedication of these two partners. Staff and colleagues can only strive to emulate such a shining example of these community leaders.

Honourable mention was given to **Newmont Exploration of Canada Ltd.** In the fall of 2001 this company completed extensive reclamation of trenches on the Aurex property in the Mayo mining district.

Trenches were backfilled and contoured, and a drag-back technique was used to replace the vegetative mat (Fig. 4). This gave the area a consistent and rough finish of soil, scattered brush and trees, which had been removed at the time of excavation. Redistribution of the organic material over recontoured trenches contributes largely to the revegetation success of a disturbed site.

Newmont Exploration of Canada Ltd. is commended for excellent reclamation in an area of ongoing exploration.



**Figure 4.** Road reclaimed on the Aurex property using dragback technique, which prohibits access by snowmachines, ATVs and other off-road vehicles.





## GEOLOGICAL FIELDWORK

<i>Late Wisconsinan McConnell ice-flow and sediment distribution patterns in the Pelly Mountains, Yukon</i> J.D. Bond and K.E. Kennedy .....	67
<i>Quaternary, structural and engineering geology of the Aishihik River landslide, Cracker Creek area (NTS 115A/15), Yukon</i> M-A. Brideau, D. Stead, C. Huscroft and K. Fecova.....	83
<i>Preliminary investigation of the bedrock geology of the Livingstone Creek area (NTS 105E/8), south-central Yukon</i> M. Colpron .....	95
<i>Flood basalts of the Wrangellia Terrane, southwest Yukon: Implications for the formation of oceanic plateaus, continental crust and Ni-Cu-PGE mineralization</i> A.R. Greene, J.S. Scoates, D. Weis and S. Israel.....	109
<i>Lead isotope signatures of Tintina Gold Province intrusions and associated mineral deposits from southeastern Yukon and southwestern Northwest Territories: Implications for exploration in the southeastern Tintina Gold Province</i> R.S. Heffernan, J.K. Mortensen, J.E. Gabites and V. Sterenberg.....	121
<i>Preliminary geology of the Quill Creek map area, southwest Yukon parts of NTS 115C/5, 6 and 12</i> S. Israel and D.P. Van Zeyl .....	129
<i>Character and metallogeny of Permian, Jurassic and Cretaceous plutons in the southern Yukon-Tanana Terrane</i> T. Liverton, J.K. Mortensen and C.F. Roots .....	147
<i>Sedimentology and hydrocarbon potential of fluvial strata in the Tantalus and Aksala formations, northern Whitehorse Trough, Yukon</i> D.G.F. Long .....	167
<i>Sedimentology, stratigraphy and source rock potential of the Richthofen formation (Jurassic), northern Whitehorse Trough, Yukon</i> G.W. Lowey.....	177
<i>Landslide processes in discontinuous permafrost, Little Salmon Lake (NTS 105L/1 and 2), south-central Yukon</i> R.R. Lyle, D.J. Hutchinson and Y. Preston.....	193
<i>Application of placer and lode gold geochemistry to gold exploration in western Yukon</i> J.K. Mortensen, R. Chapman, W. LeBarge and L. Jackson .....	205
<i>Reconnaissance geological and geochemical studies of the Joe Mountain Formation, Joe Mountain region (NTS 105D/15), Yukon</i> S.J. Piercey .....	213
<i>The isotopic sulphur composition of two barite samples from Rose Mountain area near Faro, Yukon</i> L.C. Pigage.....	227
<i>Structural evolution of the Tally Ho shear zone (NTS 105D), southern Yukon</i> A. Tizzard and S. Johnston .....	237
<i>Case study of Donjek debris flow, southwest Yukon</i> D.P. Van Zeyl and J.G. Cogley .....	247





# Late Wisconsinan McConnell ice-flow and sediment distribution patterns in the Pelly Mountains, Yukon

*Jeffrey D. Bond<sup>1</sup> and Kristen E. Kennedy*  
*Yukon Geological Survey*

Bond, J.D. and Kennedy, K.E., 2005. Late Wisconsinan McConnell ice-flow and sediment distribution patterns in the Pelly Mountains, Yukon. *In: Yukon Exploration and Geology 2004*, D.S. Emond, L.L. Lewis and G.D. Bradshaw (eds.), Yukon Geological Survey, p. 67-82.

## ABSTRACT

Late Wisconsinan McConnell glaciation (ca. 24-11 ka) occurred in four phases in the Pelly Mountains of southern Yukon. Phase 1 marked the onset of ice accumulation in cirques above 1524 m above sea level (a.s.l.). These local glaciers expanded and fed valley glaciers that extended into the surrounding lowlands (after 26.3 ka). At glacial maximum or phase 2, the development of ice-divides to the east and south of the Pelly Mountains permitted Cordilleran ice lobes to invade the lesser glaciated Pelly Mountains, which resulted in up-valley ice-flow. This ice-flow arrangement continued into early deglaciation (phase 3), a period characterized by re-advances of the invading ice lobes. Following retreat of the ice lobes from the Pelly Mountains, some local cirque glaciers above 1600 m a.s.l. resumed limited down-valley flow (phase 4).

For drift prospecting purposes, the dominant glacial dispersion trajectory in these high relief areas is controlled by the last phases of ice-flow (either phase 3 or 4).

## RÉSUMÉ

La glaciation McConnell du Wisconsinien tardif (de 24 à 11 ka environ) s'est déroulée en quatre phases dans les monts Pelly, au sud du Yukon. La phase 1 correspond au début de l'accumulation de glace dans les cirques situés à plus de 1524 m d'altitude. Ces glaciers locaux ont pris de l'expansion et ont alimenté des glaciers de vallée qui s'étendaient au-delà du front des montagnes dans les basses terres avoisinantes (après 26,3 ka). Au maximum glaciaire, soit la phase 2, l'apparition de lignes de partage glaciaire à l'est et au sud des monts Pelly a permis à des lobes glaciaires de la Cordillère d'envahir les monts Pelly, moins englacés, ce qui a causé de l'écoulement glaciaire vers l'amont des vallées. Cette configuration de l'écoulement glaciaire s'est poursuivie jusqu'au début de la déglaciation (phase 3), période caractérisée par de nouvelles avancées des lobes glaciaires envahissants. Après le recul des lobes glaciaires dans les monts Pelly, certains glaciers locaux à plus de 1600 m se sont remis à s'écouler, de façon limitée, vers l'aval des vallées (phase 4).

Aux fins de la prospection glacio-sédimentaire, il faut savoir que, dans ces régions de relief élevé, la trajectoire dominante de dispersion glaciaire semble dépendre de la dernière phase d'écoulement glaciaire (phase 3 ou 4).

<sup>1</sup>jeff.bond@gov.yk.ca

## INTRODUCTION

Predictive models of glacial dispersion and paleo-ice dynamics are an important component of mineral exploration in glaciated terrain. Exploration programs that utilize soil geochemistry and boulder tracing benefit from a comprehensive understanding of ice sheet models and the interplay between distinct ice accumulations throughout the many phases of a glaciation. Furthermore, empirical evidence regarding the nature of subglacial processes cannot be undervalued. Glacial erosion, transport and deposition are reflected in the clastic sedimentology of Quaternary sediments and sedimentary successions. A detailed understanding of the complexities of these processes is beneficial for the effective application of drift prospecting techniques.

Mineral exploration in the Seagull Creek drainage of the Pelly Mountains (Fig. 1) provides a good example of the challenges that are faced while drift prospecting in mountainous terrain. Since the 1980s, prospecting for a lode source for gold-bearing float boulders in Seagull Creek has been hindered by thick glacial deposits in the valley bottom. In 2003, Kennedy and Bond (2004) indicated that the last phase of ice movement in Seagull Creek was up-valley. This realization had important ramifications for the interpretation of previously collected geochemical and geophysical data from Seagull Creek. The glacial history of Seagull Creek is consistent with findings in the Lapie River drainage to the north where Plouffe (1989), and Plouffe and Jackson (1992) provided evidence for late glacial up-valley ice movement by the Selwyn Lobe of the Cordilleran ice sheet. This was restated in a broader context by Jackson and MacKay (1991) who suggested that ice-flow in some mountainous areas of southern Yukon could have been in the opposite direction to that of the modern drainage. These ice-flow complexities, and their potential implications to mineral exploration, provide the impetus for developing a clearer understanding of the glacial history, particularly processes of glacial erosion, transport and deposition, within the Pelly Mountains. In 2004, a study was initiated to further understand the late Wisconsinan McConnell glacial history within the Pelly Mountains. Results from this work are presented in this paper and have direct implications for drift prospecting in previously glaciated regions of Yukon and in other areas of the Cordillera where ice-flow reversals may have occurred.

## PHYSIOGRAPHY, DRAINAGE AND BEDROCK GEOLOGY

The Pelly Mountains are located in south-central Yukon and form a physiographic divide between the Pelly River drainage to the north and the Nisutlin, Big Salmon and Liard river basins to the south (Fig. 1). Summits within the highland reach elevations of 2404 m (7887 ft). Narrow, steep-sided valleys characterize drainages flowing north out of the Pelly Mountains, whereas main valleys draining to the south have a broader character. The area investigated for this study included the central part of the Pelly Mountains (Fig. 1).

### REGIONAL BEDROCK GEOLOGY

The geology of the Pelly Mountains includes rocks of Yukon-Tanana Terrane in the northwest, rocks of the Cassiar Platform through the central part of the range and displaced Yukon-Tanana Terrane rocks in the southeast. The Tintina Fault forms an important geological boundary between rocks of Cassiar Platform and those of the Yukon-Tanana Terrane. The study area is mostly underlain by rocks of the Cassiar Platform, which consist of a thick succession of Cambrian through Mississippian limestone and sandstone that represent one billion years of sediment accumulation off the margin of ancient North America (Tolbert, 2000; Gordey and Makepeace, 2003). The platform has since been folded and faulted into the 70-km-wide and 600-km-long massif of the Pelly Mountains. This assemblage of sedimentary rocks was intruded by granitic rocks in the Cretaceous.

### REGIONAL QUATERNARY GEOLOGY

Yukon has been glaciated numerous times since the late Pliocene (Froese et al., 2000; Duk-Rodkin and Barendregt, 1997; Duk-Rodkin et al., 2001; Jackson et al., 1991). Centres of ice accumulation included: the St. Elias, interior Coast and Cassiar mountains in southern Yukon; the Pelly and Selwyn mountains in eastern Yukon; and the Ogilvie and Wernecke mountains in central Yukon. Ice from each of these accumulation zones flowed radially outward into lowland areas. Thickening ice masses on the landscape developed into separate ice lobes that eventually merged to form a continuous carapace of ice across southern and eastern Yukon (Fig 2; Jackson et al. 1991). This ice mass formed the northern extent of the Cordilleran ice sheet (Fulton, 1991). The limited ice extent in central Yukon is likely to be a function of aridity (Armentrout, 1983; Ward and Jackson, 1992).



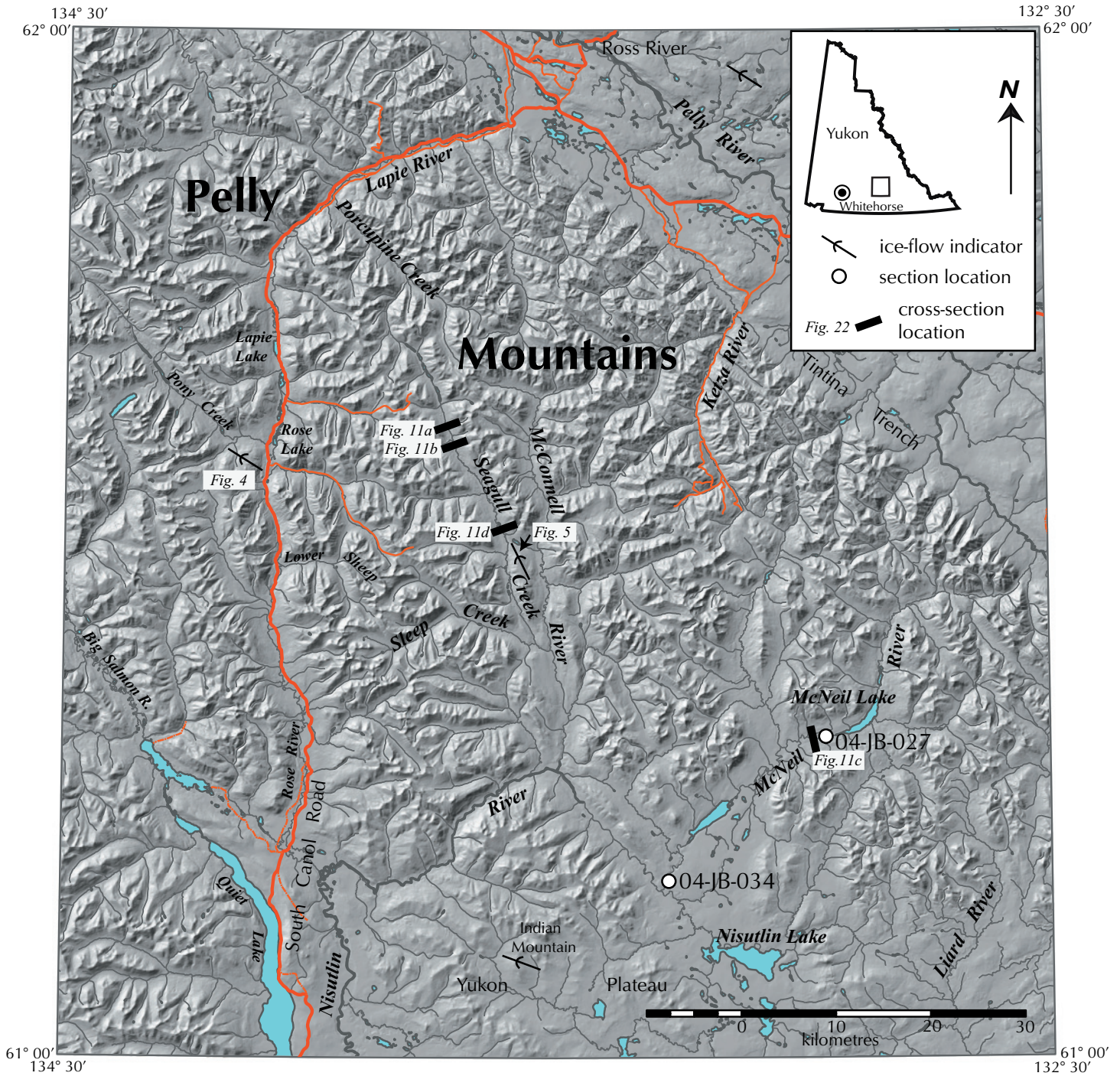
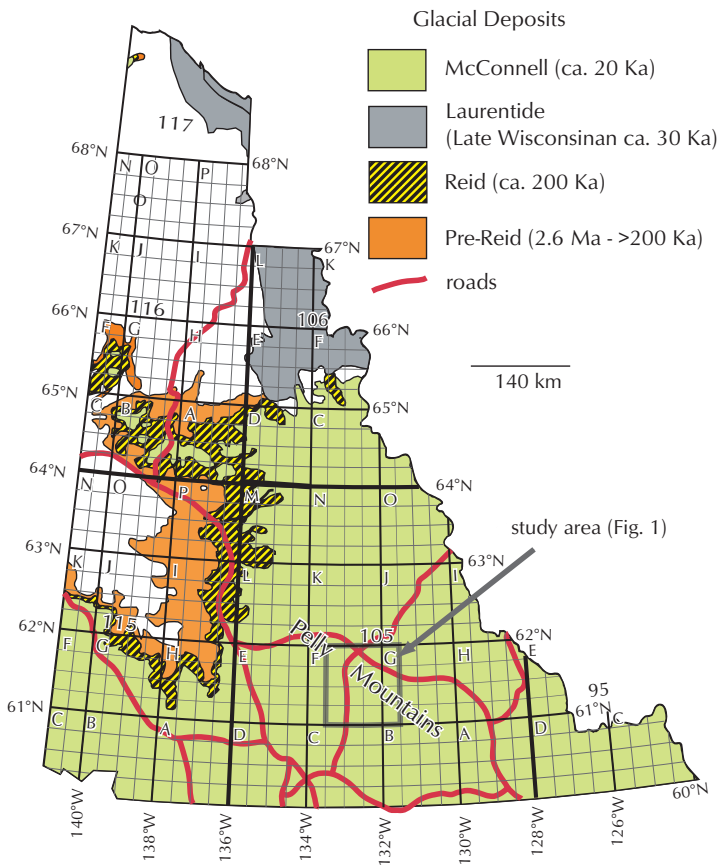


Figure 1. Location map of the study area within the Pelly Mountains.





**Figure 2.** Glacial limits map of Yukon (after Duk-Rodkin, 1999).

The current study area lies entirely within the late Wisconsinan McConnell glacial limit (Fig. 2). There is little evidence of prior glacial or interglacial deposits in this area. Where pre-McConnell organic material has been identified, pollen assemblages suggest that a cooler climate was associated with the onset of glaciation approximately 29 600 years BP (Matthews et al., 1990). In the Tintina Trench, at the foot of the Pelly Mountains, bone-bearing gravel beneath McConnell till was dated at  $26\,350 \pm 280$  BP, suggesting ice had not yet expanded out of the Pelly Mountains by this date (Jackson and Harington, 1991). Similarly, McConnell glaciers had not yet inundated the Watson Lake area in southeast Yukon by  $23\,900 \pm 1140$  BP (GSC-2811; Klassen, 1987). The retreat of ice from glacial maximum had begun by  $13\,660 \pm 180$  BP (GSC-1110) according to a radiocarbon age near the terminus of the St. Elias Mountains piedmont lobe complex (Rampton, 1971). A radiocarbon age of 10 700 BP from macrofossils in Marcella Lake (Kettlehole Pond), southern Yukon, suggests ice-free conditions by this date (Anderson et al., 2002).

## RESULTS

### GEOMORPHOLOGY

The identification of landforms used to reconstruct ice-flow during the last glaciation in the study area was completed using existing surficial geology maps (Jackson, 1993a,b,c,d) and new air photo interpretation. Landforms such as ice marginal melt-water channels, kame terraces and moraines were used to reconstruct ice-flow patterns and the style of ice retreat (Fig. 3). Four distinct phases of the McConnell glaciation were recognized in the Pelly Mountains (discussed later), although not all phases of the glaciation are well represented in the landform record. In many cases, later stages of a glaciation are preferentially preserved, which provides important information about late-stage ice-flow, but little about earlier ice-flow phases such as glacial maximum and the onset of glaciation. The reconstruction of glacial maximum depended on the identification of high-elevation landforms such as crag-and-tail features.

#### *Glacial landforms above 1524 m (5000 ft) above sea level*

Glacially streamlined crag-and-tail landforms occur near the summit of a 1524-m a.s.l. plateau west of Rose Lake, near the drainage divide within the Pelly Mountains (Fig. 4). The orientation ( $302^\circ$  trend) and morphology of these bedforms suggests ice was moving northwest, an orientation nearly perpendicular to the Rose River valley (Fig. 1). Meltwater channels mapped by Jackson (1993a)

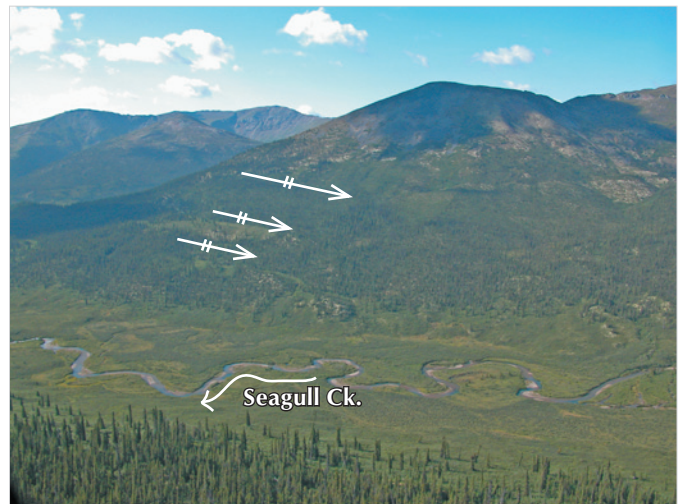


**Figure 3.** Flights of meltwater channels descending up the Seagull Creek valley (arrows) indicate a former ice front retreating down-valley. View is to the southwest. Seagull Creek flows to the left.

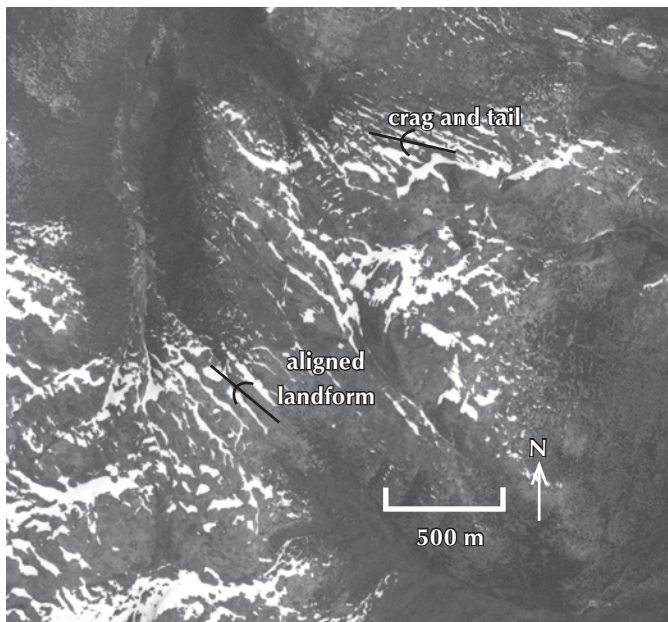


**Figure 4.** Crag-and-tail landforms near Rose Lake at 5200 ft (1524 m). The ice direction that created these landforms was to the northwest.

spill over this plateau and indicate that during early deglaciation, ice was thicker on the south side of the plateau than the north. This supports a northwest-flowing ice mass at or near glacial maximum within the western part of the study area.

Meltwater channels breaching passes above 1524 m between the Seagull Creek and Rose River valleys have paleo-flow trajectories toward the west, suggesting ice was thicker to the east. Likewise, between Seagull and Porcupine creeks, meltwater flow at high elevations was to the north.

Further east, similar meltwater channel orientations were observed. At the headwaters of a south-flowing tributary to the McNeil River, lateral meltwater channels at 1600 m elevation breach a pass and extend north into the Ketza River.

#### *Glacial landforms below 1524 m (5000 ft) a.s.l.*

Many depositional and erosional landforms within the Pelly Mountains are remnant from the latest period of the McConnell deglaciation, when ice was thinner and dominantly confined to local valleys. Morainal landforms and associated lateral meltwater channels are plentiful and well preserved. Deposits from local alpine glacial activity are also present.

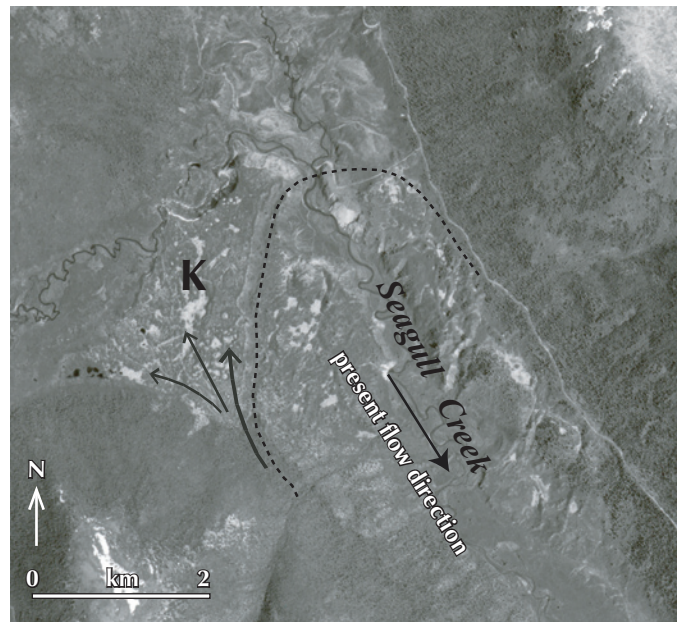


**Figure 5.** A kame terrace (K) and moraine (dashed line) mark a recessional position of the Cassiar lobe that flowed up Seagull Creek. Seagull Creek is presently flowing south-southeast.

Seagull Creek valley provides an example of remnant landforms preserved at these elevations. Multiple moraine complexes and erosional meltwater channels are present (Fig. 3). In the upper reaches of the drainage, a kame terrace and moraine complex clearly reflect a former ice front from an up-valley-flowing glacier (Kennedy and Bond, 2004; Fig. 5). Up-valley-trending moraines and meltwater channels were also documented in other valleys within the study area, and include extensive moraine deposits near Rose and Lapie lakes (Fig. 6) and at the headwaters of the McNeil River.

Glaciolacustrine deposits are widespread in many of the upper valleys of the study area. Drainage outlets for these lakes were northward and often dissected the moraine complexes mentioned above. The thickness and distribution of glacial lake sediment is variable and likely depends on how long the lake existed and the height of its outlet. For example, in upper Seagull Creek, glaciolacustrine sediments are <1 m thick and extend to 60 m above the valley bottom, whereas in the neighbouring upper McConnell River valley, glaciolacustrine sediments are 10 to 20 m thick and blanket slopes 90 m above the valley bottom (Kennedy and Bond, 2004; Jackson, 1993c).

Locally derived down-valley-trending moraines were observed in many cirques within the study area. The



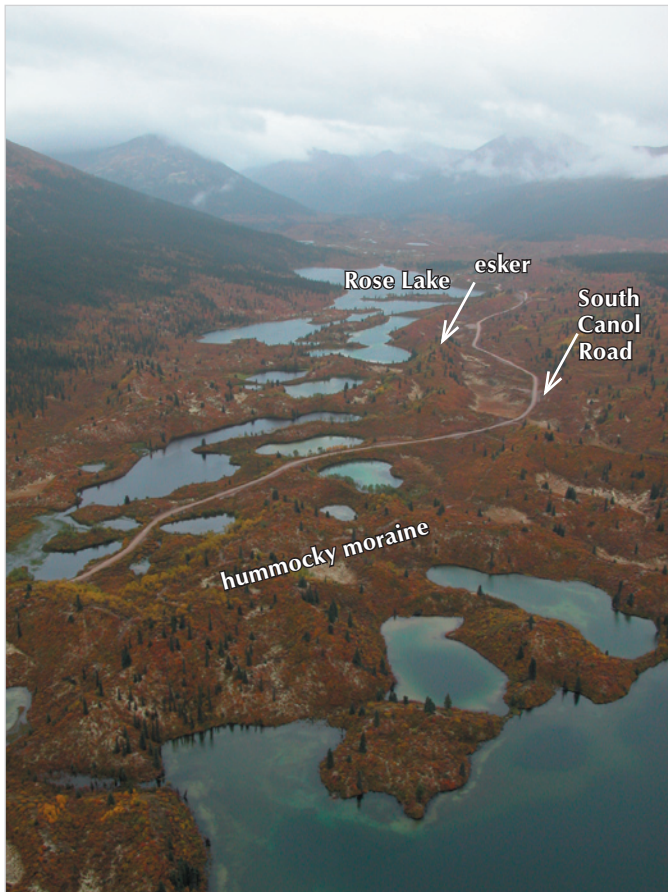


**Figure 6.** Hummocky moraine near Rose Lake shows typical ablation sediment accumulations found at drainage divides in the study area. View is to the south.

distance of these moraines from their source accumulation area is commonly limited to 1 to 2 km. The exception to this is Sleep Creek, a large east-trending tributary to lower Seagull Creek and the McConnell River. Local moraine and till from Sleep Creek are found in the McConnell River valley, approximately 20 km from its headwaters.

## QUATERNARY STRATIGRAPHY

Quaternary stratigraphic observations were used to advance our understanding of the sequence of ice-flow patterns representing various phases of glaciation. Likewise, the sub-glacial processes associated with each glacial phase were identified and characterized. Ultimately, these data were used to develop a model for glacial dispersion in the mountain valleys.

Information such as texture, colour, cohesion, structure, till fabric, till geochemistry and pebble lithology were collected at natural exposures. Till fabric analyses were based on the measurement of 50 clasts ( $n$  = number of clasts) using the long-axis of elongated pebbles to determine orientation and dip. Fabric results also list the mean orientation from the population of measured clasts (V1) and the statistical significance or reliability of the data (S1). Statistical significance was measured between 0 and 1, where 1 corresponds to perfectly aligned data and 0 corresponds to perfectly random data. Fabric data with significance values of less than 0.5 were considered unreliable as indicators of flow direction.

Till geochemistry and pebble lithology samples were collected from the clastic units in order to characterize source areas. An initial assessment of this data set indicated that no unique clast lithologies or geochemical fingerprints were present to assist in characterizing the respective glacial units. This result may be due to the uniformity of the underlying bedrock in the study area. Further analysis of these data sets are required.

The term diamict is used widely in the sedimentology descriptions. It is used as a non-genetic descriptive term for any poorly-sorted gravel-sand-mud mixture. For example, a till is a diamict with a glacial origin, whereas a colluvium can also be a diamict but is derived from slope-related processes.

Exposed glacial sediments studied in the Pelly Mountains were deposited during the late Wisconsinan McConnell glaciation. Where multiple tills were identified, there was no conclusive evidence, in the form of paleosols or organic material from previous interglacials for example, that suggested pre-McConnell deposits were present. Erosion and reworking of non-glacial and older glacial deposits during the McConnell glaciation, however, cannot be ruled out.

Quaternary sections that depict the glacial history and stratigraphy of the study area are presented below and illustrated in Figures 7a and 7b. Figure 1 shows the locations of the sections.

### 04-JB-027

This section is situated on the McNeil River immediately downstream from McNeil Lake (Fig. 1) and is illustrated in Figure 7a. The 27-m exposure contains outwash gravel at the base of the section overlain by multiple till units, which are in turn capped by a thin glaciolacustrine deposit.



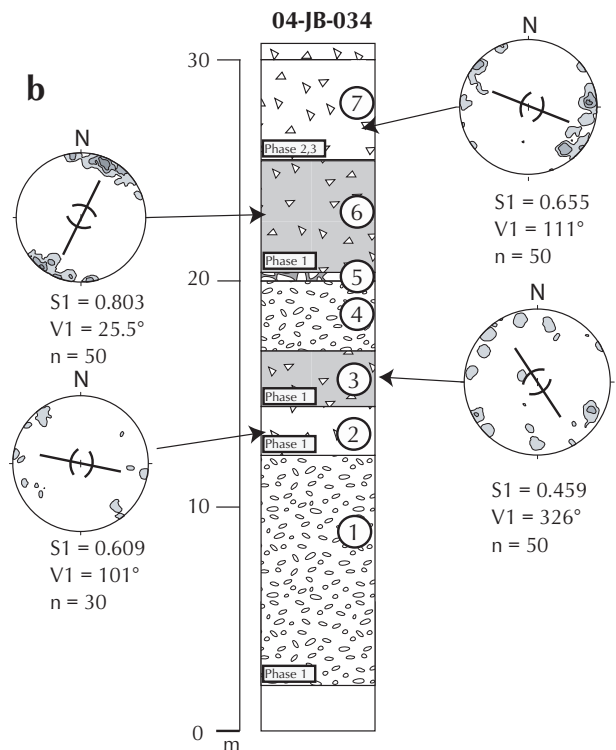
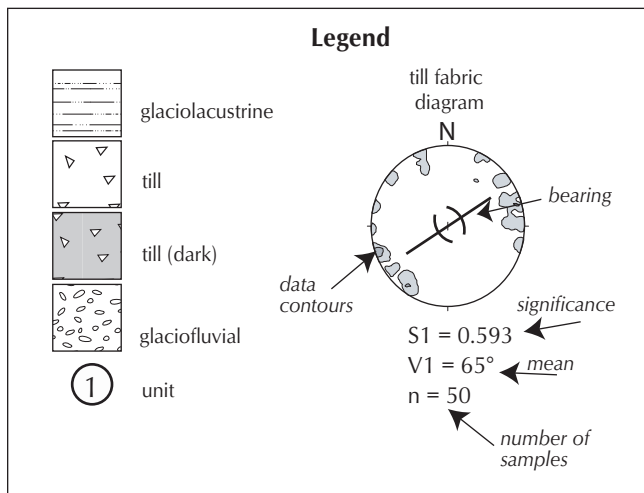
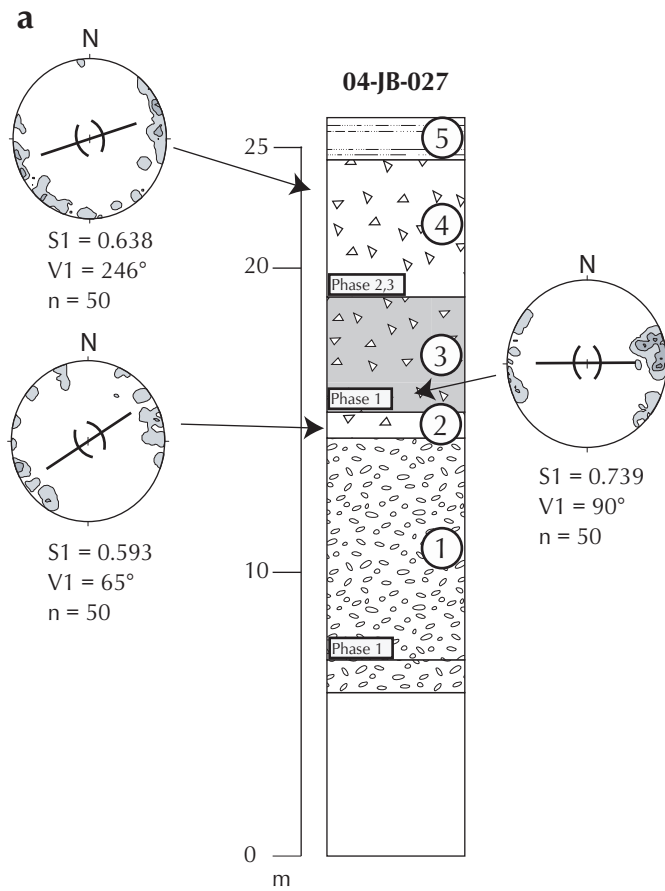


**Figure 7. (a)** Stratigraphic section 04-JB-027 consists of stacked glacial deposits. The exposure is located west of McNeil Lake along the McNeil River. **(b)** Stratigraphic section 04-JB-034 on the lower McNeil River near its junction with the Nisutlin River. A similar stratigraphy to 04-JB-027 is recorded at this site.

**Unit 1** is outwash gravel that has a paleo-flow structure concurrent with the modern McNeil River. Importantly, the unit coarsens upward from a well-sorted pebble gravel into a boulder-dominated gravel at the contact with unit 2 till. Unit 1 is interpreted as advance outwash gravel originating from Pelly Mountain glaciers.

**Units 2, 3 and 4** consist of a series of stacked diamicts (Fig. 7a). Unit 2 is a coarse-textured, cemented diamict in gradational contact with unit 1. Based on this relationship, unit 2 is interpreted to be till derived from a local glacier that advanced down-valley. The southwest-trending pebble fabric suggests that unit 2 was sourced from the upper McNeil River. The contact between units 2 and 3 is gradational. Unit 3 is a cohesive, matrix-dominated dark grey diamict. It contains many polished, striated and faceted clasts and has a well-defined fabric that is oriented east-west ( $90^\circ$ ). On this basis, it is interpreted to be a lodgement till. Its fabric parallels a nearby tributary valley entering the McNeil River, suggesting that unit 3 may have originated from west-trending ice-flow (Fig. 1). Unit 4 is a cohesive olive-grey diamict that weathers beige (Fig. 7a). The mean orientation of the clast fabric within this unit is  $246^\circ$ . It is also interpreted to be till because of its well-aligned fabric ( $S1=0.638$ ; Fig. 7a). It is capped by a laminated silty-clay deposit containing drop-stones, which is interpreted to be a glaciolacustrine unit (unit 5) that formed in a lake proximal to the ice front following deposition of unit 4 and recession of ice from the immediate area. Unit 4, the upper-most ice-deposited unit, can also be correlated with up-valley-trending meltwater channels within the valley. The presence of the glaciolacustrine silt and the meltwater channels in this part of the McNeil River drainage suggest that unit 4 is derived from an up-valley-flowing glacier.

#### 04-JB-034

This section is located on the lower McNeil River, 1 km above its confluence with the Nisutlin River and is illustrated in Figure 7b. The 31.5-m exposure consists of a stacked sequence of glacial outwash and till and is similar to section 04-JB-027.

**Unit 1** is poorly stratified, coarse gravel with diamict lenses. Boulders within this unit are angular and locally derived. It is interpreted as an ice proximal proglacial outwash. No paleo-flow measurements were taken from this unit.

**Unit 2** is a cohesive, clast-rich diamict in gradational contact with Unit 1. Clast fabric within this unit has a well-

aligned orientation of  $101^\circ$  (Fig. 7b). This unit's proximity to the underlying outwash and its clast fabric suggest that it is a till originating from a local glacier flowing out of the Pelly Mountains from the northwest.

**Unit 3** is a cohesive, matrix-supported, dark grey diamict. Smearing and reworking of unit 2 into unit 3 in a southward trajectory suggests that the contact between units 2 and 3 is erosional. The clast fabric from unit 3 has no well defined orientation (Fig. 7b); however, the presence of southward-oriented erosional smearing suggests that it was deposited from a glacier originating in the Pelly Mountains. A well-sorted sandy gravel unit (unit 4) and a discontinuous, stony diamict to muddy cobble gravel unit (unit 5) overlie unit 3. The coarse texture and muddy matrix of unit 5 is indicative of a debris-flow deposit and/or a high-energy muddy stream. Based on this reconstruction, units 4 and 5 were likely deposited in an ice proximal environment.

**Unit 6** is a compact and cohesive diamict containing well-polished, striated and faceted clasts. The clast fabric within this unit is strongly aligned parallel to the McNeil River valley ( $205.5^\circ$ ; Fig. 7b). It is interpreted as a lodgement till that was deposited by a glacier flowing out of the McNeil River valley.

**Unit 7** is a compact, matrix-supported diamict that is also interpreted as a lodgement till based on a well-aligned clast fabric ( $291^\circ$ ; Fig. 7b). The source of this upper-most ice-flow deposit is perhaps best shown by the orientation of glacially streamlined crag-and-tail landforms on top of Indian Mountain (located 13 km to the southwest of this section; Fig. 1) that trend at  $290^\circ$  and were created by ice flowing to the northwest into the Pelly Mountains. Unit 7 is interpreted to be correlative with these surficial features based on its stratigraphic position. This unit is capped by non-cohesive gravel-rich ablation sediment that extends to the top of the section.

## DISCUSSION

### MCCONNELL GLACIAL HISTORY

The late Wisconsinan McConnell glacial history of the Pelly Mountains can be separated into four phases based on changes in regional ice-flow direction and ice dynamics.

*McConnell advance: Phase 1*

Initial ice-flow within the Pelly Mountains is from the accumulation and advance of local valley glaciers (Fig. 8a) out of the mountains and into neighbouring lowlands such as the Tintina Trench and the upper Nisutlin River area. On the north side of the Pelly Mountains, local ice from the Lapie River flowed eastward into Tintina Trench prior to the arrival of the Selwyn lobe of the Cordilleran ice sheet (Plouffe, 1989; Fig. 8a). The timing of this advance into Tintina Trench post-dates 26.3 ka (Jackson and Harington, 1991). Likewise, stratigraphy in sections 04-JB-027 and 04-JB-034 on the south side of the mountains suggests that local ice advanced down the McNeil and McConnell rivers after an initial phase of glaciofluvial deposition (Figs. 7a and 7b). The clast fabric and structural data suggests that the lower tills deposited at these sections originated locally from Pelly Mountain glaciers. Deposition of multiple till units in this period could be controlled by the physiography, given that multiple valleys converge on a similar location. This would funnel glaciers into the area at slightly different times and allow for till stacking to occur. In addition, glaciofluvial deposits separating units 3 and 6 at section 04-JB-034 suggest that these valley glaciers may have advanced, retreated slightly and re-advanced at the mountain front during this time (Fig. 7b).

The details of the phase 1 ice-flow and the extent of ice originating from individual cirques cannot be clearly defined, and is therefore assumed to largely resemble the current fluvial drainage.

*McConnell glacial maximum: Phase 2*

At the height of the McConnell glaciation, ice-flow in the Pelly Mountains was controlled by ice-divides associated with the Selwyn and Cassiar lobes of the Cordilleran ice sheet (Fig. 8b). Local ice accumulations within the Pelly Mountains remained sufficiently thin to permit Cordilleran ice to advance into the mountains from the south (Cassiar lobe) and east (Selwyn lobe). By glacial maximum, the massif was largely overridden and incorporated into the neighbouring ice lobes. Cordilleran ice within the Pelly Mountains reached a minimum elevation of 1676 m (5500 ft) and was >600 m thick. High-elevation landforms within the McConnell and McNeil river drainages suggest ice-flow was directed by underlying topography. In contrast, west of the Rose River valley, ice-flow had less topographic control (Fig. 8b). Topographically uncontrolled ice-flow was likely restricted to the southern parts of the Pelly Mountains where the Cassiar lobe was

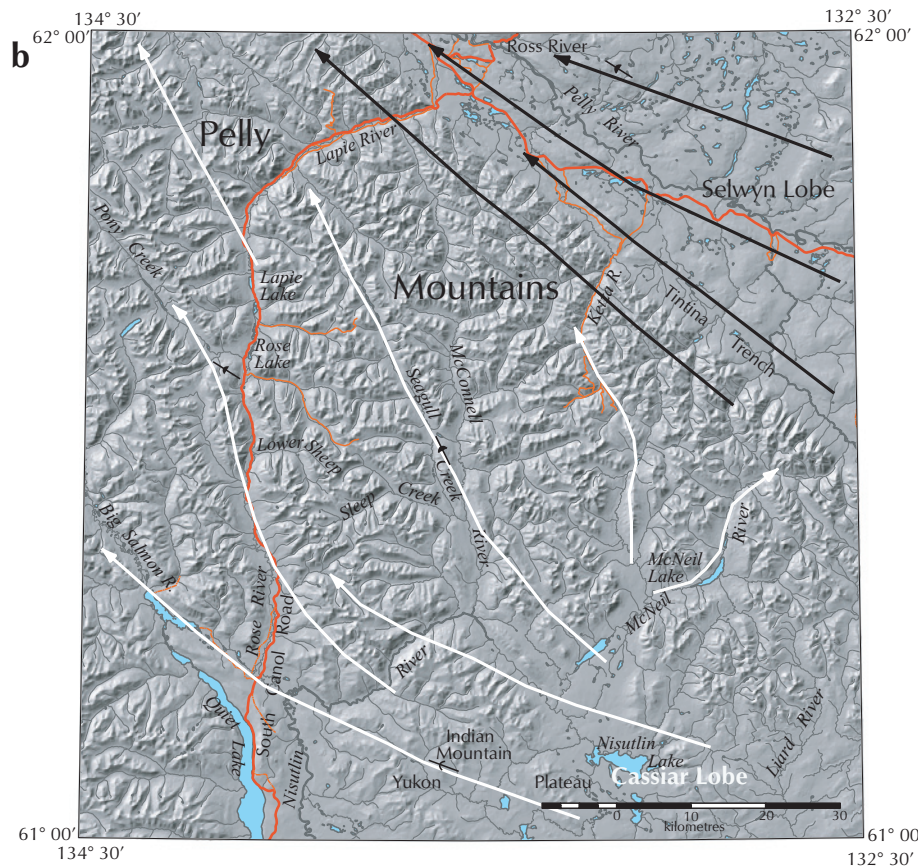
thicker. Further northwest, the ice sheet thinned and became valley controlled. Selwyn lobe ice-flow along the northeastern margin of the Pelly Mountains extended above the mountain summits adjacent to the Tintina Trench and flowed to the northwest. The orientation of high-elevation meltwater channels in this area suggests ice flowed perpendicular to the valleys entering Tintina Trench during glacial maximum (Fig. 8b).

*McConnell early deglaciation: Phase 3*

Well-defined, up-valley-trending moraine and meltwater channels identified in upper Seagull Creek suggest that retreat of the Cassiar lobe from the southern Pelly Mountains was punctuated by re-advances and prolonged recessional pauses (Fig. 8c). Similar extensive hummocky moraine accumulations were observed at drainage divides of many of the main valleys draining south out of the study area. Whether or not these landforms are chronologically correlative is uncertain; however, it does imply that ice in each of the valleys was influenced by similar climate fluctuations and ice responses. It also suggests a relative lack of local ice in the Pelly Mountains at this time. Glaciation of the Glenlyon Range to the northwest at glacial maximum could be an analogue for the Pelly Mountains in early deglaciation (Ward and Jackson, 1992). Local cirque glaciers in the Glenlyon Range advanced <3 km at glacial maximum and in most areas did not converge with the Selwyn Lobe that invaded the upland. Aridity likely played an important role in limiting the extent of local cirque glaciers (Ward and Jackson, 1992).

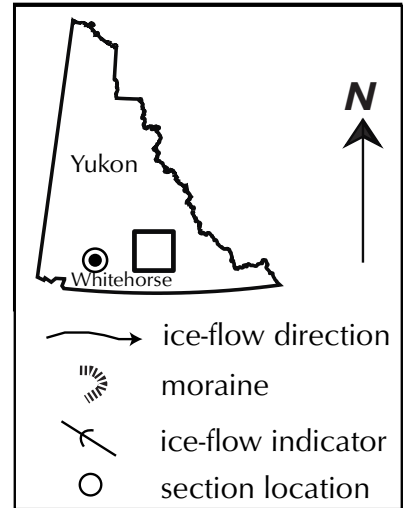
The cumulative evidence from the Pelly Mountains suggests that the Selwyn and Cassiar lobes responded to similar climatic shifts during deglaciation (Plouffe, 1989; Kennedy and Bond, 2004). Likewise, comparable deglacial characteristics are documented for paleo-glaciers in the Logan Mountains to the east (Dyke, 1990), in the Whitehorse map area to the west (Bond, 2004) and the Anvil District to the north (Bond, 1999). This evidence suggests that frontal retreat was the dominant recessional process, which contradicts Jackson's (1994) proposal for wholesale stagnation of the Selwyn Lobe at the end of the last glaciation. Jackson did recognize, however, that uniform stagnation could not explain the glacial lake that existed in the Lapie River valley. To account for this, he concurred with Plouffe (1989) and suggested that the Selwyn lobe re-advanced into the mountains. This growing body of evidence from southern Yukon suggests that deglaciation was an active period of ice-flow





**Figure 8.** Phases of the McConnell glaciation in the Pelly Mountains.

(a) Phase 1: glacial onset characterized by local ice-flow;  
 (b) Phase 2: glacial maximum ice-flow reconstruction, where flow originates from the Cassiar and Selwyn lobes of the Cordilleran ice sheet.





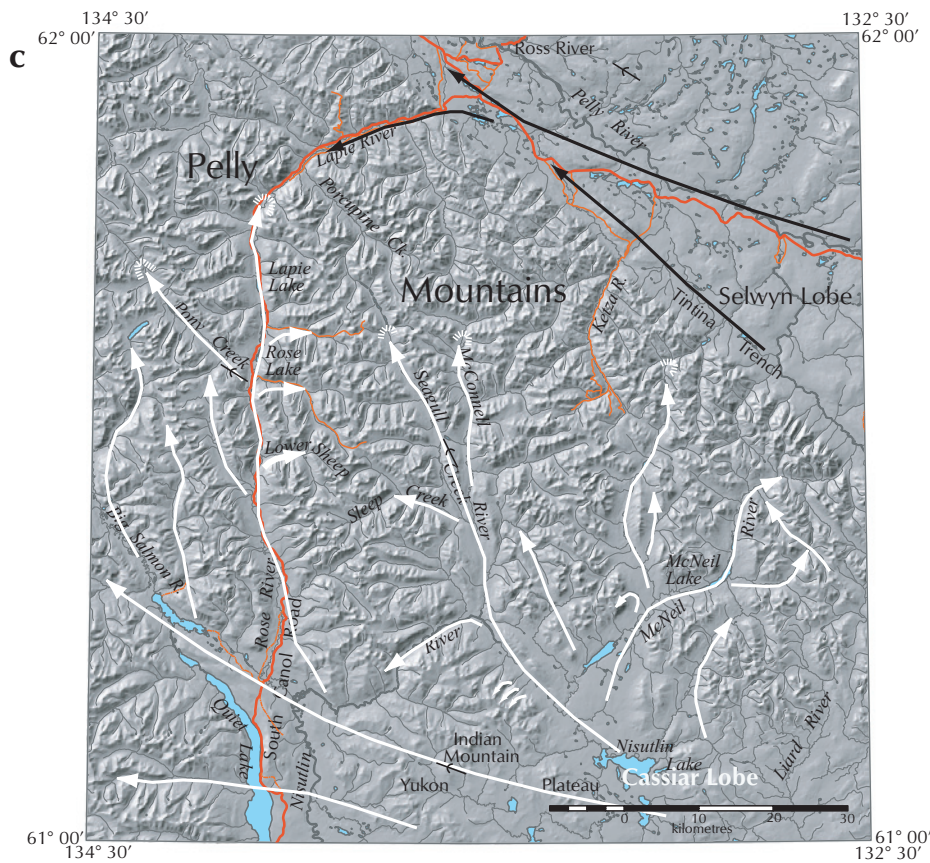


**Figure 8.** (continued) Phases of the McConnell glaciation in the Pelly Mountains. **(c)** Phase 3: early deglaciation characterized by the retreat and periodic re-advance of Cordilleran ice; **(d)** Phase 4: Late McConnell to early Holocene re-advance of local cirque glaciers.



characterized by a combination of frontal retreat, dynamic equilibrium or recessional stand-stills, and re-advances. In terms of climate reconstructions, this evidence shows that deglaciation continued to be interrupted by periods of renewed precipitation and/or cooler temperatures.

#### *McConnell late deglaciation: Phase 4*

A re-activation of local glaciers at the highest elevations was the final phase of glacial activity in the Pelly Mountains (Fig. 8d). The timing of this re-advance relative to the retreating Cordilleran ice sheet is uncertain. Evidence from Sleep Creek shows that ice flowed freely into the McConnell River valley, which suggests the northern margin of the Cordilleran ice sheet was at least as far south as the Sleep Creek outlet. The extent of this local re-advance was limited to <5 km in most drainages with the exception of Sleep Creek where glaciers advanced over 20 km (Fig. 8d). This may have been due to a lingering ice cap that spanned the drainage divide between Sleep Creek and lower Sheep Creek. The cirques associated with these known moraines typically exceed 1600 m (5250 ft) a.s.l. Air photo interpretation of the surficial geology in this region indicates extensive glacial erosion within the limit of this re-advance, but no field-based exposures were documented to verify this.

### GLACIAL PROCESSES AND IMPLICATIONS FOR DRIFT PROSPECTING:

The four-phase model proposed for the McConnell glaciation in the Pelly Mountains has implications for mineral exploration. Previous exploration projects in Seagull Creek valley assumed down-valley dispersal for mineralized float. Up-valley ice-flow dominated phases 2 and 3 of the last glaciation, however, which resulted in the reworking and redistributing of phase 1 sediment in the opposite dispersal direction (Fig. 9). In other words, the down-valley direction would be the likely source for anomalous sediment and float samples. In the hypothesized dispersal diagram (Fig. 9), a remnant geochemical anomaly may be preserved down-valley from mineralized outcrop if reworking of phase 1 sediment is incomplete. The amount of sediment reworking and erosion by successive ice-flow phases is the pivotal question in determining the dominant glacial sediment dispersion direction. To address this question, four Pelly Mountain valley profiles are described below. These field-based profiles show the distribution of surficial sediment within a typical valley cross-section, and thereby provide

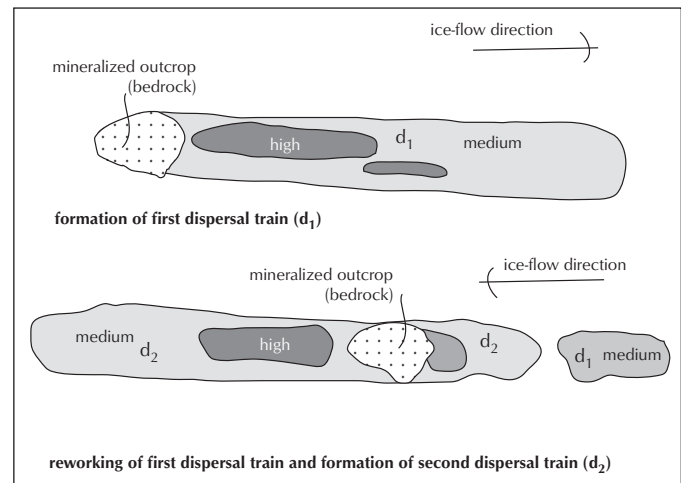


**Figure 9.** A glacial dispersion model for the Pelly Mountains. This model is most applicable for the upper reaches of the southward draining valleys that experienced ice-flow reversals during phases 2-4 of the McConnell glaciation.

a clearer understanding of the degree of deposition and inferred erosion.

The surficial geology shown in the following diagrams is based on field observations within the McNeil River, Seagull Creek and Rose-Lapie Lakes valleys. These diagrams illustrate the general characteristics of the surficial geology and its variability within a valley cross-section. These profiles are not necessarily applicable to a particular property, but can be used as a guide in the construction of new profile models that reflect the unique surficial attributes observed at that property. The general location of these cross-sections is shown in Figure 1.

#### *Upper Seagull Creek*

The surficial sediment distribution in upper Seagull Creek reflects the staggered retreat of the Cordilleran ice sheet from the Pelly Mountains. Multiple thick moraine complexes deposited during recessional pauses are separated by zones of thinner surficial cover where glacial retreat was relatively constant and rapid (Fig. 10). Two profiles have been constructed to illustrate the surficial sediment distribution in each of these zones.

Surficial geology profile 1 (Fig. 11a) illustrates an area within the Seagull Creek valley where phase 3 glaciers retreated relatively constantly and rapidly. Glacial deposits are thin (<4 m) on the valley sides and bottom (Fig. 10).



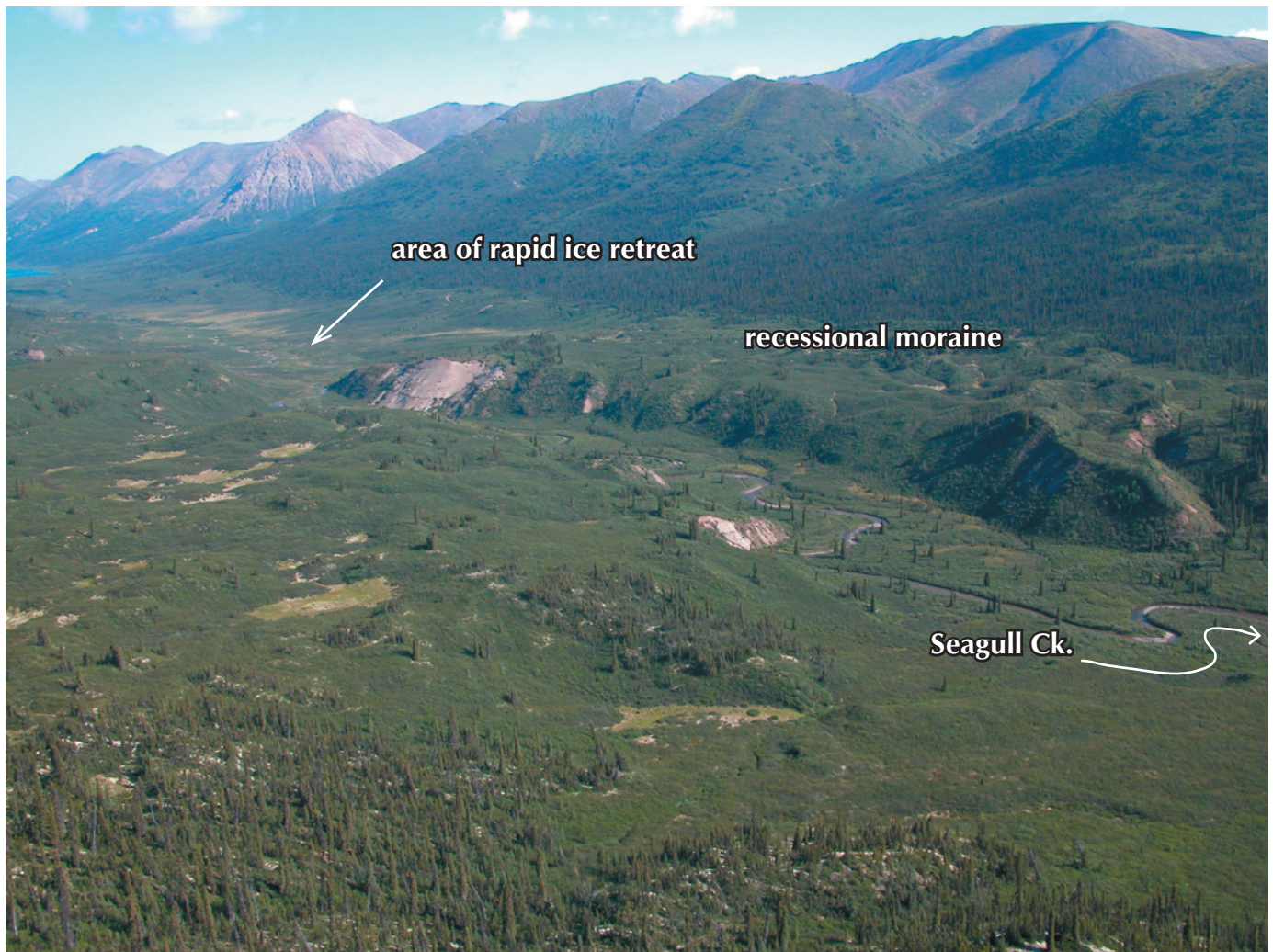


**Figure 10.** A view to the northeast up Seagull Creek showing the surficial sediment variability that is typical in the Pelly Mountains. In the foreground is a recessional moraine/kame accumulation with thicknesses exceeding 30m. In the background is an area of thin glacial cover (<4 m) indicative of clean glacial retreat.

Surficial geology profile 2 (Fig. 11b) illustrates a cross-section through a moraine complex in the Seagull Creek valley. A kame terrace is visible on the valley side and thick ablation sediment overlies basal till in the valley bottom. A deep incision by the modern creek is common (Fig. 10).

#### *Lower McNeil River*

The surficial geology in valleys of lower elevation have fewer moraines, which suggests that the Cordilleran ice sheet retreated more uniformly during the later stages of retreat from the Pelly Mountains.

In profile 3 (Fig. 11c), sediment accumulations are relatively thin on valley benches (<4 m) compared to thick accumulations in valley bottoms (>30 m) where sediment stacking occurred. Earlier glacial deposits are likely eroded from the benches by later ice-flow, whereas deposition dominates in valley bottoms and earlier deposits are preserved.

#### *Glaciolacustrine deposits*

The down-valley retreat of ice in many Pelly Mountain valleys caused ponding of fluvial and glaciofluvial drainage against the ice front. As a result, glaciolacustrine sediment was deposited into pro-glacial lakes. Controls on

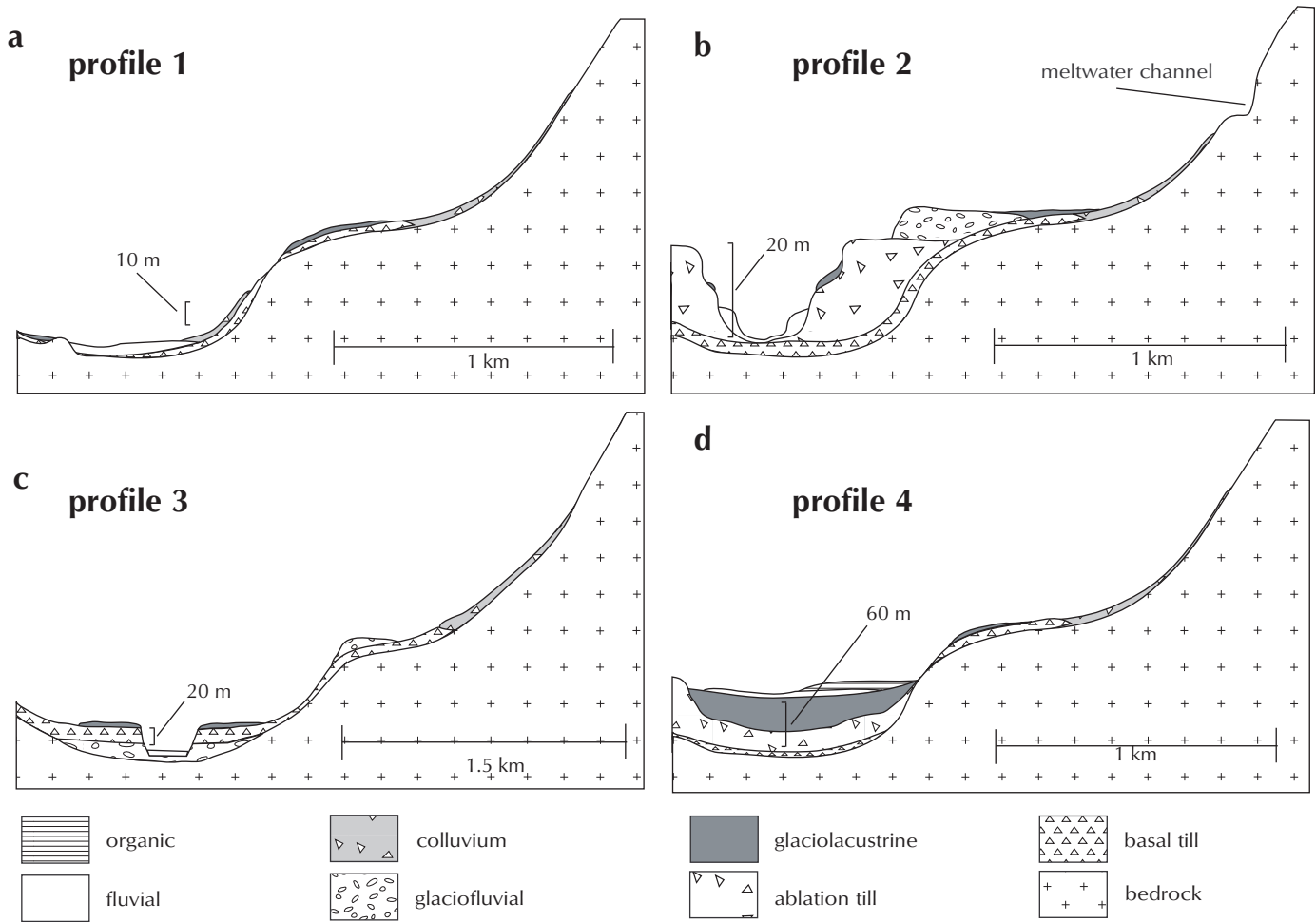


**Figure 11.** Surficial geology profiles of (a) upper Seagull Creek; (b) middle Seagull Creek; (c) McNeil Lake area- and (d) lower Seagull Creek.

the extent of glaciolacustrine sedimentation in a given valley depended on the elevation of the lake outlet, the subglacial hydrology and perhaps the style of ice retreat. Where lake outlets were relatively high, there are thicker and more widespread glaciolacustrine deposits than in drainages having lower outlets. A lower outlet may have allowed for greater circulation of water through the valley, thereby permitting sediment to be carried through in suspension. As ice retreated further down-valley, glacial lakes would have grown in extent, assuming drainage outlets remained constant. These lakes would have lasted through a significant period of deglaciation and would undoubtedly have left behind thick glaciolacustrine sediments over the valley bottoms. While some glaciolacustrine deposits are thick, particularly in the upper-reaches of the main valleys, they are not longitudinally continuous into the lower valley reaches. Reasons for this distribution of glaciolacustrine deposits

are uncertain, however, and could be explained by the style or rate of ice retreat.

Sediment accumulations in profile 4 (Fig. 11d) are characterized by thick glaciolacustrine deposits that overlie till in the valley bottom. In some valleys, fluvial erosion has incised the thick glacial sediment package, whereas in others, like lower Seagull Creek, post-glacial stream base-level changes have not been sufficient to encourage fluvial incision. Surficial sediment thicknesses on the valley sides are considerably thinner compared to the valley bottom in this environment.

In terms of mineral exploration, glaciolacustrine sediment is not derived directly from local bedrock and therefore is a poor sample medium that should be avoided when conducting standard soil geochemistry surveys. In order to illustrate the geochemical variability between glaciolacustrine sediment and till, several samples from





**Figure 12.** A surficial sediment profile in Seagull Creek valley showing a veneer of glaciolacustrine sand overlying a till. The gold concentrations from each unit show the geochemical variability within the surficial geology and highlights the need for surficial mapping early in the exploration process.

Ross River Mineral's Tay-LP property in Seagull Creek were analysed (Fig. 12). Assays showed that the anomalous gold concentration present in the till is absent within the glaciolacustrine veneer. Standard B-horizon soil geochemistry techniques would therefore be misleading in this environment.

## CONCLUSION

A proposed four-phase ice-flow model was developed to describe the McConnell glacial history for the Pelly Mountains. At the onset of glaciation, local valley glaciers advanced down-valley to the mountain front. By glacial maximum, the control on ice-flow shifted to ice-divides located south (Cassiar lobe) and east (Selwyn lobe) of the Pelly Mountains. This resulted in an ice-flow reversal into the mountains. During deglaciation, the neighbouring ice-divides continued to control ice-flow within the Pelly Mountains. The down-valley recession of glaciers was characterized by periods of rapid retreat and periodic up-valley re-advances or recessional pauses. Glacial lakes developed at the margin of the ice front where drainages were blocked. The final phase of ice activity in the Pelly Mountains was a resumption of ice-flow from local cirques above 1600 m a.s.l. This re-advance was limited to <5 km in most valleys and occurred after the invading ice lobes had retreated down-valley to the mountain fronts.

Future drift prospecting in the Pelly Mountains should consider ice-flow complexities that occurred in this area. Surficial geology investigations showed that the dominant glacial sediment dispersal trains were likely created by phases 3 and 4 ice-flow, which means that many valleys in the study area have up-valley-trending sediment dispersal records.

## ACKNOWLEDGEMENTS

Funding for this project was provided by the Yukon Territorial government through the Yukon Geological Survey. Much appreciated and enthusiastic field assistance was provided by Angela Johnson (University of Alberta). Reliable and efficient helicopter support was provided by Barry at Trans North Helicopters. This paper benefited from constructive reviews by Lionel Jackson (Geological Survey of Canada), Leyla Weston and Geoff Bradshaw (Yukon Geological Survey). Cooperation by Ross River Minerals Ltd. during our studies in Seagull Creek on the Tay-LP property was much appreciated and greatly assisted in our understanding of Pelly Mountain glacial history.

## REFERENCES

- Anderson, L., Abbott, M., Finney, B. and Edwards, M.E., 2002. The Holocene lake-level history of Marcella Lake, southern Yukon Territory, Canada. *In: The Geological Society of America Northeastern Section – 37th Annual Meeting, Springfield, Massachusetts, Session No. 19 Program Abstract.*
- Armentrout, J.M., 1983. Glacial lithofacies of the Neogene Yakataga Formation, Robinson Mountains, southern Alaska Coast Range, Alaska. *In: Glacial-marine sedimentation, B.F. Molnia, (ed.), Plenum Press, New York, New York, p. 629-665.*
- Bond, J.D., 1999. The Quaternary history and till geochemistry of the Anvil District, east-central Yukon. *In: Yukon Exploration and Geology 1998, C.F. Roots and D.S. Emond (eds.), Exploration and Geological Services Division, Yukon Region, Indian and Northern Affairs Canada, p. 105-116.*
- Bond, J.D., 2004. Late Wisconsinan McConnell glaciation of the Whitehorse map area (105D), Yukon. *In: Yukon Exploration and Geology 2003, D.S. Emond and L.L. Lewis (eds.), Yukon Geological Survey, p. 73-88.*



- Duk-Rodkin, A., 1999. Glacial limits map of Yukon Territory. Geological Survey of Canada, Open File 3694; Exploration and Geological Services Division, Yukon Region, Indian and Northern Affairs Canada, Geoscience Map 1999-2, scale 1:1 000 000.
- Duk-Rodkin, A. and Barendregt, R.W., 1997. Glaciation of Gauss and Matuyama age, Tintina Trench, Dawson area, Yukon. Canadian Quaternary Association Biannual Meeting, May 22-24, 1997, Université de Québec à Montréal, Montréal, Québec.
- Duk-Rodkin, A., Barendregt, R.W., White, J.M. and Singhroy, V.H., 2001. Geologic evolution of the Yukon River: implications for placer gold. *Quaternary International*, vol. 82, p. 5-31.
- Dyke, A., 1990. Quaternary geology of the Frances Lake map area, Yukon and Northwest Territories. Geological Survey of Canada, Memoir 426, 39 p.
- Froese, D.G., Barendregt, R.W., Enkin, R.J. and Baker, J., 2000. Paleomagnetic evidence for multiple late Pliocene-early Pleistocene glaciations in the Klondike area, Yukon Territory. *Canadian Journal of Earth Sciences*, vol. 37, p. 863-877.
- Fulton, R.J., 1991. A conceptual model for growth and decay of the Cordilleran Ice Sheet. *Geographie physique et Quaternaire*, vol. 45, no. 3, p. 281-286.
- Gordey, S.P. and Makepeace, A.J. (comps.), 2003. Yukon Digital Geology, version 2. Geological Survey of Canada, Open File 1749, and Yukon Geological Survey, Open File 2003-9(D), 2 CD-ROMS.
- Jackson, L.E., Jr. and Mackay, T.D., 1991. Glacial limits and ice-flow directions of the last Cordilleran Ice Sheet between 60 and 63 degrees north. Geological Survey of Canada, Open File 2329, scale 1:1 000 000.
- Jackson, L.E., Jr. and Harington, C.R., 1991. Pleistocene mammals, stratigraphy, and sedimentology at the Ketza River site, Yukon Territory. *Geographie physique et Quaternaire*, vol. 45, p. 69-77.
- Jackson, L.E., Jr., Ward, B., Duk-Rodkin, A. and Hughes, O.L., 1991. The last Cordilleran ice sheet in southern Yukon. *Geographie physique et Quaternaire*, vol. 45, p. 341-354.
- Jackson, L.E., Jr., 1993a. Surficial Geology, Lapie Lakes, Yukon Territory. Geological Survey of Canada, Map 1790A, scale 1:100 000.
- Jackson, L.E., Jr., 1993b. Surficial Geology, Bruce Lake, Yukon Territory. Geological Survey of Canada, Map 1791A, scale 1:100 000.
- Jackson, L.E., Jr., 1993c. Surficial Geology, McConnell River, Yukon Territory. Geological Survey of Canada, Map 1793A, scale 1:100 000.
- Jackson, L.E., Jr., 1993d. Surficial Geology, Lonely Creek, Yukon Territory. Geological Survey of Canada, Map 1796A, scale 1:100 000.
- Jackson, L.E., Jr., 1994. Terrain inventory and Quaternary history of the Pelly River area, Yukon Territory. Geological Survey of Canada, Memoir 437, 41 p.
- Kennedy, K.E. and Bond, J.D., 2004. Evidence for a late-McConnell re-advance of the Cassiar lobe in Seagull Creek, Pelly Mountains, central Yukon. *In: Yukon Exploration and Geology 2003*, D.S. Emond and L.L. Lewis (eds.), Yukon Geological Survey, p. 121-128.
- Klassen, R.W., 1987. The Tertiary-Pleistocene stratigraphy of the Liard Plain, southeastern Yukon Territory. Geological Survey of Canada, Paper 86-17, 16 p.
- Matthews, J.V., Schweger, C.E. and Hughes, O.L., 1990. Plant and insect fossils from the Mayo Indian Village section (central Yukon): new data on middle Wisconsinan environments and glaciation. *Geographie physique et Quaternaire*, vol. 44, p. 15-26.
- Plouffe, A., 1989. Drift prospecting and till geochemistry in Tintina Trench, Southeastern Yukon. Unpublished MSc thesis, Carleton University, Ottawa, Ontario, 81 p.
- Plouffe, A. and Jackson, L.E., 1992. Drift prospecting for gold in the Tintina Trench. *In: Yukon Geology*, vol. 3, Exploration and Geological Services Division, Yukon Region, Indian and Northern Affairs Canada, p. 196-213.
- Rampton, V.N., 1971. Late Quaternary vegetational and climatic history of the Snag-Klutlin area, Yukon Territory, Canada. *Geological Society of America Bulletin*, vol. 82, p. 959-978.
- Tolbert, R.S., 2000. Assessment report on selective leach soil geochemistry and prospecting. Ross River Minerals Ltd., Assessment Report #94143, 17 p.
- Ward, B.C., and Jackson, L.E., Jr. 1992. Late Wisconsinan glaciation of the Glenlyon Range, Pelly Mountains, Yukon Territory, Canada. *Canadian Journal of Earth Sciences – Journal Canadien des Sciences de la Terre*, 29 (9), p. 2007-2012.

# Quaternary, structural and engineering geology of the Aishihik River landslide, Cracker Creek area (NTS 115A/15), Yukon

**Marc-André Brideau<sup>1</sup>**

*Department of Earth Sciences, Simon Fraser University*

**Doug Stead**

*Department of Earth Sciences, Simon Fraser University*

**Crystal Huscroft**

*Department of Geography, University College of the Cariboo*

**Karin Fecova**

*Department of Earth Sciences, Simon Fraser University*

Brideau, M.-A. et al., 2005. Quaternary, structural and engineering geology of the Aishihik River landslide, Cracker Creek area (NTS 115A/15), Yukon. *In: Yukon Exploration and Geology 2004*, D.S. Emond, L.L. Lewis and G.D. Bradshaw (eds.), Yukon Geological Survey, p. 83-94.

## ABSTRACT

The Aishihik River landslide is a prehistoric slope failure located on a southwest-facing slope of the Ruby Range along the Alaska Highway. The failed mass consists of gneissic material from the Kluane metamorphic assemblage. Shoreline sediments from glacial lake Champagne were deposited on top of the landslide debris, suggesting that the slope failure occurred after the ice retreat but before the Dezadeash valley drained. Three dominant discontinuity sets were recognized and correlated to the fracturing associated with the formation of the Ruby Range antiform. Rock engineering classification and laboratory tests suggest that the rock mass present in the headscarp of the failure is of lower quality than on its sidescarps. This rock mass degradation was attributed to two intersecting fault sets at the headscarp. Tension cracks and trenches are present on all sides of the slope failure. Exposed soil and disturbed vegetation observed in trenches suggest continued instability.

## RÉSUMÉ

Le glissement de terrain de la rivière Aishihik s'est produit à la préhistoire sur une pente de la chaîne Ruby faisant face au sud-ouest, le long de la route de l'Alaska. La masse effondrée est formée de matériau gneissique de l'assemblage métamorphique de Kluane. Des sédiments littoraux du lac glaciaire Champagne se sont déposés sur les débris du glissement de terrain, ce qui porte à croire que ce dernier s'est produit après la récession glaciaire mais avant que la vallée de la Dezadeash ne se draine. Trois ensembles de discontinuités dominants ont été relevés et corrélés aux fractures associées à la formation de l'antiforme de Ruby Range. La classification de la mécanique des roches et des essais en laboratoire portent à croire que la masse de roches présente dans l'escarpement à la tête du glissement est de moins bonne qualité que les roches dans les escarpements sur les côtés du glissement. Cette dégradation de la masse de roches est attribuée à deux séries de failles croisées à l'escarpement de tête. Des fissures et fossés de tension sont présents sur tous les côtés du glissement. Le sol exposé et la végétation perturbée qui ont été observés dans les fossés semblent indiquer que l'instabilité se poursuit.

<sup>1</sup>Department of Earth Sciences, Simon Fraser University, 8888 University Drive, Burnaby, British Columbia, Canada, V5A 1S6, mbrideau@sfu.ca

## INTRODUCTION

The Aishihik River landslide is a large prehistoric slope failure that occurred on a southwest-facing slope of the Ruby Range near the intersection of the Aishihik Road and the Alaska Highway (Fig. 1). The landslide was originally mapped as alpine moraines by Kindle (1952), and was only recently analysed as a slope failure (Huscroft et al., 2004; Fig. 2). Its volume has been estimated at 22 million m<sup>3</sup>. The debris deposit consists predominantly of large subangular boulders (Huscroft et al., 2004). Examples from southern British Columbia have demonstrated that sites of prehistoric slope failures can be catastrophically reactivated (e.g., Mathews and McTaggart, 1969; Couture and Evans, 2000), and emphasize the importance of understanding their failure mechanisms and evaluating their present day stability. The fieldwork performed for this study combined elements of structural and engineering geology mapping. A total of 11 ground traverses were conducted and 1000 structural measurements were taken. GIS software was used to store, manage and display the field data. The role of each of the discontinuity sets on slope stability and failure mechanisms were investigated. This study is part of a

larger project initiated to investigate the influence of tectonic structures, such as faults, shear zones and folds, on the quality of a rock mass and their effect on the stability of rock slopes.

## BEDROCK GEOLOGY

The Aishihik River landslide occurred in Mesozoic gneissic rocks that are part of the newly proposed Kluane metamorphic assemblage (KMA; Mezger 1997, 2000, 2003). Petrography of the gneissic rocks at the Aishihik River landslide revealed that major phases (>5%) are plagioclase, quartz and biotite, and minor phases (<5%) are chlorite, potassium feldspar, unidentified opaque minerals and zircon. These results correlate with the petrology reported by Mezger (1997) for the KMA. The dominant structural feature in the KMA is a pervasive foliation that dips to the northeast. The Aishihik River landslide occurred near the contact between the Ruby Range Batholith (RRB) and the KMA. The Ruby Range Batholith is a 200-km-long northwest-trending Eocene granodiorite (Muller, 1967). The contact between the KMA and RRB was not observed directly at the study area. Intermediate dykes and sills are more prevalent in

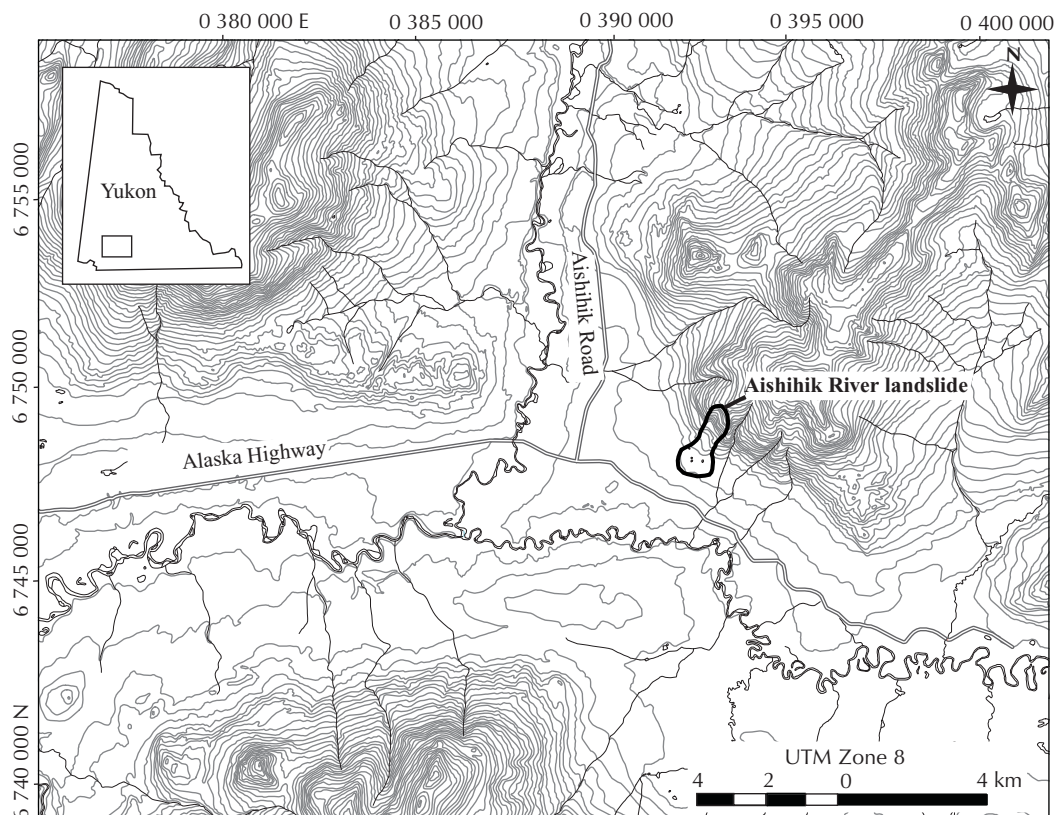


**Figure 1.** Location map of the Aishihik River landslide.



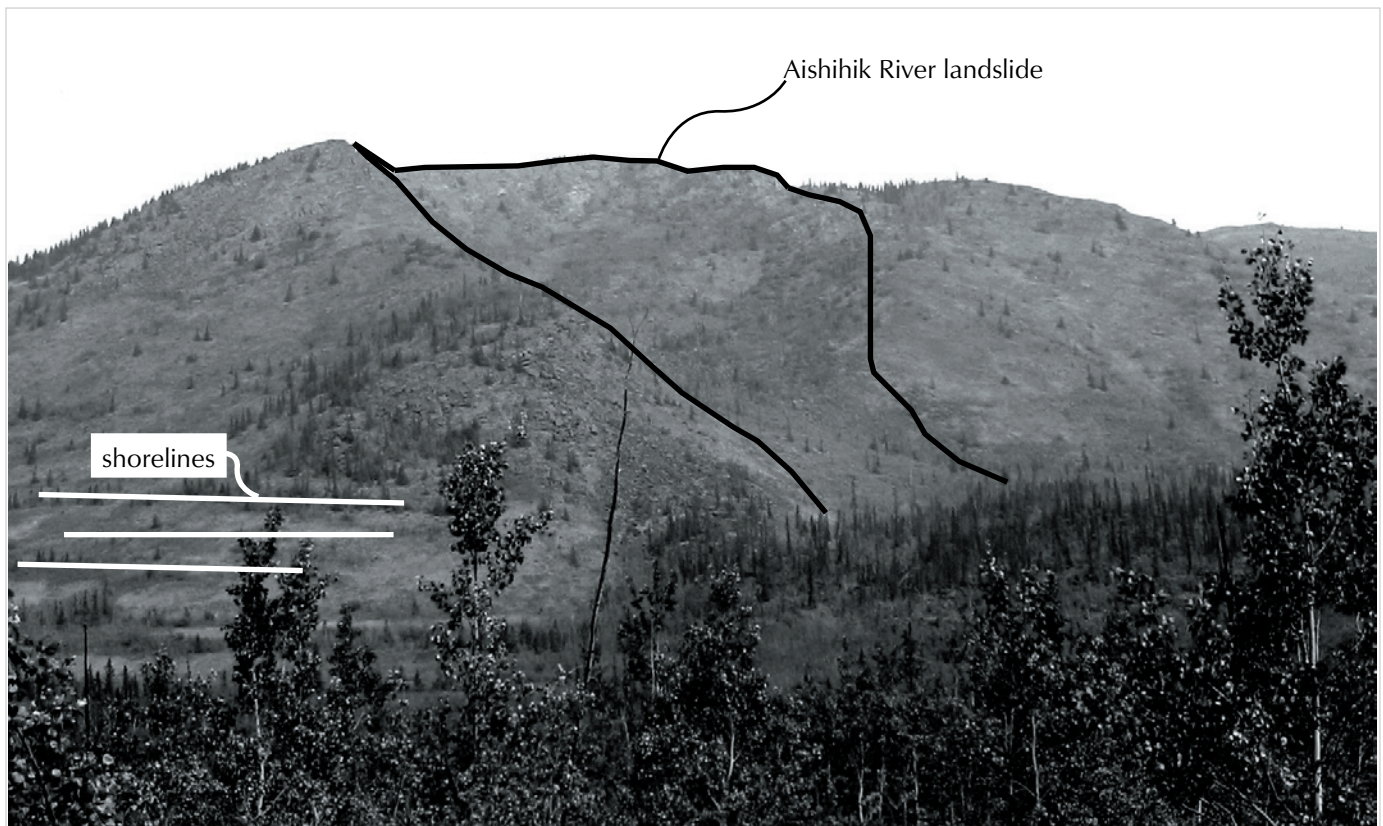


**Figure 2.** Overview of the Aishihik River landslide. View looking north.

the northeastern section of the slope failure, and this increase in minor intrusive bodies is likely related to the proximity of the contact between the KMA and RBB. Contact metamorphism related to the intrusion of the RRB caused the predominantly schistose rocks of the KMA to be metamorphosed into gneissic rocks (Mezger, 1997, 2000).

## QUATERNARY GEOLOGY

The study area was last glaciated during the late Wisconsinan McConnell glaciation. At that time, ice in southwestern Yukon generally flowed out of ice centres in the most mountainous regions, such as the St. Elias and Coast Mountain belts, and along major structural trenches. Locally, ice flowed to the north across the Dezadeash River valley and up the Aishihik River valley (Hughes et al., 1989).

Glacial recession had initiated by  $13\,660 \pm 460$  years BP and occurred in a series of intervals of retreat and stagnation, with ice lobes occupying valley bottoms and damming numerous drainage routes (Hughes et al., 1989). Large glacial lakes were impounded in most of the main

valleys, and included the Dezadeash and Aishihik river valleys. The intervals of stagnation resulted in the deposition of extensive glaciolacustrine deposits in valley bottoms and the formation of shoreline features on valley sides. Glacial lake shorelines eroded into the debris of the Aishihik River landslide are traceable between 810 and 850 m in elevation (Fig. 2). This lake level correlates with the earliest stages of the formation of glacial lake Champagne (Rampton and Paradis, 1982; Barnes, 1997; Barnes, 2000). Glacial lake Champagne was dammed by glacial ice and likely existed at its largest extent some time between 13 660 and 9500 BP (Hughes et al., 1989; Barnes, 1997).

## STRUCTURAL GEOLOGY

### DISCONTINUITY SETS AND STRUCTURAL DOMAINS

Three dominant discontinuity sets are prevalent over much of the study area (Fig. 3). The spacing and persistence categories proposed by the International Society for Rock Mechanics (ISRM1978) are employed in

this paper. The first discontinuity set (I) trends west-northwest to northwest and dips subvertically. The second discontinuity set (II) trends northeast and also dips subvertically. Discontinuity sets I and II are nearly perpendicular to each other. Discontinuity set III trends north-northeast to northeast and dips at  $\sim 30^\circ$ . Discontinuity set III is sub-parallel to the gneissic fabric. Three joint sets with similar orientations and spacings of less than 1 m were reported by Mezger (1997) for an area 20 km northwest of the Aishihik River landslide. Discontinuity set IV trends northwest and dips subvertically to the northeast. There is also a subordinate joint set that is not highlighted in the stereonet, since its spacing is wider than the area usually investigated at individual field stations. This joint set trends northeast and dips ( $40\text{-}50^\circ$ ) southeast, has a high strike and dip persistence (10 to 20 m), and an extremely wide spacing ( $>6$  m).

The area of the Aishihik River landslide is divided into nine structural domains (Fig. 3A-I). The three discontinuity sets discussed above are present in domains A to E but have

different orientations in each. These minor differences in orientation in domains A to E illustrate that the western sidescarp of the slope failure comprises a series of down-dropped blocks. Domain G, which encompasses the headscarp, is the only domain with a markedly different discontinuity pattern. The fault-parallel discontinuities related to the three northeast-trending minor faults mapped in the headscarp areas are part of discontinuity set II. A closely spaced joint set parallel to the headscarp was noted in the field and corresponds to discontinuity set IV in domain G. Discontinuity set IV is interpreted to be the field expression of a regional fault with a similar attitude (Fig. 4). Domain H on the eastern sidescarp of the slope failure is similar to domains A to E on the western sidescarp. Domains F and I have twice the number of discontinuity sets as the other domains. This is likely because the relatively few stations in these domains are located on blocks that have moved relative to one another. The spacing of the discontinuities is larger on the sidescarps (domains A to E, I, and part of H) than on the headscarp region (domain F, G, and part of H; Fig. 5). This

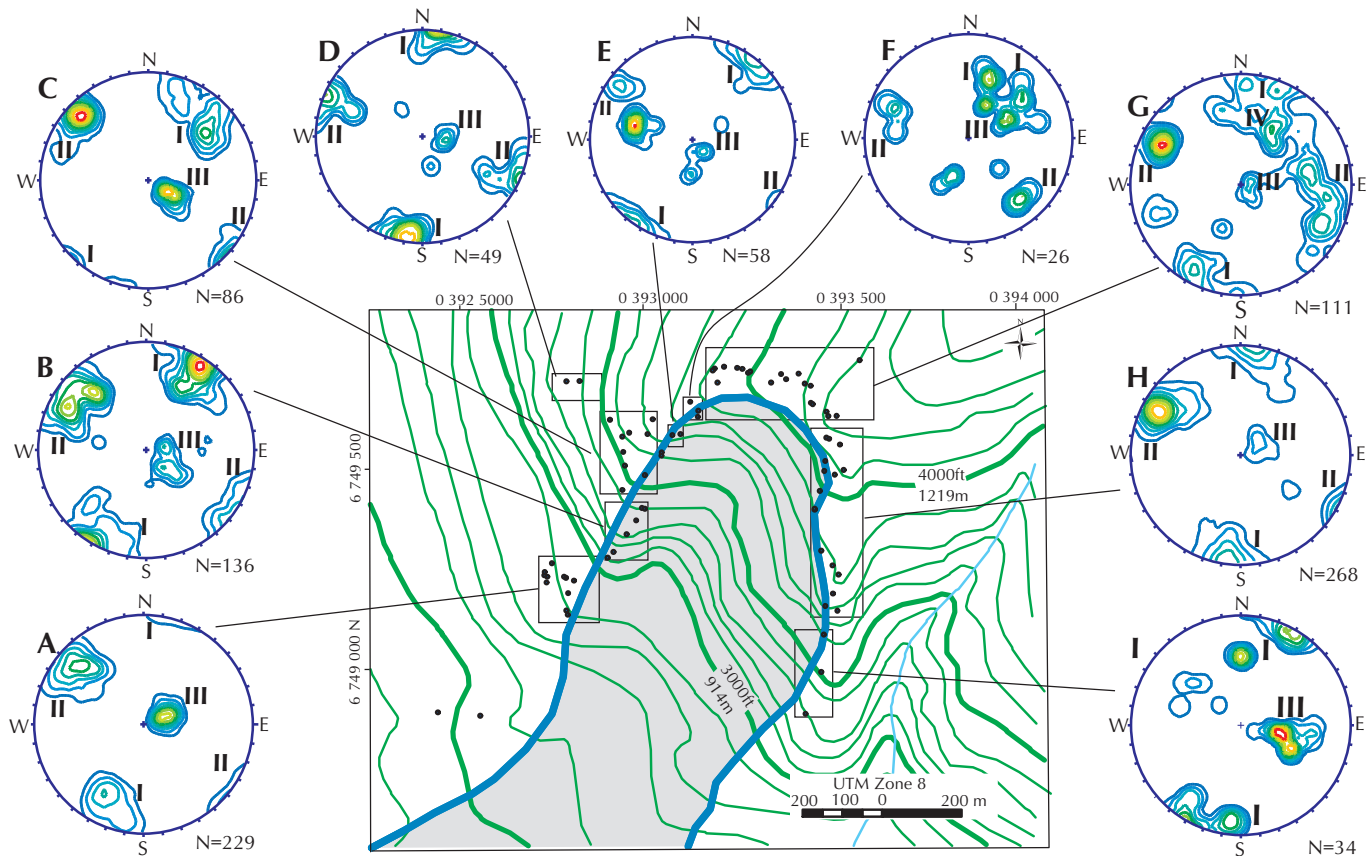


**Figure 3.** Structural domains and accompanying contour plots of poles to the discontinuities. Stereonets are lower hemisphere Schmidt nets.





**Figure 4.** Dominant discontinuity set IV in the headscarp area of the Aishihik River landslide. Note the close spacing (60 to 200 mm) of the discontinuity set.

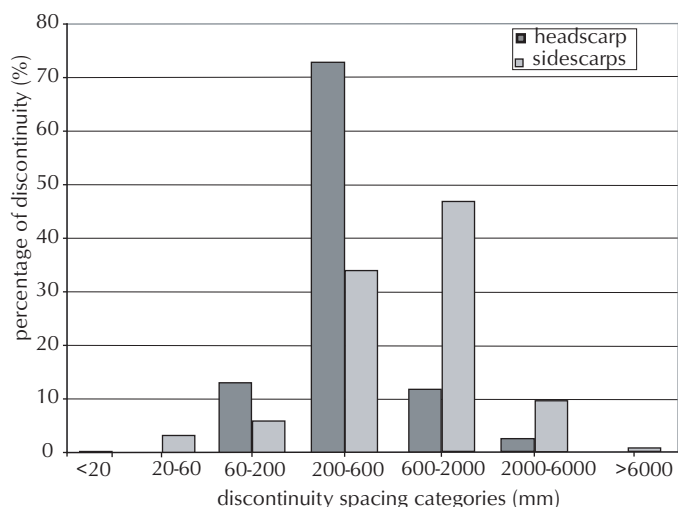


**Figure 5.** Percentage of discontinuity spacing categories at the Aishihik River landslide along the sidescarps and headscarp.

correlates with the lower rock mass quality in the headscarp area (Fig. 4).

## FOLDING

The presence of a 20-km-wide antiform, termed the Ruby Range antiform, with its fold axis trending east-southeast in the McKinley River valley was proposed by Mezger (1997). The average gneissic mineral foliation measured at the study site strikes north-northwest and dips east-northeast at  $\sim 30^\circ$ . This mineral foliation attitude indicates

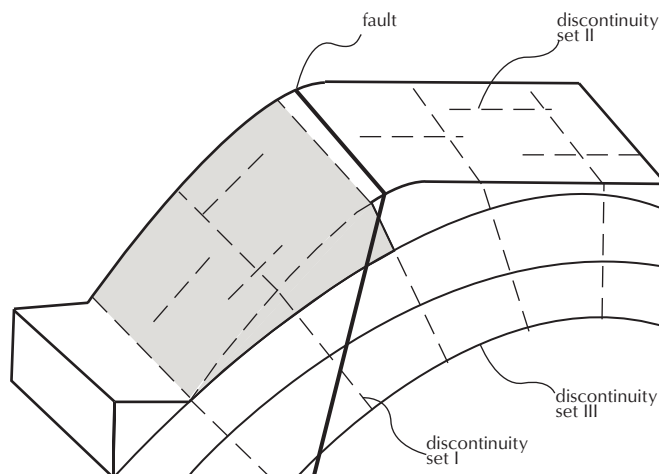


**Figure 6.** Geometry of fold, fault, discontinuities and slope at the Aishihik River landslide. The shaded area represents the unstable section of the slope.

that the Aishihik River landslide is located on the southwestern limb of the Ruby Range antiform. The discontinuity sets present at the Aishihik River landslide can be related to simple fracturing models related to folding (e.g., Price and Cosgrove, 1990; Twiss and Moore, 1992; Davis and Reynolds, 1996; Fig. 6). Discontinuity set I consists of tensile fractures parallel to the fold axis, while discontinuity set II consists of tensile fractures perpendicular to the fold axis. Discontinuity set III consists of shear fractures that formed preferentially along pre-existing foliation planes during flexural folding.

## TENSION CRACKS AND TRENCHES

Twenty-five tension cracks and trenches were observed and described. Linear depressions clearly bounded by discontinuity sets are referred to as tension cracks whereas unbounded linear depressions in the landscape or soil cover are referred to as trenches. The tension cracks are concentrated on the western sidescarp of the slope failure, and are 2.5 to 30 m long and 0.5 to 14 m deep (Fig. 7). The trenches are concentrated behind the headscarp and along the eastern sidescarp, and are 5 to 150 m long and 0.3 to 5 m deep (Fig. 7).

The trenches behind the headscarp of the landslide exposed a thin ( $\sim 20$  cm) soil profile, which contained a discontinuous 2- to 5-cm-thick tephra layer 10 cm from the present day surface. The tephra layer likely represents deposits of the eastern lobe of the White River Ash (Lerbekmo and Campbell, 1969; Clague et al., 1995). The



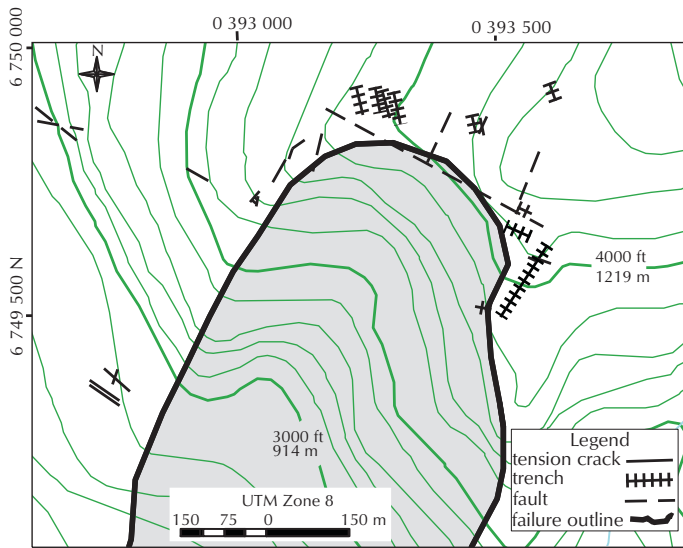


**Figure 7.** Location and orientation of faults, tension cracks and trenches described at the Aishihik River landslide.

latest age constraints on the eastern lobe suggest deposition ~1150 years BP (Clague et al., 1995).

Two movement directions of slope material are highlighted by the tension cracks and trenches (Fig. 7). A first group of north-northwest trending tension cracks and trenches indicate a down-valley movement of material due to gravity. This group contains the trenches where soil and tephra are exposed. The second group of northeast-trending tension cracks and trenches reflects the dilational movement of the rock mass material associated with loss of restraint due to the prehistoric slope failure. Mature living trees were observed within some features of this group.

**FAULTS AND BEDROCK LINEAMENTS**

Previously mapped faults (Gordey and Makepeace, 2000) within a 10-km radius of the Aishihik River landslide were compiled together with bedrock lineaments identified from air photographs (National Air Photo Library A25275-13,14; A31724-89,90) in a review of regional structures. Rose diagrams that illustrate the orientations of discontinuities, tension cracks and trenches, faults and bedrock lineaments are presented in Figure 8. All three types of structures have a well defined northeast trend concentration. The slope failure and runout direction also follow a northeast direction. Three minor faults with a northwest orientation were recorded at the headscarp of the Aishihik River landslide (Fig. 7). Timing constraints regarding the formation of the three types of structures

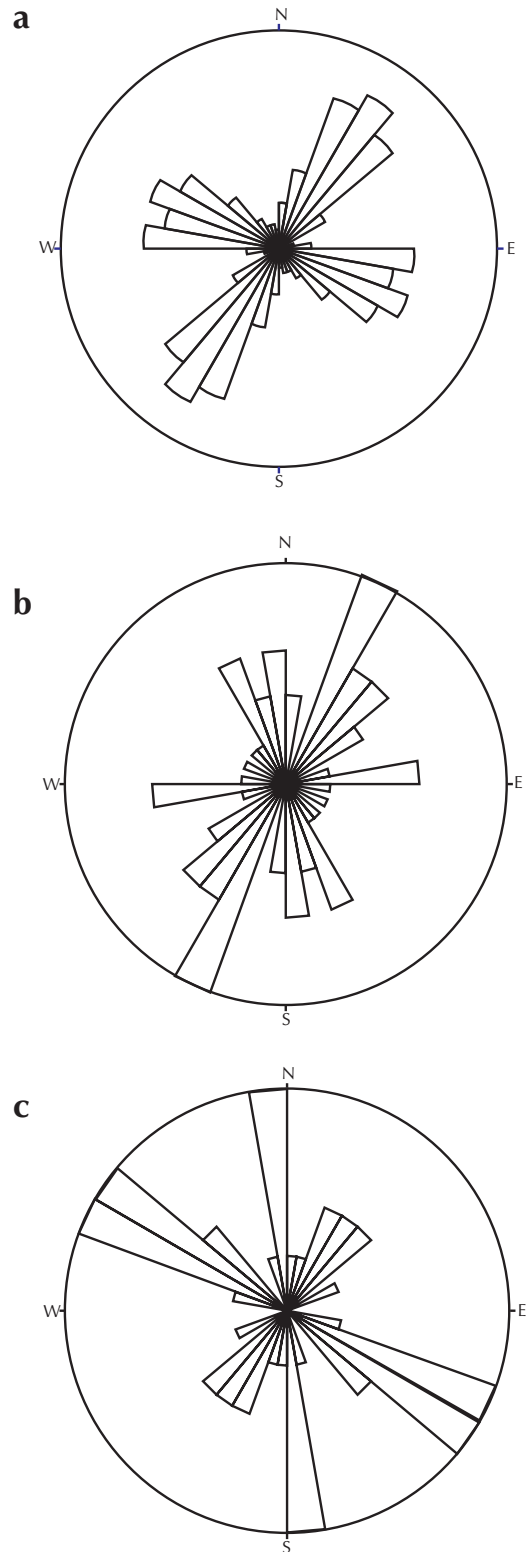


**Figure 8.** Symmetric rose diagrams comparing the orientation of discontinuities, faults and tension cracks. (a) discontinuities, (b) faults and bedrock lineaments, (c) tension cracks and trenches.

were not evaluated at the Aishihik River landslide. A second west-northwest structural trend is dominant in the discontinuities and is present to a lesser extent in the faults and bedrock lineaments. This trend corresponds to the orientation of the headscarp. A third north-northwest structural trend was only present in the faults/bedrock lineaments and tension cracks/trenches rose diagrams. This orientation corresponds to the trenches with evidence of recent activity.

## ENGINEERING GEOLOGY

### GEOLOGICAL STRENGTH INDEX (GSI)

The GSI was developed by Hoek and Brown (1997) as a quantitative way of relating field observations to the rock mass quality. It is based on the structure conditions (e.g., number of joints, joint density, bedding, shearing) and surface/weathering conditions observed in a homogeneous rock mass. The distribution of GSI estimates obtained at the Aishihik River landslide is shown in Figure 9. The average GSI value for both sidescarps was

approximately 50-60. This corresponds to a blocky rock mass (i.e., three discontinuity sets) and fair surface conditions. The average GSI value for the backscarp of the slope failure was approximately 30 to 40. This indicates a very blocky rock mass (angular blocks due to the intersection of four discontinuity sets or more) with poor surface conditions.

### SCHMIDT HAMMER

The Schmidt Hammer is a non-destructive field test originally developed to test concrete hardness and first applied in rock engineering by Deere and Miller (1966). The average rebound values (R) can be correlated to the unconfined compressive strength (UCS) of the intact rock. Empirical relations between R and the UCS are specific to the rock lithology and weathering conditions (Dincer et al., 2004). The analysis in this study is conducted as a function of R, because empirical relations between R and UCS have not been derived for gneissic rock. Figure 10 illustrates the average rebound values obtained. The average rebound value calculated at each station ranged from 24 to 42. Four of the five average rebound values

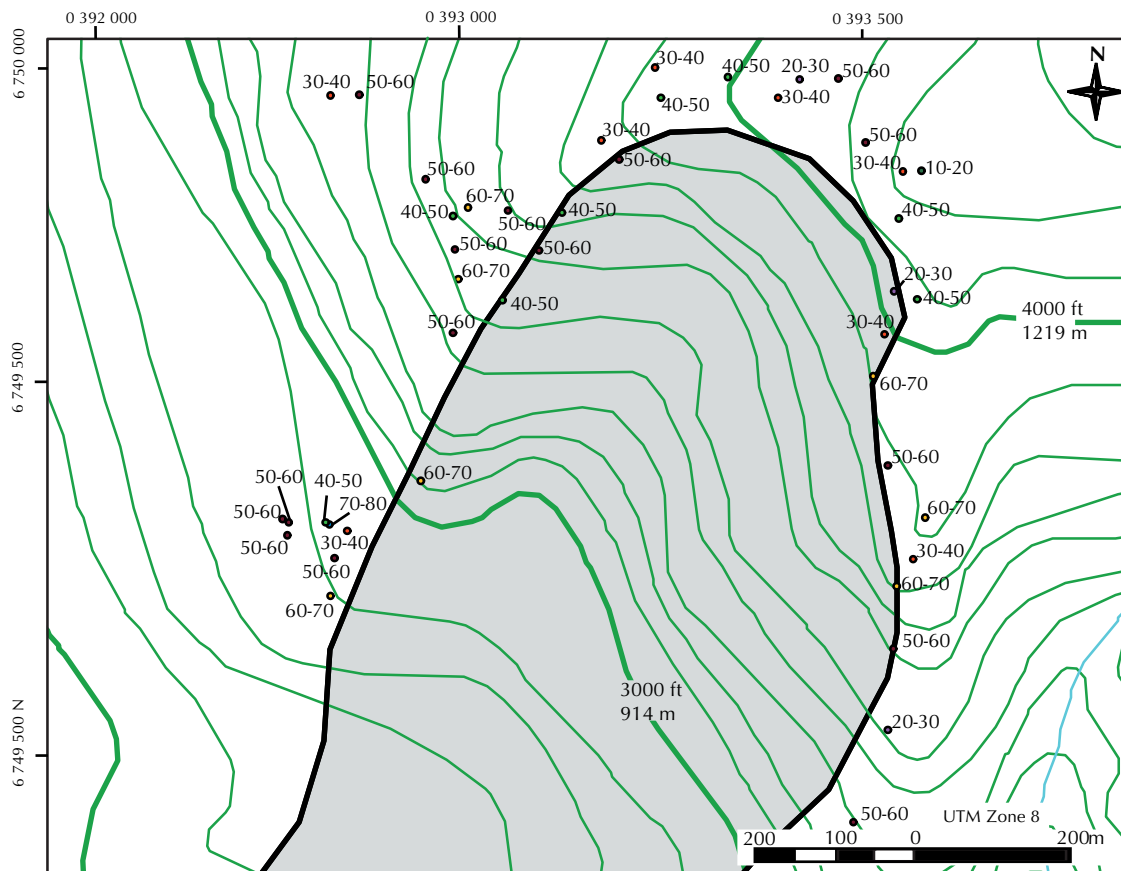


**Figure 9.** GSI values recorded at the Aishihik River landslide.

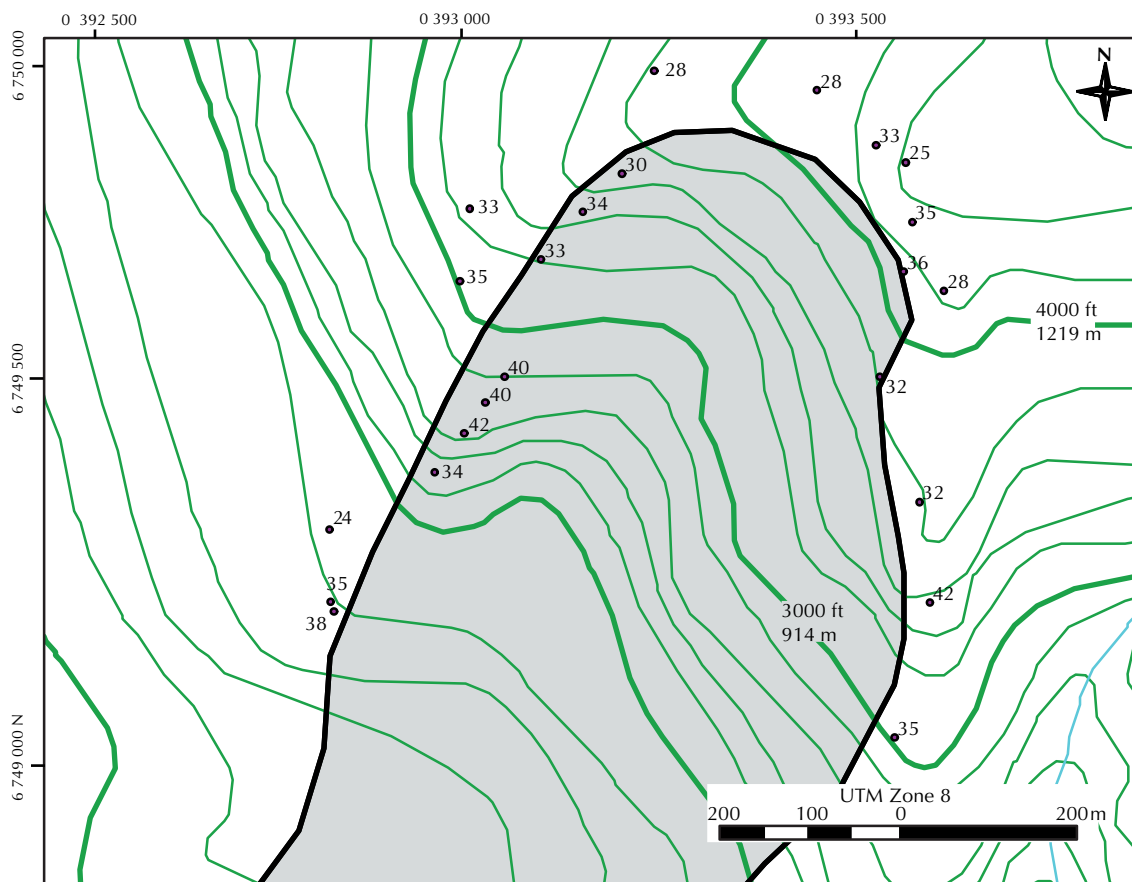


**Figure 10.** Average Schmidt Hammer rebound number values obtained at the Aishihik River landslide.

that were below thirty were recorded in the backscarp area. The lower rebound values from the headscarp area of the Aishihik River landslide correlate with the lower rock mass quality (GSI values).

**POINT LOAD TESTS**

Point load tests were used to test the strength of rock samples collected at different locations around the slope failure. Tests were done according to the ISRM standard for irregular blocks (ISRM, 1985). Table 1 summarizes the

point load index and corresponding uniaxial compressive strength (UCS) estimates obtained for the different lithologies. There was minimal variation in point load index between gneissic rocks that were tested perpendicular ( $Is_{50\text{perpendicular}}$ ) and the samples tested parallel to the mineral foliation ( $Is_{50\text{parallel}}$ ). A point load anisotropy index ( $Is_{50\text{perpendicular}}/Is_{50\text{parallel}}$ ) of 1.09 was calculated. The intact gneissic material is therefore considered to have isotropic strength characteristics. Point load index values obtained for the gneissic rocks correspond to values reported by Kulhawy (1975). The

**Table 1.** Average point load index values and uniaxial compressive strength estimates obtained for the lithologies present at the Aishihik River landslide.

Lithology	point load index $Is_{50}$ (MPa)	uniaxial compressive strength (MPa)	number of samples tested	number of tests performed
fresh grey intrusive	13.3	293	4	7
slightly ( $W_1$ ) weathered intermediate intrusive	2.1	46	1	2
gneissic material parallel to foliation	5.4	119	5	9
gneissic material perpendicular to foliation	5.9	130	4	9
slightly ( $W_1$ ) weathered fault material	0.72	16	3	3



weathered materials had significantly lower point load index values (Table 1). The weathered samples were collected in zones that contained tectonic structures and their low point load index values could also be due to strength degradation related to tectonic damage of the rock mass. Results from point load tests on grey sills in the area demonstrate that these rocks have point load index values that are more than twice than those of the gneissic rocks.

## DISCUSSION

### TECTONIC DAMAGE

The influence of tectonic structures on slope stability was previously investigated in the southwestern Yukon by Everard (1994). An inventory of landslides and bedrock lineaments was derived from air photographs for the Kluane Lake, Mt. St. Elias, and the western half of the Dezadeash map areas. Bedrock lineaments were interpreted to represent the surface expression of faults by Everard (1994). The spatial distribution of landslides in southwestern Yukon is related to the presence of faults. Lithology and clusters of low-level earthquakes were also found to influence the spatial distribution of slope failures (Everard, 1994). Vanicek and Nagy (1981) reported that the highest 'present day' vertical crustal movement in Canada (24 mm/yr) was occurring in the southwestern Yukon at that time. This rate of uplift correlates to the 237 m of isostatic rebound in the Aishihik map area since deglaciation (Hughes, 1990). This large rebound and/or tectonic uplift rate is the principle cause of earthquakes and subsequent slope instability in southwestern Yukon (Clague, 1981).

The present study documents the tectonic structures in the region of the Aishihik River landslide, measures their effects on rock mass quality, and thereby provides an assessment of the implications for rock slope stability. Badger (2002) investigated fracturing related to anticlines and its influence on slope stability in a study of five sites in Washington State. Conceptual models suggest that when the fold-axis trend is parallel to the slope aspect but behind the slope crest, the slope would be predisposed to planar failure along shear fractures with tensile fractures acting as rear and lateral-release surfaces (Fig. 6). In the case of the Aishihik River landslide, the development of lateral-release surfaces would also be facilitated by faults perpendicular to the headscarp. The lower GSI, Schmidt Hammer rebound values, closer

discontinuity spacing and complex discontinuity pattern collectively suggest that the headscarp area of the Aishihik River landslide is composed of a more damaged rock mass than the sidescarps. This lower rock mass quality facilitated the development of rear-release surfaces. The undercutting and subsequent debuttressing of the slope by glaciers during the last glaciation may have triggered the prehistoric Aishihik River landslide.

### FAILURE MECHANISMS

A kinematic analysis (Richards et al., 1978) that considers sliding, toppling and wedge failure mechanisms was performed (Fig. 11) to evaluate the model presented in Figure 6. The kinematic analysis was performed for two angles of friction (20° and 30°). The zone where each failure mechanism was kinematically feasible was delineated by a bold outline in each stereonet. Since the slope angle and discontinuity set III dip at ~30° the kinematic analysis performed for a friction angle of 30° suggests marginally stable conditions. The kinematic analysis performed using a friction angle of 20° suggests that sliding, toppling and wedge failures are all feasible failure mechanisms. Sliding and toppling failure mechanisms as represented in the conceptual model in Figure 6 would therefore only be kinematically feasible if the friction angle was below 30°. The shorelines deposited onto, and eroded into, the debris deposit suggest that the valley was still occupied by glacial lake Champagne when the slope failure occurred. The presence of water in the lower section of the slope could have reduced the effective friction angle along the discontinuities to the 20° value considered in the kinematic analysis.

Caution must be exerted when basic kinematic analysis techniques originally applied at the road-cut scale are to be applied to the mountain scale. Scale effects on the failure mechanism have been documented in physical and numerical models (Bandis and Barton, 1980; Hencher et al., 1996; Bhasin and Hoeg, 1998). Numerical and physical models suggest that rotation has a more important role in the failure mechanism of a region composed of a large number of blocks than the same region composed of fewer blocks (Bhasin and Hoeg, 1998). The number and size of blocks can be estimated during field investigation of rock slope by the spacing and persistence of discontinuities. For example, large rock slides in the Canadian Cordillera suggest that either wide spacing or a poor persistence of the subvertical discontinuity combined with a higher persistence of the

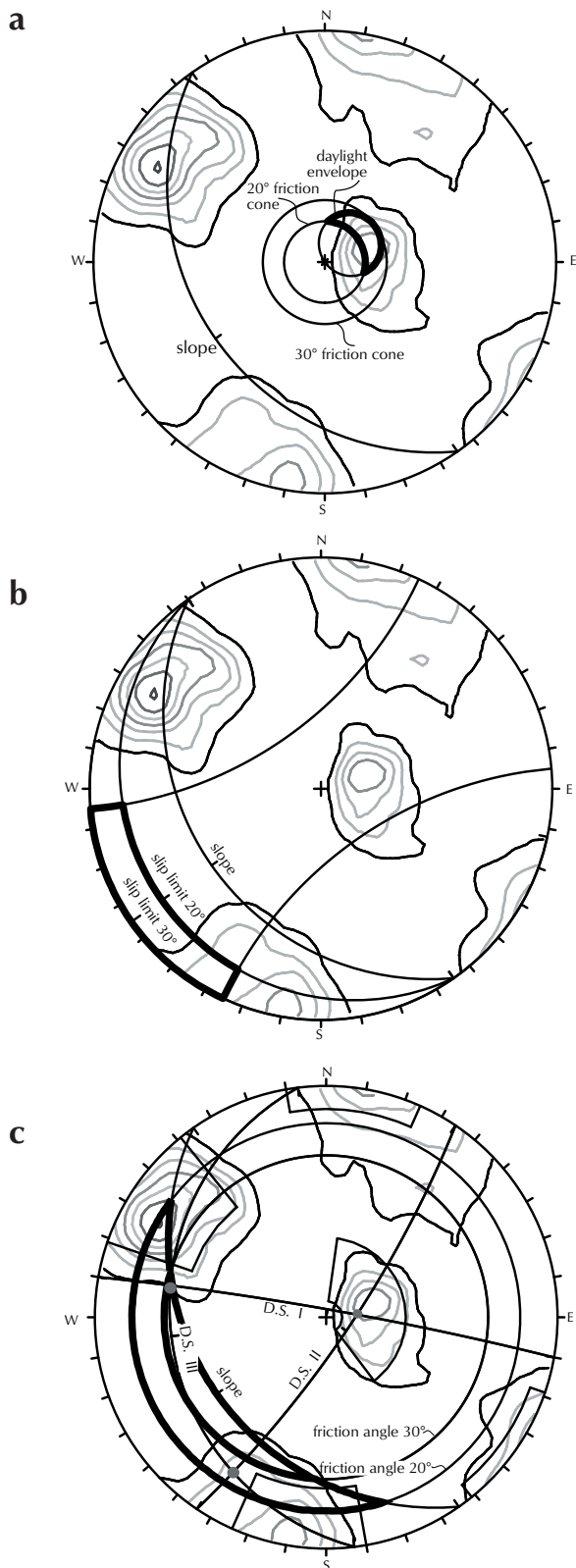


**Figure 11.** Kinematic analysis of the discontinuity sets recorded at the Aishihik River landslide. Analysis for (a) sliding, (b) toppling and (c) wedge failure mechanism.

diagonal discontinuity was present. One of the largest rock slides in Canada, near Avalanche Lake (200 m<sup>3</sup>) in the Northwest Territories, was described as a slope failure along a 150-m-thick massive carbonate bed (Eisbacher, 1979; Evans et al., 1994). The moderate to wide spacing and low to medium persistence of all three discontinuity sets present at the Aishihik River landslide create a blocky rock mass (Fig. 12) which is unlikely to fail as a simple translational planar event. Numerical simulation will be used to further investigate possible failure mechanisms.

### PRESENT STABILITY CONDITIONS

Observations made during fieldwork and a review of the air photographs provide a preliminary assessment of the current stability of the rock slope adjacent to the slope failure. Recent movement at the study site is indicated in the headscarp area by exposed soil and White River Ash in trenches, and disturbance to the vegetation (Huscroft et al., 2004). Both sidescarps are composed of a series of down-dropped blocks. The headscarp of the Aishihik River landslide extends beyond the western limit of failed material. Active block toppling and rock fall zones are present on the western sidescarp.

Such signs of ongoing instability over much of a prehistoric failure area and adjacent area along the valley side have important implications for hazard assessment. Further study and a hazard assessment should precede any development of the area proximal to the Aishihik River landslide. This study should investigate the rate of movement on the trenches and tension cracks and include a runout analysis. Runout analyses investigate how far a landslide will likely travel. They are important in evaluating which infrastructures are at risk. Field observations acquired during this project suggest that there is the potential for a future failure of a similar



**Figure 12.** Blocky nature of the southwestern ridge. View looking northeast.

volume to the prehistoric Aishihik River landslide. A travel distance similar to that of the previous slope failure should be considered a minimum.

## CONCLUSIONS

The origin of the three dominant discontinuity sets present at this landslide are explained by a simple fracture model related to the formation of the regional antiform. The structural domains, discontinuity spacing, Geological Strength Index and average Schmidt Hammer measurements suggest that the headscarp region of the slope failure comprises lower quality rock than the regions on either side. Analysis of known faults, bedrock lineaments, discontinuities, tension cracks and trenches reveals a preferential northeast orientation that corresponds to the orientation of the failed material and transport direction. Pre-existing tectonic conditions have played an important role in reducing the rock mass quality and strength in the headscarp of the Aishihik River landslide, thereby facilitating the development of a rear-release surface. Point load tests suggest that the rock mass has a nearly isotropic intact rock strength. Geomorphic evidence of present-day slope instability at the Aishihik River landslide was observed during this project and by previous workers, and has implications for future development in the area.

## ACKNOWLEDGEMENTS

The authors would like to thank B. Ward for his critical review of the manuscript. We would also like to thank J.E. Mezger for access to his field notes and discussions on the regional structural geology, J. Bond for discussions on the glacial lakes in southern Yukon and D. Froese for discussions on the tephra found in the southwestern Yukon. Funding for this project was provided by an NSERC Discovery grant to D. Stead and an NSTP grant to M.-A. Brideau.

## REFERENCES

- Badger, T.C., 2002. Fracturing within anticlines and its kinematic control on slope stability. *Environmental and Engineering Geoscience*, vol. VIII, no. 1, p. 19-33.
- Bandis, S.C. and Barton, N.R., 1980. Some effects of scale on the shear strength of joints. *International Journal of Rock Mechanics, Mining Sciences and Geomechanic Abstract*, vol. 17, p. 69-73.
- Barnes, S.D., 1997. The sedimentology and paleogeography of glacial lake Champagne, southern Yukon Territory. Unpublished M.Sc. thesis, Carleton University, Ottawa, Ontario, 109 p.
- Barnes, S.D., 2000. The paleogeography of glacial lake Champagne, southern Yukon: Implications for the last deglaciation. 30th International Arctic Workshop, Program and Abstracts, 2000, Institute of Arctic and Alpine Research, University of Colorado, Boulder, Colorado, p. 17-19.
- Bhasin, R. and Hoeg, K., 1998. Numerical modelling of block size effects and influence of joint properties in multiply jointed rock. *Tunneling and Underground Space Technology*, vol. 13, no. 2, p. 181-188.
- Clague, J.J., Evans, S.G., Rampton, V.N., and Woodsworth, G.J., 1995. Improved age estimates for the White River and Bridge River tephra, Western Canada. *Canadian Journal of Earth Sciences*, vol. 32, no. 8, p. 1172-1179.
- Clague, J.J., 1981. Landslides at the south end of Kluane Lake, Yukon Territory. *Canadian Journal of Earth Sciences*, vol. 18, p. 959-971.
- Couture, R. and Evans, S.G., 2000. The East Gate Landslide, Beaver Valley, Glacier National Park, Columbia Mountains, British Columbia. *Geological Survey of Canada, Open File 3877*, p. 1-26.
- Davis G.H. and Reynolds, S.J., 1996. *Structural Geology of Rocks and Regions*, 2nd Edition. Wiley Publishing, New York, New York, 776 p.
- Deere, D.U. and Miller, R.P., 1966. Engineering classification and index properties for intact rock, Report AFWL-TR-65-116, Air Force Weapons Laboratory, 300 p.
- Dincer, I., Acar, A., Cobano, I. and Uras, Y., 2004. Correlation between Schmidt hardness, uniaxial compressive strength and Young's modulus for andesites, basalts and tuffs. *Bulletin of Engineering Geology and the Environment*, vol. 63, no. 2, p. 141-148.
- Eisbacher, G.H., 1979. Cliff collapse and rock avalanches (sturzstroms) in the Mackenzie Mountains, Northwestern Canada. *Canadian Geotechnical Journal*, vol. 16, p. 309-334.
- Evans, S.G., Hungr, O. and Enegren, E.G., 1994. The Avalanche Lake rock avalanche, Mackenzie Mountains, Northwest Territories, Canada: Description, dating, and dynamics. *Canadian Geotechnical Journal*, vol. 31, p. 749-768.



- Everard, K.A., 1994. Regional characterization of large landslides in southwest Yukon, with emphasis on the role of neotectonics. Unpublished M.A.Sc., University of British Columbia, Vancouver, British Columbia, 165 p.
- Gordey, S.P. and Makepeace, A.J., (compilers), 2000. Yukon Digital Geology. Geological Survey of Canada, Open File D3826 or Exploration and Geological Services Division, Yukon Region, Indian and Northern Affairs Canada, Open File 1999-1(D), 2 CD-ROMs.
- Hencher, S.R., Liao, Q-H. and Monaghan, B.G., 1996. Modelling slope behaviour for open-pits. Transactions of the Institution of Mining and Metallurgy Section A-Mining Industry, vol. 105, p. A37-A47.
- Hoek, E. and Brown, E.T., 1997. Practical estimates of rock mass strength. International Journal of Rock Mechanics and Mining Sciences, vol. 34, no. 8, p. 1165-1186.
- Hughes, O.L., 1990. Surficial geology and geomorphology, Aishihik Lake, Yukon Territory. Geological Survey of Canada, Paper 87-29, 23 p.
- Hughes, O.L., Rutter, N.W. and Clague, J.J., 1989. Yukon Territory (Quaternary stratigraphy and history, Cordilleran Ice Sheet). *In*: Chapter 1 of Quaternary Geology of Canada and Greenland Volume, R.J. Fulton (ed.); Quaternary; Geological Survey of Canada; also Geological Society of America, The Geology of North America vol. K-1, p. 58-62.
- Huscroft, C., Lipovsky, P. and Bond, J., 2004. A regional characterization of landslides in the Alaska Highway Corridor, Yukon. Yukon Geological Survey Open File 2004-18, 65 p, includes CD-ROM.
- ISRM, 1978. Suggested methods for the quantitative description of discontinuities in rock masses. International Journal of Rock Mechanics and Mining Sciences and Geomechanics Abstracts, vol. 15 p. 319-368.
- ISRM, 1985. Suggested method for determining point load strength. International Journal of Rock Mechanics and Mining Sciences and Geomechanics Abstracts, vol. 22, no. 2, p. 51-60.
- Kindle, E.D., 1952. Dezadeash map-area, Yukon Territory. Memoir 268, Geological Survey of Canada, 68 p.
- Kulhawy, F.H., 1975. Stress deformation properties of rock and rock discontinuities. Engineering Geology, vol. 9, p. 327-350.
- Lerbekmo, J.F. and Campbell, F.A., 1969. Distribution, composition, and source of the White River Ash, Yukon Territory. Canadian Journal of Earth Sciences, vol. 6, no. 1, p. 109-116.
- Mathews, W.H. and McTaggart, K.C., 1969. The Hope landslide, British Columbia. In The Geological Association of Canada, vol. 20, p. 65-75.
- Mezger, J.E., 1997. Tectonometamorphic evolution of the Kluane metamorphic assemblage, SW Yukon: Evidence for Late Cretaceous eastward subduction of oceanic crust underneath North America. Unpublished Ph.D. Thesis, University of Alberta, Edmonton, Alberta, 324 p.
- Mezger, J.E., 2000. 'Alpine-type' ultramafic rocks of the Kluane metamorphic assemblage, southwest Yukon: Oceanic crust fragments of a late Mesozoic back-arc basin along the northern Coast Belt. *In*: Yukon Exploration and Geology 1999, D.S. Emond and L.H. Weston (eds.), Exploration and Geological Services Division, Yukon Region, Indian and Northern Affairs Canada, p. 127-138.
- Mezger, J.E., 2003. Geology of the Dezadeash Range and adjacent northern Coast Mountains (115A), southwestern Yukon: Re-examination of a terrane boundary. *In*: Yukon Exploration and Geology 2002, D.S. Emond and L.L. Lewis (eds.), Exploration and Geological Services Division, Yukon Region, Indian and Northern Affairs Canada, p. 149-163.
- Muller, J.E., 1967. Kluane Lake map-area, Yukon Territory (115G, 115F E1/2). Geological Survey of Canada Memoir 340, 137 p.
- Price, N.J. and Cosgrove, J.W., 1990. Analysis of geological structures. Cambridge University Press, Cambridge, UK, 502 p.
- Rampton, V.N. and Paradis, S., 1981. Surficial geology and geomorphology Teye Lake, YT. Geological Survey of Canada, Map 14-1981, 1:100 000 scale
- Richards, L.R., Leg, G.M.M. and Whittle, R.A., 1978. Appraisal of stability conditions in rock slopes. *In*: Foundation Engineering in Difficult Ground, F.G. Bell (ed.). Newnes-Butterworth, London, UK, p. 449-512.
- Twiss, R.J. and Moore, E.M., 1992. Structural geology. W.H. Freeman and Company, New York, New York, 532 p.
- Vanicek, P. and Nagy, D., 1981. On the compilation of the map of contemporary vertical crustal movements in Canada. Tectonophysics, vol. 71, p. 75-86.

# Preliminary investigation of the bedrock geology of the Livingstone Creek area (NTS 105E/8), south-central Yukon

*Maurice Colpron<sup>1</sup>*  
*Yukon Geological Survey*

Colpron, M., 2005. Preliminary investigation of the bedrock geology of the Livingstone Creek area (NTS 105E/8), south-central Yukon. *In: Yukon Exploration and Geology 2004*, D.S. Emond, L.L. Lewis and G.D. Bradshaw (eds.), Yukon Geological Survey, p. 95-107.

## **ABSTRACT**

The Livingstone Creek area is underlain by metasedimentary and metaigneous rocks of Yukon-Tanana Terrane. It is intruded by at least five distinct suites of intrusive rocks of probable Mississippian to Late Cretaceous ages, at least three of which provide timing constraints on the development of tectonic foliations. Two phases of isoclinal folding, the development of a transposition foliation and late, northeast-vergent open folds characterize the ductile deformation in the area. Brittle-ductile dextral strike-slip deformation is localized along the north-trending d'Abbadie fault zone in the eastern part of the area. Bedrock in the area has potential for lode gold, copper-gold massive sulphide and nickel (platinum-group element?) mineralization along d'Abbadie Fault.

## **RÉSUMÉ**

La région du ruisseau Livingstone est occupée par les roches métasédimentaires et métaignées du terrane de Yukon-Tanana. Elles sont recoupées par au moins cinq suites de roches intrusives distinctes, dont les âges probables varient du Mississippien au Crétacé tardif, et dont trois d'entre elles permettent de dater la formation de foliations tectoniques. Deux phases de plissement isoclinaux, le développement d'une foliation de transposition et des plis ouverts tradifs de vergence nord-est caractérisent la déformation ductile dans la région. Une déformation de type décrochement dextre cassant-ductile est localisée le long de la zone de faille d'Abbadie, dans le secteur oriental de la région. Les roches de cette région sont propices à une minéralisation d'or en filon, de sulfures de cuivre-or massifs, et de nickel (platine?) le long de la faille d'Abbadie.

<sup>1</sup>maurice.colpron@gov.yk.ca

## INTRODUCTION

The Livingstone Creek area, 80 km northeast of Whitehorse (Fig. 1), is a placer camp which has seen intermittent mining operations since the 1898 discovery of gold in the area (Bostock and Lees, 1938; Levson, 1992), but for which a lode source remains elusive. Published bedrock geology maps of the area are limited to reconnaissance-scale (1:250 000) studies of Bostock and Lees (1938) and Tempelman-Kluit (1984). Subsequent studies of the Livingstone Creek and surrounding areas provided more detailed descriptions of the bedrock geology. They primarily focused on the structural evolution of the region (e.g., Hansen, 1989; Harvey et al., 1996, 1997; Gallagher et al., 1998; de Keijzer et al., 1999; Gallagher, 1999; de Keijzer, 2000).

The Livingstone Creek area is underlain primarily by metasedimentary and metaigneous rocks of Yukon-Tanana Terrane (YTT; Figs. 1 and 2). Metasedimentary rocks in the east and northeast part of the area are traditionally assigned to Cassiar Terrane. For reasons outlined in this paper, I entertain the hypothesis that these rocks may also be part of YTT. To the west, YTT is

juxtaposed against Late Paleozoic rocks of the Semenof Block along the Big Salmon Fault (Simard, 2003). The eastern part of the Livingstone Creek area is dissected by the north-striking d'Abbadie fault zone (Fig. 2).

In this region, YTT is traditionally considered to be only ~10-15 km wide. This narrow part of the terrane corresponds to the Teslin Suture Zone of Tempelman-Kluit (1979), a zone of highly strained rocks which were originally interpreted to have developed in a subduction zone setting during Early Mesozoic convergence of Stikinia and North America (e.g., Tempelman-Kluit, 1979; Hansen, 1989, 1992). Subsequent studies of this portion of YTT have shown that ductile deformation features in the Teslin zone are the result of development of an early (late Paleozoic?) transposition foliation superposed by younger (early Mesozoic?) northeast-verging folds (e.g., de Keijzer et al., 1999; Gallagher, 1999). Regional studies of YTT have shown that the terrane is composed of a series of mid- to late-Paleozoic arc and back-arc successions built upon a metasedimentary basement of continental margin affinity (Colpron and Yukon-Tanana Working Group, 2001; Colpron, 2003). Detailed structural

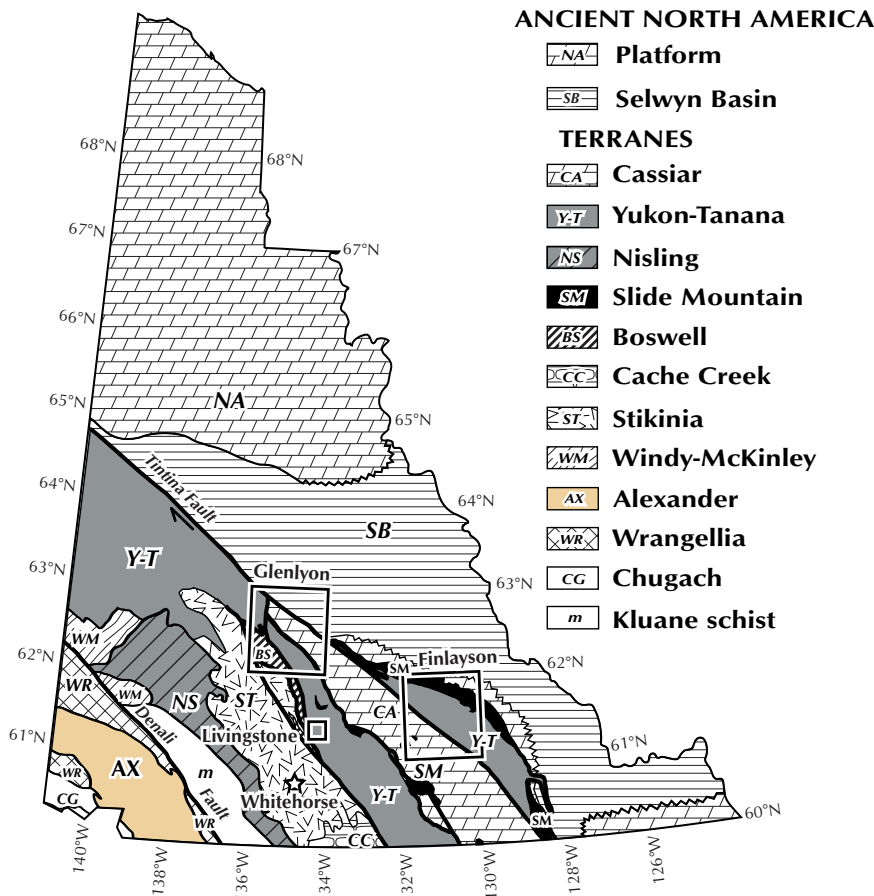


**Figure 1.** Terrane map of Yukon showing the location of the Livingstone Creek area with respect to the Glenlyon and Finlayson Lake areas (modified after Wheeler et al., 1991).



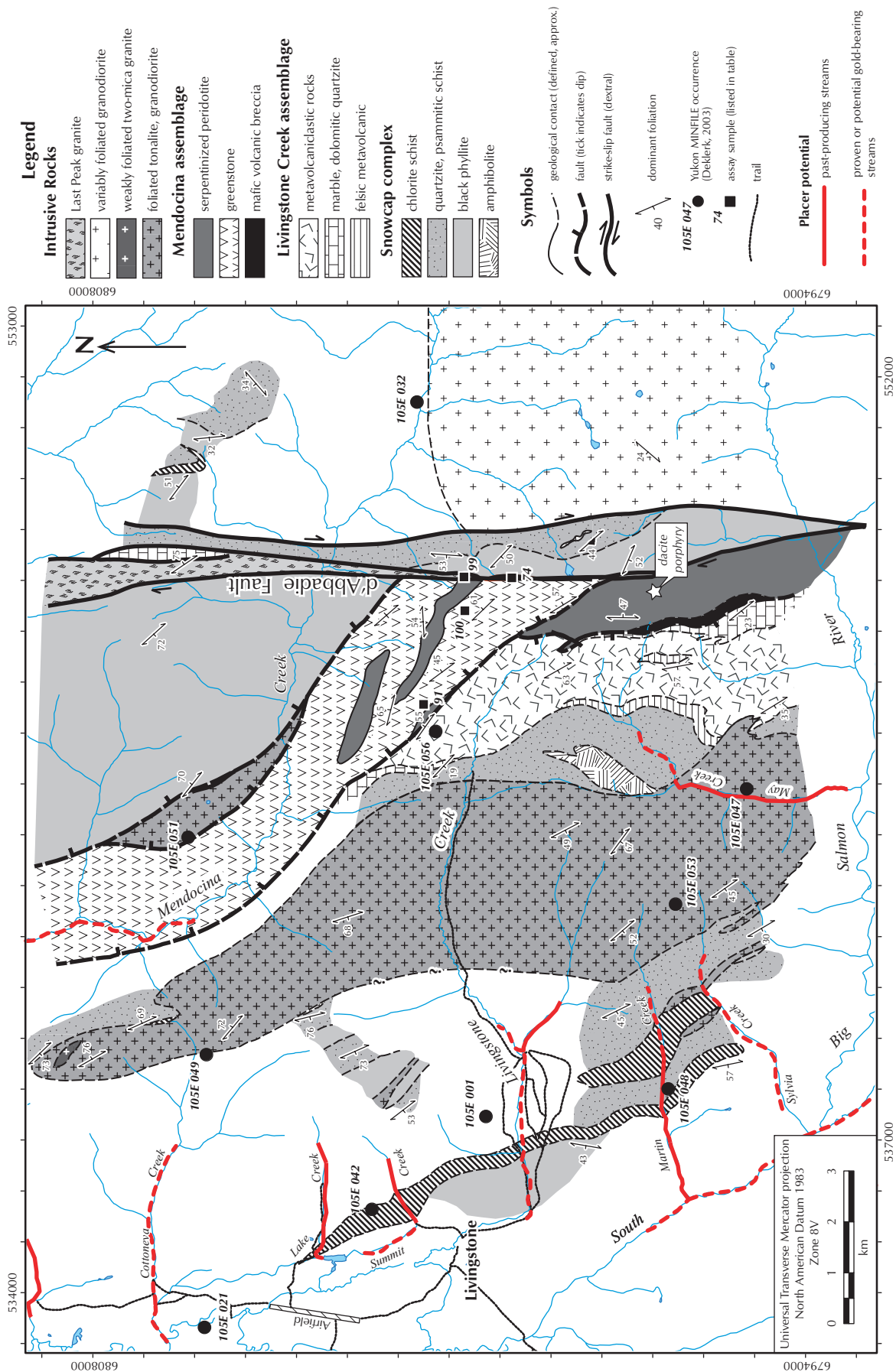


Figure 2. Preliminary bedrock geology map of the Livingstone Creek area. Placer potential from Lipovsky et al. (2001).

and geochronological studies of the Livingstone Creek area, and the adjacent Dycer Creek area to the north, were most recently conducted by Harvey et al. (1996, 1997) and Gallagher (1999).

Bedrock mapping of the Livingstone Creek area at 1:50 000-scale by the Yukon Geological Survey was initiated in 2004 to establish the stratigraphic framework of Yukon-Tanana Terrane (YTT) in the area, and to place the Livingstone Creek area within the context of recent studies of YTT in the Finlayson Lake and Glenlyon areas of Yukon (e.g., Colpron and Yukon-Tanana Working Group, 2001; Colpron, 2003, Fig. 1). This study will provide the basis for compiling unpublished maps produced as part of the graduate theses of Gallagher (1999) and de Keijzer (2000), and unpublished preliminary observations made by J.L. Harvey in 1995-1996. This report summarizes preliminary observations of the bedrock geology of the Livingstone Creek area and some hypotheses to be tested with future field and geochronological studies.

## LAYERED ROCKS

Three distinct successions of metasedimentary and metavolcanic rocks are recognized in YTT of the Livingstone Creek area (Fig. 2). They are, from west to east, the Snowcap complex, the Livingstone Creek assemblage and the Mendocina assemblage. Metasedimentary rocks northeast of Mendocina Creek, and those that occur in strands within and to the east of d'Abbadie fault zone, were previously assigned to Cassiar Terrane by Tempelman-Kluit (1979), Wheeler et al. (1991) and Gordey and Makepeace (2000). However, they are lithologically similar to rocks of the Snowcap complex to the west and are therefore described with this succession. Their terrane affinity is briefly discussed below.

## SNOWCAP COMPLEX

Quartzite, psammitic schist, carbonaceous phyllite and chlorite schist exposed on alpine ridges along Livingstone Creek resemble the Snowcap complex of Glenlyon map area (Colpron et al., 2002, 2003) and are thus tentatively correlated with it. These rocks are divided into two belts by a sheet of tonalite orthogneiss which dips moderately to the southwest (Fig. 2). To the west, and structurally above the orthogneiss, the few exposures of Snowcap complex visited in 2004 consist of intercalated platy quartzite and quartz-muscovite-biotite schist (Fig. 3a). The schist and quartzite are locally graphitic and typically strongly foliated. The quartzite is locally fractured and

injected with quartz veins on the ridge above Summit and Lake creeks. Calcareous chloritic schist is present in ridge exposures between Livingstone and Sylvia creeks. The rock is light to medium green in colour and variably siliceous, suggesting a metasedimentary protolith for this unit. Between Martin and Sylvia creeks, the chlorite schist is associated with <10-cm-thick buff-weathering siliceous marble layers. A single marble layer, ~3 m thick, occurs at the contact between Snowcap quartzite and the tonalite orthogneiss body north of Livingstone Creek.

To the east of, and structurally below the tonalite orthogneiss sheet, the Snowcap complex is only poorly exposed and consists predominantly of psammitic schist, quartzite and amphibolite. The schist is light grey to light green in colour, fine- to medium-grained and composed primarily of muscovite, plagioclase, quartz and minor chlorite. Quartzite exposures are restricted to the immediate vicinity of the tonalite orthogneiss body. It is light grey to white in colour and strongly foliated. North of Livingstone Creek, the quartzite contains biotite porphyroblasts. East of May Creek, garnet porphyroblasts in the quartzite are partially pseudomorphed by chlorite. Dark green to black, fine-grained garnet amphibolite is restricted to a few exposures on the ridge between Livingstone and May creeks (Fig. 2).

A similar succession of graphitic phyllite, quartzite and minor chlorite schist and marble also occurs northeast of Mendocina Creek, within the eastern slice of the d'Abbadie fault zone and along one alpine ridge east of the fault (Fig. 2). Although only a cursory examination of these rocks was conducted in 2004, there is no apparent reason to separate them from those of the Snowcap complex to the west. Harvey et al. (1997) and de Keijzer (2000) reached similar conclusions but considered these rocks as part of Cassiar Terrane following Tempelman-Kluit (1977, 1979, 1984). It is proposed here that these metasedimentary rocks may be part of YTT because they were intruded by Mississippian granitoid plutons to the north of the Livingstone Creek area (Hansen et al., 1989; Gallagher, 1999; de Keijzer, 2000; S.D. Carr, pers. comm., 2000). Tonalite to granodiorite plutons of Mississippian age are characteristic of the metasedimentary basement of YTT (Snowcap complex, Colpron, 2003; Colpron et al., 2003), but not of the miogeoclinal rocks of Cassiar Terrane which only contain rare alkalic plutons of Devonian age.





**Figure 3.** (a) Interlayered and folded quartzite and pelite of the Snowcap complex near Martin Creek; (b) plagioclase-rich aggregates in metavolcanic rock of the Livingstone Creek assemblage, east of May Creek; (c) band of felsic metavolcanic rock (white) folded within quartz-plagioclase-chlorite schist of the Livingstone Creek assemblage, east of May Creek; (d) serpentinite injected by felsic dyke at the headwater of May Creek. Note silicification halo (light grey) near felsic veins.

### LIVINGSTONE CREEK ASSEMBLAGE

The succession of light green to light grey quartzite, quartz-muscovite-plagioclase-chlorite schist and minor greenstone exposed at the headwaters of May and Livingstone creeks was informally named the Livingstone Creek assemblage by Harvey et al. (1997). This name is provisionally retained in this report. The rock is generally fine grained, but locally contains chlorite discs up to 5 mm in diameter and plagioclase-rich aggregates up to 5 cm long (lapillis?) suggesting a volcanoclastic origin (Fig. 3b). Massive chlorite schist is rare and commonly contains fine-grained hornblende in addition to chlorite, plagioclase and

epidote. Rocks of the Livingstone Creek assemblage are generally less penetratively deformed than rocks of the Snowcap complex to the west.

Light green quartzite and schist of the Livingstone Creek assemblage are gradational with buff-weathering dolomitic quartzite and marble to the east. The quartzite preserves well-rounded quartz grains and contains 1- to 2-cm-thick marble horizons. It grades into massive dolomitic marble to the east. Light grey marble also occurs as 1- to 2-m-thick layers in the metavolcanoclastic rock, most abundantly north of Livingstone Creek.



Fine-grained, white-weathering muscovite-plagioclase-quartz schist occurs in horizons 10 cm to 1 to 2 m thick along the western contact of the Livingstone Creek assemblage, as well as within the metavolcanic rocks (Fig. 2). This white schist is typically finely laminated and intercalated with the light green schist and quartzite (Fig. 3c). It locally contains 1 to 2 mm quartz eyes. This rock is interpreted as a felsic metavolcanic rock and is likely derived from a tuffaceous protolith.

Rocks of the Livingstone Creek assemblage resemble metavolcanic rocks of the Lower Mississippian Little Kalzas formation in the Glenlyon map area (Colpron, 1999; Colpron et al., 2002, 2003). Like the Little Kalzas formation, rocks of the Livingstone Creek assemblage were likely deposited in an arc setting.

### MENDOCINA ASSEMBLAGE

The ~3-km-wide, northwest-trending belt of greenstone and associated serpentinite which extends from the headwaters of Livingstone Creek into lower Mendocina Creek were described by Harvey et al. (1997) as the Mendocina assemblage. This name is provisionally retained for this report. The greenstone is generally fine grained and phyllitic, rarely massive. Patches of medium- to coarse-grained plagioclase-hornblende-rich greenstone occur sporadically in the finer grained rock and likely represent dismembered gabbro dykes. Metagabbro is most commonly found in proximity to, and within, the serpentinite.

Serpentinite forms a large massif at the headwater of May Creek, and occurs as smaller bodies within the greenstone north of Livingstone Creek (Fig. 2). The rock is generally bottle-green in colour and soft, although silicification patches within the serpentinite are common. They form centimetre to metre patches and appear related to abundant small felsic dykes and a dacite porphyry plug found in the May Creek massif (Fig. 3d). Coarse magnetite is common in association with silicification patches.

A few thin (<5 m) marble layers are present in the greenstone near d'Abbadie Fault. A single band (<20 m wide) of felsic schist occurs in association with carbonaceous phyllite within greenstone of the Mendocina assemblage. Graphitic phyllite is common at the contacts between greenstone and serpentinite north of Livingstone Creek.

The association of greenstone, metagabbro, serpentinite and minor carbonaceous phyllite and felsic schist of the

Mendocina assemblage resembles the Upper Devonian Fire Lake formation of the Finlayson Lake district (Murphy et al., 2001, 2002) and is tentatively correlated with this unit. The Fire Lake formation is host to the Fyre Lake polymetallic massive sulphide deposit (Yukon MINFILE 105G 034, Deklerk, 2003).

### INTRUSIVE ROCKS

At least five distinct suites of intrusive rocks are present in the Livingstone Creek area. The oldest suite corresponds to strongly foliated and locally gneissic tonalite to granodiorite. This suite occurs as one large sheet and a few dykes within metasedimentary rocks of the Snowcap complex (Fig. 2). The rock is generally fine-grained and light to medium grey in colour. Hornblende and biotite are common constituents and are locally concentrated in melanocratic bands up to 10 cm wide (Fig. 4a). Muscovite locally makes up to 15% of the granodiorite. These rocks resemble foliated tonalite-granodiorite of the Simpson Range plutonic suite (ca. 345 to 355 Ma) which is typical of YTT in Yukon (e.g., Mortensen and Jilson, 1985; Stevens, 1994; Colpron et al., 2002; Ryan and Gordey, 2004).

Weakly foliated two-mica granite is a volumetrically small but widespread intrusive suite in the Livingstone Creek area. It occurs as: (1) small dykes in psammitic schist of the Snowcap complex south of Livingstone Creek; (2) a >3-m-wide lens at the contact between greenstone and serpentinite of the Mendocina assemblage north of Livingstone Creek; and (3) a small plug (<100 m) and a dyke swarm (Fig. 4b) in metatonalite north of the headwaters of Cottoneva Creek. The rock is usually white in colour, medium- to coarse-grained and locally pegmatitic. Dykes of two-mica granite are typically 10 to 20 cm wide (up to 40 cm locally) and concordant with the dominant foliation. The dykes are invariably weakly foliated and locally display pinch-and-swell structures suggesting that the granite was emplaced during development of the dominant foliation (Fig. 4c).

Variably foliated diorite to granodiorite exposed east of d'Abbadie Fault, between Mendocina Creek and the South Big Salmon River, is generally considered to be Paleozoic in age on the basis of the localized high strain in the granodiorite and of a poorly resolved discordant U-Pb zircon age (Tempelman-Kluit, 1984; Hansen et al., 1989; Harvey et al., 1997). The rock is most commonly K-feldspar porphyritic and weakly foliated (Fig. 4d), but locally has a shallow, northwest-dipping protomylonitic



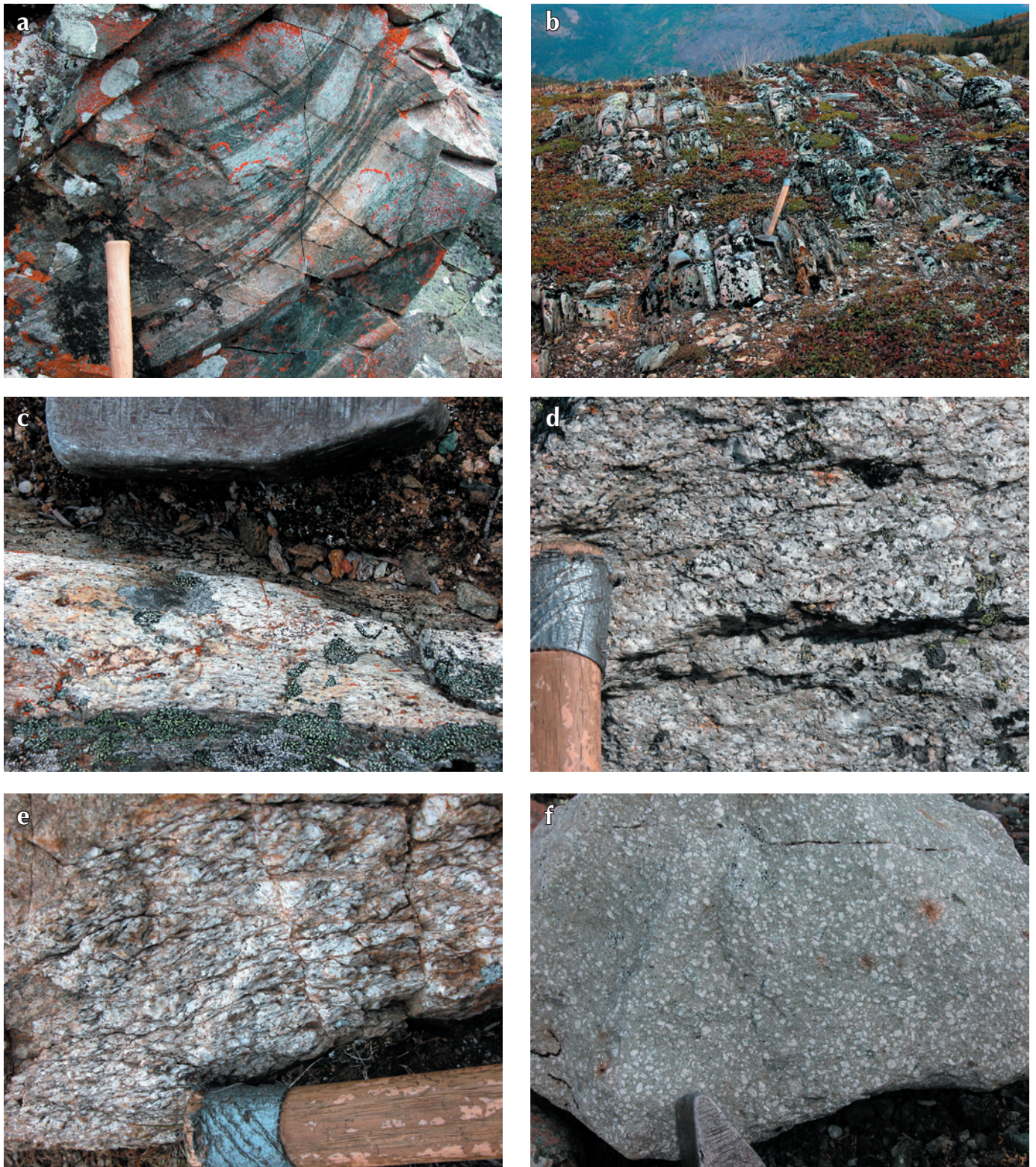


**Figure 4.** (a) Banded hornblende tonalite gneiss, south of Livingstone Creek; (b) steeply dipping two-mica granite dykes (white) intruding grey tonalite gneiss; headwaters of Cottoneva Creek; (c) close-up of a granite dyke (white) showing development of the regional foliation in the dyke. Wall rocks are grey tonalite orthogneiss; headwaters of Cottoneva Creek; (d) weakly foliated K-feldspar porphyritic granodiorite east of d'Abbadie Fault; (e) coarse-grained, foliated Last Peak leucogranite (ca. 96 Ma, Gallagher, 1999) within the d'Abbadie fault zone north of Mendocina Creek; (f) dacite porphyry.



fabric with K-feldspar porphyroclasts, and shear bands indicating a top-to-the-east sense of shear. The granodiorite is cut by a less deformed, fine-grained hornblende-biotite diorite. Along its western edge, the granodiorite body is strongly altered and truncated by the vertical d'Abbadie fault zone (Fig. 2). Although it is locally highly strained, the granodiorite has similar composition to granodiorite of the Cretaceous Quiet Lake Batholith to the southeast, which is locally foliated (Tempelman-Kluit, 1977), and for which preliminary geochronological analysis indicates a complex zoning pattern of zircons with Proterozoic-, Paleozoic- and Cretaceous-age domains (C.J.R. Hart, pers. comm., 2004). Further field and geochronological studies of this granodiorite body are required to precisely determine its age and relationship to the adjacent Quiet Lake Batholith.

The Last Peak granite (Harvey et al., 1997; Gallagher, 1999) occurs in the northern part of the map area within the western strand of the d'Abbadie fault zone (Fig. 2). It consists of a variably foliated and altered, medium- to coarse-grained white biotite granite (Fig. 4e). Gallagher (1999) reported a U-Pb monazite age of ca. 96 Ma from the Last Peak granite and suggested that the granite was emplaced during deformation along the d'Abbadie fault zone.

Finally, a small plug of dacite porphyry (30 x 80 m) intruded the serpentinite at the headwaters of May Creek (Fig. 2). The porphyry consists of a light green fine-grained dacite matrix which supports up to 25% plagioclase (up to 7 mm long) and rare quartz phenocrysts (Fig. 4f). Contacts with the serpentinite are covered by talus, but the fresh and undeformed nature of the dacite clearly suggests a relatively young age for this rock. Numerous small felsic dykes commonly found in brecciated parts of the serpentinite are inferred to be related to this dacitic phase of intrusion.

## STRUCTURE

At least three generations of ductile structures are preserved in rocks of the Livingstone Creek area. The earliest structures correspond to a pervasive foliation and rare isoclinal folds (Fig. 5a) which are for the most part transposed by the second generation of structures. The second phase of deformation resulted in the development of a regional, penetrative transposition foliation, which is axial planar to tight to isoclinal folds. The transposition fabric is locally protomylonitic within the tonalite gneiss body and along lithological contacts in the western part

of the area. It generally dips moderately to the southwest in the western part of the Livingstone Creek area, and moderately to steeply to the northeast, northeast of the fault inferred to mark the contact between the Mendocina assemblage and rocks to the west (Fig. 2). It commonly contains an elongation lineation. East of d'Abbadie fault zone, the dominant foliation typically dips gently to the west-northwest. The dominant foliation is everywhere folded by northeast-verging open folds (Fig. 5b).

The d'Abbadie fault zone is a steep, north-striking brittle-ductile fault zone which extends across the eastern part of the Livingstone Creek area (Figs. 2, 5c). Deformation features related to the d'Abbadie Fault are restricted to localized cataclastic structures (cm-scale) and development of a steeply dipping anastomosing cleavage (Fig. 4e). Gallagher (1999) reports the presence of kinematic indicators consistent with dextral strike-slip displacement along d'Abbadie Fault. He also suggested that the ca. 96 Ma Last Peak granite was emplaced during displacement along d'Abbadie Fault. An apparent dextral offset of ~4 km has been estimated on d'Abbadie Fault (Harvey et al., 1996). Detailed descriptions of the structural style and evolution of adjacent areas to the north are presented in Gallagher (1999) and de Keijzer (2000).

## MINERAL POTENTIAL

An estimated 50,000 ounces (1.6 million grams) of gold has been recovered from placers of the Livingstone Creek area since 1898 (W. LeBarge, pers. comm., 2004); however, its lode source remains elusive. The gold typically occurs as coarse (>1 cm) nuggets and is commonly associated with magnetite, suggesting a nearby source and potentially a skarn style of mineralization. Alternatively, the coarse magnetite (and the gold) may have been derived from serpentinite of the Mendocina assemblage to the east; although this would have required more than 10 km of westerly glacial transport of the gravels prior to deposition in the gold-bearing streams (Fig. 2).

Quartz veins containing disseminated sulphide minerals occur as foliaform veins in the bedrock at the headwaters of the past-producing streams and were considered a potential source for some of the gold (Stroink and Friedrich, 1992). However, the lack of magnetite and coarse gold in the veins argues against them being the major source for the placer gold. Despite the numerous



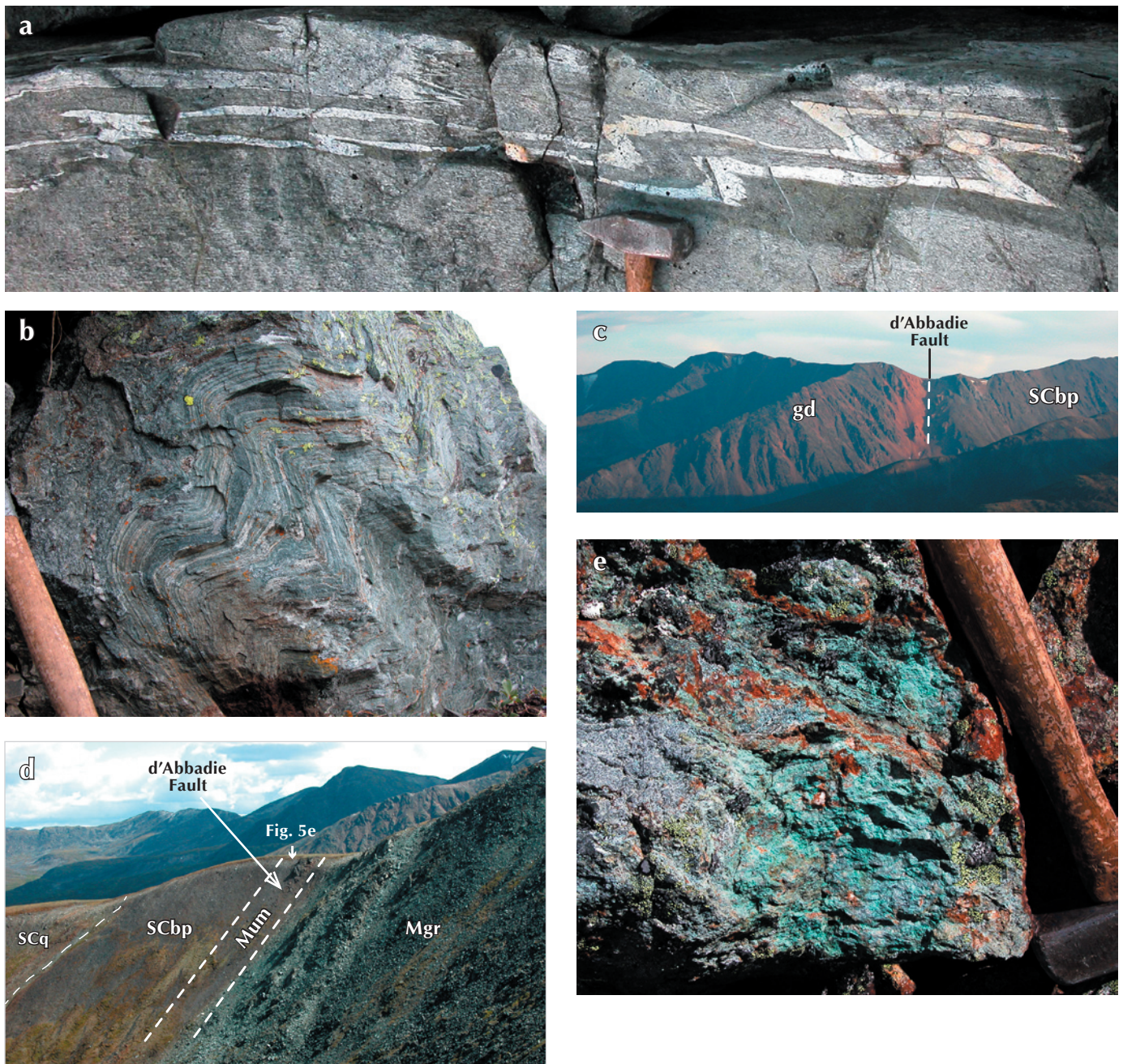


**Figure 5.** (a) Two phases of folds in tonalite orthogneiss south of Livingstone Creek. Early isoclinal folds are refolded by tight folds associated with the regional transposition foliation; (b) looking south at northeast-vergent open folds of the transposition foliation in light green quartzite of the Livingstone Creek assemblage, north of Livingstone Creek; (c) looking south at d'Abbadie fault zone between Mendocina Creek and South Big Salmon River. At this location, the fault juxtaposes black graphitic phyllite of the Snowcap complex (SCbp) against variably foliated granodiorite (gd) to the east. Note strong gossan along the fault; (d) oblique view to the southeast of the d'Abbadie Fault near Mendocina Creek. Here the fault juxtaposes greenstone of the Mendocina assemblage (Mgr) against black phyllite (SCbp) and quartzite (SCq) of the Snowcap complex to the east. A sliver of silicified ultramafic rock (Mum) occurs within the fault; (e) silicified ultramafic rock with annabergite and nickeline mineralized rock in the d'Abbadie fault zone (sample 74-1 to -4; Table 2).

**Table 1.** Yukon MINFILE occurrences for the Livingstone Creek area (Deklerk, 2003).

MINFILE	Name	Status	Deposit type	Commodities
105E 001	Livingston	showing	vein	Au-Ag-Pb-Cu
105E 020	Sylvia	showing	vein	Pb-Zn-Cu-Au-Ag
105E 021	Cottoneva	unknown	unknown	
105E 032	Mendocina	unknown	unknown	
105E 042	Lake	unknown	unknown	
105E 047	Maybe	anomaly	unknown	Pb-Au
105E 048	Marbee	unknown	unknown	
105E 049	Little Violet	unknown	unknown	
105E 051	Gord	unknown	unknown	
105E 053	Deet	showing	vein	Ag-Au-Zn-Sb-Pb-As
105E 056	Brenda	unknown	unknown	

signs of past bedrock exploration activity in the area, there is very little documentation of this work (Table 1).

The possible correlation of greenstone and serpentinite of the Mendocina assemblage with the Fire Lake formation opens the potential for this belt to host copper-cobalt-gold massive sulphide mineralization similar to that at the Fyre Lake deposit in the Finlayson Lake district (Yukon MINFILE 105G 034, Deklerk, 2003; Sebert et al. 2004; Hunt, 2002). Disseminated pyrite and pyrrhotite occur at several locations within the greenstone, and malachite and chalcopyrite were observed at one locality (Fig. 2; Table 2, samples 91, 100).

Silicified ultramafic rock in the d'Abbadie fault zone are mineralized in nickeline and annabergite (Figs. 5d,e) and samples returned anomalous values in nickel, cobalt, arsenic and antimony (sample 74-1 to -4; Table 2). This rock was likely altered by circulation of hydrothermal fluids along d'Abbadie Fault, thereby establishing the potential for further mineralization along this fault zone. Well-developed gossans along segments of the d'Abbadie Fault (Fig. 5c) are consistent with fluid migration along the fault.

## ACKNOWLEDGEMENTS

Eri Boye and Jim Coates provided assistance in the field. Karl Ziehe of Heli Dynamics Ltd. of Whitehorse got us there, and back, safely. Dr. Sharon Carr of Carleton University is thanked for providing unpublished notes and maps from her students (C. Gallagher and J.L. Harvey), reading an earlier version of this report and continuing discussions.

## REFERENCES

- Bostock, H.S. and Lees, E.J., 1938. Laberge map-area, Yukon. Geological Survey of Canada, Memoir 217, 33 p.
- Colpron, M., 1999. Glenlyon Project: Preliminary stratigraphy and structure of Yukon-Tanana Terrane, Little Kalzas Lake area, central Yukon (105L/13). *In: Yukon Exploration and Geology 1998*, C.F. Roots and D.S. Emond (eds.), Exploration and Geological Services Division, Yukon Region, Indian and Northern Affairs Canada, p. 63-72.
- Colpron, M., 2003. A stratigraphic framework for the pericratonic terranes of the northern Cordillera. Geological Association of Canada – Mineralogical Association of Canada – Society of Economic Geologists Joint Annual Meeting, Abstracts, vol. 28.
- Colpron, M. and Yukon-Tanana Working Group, 2001. Ancient Pacific Margin – An update on stratigraphic comparison of potential volcanogenic massive sulphide-hosting successions of Yukon-Tanana Terrane, northern British Columbia and Yukon. *In: Yukon Exploration and Geology 2000*, D.S. Emond and L.H. Weston (eds.), Exploration and Geological Services Division, Yukon Region, Indian and Northern Affairs Canada, p. 97-110.



**Table 2.** Selected assay results from the Livingstone Creek area.

		74-1	74-2	74-3	74-4	91	99-1	99-2	100
		silicified ultramafic rock nickeline + annabergite				disseminated pyrite- pyrrhotite	altered granite		disseminated pyrite- chalcopyrite
Mo	ppm	1.11	1.35	1.05	1.53	0.77	1.28	2.05	0.65
Cu	ppm	9.69	12.44	5.02	18.83	73.98	102.01	49.14	280.00
Pb	ppm	1.30	9.25	1.63	3.39	0.43	2.26	7.39	0.52
Zn	ppm	6.1	34.6	14.3	20.7	47.0	56.9	121.7	41.0
Ag	ppb	38	57	33	69	14	82	49	895
Ni	ppm	741.1	79.7	45.8	3409.5	35.9	26.9	42.4	35.3
Co	ppm	32.7	6.9	2.8	140.3	30.8	4.1	7.2	48.6
Mn	ppm	47	30	42	35	617	41	88	459
Fe	%	1.19	0.76	1.23	1.75	4.50	1.92	3.63	4.79
As	ppm	1414.9	1576.6	426.8	3068.6	1.6	10.2	10.0	1.0
U	ppm	0.1	0.1	0.1	0.1	<0.1	0.3	0.4	<0.1
Au	ppb	4.0	0.4	0.8	3.4	0.5	0.9	2.2	2.5
Th	ppm	0.1	<0.1	0.1	<0.1	<0.1	0.3	0.8	<0.1
Sr	ppm	5.2	11.9	17.2	1.5	6.5	6.1	4.1	12.1
Cd	ppm	0.06	0.16	0.05	0.34	0.04	0.11	0.17	0.04
Sb	ppm	137.25	271.86	35.14	1822.10	0.68	8.80	10.20	0.24
Bi	ppm	0.03	0.03	0.07	0.03	<0.02	0.05	0.08	<0.02
V	ppm	9	21	8	22	102	100	30	81
Ca	%	0.02	0.02	0.01	0.01	0.85	0.01	0.01	0.92
P	%	0.001	0.001	0.003	<0.001	0.096	0.036	0.034	0.134
La	ppm	1.1	<0.5	0.6	<0.5	1.6	0.9	2.7	0.9
Cr	ppm	173.4	217.1	66.2	269.5	42.4	49.9	26.0	39.0
Mg	%	0.02	0.02	0.01	0.02	1.70	0.01	0.02	1.97
Ba	ppm	112.2	12.1	38.3	34.1	15.1	9.9	31.5	40.1
Ti	%	<0.001	<0.001	0.001	<0.001	0.332	0.003	0.003	0.430
B	ppm	<1	<1	<1	<1	1	1	1	<1
Al	%	0.19	0.25	0.19	0.28	1.90	0.74	0.33	1.85
Na	%	0.007	0.002	0.001	0.001	0.055	0.003	0.002	0.011
K	%	0.01	0.01	0.03	<0.01	0.05	0.01	0.06	0.01
W	ppm	0.1	0.2	<0.1	0.2	<0.1	0.3	0.4	<0.1
Sc	ppm	0.6	1.4	0.6	1.6	3.3	6.7	2.6	1.6
Tl	ppm	0.13	0.37	0.04	0.67	<0.02	0.02	0.07	<0.02
S	%	0.11	0.01	<0.01	1.24	0.43	<0.01	<0.01	1.5
Hg	ppb	91	157	51	158	<5	31	41	<5
Se	ppm	0.7	0.9	0.3	2.9	0.9	0.2	0.2	1.7
Te	ppm	0.02	0.04	0.03	0.07	<0.02	0.04	0.04	0.03
Ga	ppm	1.9	1.7	0.8	13.4	4.9	2.7	1.3	3.0
UTM-E		548085	548085	548085	548085	545566	548078	548078	547410
UTM-N		6799693	6799693	6799693	6799693	6801492	6800718	6800718	6800686

Note: Sample were analysed by ICP-MS at Acme Analytical Laboratories in Vancouver, British Columbia.



- Colpron, M., Murphy, D.C., Nelson, J.L., Roots, C.F., Gladwin, K., Gordey, S.P. and Abbott, J.G., 2003. Yukon Targeted Geoscience Initiative, Part 1: Results of accelerated bedrock mapping in Glenlyon (105L/1-7,11-14) and northeast Carmacks (115I/9,16) areas, central Yukon. *In: Yukon Exploration and Geology 2002*, D.S. Emond and L.L. Lewis (eds.), Exploration and Geological Services Division, Yukon Region, Indian and Northern Affairs Canada, p. 85-108.
- Colpron, M., Murphy, D.C., Nelson, J.L., Roots, C.F., Gladwin, K., Gordey, S.P., Abbott, G. and Lipovsky, P.S., 2002. Preliminary geological map of Glenlyon (105L/1-7,11-14) and northeast Carmacks (115I/9,16) areas, Yukon Territory (1:125 000 scale). Exploration and Geological Services Division, Yukon Region, Indian and Northern Affairs Canada, Open File 2002-9; also Geological Survey of Canada, Open File 1457.
- de Keijzer, M., Williams, P.F. and Brown, R.L., 1999. Kilometre-scale folding in the Teslin zone, northern Canadian Cordillera, and its tectonic implications for the accretion of the Yukon-Tanana Terrane to North America. *Canadian Journal of Earth Sciences*, vol. 39, p. 479-494.
- de Keijzer, M., 2000. Tectonic evolution of the Teslin zone and the western Cassiar terrane, northern Canadian Cordillera. Unpublished Ph.D. thesis. University of New Brunswick, 391 p.
- Deklerk, R., 2003. Yukon MINFILE 2003 - A database of mineral occurrences. Yukon Geological Survey, CD-ROM.
- Gallagher, C., Brown, R.L. and Carr, S.D., 1998. Structural geometry of the Cassiar Platform and Teslin zone, Dycer Creek area, Yukon. *In: Slave-Northern Cordillera Lithospheric Evolution (SNORCLE) Transect and Cordilleran Tectonic Workshop Meeting*, F. Cook and P. Erdmer (eds.), Lithoprobe Report No. 64, p. 139-151.
- Gallagher, C.S., 1999. Regional-scale transposition and late large-scale folding in the Teslin Zone, Pelly Mountains, Yukon. Unpublished M.Sc. thesis. Carleton University, 199 p.
- Gordey, S.P. and Makepeace, A.J., 2000. Bedrock geology, Yukon Territory. Geological Survey of Canada, Open File 3754, 1:1 000 000; also Exploration and Geological Services Division, Yukon, Indian and Northern Affairs Canada, Open File 2001-1.
- Hansen, V.L., 1989. Structural and kinematic evolution of the Teslin suture zone, Yukon: Record of an ancient transpressional margin. *Journal of Structural Geology*, vol. 11, p. 717-733.
- Hansen, V.L., 1992. Backflow and margin-parallel shear within an ancient subduction complex. *Geology*, vol. 20, p. 71-74.
- Hansen, V.L., Mortensen, J.K. and Armstrong, R.L., 1989. U-Pb, Rb-Sr, and K-Ar isotopic constraints for ductile deformation and related metamorphism in the Teslin suture zone, Yukon-Tanana Terrane, south-central Yukon. *Canadian Journal of Earth Sciences*, vol. 26, p. 2224-2235.
- Harvey, J.L., Brown, R.L. and Carr, S.D., 1996. Progress in structural mapping in the Teslin suture zone, Big Salmon Range, central Yukon Territory. *In: Slave-Northern Cordillera Lithospheric Evolution (SNORCLE) Transect and Cordilleran Tectonic Workshop Meeting*, F. Cook and P. Erdmer (eds.), Lithoprobe Report No. 50, p. 33-44.
- Harvey, J.L., Carr, S.D., Brown, R.L. and Gallagher, C., 1997. Deformation history and geochronology of plutonic rocks near the d'Abbadie Fault, Big Salmon Range, Yukon. *In: Slave-Northern Cordillera Lithospheric Evolution (SNORCLE) Transect and Cordilleran Tectonic Workshop Meeting*, F. Cook and P. Erdmer (eds.), Lithoprobe Report No. 56, p. 103-114.
- Hunt, J.A., 2002. Volcanic-associated massive sulphide (VMS) mineralization in the Yukon-Tanana Terrane and coeval strata of the North American miogeocline, in the Yukon and adjacent areas. Exploration and Geological Services Division, Yukon Region, Indian and Northern Affairs Canada, Bulletin 12, 107 p.
- Levson, V., 1992. The sedimentology of Pleistocene deposits associated with placer gold bearing gravels in the Livingstone Creek area, Yukon Territory. *In: Yukon Geology*, Exploration and Geological Services Division, Yukon Region, Indian and Northern Affairs Canada, Volume 3, p. 99-132.
- Lipovsky, P.S., LeBarge, W., Bond, J.D. and Lowey, G., 2001. Yukon placer activity map. Exploration and Geological Services Division, Yukon Region, Indian and Northern Affairs Canada, Open File 2001-30, 1:1 000 000 scale.

- Mortensen, J.K. and Jilson, G.A., 1985. Evolution of the Yukon-Tanana terrane: evidence from southeastern Yukon Territory. *Geology*, vol. 13, p. 806-810.
- Murphy, D.C., Colpron, M., Roots, C.F., Gordey, S.P. and Abbott, J.G., 2002. Finlayson Lake Targeted Geoscience Initiative (southeastern Yukon), Part 1: Bedrock geology. *In: Yukon Exploration and Geology 2001*, D.S. Emond, L.H. Weston and L.L. Lewis (eds.), Exploration and Geological Services Division, Yukon Region, Indian and Northern Affairs Canada, p. 189-207.
- Murphy, D.C., Colpron, M., Gordey, S.P., Roots, C.F., Abbott, G. and Lipovsky, P.S., 2001. Preliminary bedrock geological map of northern Finlayson Lake area (NTS 105G), Yukon Territory (1:100 000 scale). Exploration and Geological Services Division, Yukon Region, Indian and Northern Affairs Canada, Open File 2001-33.
- Ryan, J.J. and Gordey, S.P., 2004. Geology, Stewart River area (Parts of 115 N/1,2,7,8 and 115 O/2-12), Yukon Territory. Geological Survey of Canada, Open File 4641, 1:100 000 scale.
- Sebert, C., Hunt, J.A. and Foreman, I.J., 2004. Geology and lithogeochemistry of the Fyre Lake copper-cobalt-gold sulphide-magnetite deposit, southeastern Yukon. Yukon Geological Survey, Open File 2004-17, 46 p.
- Simard, R.-L., 2003. Geological map of southern Semenof Hills (part of NTS 105E/1,7,8), south-central Yukon (1:50 000 scale). Yukon Geological Survey, Open File 2003-12.
- Stevens, R.A., 1994. Geology of the Teslin suture zone in parts of Laberge (105E/1), Quiet Lake (105F/4) and Teslin (105C/11, 13, 14) map areas, Yukon Territory. Geological Survey of Canada, Open File 2768, 1:50 000 scale.
- Stroink, L. and Friedrich, G., 1992. Gold-sulphide quartz veins in metamorphic rocks as a possible source for placer gold in the Livingstone Creek area, Yukon Territory, Canada. *In: Yukon Geology, Exploration and Geological Services Division, Yukon Region, Indian and Northern Affairs Canada*, vol. 3, p. 87-98.
- Tempelman-Kluit, D.J., 1977. Quiet Lake (105F) and Finlayson Lake (105G) map areas, Yukon Territory. Geological Survey of Canada, Open File 486, 1:250 000 scale.
- Tempelman-Kluit, D.J., 1979. Transported cataclasite, ophiolite and granodiorite in Yukon: evidence of arc-continent collision. Geological Survey of Canada, Paper 79-14, 27 p.
- Tempelman-Kluit, D.J., 1984. Geology, Laberge (105E) and Carmacks (105I), Yukon Territory. Geological Survey of Canada, Open File 1101, 1:250 000 scale.
- Wheeler, J.O., Brookfield, A.J., Gabrielse, H., Monger, J.W.H., Tipper, H.W. and Woodsworth, G.J., 1991. Terrane Map of the Canadian Cordillera. Geological Survey of Canada, Map 1713A, 1:2 000 000 scale.





# Flood basalts of the Wrangellia Terrane, southwest Yukon: Implications for the formation of oceanic plateaus, continental crust and Ni-Cu-PGE mineralization

*Andrew R. Greene<sup>1</sup>, James S. Scoates and Dominique Weis*  
*Pacific Centre for Isotopic and Geochemical Research<sup>2</sup>*

*Steve Israel*  
*Yukon Geological Survey*

Greene, A.R., Scoates, J.S., Weis, D. and Israel, S., 2005. Flood basalts of the Wrangellia Terrane, southwest Yukon: Implications for the formation of oceanic plateaus, continental crust and Ni-Cu-PGE mineralization. *In: Yukon Exploration and Geology 2004*, D.S. Emond, L.L. Lewis and G.D. Bradshaw (eds.), Yukon Geological Survey, p. 109-120.

## ABSTRACT

The Wrangellia Terrane along the northwest margin of North America is an extensive accreted oceanic plateau. These volcanic sequences erupted onto an extinct island arc in less than 5 million years at ca. 230 Ma. Triassic Wrangellia basalts and intrusions form a 1 to 10 km-wide linear belt of mafic and ultramafic rocks extending 300 km across southwest Yukon. A total of 85 samples were collected for geochemical and isotopic analysis from 10 widespread areas along the entire length of the linear belt. Field observations during the summer of 2004, and a synthesis of previous research for the Yukon portion of Wrangellia, are part of a larger research project involving Wrangellia basalts extending from Vancouver Island to central Alaska. The Wrangellia volcanic sequences represent one of the finest examples of an accreted oceanic plateau worldwide. They provide an excellent opportunity to gain a better understanding of the mantle source of oceanic plateaus and to assess the role of accretion of oceanic plateaus in continental growth.

## RÉSUMÉ

La Wrangellie est un vaste terrane constitué d'un plateau océanique accrété le long de la marge nord-ouest de l'Amérique du Nord. Ces séquences volcaniques se sont formées sur un arc insulaire éteint en moins de 5 millions d'années vers 230 Ma. Les basaltes et intrusions triasiques de la Wrangellie forment une zone linéaire de roches mafiques et ultramafiques de un à dix kilomètres de largeur qui s'allonge sur 300 km dans le sud-ouest du Yukon. Au total, 85 échantillons ont été recueillis pour des analyses géochimiques et isotopiques dans dix régions réparties sur toute la longueur de la zone linéaire. Les observations de terrain faites à l'été 2004 et la synthèse des recherches antérieures dans la partie de la Wrangellie située au Yukon s'inscrivent dans le cadre d'un vaste projet de recherche portant sur les basaltes de la Wrangellie qui s'étendent de l'île de Vancouver jusqu'au centre de l'Alaska. Les séquences volcaniques de la Wrangellie, qui constituent un des meilleurs exemples de plateau océanique accrété au monde, offrent une excellente occasion de mieux comprendre la source mantellique des plateaux océaniques et d'évaluer le rôle de l'accrétion de ces plateaux dans l'expansion des continents.

<sup>1</sup>agreene@eos.ubc.ca

<sup>2</sup>Department of Earth and Ocean Sciences, University of British Columbia, Vancouver, British Columbia, Canada V6T 1Z4

## INTRODUCTION

A large part of the Wrangellia Terrane consists of an oceanic plateau, a vast outpouring of basalt and more Mg-rich magma that erupted onto the ocean floor, which was then subsequently accreted to the western margin of the North American plate. Wrangellia flood basalts exposed in southwest Yukon are believed to have originated by melting in a mantle plume and they constitute the oceanic variety of a Large Igneous Province (LIP) that erupted onto the extinct Pennsylvanian and Permian Sicker-Skolai island arc.

Oceanic plateaus represent the largest known magmatic events on Earth. Enormous volumes of magma erupt in ocean basins over geologically short time intervals (several million years), and are suspected to have catastrophic effects on the climate and biosphere (Wignall, 2001). Throughout Earth's history, the formation and accretion of oceanic plateaus may have significantly contributed to the growth of continents (Kroenke, 1974; Ben-Avraham et al., 1981; Nur and Ben-Avraham, 1982; Schubert and Sandwell, 1989; Abouchami et al., 1990; Richards et al., 1991; Boher et al., 1992; Abbott and Mooney, 1995; Kimura and Ludden, 1995; Saunders et al., 1996; Stein and Goldstein, 1996; Albarède, 1998; Kerr et al., 2000; Kerr, 2003). However, accreted oceanic plateaus can be difficult to distinguish in the geological record, and well-preserved examples are rare. Exposures of Triassic Wrangellia flood-volcanic sequences represent one of the finest examples of an accreted oceanic plateau worldwide and offer an exceptional opportunity to closely examine the on-land remains of such a phenomenon.

The present overview is a preliminary report of fieldwork within the Kluane Ranges of southwest Yukon and a summary of previous research on the Wrangellia Terrane. This paper represents one component of a larger research project on Wrangellia flood basalts extending from Vancouver Island to central Alaska. The principal objectives of this project are to gain a better understanding of the mantle source of oceanic plateaus and to determine the role of accretion of oceanic plateaus in the growth of continental crust. Ultimately, the goal of the ongoing larger study is to characterize the composition of the Wrangellia oceanic plateau. Then, using this constrained elemental reservoir, we aim to model the effect of adding oceanic plateaus to continental crust.

Intrusive complexes within the Wrangellia Terrane have distinct similarities to intrusions related to some of the

world's richest ore deposits. For example, intrusions related to the Siberian LIP, the continental equivalent of an oceanic plateau, host the Noril'sk deposit in Siberia, which is arguably the richest ore deposit in the world. To date, no large economically exploitable copper-nickel-PGE (platinum group elements) deposits have been discovered in the Yukon segment of the Wrangellia Terrane despite the fact that mineralization in the intrusive complexes resembles that at Noril'sk (Hulbert, 1997). This is surprising, because the essential conditions required to form a Noril'sk-type deposit, specifically the emplacement of hot, Ni- and PGE-rich picritic magmas into S-bearing sediments, appear to be present in the Wrangellia Terrane. In this respect, this project will provide information to allow better evaluation of the potential for magmatic Ni-Cu-PGE mineralization in the Wrangellia Terrane.

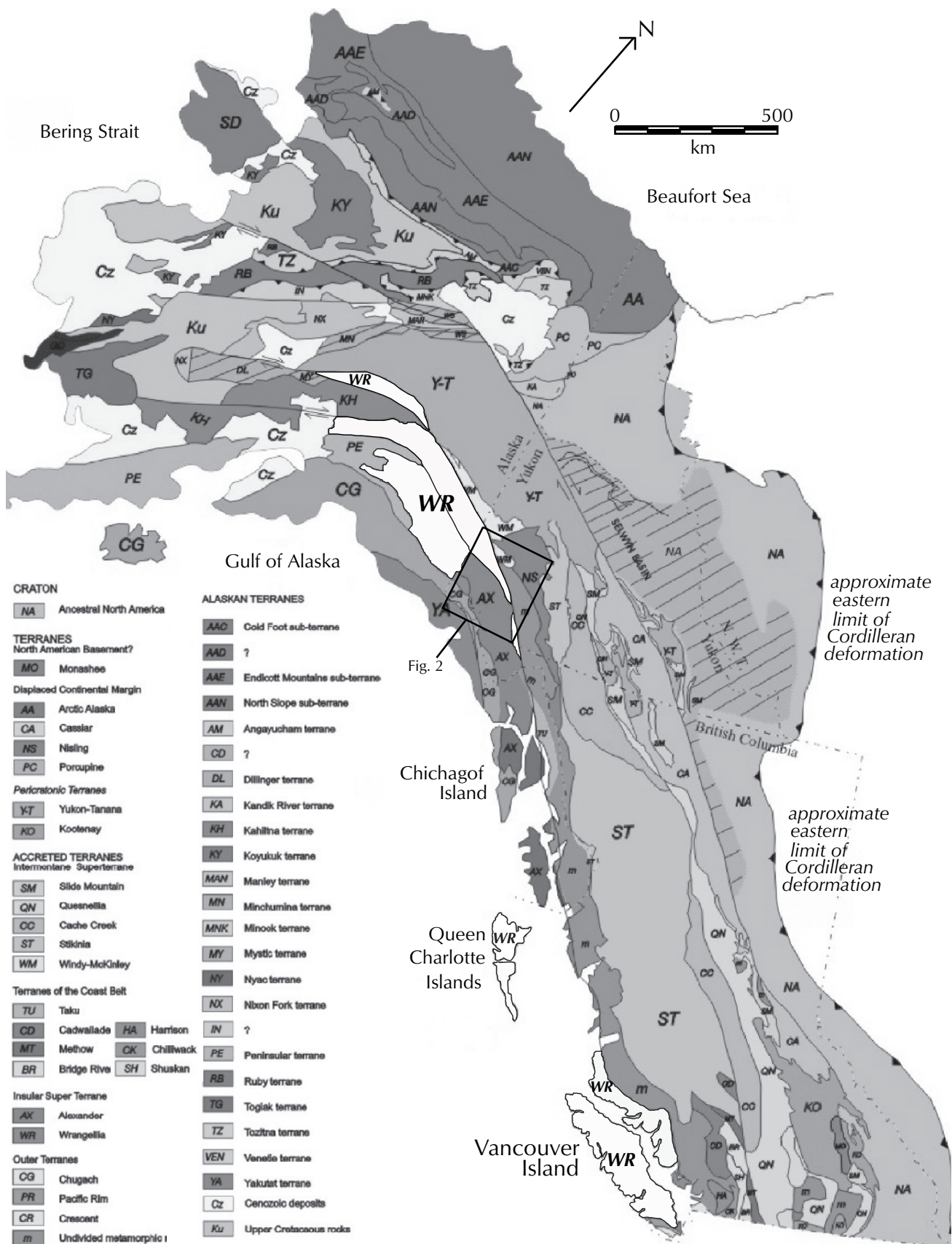
## TECTONIC SETTING OF THE WRANGELLIA TERRANE

The Wrangellia Terrane is a complex and variable terrane that extends from Vancouver Island to central Alaska (Fig. 1). The northernmost part of Wrangellia, which underlies large areas of east-central Alaska, is divided into two narrow linear belts to the south, which are separated by the Alexander Terrane. In the Yukon, the eastern belt is the narrowest section of Wrangellia rocks currently exposed.

Wrangellia is most commonly characterized by widespread exposures of Triassic flood basalts and complementary intrusive rocks (Jones et al., 1977). Triassic flood basalts extend in a discontinuous belt from Vancouver Island and the Queen Charlotte Islands (Karmutsen Formation), through southeast Alaska and the Kluane Ranges in southwest Yukon, and into the Wrangell Mountains and Alaska Range in east-central Alaska (Nikolai formation). The flood basalt sequences in this belt have distinct similarities and are recognized as a once-contiguous terrane (Jones et al., 1977).

Wrangellia has a long and diverse geologic history that spans much of the Phanerozoic. In Yukon, Wrangellia lies on the west side of the Denali Fault, where Nikolai basalt

**Figure 1 (facing page).** Terrane map of western Canada and Alaska (modified after Wheeler et al., 1991) showing the distribution of the Wrangellia Terrane (WR; in white) in B.C., the Yukon and Alaska.





overlies Pennsylvanian to Permian marine sediments and arc sequences of the Hasen Creek and Station Creek formations (Read and Monger, 1976; Campbell, 1981). In the Late Triassic, rapid uplift associated with a rising plume head led to eruption of voluminous flood basalts as part of an extensive oceanic plateau (Richards et al., 1991). As volcanism ceased, the oceanic plateau soon began to subside and accumulate deep-water carbonate sediments, represented by the Upper Triassic to Lower Jurassic Chitstone and Nizina limestones and McCarthy Formation (Armstrong et al., 1969; MacKevett, 1970a, 1970b, 1971, 1972; Armstrong and MacKevett, 1977; MacKevett, 1978; Armstrong and MacKevett, 1982). Thick, deep marine fan deposits of the Dezadeash Formation overlap the Alexander and Wrangellia terranes (Smith and MacKevett, 1970; MacKevett, 1971; Read and Monger, 1976).

The enormous exposures of the Nikolai appear to represent a single flood basalt event (Richards et al., 1991). A mantle plume initiation model has been proposed for the Wrangellia flood basalts based on: (1) relatively limited geochemical data; (2) the nature of the underlying and overlying formations; (3) rapid uplift prior to volcanism; (4) the lack of evidence of rifting associated with volcanism; and (5) the short duration and high eruption rate of volcanism (Richards et al., 1991). The basalt flows are estimated to have erupted a minimum volume of  $1 \times 10^6 \text{ km}^3$  (Panuska, 1990) within a maximum of 5 million years (Carlisle and Suzuki, 1974).

During the approximately 80 million years between arc activity and emergence of oceanic plateau flood basalts, as the continents gathered into a great landmass, Wrangellia became part of a composite terrane (Plafker et al., 1989). By the Middle Pennsylvanian, Wrangellia may have joined or been in close proximity (stratigraphic continuity) with the Alexander Terrane (Gardner et al., 1988; Yorath et al., 1999). The ocean-bound Wrangellia terrane amalgamated with the Taku terrane of southeast Alaska and the Peninsular terrane of southern Alaska by as early as the Late Triassic (Plafker et al., 1989). Paleomagnetic and faunal evidence indicate that the Wrangellia Terrane originated far to the south of its present position (Hillhouse, 1977; Yole and Irving, 1980; Hillhouse et al., 1982; Hillhouse and Gromme, 1984). Wrangellia accreted to the North American craton by the Late Jurassic or Early Cretaceous (Monger et al., 1982; Tipper, 1984; Plafker et al., 1989; Gehrels and Greig, 1991; van der Heyden, 1992; Monger et al., 1994).

## GEOLOGIC SETTING OF THE NIKOLAI FORMATION

Flood basalts of the Nikolai formation are preserved in a discontinuous, southeast-trending linear belt 30-60 km wide, extending over 300 km in the southwest corner of Yukon (Fig. 2). Marine sedimentary rocks of the Paleozoic Station Creek Formation and island arc rocks of the Hasen Creek Formation and Nikolai formation are intruded by mafic-ultramafic sills considered to be associated with eruption of the flood basalts. The Nikolai formation is commonly intercalated with thin, discontinuous lenses of marine sedimentary rocks and is capped by shallow-water limestone (Armstrong et al., 1969; Read and Monger, 1976).

The earliest geological mapping of the Kluane Ranges was done by McConnell (1905). Reconnaissance mapping was done periodically in the early 1900s until prospecting and exploration increased in the 1950s as the result of several discoveries (Hulbert, 1997). For the northern segment of Wrangellia, mapping was primarily accomplished by MacKevett (1970, 1970, 1971, 1972, 1978) in Alaska and J.E. Muller, P.B. Read, and R.B. Campbell (Muller, 1967; Read and Monger, 1976; Campbell and Dodds, 1982, 1985) in southwest Yukon. This initial work established the location, characteristics and depositional history of the Triassic volcanic sequences. Muller (1967) produced the first regional geologic map of the Kluane Ranges at 1:250 000 scale and proposed the correlation between the flood basalts in Yukon and those underlying extensive areas of east-central Alaska. Numerous exploration companies have since investigated the mineralization potential of mafic-ultramafic intrusions in the Kluane Ranges, and some of this work is reviewed in Hulbert (1997) and Carne (2003). Hulbert (1997) studied the intrusive complexes in the Yukon segment of the Wrangellia Terrane and refers to these bodies as the Kluane Mafic-Ultramafic Belt. The most recent summary of the geology of the Kluane Ranges is by Gordey and Makepeace (2000). The Yukon Geological Survey recently initiated a bedrock mapping project in the Kluane Ranges, the preliminary results of which are summarized by Israel and Van Zeyl (this volume).

The Nikolai formation in southwest Yukon is preserved in thin flood-volcanic sequences with minimal lithologic variation. The extrusive marine sequences locally exceed 1000 m in thickness. Extensive faulting and folding throughout the Yukon segment of Wrangellia, however, makes reconstruction of the stratigraphic thickness

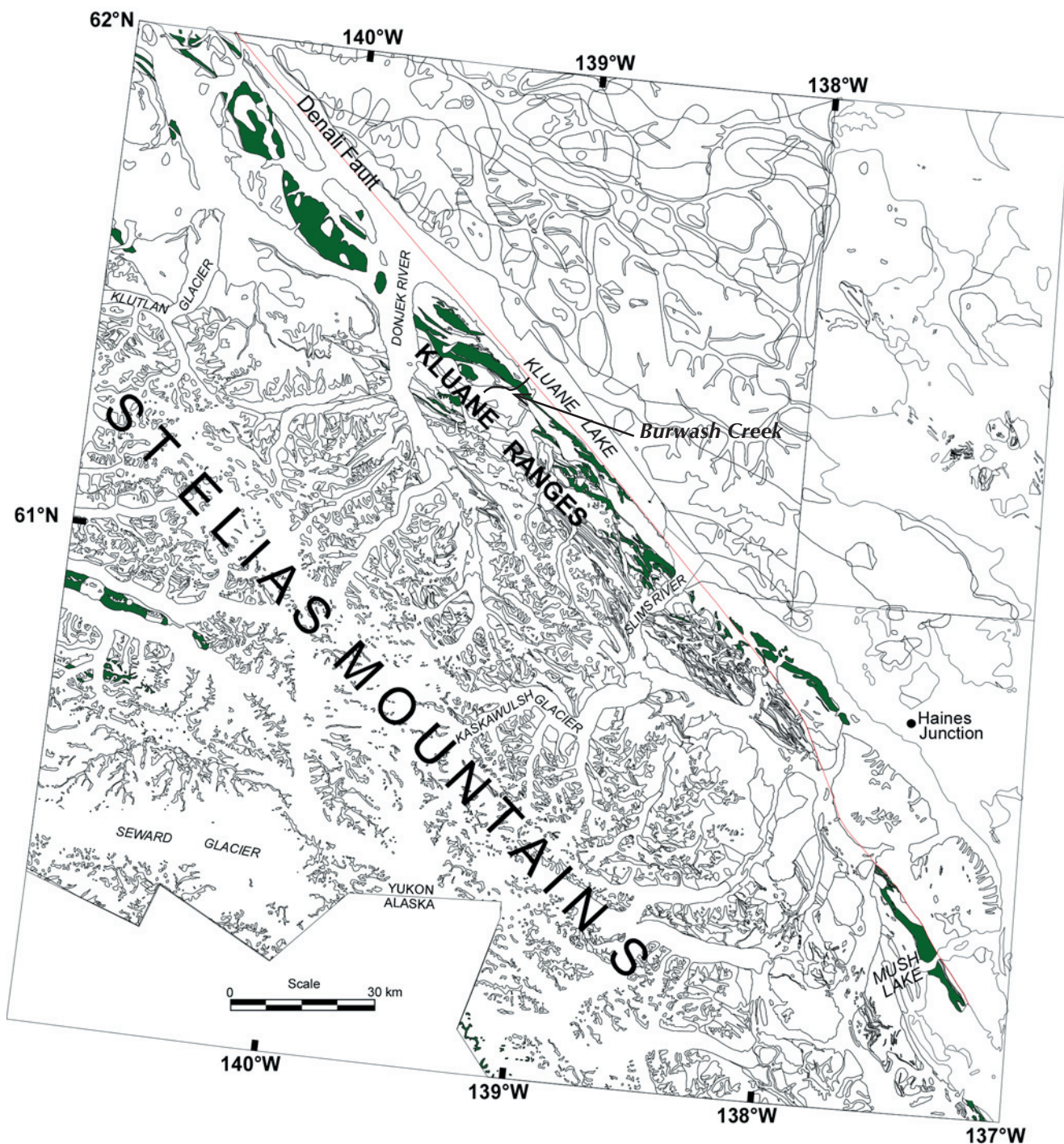


**Figure 2.** Geologic map of southwest Yukon showing exposures of flood basalt from the Triassic Nikolai formation (dark shading). This map was modified from Israel (2004).



challenging. The basalts preserve both a submarine and subaerial history of eruption for the oceanic plateau. In the Kluane Ranges, the base of the volcanic section is a thin zone of volcanic breccia, pillow lava and conglomerate that is typically less than 100 m thick (Fig. 3). The remaining sequences of flood basalt are almost exclusively massive flows with undulating contacts and abundant amygdules. The concordant subaerial flows preserve minimal evidence of erosional surfaces between them and lack significantly thick or laterally continuous intravolcanic sedimentary rocks (Read and Monger, 1976). The “essentially homogeneous” flood basalts (Barker et al., 1989; Richards et al., 1991; Lassiter et al., 1995; Yorath et al., 1999) formed as an enormous lava pile beneath, close to, and above the surface of the ocean within a geologically short time span.

There are distinct differences between the nature of the flood basalt sequences in Yukon and those in the southern portion of the Wrangellia Terrane in British Columbia. The correlative Karmutsen Formation on Vancouver Island contains a much larger proportion of submarine basalts than the predominantly subaerial Nikolai. However, there are subaerial flows in the uppermost sequences of the Karmutsen and submarine basalts near the base of the Nikolai formation (Muller et al., 1974; Read and Monger, 1976; Jones et al., 1977). On Vancouver Island, Wrangellia flood basalts reach thicknesses of nearly 6000 m, whereas in the Yukon the total thickness is ~1000 m. On Vancouver Island, the Karmutsen volcanics are commonly distinguished by (1) a lower member of exclusively pillow lava (2500 ± 150 m) (2) a middle member of pillow breccia and aquagene tuff (600 to 1100 m) and (3) an upper member of massive basalt flows (2600 ± 150 m; Carlisle and Suzuki, 1974). With the exception of a thin zone of submarine basalt near the base, the Nikolai formation consists primarily of subaerial lava flows.

The timing of the eruption of Wrangellia flood basalts is poorly constrained. The age of Wrangellia flood basalts is bracketed by fossils in the underlying and overlying sedimentary units and corroborated with several radiometric dates (Fig. 3). The entire eruption and deposition of Wrangellia flood basalts on Vancouver Island possibly occurred within 2.5 to 3.5 million years (early Upper Ladinian to early Upper Carnian-middle Triassic; Carlisle and Suzuki, 1974). Zircon ages for related intrusive units on Vancouver Island corroborate bracketing ages of 217 to 222 Ma (Isachsen et al., 1985) and 227 ± 3 Ma (Parrish and McNicoll, 1992). In Yukon,

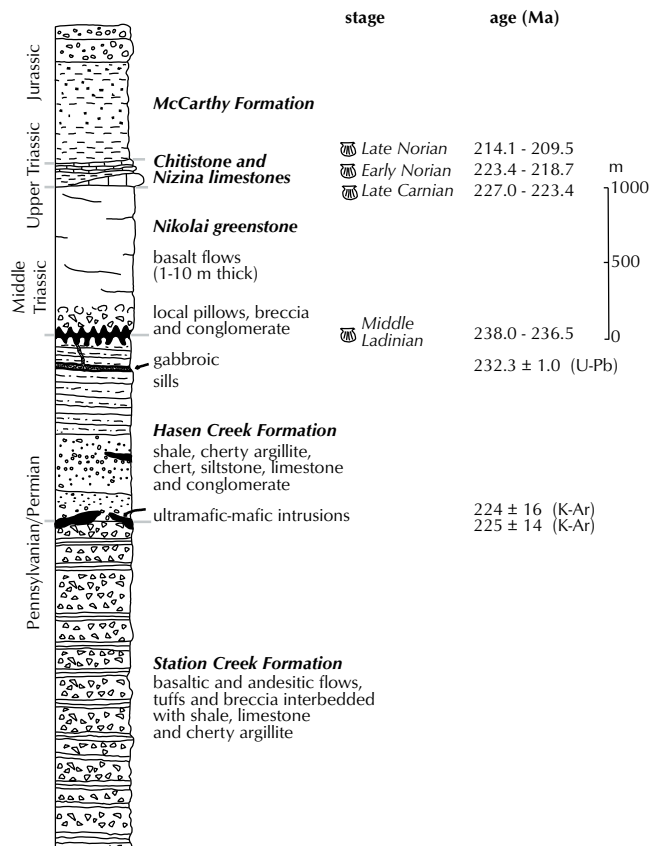


**Figure 3.** Composite stratigraphic column depicting flood basalt sequences of the Nikolai formation and other major sedimentary sequences in the Kluane Ranges in southwest Yukon. Modified after Read and Monger (1976) and Hulbert (1997).

K-Ar ages for phlogopite in peridotite from two intrusive complexes yield ages of 224 ± 16 Ma and 225 ± 14 Ma (Campbell, 1981). A U-Pb age for zircon from a gabbro sill contemporaneous with eruption of the Nikolai volcanics yielded an age of 232.2 ± 1.0 Ma (Mortensen and Hulbert, 1991). Conodonts from the Nikolai volcanics in Alaska also indicate a latest Carnian to earliest Norian age (Plafker et al., 1989).

## DESCRIPTION OF THE STUDY AREA

Field studies were undertaken in August, 2004 to investigate Wrangellia flood basalts in southwest Yukon. Published literature and maps were evaluated for the selection of target areas prior to commencing fieldwork. Field areas were selected based on accessibility, potential for exposure of thick stratigraphic sequences, and an even distribution throughout the linear belt of exposures.



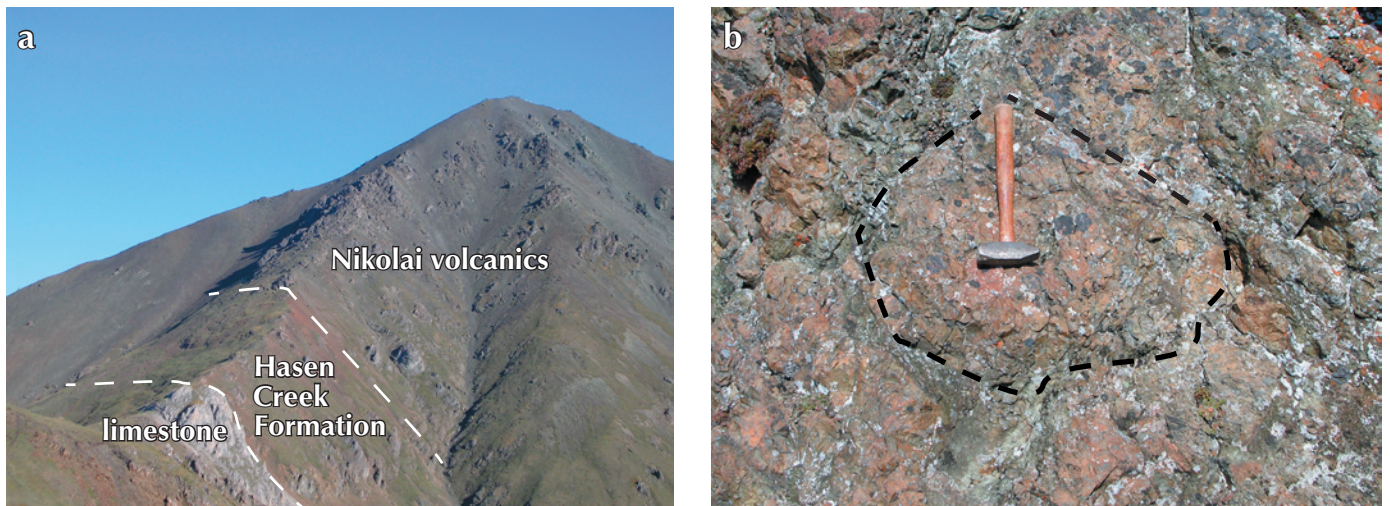


**Figure 4.** (a) Base of the Nikolai formation adjacent to marine sedimentary units, above the Wellgreen Mine; (b) Cross-section of weathered basalt pillows at the base of the Nikolai formation; (c) Pillow breccia with angular, blocky clasts in a fine-grained matrix, in a zone <40 m thick at the base of the Nikolai formation.

Sampling was undertaken from the area near Mush Lake in the south, to as far north as the Donjek River (Fig. 2).

Reconnaissance of these areas revealed that complete sections of the volcanic flood basalt sequences are not present in any one area. Small sequences of pillow lavas and breccia underlying more extensive sequences of massive flows, however, are well-exposed and easily accessible. The degree of faulting made assessment of the stratigraphy difficult in most areas. Eighty-five evenly-distributed samples were collected for petrographic and geochemical analysis. Special care was taken to sample the freshest-appearing basalts and to cover the extent of the exposed Triassic stratigraphy.

Of the ten areas investigated, nearly half of the time was spent between Burwash Creek and the Donjek River. In several areas where the base of the Nikolai formation is exposed adjacent to Middle Triassic marine sediments, it is marked by a thin zone, commonly <40 m thick, of breccia or conglomerate with angular volcanic clasts (Read and Monger, 1976; Fig. 4). Pillow lavas near the



base of the Nikolai formation are difficult to distinguish and are closely associated with this thin zone of breccia, which preserves no easily-recognizable bedding (Fig. 4a). The pillow breccia may have formed as the result of a varied eruptive stage where stacks of pillows emerging from young lava centers collapsed due to an increased level of magma flux or seismic activity (Yorath et al., 1999).

The exposed thickness of the Nikolai formation varies throughout the linear belt. Massive lava flows in each of the investigated areas are generally 1 to 15 m thick (Fig. 5a). Amygdules are prevalent throughout individual flows, which commonly reveal uneven contacts with no discernible erosional surface or columnar jointing. Phenocrysts are common throughout many of the flows. The basalt flows are rarely interbedded with thin, lenticular beds of marine sediments (Fig. 5b). Most of the flows appear to have erupted subaerially or in shallow water, which likely precluded significant deposition of sedimentary rocks (Carlisle and Suzuki, 1974).





**Figure 5.** (a) Vertically oriented basalt flows near Tatamagouche Creek, with Dall Sheep for scale; (b) Intercalated marine sediments within the Nikolai formation; (c) Vertically oriented Chitistone Limestone adjacent to the Nikolai formation on Sheep Mountain.

## MAGMATIC SULPHIDE DEPOSITS IN THE WRANGELLIA TERRANE IN YUKON?

The intrusive centres linked to the overlying Wrangellia flood basalts represent one of the largest belts of Ni-Cu-PGE-bearing mafic and ultramafic rocks in North America (Hulbert, 1997). Numerous deposits and occurrences in Yukon and adjacent parts of Alaska have seen considerable attention (e.g., Wellgreen, Yukon MINFILE 115G 024; Canalask, Yukon MINFILE 115F 045) and the characteristics of some of these are summarized by Hulbert (1997). Geochemical variations in the Wrangellia flood basalts preserve a record, as yet undeciphered, of the evolution of magmas within upper crustal magma chambers or sills and their interaction with local contaminants and deep crustal contaminants during ascent. At Noril'sk, the geochemistry of the flood basalts

has been used as an indication of the likelihood that complementary intrusive rocks contain Ni-Cu-PGE deposits (e.g., Naldrett and Lightfoot, 1993) and the geochemistry of the intrusive rocks has been successfully used to constrain the role of staging chambers for crustal contamination and sulphide segregation within magmas prior to eruption (Arndt et al., 2003). These studies concluded that the assimilation of S-bearing sedimentary rocks by picritic (high-MgO) magma led to the segregation of Ni- and PGE-rich magmatic sulphides.

In this ongoing study, detailed geochemical and isotopic studies of the Wrangellia flood basalts may provide insight into the relative importance of different components on the formation of magmatic sulphide deposits. These components include magma composition, nature and relative age of wallrock, extent of contamination, prior sulphide segregation and tectonic setting. Hulbert (1997) suggested that olivine-rich basalt flows (picritic basalts)

and mafic and ultramafic intrusions may be restricted to the Yukon segment of Wrangellia, as a result of their formation in proximity to the hotter axial “jet” of the mantle plume. However, this aspect of the Wrangellia flood basalt province is poorly understood due to the lack of comparative studies. To assess the significance of primitive S-undersaturated magmas, crustal contamination and high-level magmatic processes, it is important to understand the relative contributions to the magmas from the plume source and the lithosphere (Lightfoot and Hawkesworth, 1997).

The nature of the basement rock is likely crucial to the formation of magmatic Ni-Cu-PGE deposits in flood basalt provinces. Late Paleozoic marine sediments and arc volcanics underlie Wrangellia flood basalts in the Kluane Ranges and throughout most of the Wrangellia Terrane (Muller, 1967; Read and Monger, 1976; Jones et al., 1977; Campbell, 1981). Zoned, sill-like mafic and ultramafic bodies, representing subvolcanic magma chambers for the overlying Triassic flood basalts, appear to preferentially intrude at or near the contact between the Hasen and Station Creek Formations in the Kluane Ranges. Many of these mafic and ultramafic sills have anomalous magmatic sulphide concentrations (Hulbert, 1997). These relationships indicate that S- and Ba-rich sediments may have been integral to contaminating magmas and initiating sulphide immiscibility (Hulbert, 1997). One of the aims of this study is to determine what the geochemistry of the Wrangellia flood basalts can tell us about the likelihood of discovering additional Ni-Cu-PGE deposits in this part of the terrane.

## ONGOING AND PLANNED RESEARCH

We are presently preparing 85 samples of flood basalt and basement rock from the Wrangellia Terrane in Yukon for high-precision geochemical and isotopic analytical work at the Pacific Centre for Isotopic and Geochemical Research (PCIGR) at the University of British Columbia (UBC). Additionally, we are preparing 50 samples from Vancouver Island for analysis. Careful procedures are being used to avoid any contamination of samples during crushing. Petrographic thin-sections for all the samples are also currently being analyzed for their mineralogy and texture.

We plan a thorough evaluation of the petrology, geochronology and geochemistry of flood basalts in the Wrangellia Terrane. Due to the lack of a comprehensive published geochemical database for Wrangellia, this

evaluation will require the acquisition of a large, internally consistent database with element concentrations and isotopic ratios measured in the same lab. Ratios of low-abundance trace elements, such as Nb/La, La/Sm, Ba/Th, Sr/Nd and Pb/Nd, are very sensitive to differences in sources and contaminants, and are therefore used to determine the extent of crustal contamination. Furthermore, combinations of different radiogenic isotopic systems such as Pb-Pb, Rb-Sr, Sm-Nd and Lu-Hf with different geochemical behaviours and relative ratios for the parent and daughter isotopes can precisely fingerprint potential source components (e.g., enriched mantle, depleted mantle, arc crust, sedimentary rocks). Select samples will be precisely dated by Ar-Ar methods to provide absolute time constraints on magmatism in the Wrangellia Terrane. Particular emphasis will be placed on determining the extent of crustal contamination in the Wrangellia magmatic suite by local sedimentary rock sources and/or by lower crustal material. Geochemical modeling will help to elucidate trends in compositional evolution and will determine whether arc assimilation may have given the Wrangellia flood basalts their distinct geochemical signature.

We plan to complete the compilation of geological information for the entire Wrangellia Terrane in B.C., Yukon and Alaska. The major goal of the compilation work is to constrain the location, aerial significance, and stratigraphic location of intrusions and sedimentary sequences. Additional field studies planned in Alaska during the summer of 2005 will supplement the work in Yukon. Ultimately, the goal of this project is to characterize the chemical composition of Wrangellia flood basalts in order to better understand the origin and evolution of oceanic plateaus, from their initiation at the mantle source to their accretion in the continental graveyard.

## ACKNOWLEDGEMENTS

Funding for this project has been generously provided by the Yukon Geological Survey. We would like to thank Bruno Kieffer, Frederico Henriques and Dave Van Zeyl for their dedicated help with fieldwork.



## REFERENCES

- Abbott, D. and Mooney, W., 1995. The structural and geochemical evolution of the continental crust: support for the oceanic plateau model of continental growth. *In: US National Report to IUGG 1991-1994. Reviews of Geophysics - Supplement*, vol. 33, p. 231-242.
- Abouchami, W., Boher, M., Michard, A. and Albarède, F., 1990. A major 2.1 Ga old event of mafic magmatism in West Africa: an early stage of crustal accretion. *Journal of Geophysical Research*, vol. 95, p. 17605-17629.
- Albarède, F., 1998. The growth of continental crust. *Tectonophysics*, vol. 296, p. 1-14.
- Armstrong, A.K. and MacKevett, E.M., Jr., 1977. The Triassic Chitistone Limestones, Wrangell Mountains, Alaska. U.S. Geological Survey, Open-File Report 77-217, p. D49-D62.
- Armstrong, A.K. and MacKevett, E.M., Jr., 1982. Stratigraphy and diagenetic history of the lower part of the Triassic Chitistone Limestone, Alaska. U.S. Geological Survey, Professional Paper 1212-A, p. 26.
- Armstrong, A.K., MacKevett, E.M., Jr. and Silberling, N.J., 1969. The Chitistone and Nizina limestones of part of the southern Wrangell Mountains – a preliminary report stressing carbonate petrography and depositional environments. U.S. Geological Survey, Professional Paper 650-D, p. D49-D62.
- Arndt, N.T., Czamanske, G.K., Walker, R.J., Chauvel, C. and Federenko, V.A., 2003. Geochemistry and origin of the intrusive hosts of the Noril'sk-Talnakh Cu-Ni-PGE sulfide deposits. *Economic Geology*, vol. 98, p. 495-515.
- Barker, F., Brown, A.S., Budahn, J.R. and Plafker, G., 1989. Back-arc with frontal-arc component origin of Triassic Karmutsen basalt, British Columbia, Canada. *Chemical Geology*, vol. 75, p. 81-102.
- Ben-Avraham, Z., Nur, A., Jones, D.L. and Cox, A., 1981. Continental accretion: From oceanic plateaus to allochthonous terranes. *Science*, vol. 213, p. 47-54.
- Boher, M., Abouchami, W., Michard, A., Albarède, F. and Arndt, N.T., 1992. Crustal growth in West Africa at 2.1 Ga. *Journal of Geophysical Research*, vol. 97, p. 345-369.
- Campbell, R.B. and Dodds, C.J., 1982. Geology of the S.W. Kluane Lake map area (115F and 115 G), Yukon Territory. Canadian Geological Survey, Open-File Report 829, 1:250 000 scale.
- Campbell, R.B. and Dodds, C.J., 1985. Geology of the Mount St. Elias map area (115B and 115C[E1/2]). Canadian Geological Survey, Open-File Report 830, 1:250 000 scale.
- Campbell, S.W., 1981. Geology and genesis of copper deposits and associated host rocks in and near the Quill Creek area, southwestern Yukon. Unpublished PhD thesis, University of British Columbia, Vancouver, British Columbia, 215 p.
- Carlisle, D. and Suzuki, T., 1974. Emergent basalt and submergent carbonate-clastic sequences including the Upper Triassic Dilleri and Welleri zones on Vancouver Island. *Canadian Journal of Earth Science*, vol. 11, p. 254-279.
- Carne, R.C., 2003. Metallogeny of the Kluane Ranges, Southwest Yukon Territory. Archer, Cathro & Associates (1981) Limited, <http://www.geology.gov.yk.ca/metallogeny/kluane/index.html>.
- Gardner, M.C., Bergman, S.C., Cushing, G.W., MacKevett, E.M. Jr., Plafker, G., Campbell, R.B., Dodds, C.J., McClelland, W.C. and Mueller, P.A., 1988. Pennsylvanian pluton stitching of Wrangellia and the Alexander terrane, Wrangell Mountains, Alaska. *Geology*, vol. 16, p. 967-971.
- Gehrels, G.E. and Greig, C.J., 1991. Late Jurassic detrital zircon link between the Alexander-Wrangellia terrane and Stikine and Yukon-Tanana terranes. *Geological Society of America, Abstracts with Programs*, vol. 23, p. A434.
- Gordey, S.P. and Makepeace, A.J., (compilers), 2000. Yukon digital geology (version 2). Geological Survey of Canada, Open File 2003-9(D) and Exploration and Geological Services Division (EGSD), Yukon Region, Indian and Northern Affairs Canada (DIAND).
- Hillhouse, J.W., 1977. Paleomagnetism of the Triassic Nikolai Greenstone, McCarthy Quadrangle, Alaska. *Canadian Journal of Earth Science*, vol. 14, p. 2578-3592.
- Hillhouse, J.W. and Gromme, C.S., 1984. Northward displacement and accretion of Wrangellia: New paleomagnetic evidence from Alaska. *Journal of Geophysical Research*, vol. 89, p. 4461-4467.
- Hillhouse, J.W., Gromme, C.S. and Vallier, T.L., 1982. Paleomagnetism and Mesozoic tectonics of the Seven Devils volcanic arc in northeastern Oregon. *Journal of Geophysical Research*, vol. B. 87, p. 3777-3794.

- Hulbert, L.J., 1997. Geology and metallogeny of the Kluane mafic-ultramafic belt, Yukon Territory, Canada: eastern Wrangellia – a new Ni-Cu-PGE metallogenic terrane. Geological Survey of Canada, Bulletin 506, 265 p.
- Isachsen, C., Armstrong, R.L. and Parrish, R.R., 1985. U-Pb, Rb-Sr, and K-Ar geochronometry of Vancouver Island igneous rocks. Geological Association of Canada – Victoria Section Symposium (abstract), p. 21-22.
- Israel, S., 2004. Geology of southwest Yukon. Yukon Geological Survey, Open File 2004-16.
- Jones, D.L., Silberling, N.J. and Hillhouse, J., 1977. Wrangellia; a displaced terrane in northwestern North America. Canadian Journal of Earth Sciences, vol. 14, p. 2565-2577.
- Kerr, A.C., 2003. Oceanic Plateaus. *In*: Treatise on Geochemistry, H.C. Holland and K. Turekian (series eds.), The Crust, R. Rudnick (ed.), Elsevier Science, Oxford. p. 537-565.
- Kerr, A.C., White, R.V. and Saunders, A.D., 2000. LIP Reading: Recognizing Oceanic Plateaux in the Geological Record. Journal of Petrology, vol. 41, p. 1041-1056.
- Kimura, G. and Ludden, J., 1995. Peeling oceanic crust in subduction zones. Geology, vol. 23, p. 217-220.
- Kronke, L.W., 1974. Origin of continents through development and coalescence of oceanic flood basalt plateaus. Eos, vol. 55, p. 443.
- Lassiter, J.C., DePaolo, D.J. and Mahoney, J.J., 1995. Geochemistry of the Wrangellia Flood Basalt Province: Implications for the Role of Continental and Oceanic Lithosphere in Flood Basalt Genesis. Journal of Petrology, vol. 36, p. 983-1009.
- Lightfoot P.C. and Hawkesworth C.J., 1997. Flood basalts and magmatic Ni, Cu, and PGE Sulphide mineralization: Comparative geochemistry of the Noril'sk (Siberian Traps) and West Greenland sequences. *In*: Large igneous provinces: continental, oceanic, and planetary flood volcanism, J.J. Mahoney and M.F. Coffin (eds.), American Geophysical Union, Geophysical Monograph 100, p. 357-380.
- MacKevett, E.M., Jr., 1970a. Geologic map of the McCarthy C-4 Quadrangle, Alaska. U.S. Geological Survey, Geological Quadrangle Map, 1:63 360 scale.
- MacKevett, E.M., Jr., 1970b. Geologic map of the McCarthy C-5 Quadrangle, Alaska. U.S. Geological Survey, Geological Quadrangle Map, 1:63 360 scale.
- MacKevett, E.M., Jr., 1971. Stratigraphy and general geology of the McCarthy C-5 Quadrangle, Alaska. U.S. Geological Survey, Bulletin 1323 p. 35.
- MacKevett, E.M., Jr., 1972. Geologic map of the McCarthy C-6 Quadrangle, Alaska. U.S. Geological Survey, Geological Quadrangle Map, 1:63 360 scale.
- MacKevett, E.M., Jr., 1978. Geologic map of the McCarthy Quadrangle, Alaska. U.S. Geological Survey, Miscellaneous Investigations Series Map, 1:250 000 scale.
- McConnell, R.G., 1905. The Kluane mining district. Geological Survey of Canada, Annual Report 1904, v. 16, p. 1A-18A.
- Monger, J.W.H., Price, R.A. and Tempelman-Kluit, D.J., 1982. Tectonic accretion and the origin of the two major metamorphic and plutonic belts in the Canadian Cordillera. Geology, vol. 10, p. 70-75.
- Monger, J.W.H., van der Heyden, P., Journeay, J.M., Evenchick, C.E. and Mahoney, J.B., 1994. Jurassic-Cretaceous basins along the Canadian Coast Belt: Their bearing on pre-mid-Cretaceous sinistral displacements. Geology, vol. 22, p. 175-178.
- Mortensen, J.K. and Hulbert, L.J., 1991. A U-Pb zircon age for a Maple Creek gabbro sill, Tatamagouche Creek area, southwestern Yukon Territory. *In*: Radiogenic Age and Isotopic Studies: Report 5, Geological Survey of Canada, Paper 91-2, p. 175-179.
- Muller, J.E., 1967. Kluane Lake map area, Yukon Territory (115G, 115F/E 1/2). Geological Survey of Canada, Memoir 340, 137 p.
- Muller, J.E., Northcote, K.E. and Carlisle, D., 1974. Geology and mineral deposits of Alert Bay - Cape Scott map area, Vancouver Island, British Columbia. Geological Survey of Canada, Paper 74-8, p. 77.
- Naldrett, A.J. and Lightfoot, P.C., 1993. A model for giant magmatic sulphide deposits associated with flood basalts. *In*: Giant Ore Deposits, B.H. Whiting, R. Mason and C.J. Hodgson (eds.), Society of Economic Geologists, Special Publication, p. 81-123.
- Nur, A. and Ben-Avraham, Z., 1982. Oceanic plateaus, the fragmentation of continents, and mountain building. Journal of Geophysical Research, vol. 87, p. 3644-3661.

- Panuska, B.C., 1990. An overlooked, world class Triassic flood basalt event. Geological Society of America, Abstracts with Programs, vol. 22, p. A168.
- Parrish, R.R. and McNicoll, V.J., 1992. U-Pb age determinations from the southern Vancouver Island area, British Columbia. *In: Radiogenic Age and Isotopic Studies: Report 5*, Geological Survey of Canada, Paper 91-2, p. 79-86.
- Plafker, G., Nokleberg, W.J. and Lull, J.S., 1989. Bedrock geology and tectonic evolution of the Wrangellia, Peninsular, and Chugach terranes along the Trans-Alaskan Crustal Transect in the northern Chugach Mountains and southern Copper River basin, Alaska. *Journal of Geophysical Research*, vol. 94, p. 4255-4295.
- Read, P.B. and Monger, J.W.H., 1976. Pre-Cenozoic volcanic assemblages of the Kluane and Alsek Ranges, southwestern Yukon Territory. Geological Survey of Canada, Open-File Report 381, p. 18.
- Richards, M.A., Jones, D.L., Duncan, R.A. and DePaolo, D.J., 1991. A mantle plume initiation model for the Wrangellia flood basalt and other oceanic plateaus. *Science*, vol. 254, p. 263-267.
- Saunders, A.D., Tarney, J., Kerr, A.C. and Kent, R.W., 1996. The formation and fate of large oceanic igneous provinces. *Lithos*, vol. 37, p. 81-95.
- Schubert, G. and Sandwell, D., 1989. Crustal volumes of the continents and of oceanic and continental submarine plateaus. *Earth and Planetary Science Letters*, vol. 92, p. 234-246.
- Smith, J.G. and MacKevett, E.M., Jr., 1970. The Skolai Group in the McCarthy B-4, C-4, C-5 Quadrangles, Wrangell Mountains, Alaska. U.S. Geological Survey, Bulletin 1274-Q, p. Q1-Q26.
- Stein, M. and Goldstein, S.L., 1996. From plume head to continental lithosphere in the Arabian-Nubian shield. *Nature*, vol. 382, p. 773-778.
- Tipper, H.W., 1984. The allochthonous Jurassic-Lower Cretaceous terranes of the Canadian Cordillera and their relation to correlative strata of the North American craton. Geological Association of Canada, Special Paper 27, p. 113-120.
- van der Heyden, P., 1992. A middle Jurassic to early Tertiary Andean-Sierran arc model for the coast belt of British Columbia. *Tectonics*, vol. 11, p. 82-97.
- Wheeler, J.O., Brookfield, A.J., Gabrielese, H., Monger, J.W.H., Tipper, H.W. and Woodsworth, G.J., 1991. Terrane map of the Canadian Cordillera. Geological Survey of Canada, Map 1713, 1:1 000 000 scale.
- Wignall, P.B., 2001. Large igneous provinces and mass extinctions. *Earth-Science Reviews*, vol. 53, p. 1-33.
- Yole, R.W. and Irving, E., 1980. Displacement of Vancouver Island, paleomagnetic evidence from the Karmutsen Formation. *Canadian Journal of Earth Sciences*, vol. 17, p. 1210-1228.
- Yorath, C.J., Sutherland Brown, A. and Massey, N.W.D., 1999. LITHOPROBE, southern Vancouver Island, British Columbia. Geological Survey of Canada, Bulletin 498, p. 145.



# Lead isotope signatures of Tintina Gold Province intrusions and associated mineral deposits from southeastern Yukon and southwestern Northwest Territories: Implications for exploration in the southeastern Tintina Gold Province

**R. Scott Heffernan<sup>1</sup>**

*Equity Engineering Ltd.*

**James K. Mortensen<sup>2</sup> and Janet E. Gabites<sup>3</sup>**

*Pacific Centre for Isotopic and Geochemical Research at the University of British Columbia*

**V. Sterenberg**

*Department of Indian and Northern Affairs, Government of the Northwest Territories<sup>4</sup>*

Heffernan, R.S., Mortensen, J.K., Gabites, J.E. and Sterenberg, V., 2005. Lead isotope signatures of Tintina Gold Province intrusions and associated mineral deposits from southeastern Yukon and southwestern Northwest Territories: Implications for exploration in the southeastern Tintina Gold Province. *In: Yukon Exploration and Geology 2004*, D.S. Emond, L.L. Lewis and G.D. Bradshaw (eds.), Yukon Geological Survey, p. 121-128.

## ABSTRACT

This paper presents new lead isotope data from intrusive rocks and several mineral deposits from the southeastern portion of the Tintina Gold Province (TGP). Lead isotopic studies of feldspars separated from various mid-Cretaceous intrusions in the study area and sulphide minerals from a number of mineral occurrences that are spatially associated with the intrusions were done in order to investigate possible relationships between the mineralization and magmatism. These data provide insight on metal sources within these systems and hence help to constrain exploration models. Results from this study indicate that: 1) the metals in many mineral deposits and prospects in the region are mostly derived from the mid-Cretaceous TGP intrusions; 2) the Sa Dena Hes deposit is broadly mid-Cretaceous in age; and 3) metals in apparently distal styles of intrusion-related gold mineralization are not entirely derived from magmatic sources.

## RÉSUMÉ

Nous présentons de nouvelles données sur les isotopes du plomb dans les roches intrusives et plusieurs gîtes minéraux dans la partie sud-est de la province aurifère de Tintina (PAT). Pour étudier les relations possibles entre la minéralisation et le magmatisme, nous avons aussi analysé les isotopes du plomb dans des feldspaths séparés de diverses intrusions datant du Crétacé moyen dans l'aire d'étude, ainsi que dans des minéraux sulfurés provenant d'un certain nombre d'occurrences minéralisées associées aux intrusions. Ces données renseignent sur les sources de métaux dans ces systèmes et permettent ainsi d'imposer des limites aux modèles d'exploration. Les résultats de cette étude indiquent 1) que les métaux présents dans de nombreux gîtes (et occurrences) minéraux de la région proviennent surtout d'intrusions du Crétacé moyen dans la PAT, 2) que le gîte Sa Dena Hes remonte à peu près au Crétacé moyen, et 3) que les métaux présents dans des types apparemment distaux de minéralisations en or liées aux intrusions ne proviennent pas entièrement de sources magmatiques.

<sup>1</sup>scotth@equityeng.bc.ca

<sup>2</sup>jmortensen@eos.ubc.ca

<sup>3</sup>jpgabites@eos.ubc.ca

<sup>4</sup>Yellowknife, Northwest Territories, Canada

## INTRODUCTION

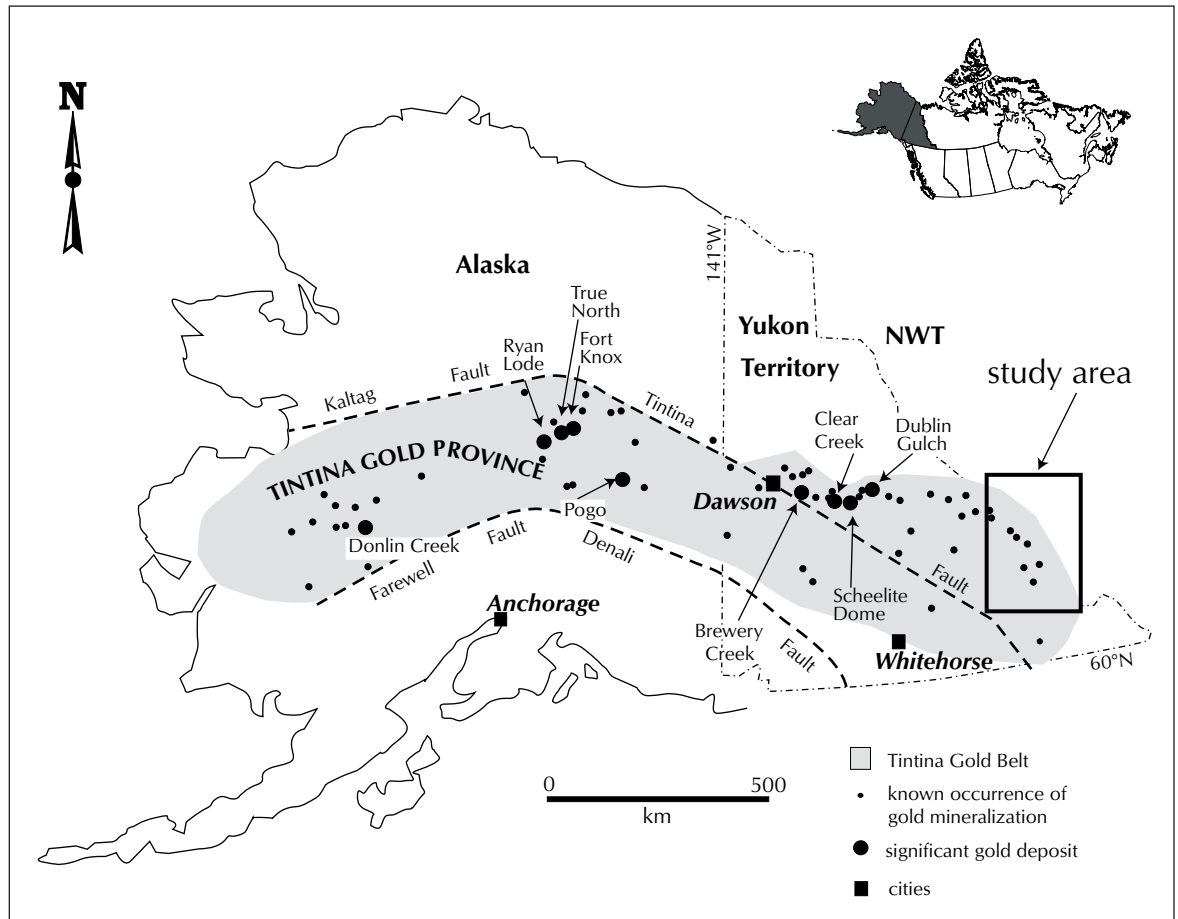
The Tintina Gold Province (TGP) in east-central Alaska, Yukon Territory, and southwestern Northwest Territories is host to numerous styles of precious- and base-metal mineralization thought to be genetically associated with widespread Early to Late Cretaceous magmatism (Fig. 1). Styles of mineralization in the TGP are highly variable and include sheeted quartz-feldspar veins, polymetallic replacement bodies, auriferous breccias, disseminated mineralization, gold-rich skarns, and epithermal vein systems (especially associated with Late Cretaceous intrusive and volcanic rocks). In the early 1990s, the discovery of gold deposits such as Fort Knox and Brewery Creek spurred exploration activity which led to further discoveries at Pogo, Donlin Creek, True North, Dublin Gulch, Ryan Lode, and Scheelite Dome. The rush of exploration success was accompanied by significant research directed at the development of genetic and exploration models. The resulting "Intrusion-Related Gold Systems" (IRGS) model has been continuously evolving since its inception (Thompson et al., 1999; Lang, 2000; Hart et al, 2000; Lang and Baker, 2001).

This paper presents new lead isotope data from intrusive rocks and several mineral deposits from the southeastern portion of the TGP. These data help to constrain metal sources within these systems and hence provide insight into possible relationships between magmatism and mineralization. The results of this study will help to refine exploration models that target mineralization in this region.

## REGIONAL METALLOGENY

A variety of intrusion-hosted and (probably) intrusion-related deposits and occurrences are known in the eastern Selwyn Basin, including tungsten ( $\pm$  base metal) skarns such as Mactung, Cantung and Lened, silver-rich base metal skarns and mantos such as Sa Dena Hes, gold-bearing sheeted quartz-feldspar veins (e.g., within the Mactung intrusion), distal, apparently structurally controlled deposits such as Hyland, and massive sulphide replacement deposits such as Quartz Lake (McMillan; Fig. 2). Indeed, at least 45% of the 325 MINFILE occurrences (Deklerk and Traynor, 2004) listed for the six

**Figure 1.** Map of Alaska State and Yukon Territory showing the extent of the Tintina Gold Province and significant gold deposits and occurrences within (after Mortensen et al., 2000). The main study area is outlined at right.



map sheets that compose the study area (105-A, -H, -I, and 95-D, -E, -L) are definitely or arguably intrusion-related. A discussion on the mineral potential of the eastern Selwyn Basin would not be complete without mention of the numerous sedimentary-exhalative (SEDEX)-type occurrences such as the Howard's Pass deposit and the Matt Berry prospect. The combination of both syngenetic and epigenetic exploration targets has led to a considerable amount of interest from exploration companies in the mineral potential of this region in the past several decades.

### GEOLOGIC OVERVIEW

One of the most striking features of the southeastern TGP is the great volume of granitic intrusions present; more than 5000 km<sup>2</sup> of mid-Cretaceous intrusive rocks are exposed within the study area (Fig. 2). These intrusions

consist of simple to complex, single- to multi-phase stocks, plutons and batholiths. Major intrusive phases consist mainly of medium-grained, massive to megacrystic granodiorite, quartz monzonite and granite. Intrusions of the southeastern TGP were emplaced into Late Precambrian to Mesozoic strata of the Selwyn Basin. Stratigraphy of the Selwyn Basin in this region consists mainly of turbiditic sandstone, deep water limestone, shale and chert that were deposited contemporaneously with shallow water carbonate and sandstone of the Mackenzie platform to the north and east (Gordey and Anderson, 1993). Results of geochronological, geochemical and isotopic investigations (Heffernan, 2004) indicate that the known plutonic suites of the western and northern portions of the TGP (Mortensen et al., 2000) do continue into southeastern Yukon and southwestern Northwest Territories.

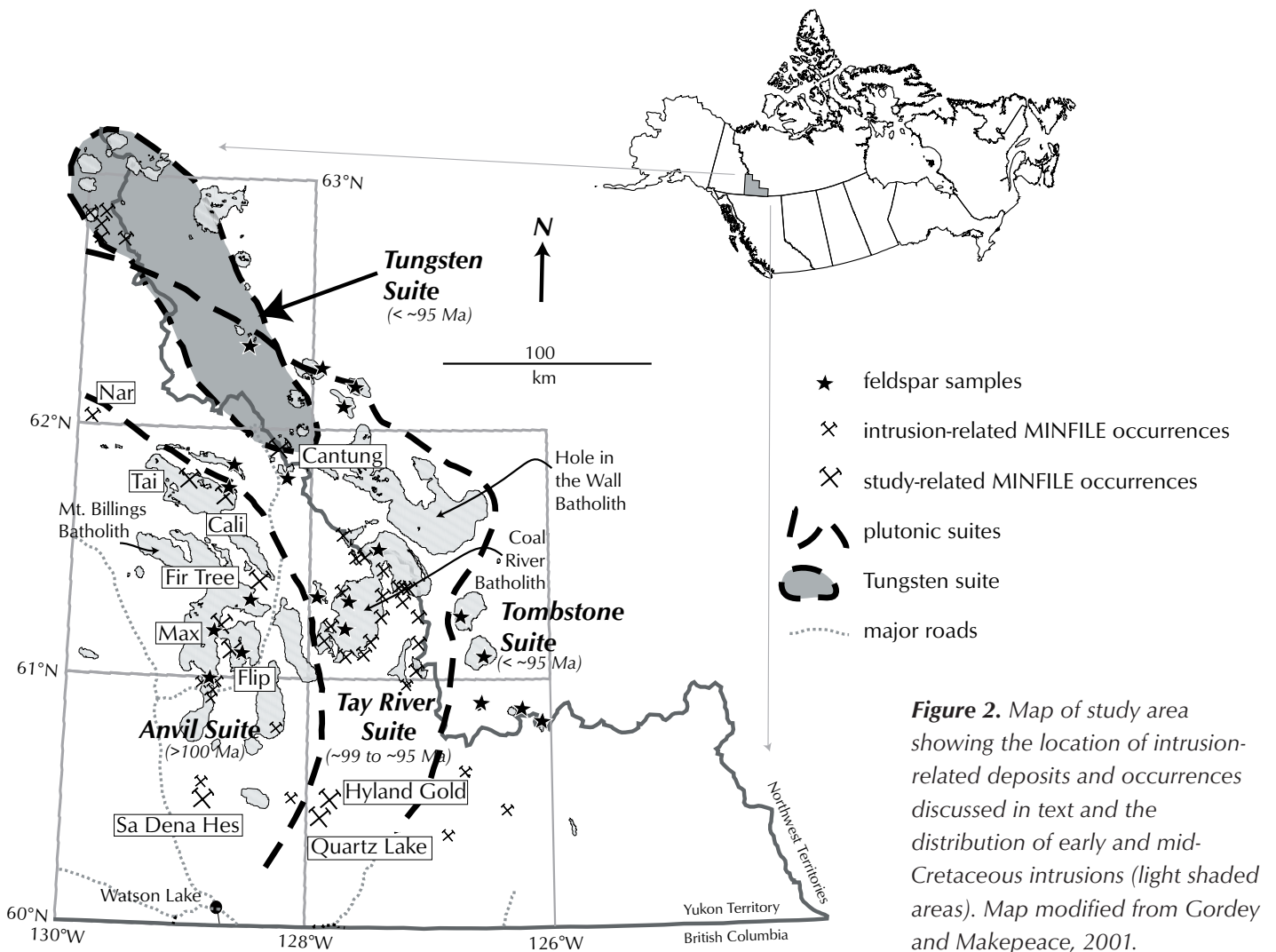


**Figure 2.** Map of study area showing the location of intrusion-related deposits and occurrences discussed in text and the distribution of early and mid-Cretaceous intrusions (light shaded areas). Map modified from Gordey and Makepeace, 2001.



## LEAD ISOTOPE STUDY

Pb isotope studies of feldspars separated from various mid-Cretaceous intrusions in the study area and of sulphide minerals from a number of precious- and base-metal deposits and occurrences have been carried out in order to investigate possible genetic relationships between mineralization and magmatism.

## SAMPLES AND ANALYTICAL TECHNIQUES

Sulphide samples were collected from numerous mineral deposits and occurrences that were examined during the course of this study. Names and brief descriptions of the sampled occurrences are presented in Table 1, and sample locations are shown in Figure 2. All sample preparation, geochemical separations and isotopic measurements were done at Pacific Centre for Isotopic and Geochemical Research (PCIGR) at the University of British Columbia. Additional discussion of the samples and the analytical techniques that were employed is presented in Heffernan (2004). For trace lead sulphide samples, approximately 10 to 50 milligrams of hand-picked sulphide minerals were first leached in dilute hydrochloric acid to remove surface contamination and then dissolved in dilute nitric acid. Samples of galena required no leaching and were directly dissolved in dilute hydrochloric acid. Following ion exchange chemistry, approximately 10 to 25 nanograms of lead in chloride form was loaded on rhenium filaments using a phosphoric acid-silica gel emitter. Isotopic ratios were determined with a modified VG54R thermal ionization mass spectrometer in peak-switching mode on a Faraday detector. Measured ratios were corrected for instrumental mass fractionation of 0.12%/amu based on repeated measurements of the NBS 981 standard and the values

recommended by Thirwall (2000). Errors were numerically propagated throughout all calculations and are reported at the  $2\sigma$  level (Table 2).

## RESULTS

The results from Pb isotope analyses of feldspar and sulphide mineral separates are presented in Table 2 and are plotted in Figure 3 with reference to the upper-crustal Pb evolution model (Shale Curve) of Godwin and Sinclair (1982). The Shale Curve is of particular relevance to this study as it is based on the Pb isotope compositions of shale-hosted lead-zinc deposits located within the Canadian Cordillera miogeocline. The new data are plotted together with previously determined lead isotopic compositions for other sulphide occurrences in the area (discussed later).

Lead isotopic analyses of feldspar collected from intrusions throughout the region generally yield quite consistent lead isotopic compositions (Table 2) with the exception of one sample (SH-011E-INT) collected from the Mt. Billings occurrence, which returned significantly more radiogenic values. With that single exception, the lead isotopic compositions ( $n=19$ ) show little variation in  $^{206}\text{Pb}/^{204}\text{Pb}$ ,  $^{207}\text{Pb}/^{204}\text{Pb}$ ,  $^{208}\text{Pb}/^{204}\text{Pb}$ ,  $^{207}\text{Pb}/^{206}\text{Pb}$  and  $^{208}\text{Pb}/^{206}\text{Pb}$  ratios, with narrow ranges of 19.397 to 19.651, 15.697 to 15.829, 39.461 to 39.883, 0.805 to 0.811 and 2.020 to 2.037, respectively.

Lead isotopic analyses for sulphide samples from mineral occurrences that are spatially associated with the intrusions also generally yield similar lead isotopic compositions (Table 2). Exceptions include three samples (SH-073-1, SH-070-1 and -2) from the Tai and Cali mineral occurrences at the north end of the Mt. Billings Batholith (Fig. 2), which returned the least radiogenic  $^{207}\text{Pb}/^{206}\text{Pb}$

**Table 1.** Location and basic descriptions of deposits and occurrences examined during this study.

Occurrence/ deposit	MINFILE reference	Commodities	Location		Status	Samples
			Northing	Easting		
Tai	105H 073	W, Cu, Zn, Mo	6854191	497966	drilled prospect	SH-073-1, SH-073-2
Cali	105H 070	W, Cu, Ag	6845327	518253	drilled prospect	SH-070, SH-070s
Flip	105H 005	Ag, Pb, Zn, W, Cu	6778677	518322	prospect	SH-005-1
Max	105H 011	Pb, Zn, Ag, W, Cu	6795031	515542	drilled prospect	SH-011E-1 to -4
Fir Tree	105H 029	Pb, Zn, Ag, Cu, W	6808645	529674	drilled prospect	SH-028-1, SH-029-2
Sa Dena Hes (Mt. Hundere)	105A 012	Zn, Pb, Ag	6709115	506817	past underground producer	SH-SDH (this study), 10138-001, -002, 501

**Table 2.** Pb isotope data from feldspar and sulphide mineral separates analysed during this study. All analyses were conducted in the Pacific Centre for Isotopic and Geochemical Research at the University of British Columbia. Mineral abbreviations: fs – feldspar; po – pyrrhotite; gl – galena; cp – chalcopyrite; py – pyrite. Samples SH-HY-01 to 04 are from the Hyland Au occurrence (Fig. 2) and were provided to the primary author by StrataGold Corp. Italicized samples are from intrusions and not necessarily associated with a specific mineral occurrence. Locations are shown as stars on Figure 2.

Sample	Source	Mineral	$^{206}\text{Pb}/^{204}\text{Pb}$	$2\sigma, \%$	$^{207}\text{Pb}/^{204}\text{Pb}$	$2\sigma, \%$	$^{208}\text{Pb}/^{204}\text{Pb}$	$2\sigma, \%$	$^{207}\text{Pb}/^{206}\text{Pb}$	$2\sigma, \%$	$^{208}\text{Pb}/^{206}\text{Pb}$	$2\sigma, \%$
<i>98-HAS-02</i>	Mt. Appler pluton	fs	19.490	0.03	15.757	0.04	39.541	0.06	0.80844	0.02	2.02878	0.03
<i>98-HAS-03</i>	Faille pluton	fs	19.440	0.03	15.731	0.04	39.480	0.06	0.80920	0.02	2.03090	0.03
<i>98-HAS-06</i>	Mulholland (Cirque) pluton	fs	19.487	0.04	15.751	0.05	39.578	0.07	0.80830	0.02	2.03103	0.04
<i>98-HAS-07</i>	Jorgensen pluton	fs	19.560	0.04	15.754	0.05	39.673	0.07	0.80541	0.02	2.02830	0.03
<i>98-HAS-12</i>	Patterson pluton	fs	19.534	0.08	15.771	0.08	39.757	0.10	0.80736	0.04	2.03530	0.04
<i>98-HAS-14</i>	McLeod pluton	fs	19.594	0.03	15.772	0.05	39.577	0.06	0.80496	0.02	2.01991	0.03
<i>98-Z-12</i>	Powers pluton	fs	19.651	0.11	15.829	0.12	39.883	0.13	0.80553	0.02	2.02960	0.03
<i>98-Z-C028</i>	Rudi Pluton	fs	19.493	0.03	15.750	0.05	39.569	0.06	0.80797	0.02	2.02993	0.03
<i>99SH-001</i>	Shannon Creek pluton	fs	19.404	0.03	15.732	0.04	39.461	0.06	0.81076	0.02	2.03365	0.03
<i>99SH-006</i>	Coal River Batholith	fs	19.477	0.10	15.771	0.10	39.640	0.11	0.80975	0.02	2.03526	0.03
<i>99SH-008</i>	Coal River Batholith	fs	19.460	0.09	15.741	0.09	39.596	0.10	0.80893	0.02	2.03480	0.03
<i>99SH-011</i>	Big Charlie pluton	fs	19.585	0.03	15.788	0.04	39.618	0.06	0.80612	0.02	2.02294	0.03
<i>99SH-023</i>	Mt. Billings Batholith	fs	19.447	0.04	15.749	0.05	39.598	0.07	0.80983	0.02	2.03621	0.04
<i>SH-005-INT</i>	Mt. Billings Batholith	fs	19.447	0.24	15.697	0.24	39.528	0.25	0.80718	0.05	2.03259	0.05
<i>SH-073-INT</i>	Mt. Billings Batholith	fs	19.473	0.03	15.762	0.05	39.591	0.06	0.80943	0.02	2.03317	0.03
<i>99SH-009</i>	Coal River Batholith	fs	19.545	0.04	15.757	0.05	39.670	0.07	0.80621	0.02	2.02969	0.03
<i>99SH-013</i>	Caesar Lakes pluton	fs	19.397	0.03	15.713	0.05	39.469	0.07	0.81007	0.02	2.03484	0.03
<i>99SH-016</i>	Tuna Stock	fs	19.530	0.04	15.798	0.05	39.774	0.07	0.80890	0.03	2.03658	0.04
<i>SH-011E-INT</i>	Mt. Billings Batholith	fs	19.772	0.04	15.810	0.05	39.786	0.07	0.79962	0.02	2.01221	0.03
<i>SH-029-INT</i>	Mt. Billings Batholith	fs	19.444	0.03	15.730	0.05	39.467	0.07	0.80899	0.02	2.02983	0.03
<i>SH-005-1</i>	Flip	po	19.579	0.05	15.775	0.06	39.750	0.07	0.80569	0.02	2.03022	0.03
<i>SH-011E-1</i>	Max	gl	19.473	0.03	15.731	0.04	39.482	0.06	0.80787	0.02	2.02757	0.03
<i>SH-011E-2</i>	Max	gl	19.491	0.03	15.752	0.05	39.545	0.06	0.80817	0.02	2.02888	0.03
<i>SH-011E-3</i>	Max	cp	19.615	0.04	15.904	0.05	40.039	0.07	0.81080	0.02	2.04126	0.03
<i>SH-011E-4</i>	Max	py	19.494	0.03	15.758	0.05	39.594	0.07	0.80832	0.02	2.03107	0.03
<i>SH-029-1</i>	Fir Tree	gl	19.396	0.04	15.728	0.05	39.445	0.07	0.81092	0.02	2.03373	0.03
<i>SH-029-2</i>	Fir Tree	po	19.467	0.03	15.795	0.05	39.709	0.06	0.81136	0.02	2.03979	0.03
<i>SH-070</i>	Cali	po	20.550	0.05	15.702	0.05	40.003	0.07	0.76406	0.03	1.94663	0.04
<i>SH-070s</i>	Cali	po	21.106	0.15	15.843	0.21	42.657	0.28	0.75066	0.07	2.02121	0.14
<i>SH-073-1</i>	Tai	po	19.915	0.15	15.797	0.21	39.648	0.28	0.79325	0.07	1.99101	0.14
<i>SH-073-2</i>	Tai	po	19.513	0.10	15.780	0.11	39.500	0.12	0.80873	0.02	2.02436	0.03
<i>SH-SDH</i>	Sa Dena Hes	gl	19.397	0.03	15.711	0.05	39.391	0.07	0.80998	0.02	2.03081	0.04
<i>SH-HY-01</i>	Hyland	py	20.066	0.11	15.779	0.10	40.174	0.06	0.78640	0.08	2.00210	0.06
<i>SH-HY-02</i>	Hyland	py	20.182	0.05	15.807	0.07	40.167	0.04	0.78320	0.03	1.99020	0.05
<i>SH-HY-03</i>	Hyland	py	20.236	0.05	15.871	0.07	40.391	0.04	0.78430	0.03	1.99600	0.04
<i>SH-HY-04</i>	Hyland	py	20.475	0.05	15.889	0.07	40.366	0.04	0.77600	0.02	1.97150	0.05

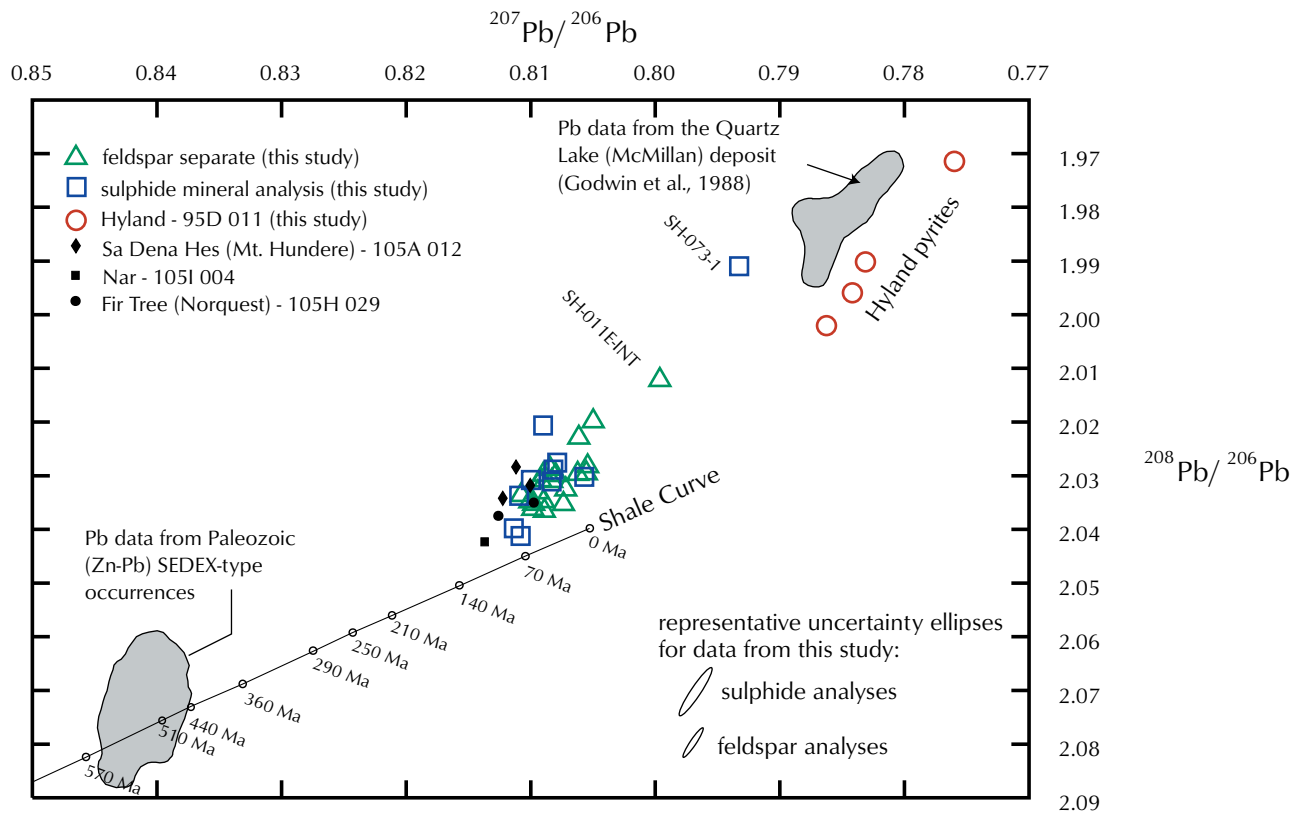


**Figure 3.**  $^{207}\text{Pb}/^{206}\text{Pb}$  versus  $^{208}\text{Pb}/^{206}\text{Pb}$  plot of Pb data from this study and similar data compiled from Godwin et al. (1988) for other mineral occurrences and deposits from within the study area (see text for discussion). Lead data for the Paleozoic SEDEX-type occurrences includes data from the Howard's Pass, Matt Berry, Mel-Hoser, Maxi, and Pas occurrences (Godwin et al., 1988). The Shale Curve of Godwin and Sinclair (1982) is shown for reference.

and  $^{208}\text{Pb}/^{206}\text{Pb}$  ratios in this study, and four analyses of pyrite from the Hyland gold occurrence, which yielded the most radiogenic lead isotopic compositions. The majority of analyses ( $n=9$ ) yield narrow ranges of  $^{206}\text{Pb}/^{204}\text{Pb}$ ,  $^{207}\text{Pb}/^{204}\text{Pb}$ ,  $^{208}\text{Pb}/^{204}\text{Pb}$ ,  $^{207}\text{Pb}/^{206}\text{Pb}$ , and  $^{208}\text{Pb}/^{206}\text{Pb}$  ratios with values of 19.396 to 19.615, 15.711 to 15.904, 39.391 to 40.039, 0.806 to 0.811, and 2.024 to 2.041, respectively.

## DISCUSSION

The feldspar lead isotopic compositions are highly radiogenic and plot above the Shale Curve of Godwin and Sinclair (1982), which indicates that the intrusions are largely, if not entirely, the product of partial melting of Selwyn Basin-like sedimentary rocks (see Heffernan, 2004, for further discussion). Lead isotopic compositions of most sulphide minerals from occurrences proximal to the

plutons are very similar to feldspar lead isotopic compositions from the plutons themselves. This is consistent with the metals having been derived mainly from the plutons.

Sulphide lead isotopic compositions from the past producing Sa Dena Hes zinc-lead-silver skarn deposit plot within the cluster of lead analyses for feldspars from Cretaceous intrusions and for associated sulphide minerals. Rare felsic and andesitic dykes are known to be associated with, and possibly related to, mineralization at the mine but have not been dated directly. The similarity in lead isotopic compositions suggests that the deposit is also mid-Cretaceous in age and probably related to a Cretaceous intrusion that is not exposed in the area.

Lead isotopic compositions from the Quartz Lake (McMillan) occurrence in the southeastern part of the study area and from the Hyland gold occurrence (Fig. 2),



a gold-rich, base metal poor deposit located near the Quartz Lake occurrence, are much more radiogenic than any of the other sulphide minerals or feldspars from the area. The Hyland gold occurrence may represent a distal style of intrusion-related, structurally controlled disseminated gold mineralization, whereas the Quartz Lake deposit consists of massive sulphide replacement bodies. The similar lead isotopic compositions from these occurrences suggest similar sources for the metals; however, the measured lead isotopic compositions are very different from that of any of the Cretaceous intrusions in the study area. The implications of this are uncertain. It could indicate that: (1) the metals in the Quartz Lake and Hyland deposits were derived from an unidentified intrusive phase that is much more radiogenic than any recognized thus far in the study area; or (2) the metals were derived mainly from sedimentary sources and are completely unrelated to the plutons; or (3) the lead in these deposits represents a mixture of lead from igneous and sedimentary sources. The lead isotopic compositions of sulphide minerals from epigenetic occurrences sampled in this study are very different from typical SEDEX-type lead-zinc occurrences in the Selwyn Basin (Fig. 3), and thus indicates that these occurrences do not represent remobilized SEDEX-type mineralization.

## CONCLUSIONS

The primary goal of this study was to compare and contrast the lead isotopic compositions of feldspars from various intrusions and sulphides from associated precious- and base-metal deposits and occurrences within the southeastern TGP in order to investigate possible linkages between magmatism and mineralization. Results from this study indicate that: (1) the metals in many mineral deposits and prospects in the region are mostly derived from the mid-Cretaceous TGP intrusions; (2) the Sa Dena Hes deposit is broadly mid-Cretaceous in age; and (3) metals in apparently distal styles of intrusion-related gold mineralization in this region are not entirely derived from magmatic sources. In an area with such voluminous magmatism and few mineral deposits, these results also serve to highlight the exploration potential throughout the study area.

## ACKNOWLEDGEMENTS

This work was completed as part of the author's MSc thesis at the University of British Columbia in conjunction with the Pacific Centre for Isotopic and Geochemical Research (PCIGR) and the Mineral Deposit Research Unit (MDRU). Funding and support for this project were provided by an NSERC Research Grant (to J.K. Mortensen), an NSERC Collaborative Research and Development Grant (to J.K. Mortensen and the MDRU), the Yukon Geological Survey, Hudson Bay Exploration and Development Co. Ltd., and a Hugh E. McKinstry Grant (to R.S. Heffernan). Thanks to Dave Hladky and StrataGold Corporation for providing samples from Hyland. Also, thanks goes to Dick Tosdal of the MDRU for providing a critical review of this paper.

## REFERENCES

- Deklerk, R. and Traynor, S., 2004 (compilers.). Yukon MINFILE – A database of mineral occurrences. Yukon Geological Survey, CD-ROM.
- Godwin, C.I. and Sinclair, A.J., 1982. Average lead isotope growth curves for shale-hosted zinc-lead deposits, Canadian Cordillera. *Economic Geology*, vol. 77, p. 208-211.
- Godwin C.I., Gabites, J.E. and Andrew, A., 1988. Leadtable: A galena lead isotope database for the Canadian Cordillera. *In: British Columbia Ministry of Energy and Mines and Petroleum Resources Paper 1988-4*, 214 p.
- Gordey, S.P. and Anderson, R.G. 1993. Evolution of the northern Cordillera Miogeocline, Nahanni Map Area (1051), Yukon and Northwest Territories. *Geological Survey of Canada Memoir 428*, 214 p.
- Gordey, S.P. and Makepeace, A.J. (compilers), 2001. *Bedrock Geology, Yukon Territory. In: Geological Survey of Canada, Open File 3754 and Exploration and Geological Services Division, Yukon Region, Indian and Northern Affairs Canada, Open File 2001-1*, 1:1 000 000 scale.
- Hart, C.J.R., McCoy, D.T., Goldfarb, R.J., Smith, M., Roberts, P., Hulstein, R., Bakke, A.A. and Bundtzen, T.K., 2002. Geology, exploration and discovery in the Tintina Gold Province, Alaska and Yukon. *In: Society of Economic Geologists Special Publication 9, Integrated Methods for Discovery: Global Exploration in the 21st Century*, p. 241-274.

- Heffernan, R.S., 2004. Temporal, geochemical, isotopic, and metallogenic studies of mid-Cretaceous magmatism in the Tintina Gold Province, southeastern Yukon and southwestern Northwest Territories, Canada. Unpublished MSc thesis, University of British Columbia, British Columbia, Canada, 83 p.
- Lang, J.R. and Baker, T., 2001. Intrusion-related gold systems: the present level of understanding. *Mineralium Deposita*, vol. 36, no. 6, p. 477-489.
- Lang, J.R. (ed.), 2000. Regional and system-scale controls on the formation of copper and/or gold magmatic-hydrothermal mineralization: Final Report, Mineral Deposit Research Unit Special Publication no. 2, 115 p.
- Mortensen, J.K., Hart, C.J.R., Murphy, D.C. and Heffernan, S., 2000. Temporal evolution of Early and mid-Cretaceous magmatism in the Tintina Gold Belt. *In: The Tintina Gold Belt: Concepts, Exploration and Discoveries*, British Columbia and Yukon Chamber of Mines, Special Volume 2, p. 49-58.
- Thompson, J.F.H., Sillitoe, R.H., Baker, T., Lang, J.R. and Mortensen, J.K., 1999. Intrusion-related gold deposits associated with tungsten-tin provinces. *Mineralium Deposita*, vol. 34, no. 4, p. 323-334.
- Thirwall, M.F., 2000. Inter-laboratory and other errors in Pb isotope analyses investigated using a  $^{207}\text{Pb}$ - $^{204}\text{Pb}$  double spike. *Chemical Geology*, vol. 163, p. 299-322.

# Preliminary geology of the Quill Creek map area, southwest Yukon parts of NTS 115G/5, 6 and 12

*Steve Israel<sup>1</sup>*

*Yukon Geological Survey*

*David P. Van Zeyl*

*Department of Geography, Trent University*

Israel S. and Van Zeyl, D.P., 2005. Preliminary geology of the Quill Creek map area, southwest Yukon parts of NTS 115G/5, 6 and 12. *In: Yukon Exploration and Geology 2004*, D.S. Emond, L.L. Lewis and G.D. Bradshaw (eds.), Yukon Geological Survey, p. 129-146.

## **ABSTRACT**

Geologic mapping within the Quill Creek area identified complex stratigraphic and structural relationships that characterize much of the Kluane Ranges in southwest Yukon. Bedrock in the Quill Creek area consists of Late Paleozoic to mid-Mesozoic volcanic and sedimentary rocks belonging to the Wrangellia Terrane. These rocks are intruded by Upper Triassic mafic and ultramafic sills and dykes and Early Cretaceous to Oligocene granitic rocks. At least two phases of folding are recognized that affect rocks throughout the mapped area. Early phase folds are likely associated with large, low-angle thrust faults. Reactivation of thrusts during younger strike-slip faulting may be responsible for refolding of the early folds.

Several known mineralized showings occur within the Quill Creek area, including extensive nickel-copper-platinum group element mineralization associated with the ultramafic sills. Samples collected during 2004 mapping indicate potential for copper-silver mineralization at the base of Upper Triassic volcanic rocks.

## **RÉSUMÉ**

La cartographie géologique de la région de Quill Creek a permis de mettre en évidence des relations stratigraphiques et structurales complexes qui caractérisent une bonne partie des chaînes Kluane dans le sud-ouest du Yukon. L'assise rocheuse de la région de Quill Creek est formée de roches volcaniques et sédimentaires qui datent de la période allant du Paléozoïque tardif au Mésozoïque moyen et appartiennent à la Wrangellie. Ces roches sont pénétrées par des filons-couches et dykes mafiques et ultramafiques du Trias supérieur et des roches granitiques de la période allant du Crétacé précoce à l'Oligocène. Au moins deux phases de plissement ont touché les roches dans l'ensemble de la région cartographiée. Les plis de la première phase sont sans doute associés à de grandes failles chevauchantes à faible pendage. La réactivation du chevauchement lors de la formation de failles décrochantes pourrait avoir causé le replissement des plis initiaux.

Plusieurs indices minéralisés sont connus dans la région de Quill Creek, y compris des minéralisations importantes en nickel, en cuivre et en éléments du groupe du platine, lesquelles sont associées aux filons-couches ultramafiques. Les échantillons recueillis en 2004 indiquent la possibilité de minéralisation en cuivre et en argent à la base des roches du Trias supérieur.

<sup>1</sup>steve.israel@gov.yk.ca



## INTRODUCTION

This paper presents preliminary results from 1:50,000-scale bedrock mapping within the Quill Creek area, southwest Yukon. Work completed in the summer of 2004 sets the groundwork for a multi-year project within the Kluane Ranges with the aim of deciphering complex geologic relationships found in Late Paleozoic to Tertiary sedimentary and volcanic rocks associated with the Wrangellia Terrane and younger overlap assemblages. Mapping began in June 2004 and focused on the area between the Donjek River and Burwash Creek (Fig. 1) and is meant to build on data collected by previous

workers. A study by Greene et al. (this volume) will focus on the Upper Triassic volcanic rocks of the Wrangellia Terrane and will help to place these rocks within the regional tectonic framework for the Quill Creek area and the surrounding Kluane Ranges.

## PREVIOUS WORK

Exploratory geological mapping of the Kluane Ranges and surrounding regions was first conducted by McConnell (1905) and later by Cairnes (1915) and Sharp (1943) within the White River and Steele Creek areas, respectively. In 1951, nickel-copper mineralization was discovered along

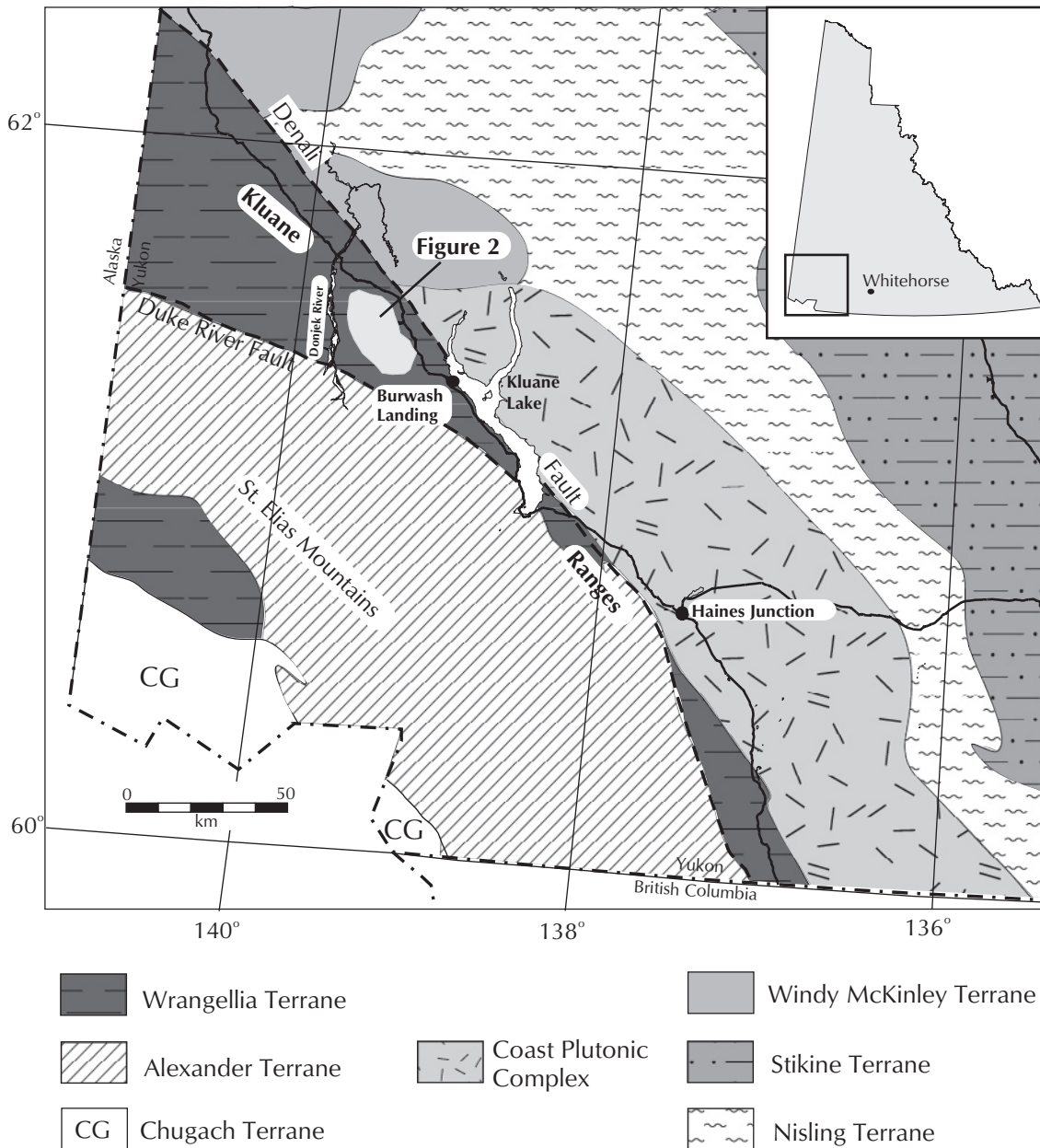


**Figure 1.** Terrane map of southwest Yukon, showing the distribution of the Wrangellia Terrane. The location of Figure 2, the Quill Creek map area, is highlighted for reference (after Wheeler et al., 1991).

Quill Creek. This led to a staking rush and an increase in industry activity that was followed by the preliminary geological investigations of Bostock (1952). Subsequent regional mapping of parts of the southwest Dezadeash (Kindle, 1953), southwest Kluane Lake (Muller, 1967), Tatshenshini (Watson, 1948) and Mount St. Elias (Wheeler, 1963) map sheets was carried out by the Geological Survey of Canada (GSC). Between 1973 and 1987, the GSC mapped the entire St. Elias Mountains, including the Kluane Ranges, at a scale of 1:250 000 under the auspices of Operation St. Elias. The objective of this project was to gain a better understanding of an area for which limited geological information existed. Several reports were produced from this study including a summary of the pre-Cenozoic rocks of the Kluane and Alsek ranges (Read and Monger, 1976), an investigation of the Ni-Cu mineralization within the Kluane Ranges (Campbell, 1976) and 1:250 000 compilations of bedrock geology for 115 A, 115 B/C, 115 G/F and 114 P (Dodds and Campbell, 1992). Detailed investigations of ultramafic intrusions associated with Ni-Cu-PGE mineralization in the Kluane Ranges by Hulbert (1997) led to identification of the 'Kluane mafic-ultramafic belt,' which underlies the Kluane Ranges from southern Kluane Lake to the Alaska-Yukon border. Geologic mapping of the Quill Creek and surrounding area accompanied this project (T. Bremner, unpublished data).

## GEOLOGIC SETTING

The Kluane Ranges are composed of Late Paleozoic to Middle Mesozoic rocks of the Wrangellia Terrane and portions of the Alexander Terrane, and younger Mesozoic to Cenozoic overlap assemblages. The Wrangellia Terrane and the Alexander Terrane were amalgamated prior to Middle Jurassic, and perhaps as early as Pennsylvanian time, to form the Insular Superterrane. This large composite terrane spans much of the western margin of the North American Cordillera from Vancouver Island to southern Alaska (Gardner et al., 1988; Gehrels, 2002) and was accreted to the North American margin by at least the Middle Jurassic (McClelland et al., 1992; van der Heyden, 1992; Gehrels, 2001; Ridgeway et al., 2002). Late Mesozoic and Cenozoic dextral strike-slip faulting along the Denali and related faults dissected the amalgamated terranes and offset portions of the terranes by as much as 350 to 400 km (Lowey, 1998). This event included reactivation of the Wrangellia/Alexander suture, now defined in southwestern Yukon by the Duke River Fault (Fig. 1). The Wrangellia Terrane in the Kluane Ranges

forms a fault-bounded wedge that widens to the northwest and is juxtaposed against the Coast Plutonic complex along the Denali Fault to the northeast and against the Alexander Terrane along the Duke River Fault to the southwest (Fig. 1).

The Quill Creek map area is underlain entirely by rocks of the Wrangellia Terrane. It contains much of the Late Paleozoic to Upper Triassic stratigraphy that defines the terrane.

## STRATIGRAPHY

### SKOLAI GROUP

Pennsylvanian to Lower Permian volcanic and sedimentary rocks of the Quill Creek area have been correlated with the Skolai Group of eastern Alaska (Read and Monger, 1976) where it is divided into a lower volcanic unit, the Station Creek Formation, and an upper sedimentary unit, the Hasen Creek Formation (Smith and MacKevett, 1970). The Skolai Group consists of the Late Paleozoic 'Skolai arc' with the Station Creek Formation representing arc volcanism and the Hasen Creek Formation representing the basin infill during arc subsidence (Nokleberg et al., 1994).

#### *Station Creek Formation*

The Station Creek Formation outcrops extensively throughout the Quill Creek area where it is gradationally overlain by rocks of the Hasen Creek Formation and is locally in fault contact with the Upper Triassic Nikolai formation (Fig. 2). Thickness of the Station Creek Formation is unknown since the only exposures of its base are fault contacts (Smith and MacKevett, 1970; Read and Monger, 1976). Outcrops of the Station Creek Formation on the northern slopes of the Kluane Ranges, within the northwestern portion of the Quill Creek area, suggest that it is at least several hundred metres thick. Read and Monger (1976) suggest the unit could be upwards of 3000 m thick in places. Structural complexities, however, likely affect the accuracy of these estimates.

At its type section, within the McCarthy Quadrangle of eastern Alaska, Smith and MacKevett (1970) divide the Station Creek into a lower volcanic flow-dominated member and an upper volcanoclastic-dominated member. In the Quill Creek area the volcanoclastic member dominates with only local exposures of volcanic flows. Volcanic breccia, tuff and tuffaceous sandstone make up the majority of rock types within the Station Creek

Formation in the study area (Fig. 3). The breccia is composed of dark to light green, angular to subangular clasts within a tuffaceous to sandy matrix (Fig. 4a). The clasts are up to several tens of centimeters in diameter and are mainly composed of pyroxene-±plagioclase-phyric basalt and minor light green tuff. The breccia is generally clast-supported but locally shows grading to become more matrix-supported. The tuff is much more variable, ranging from a light green, very fine-grained vitric

tuff to a light grey/green coarse-grained crystal rich, volcanoclastic sandstone. Flows composed of pyroxene-±plagioclase-phyric basalt constitute a minor portion of the Station Creek Formation within the study area; however, where they do occur they make up a substantial portion of the outcrops. Campbell (1981) included a 'Transition Zone' within the uppermost Station Creek Formation that consists of argillite, limestone and chert. The Transition Zone marks the gradational boundary

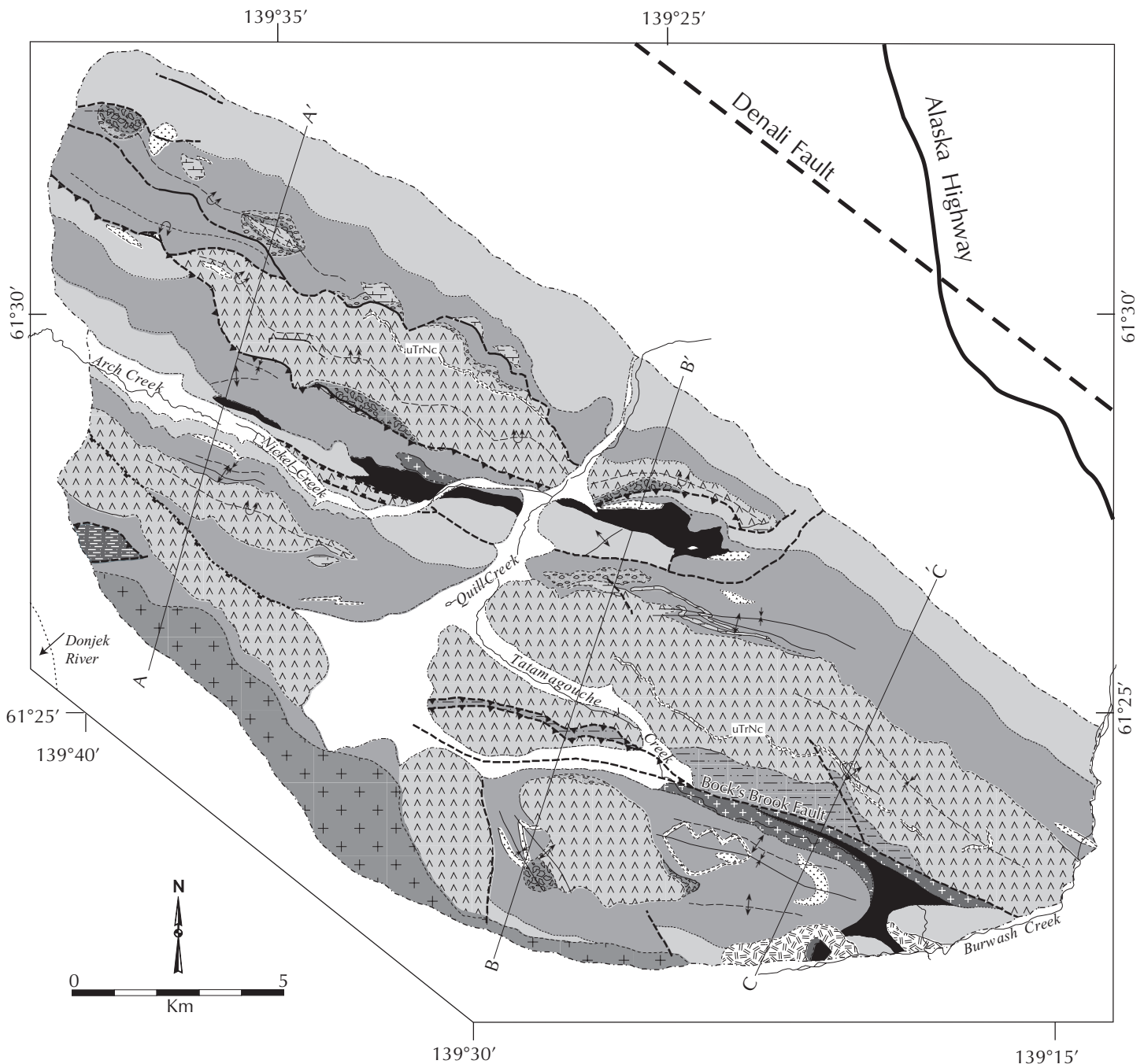
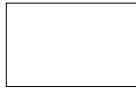


Figure 2. Generalized geological map of the Quill Creek area (after Israel and Van Zeyl, 2004).



STRATIGRAPHY

QUATERNARY



unconsolidated alluvium, colluvium and glacial deposits

STRATIGRAPHIC ROCKS

TRIASSIC TO CRETACEOUS

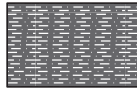
**Tatamagouche succession**



dark to light grey phyllite, minor greywacke and pebble conglomerate, may include upper parts of McCarthy Formation

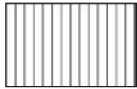
UPPER TRIASSIC

**McCarthy Formation**



light to dark grey shale and argillite interbedded with buff-coloured limestone

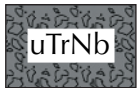
**Nikolai formation**



thinly bedded grey limestone and minor maroon to olive green argillite



dark green to maroon amygdaloidal basalt and andesitic/basalt flows, pyroxene and plagioclase porphyritic; locally developed pillows and pillow breccia.



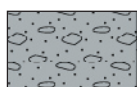
uTrNb

light to dark green volcanic breccia. Angular clasts of amygdaloidal and pyroxene porphyritic volcanic rocks and minor argillite

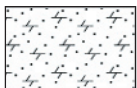
PENNSYLVANIAN (?) AND PERMIAN

**Skolai Group**

**Hasen Creek Formation**



pebble to cobble conglomerate, rounded to sub-angular clasts of siltstone, chert, greywacke and minor mafic volcanic rocks; massive to graded beds several metres thick



limestone, light to dark grey, fossiliferous and frequently pebbly; commonly graded and cross-bedded



light grey to white bioclastic limestone, local cherty interbeds



dark to light grey/brown siltstone turbidites, siliceous argillite, chert and minor volcanoclastic sandstone and tuffs

**Station Creek Formation**



dark to light green volcanic breccia, crystal tuff and tuffaceous sandstone; breccia clasts consist of augite phyric basalt clasts within tuffaceous matrix; minor augite porphyry, locally amygdaloidal

INTRUSIVE ROCKS

OLIGOCENE

**Tkope suite**



fine- to medium-grained, equigranular hornblende± biotite quartz-feldspar porphyry

CRETACEOUS

**Kluane Ranges suite**



fine- to medium-grained, equigranular hornblende ± pyroxene diorite and gabbro

UPPER TRIASSIC

**Maple Creek gabbro**



fine- to coarse-grained diabase and gabbro sills and dykes, locally abundant epidote and chlorite altered; commonly columnar jointed

**Kluane mafic-ultramafic complex**



coarse-grained and pegmatitic gabbro



peridotite, dunite and clinopyroxenite, layered intrusions, locally with gabbroic chilled margins

SYMBOLS

geologic contacts (defined, approximate, inferred).....	
limit of mapping.....	
limit of outcrop.....	
fault movement not known (known, approximate).....	
thrust fault (known, approximate).....	
normal fault (approximate, inferred).....	
fold axial trace antiform: (upright, overturned).....	
synform: (upright, overturned).....	

Figure 2. Legend for Quill Creek map area, facing page.

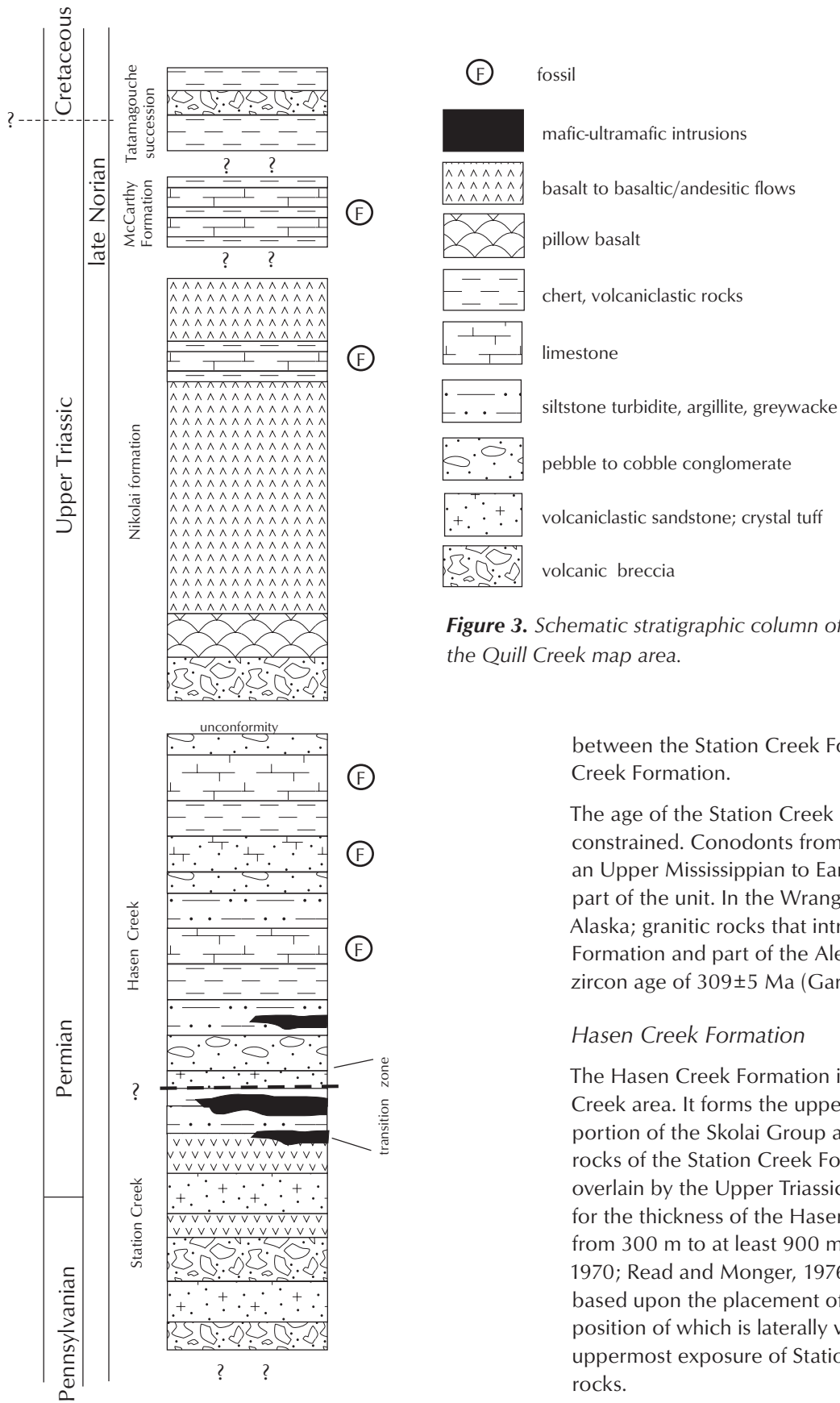


**Figure 3.** Schematic stratigraphic column of the rocks found within the Quill Creek map area.

between the Station Creek Formation and the Hasen Creek Formation.

The age of the Station Creek Formation is not well constrained. Conodonts from the Transition Zone suggest an Upper Mississippian to Early Permian age for the upper part of the unit. In the Wrangell Mountains of east-central Alaska; granitic rocks that intrude the Station Creek Formation and part of the Alexander Terrane have a U-Pb zircon age of  $309 \pm 5$  Ma (Gardner et al., 1988).

### Hasen Creek Formation

The Hasen Creek Formation is widespread in the Quill Creek area. It forms the upper sedimentary-dominated portion of the Skolai Group and gradationally overlies rocks of the Station Creek Formation. It is unconformably overlain by the Upper Triassic Nikolai formation. Estimates for the thickness of the Hasen Creek formation range from 300 m to at least 900 m (Smith and Mackevett, 1970; Read and Monger, 1976; Campbell, 1981) and are based upon the placement of the lower contact, the position of which is laterally variable, above the uppermost exposure of Station Creek Formation volcanic rocks.



**Figure 4.** (a) Angular to sub-angular clasts of pyroxene-phyric basalt within volcanic breccia of the Station Creek Formation; (b) Pebbles to cobbles of siltstone, chert and limestone within conglomerate of the Hasen Creek Formation; (c) Typical large outcrop of limestone within the Hasen Creek Formation; outcrop is approximately 40 m high.

In the Quill Creek area, the Hasen Creek Formation is dominated by siltstone, argillite and greywacke turbidite with local development of conglomerate, limestone, chert and minor volcanoclastic rocks (Fig. 3). Turbidites locally exhibit complete Bouma sequences with graded and cross-bedded layers indicating way-up. Massive argillite beds are also widespread and are up to several metres thick. Conglomerate beds are less than 1 m to >100 m thick and are composed of pebbles to cobbles of siltstone, chert and limestone within a fine- to medium-grained sandy matrix (Fig. 4b). Light beige to white weathering limestone and dark grey limestone conglomerate occur as small lenses and as thick, laterally continuous beds in the upper half of the Hasen Creek Formation (Fig. 4c). They commonly contain solitary and colonial corals and cherty interbeds. Rare beds of volcanic breccia are several metres thick and contain angular to subangular clasts of fine-grained mafic volcanic rocks. Numerous fossils found within the unit suggest an Upper Carboniferous to Lower Permian age for the Hasen Creek Formation (Dodds et al., 1993).

#### *Nikolai formation*

The Nikolai formation is an informally named sequence of volcanic and minor sedimentary rocks also known as the Nikolai Greenstone and the Nikolai volcanics (Smith and Mackevett, 1970; Read and Monger, 1976; Campbell, 1981; Dodds and Campbell, 1992). The formation outcrops extensively within the study area, capping many of the highest mountains in the region and coring large regional overturned synclines (Fig. 2). In the Quill Creek area, the Nikolai formation unconformably overlies rocks of the Skolai Group and has uncertain contact relationships with overlying rocks of the McCarthy Formation and the Tatamagouche succession (Fig. 3). The Nikolai formation is up to 1000 m thick in the Quill Creek area and elsewhere is reported to be at least 4350 m thick (Nokleberg et al., 1994). It is a dominantly volcanic sequence that is part of a large oceanic plateau (Richards et al., 1991) that extends to the northwest into Alaska and as far south as Vancouver Island. In the Quill Creek area the Nikolai formation is divided into three units: a lowermost breccia unit (uTrNb), a middle flow unit





**Figure 5.** (a) Volcanic breccia/agglomerate found at the base of the Nikolai formation; note large clast left of hammer; (b) Pillow breccia near the base of Nikolai formation; (c) Poorly formed pillows found at the base of thick flows of the Nikolai formation; (d) Typical flows found within the main volcanic package of the Nikolai formation; note the concentration of amygdules at the top and bottom of flows; (e) Thinly bedded olive green to maroon argillite and limestone of unit uTrNc.



(uTrNv), and a sedimentary unit (uTrNc) that is found near the base and the top of the flow unit.

#### *uTrNb*

Volcanic breccia to agglomerate, at least 100 m thick, is locally developed at the base of the Nikolai formation (Fig. 3). The breccia is characterized by clasts of amygdaloidal basalt within a fine- to medium-grained matrix of the same composition (Fig. 5a). The clasts are subangular to subrounded and range in size from <1 cm up to 40 cm in diameter. It is locally difficult to distinguish between the Nikolai breccias and those of the Station Creek Formation. The main difference is the abundance of amygdules observed within clasts of the Nikolai breccias.

#### *uTrNv*

The main component of the Nikolai formation is a thick sequence of flood basalts. At the base of the sequence flows are dark green, vesicular and commonly composed of pillow breccia (Fig. 5b, c). The thickness of the pillowed section is unknown, but must be at least several tens of metres thick based on outcrop distribution. The pillows pass upward into massive basalt to basaltic andesite flows that are characteristically olive green to maroon in colour, highly vesicular and amygdaloidal. Locally, the flows are augite- and more rarely olivine-phyric. Amygdules are filled with chlorite, quartz and epidote. Flows are from one to several metres thick and are discernable by hematite-rich, highly vesicular flow tops and bottoms (Fig. 5d).

#### *uTrNc*

Thinly bedded bioclastic limestone and argillite of unit uTrNc are found near the base and near the top of the Nikolai formation. These sedimentary beds are normally less than 50 m thick but in places are nearly 100 m thick. The limestone is dirty grey, fine-grained and thinly interbedded with olive green to maroon, fine-grained argillite (Fig. 5e). This unit is ubiquitous where the Nikolai formation is thick and is laterally continuous over several kilometres (Fig. 2). The limestone has yielded conodonts and macrofossils with late Carnian to early Norian ages (Campbell, 1981; Read and Monger, 1976; Muller, 1967). These fossil constraints indicate an Upper Triassic age for the Nikolai formation.

### *McCarthy Formation*

The McCarthy Formation occurs as a fault bounded exposure at least 100 m thick in the westernmost part of the Quill Creek area (Fig. 2). It consists of interbedded light grey to beige limestone and dark grey argillite and shale that give the outcrops a very distinct striped appearance (Fig. 6a). Individual beds are generally less than 50 cm thick and are often disrupted by extensive faulting and folding. Abundant macrofossils are found throughout this unit. Samples collected during this study have yielded *Monotis subcircularis* (Gabb), a Late Norian bivalve common to the McCarthy Formation outside of the Quill Creek area (Read and Monger, 1976; Mackevett, 1971). Stratigraphic relationships with the underlying Nikolai formation are not well constrained in the Quill Creek area. Elsewhere, the McCarthy Formation conformably overlies the similarly aged Chitistone

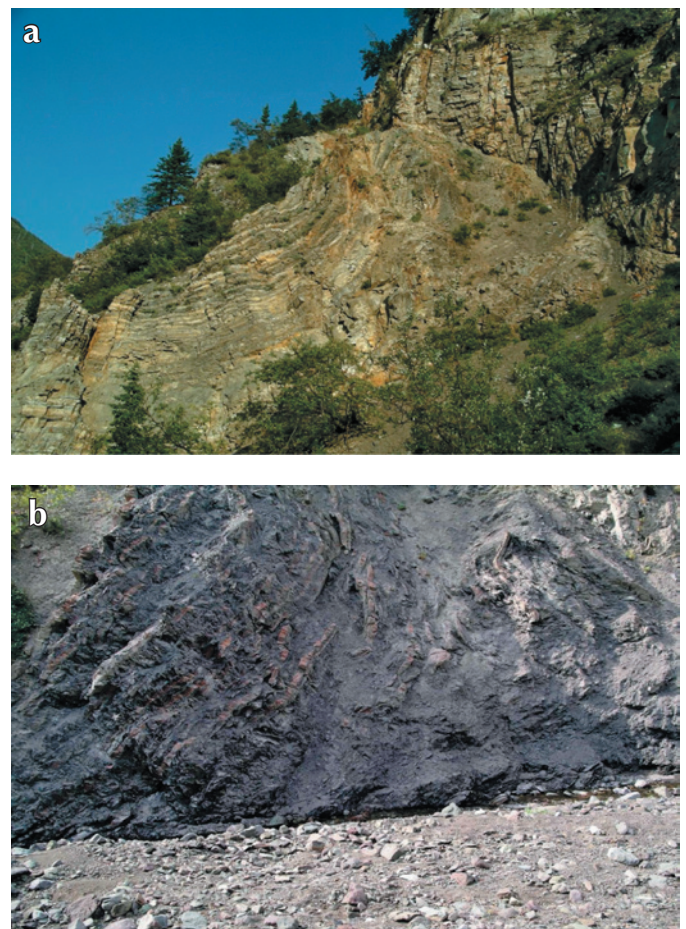


**Figure 6.** (a) Distinct striped appearance of interbedded limestone and argillite of the McCarthy Formation; (b) Highly deformed phyllites of the Tatamagouche succession, light bands are red weathering siliceous layers found only in this unit.



limestone which is in conformable contact with the underlying Nikolai formation (Read and Monger, 1976).

### TATAMAGOUCHE SUCCESSION

A sequence of highly deformed phyllite, siltstone, limestone and rare conglomerate that appears to stratigraphically overlie the Nikolai formation in one locality and is structurally interleaved with the Nikolai in another, is informally identified here as the Tatamagouche succession (Fig. 2). Outcrops of this succession along Tatamagouche Creek contain distinct, reddish, cherty bands that help to separate the unit from similar rocks within the Hasen Creek Formation (Fig. 6b). Included in the succession is a brick red conglomerate that is exposed in a creek that flows into the Tatamagouche Creek in the western part of the Quill Creek map area. This

conglomerate contains pebble- to cobble-sized clasts of grey and green chert, red siltstone, greenish intermediate volcanics and rare granitic rock. Fossils recovered from exposures of the Tatamagouche succession indicate ages for this unit that range from Upper Triassic to Cretaceous (Muller, 1967; Read and Monger, 1976). Relationships with the McCarthy Formation are not known and it may be that the Tatamagouche succession includes the upper part of the McCarthy Formation.

### INTRUSIONS

#### KLUANE MAFIC-ULTRAMAFIC BELT

Layered intrusions of the Kluane mafic-ultramafic belt are found within the rocks of the Wrangellia Terrane



**Figure 7.** (a) Typical outcrop of Kluane mafic-ultramafic belt peridotite; (b) Sill of Maple Creek gabbro (uTMg) intruding Hasen Creek Formation; (c) Salt and pepper colour typical of Kluane Ranges suite diorite; (d) Large exposure of Tkope suite quartz-feldspar porphyry (Ofp) intruding Station Creek Formation along Burwash Creek.



throughout the Kluane Ranges. They are considered to be, in part, the feeders to the Nikolai formation volcanic rocks. Several of these intrusions are found within the Quill Creek map area and include the Quill Creek complex, which hosts the Wellgreen Ni-Cu-PGE deposit (Yukon MINFILE 115G 024, Deklerk and Traynor, 2004). The intrusions occur primarily as sills and dykes near the contact between the Station Creek Formation and the Hasen Creek Formation. They are generally composed of a dunite core surrounded by peridotite and pyroxenite layers, and a pegmatitic to coarse-grained gabbro rim (Fig. 7a; Hulbert, 1997). Many of the sills are ubiquitously altered and locally are almost entirely serpentinized. The thickness of the ultramafic bodies is variable, ranging from several metres to several hundred metres (Hulbert, 1997). No direct, reliable age determinations have been made for the Kluane mafic-ultramafic belt; however, it is believed to be genetically linked to the Maple Creek gabbro that has an associated age of  $232\pm 1$  Ma (Mortensen and Hulbert, 1991; Hulbert, 1997).

### MAPLE CREEK GABBRO

Gabbroic dykes and sills of the Maple Creek gabbro outcrop extensively throughout the Quill Creek area (Fig. 2). These range from small (less than one metre) dykes to larger (over several tens of metres) sills. The Maple Creek gabbros are found almost exclusively within the Skolai Group and only rarely within the lower part of the Nikolai formation (Fig. 7b). They are composed of coarse- to medium-grained, pyroxene gabbro and fine-grained diabase. Where they intrude as sills, the bodies

commonly show columnar jointing. They are distinguished from the gabbro of the Kluane mafic-ultramafic belt by their much fresher appearance and lack of pegmatitic phases. The Maple Creek gabbro and the Kluane mafic-ultramafic belt are interpreted as feeders to the Nikolai formation (Hulbert, 1997). U-Pb zircon analyses of the Maple Creek gabbro indicate a crystallization age of  $232\pm 1$  Ma (Mortensen and Hulbert, 1991).

### KLUANE RANGES SUITE

Intrusive bodies of the Kluane Ranges suite extend along the entire length of the Kluane Ranges from the British Columbia/Yukon border to the Alaska/Yukon border in southwest Yukon. One intrusion outcrops along the southwestern margin of the Quill Creek area (Fig. 2) and is composed of salt and pepper coloured, fine- to medium-grained, hornblende-pyroxene diorite to gabbro (Fig. 7c). Outcrops are relatively fresh with little deformation or alteration, with the exception of small epidote veins. Imprecise K-Ar dates for the Kluane Ranges suite in the Quill Creek area indicate a mid-Cretaceous age (117 to 115 Ma; Christopher et al., 1972).

### TKOPE SUITE

Outcrops of the Tkope suite are exclusively found along Burwash Creek at the southern extent of the Quill Creek map area (Fig. 2). The suite is a light grey to cream coloured quartz-feldspar porphyry with acicular hornblende and minor biotite phenocrysts (Fig. 7d). The age of the Tkope suite is 28-26 Ma based on K-Ar analyses

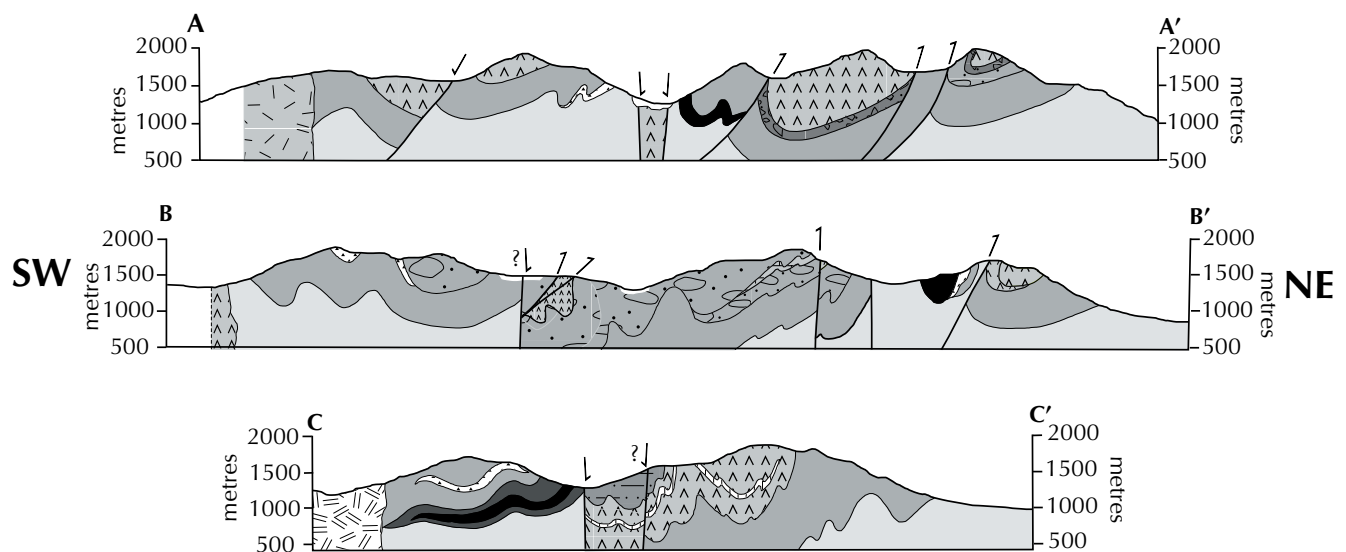


**Figure 8.** Schematic cross-sections through the Quill Creek map area. Location of section lines shown on Figure 2. Rock unit fills are the same as Figure 2.

of biotite from samples collected within and outside of the Quill Creek area (Read and Monger, 1976).

## STRUCTURE

The Quill Creek map area is characterized by complex structural relationships that are associated with two major terrane boundaries and reactivation along these boundaries during younger events. The boundaries are now represented by the Duke River Fault and the Denali Fault which bound the map area to the southwest and northeast, respectively, and separate rocks of the Wrangellia Terrane from those of the Alexander Terrane and the Coast Plutonic Complex (Fig. 1).

The oldest and most pervasive structural features evident within the study area are map-scale, northwest trending,

and northeast verging overturned folds (Fig. 2). The folds are likely related to northeast-directed contraction that occurred along southwest-dipping faults that are most prominent in the northwest part of the Quill Creek area. These faults apparently place Skolai Group rocks over Nikolai formation locally (Fig. 8). Associated outcrop-scale features indicate that the folds are tight to isoclinal (Fig. 9a, b) and plunge shallowly to moderately to the southwest and southeast. Cleavage formed during folding is generally moderately southwest-dipping but changes to northeast-dipping near Tatamagouche Creek in the southern portion of the map area (Fig. 2, 8).

A second folding event is locally developed within the study area. This second event is best represented by the refolding of the first phase folds that resulted in southwest and southeast plunges of the first phase fold axes.



**Figure 9.** (a) Tight fold in interbedded Hasen Creek Formation limestone and argillite; (b) Tight to isoclinal folds in limestone of the Hasen Creek Formation, located near the core of a large regional syncline; (c) Elongated clast within strongly deformed volcanic breccia of the Station Creek Formation. Stretching is parallel to pen and occurs along a southwest-dipping structure reactivated during strike-slip faulting; (d) North- to northwest-striking, steeply dipping shear zone several metres wide within ultramafic rocks of the Kluane mafic-ultramafic belt.



Cleavage development related to this folding event suggests that these folds are fairly upright and bedding cleavage relationships indicate that fold axes plunge gently to the south-southwest. It is likely that the second phase of folding is related to deformation along northwest-striking steeply dipping faults. Numerous northwest-striking faults are present at all scales within the Quill Creek area. They are undoubtedly related to the Denali and Duke River faults (Fig. 2). Reactivation of the large southwest-dipping structures responsible for the first contractional event is indicated by shallowly plunging lineations, stretched pebbles and asymmetric crenulations developed within these fault zones (Fig. 9c).

A number of normal faults are inferred by stratigraphic relationships observed in the Quill Creek map area (Fig. 8). These faults are concealed beneath the Quaternary cover. They are required to explain the position of Nikolai formation rocks, particularly along Nickel and Arch creek valleys (Fig. 2). Campbell (1981) suggested the presence of a graben



**Figure 11.** Photograph of area that sample 04-SIS-137-3-1 was taken from. Zone just below hammer in centre of photograph is composed of chalcopyrite, pyrite and malachite.

**Table 1.** Yukon MINFILE occurrences and associated deposit types found within the Quill Creek area (from Deklerk and Traynor, 2004).

MINFILE	Name	Deposit type	Status
115G 014	Amp	Porphyry Cu-Mo-Au	anomaly
115G 015	Cork	Porphyry Cu-Mo-Au	drilled prospect
115G 016	Glen	Gabbroid Cu-Ni	drilled prospect
115G 017	Burwash	Besshi massive sulphide	drilled prospect
115G 018	Nelms	Unknown	unknown
115G 019	Jaquot	Gabbroid Cu-Ni	drilled prospect
115G 020	Vug	Unknown	unknown
115G 021	Quill	Gabbroid Cu-Ni	drilled prospect
115G 022	Versluce	Gabbroid Cu-Ni	drilled prospect
115G 023	Callinan	Unknown	unknown
115G 024	Wellgreen	Gabbroid Cu-Ni	underground past producer
115G 025	Airways	Gabbroid Cu-Ni	drilled prospect
115G 026	Musketeer	Besshi massive sulphide	showing
115G 027	Swede Johnson	Gabbroid Cu-Ni	showing
115G 094	Linda	Alaskan Type ultramafic	drilled prospect
115G 095	Arby	Unknown	unknown
115G 102	Tremblay	Cu ± Ag quartz vein	unknown

structure in this area and of normal faults along the Bock's Brook Fault in Tatamagouche Creek.

Several north-northeast- and north-northwest-striking, steeply dipping structures are present throughout the area and appear to offset many of the other structures (Fig. 2, 9d).

## MINERALIZATION

Several different mineral occurrences, associated with a variety of deposit types, are found within the Quill Creek map area (Table 1; Fig. 10 [see next page]). The most prevalent are gabbroid Ni-Cu-PGE occurrences associated with the Kluane mafic-ultramafic belt. A detailed investigation of the Kluane mafic-ultramafic belt by Hulbert (1997) identified a number of ultramafic complexes. Of these, the Quill Creek complex, which hosts the Wellgreen deposit (Yukon MINFILE 115G 024), has received the most attention. Drilling by Kluane Joint Ventures in 1988 and 1989 led to an estimate of probable reserves at Wellgreen of approximately 42.3 million tonnes grading 0.36% Ni, 1.42% Cu, 0.51 g/t Pt and 0.34 g/t Pd (Deklerk and Traynor, 2004). Other ultramafic complexes have received little attention recently, but have high potential for similar mineralization. In the Quill Creek map area, the Linda Creek and the Tatamagouche are two





other notable ultramafic complexes (Fig. 10). Of these, the Linda Creek complex has seen the most exploration work, whereas relatively little attention has been given to the Tatamagouche complex. The Tatamagouche complex is considered to be the largest ultramafic complex within the belt and is a highly prospective target for Ni-Cu-PGE mineralization (Hulbert, 1997).

Two porphyry Cu-Mo-Au occurrences, the Amp and Cork, are found within the Quill Creek area (Fig. 11; Yukon MINFILE 115G 014 and 115G 015, Deklerk and Traynor, 2004). The Amp is related to the mid-Cretaceous Kluane Ranges suite and the Cork is associated with feldspar-porphry of the Tkope suite (Read and Monger, 1976; Deklerk and Traynor, 2004).

The Musketeer and Burwash (Yukon MINFILE 115G 017 and 115G 026) are possible Besshi-type massive sulphide occurrences. Exploration work on the Burwash occurrence included drilling by Nathan Minerals Inc. in 1989 that resulted in assays from drill core up to 1025 ppb Au (Halferdahl, 1991).

Several samples collected during mapping in 2004 were assayed and the results are presented in Table 2. One notable sample (04-SIS-137) returned 2.9% Cu, 43.3 g/t Ag and anomalous Ni and Au values. This sample was taken from the base of the Nikolai formation where chalcopyrite, pyrite and malachite occur within thin quartz veins and altered sediments of the Hasen Creek Formation (Fig. 11).

## DISCUSSION

Mapping of the Quill Creek area has identified stratigraphy that is common to the Wrangellia Terrane and reflects several tectonic events. The Skolai Group represents a Late Paleozoic volcanic arc that may be related to subduction of oceanic crust during the amalgamation of the Alexander Terrane and the Wrangellia Terrane to form the Insular Superterrane. Sedimentary rocks of the Slokai Group reflect later basin development during arc subsidence. Upper Triassic oceanic flood basalts of the Nikolai formation represent accumulation of a large amount of igneous material on top of the Paleozoic arc after uplift of the arc, which is indicated by the unconformable upper contact with the Nikolai formation. This was also the time of intrusion of the Kluane mafic-ultramafic belt and the Maple Creek gabbros. Subsidence of the Nikolai plateau led to the formation of the carbonate and sedimentary rocks that

overlie the volcanic rocks. Accretion of the Insular superterrane in Middle Jurassic time resulted in the large-scale folding and faulting that is evident within the Quill Creek map area. Late Mesozoic to Cenozoic strike-slip faulting along the entire length of Cordilleran margin overprinted earlier structural features.

## ACKNOWLEDGEMENTS

The authors would like to thank Rob Carne for discussion on the geology of the Kluane Ranges. Safe and reliable helicopter service was provided by Trans North Helicopters out of Haines Junction. Thanks to Grace Cohoe and Luke Johnson of Kluane First Nation for sharing their knowledge of the Quill Creek region. Parks Canada is acknowledged for their cooperation in providing access to Kluane National Park and Reserve. Comments by Maurice Colpron and Geoff Bradshaw on an early version made for a better manuscript.

## REFERENCES

- Bostock, H.S., 1952. Geology of the northwest Shakwak Valley, Yukon Territory. Geological Survey of Canada, Memoir 267.
- Cairnes, D.D., 1915. Exploration in southwest Yukon. Geological Survey of Canada, Summary Report 1914, p. 10-37.
- Campbell, S.W., 1981. Geology and genesis of copper deposits and associated host rocks in and near the Quill Creek area, southwestern Yukon. Unpublished PhD thesis, University of British Columbia, Vancouver, British Columbia, 215 p.
- Campbell, S.W., 1976. Nickel-copper sulphide deposits in the Kluane Ranges, Yukon Territory. Department of Indian and Northern Affairs, Open File EGS 1976-10, 17 p.
- Christopher, P.A., White, W.H. and Harakal, J.E., 1972. K-Ar dating of the 'Cork' (Burwash Creek) Cu-Mo prospect, Burwash Landing area, Yukon Territory. Canadian Journal of Earth Science, vol. 9, p. 918-921.
- Deklerk, R. and Traynor, S. (comps.), 2004. Yukon MINFILE – A database of mineral occurrences. Yukon Geological Survey, CD-ROM.

- Dodds, C.J. and Campbell, R.B., 1992. Overview, legend and mineral deposit tabulations for: Geological Survey of Canada Open File 2188, Geology of SW Kluane Lake map area (115G and F[East half]), Yukon Territory; Open File 2189, Geology of Mount St. Elias map area (115B and C[East half]), Yukon Territory; Open File 2190, Geology of SW Dezadeash map area (115A), Yukon Territory; Open File 2191, Geology of NE Yakutat (114O) and Tatshenshini River (114P) map areas, British Columbia. Geological Survey of Canada, Summary Report, 85 p.
- Dodds, C.J., Campbell, R.B., Read, P.B., Orchard, M.J., Tozer, E.T., Bamber, E.W., Pedder, A.E.H., Norford, B.S., McLaren, D.J., Harker, P., McIver, E., Norris, A.W., Ross, C.A., Chatterton, B.D.E., Cooper, G.A., Flower, R.H., Haggart, J.W., Uyeno, T.T. and Irwin, S.E.B., 1993. Macrofossil and conodont data from: SW Kluane Lake (115G and F [East half]), Mount St. Elias (115B and C [East half]), SW Dezedeash (115A), NE Yakutat (114O) and Tatshenshini River (114P) map areas, southwestern Yukon and northwestern British Columbia. Geological Survey of Canada, Open File 2731, 137 p.
- Gardner, M.C., Bergman, S.C., Cushing, G.W., MacKevett, E.M. Jr., Plafker, G., Campbell, R.B., Dodds, C.J., McClelland, W.C. and Mueller, P.A., 1988. Pennsylvanian pluton stitching of Wrangellia and the Alexander terrane, Wrangell Mountains, Alaska. *Geology*, vol. 16, p. 967-971.
- Gehrels, G., 2001. Geology of the Chatham Sound region, southeast Alaska and Coastal British Columbia. *Canadian Journal of Earth Science*, vol. 38, p. 1579-1599.
- Gehrels, G., 2002. Detrital zircon geochronology of the Taku terrane, southeast Alaska. *Canadian Journal of Earth Science*, vol. 39, p. 921-931.
- Greene, A.R., Scoates, J.S., Weis, D. and Israel, S., 2005. Flood basalts of the Wrangellia Terrane, southwest Yukon: Implications for the formation of oceanic plateaus, continental crust and Ni-Cu-PGE mineralization. *In: Yukon Exploration and Geology 2004*, D.S. Emond, L.L. Lewis and G.D. Bradshaw (eds.), Yukon Geological Survey, p. 109-120.
- Halferdahl, L.B., 1991. Nathan Minerals Incorporated, Burwash Creek Area, Yukon. Energy, Mines and Resources, Mineral Assessment Report #092950.
- Hulbert, L., 1997. Geology and metallogeny of the Kluane mafic-ultramafic belt, Yukon Territory, Canada: eastern Wrangellia – A new Ni-Cu-PGE metallogenic terrane. Geological Survey of Canada, Bulletin 506, 265 p.
- Israel, S. and Van Zeyl, D., 2004. Preliminary geological map of the Quill Creek area, (parts of NTS 115G/5, 6, 12), southwest Yukon (1:50 000 scale). Yukon Geological Survey, Open File 2004-20.
- Kindle, E.D., 1953. Dezadeash map-area, Yukon Territory. Canadian Geological Survey, Memoir 268, 68 p.
- Lowey, G., 1998. A new estimate of the amount of displacement on the Denali Fault system based on the occurrence of carbonate megaboulders in the Dezadeash formation (Jura-Cretaceous), Yukon, and the Nutzotin Mountains sequence (Jura-Cretaceous), Alaska. *Bulletin of Canadian Petroleum Geology*, vol. 46, no. 3, p. 379- 386.
- MacKevett, E.M., Jr., 1971. Stratigraphy and general geology of the McCarthy C-5 Quadrangle, Alaska. United States Geological Survey, Bulletin 1321, 35 p.
- McConnell, R.G., 1905. The Kluane mining district. Canadian Geological Survey, Summary report 1904, report A, p. 1A-18A.
- McClelland, W.C., Gehrels, G.E. and Saleeby, J.B., 1992. Upper Jurassic-Lower Cretaceous basinal strata along the Cordilleran margin: implications for the accretionary history of the Alexander-Wrangellia-Peninsular Terrane. *Tectonics*, vol. 11, p. 823-835.
- Mortensen, J.K. and Hulbert, L.J., 1991. A U-Pb zircon age for a Maple Creek gabbro sill, Tatamagouche Creek area, southwest Yukon Territory. *In: Radiogenic age and isotopic studies: Report 5*, Geological Survey of Canada, paper 91-2, p. 175-179.
- Muller, J.E., 1967. Kluane Lake map-area, Yukon Territory. Canadian Geological Survey, Memoir 340, 137 p.
- Nokelburg, W.J., Plafker, G. and Wilson, F.H., 1994. Geology of south-central Alaska. *In: The Geology of Alaska*, G. Plafker and H.C. Berg (eds.), Geological Society of America, The Geology of North America, vol. G-1, p. 311-366.
- Read, P.B. and Monger, J.W.H., 1976. Pre-Cenozoic volcanic assemblages of the Kluane and Alsek Ranges, southwestern Yukon Territory. Geological Survey of Canada, Open File 381, 96 p.



- Richards, M.A., Jones, D.L., Duncan, R.A. and DePaolo, D.J., 1991. A mantle plume initiation model for the Wrangellia flood basalt and other oceanic plateaus. *Science*, vol. 254, p. 263-267.
- Ridgeway, K.D., Trop, J.M., Nokelburg, W.J., Davidson, C.M. and Eastham, K.R., 2002. Mesozoic and Cenozoic tectonics of the eastern and central Alaska Range: Progressive basin development and deformation in a suture zone. *Geological Society of America, Bulletin* 114, no. 12, p. 1480-1504.
- Sharp, R.P., 1943. Geology of the Wolf Creek area, St. Elias Range, Yukon Territory, Canada. *Geological Society of America, Bulletin* 54, p. 625-650.
- Smith, J.G. and MacKevett, E.M., Jr., 1970. The Skolai Group in the McCarthy B-4, C-4 and C-5 quadrangles, Wrangell Mountains, Alaska. *United States Geological Survey, Bulletin* 1274-Q, 26 p.
- van der Heyden, P., 1992. A Middle Jurassic to early Tertiary Andean-Sierran arc model for the Coast belt of British Columbia. *Tectonics*, vol. 11, p. 82-97.
- Watson, K. DeP., 1948. The Squaw Creek-Rainy Hollow area, northern British Columbia. *British Columbia Department of mines, Bulletin* 25, 74 p.
- Wheeler, J.O., 1963. Kaskawulsh, Yukon Territory. *Canadian Geological Survey, Map* 1134A.
- Wheeler, J.O., Brookfield, A.J., Gabrielse, H., Monger, J.W., Tipper, H.W. and Woodsworth, G.J., 1991. Terrane map of the Canadian Cordillera. *Geological Survey of Canada, Map* 1713A.

## APPENDIX

### FOSSIL IDENTIFICATION

Field no.: 04-SIS-138-1 GSC Loc. C-307261

Locality: Yukon Territory

UTM: Zone 7, 571103E, 6814288N

NTS: 115G/05

Loc: 4 km east of Donjek River

Strat: "Carbonaceous Siltstone"

Lith: Interbedded dirty limestone and carbonaceous siltstone

Fossils: *Monotis subcircularis* (Gabb)

Age: Late Triassic, Late Norian

# Character and metallogeny of Permian, Jurassic and Cretaceous plutons in the southern Yukon-Tanana Terrane<sup>1</sup>

**Tim Liverton<sup>2</sup>**

*Rhyoflow Inc.*

**Jim K. Mortensen**

*Pacific Centre for Isotopic and Geochemical Research, University of British Columbia<sup>3</sup>*

**Charlie F. Roots**

*Geological Survey of Canada<sup>4</sup>*

Liverton, R., Mortensen, J.K. and Roots, C.F., 2005. Character and metallogeny of Permian, Jurassic and Cretaceous plutons in the southern Yukon-Tanana Terrane. *In: Yukon Exploration and Geology 2004*, D.S. Emond, L.L. Lewis and G.D. Bradshaw (eds.), Yukon Geological Survey, p. 147-165.

## ABSTRACT

Between the Swift and Nisutlin rivers, unmetamorphosed granite to ultramafic intrusions of four ages (from Permian through Cretaceous) span the amalgamation of Cassiar Platform with Yukon-Tanana and Cache Creek terranes. The mid-Permian granitic Ram Stock and two plutons cutting the Sylvester Allochthon lie at the edge of the Dorsey Complex, a remnant of an ancient passive margin succession that underlies the volcanic arcs of Yukon-Tanana Terrane. Middle Jurassic, locally foliated granodiorite to gabbro intrusions are metaluminous, and high in Sr and low in Ti compared to the Cretaceous suite. These 'I-type' volcanic arc plutons may be the remnants of an overlapping arc correlative with the Quesnel Terrane. The Cretaceous (113 to 98 Ma) meta- to peraluminous granites are late orogenic incipient 'A-type' plutons from highly fractionated F- and Cl-rich magmas. These generated extensive hydrothermal systems that produced tin, tungsten, molybdenum and beryl occurrences.

## RÉSUMÉ

Entre les rivières Swift et Nisutlin, des intrusions granitiques à ultramafiques non métamorphisées de quatre âges (allant du Permien au Crétacé) couvrent la limite entre la plate-forme de Cassiar et les terranes de Yukon-Tanana et de Cache Creek. Le stock granitique de Ram et deux plutons du Permien moyen, recoupant l'Allochthone de Sylvester, reposent à la bordure du Complexe de Dorsey, vestige d'une ancienne succession de marge passive sous-jacente aux arcs volcaniques du terrane de Yukon-Tanana. Des intrusions de granodiorite et de gabbro foliés par endroits, datant du Jurassique moyen, sont métalumineuses, ainsi que riches en Sr et pauvres en Ti en comparaison avec la série du Crétacé. Ces plutons de type I d'arcs volcaniques peuvent représenter les vestiges d'un arc chevauchant corrélatif au terrane de Quesnel. Les granites métalumineux à hyperalumineux du Crétacé (113 à 98 Ma) sont des plutons embryonnaires tardiorogéniques de type A, qui ont pour origine des magmas très fractionnés, riches en F et en Cl. Les vastes systèmes hydrothermaux générés ont donné lieu à des occurrences d'étain, de tungstène, de molybdène et de béryl.

<sup>1</sup>Contribution to Ancient Pacific Margin NATMAP 2004286

<sup>2</sup>Box 393, Watson Lake, Yukon, Canada Y0A 1C0

<sup>3</sup>6339 Stores Rd., Vancouver, British Columbia, Canada V6B 1Z4

<sup>4</sup>Box 2703 K-10, Whitehorse, Yukon, Canada Y1A 2C6



## INTRODUCTION

Almost 40% of the exposed bedrock in south-central Yukon and adjacent northern British Columbia is of felsic plutonic origin. Most of the plutons were intruded after the last major deformational episode and are termed post-tectonic. Isotopic dating has refined their ages (e.g., Stevens et al., 1993; Gordey et al., 1998; Roots et al., 2002; Nelson and Friedman, 2004): several are mid-Permian, many are Early Jurassic and mid-Cretaceous, and a few are Early Eocene.

Mineral occurrences are spatially associated with these plutons in the region. The occurrences which follow are from the Yukon MINFILE (Deklerk, 2003). A couple are also noted from BC MINFILE (Bradford and Jakobsen, 1988). At least ten mineral occurrences in greisen, skarn and fracture-fillings are associated with the Cretaceous Seagull Batholith (Dick, 1979; Mato et al., 1983; 105B 040) and the Thirtymile Range (50 km northwest; Liverton, 1990; 105C 038). Other deposit types are veins with chalcophile elements (silver and gold; Logjam, 105B 038), tungsten-molybdenum-bismuth-beryllium (beryl, aquamarine) porphyries (Logtung: Yukon MINFILE 105B 039, and BC MINFILE 104 016) and cassiterite-chalcopyrite breccias (STQ/Verley; 105B 078). Understanding the relationship of mineralization to the plutonic suites can be a useful tool in the continuing search for mineral deposits in the region.

In this paper we summarize the mineralogical and chemical character of three of these age-determined suites, and speculate on their origin. Isotopic age data for the Ram Stock is presented because this intrusion is important in resolving the tectonic history of southern Yukon-Tanana Terrane.

## REGIONAL GEOLOGY

The plutons intrude an 80-km-wide northwest-trending belt of Yukon-Tanana Terrane (YTT). This terrane consists of polydeformed sedimentary, volcanic and plutonic rocks that have been resolved into time- and protolith-determined arc successions, above metasedimentary units of probable continental-shelf origin (e.g., Colpron and the Yukon-Tanana Working Group, 2001). Southern YTT as used in this paper corresponds to the former Dorsey Terrane (e.g., Monger et al., 1991), now an obsolete term as the units within it have direct parallels with those of YTT.

YTT is separated by transcurrent faults from Cache Creek Terrane to the west, and Slide Mountain Terrane to the

east. These terranes contain stratigraphy that mainly records the evolution of mid-Paleozoic to Jurassic ocean basins, for the most part synchronous with the history of YTT. Slide Mountain Terrane is faulted to the east against marginal sedimentary rocks of ancient North America, a miogeoclinal succession of Cambrian to Permian age. In northern BC, between Dease Lake and the Rancheria River, is a klippe atop the miogeocline, which contains thrust slices of Slide Mountain and YTT (Fig. 1). This is the Sylvester Allochthon (e.g., Nelson, 1993), and is important because Slide Mountain Terrane is preserved here, while it is very thin or faulted out between YTT and ancient North America in Yukon.

The recent redefinition of YTT is based upon time-sequences rather than geographic area (c.f., Mortensen, 1992); currently, the term is restricted to the Devonian-Mississippian series of arc assemblages. In the BC-Yukon border area of YTT, these arc successions are the Big Salmon and Ram Creek complexes (Mihalynuk et al., 2000; Roots and Heaman, 2001). They lie along the west and east sides of YTT; between them a central area is underlain by Dorsey Complex, a highly strained 'basement' of siliciclastic sediments and amphibolite (Nelson, 2000), structurally overlain by basin and off-shelf sediment (Swift River Group; Nelson, 2001).

Overlapping the three complexes of southern YTT is a Late Mississippian to Triassic series of arc-related successions equivalent to the Quesnel Terrane of the southern Cordillera (Simard et al., 2003; Nelson and Friedman, 2004). An erosional unconformity and locally prominent conglomerate beneath the Klinkit Group (Simard et al., 2003) defines the irregular boundary between Quesnellia and underlying YTT.

A Permian intrusion (the Ram Stock), described in this paper, intrudes YTT just north of the Seagull Batholith. Two very large, subcircular Jurassic intrusions, the Simpson Peak and Nome Lake batholiths, in northern BC, could have supplied volcanic arc systems (Nelson and Friedman, 2004). Cretaceous and early Eocene plutons are considered post-tectonic because they intruded after these terranes were joined together. They occur in many suites (Breitsprecher et al., 2004), but we shall focus here upon the Cretaceous Hake and Thirtymile plutons, which are peculiar to southern YTT.

## GRANITIC SUITES

Table 1 provides a summary of dates for plutonic rocks in the BC-Yukon border area. These dates indicate four age groupings: Late Permian (270 to 255 Ma), Early Jurassic (ca. 188 Ma), early Late Cretaceous (101 Ma), and early Eocene (58 Ma). The physical characteristics are summarized below.

### LATE PERMIAN SUITE

Representatives of the Permian suite include the Ram Stock in southern Yukon, two smaller plutons in Sylvester Allochthon (Gabrielse et al., 1993), and several muscovite-bearing pegmatite dykes in northern BC (Nelson and Friedman, 2004). Only the Ram Stock is described here. It is a 26-km-long body, elongated northwest and parallel to the regional structural grain (Fig. 1). Width varies up to

3 km, the product of vertical offset on northeast-trending faults that expose different levels of a steeply dipping tabular or lenticular intrusion.

Almost all of Ram Stock is coarse-grained, equigranular hornblende>biotite quartz monzonite to granodiorite. The classic description of Poole (1956) includes microperthitic orthoclase, strained quartz and corroded ferromagnesian minerals. The range of modal analyses is shown in Table 2. It was known as the 'green granite' due to the abundant chlorite and pervasive sausseritization, yet it remains massive and resistant (Fig. 2).

The significance of the Ram Stock was first raised by R. Stevens during revision mapping (Stevens and Harms, 1995; Stevens, 1996). The top of the body (southwest contact) is intrusive into lower Dorsey Complex (Fig. 3). Within the stock, xenoliths show the same high-strain

fabric as does the Dorsey host rock to the southwest. In contrast, the dykes and offshoots of Ram Stock are relatively undeformed. Thus a date for the Ram Stock provides a minimum age for the deformation that imparted a distinct texture to rocks of the Dorsey Complex. Without the date, this deformational episode cannot be conclusively distinguished from that stemming from obduction of allochthons onto ancient North America (Cordilleran orogeny). A hornblende separate analysed by the Rb-Sr method gave a  $235 \pm 12$  Ma date (Hunt and Roddick, 1987).

The base of Ram Stock (northeast contact, and well exposed across ridge spurs west of Hidden Lake (Fig. 2)) is a 10- to 20-m-wide mylonitic shear zone. This is the Hidden Lake Thrust, an intra-terrane fault separating Dorsey Complex from Ram Creek Complex. It extends many tens of kilometres southeast, where top-to-the-east motion is indicated (Nelson et al., 2001).

Determination of the age of the Ram Stock provides a maximum age of this key thrust fault.

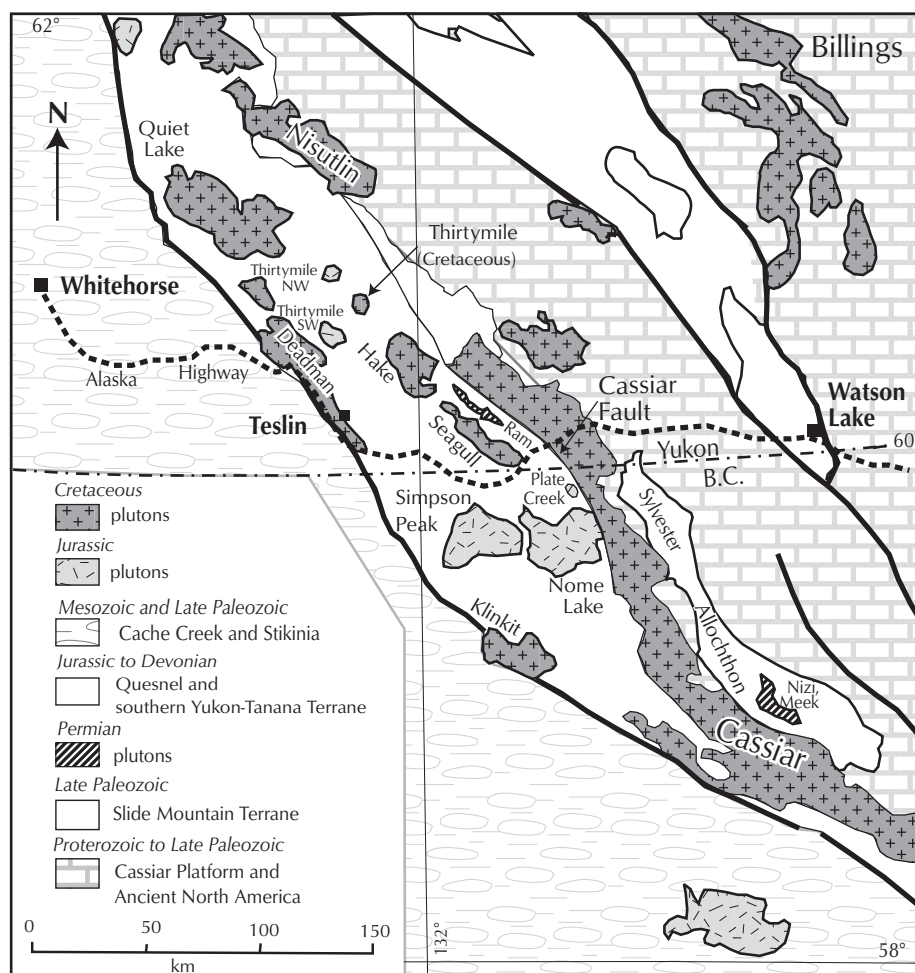


**Figure 1.** The area of southern Yukon-Tanana Terrane in northern BC and Yukon, showing the distribution of major post-tectonic plutons. The outlines of Quesnellian and Yukon-Tanana Terrane rock units is from Nelson and Friedman (2004; for BC) and Colpron (draft map; for Yukon).

**Table 1.** Summary of isotopic dates for post-tectonic plutons within Yukon-Tanana Terrane.

Name of pluton	Size	Main rock type	Minor types	Mineral occurrence (not necessarily same age)	Age, method	Reference for age
<b>Eocene</b>						
<b>Logtung</b>	2.5 km <sup>2</sup>	monzonitic granite	felsic dykes	scheelite, molybdenite, beryl	58.6±1.5 U-Pb zircon	Mihalynuk and Heaman, 2001
<b>Cretaceous</b>						
<b>Thirtymile</b>	15 km <sup>2</sup>	monzo- and syenogranite		Sn (tin) skarn	99±3 K-Ar on biotite hornfels	Liverton, 1990
		K-feldspar leucogranite		beryl	101±5.6 Rb/Sr	Liverton et al., 2001
<b>Seagull</b>	43 x 8 km	leuco quartz monzonite	alaskite	Sn, Pb, Zn skarn, wolframite	100±2.8 K-Ar	Mato et al. 1983
<b>Hake</b>	30 x 15 km	coarse biotite granite		Au skarn	98.3±2.9 Rb/Sr	Liverton et al., 2001
<b>STQ</b>	< 1 km <sup>2</sup>	granite	alaskite	cassiterite, scheelite, molybdenite, chalcopyrite	108±2 K-Ar on biotite	Hunt and Roddick, 1987 (GSC 87-152)
<b>Klinkit</b>	35 x 25 km	bt-hb granite		unknown	109.4 U-Pb zircon	Roots et al., 2002
<b>Jurassic</b>						
<b>Logjam pluton</b>	4 x 3 km	hb quartz monzonite, monzogranite	diorite, peridotite	unknown	181±14 K-Ar	Hunt and Roddick, 1987 (GSC 87-151)
<b>NW Thirtymile</b>	12 km <sup>2</sup>	monzogranite to granodiorite		unknown		
<b>SW Thirtymile</b>	20 km <sup>2</sup>	quartz diorite, hb granodiorite	gabbro		181.5±2.5 Rb-Sr	Liverton et al., 2001
<b>Simpson Peak</b>	20 x 40 km	granite, quartz monzonite	hb gabbro	unknown	185±14 K-Ar on hb	Mihalynuk et al., 1998
<b>Nome Lake</b>	36 x 28 km	hb-bt quartz diorite to quartz monzonite	bt-hb quartz diorite margin	unknown	187±9 K-Ar on hb, bt	Mihalynuk et al., 1998
<b>Plate Creek</b>	12 x 6 km	hb diorite	quartz diorite	stibnite in quartz vein (Tan showing)	ca. 203 U-Pb; 197.3±0.9 U-Pb zircon	L. Heaman, pers. comm., 2002; Nelson and Friedman, 2004
<b>Logjam diorite</b>	7 x 1 km	hb diorite	granite to gabbro	veins w/ galena, sphalerite (Au, Ag)	186.6±5.8 <sup>207</sup> Pb/ <sup>206</sup> Pb	Nelson and Friedman, 2004
<b>Swift River sills</b>	24 x 2 km	hb diorite, tonalite	quartz diorite	Zn, Pb (Ag) skarns		
<b>Permian</b>						
<b>Ram Stock</b>	26 x 2 km	quartz monzonite, granodiorite		unknown	258±2; 258.5±1.1 U-Pb zircon	this paper
<b>Nizi</b>	10 x 8 km	gabbro to diorite		gossans with Cu, Ag, Zn	262±8 K-Ar on hb	Nelson and Friedman, 2004
<b>Meek</b>	11 x 5 km	granite		quartz veins w/ Ag-Pb-Zn±Au; gossans	270±4 U-Pb zircon; 262±2 U-Pb titanite	Nelson and Friedman, 2004

Abbreviations: bt=biotite; hb=hornblende





**Figure 2.** The Ram Stock is a steeply dipping tabular intrusion; here it's about 700 m wide. This northeast view is from 364800E 6679700N in northwest corner of 105B/3 (Roots et al., 2004c). The intrusive contact is at right (here offset by a minor fault, indicated), and the granite extends to the Hidden Lake Thrust (unseen, at far left).

**Table 2.** Rock type and modal mineralogy for representative samples. Modes are estimated by the authors, except: Seagull NW (average of 24 modes, Mato et al., 1983), Thirtymile, NW and SW (point-counted, Liverton, 1990), Simpson Peak (range in 17 granitoid samples, L'Heureux, 2000).

Granite suite	rock type	grain size	alkali feldspar	quartz	plagioclase	ferromagnesian minerals	accessory minerals
<b>Cretaceous</b>							
Seagull SE	quartz syenite	medium	50	25	18	5 bt	fl, ap, topaz
Seagull NW	leucogranite	fine	35 (por)	38	24	3 bt	tour orbicules, fl, ap
Thirtymile	microgranite	fine	30-40	40-55	10-15	1 bt	fl, mon, zr, py
Thirtymile	megacrystic	coarse	30-40	40-45	10-20	1-5 bt	tour cavities
<b>Jurassic</b>							
NW Thirtymile	monzogranite	medium	32	27	6	23 bt, 33 hb	sph, ap
SW Thirtymile	quartz diorite	fine	8	17	49	5 bt, 20 hb	ap, sph
SW Thirtymile	gabbro	fine	0	1	55	12 bt, 9 hb, 22 aug	
Logjam	granite	fine	30	25	<20	7 bt, 7 hb, 3 cpx	
Logjam	diorite	medium	0		10	40 hb, 15 opx, 2 ol	
Swift River	tonalite	fine	5	25	55	15 hb, allanite	ap, sulphide minerals, allanite?
Swift River	diorite	medium	0		45	45 hb	sulphide minerals siderite
Plate Creek	granodiorite	medium	3	20	70, zoned	4 bt, 2 hb	sulphide minerals
Simpson Pk	granite	medium	32-55	25-35	10-28	<5 bt; 1-12 hb	titanite, ap, zircon
<b>Permian</b>							
Ram	granite	medium	50	18	perthitic	bt (chloritized)	rutile

Abbreviations: ap=apatite; aug=augite; bt=biotite; cpx=clinopyroxene; fl=fluorite; hb=hornblende; mon=monazite; por=porphyritic; py=pyrite; sph=sphene; tour=tourmaline; zr=zircon

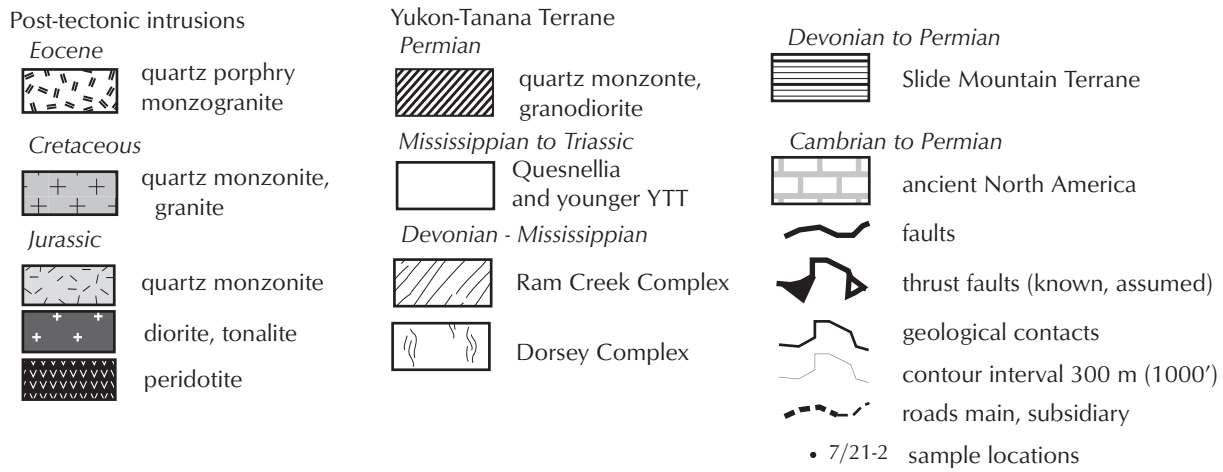
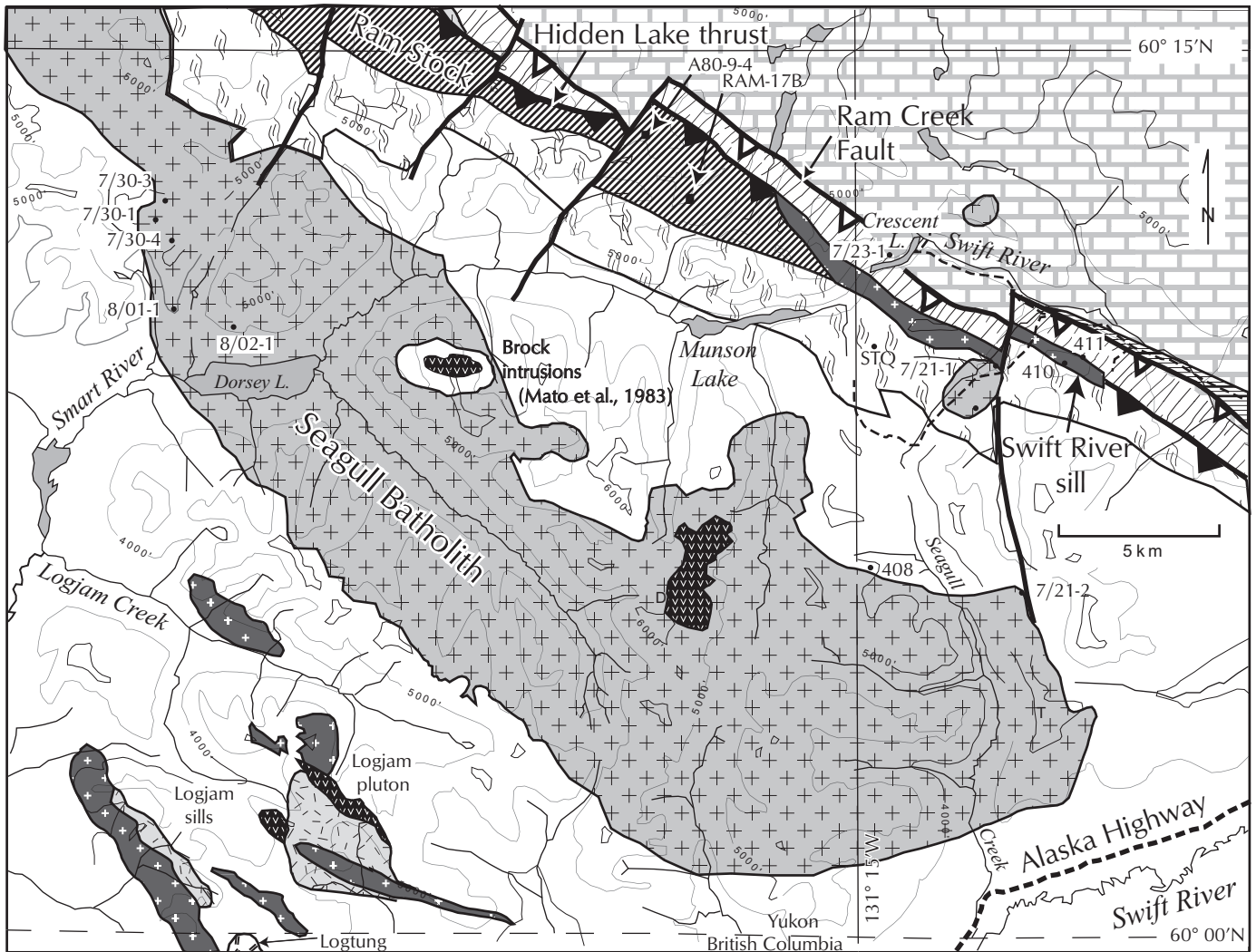


**Figure 3.** Location of samples for dates and geochemistry in southeastern Ram Stock, Seagull Batholith and Swift River (Jurassic) sill. Geological contacts are simplified from Roots et al., 2004.

Not dated, but correlated with Ram Stock on the basis of composition, is a diorite dyke on the west side of Crescent Lake that was observed to be cross-cut by the Ram Stock (Poole, 1956; J.G. Abbott, pers. comm., 1980).

### Age of the Ram Stock

Two samples of the Ram Stock yielded zircon for uranium-lead dating. Sample A80-9-4 was a hand sample collected during regional mapping in the area (Abbott, 1981) that weighed ~0.3 kg. Sample RAM-17B was a larger (~10 kg) sample collected during a field trip in 2002 (locations on Fig. 3). Geochronological analyses were carried out at the Pacific Centre for Isotopic and Geochemical Research at

the University of British Columbia, Vancouver, BC. Mineral separation and U-Pb analytical techniques employed are those described in Friedman et al. (2001).

### Results

U-Pb analytical data are listed in Table 1 and the analytical results are plotted on a conventional concordia diagram in Figure 4. Zircons from both samples were stubby, euhedral, pale pink grains, with no internal zoning or visible cores. Two strongly abraded and two unabraded fractions were analysed from sample A80-9-4 (Table 1). The two abraded fractions (C and D) give overlapping error ellipses that lie on or near concordia, and fraction D

**Table 3.** U/Pb analytical data for samples of Ram Stock.

Sample description <sup>1</sup>	Weight (mg)	U (ppm)	Pb <sup>2</sup> (ppm)	<sup>206</sup> Pb/ <sup>204</sup> Pb (measured) <sup>3</sup>	Total common Pb (pg)	% <sup>208</sup> Pb <sup>2</sup>	<sup>206</sup> Pb/ <sup>238</sup> U <sup>4</sup> (± 1σ)	<sup>207</sup> Pb/ <sup>235</sup> U <sup>4</sup> (± 1σ)	<sup>207</sup> Pb/ <sup>206</sup> Pb <sup>4</sup> (± 1σ)	<sup>206</sup> Pb/ <sup>238</sup> U age (Ma; ± 2σ)	<sup>207</sup> Pb/ <sup>206</sup> Pb age (Ma; ± 2σ)
<b>Sample A80-9-4</b>											
A: N2, 62-74,u	0.089	1330	53.8	6392	48	9.5	0.04050(0.07)	0.2875(0.11)	0.05150(0.06)	255.9(0.4)	263.2(2.9)
B: N2, 62-74,u	0.182	1382	55.8	5921	108	10.0	0.04018(0.18)	0.2846(0.20)	0.05138(0.06)	253.9(0.9)	257.7(2.9)
C: N2, 74-134	0.060	1074	43.7	8929	20	9.1	0.04089(0.09)	0.2901(0.10)	0.05145(0.07)	258.4(0.5)	261.2(3.1)
D: N2, 75-104	0.058	1119	45.3	9153	19	8.7	0.04091(0.08)	0.2899(0.10)	0.05140(0.05)	258.4(0.4)	258.9(2.4)
<b>Sample RAM-17B</b>											
A: N2,+104	0.027	1149	46.9	7187	11	9.3	0.04091(0.22)	0.2897(0.27)	0.05137(0.11)	258.5(1.1)	257.3(5.0)
B: N2,+104	0.035	1142	48.1	1080	10	11.1	0.04145(0.13)	0.2959(0.29)	0.05178(0.20)	261.8(0.7)	275.9(9.2)
C: N2,+104	0.050	1189	49.6	7952	19	9.8	0.04154(0.14)	0.2968(0.19)	0.05181(0.10)	262.4(0.7)	277.2(4.7)
D: N2,+104	0.062	995	40.9	2184	71	9.7	0.04106(0.12)	0.2921(0.22)	0.05161(0.13)	259.4(0.6)	268.1(5.9)
E: N2,+104	0.044	749	30.8	3137	27	9.6	0.04111(0.09)	0.2931(0.19)	0.05172(0.11)	259.7(0.5)	273.1(5.1)

<sup>1</sup>N2 = non-magnetic at 2 degrees side slope on Frantz magnetic separator; grain size given in microns; u = unabraded

<sup>2</sup>radiogenic Pb; corrected for blank, initial common Pb, and spike

<sup>3</sup>corrected for spike and fractionation

<sup>4</sup>corrected for blank Pb and U, and common Pb

**Location of samples** (UTM in Zone 9, NAD 83)

Sample A80-9-4 : 369815E 6678495N ; in northwest-facing cirque

Sample RAM 17-8 : 370715E 6678492N; on ridge crest

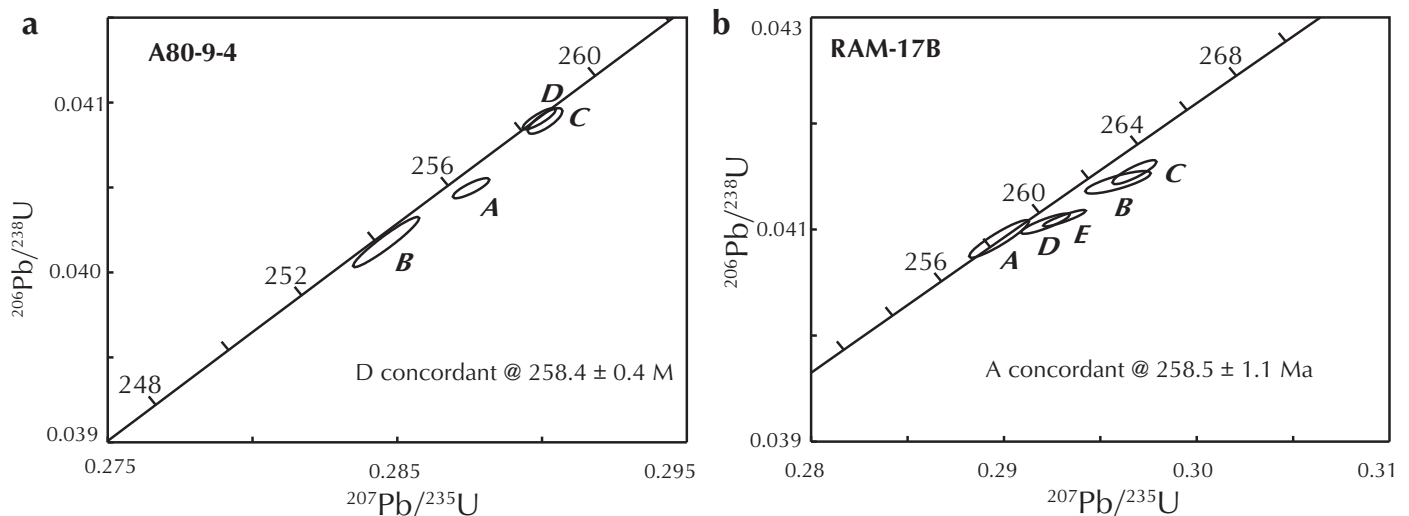


**Figure 4.** Concordia plot for Ram Creek stock. The lettered fractions are described in Table 1.



gives a concordant analysis with a  $^{206}\text{Pb}/^{238}\text{U}$  age of  $258.4 \pm 0.4$  Ma, which is interpreted to be the crystallization age of the sample. The two unabraded fractions give younger  $^{206}\text{Pb}/^{238}\text{U}$  ages (Fig. 4a) and are interpreted to have experienced minor post-crystallization Pb-loss. Five fractions of strongly abraded zircon were analysed from sample RAM-17B (Table 1, Fig. 4b). Fraction A gives a concordant analysis with a  $^{206}\text{Pb}/^{238}\text{U}$  age of  $258.5 \pm 1.1$  Ma, which gives the crystallization age of the sample. The other four fractions yield slightly older Pb/U and Pb/Pb ages, indicating the presence of minor 'cryptic' inherited zircon components in each fraction.

### Discussion

The Late Permian age for the Ram Stock: 1) indicates the penetrative strain of the Dorsey Complex is older than Permian; 2) places a maximum age on the Hidden Lake thrust and 3) represents a significant regional event in the superimposition history of YTT and Quesnellia. The dykes at the tip of the southern part of the stock yielded Permian U-Pb ages ( $269.8 \pm 3.2$  Ma), while dates on the two plutons in Sylvester Allochthon (Gabrielse et al., 1993) are within the margin of error of Ram Stock (restoration of about 100 km dextral movement of the Cretaceous Cassiar Fault (Gabrielse, 1985) places the Ram Stock where the Sylvester Allochthon may have been physically connected, before uplift and intrusion of the intervening Cassiar Batholith; Nelson and Friedman, 2004). Other parts of YTT expose volcanic and plutonic rocks between 270 and 260 Ma that are considered a magmatic cycle (S. Piercey, 2004), although its significance remains unclear.

### EARLY JURASSIC SUITE

This suite includes subcircular granite bodies ranging from tens of metres to several hundred kilometres in area, sill-like diorite to tonalite, and several dunite to pyroxenite bodies. The age of these bodies is typically 186 to 188 Ma (Table 1), but the Plate Creek stock is 10 Ma older (Nelson and Friedman, 2004). The Southwest Thirtymile is 181.5 Ma (Liverton et al., 2001); note that an adjacent pluton of Cretaceous age is called Thirtymile – an unfortunate opportunity for confusion.

Most of the felsic intrusions have steeply dipping, locally sheared margins and insignificant stoping or xenolithic screens. Many are surrounded by a broad contact metamorphic aureole. Simpson Peak and Nome Lake batholiths (Fig. 1) consist primarily of hornblende-biotite granodiorite with blade-like K-feldspar megacrysts inside a

peripheral zone of foliated biotite-hornblende quartz diorite (Gabrielse, 1969). Less common are hornblende or clinopyroxene gabbro, and foliated lithodemes (Mihalynuk et al., 2000). The western side of Simpson Peak Batholith includes a late-stage, medium-grained biotite granite, characterized by white intergrowths of plagioclase and K-feldspar, as well as a leucocratic porphyry (L'Heureux, 2000).

Extreme variations in lithology, both between stocks and over a few tens of metres within them, are characteristic of the Early Jurassic suite. The intrusion at the head of Logjam Creek contains three lithodemes (Fig. 3). The earliest, of olivine clinopyroxenite to dunite (peridotite), is exposed in two bodies, separated by the second, of hornblende quartz monzonite, including a zone with blade-like K-feldspar megacrysts (Poole, 1956). The third lithodeme is massive hornblende diorite to quartz diorite, which cross-cuts the quartz monzonite and extends several kilometres as large lozenge-shaped bodies. These attest to structural anisotropy; they coincide with old faults or contacts between major rock units. For example, the tonalite-diorite sill at the head of Swift River plugs the Hidden Lake Thrust that separates the Dorsey and Ram Creek complexes (Fig. 3).

Texturally the tonalite is massive to slightly porphyritic, with locally zoned plagioclase, pink microperthite and interstitial unstrained quartz. Jurassic intrusions are characterized by the presence of hornblende (constitutes 6 to 8% of most rocks according to Poole (1956); our samples typically contained more). This contrasts with the Cretaceous granites of the region, which are virtually hornblende-free. Biotite, partly altered to chlorite and iron-oxide?, is commonly 2 to 5%. In the gabbroic lithodeme, hornblende or clinopyroxene (locally pseudomorphed by hornblende) is present. No miarolitic cavities or hydrothermal evidence was observed in the Jurassic intrusions; likely they cooled at least several kilometres beneath the surface

### EARLY LATE CRETACEOUS SUITE

Cretaceous granites intrude every tectonic belt in southern Yukon, and in some cases demonstrably plug faults that separate the terranes. Most are biotite leuco-quartz monzonite, but the Seagull Batholith is about 10 Ma younger than its neighbours: the Cassiar Batholith to the east, and the Dead Creek Batholith to the west (Gordey et al., 1998).

Information is presented here on the northwest-trending Seagull Batholith, Hake Batholith and Thirtymile pluton. These intrusions are compositionally identical, and they are likely linked beneath the surface (hereafter referred to as the Seagull-Thirtymile granite). More mineral occurrences surround these than other intrusions to east and west (Table 2). The Seagull-Thirtymile granite is not unusual in general composition (biotite leuco-quartz monzonite), but it hosts pockets and zones with unusual mineralogy and composition that have seen intensive exploration (Mato et al., 1983).

A first-order difference between the Seagull-Thirtymile granites and others is map pattern. In particular, the Seagull Batholith has an irregular outline with numerous satellite stocks (Fig. 3). Valley exposures of granite between ridges of hornfelsed and hydrothermally altered country rock, and (in places) gently dipping intrusive contacts, attest that the Seagull-Thirtymile granite is barely unroofed. It also carries large pendants; these include volcanoclastic rocks, the Brock intrusion of Mato et al. (1983; Fig 3), and a gabbro body south of Munson Lake that is probably an isolated, uplifted part of the Early Jurassic suite. The northwest trend of the Seagull-Thirtymile granite parallels that of the Jurassic diorite sills and the Ram Stock, perhaps indicative of a fundamental crustal break that focused upwelling magma in three episodes over 150 million years.

The Seagull-Thirtymile granites are characterized by high silica content and biotite is the only ferromagnesian mineral. Appreciable hornblende is only present in the porphyry lithodeme of the Thirtymile stock (Liverton, 1990). The granite has an equigranular or slightly porphyritic texture. Potash feldspar grains typically overgrow quartz and plagioclase grains at their borders, indicating partial replacement (Poole, 1956). Biotite is commonly slightly altered to chlorite.

The special areas of the granite are characterized by abundant cavities rimmed with quartz and black tourmaline, purple and green fluorite with rarer blue-green beryl and topaz. Li-rich micas in Thirtymile pluton were described by Liverton and Alderton (1994). These are zones where late-stage volatiles were concentrated, and likely were the highest points in the intrusion, now exposed by erosion.

## EOCENE SUITE

The stock that hosts the Logtung tungsten-molybdenum-bismuth-beryllium (beryl, aquamarine) porphyry deposit

along its northern edge yielded a U-Pb age of 58 Ma  $\pm$  1.5 (Mihalynuk and Heaman, 2001). It is a highly differentiated hypabyssal monzogranite with related felsic dykes. Different compositional lithodemes resulted from periodic tapping of an almost completely crystallized, fractionating magma chamber (Stewart and Evensen, 1983). Interaction between magmatic and other hydrothermal processes led to a texturally distinctive 'brain-rock' texture consisting of alternate-banded felsic porphyry and drusy quartz (Noble et al., 1984).

## CHEMICAL CHARACTERISTICS OF THE PLUTONS

Clean, fresh, fist-sized rock samples were selected from various plutons. The trace element analyses augment previous data from the Thirtymile and Hake intrusions (Liverton, 1992; Liverton and Alderton, 1994; Liverton and Botelho, 2001). New major and minor whole-rock analyses were made for Permian and Jurassic intrusions in the Swift River area.

## RESULTS

Tables 4 and 5 present the major, minor and trace element compositions of the plutonic samples, organized by age. Relatively immobile and incompatible elements are the primary basis for discussion of tectonic origin.

In terms of silica content, the Permian and Jurassic samples span an SiO<sub>2</sub> range from 52 to 72%, whereas all the Cretaceous granites are > 70% SiO<sub>2</sub>. On silica bivariate plots, the Rb/Zr ratio (Fig 5a) and Ga/Al ratio (Fig. 5b) are relatively uniform for Permian and Jurassic samples (in the volcanic arc granites field of Harris et al., 1986), whereas the Cretaceous Seagull-Thirtymile samples have higher ratios, in the realm of anorogenic granites.

Rubidium and high field strength elements rise proportionally in Cretaceous granites, but not in Permian and Jurassic samples (Fig. 6a) which also have relatively low Fe/Mg, whereas the Cretaceous samples show an order of magnitude higher (Fig. 6b). The position of the samples on this diagram correspond to the fields for 'Normal' S- and I-types for the former, and A-type for the latter (according to Sylvester, 1989). The iron-rich Seagull-Thirtymile trend is unusual for S-type tin plutons worldwide, but is typical of late-orogenic (sub-alkaline in the sense of Barbarin, 1990) and anorogenic types.

A similar distinction is shown on the ternary Rb-Ba-Sr diagram (Fig. 7). The Jurassic samples cluster near the

baseline, in the volcanic arc granites' field of El Bouseily and El Sokkary (1975). The Permian granite has relatively higher Ba (in the field of high-Ca granites). In contrast, the Cretaceous suite forms a steep trend along the boundary between 'within-plate' and 'collisional' granites field.

Notably samples from each pluton constitute lines with slightly different slopes, and in each case, the most evolved samples are near the top (higher Rb/Sr ratio).

A common measure of fractionation of granitic magmas is the Thornton-Tuttle, or Differentiation Index, in which the

**Table 4.** Major oxides, and normative mineralogy for selected samples. Oxides are in weight %. Four Cretaceous samples were analysed in 1990 at University of London using long count INAA (from Liverton and Botelho, 2001); others were done by Activation Laboratories, Ontario (#40273) using Induction-coupled optical emission spectroscopy.

Location	Cretaceous					Jurassic			Permian
	STQ Dyke	Seagull NE		Seagull NW		DY-12	410	411	16-10
Sample	07/24-1	07/21-1	408	07/30-1	07/30-4	DY-12	410	411	16-10
UTM Easting**	0375600	0378580	0374410	0353430	0353800	0374410	0382117	0382265	0357595
UTM Northing	6671800	6669250	6664600	6676560	6675890	6664600	6670830	6670903	6685600
<b>Major oxide</b>									
SiO <sub>2</sub>	76.08	76.53	77.13	76.11	78.48	64.8	60.43	49.88	69.43
Al <sub>2</sub> O <sub>3</sub>	13.54	12.65	11.76	12.62	11.91	16.5	18.23	14.39	14.87
Fe <sub>2</sub> O <sub>3</sub> *	1.04	1.64	1.71	1.73	1.34	4.51	5.83	9.58	2.24
MnO	0.12	0.08	0.015	0.04	0.05	0.115	0.086	0.159	0.057
MgO	0.27	0.57	0.05	0.59	0.33	1.49	1.79	7.77	0.31
CaO	3.51	3.4	0.44	3.53	3.18	4.88	5.38	10.4	1.64
Na <sub>2</sub> O	4.75	4.91	3.2	4.92	5.02	3.46	4.36	2.76	3.45
K <sub>2</sub> O	0.06	0.12	4.77	0.09	0.09	2.63	0.89	0.87	5.18
TiO <sub>2</sub>	0.01	0.02	0.103	0.01	0.01	0.485	0.66	1.28	0.231
P <sub>2</sub> O <sub>5</sub>	0.02	0.04	0.01	0.01	0.02	0.22	0.23	0.21	0.07
S			0.004			0.004	0.001	0.008	0.004
LOI	1.33	0.44	0.46	0.63	0.43	1.04	1.98	1.85	1.13
<b>Total</b>	<b>99.4</b>	<b>99.96</b>	<b>99.63</b>	<b>99.65</b>	<b>100.43</b>	<b>100.13</b>	<b>99.88</b>	<b>99.14</b>	<b>98.6</b>
<b>C.I.P.W. Normative minerals (calculated from above analyses)</b>									
% iron used	10	10	10	10	10	20	20	20	20
quartz	36.14	35.72	38.24	34.38	39.22	20.67	15.47	0	24.7
orthoclase	28.1	29.06	28.19	29.12	29.7	15.54	5.26	5.14	30.61
albite	29.73	28.81	27.08	29.92	26.94	29.28	36.89	23.35	29.19
anorthite	1.21	2.57	2.12	2.87	1.51	21.73	25.19	24.31	7.68
calcite	2.18	0.8	0.56	0.44	0.69	0	0.86	0	0.77
diopside	0.3	0.2	0	0.1	0.13	0.87	0	20.96	
hypersthene	1.49	2.34	2.38	2.47	1.92	7.9	10.25	13.4	3.09
olivine	0.14	0.22	0	0.23	0.177	0	0	3.67	0
magnetite	0	0	0.25	0	0	1.31	1.69	2.78	0.65
ilmenite	0.05	0.09	0.2	0.02	0.05	0.92	1.25	2.43	0.44
hematite	0	0	0	0	0	0	0	0	0
apatite	0.1	0.1	0.02	0.1	0.1	0.51	0.53	0.49	0.16
<b>D***</b>	<b>93.97</b>	<b>93.59</b>	<b>93.51</b>	<b>93.42</b>	<b>95.86</b>	<b>65.49</b>	<b>57.62</b>	<b>28.49</b>	<b>84.5</b>

\*Total iron expressed as Fe<sub>2</sub>O<sub>3</sub> \*\*NAD83 \*\*\*Differentiation index + Normative q+or+ab+an



**Table 5.** Minor and trace elements, in parts per million. Analyses by Activation Laboratories, Ontario (A04-273) using a combination of ICP-MS, ICP-OES and INAA.

Sample	STQ	Seagull Batholith									Hake		Thirtymile			Plate Creek	Swift River sill		Ram Stock	Crescent Lake
	dyke	NE			NW						margin	core	even	mega	porph	diorite	tonal	diorite	gran	diorite
	7/24-2	7/21-1	7/21-2	408	7/30-1	7/30-3	7/30-4	8/1-01	8/1-02	8/02-1A	8/17-2	8/17-3	97/29-1	97/28-5	HPG	DY-12	410	411	16-10	7/23-1
Ag	na	na	na	bd	na	na	na	na	na	na	na	na	na	na	bd	0.03	bd	bd	na	
As	22.0	93.0	82.0	20.0	8.0	bd	bd	bd	14.0	12.0	bd	bd	bd	bd	bd	bd	1.0	1.0	bd	
Ba	29.0	45.0	17.0	29.0	15.0	93.0	43.0	278.0	354.0	408.0	375.0	270.0	108.0	322.0	756.0	1970.0	574.0	466.0	1115.0	1540.0
Be	na	na	na	6	na	na	na	na	na	na	na	na	na	na	na	2.0	2.0	2.0	3.0	na
Bi	0.3	7.2	0.1	bd	11.4	0.2	bd	0.2	0.7	0.7	bd	4.3	0.3	bd	bd	bd	bd	bd	bd	bd
Cd	na	na	na	bd	na	na	na	na	na	na	na	na	na	na	na	0.4	0.05	0.06	0.03	na
Ce	156.0	142.0	165.0	154.0	144.0	140.0	117.0	148.0	125.0	127.0	118.0	110.0	79.3	76.4	103.0	56.0	25.0	30.0	45.0	45.7
Cs	15.1	17.4	17.9	16.0	11.6	11.1	14.0	8.1	11.2	11.1	13.2	12.6	17.2	24.0	6.0	0.9	1.2	1.2	2.6	3.7
Cu	na	na	na	10	na	na	na	na	na	na	na	na	na	na	na	20	16	43	15	na
Dy	18.1	16.4	19.8	na	21.6	15.1	11.6	5.68	7.89	9.19	5.06	5.41	8.82	5.52	5.45	na	na	na	na	2.87
Er	13.3	11.1	14.0	na	14.7	9.92	8.11	3.17	5.01	5.94	3.43	3.66	6.47	3.89	3.45	na	na	na	na	1.72
Eu	0.02	0.078	0.031	bd	0.029	0.114	0.069	0.321	0.344	0.374	0.533	0.376	0.164	0.391	0.762	1.23	0.85	1.17	0.73	1.13
Ga	34.0	26.0	26.0	28.0	26.0	23.0	22.0	20.0	21.0	21.0	19.0	19.0	22.0	21.0	19.0	21.0	19.0	17.0	17.0	18.0
Gd	13.7	13.2	15.8	na	16.9	12.7	9.88	7.08	8.01	9.02	5.35	5.52	6.47	5.02	5.24	na	na	na	na	3.68
Ge	2.8	2.7	2.5	na	2.9	2	1.8	1.5	1.9	1.9	1.4	1.7	2.4	1.8	1.3	na	na	na	na	1.4
Hf	8.1	7.1	8.9	6.9	8.5	9.4	6.5	5.1	6.7	6.4	5.5	5.5	6.4	6.6	7.0	na	na	na	na	3.7
Ho	3.92	3.47	4.34	na	4.59	3.16	2.51	1.08	1.62	1.93	1.07	1.11	1.93	1.21	1.1	na	na	na	na	0.57
La	81.5	68.7	82.9	80.1	72.6	69.0	59.5	76.2	64.2	64.4	65.8	58.3	38.3	39.8	57.8	29.0	15.6	13.3	21.5	24.2
Lu	2.3	1.61	1.95	1.48	2.03	1.37	1.18	0.462	0.765	0.868	0.566	0.625	1.26	0.638	0.561	0.29	0.17	0.37	0.15	0.271
Nb	99.8	70.7	80.7	77.0	72.7	68.6	50.2	36.2	39.5	40.0	45.8	43.8	63.3	50.0	48.1	13.0	bd	8.0	10.0	14.1
Nd	60.5	54.3	61.1	51.0	60.6	54.9	44.3	52.6	46.7	47.9	37.4	35.5	28.6	26.7	35.0	27.0	9.0	14.0	12.0	20.1
Ni	bd	bd	bd	5.0	bd	bd	bd	bd	bd	bd	bd	bd	bd	bd	bd	9.0	9.0	56.0	6.0	bd
Pb	24.0	26.0	20.0	36.0	36.0	27.0	15.0	28.0	24.0	22.0	14.0	111.0	25.0	15.0	26.0	11.0	7.0	3.0	10.0	23.0
Pr	19.4	15.7	18.1	bd	17.0	15.4	13.1	15.6	13.7	13.9	11.9	11.2	8.64	8.02	10.5	na	na	na	na	5.3
Rb	863.0	584.0	615.0	652.0	593.0	429.0	421.0	242.0	347.0	350.0	329.0	414.0	579.0	428.0	236.0	63.0	29.0	33.0	151.0	112.0
Sb	0.2	0.6	0.7	1.2	0.3	0.6	0.4	0.5	0.4	0.4	0.5	0.5	0.3	0.5	0.2	na	na	na	na	1.3
Sm	14.7	13.1	15.0	10.6	16.0	13.1	10.1	8.9	9.3	10.0	6.5	6.8	6.6	5.4	6.2	4.5	1.4	3.6	2.17	4.03
Sn	25.0	37.0	21.0	bd	6.0	7.0	6.0	20.0	7.0	6.0	9.0	13.0	7.0	9.0	6.0	bd	bd	bd	bd	5.0
Sr	10.0	13.0	3.0	9.0	5.0	12.0	6.0	33.0	43.0	45.0	91.0	61.0	25.0	67.0	128.0	827.0	400.0	332.0	325.0	427
Ta	19.0	9.65	9.59	10.9	9.71	6.61	7.31	4.20	5.33	5.17	4.83	6.39	10.8	8.76	4.06	0.90	bd	bd	0.7	0.95
Tb	3.0	2.75	3.34	1.9	3.58	2.56	2.0	1.09	1.42	1.62	0.91	0.97	1.36	0.94	0.94	0.5	0.4	0.7	0.3	0.55
Th	67.0	65.7	93.0	44.9	83.2	47.9	52.9	42.5	50.5	49.7	66.6	69.6	57.4	55.4	43.0	5.7	4.3	1.4	16.4	14.7
Tl	6.31	5.33	4.14	na	5.17	3.45	3.14	2.04	3.22	3.28	2.24	3.38	4.83	2.84	1.32	na	na	na	na	0.75
Tm	2.19	1.66	2.08	na	2.23	1.45	1.21	0.47	0.76	0.87	0.52	0.57	1.07	0.59	0.52	na	na	na	na	0.25
U	39.7	24.9	25.3	6.7	19.4	22.1	13.2	6.01	12.8	12.9	18.3	20.4	31.3	19.5	9.35	1.6	2.0	0.5	3.2	4.66
V	bd	bd	bd	7.0	bd	bd	bd	bd	bd	bd	8.0	bd	bd	bd	15.0	76.0	27.0	238.0	22.0	96.0
Y	154.0	123.0	156.0	86.0	160.0	108.0	82.5	33.6	53.4	61.0	36.9	40.0	72.2	40.6	38.0	16.0	7.0	24.0	8.0	19.0
Yb	14.5	10.5	12.6	10.1	13.6	9.15	7.56	2.95	4.86	5.58	3.54	3.88	7.56	3.91	3.47	1.91	1.14	2.45	1.06	1.59
Zn	bd	66.0	bd	38.0	46.0	46.0	n.d.	50.0	bd	35.0	37.0	7990.0	bd	bd	bd	68.0	36.0	66.0	32.0	98.0
Zr	140	181.0	229.0	182.0	208.0	310.0	153.0	188.0	232.0	224.0	212.0	197.0	165.0	209.0	306.0	179.0	324.0	97.0	411.0	151.0

Abbreviations: marg=margin; even=equigranular lithodeme; mega=megacrystic; porph=porphyritic; tonal=tonalite; gran=granite; na=not analysed; bd=below detection

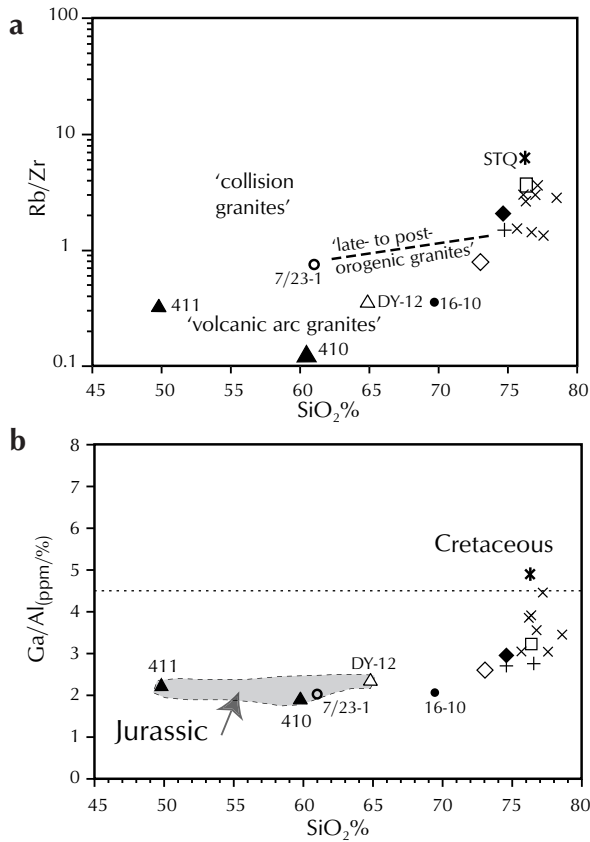


**Figure 5.** Silica-variation diagrams highlight the distinction between Jurassic and Cretaceous suites: (a) Rb/Zr vs SiO<sub>2</sub> (fields from Harris et al., 1986); (b) Ga/Al vs SiO<sub>2</sub>. Note that the two Permian samples (16-10 and 7/23-1) typically have an intermediate position between the relatively flat Jurassic, and the steeply rising Cretaceous fields.

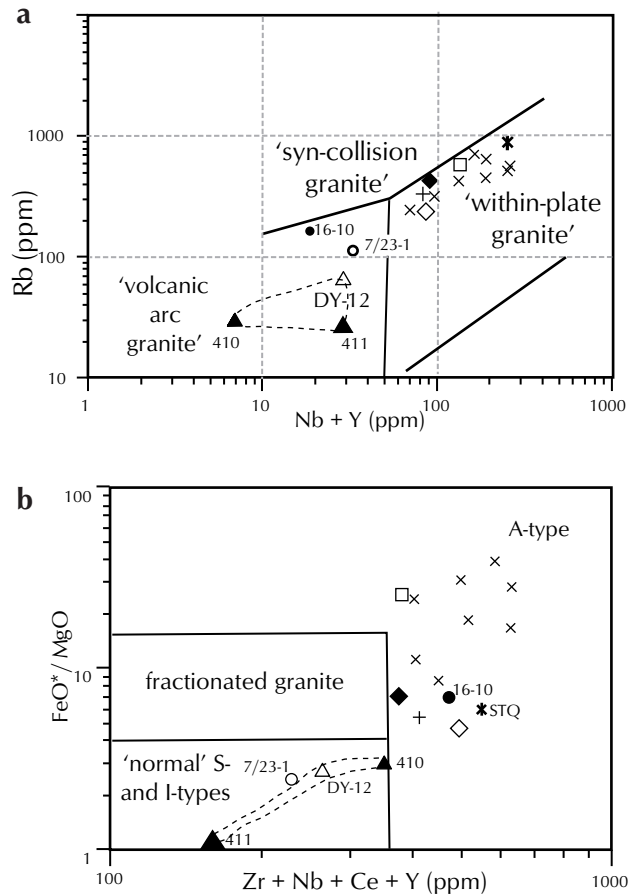


**Figure 6.** Tectonic discrimination diagrams, with fields according to Pearce et al. (1984) and Sylvester (1989) and Harris et al. (1986): FeO\*=total iron.

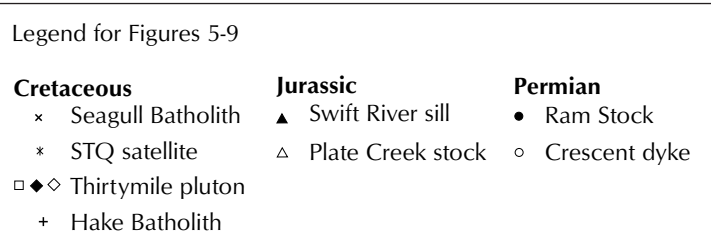
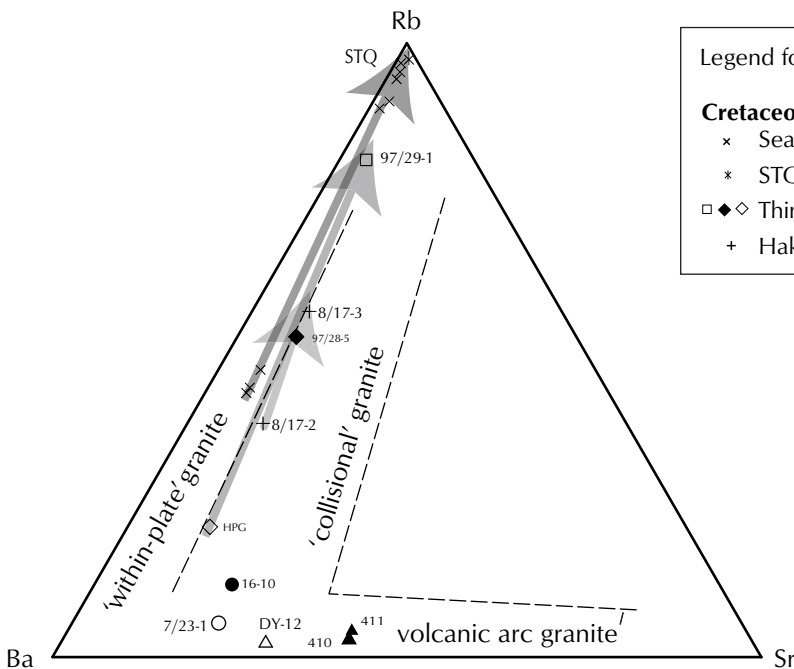


**Figure 7.** Distribution of Permian, Jurassic and Cretaceous samples on the Rb-Ba-Sr ternary plot. Boundaries between the volcanic-arc granite (VAG), within-plate and collisional granites are from El Bouseilly and El Sockary (1975). Shaded arrows highlight the steep trends of Seagull, Hake and Thirtymile samples toward the Rb apex, the result of fractionation.

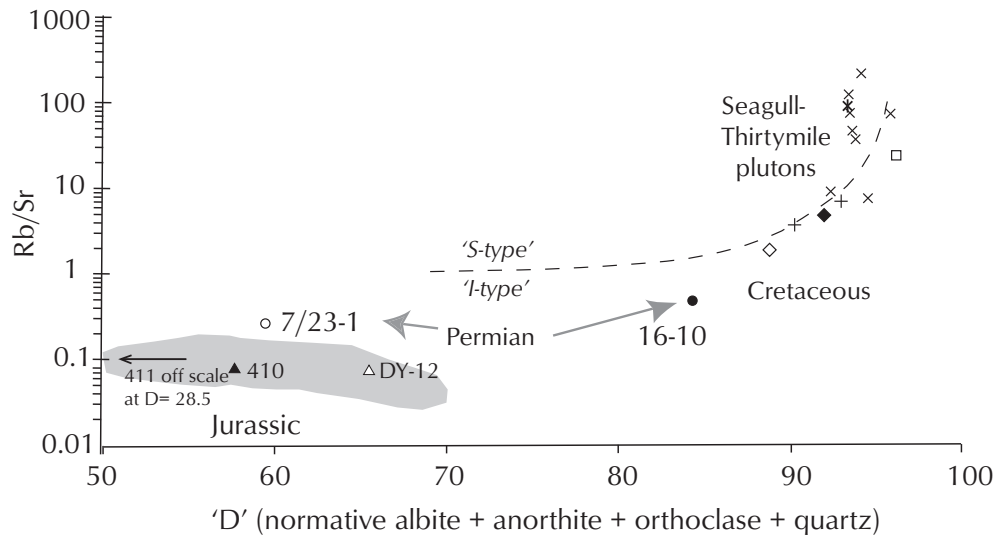


**Figure 8.** Cobbing (1990) diagram shows the I-type nature of Jurassic intrusions and the intermediate nature of the Permian samples. Legend on facing page. The Cretaceous granites straddle the line separating I- and S-type granitoids, and their Rb content rises steeply when the Differentiation Index ('D') is greater than 90.

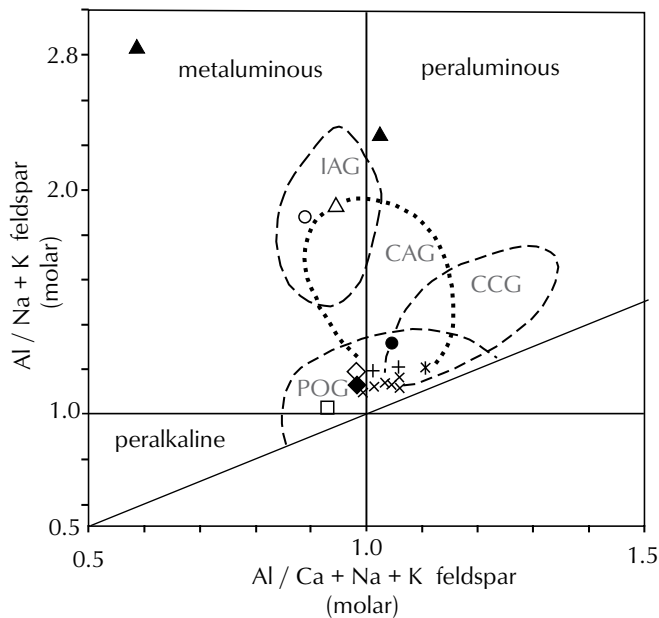


**Figure 9.** The aluminum saturation (Shand) index ( $A/CNK = \text{molar Al} / \text{Ca} + \text{Na} + \text{K}$ , with correction for fugacity of Ca for apatite content). Legend on facing page. Major element compositions separate the Jurassic, as a metaluminous suite, from the Cretaceous samples, which tightly cluster in the 'post-orogenic granites' (POG) field. IAG: island-arc granite; CAG: continental-arc granites; CCG: continental collisional granite from Maniar and Piccoli (1989).

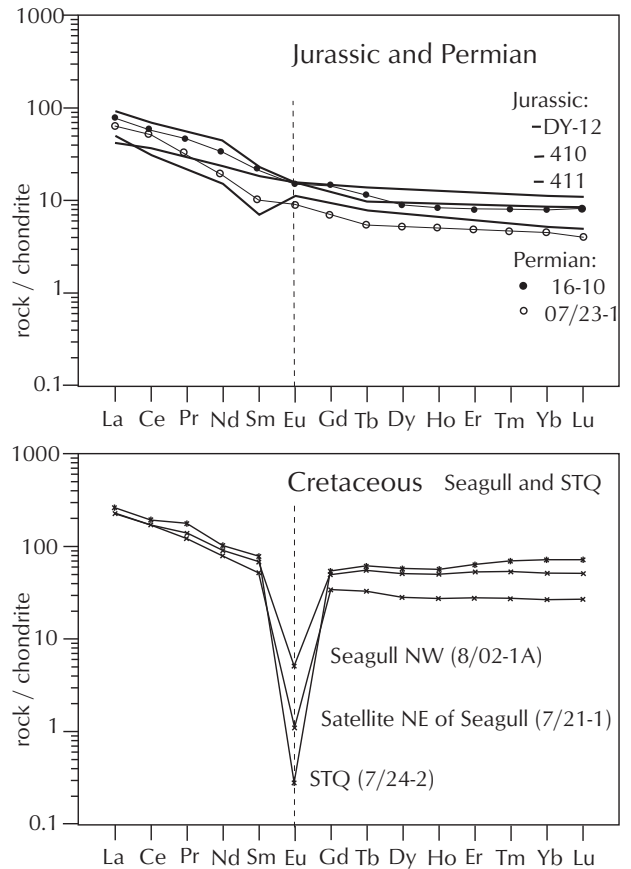


**Figure 10.** Rare-earth element abundances for granites, normalized to chondrite values of Sun (1980).



sum of the CIPW normative feldspars + quartz comprise the x-axis. On Figure 8 the Cretaceous samples form a cluster around the upward curve, rising at higher indices of differentiation. For example, the samples of Thirtymile pluton define evolution from porphyritic, to megacrystic, to equigranular lithodemes, an increase of Rb/Sr from 2 to 12. This change matches the emplacement sequence determined from cross-cutting relationships (Liverton, 1992). The STQ sample has the highest Rb (863 ppm) of any of the samples in this dataset. It is a satellite stock of Seagull Batholith that is interpreted to have fractionated toward quartz enrichment.

The Shand Index plot (Fig. 9) demonstrates a clear distinction between the Permian and Jurassic samples, which are metaluminous and in either the island-arc or continental-arc field. The more alkaline, metaluminous to peraluminous Cretaceous plutons cluster tightly in the "post-orogenic granites" field (Maniar and Piccoli, 1989).

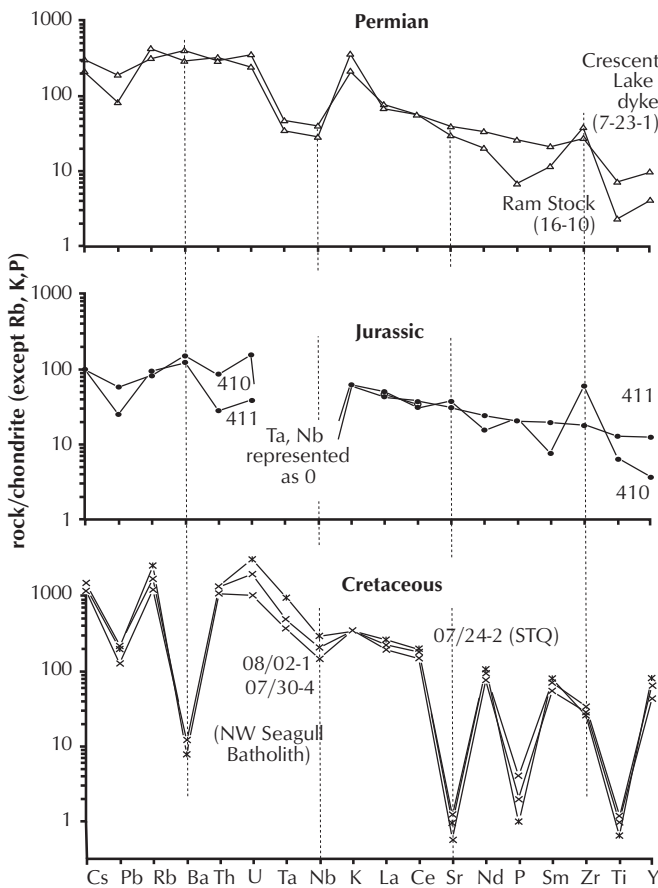


**Figure 11.** Minor and trace element abundance, normalized to chondrite (Sun, 1980) shows relatively smooth trends for Permian and Jurassic intrusions diagrams. The Cretaceous samples show strong depletion in Ba, Sr, P and Ti.

Rare-earth element plots (spidergrams) are used to display the type of fractionation. In Figure 10, the curves for samples are uniform and descend gently (more enriched in LREE than HREE), a classic within-plate signature. In contrast, the most fractionated samples, from the northwest cupola of Seagull Batholith (DU area), and the STQ satellite stock, have the deepest Eu trough, as this element is taken up in the crystallization of plagioclase. Even higher fractionation is shown at the Ork (Mindy, 105C 038B, Deklerk, 2003) near the Thirtymile pluton, where lithium-rich mica is present (Liverton, 1990).

Trace and rare-earth elements abundances normalized to chondrite show negative slopes for all the granites (Fig. 11). Among Jurassic and Permian samples, the trend is comparatively smooth, with anomalous increase in K. The Ram Stock is similar to the Meek granite pluton which displays a flat REE pattern with respect to upper mantle crustal values (Nelson and Friedman, 2004, p. 1212). The Jurassic suite has large-ion lithophile elements enriched about 100 times, and the incompatible elements about 10 times that of chondrite. Nb and Ta are very low, similar to the large Triassic-Jurassic suites in Quesnellia of southern BC, which are derived from mafic parents (Preto et al., 1979; Ghosh, 1995). All the Cretaceous samples show significant troughs for Ba, Sr, P, Ti and Pb, likely a result of the early crystallization of minerals such as feldspar and ilmenite within the magma chamber.

## PLUTON COMPOSITION AND TECTONIC ORIGIN

The trace element abundances of the Permian plutons suggest that they were likely derived from an influx of enriched mantle-derived magma, accompanied by melting of the lower crust (S. Piercey, pers. comm., 2003). These Permian igneous rocks thus contrast sharply with the contemporaneous mid-oceanic ridge basalt lavas in the Campbell Range (southeast Yukon) and in the Slide Mountain Terrane, both on the east side of Yukon-Tanana Terrane (YTT). Possibly these intrusions were the last stage of a Permian magmatic event that began with arc volcanism recorded by the Klinkit Group. The rare-earth element abundances and Nd isotopic ratio of the Klinkit volcanic rocks show little evidence of crust in their genesis, and the arc is interpreted to lie above an east-dipping subduction (Simard et al., 2003). Possibly the heated lower crust at the end of this cycle gave rise to the Ram Stock and other plutons.

The composition of our samples corroborates the results of Nelson and Friedman (2004), who interpreted the magmas as being derived from melting of a previously metasomatized mantle wedge. This reflects a continental arc setting. Where was the subduction zone? Liverton et al. (2001) proposed that the subduction zone was west-dipping and led to closure of the Slide Mountain ocean beneath the leading eastern edge of YTT. The southwest dip of the units, and top-to-the-northeast sense of motion on intra-terrane faults support this hypothesis. The mafic volcanic and sedimentary rocks of Slide Mountain terrane are interpreted to have melted in the subduction zone and risen in what was likely the thickest zone of the shortened width of YTT.

The three Jurassic samples are similar to the dykes analysed by Nelson and Friedman (2004) in showing a strong arc affinity, particularly using Rb as a discriminant (Figs. 5,6 and 7). Unlike theirs, however, the Swift River sill and Plate Creek stock lack the potassic character that is typical of the Late Triassic-Early Jurassic suite that is a hallmark of Quesnellia (Mortimer, 1987; Nelson and Friedman, 2004).

The Cretaceous Seagull-Thirtymile plutons have compositions consistent with A-type or collisional granites (Figs. 5a, 6b). Their initial Sr isotopic ratios are high (0.712; Mato et al., 1983), reflecting an old, sialic source. Among the least-differentiated lithodemes, trace-element abundances are typical for such granites throughout the Cordilleran interior, and consistent with a simple Rayleigh crystal-liquid fractionation process. In samples displaying highly differentiated compositions (above 90 on the Thornton-Tuttle Differentiation Index), however, the large-ion lithophile element content rises dramatically. Ultrafractionation occurs in the presence of abundant, halogen-rich volatiles, and water vapour promotes liquid-liquid fractionation (early phase), leading to scavenging of certain metals (e.g., Newberry et al., 1990). Fluorine facilitates fractionation by inhibiting the nucleation, depolymerizing silicates and depressing the solidus so that elements such as lithium and boron can move upward through the magma (C. Hart, pers. comm., 2003). The presence of lithium-bearing micas at Thirtymile pluton (Liverton and Alderton, 1994), and tourmaline orbicules and linings ofmiarolitic cavities in cupolas at the northwest end of Seagull Batholith, attest to this process.

## METALLOGENY RELATED TO PLUTONIC SUITES

The Permian intrusions lack a distinctive metallogenic character. McPres (105B 087, Deklerk, 2003) is a copper-molybdenum-rich gossan within the Ram Stock. The Nizi pluton in the Sylvester Allochthon hosts numerous gossans with chalcopyrite in shear zones, and gold-silver-lead-zinc in quartz veins (Nelson, 2001). Some spatially associated skarns, such as Hidden (lead, zinc, silver; 105B 025, Deklerk, 2003), were probably distant from the Ram Stock, prior to movement on the Hidden Lake Thrust fault.

The Jurassic suite has associated vein and skarn occurrences. The Tan (Bradford and Jakobsen, 1988) showing is a quartz vein with stibnite and pyrite, and nearby anomalous stream sediments (Jackaman, 2000) occur near the Plate Creek stock. The Logjam occurrence (105B 038, Deklerk, 2003) consists of six quartz veins (gold, silver, lead-zinc) within a Jurassic diorite sill, but is likely younger because quartz veins are also present in the nearby Logtung (Early Eocene) intrusion.

At the head of the Swift River, along the northeast edge of YTT, are several large pyrrhotite-galena-sphalerite lenses hosted in calc-silicate layers (Bar (better known as Dan), Atom, Bom, and Munson (better known as TBMB); Deklerk, 2003 105B 026, 027, 028, 029). Some exploration programs have investigated the possibility that the adjacent volcanic rock and tuffaceous textures could indicate a syn-sedimentary (volcanogenic) origin. Galena and pyrrhotite samples from these occurrences have lead isotopic ratios that are midway between clearly epigenetic veins, and probable volcanogenic deposits in YTT, however, their modal age is broadly mid-Triassic to mid-Jurassic (Mortensen and Gabites, 2002).

Cretaceous plutons of the Seagull-Thirtymile trend were the focus of considerable exploration activity during the late 1970s as the price of tin briefly soared. Among the most explored properties were the JC, a 600-m-long tin skarn (105B 040, Deklerk, 2003) and the nearby MC sheeted tin- and sulphide-bearing veins (Mato et al., 1983; 105B 088 (called Smith), Deklerk, 2003). At the JC, tin was precipitated in an early stage within andradite skarn, but later replaced by cassiterite within 90 m of the top of the granite (Layne and Spooner, 1991). At MC, cassiterite coats 'dry' (lacking quartz) fractures in country rock (DIAND, 1981, p. 150). The mineralogy and conditions of formation of the Mindy prospect, a skarn south of the Thirtymile pluton, is documented by Liverton (1992).

## CONCLUSIONS

A primary mineralogical distinction between the igneous suites is the dominance of hornblende (and in the mafic phases, clinopyroxene) in the Jurassic plutons, whereas the Seagull-Thirtymile granite lacks hornblende but is biotite-bearing. Our geochemical data, combined with previously published results for plutonic rocks, shows distinct differences between intrusive rocks 80 million years apart.

Most distinctive are Jurassic rocks, which are rich in MgO, TiO<sub>2</sub> and have low K<sub>2</sub>O/Na<sub>2</sub>O ratios, Rb and Nb. As indicated by Mortensen et al. (2000), these are metaluminous, I-type and likely derived from a mantle source.

By contrast, the Cretaceous granites are silica- and iron-rich. The K<sub>2</sub>O/Na<sub>2</sub>O ratio is high, Rb is very high (in the most fractionated samples), and high field-strength elements are enriched in these rocks relative to chondrites, except for Ba, Sr, Ti and P. It is a peraluminous, and A-type on discriminant diagrams (Figs. 6b and 9). Following the discussion by Creaser et al. (1991) the Seagull-Thirtymile granite could be derived from an igneous source within the lower continental crust, such as a partial melt of granodiorite to tonalite residue from previous magmatic episodes. This may explain the parallel geometry of the Seagull-Thirtymile granite with both Jurassic and Permian Ram Stock precursors.

The unusual character of the Seagull-Thirtymile granite reflects late-stage fractionation when halogen concentrations rose quickly toward the end of crystallization. This fortunate occurrence mobilized the metals and resulted in a high incidence of mineral showings. The degree of fractionation of granite samples indicated by normative minerals, Ga/Al, Rb/Zr or Rb/Sr ratios, could be used as an exploration tool.

Samples of the Permian suite are too sparse for any but the broadest conclusions. The Ram granite has high field strength element abundances, intermediate between the Jurassic and Cretaceous plutons. It lies within the range of some arc magmas, but has more crustal enrichment, indicated by higher large-ion lithophile-element abundances. Its presence indicates the Early Permian magmatism occurred beneath southern Yukon-Tanana Terrane (YTT), and prior to contraction that welded the island arcs into YTT.

## ACKNOWLEDGEMENTS

The Ancient Pacific Margin NATMAP project initiated this investigation, and geochronology was supported by Natural Science and Engineering Research Council grants to the second author. The paper was improved by reviews from Craig Hart, Bob Anderson and Diane Emond.

## REFERENCES

- Abbott, J.G., 1981. Geology of the Seagull tin district. *In: Yukon Geology and Exploration 1979-80*. Exploration and Geological Services, Yukon Region, Indian and Northern Affairs Canada, p. 32-44.
- Bradford, J. and Jakobsen, D.E., 1988. Jennings River mineral occurrence data NTS 104O; BC Ministry of Energy and Mines, MINFILE digital data, 55 occurrences, posted Nov 2004, [www.em.gov.bc.ca/Mining/Geosurv/Minfile/mapareas/104ocov.htm](http://www.em.gov.bc.ca/Mining/Geosurv/Minfile/mapareas/104ocov.htm).
- Breitsprecher, K., Mortensen, J.K. and Villeneuve, M. (compilers), 2004. YukonAge 2004 – A database of isotopic age determinations for rock units from Yukon Territory. Yukon Geological Survey, CD-ROM.
- Cobbing, E.J., 1990. A comparison of granites and their tectonic settings from the South American Andes and the Southeast Asian tin belt. *In: Plutonism from Antarctica to Alaska*, S.M. Kay and C.W. Rapela, (eds.), Geological Society of America, Special Paper 241, p. 193-204.
- Colpron, M. and the Yukon-Tanana Working Group, 2001. Ancient Pacific Margin – An update on stratigraphic comparison of potential volcanogenic massive sulphide-hosting successions of Yukon-Tanana Terrane, northern British Columbia and Yukon. *In: Yukon Exploration and Geology 2000*, Exploration and Geological Services Division, Yukon Region, Indian and Northern Affairs Canada., p. 97-110.
- Creaser, R.A., Price, R.C. and Wormald, R.J. 1991. A-type granites revisited: Assessment of a residual-source model. *Geology*, vol. 19, p. 163-166.
- Deklerk, R. (comp.), 2003. Yukon MINFILE 2003 – A database of mineral occurrences. Yukon Geological Survey, CD-ROM.



- DIAND, 1981. Yukon Exploration and Geology 1979-80. Summaries of assessment work, descriptions of mineral properties, and mineral claims staked in 1980 – Wolf Lake. Geology Section, Yukon Region, Department of Indian and Northern Affairs, Whitehorse, Yukon, p. 142-160.
- Dick, L.A., 1979. Tungsten and base metal skarns in the northern Cordillera, Canada. Geological Survey of Canada, Paper 79-1A, p. 259-288.
- El Bouseily, A.M. and El Sokkary, A.A., 1975. The relation between Rb, Ba and Sr in granitic rocks. *Chemical Geology*, vol. 16, p. 207-220.
- Erdmer, P., Ghent, E.D., Archibald, D.A. and Stout, M.Z., 1998. Paleozoic and Mesozoic high pressure metamorphism at the margin of ancestral North America in central Yukon. *Geological Society of America Bulletin*, vol. 110, p. 615-629.
- Friedman, R.M., Diakow, L.J., Lane, R.A. and Mortensen, J.K., 2001. New U-Pb age constraints on latest Cretaceous magmatism and associated mineralization in the Fawnie Range, Nechako Plateau, central British Columbia. *Canadian Journal of Earth Sciences*, vol. 38, p. 619-637.
- Gabrielse, H., 1969. Geology of Jennings River map area, British Columbia (104O). Geological Survey of Canada, Paper 68-55, 37 p. and uncoloured 1:253 440-scale map.
- Gabrielse, H., 1985. Major dextral transcurrent displacements along the Northern Rocky Mountain Trench and related lineaments in north-central British Columbia. *Geological Society of America, Bulletin* 96, p. 1-14.
- Gabrielse, H., Monger, J.W.H., Wheeler, J.O. and Yorath, C.J., 1991. Part A: Morphogeological belts, tectonic assemblages and terranes. *In: Chapter 2 of Geology of the Cordilleran Orogen in Canada*, H. Gabrielse and C. J. Yorath (eds.), Geological Survey of Canada, *Geology of Canada*, no. 4, p. 15-28.
- Gabrielse, H., Mortensen, J.K., Parrish, R.R., Harms, T.A., Nelson, J. L. and van der Heyden, P., 1993. Late Paleozoic plutons in the Sylvester Allochthon, northern British Columbia. *In: Radiogenic age and isotopic studies, Report 7*, Geological Survey of Canada, Paper 93-1, p. 107-118.
- Ghosh, D.K., 1995. Nd-Sr isotopic constraints on the interactions of the Intermontane superterrane with the western edge of North America in the southern Canadian Cordillera. *Canadian Journal of Earth Sciences*, vol. 32, p. 1740-1758.
- Gordey, S.P., McNicholl, V.J. and Mortensen, J.K., 1998. New U-Pb ages from the Teslin area, southern Yukon, and their bearing on terrane evolution in the northern Cordillera. *In: Radiogenic Age and Isotopic Studies: Report 11*, Geological Survey of Canada, *Current Research 1998-F*, p. 129-148.
- Harris, N.B.W., Pearce, J.A. and Tindle, A.G., 1986. Geochemical characteristics of collision-zone magmatism. *In: Collision Tectonics*, M.P. Coward and A.C. Ries (eds.), Geological Society of London Special Publication 19, p. 67-81.
- Hunt, P.A. and Roddick, J.C., 1987. A compilation of K-Ar ages, Report 17. *In: Radiogenic and Isotopic Studies, Report 1*, Geological Survey of Canada, Paper 87-2, p. 143-210.
- Jackaman, W., 2000. British Columbia Regional Geochemical Survey; NTS 104O – Jennings River: Stream sediment and water geochemical map booklet. British Columbia Ministry of Energy and Mines, BC RGS 52.
- Layne, G.D. and Spooner, E.T.C., 1991. The JC skarn deposit, southern Yukon Territory: 1. Geology, paragenesis and fluid inclusion microthermometry. *Economic Geology*, vol. 86, p. 29-47.
- l'Heureux, E., 2000. Geochemical and petrological analysis of Simpson Peak batholith, NW British Columbia. Unpublished BSc thesis, University of Victoria, Department of Earth and Ocean Sciences, Victoria, British Columbia, 71 p.
- Liverton, T., 1990. Tin-bearing skarns of the Thirtymile Range, NTS sheet 105 C/9: A progress report. *In: Yukon Geology, Volume 3*, Exploration and Geological Services Division, Yukon Region, Indian and Northern Affairs Canada, p. 52-70.
- Liverton, T., 1992. Tectonics and metallogeny of the Thirtymile Range, Yukon Territory, Canada. PhD thesis, Royal Holloway, University of London, London, United Kingdom.

- Liverton, T. and Alderton, D.H.M., 1994. Plutonic rocks of the Thirtymile Range, Dorsey Terrane: Ultrafractionated tin granities in the Yukon. *Canadian Journal of Earth Sciences*, vol. 31, p. 1557-1568.
- Liverton, T. and Botelho, N.F. 2001. Fractionated alkaline rare-metal granites: Two examples. *Journal of Asian Earth Sciences*, vol. 19, p. 399-412.
- Liverton, T., Thirlwall, M.F. and McClay, K.R., 2001. Tectonic significance of plutonism in the Thirtymile Range, southern Yukon. *In: Yukon Exploration and Geology 2000*, D.S. Emond and L.H. Weston (eds.), Exploration and Geological Services Division, Yukon Region, Indian and Northern Affairs Canada, p. 171-180.
- Maniar, P.D. and Piccoli, P.M., 1989. Tectonic discrimination of granitoids. *Geological Society of America Bulletin*, vol. 101, p. 635-643.
- Mato, G., Ditson, G. and Godwin, C., 1983. Geology and geochemistry of the tin mineralization associated with the Seagull batholith, south-central Yukon Territory. *Canadian Institute of Mining and Metallurgy Bulletin*, vol. 76 (854), p. 43-49.
- Mihalynuk, M.G. and Heaman, L.H., 2001. Age of mineralized porphyry at the Logtung deposit W-Mo-Bi-Be (Beryl, aquamarine), northwest BC. *In: Geological Fieldwork 2001*, B.C. Ministry of Mines and Energy, Paper 2001-1, p. 35-39.
- Mihalynuk M.G., Nelson, J. and Friedman, R.M., 1998: Regional geology and mineralization of the Big Salmon Complex (104N NE and 104O SW). *In: Geological Fieldwork 1997*, British Columbia Department of Energy, Mines and Employment, p. 6-1 to 6-20.
- Mihalynuk, M.G., Nelson, J.L., Roots, C.F., Friedman, R.M. and de Keijzer, M., 2000. Ancient Pacific Margin, Part III: Regional geology and mineralization of the Big Salmon Complex (NTS 104N/9E,16 and 104O/12,13,14W). *In: Geological Fieldwork 1999*, British Columbia Department of Energy, Mines and Petroleum Resources, p. 27-46.
- Monger, J.W.H., Wheeler, J.O., Tipper, H.W., Gabrielse, H., Harms, T., Struik, L.C., Campbell, R.B., Dodds, C.J., Gehrels, G.E. and O'Brien, J., 1991. Cordilleran Terranes. *In: Geology of the Cordilleran Orogen in Canada*, H. Gabrielse and C.J. Yorath (eds.), Geological Survey of Canada, *Geology of Canada*, no. 4, p. 281-327.
- Mortensen, J.K., 1992: Pre-mid-Mesozoic tectonic evolution of the Yukon-Tanana terrane, Yukon and Alaska. *Tectonics*, vol. 111, no. 4, p. 836-853.
- Mortensen, J.K. and Gabites, J.E., 2002. Lead isotopic constraints on the metallogeny of southern Wolf Lake, southeastern Teslin and northern Jennings River map areas, Yukon and British Columbia: Preliminary results. *In: Yukon Exploration and Geology 2001*, D.S. Emond, L.H. Weston and L.L. Lewis (eds.), Exploration and Geological Services Division, Yukon Region, Indian and Northern Affairs Canada, p. 179-188.
- Mortensen, J.K., Emon, K., Johnston, S.T. and Hart, C.J.R., 2000. Age, geochemistry, paleotectonic setting and metallogeny of Late Triassic-Early Jurassic intrusions in the Yukon and eastern Alaska: a preliminary report. *In: Yukon Exploration and Geology 1999*, D.S. Emond and L.H. Weston (eds), Exploration and Geological Services Division, Yukon Region, Indian and Northern Affairs Canada, p. 139-144.
- Nelson, J.L., 1993. The Sylvester Allochthon: Upper Paleozoic marginal basin and island arc terranes in northern British Columbia. *Canadian Journal of Earth Sciences*, vol. 30, p. 631-643.
- Nelson, J.L., 2000. Ancient Pacific Margins Part VI: Still heading south: Potential VMS hosts in the eastern Dorsey Terrane, Jennings River (104O/1; 7,8,9,10). *In: Geological Fieldwork, 1999*. British Columbia Ministry of Employment and Investment, Geological Survey Branch, Paper 2000-1, p. 107-126.
- Nelson, J.L., 2001. Geology of north-central Jennings River area (104O/14E, 15). *In: Geological Fieldwork 2000*, B.C. Ministry of Energy and Mines, Paper 2001-1, p. 51-66.
- Nelson, J. and Friedman, R., 2004. Superimposed Quesnel (late Paleozoic-Jurassic) and Yukon-Tanana (Devonian-Mississippian) arc assemblages, Cassiar Mountains, northern British Columbia: Field, U-Pb and igneous petrochemical evidence. *Canadian Journal of Earth Sciences*, vol. 41, p. 1201-1235.
- Newberry, R.J., Burns, L.R.E., Swanson, S.E. and Smith, T.E., 1990. Comparative petrologic evolution of the Sn and W granites of the Fairbanks-Circle area, interior Alaska. *In: Ore-bearing granite systems; Petrogenesis and mineralizing processes*, H.J. Stein and J.L. Hannah (eds.), Geological Society of America, Special Paper 246, p. 121-142.

- Noble, S.R., Spooner, E.T.C. and Harris, F.R., 1984. The Logtung large tonnage, low-grade W (scheelite)-Mo porphyry deposit, south-central Yukon Territory. *Economic Geology*, vol. 79, p. 848-868.
- Pearce, J.A., Harris, N.B.W. and Tindle, A.G., 1984. Trace element discrimination diagrams for the tectonic interpretation of granitic rocks. *Annual Reviews in Earth and Planetary Science*, vol. 23, p. 251-285.
- Poole, W.H., 1956. Geology of the Cassiar Mountains in the vicinity of the Yukon-British Columbia boundary. Unpublished PhD thesis, Princeton University, Princeton, New Jersey, 247 p.
- Poole, W.H., Roddick, J.A. and Green, L.H., 1960. Geology, Wolf Lake, Yukon Territory. Geological Survey of Canada, Map 10-1960 (uncoloured, scale 1:253 440, with marginal notes).
- Preto, V.A., Osatenko, M.J., McMillan, W.J. and Armstrong, R.L., 1979. Isotopic dates and strontium isotopic ratios for plutonic and volcanic rocks in the Quesnel Trough and Nicola belt, south-central British Columbia. *Canadian Journal of Earth Sciences*, vol. 16, p. 1658-1672.
- Roots, C.F. and Heaman, L., 2001. Mississippian U-Pb dates from Dorsey Terrane assemblages in the upper Swift River area, southern Yukon Territory. *Geological Survey of Canada, Current Research 2001-A1*, 9 p.
- Roots, C.F., Harms, T.A., Simard, R-L., Orchard, M.J. and Heaman, L., 2002. Constraints on the age of the Klinkit assemblage east of Teslin Lake, northern British Columbia. *Geological Survey of Canada, Current Research 2002-A7*, 11 p.
- Roots, C., Nelson, J. and Stevens, R., 2004. Bedrock Geology, Seagull Creek (105B/3), Yukon Territory. Geological Survey of Canada, Open File 4632 and Yukon Geological Survey Open File 2004-1, 1:50 000 scale.
- Simard, R-L., Dostal, J. and Roots, C.F., 2003. Development of late Paleozoic volcanic arcs in the Canadian Cordillera: An example from the Klinkit Group, northern British Columbia and southern Yukon. *Canadian Journal of Earth Sciences*, vol. 40, p. 907-924.
- Stevens, R.A., 1996. Dorsey Assemblage: Pre-mid-Permian high temperature and pressure metamorphic rocks in the Dorsey Range, southern Yukon Territory. *In: Lithoprobe report No. 56, SNORCLE and Cordilleran Tectonics Workshop*, p. 70-75.
- Stevens, R.A. and Harms, T.A., 1995. Investigations in the Dorsey terrane, Part 1: Stratigraphy, structure and metamorphism in the Dorsey Range, southern Yukon Territory and northern British Columbia. *Geological Survey of Canada, Current Research 1995-A*, p. 117-127.
- Stevens, R.A., Mortensen, J.K. and Hunt, P.A., 1993. U-Pb and  $^{40}\text{Ar}$ - $^{39}\text{Ar}$  geochronology of plutonic rocks from the Teslin suture zone, Yukon Territory. *In: Radiogenic and Isotopic Studies: Report 7, Geological Survey of Canada, Paper 93-2*, p. 83-90.
- Stewart, J.P. and Evensen, N.M., 1983. The Logtung W (scheelite)-Mo deposit, S. Yukon: Petrology and geochemistry of spatially associated felsic igneous rocks. *Geological Association of Canada, Program with Abstracts*, vol. 8, p. A65.
- Sun, S-S., 1980. Lead isotopic study of young volcanic rocks from mid-ocean ridges, oceanic islands and island arcs. *Philosophical Transactions of the Royal Society of London*, vol. A 297, p. 409-445.





# Sedimentology and hydrocarbon potential of fluvial strata in the Tantalus and Aksala formations, northern Whitehorse Trough, Yukon

*D.G.F. Long*

*Department of Earth Sciences, Laurentian University<sup>1</sup>*

Long, D.G.F., 2005. Sedimentology and hydrocarbon potential of fluvial strata in the Tantalus and Aksala formations, northern Whitehorse Trough, Yukon. *In: Yukon Exploration and Geology 2004*, D.S. Emond, L.L. Lewis and G.D. Bradshaw (eds.), Yukon Geological Survey, p. 167-176.

## **ABSTRACT**

Extensive conglomeratic strata in the Late Jurassic to Early Cretaceous Tantalus Formation were deposited in both shallow gravel-bed braided rivers, and deeper meandering gravel bed rivers. Overbank, marsh and swamp deposits, with potential to contain abundant terrestrial organic materials, are restricted to recessive intervals associated with small sandy and gravelly high-constructive river systems. Medium- to high-volatile bituminous and anthracitic coals in these intervals have limited potential as a source of additional gaseous hydrocarbons. Most of the conglomerates have a high fracture density, which would make them good reservoirs for coal-bed methane in settings where the Tantalus Formation lies beneath a seal of younger volcanic strata. Strata of the Late Norian Mandanna member of the Aksala formation near Takhini Hotsprings do not contain fluvial strata: laminated, bioturbated, intraclast-bearing red sandstones were deposited in an intertidal setting, and may have lost most of their organic material prior to burial.

## **RÉSUMÉ**

D'importantes strates conglomératiques de la Formation de Tantalus datant du Jurassique tardif au Crétacé précoce se sont déposées à la fois dans des cours d'eau anastomosés peu profonds et dans des cours d'eau sinueux plus profonds, à fond de gravier. Des dépôts de débordement, de marais et de marécages, qui peuvent contenir des matières organiques terrestres abondantes, sont limités à des intervalles récessifs associés à de petits réseaux hydrographiques sableux et graveleux très constructifs. Dans ces intervalles, des charbons bitumineux et anthraciteux à teneur en matières volatiles de moyenne à élevée offrent un potentiel limité comme source supplémentaire d'hydrocarbures gazeux. La plupart des conglomérats présentent une grande densité de fractures qui en feraient de bons réservoirs pour du méthane de houille dans des milieux où la Formation de Tantalus repose sous une couche étanche formée de strates volcaniques plus récentes. Près de Takhini Hotsprings, les strates du membre Mandanna de la formation Aksala, datant du Norien tardif, ne renferment pas de strates fluviales : des grès rouges laminés et bioturbés à intraclastes se sont déposés dans un milieu intertidal et ont probablement perdu la majeure partie de leurs matières organiques avant leur enfouissement.

<sup>1</sup>Sudbury Ontario, Canada P3E 2C6, [dlong@laurentian.ca](mailto:dlong@laurentian.ca)

## INTRODUCTION

Terrestrial hydrocarbons, which may represent a viable source for coal-bed methane, may be present at several levels within the Whitehorse Trough in the Yukon and Northern British Columbia. K.G. Osadetz (pers. comm., 2004) suggests that within the Whitehorse Trough there may be a potential for as much as 7.3 trillion cubic feet (21 billion m<sup>3</sup>) of gas, and 0.1 billion (20 million m<sup>3</sup>) barrels of oil. Estimates for the Yukon segment of the trough are 8.12 million barrels (1.29 million m<sup>3</sup>) of recoverable oil and 196 billion cubic feet (5521 million m<sup>3</sup>) of marketable gas (National Energy Board, 2001). The major source of the gas may be from fractionation of coals within the terrestrial sequences, and algae in the marine sequences, most of which are above the grade required for methane production (Hannigan et al., 1995; Hunt, 1994; Hunt and Hart, 1993; Long, 1981, 1982a,b, 1984, 1986). Terrestrial units within the sequence have potential as both sources and reservoirs of coal-bed methane, at least in parts of the Whitehorse Trough where structural or facies closure occurs. In order to properly assess this potential, it is essential to understand the

sedimentology of the units, as this will allow preliminary estimates of the hydrocarbon potential, and the architecture, permeability structure and heterogeneity of potential reservoirs.

The objectives of the current study are to determine the age, depositional environments and hydrocarbon potential of both the Tantalus Formation, and the Mandanna member of the Aksala formation. This includes determination of the sedimentary architecture of fluvial facies in these units, and the relationship between the carbonate facies and contemporary volcanoclastic rocks in the Aksala formation. In addition, the provenance characteristics of the Tantalus Formation will be determined using petrographic analysis of clast types and isotopic dating of zircon populations. Ultimately this data may be used in conjunction with the vibra-seismic survey conducted across the Whitehorse Trough in 2004 as part of the Targeted Geoscience Initiative between the Yukon Geological Survey and the Geological Survey of Canada. The survey was initiated to identify potential hydrocarbon traps, reservoirs and seals in these units within the Whitehorse Trough.

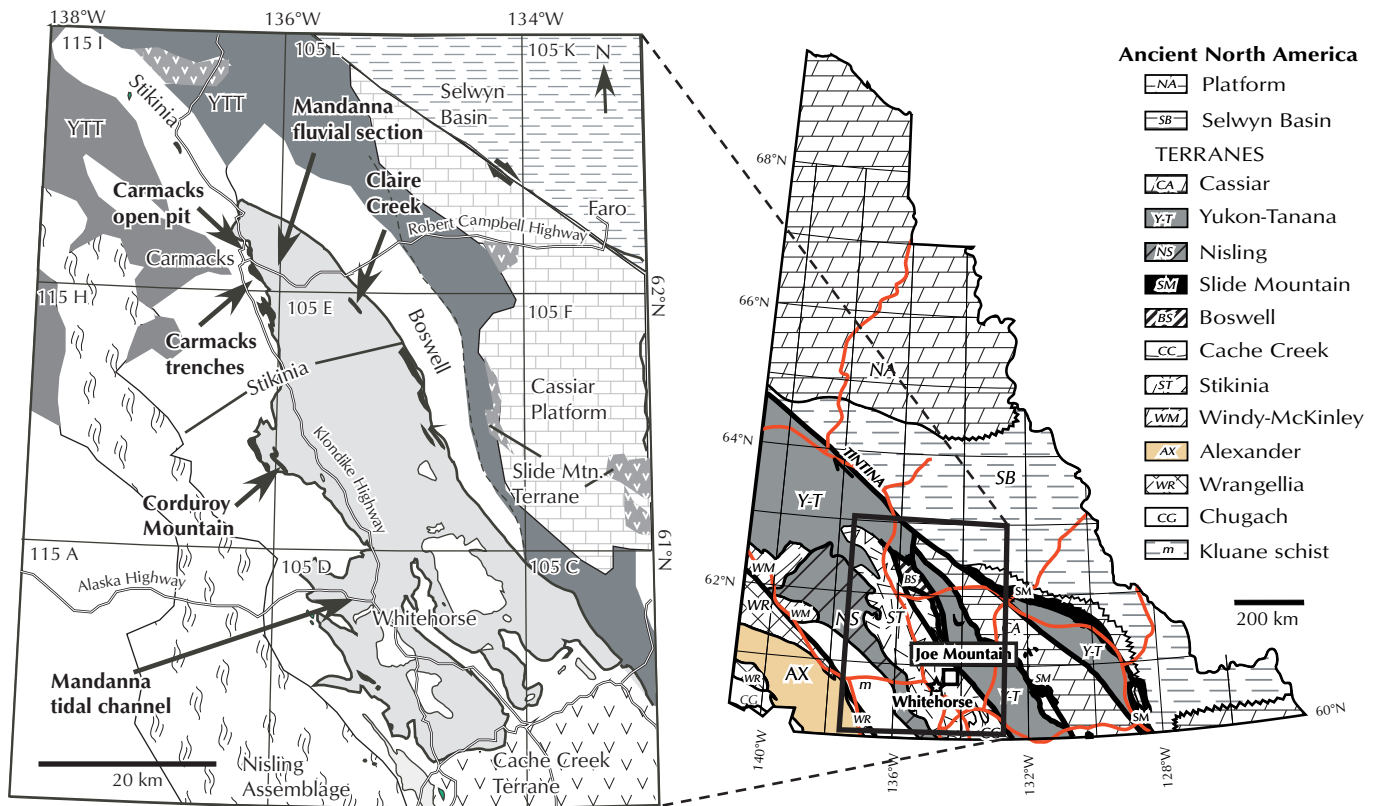


**Figure 1.** Location of strata of the Laberge and Lewes River groups (light grey) and Tantalus Formation (black) in the northern Whitehorse Trough. Location of sections mentioned in text shown in bold. YTT=Yukon-Tanana Terrane. Terrane/location map at right is modified from Colpron after Wheeler and McFeely (1991).



## GEOLOGICAL BACKGROUND

Rocks of the Whitehorse Trough form part of the Intermontane belt of the Canadian Cordillera and, according to Wheeler and McFeely (1991), constitute part of the Stikine Terrane, which is bordered to the west and east by rocks of the Yukon-Tanana Terrane, and to the south by rocks of the Cache Creek Terrane (Fig. 1). The Trough has been variably interpreted as a back-arc basin (Templeman-Kluit, 1978; Monger and Price, 1979; Bultman, 1979), a fore-arc basin (Templeman-Kluit, 1979, 1980; Dickie, 1995; Johannson et al., 1997), a simple marginal basin (Eisbacher, 1981), or part of a complex of inter-arc basins (Monger et al., 1991) and small ocean basins (Souther 1991, p. 469). Metamorphic rocks in the Stikine Terrane west of the trough (included in the Late Paleozoic Takhini assemblage by Hart, 1997) are interpreted in all models as part of an older island arc system, which developed on top of the Cache Creek Terrane (Hart et al., 1995). Strata in the Cache Creek Terrane to the south and east of the trough are interpreted as remnants of a small ocean basin (Eisbacher, 1981; Souther, 1991), an oceanic plateau, or a broader ocean basin (1100 to 5500 km wide), which may represent a fragment of an ancestral Pacific Ocean basin (Templeman-Kluit, 1979; Monger and Price, 1979; Tozer, 1982; Poulton, 1982; Poulton and Aitken, 1989).

Current models (Hart, 1997) suggest that during the Triassic, deposition of volcanic and sedimentary rocks of the Lewes River Group took place in a fore-arc or inter-arc basin associated with westward subduction. The basal tholeiitic pillowed volcanic rocks (Joe Mountain Formation) may have developed along a rift, or by sea-floor volcanism associated with arc initiation in Middle Triassic (Ladinian) time; associated sediments indicate a deep-water setting. The Whitehorse Trough appears to have become a distinct basin by Upper Triassic (Carnian) time. The basin-fill begins with a thick sequence of pillow basalts and associated volcanoclastic rocks in the Povoas Formation (Templeman-Kluit, 1984; Hart, 1997). Volcanoclastic strata are more abundant in the eastern part of the basin, where they are locally calcareous. The overlying Carnian and Norian Aksala formation reflects extension of the fore-arc basin with development of carbonate reefs along the fore-arc rise (Hart, 1997).

The paleogeographic setting of the area is further complicated by the possibility that remnants of a second arc system (the northern extension of Quesnellia) may be present in the Yukon-Tanana Terrane, east of the

Whitehorse Trough. Monger et al. (1982, 1991) suggest that this terrane amalgamated with Stikinia prior to Latest Triassic times, but may not have arrived at its present setting until the mid-Jurassic (Wernicke and Klepacki, 1988; Mihalyuk et al., 1994; Nelson and Friedman, 2004).

While no clear evidence exists for the presence of a volcanic arc east of the Whitehorse Trough in the Triassic, local emergence of the trench-slope break may be indicated in latest Norian by local southeast-directed paleocurrents in strata of the Lewes River Group along the northeast side of the Whitehorse Trough (Wheeler, 1961) and development of asymmetric reefs (Templeman-Kluit, 1978; Reid, 1982, 1987 a,b, 1988; Reid and Templeman-Kluit, 1987; Hart, 1997). In the latest Triassic, the basin appears to have collided either with the Atlin Terrane (part of Quesnellia) or the leading edge of the North American plate.

Contraction of the remnant arc basin in the early Jurassic, related to oblique collision with the North American plate, led to uplift of adjacent arc terranes and rapid accumulation of sediment gravity flows and associated slope deposits of the Laberge Group along the western (Dickie and Hein, 1992, 1995) and eastern (Wheeler, 1961) margins of the basin, with deepwater mudstones accumulating along the basin axis (Templeman-Kluit, 1984). Continued contraction, associated with obduction of parts of the eastern arc terranes, is marked by depositional hiatuses within the basin, followed by accumulation of more feldspathic sediments in the upper part of the Laberge Group in post Middle Jurassic times (Hart, 1997; Lowey, 2004).

The Laberge Group is succeeded by up to 1.3 km of predominantly medium- and large-pebble conglomerate of the (?) Upper Jurassic, to Lower Cretaceous Tantalus Formation (Templeman-Kluit, 1980; Long, 1982a,b, 1983, 1986). Clasts in the Tantalus Formation are predominantly chert, silicified mudstone and quartz, with only minor labile lithic fragments. This suggests that much of the clastic material was derived from reworking of carbonate sequences on the leading edge of the North American plate, or from chert-rich horizons within the Cache Creek Terrane, rather than from reworking of older arc systems. Analysis of zircon assemblages and clast types within the formation may provide additional clues to the late-stage evolution of the Whitehorse Trough, and provide possible links with the evolution of the Bowser Basin in northern BC.

## MANDANNA MEMBER

The Late Norian Mandanna member is the uppermost unit within the Lewes River Group (Templeman-Kluit, 1984), and lies above algal carbonates and volcanoclastic sandstones that may represent a potential marine hydrocarbon source. In the southern part of the trough, these rocks are dominated by well-bedded varicoloured siltstone, wacke, sandstone, tuff and conglomerate that conformably overlie and interfinger algal carbonates of the Hancock member. It has been suggested that the Mandanna rocks may include shallow marine, beach- and flash-flood-dominated fluvial facies (Hart, 1997). Although the carbonate reefs in the underlying Hancock member have been studied in some detail (Reid, 1981, 1982, 1986, 1987a,b; Reid and Ginsburg, 1986; Reid and Templeman-Kluit, 1987; Senowbari-Daryan and Reid, 1987; Yarnell, 2000), the exact relationships between the reefs and associated marine-reworked volcanoclastic sediments has not been documented in detail.

## TANTALUS FORMATION

The Tantalus Formation contains significant coal resources at Carmacks and other locations within the trough, and may represent another potential source for coal-bed methane, as well as being a potential reservoir for conventional oil and gas. At Carmacks, the thickest coal deposits are associated with drag-folds in fine-grained overbank deposits, formed in association with high-constructive (anastomosed or single channel) stream systems, while associated conglomerates were formed predominantly in deep gravel-bed braided and meandering systems (Long, 1986). The architecture of these systems is poorly understood and needs further detailed documentation, as this may have had a direct effect on methane migration and trapping potential.

## PRELIMINARY OBSERVATIONS

Due to extensive forest fires near Mandanna Lake and northwest of Carmacks, it was not possible to fly into any of the key localities in the northern Whitehorse Trough. Sections of the Mandanna member were examined south of Takhini Hotsprings, adjacent to the Alaska Highway at 60°48.922'N, 135°18.388'W, and possibly equivalent strata east of Carmacks adjacent to the Robert Campbell Highway near Eagle's Nest Bluff (Fig. 1). Parts of the Tantalus Formation were examined, and sampled at Corduroy Mountain and in the open-pit on Tantalus Butte at 62°08.532'N, 136°15.975'W, near Carmacks before the smoke became too dense to undertake detailed work.

## MANDANNA MEMBER

In exposures along the Alaska Highway, south of Takhini Hotsprings, exposures of the Mandanna member are dominated by flat laminated fine- to medium-grained sandstone and siltstone, with minor massive sandstone (Fig. 2). The presence of abundant bioturbation (worm tubes – Figs. 3 and 4) in the interbedded sand-mud facies supports the interpretation of an intertidal, rather than fluvial origin. Massive to flat-laminated sandstones, with some large cobbles of mud-grade material (Fig. 5), infill broad channels with stepped margins (Figs. 2,3). Faint burrows within these sands provides evidence for an intertidal origin.

Although many of the flat-laminated sandstones in the Mandanna member may be of intertidal origin, this does not preclude the existence of fluvial strata in the northern parts of the Whitehorse Trough. Strata that appear to be structurally and stratigraphically above the Hancock member in exposures immediately to the east of Eagle's Nest (adjacent to the Robert Campbell Highway: Fig 1) are thought to be a coarser grained facies of the Mandanna member. These strata contain evidence of deposition in perennial sand-bed rivers and meandering gravel-bed rivers, with stable channels, well developed levees and extensive overbank mud and sand deposits



**Figure 2.** Part of a tidal channel deposit in the Mandanna member, in exposures along north side of the Alaska Highway.



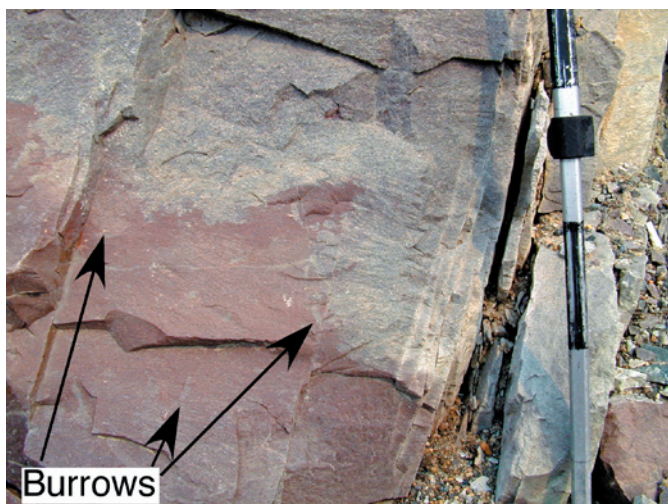


**Figure 3.** Bioturbation in the stepped bank of the tidal channel in Figure 1. Mandanna member, Alaska Highway. Scale divisions 10 cm.

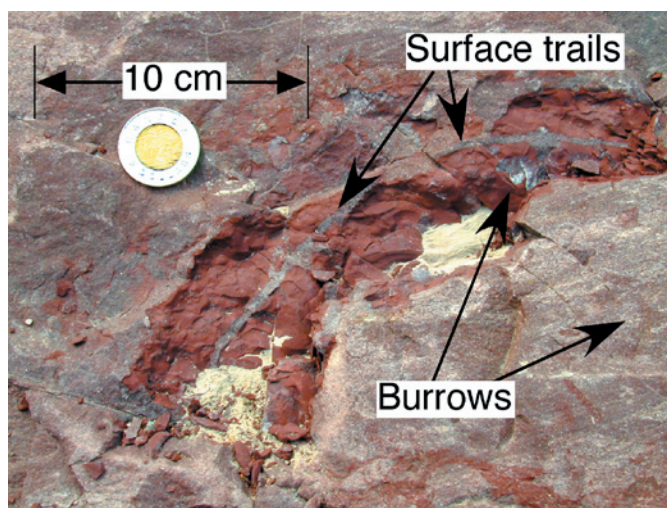


**Figure 4.** Bedding plane view of mud flaser, with sand-filled surface trails and burrows. Mandanna member, Alaska Highway.

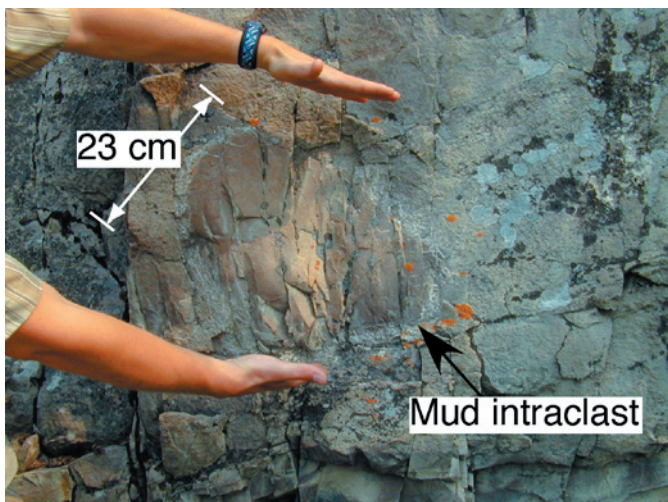


**Figure 5.** Large rounded clast of intraformational mudstone in massive sandstone fill of tidal channel shown in Figure 1.

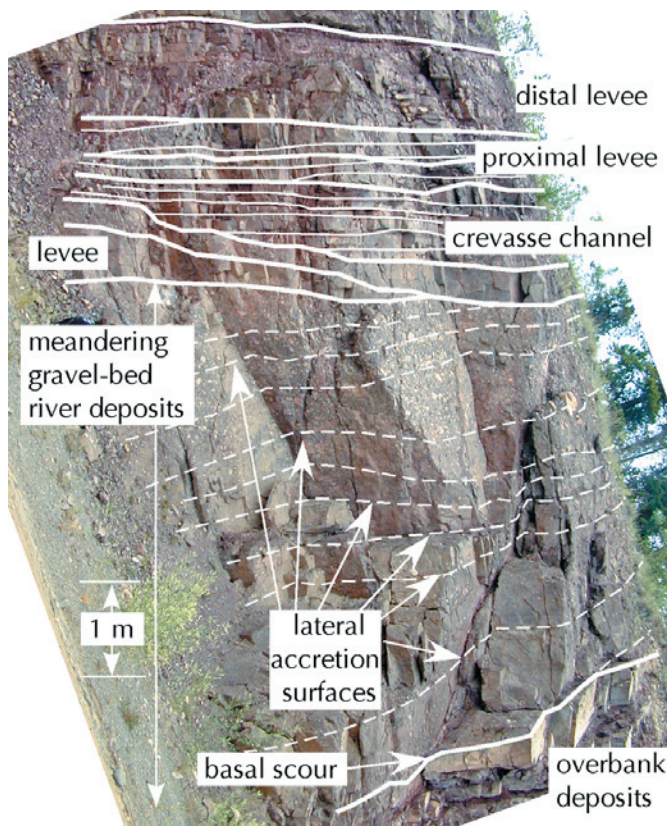


**Figure 6.** Part of an exposed section of the Mandanna member, on north side of the Robert Campbell Highway, east of Eagle's Nest Bluff. The photograph has been rotated to show well developed lateral accretion surfaces within moderately poorly sorted conglomerates, interpreted here as deposits of a gravel-bed meandering river system.



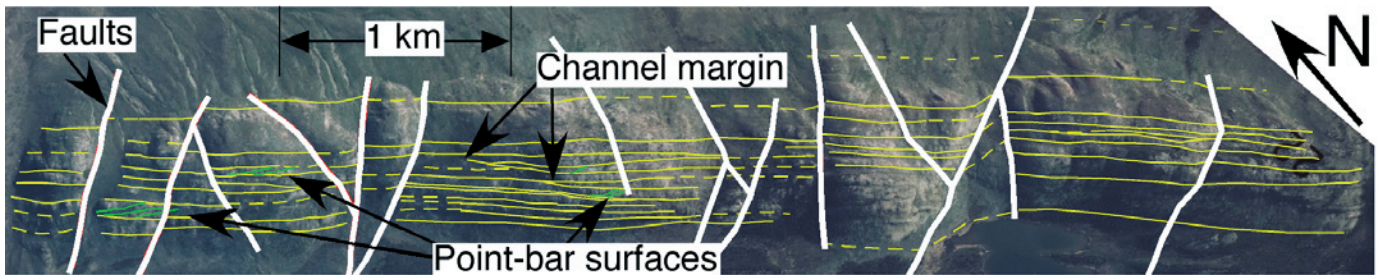


**Figure 7.** Annotated air-photograph of conglomerate exposures along Corduroy Mountain shows that some of the gravel-bed systems can be traced along strike for more than 5 km. A few channels pinch out laterally, and large-scale foresets, representing lateral accretion surfaces of gravel-bed meandering rivers, can be seen locally.

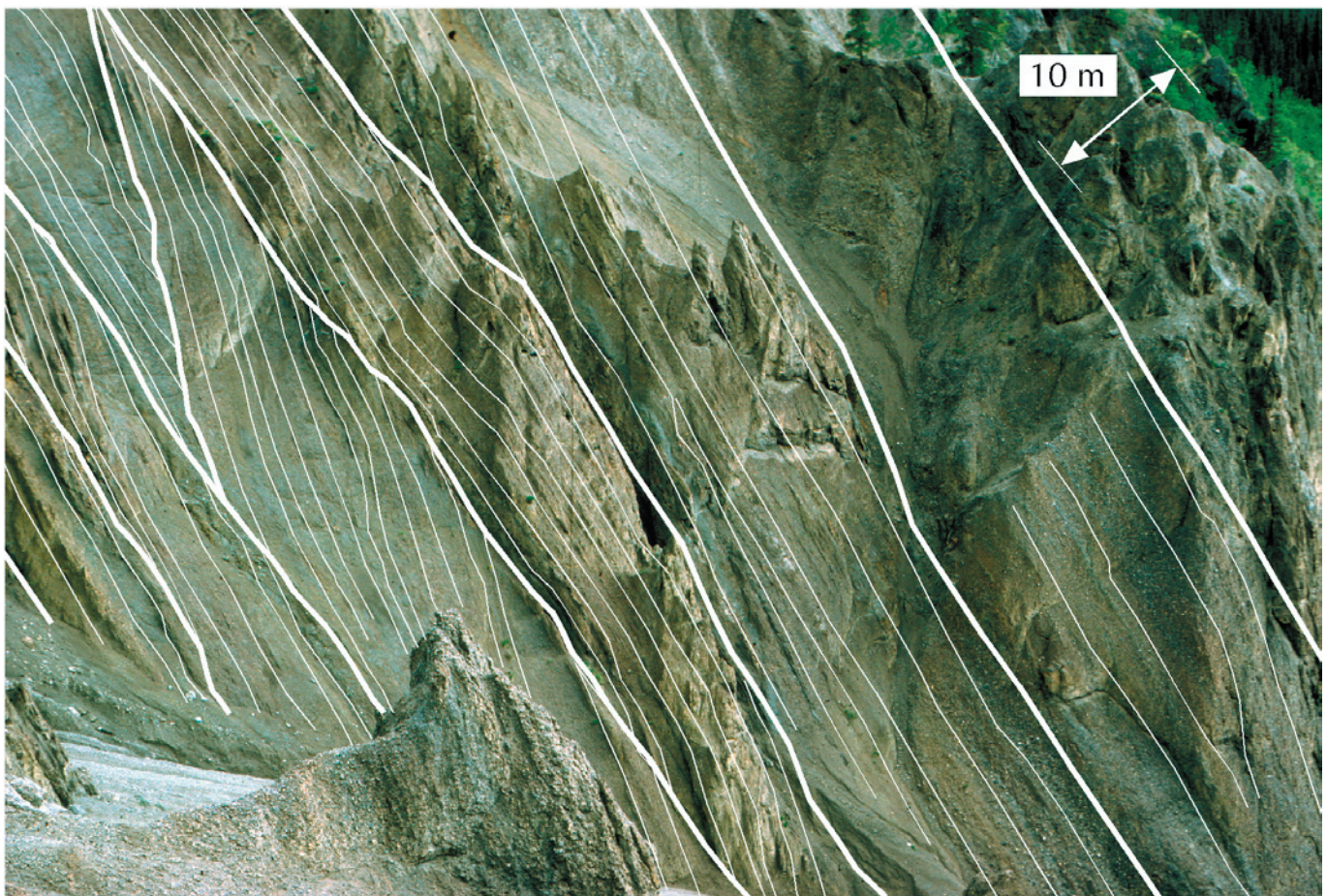


**Figure 8.** Large-scale inclined sets in conglomerates of the Tantalus Formation at Claire Creek indicates that at least part of the formation was deposited in meandering gravel-bed rivers, with little evidence for preservation of overbank sediments. Thick lines indicate channel beds and margins; thin lines outline lateral accretion surfaces.



(Fig. 6). There is no evidence for deposition under flash-flood conditions, although the rivers may have been highly seasonal.

## TANTALUS FORMATION

The Tantalus Formation contains significant coal resources at Carmacks and other locations within the Trough (Fig. 1), and may represent another potential source for coal-bed methane. At Carmacks, the thickest coal deposits are associated with drag-folds in fine-grained overbank deposits, formed in association with high-constructive (anastomosed and single channel) streams, whereas associated conglomerates were formed predominantly in deep-gravel-bed braided and meandering systems (Long, 1986).

Initial studies in the Braeburn-Kynocks area at Corduroy Mountain (Figs. 1, 7) suggest that it may be possible to determine the width and depth of some of the meandering gravel-bed systems. Exposures at Claire Creek indicate that stream depths may have been in excess of 12 m (Fig. 8).

Examination of measured sections taken in 1978 (D. Long, unpublished) reveal significant erosional intervals within the Tantalus Formation, and the development of an incised valley system with a relief in excess of 200 m. There is also significant erosion at the contact with underlying coal-bearing strata of the Tanglefoot Formation, at least in the area around Carmacks (Fig. 9).

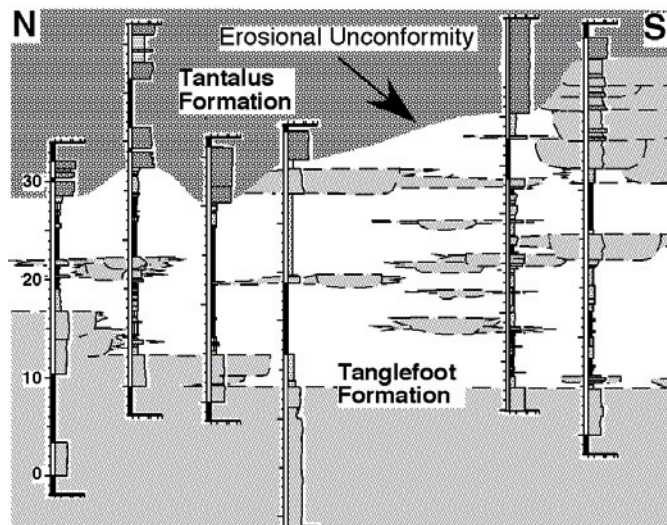


**Figure 9.** Correlation of strata in the upper part of the Tanglefoot Formation, exposed in trenches south of the Yukon River at Carmacks, indicates that there is a stepped erosion surface at the base of the Tantalus Formation. Scale in metres.

## HYDROCARBON POTENTIAL

Initial studies of the Mandanna member suggests that it has little potential as a source of hydrocarbons, as there is little evidence for transported organic material. The presence of muddy intervals in the fluvial strata in the northern part of the Whitehorse Trough may provide local seals for stratigraphic traps for hydrocarbons migrating from stratigraphically lower members of the Aksala formation.

The presence of thick coal seams in the Tantalus Formation near Carmacks indicates that there is some potential for in-situ gasification to produce coal-bed methane. Other, fine-grained parts of the formation may also contain high concentrations of organic matter, and so, may have limited potential as a source of conventional oil and gas. The formation is dominated by porous conglomerates and minor sandstones, and is highly fractured in almost all locations. This would make it a good reservoir rock in situations where structural traps exist, but leaves little potential for stratigraphic traps of the type envisaged by the National Energy Board (2001) in their analysis of the hydrocarbon potential of the Whitehorse Trough. These models typically show lenses of coarse-porous facies encapsulated in fine-grained material: a situation which is clearly not evident in the Tantalus Formation, where fines represent less than 5% of the sequence.

Given the complex structural history of the area, the most significant risks for both structural and stratigraphic traps is seal integrity. No oil stains have been encountered in the >150 thin sections of the Tantalus Formation examined to date, suggesting that liquid hydrocarbons were never abundant.

## FUTURE WORK

Field work in 2005 will concentrate on determining the character of fluvial strata in the Mandanna member of the Aksala formation, and in the Tantalus Formation. In addition, the study will be expanded to include marine strata of the Hancock and Casca members of the Aksala formation, in order to determine if these are potential sources of liquid or gaseous hydrocarbons. Representative samples will be collected and examined for hydrocarbon content, type and grade using vitrinite reflectance and RockEval analysis.

Architectural elements and discontinuity surfaces in the Tantalus Formation will be traced along strike in order to

determine the potential width/depth ratios of individual channel systems. This type of information is required to determine interconnectivity and lateral heterogeneity of potential reservoirs (c.f., Jordan and Pryor, 1992) and the tectonostratigraphic history of the basin.

Analysis of zircon assemblages from three large samples collected from the Tantalus Formation in 2004 will be used to determine if there were significant changes in provenance during deposition of the formation. Petrographic and geochemical investigation of clast types (predominantly chert) within the formation may provide additional clues to the late stage evolution of the Whitehorse Trough, and provide possible links with the evolution of the Bowser Basin in northern B.C.

## ACKNOWLEDGEMENTS

I thank the Yukon Geological Survey, Laurentian University Research Fund and the NSERC Discovery Grants program for funding parts of this study. I thank Jeremie Caza for his able assistance in the field, and Grant Lowey for continuing discussions on the sedimentology and hydrocarbon potential of the Whitehorse Trough. I thank Steve Piercey and Grant Lowey for critically reviewing an earlier version of this paper.

## REFERENCES

- Bultman, T.R., 1979. Geology and tectonic history of the Whitehorse trough west of Atlin, British Columbia. Unpublished PhD thesis, Yale University, New Haven, Connecticut, 284 p.
- Dickie, J.R., 1995. Conglomeratic fan deltas and submarine fans of the Jurassic Laberge Group, Whitehorse Trough, Yukon Territory, Canada; fore-arc sedimentation and unroofing of a volcanic island arc complex. *Sedimentary Geology*, vol. 98 (1-4), p. 263-292.
- Dickie, J.R. and Hein, F.J., 1992. A Pliensbachian submarine slope and conglomerate gully-fill succession; Richthofen to Conglomerate formation transition (Laberge Group), Brute Mountain, Yukon. *Yukon Geology* 1992, p. 71-86.
- Dickie, J.R. and Hein, F.J., 1995. Conglomeratic fan deltas and submarine fans of the Jurassic Laberge Group, Whitehorse Trough, Yukon Territory, Canada: fore-arc sedimentation and unroofing of a volcanic island complex. *Sedimentary Geology*, vol. 98, p. 263-292.
- Eisbacher, G.H., 1981. Late Mesozoic-Paleogene Bowser Basin molasse and cordilleran tectonics. *In: Sedimentation and tectonics in alluvial basins*. A.D. Miall (ed.), Geological Association of Canada, Special Paper 23, p. 125-151.
- Hannigan, P., Lee, P.J., Osadetz, K.G., Dietrich, J.R. and Olsen-Heise, K., 1995. Oil and Gas Resource Potential of the Bowser-Whitehorse Area of British Columbia. Geological Survey of Canada, Geofile 2001-5, March 1995.
- Hart, C.J.R., Dickie, J.R., Ghosh, D.K. and Armstrong, R.L., 1995. Provenance constraints for Whitehorse Trough conglomerate; U-Pb zircon dates and initial Sr ratios of granitic clasts in Jurassic Laberge Group, Yukon Territory. *In: Jurassic magmatism and tectonics of the North American Cordillera*, D.M. Miller and C. Busby (eds.), Geological Society of America, Special Paper 299, p. 47-63.
- Hart, C.J.R., 1997. A transect across Northern Stikinia: geology of the northern Whitehorse Map area, southern Yukon Territory (105D/13-16). Exploration and Geological Services Division, Yukon Region, Indian and Northern Affairs Canada, Bulletin 8, 112 p.
- Hunt, J.A., 1994. Yukon coal inventory 1994. Report prepared for Energy and Minerals Branch, Economic Development, Yukon Territorial Government, 169 p.
- Hunt, J.A. and Hart, C.J., 1993. Thermal maturation and hydrocarbon source rock potential of Tantalus Formation coals in the Whitehorse area, Yukon Territory. *In: Yukon Exploration and Geology 1993*, Exploration and Geosciences Division, Yukon Region, Indian and Northern Affairs Canada, p. 67-77.
- Johansson, G.G., Smith, P.L. and Gordey, S.P., 1997. Early Jurassic evolution of the northern Stikinian arc; evidence from the Laberge Group, northwestern British Columbia. *Canadian Journal of Earth Sciences*, vol. 34, no. 7, p. 1030-1057.
- Jordan, D.W. and Pryor, W.A., 1992. Hierarchical levels of heterogeneity in a Mississippi River meander belt and application to reservoir systems. *AAPG Bulletin*, October, 1992, vol. 76, no. 10, p. 1601-1624.
- Long, D.G.F., 1981. Coal deposits. *In: An assessment of mineral and fuel resource potential of Yukon Territory*. W.D. Sinclair, D.C. Findlay, W.H. Pool and K.M. Dawson (eds.), Geological Survey of Canada, Interim Report, August, 1981.



- Long, D.G.F., 1982a. Quesnel coalfield, Whitehorse Trough, Big Salmon coalfield, Ross River coalfield, Dawson coalfield, Amphitheater coalfield, Watson Lake coalfield, South Nahanni - Mattson coalfield, Moose Channel coalfield. *In: World Coalfields, Tectonics, Rijks Geologische Dienst, the Netherlands, I.G.C.P., 166, p. CANADA 14, 27, 28, 29, 30, 31, 32, 33, 35.*
- Long, D.G.F., 1982b. Depositional framework of coal deposits in forearc basin and molasse sequences of the Whitehorse Trough, Yukon Territory, Canada. International Association of Sedimentologists, Eleventh International Congress on Sedimentology, McMaster University, Hamilton, Ontario, Canada, August 22-27, 1982, Abstracts of Papers, p. 36.
- Long, D.G.F., 1983. Depositional setting of coal deposits in the Whitehorse Trough, Yukon Territory, Canada. Canadian Society of Petroleum Geologists, The Mesozoic of Middle North America, Program and Abstracts, p. 57
- Long, D.G.F., 1984. Carmacks-Braeburn-Whitehorse coalfield, Big Salmon coalfield, Ross River coalfield, Dawson coalfield, Amphitheater coalfield, Watson Lake coalfield, South Nahanni-Mattson coalfield. *In: World Coalfields, Tectonics, Rijks Geologische Dienst, the Netherlands, I.G.C.P., 166, p. CANADA 27T-33T.*
- Long, D.G.F. 1986. Coal in Yukon. *In: Mineral deposits of the northern Cordillera, J.D. Morin (ed.), Canadian Institute of Mining and Metallurgy, Special Volume 37, p. 311-318.*
- Lowey, G.W., 2004. Preliminary lithostratigraphy of the Laberge Group (Jurassic), south-central Yukon: implications concerning the petroleum potential of the Whitehorse Trough. *In: Yukon Exploration and Geology 2003, D.S. Emond and L.L. Lewis (eds.), Yukon Geological Survey, p. 129-142.*
- Mihalynuk, M.G., Nelson, J. and Diakow, L.J., 1994. The Cache Creek Terrane entrapment; oroclinal paradox within the Canadian Cordillera. *Tectonics, vol. 13, no. 3, p. 575-595.*
- Monger, J.W.H. and Price, R.A. 1979. Geodynamic evolution of the Canadian Cordillera, progress and problems. *Canadian Journal of Earth Sciences, vol. 16, p. 770-791.*
- Monger, J.W.H., Price, R.A. and Tempelman-Kluit, D.J., 1982. Tectonic accretion and the origin of the two major metamorphic and plutonic belts in the Canadian Cordillera. *Geology, vol. 10, p. 70-75.*
- Monger, J.W.H., Wheeler, J.O., Tipper, H.W., Gabrielse, H., Harms, T., Struik, L.C., Campbell, R.B., Dodds, G.E., Gehrels, G.E. and O'Brien, J., 1991. Part B. Cordilleran terranes. *In: Upper Devonian to Middle Jurassic assemblages, Chapter 8 of Geology of the Cordilleran Orogen in Canada, H. Gabrielse and C. Yorath (eds.), Geological Survey of Canada, Geology of Canada, vol. 4, p. 281-327.*
- National Energy Board, 2001. Petroleum Resource assessment of the Whitehorse Trough, Yukon Territory, Canada. Oil and Gas Branch, Department of Economic Development, Government of the Yukon, 59 p.
- Nelson, J. and Friedman, R., 2004. Superimposed Quesnel (late Paleozoic-Jurassic) and Yukon-Tanana (Devonian-Mississippian) arc assemblages, Cassiar Mountains, northern British Columbia: field, U-Pb, and igneous petrochemical evidence. *Canadian Journal of Earth Sciences, vol. 41, no. 10, p. 1201-1235.*
- Poulton, T.P., 1982. Paleogeographic and tectonic implications of Lower and Middle Jurassic facies patterns in northern Yukon Territory and adjacent Northwest Territories. *In: Arctic Geology and Geophysics. A.F. Embry and H.R. Balkwill (eds.), Canadian Society of Petroleum Geologists, Memoir 8, p. 13-27.*
- Poulton, T.P. and Aitken, J.D., 1989. The Lower Jurassic phosphorites of southeastern British Columbia and terrane accretion to western North America. *Canadian Journal of Earth Sciences, vol. 26, p. 1612-1616.*
- Reid, R.P., 1981. Report of field work on the Upper Triassic reef complex of Lime Peak, Laberge map-area, Yukon. *In: Yukon geology and exploration 1979-80, Exploration and Geological Sciences Division, Yukon Region, Indian and Northern Affairs Canada, p. 110-114.*
- Reid, P., 1982. Lime Peak; an Upper Triassic reef complex in Yukon. *AAPG Bulletin, vol. 66, no 5, p. 621-622.*
- Reid, R.P., 1986. Discovery of Triassic phylloid algae; possible links with the Paleozoic. *Canadian Journal of Earth Sciences, vol. 23, no. 12, p. 2068-2071.*

- Reid, R.P., 1987a. Nonskeletal peloidal precipitates in Upper Triassic reefs, Yukon Territory (Canada). *Journal of Sedimentary Petrology*, vol. 57, no. 5, p. 893-900.
- Reid, R.P., 1987b. The co-variation of lithology and geometry in Triassic reefal limestones at Lime Peak, Yukon. *In: Yukon Exploration and Geology 1981*, Department of Indian and Northern Affairs, Yukon Region, Exploration and Geological Services Division, p. 58-61.
- Reid, R.P., 1988. Lime Peak reef complex, Norian age, Yukon. *In: Reefs; Canada and adjacent areas*, H.J. Helmut, N.J. Geldsetzer and G.E. Tebbutt (eds.), Canadian Society of Petroleum Geologists, Memoir 13, p. 758-765
- Reid, R.P. and Ginsburg, R.N., 1986. The role of framework in Upper Triassic patch reefs in the Yukon. *Palaios*, vol. 1, no. 6, p. 590-600.
- Reid, R.P. and Templeman-Kluit, D.J., 1987. Upper Triassic Tethyan-type reefs in the Yukon. *Bulletin of Canadian Petroleum Geology*, vol. 35, no. 3, p. 316-332.
- Senowbari-Daryan, B. and Reid, R.P., 1987. Upper Triassic sponges (Sphinctozoa) from southern Yukon, Stikinia Terrane. *Canadian Journal of Earth Sciences*, vol. 24, no. 5, p. 882-902.
- Souther, J.G., 1991. Volcanic regimes, Chapter 14. *In: Geology of the Cordilleran Orogen in Canada*, H. Gabrielse and C. Yorath (eds.), Geological Survey of Canada, *Geology of Canada*, vol. 4, p. 457-490.
- Templeman-Kluit, D.J., 1978. Laberge (106E) map area, Yukon. Geological Survey of Canada, Open File Report 578, 1:250 000 scale.
- Templeman-Kluit, D.J., 1979. Transported cataclasite, ophiolite and granodiorite in Yukon: evidence of arc-continent collision. Geological Survey of Canada, Paper 79-14, 27 p.
- Templeman-Kluit, D.J., 1980. Highlights of field-work in the Laberge and Carmacks map areas, Yukon Territory. *In: Current Research, part A*. Geological Survey of Canada, Paper 80-1A, p. 357-362.
- Templeman-Kluit, D.J., 1984. Geology, Laberge (105E) and Carmacks (105I), Yukon Territory, Geological Survey of Canada, Open File Report 1101, 1:250 000 scale .
- Tozer, E.T., 1982. Marine Triassic faunas of North America: their significance for assessing plate and terraine movements. *Geologische Rundschau*, vol. 71, p. 1077-1104.
- Wernicke, B. and Klepacki, D.W., 1988. Escape hypothesis for the Stikine block. *Geology*, vol. 16, p. 416-464.
- Wheeler, J.O., 1961. Whitehorse map-area, Yukon Territory, 105D. Geological Survey of Canada, Memoir 312, 156 p.
- Wheeler, J.O. and McFeeley, P., 1991. Tectonic Assemblage Map of the Canadian Cordillera. Geological Survey of Canada, Map 1712A, 1:1 000 000 scale.
- Yarnell, J.M., 2000. Paleontology of two North American Triassic reef faunas; implications for terrane paleogeography. Unpublished MSc thesis, University of Montana, Missoula, Montana, 141 p.

# Sedimentology, stratigraphy and source rock potential of the Richthofen formation (Jurassic), northern Whitehorse Trough, Yukon

Grant W. Lowey<sup>1</sup>

Yukon Geological Survey

Lowey, G.W., 2005. Sedimentology, stratigraphy and source rock potential of the Richthofen formation (Jurassic), northern Whitehorse Trough, Yukon. *In: Yukon Exploration and Geology 2004*, D.S. Emond, L.L. Lewis and G. Bradshaw (eds.), Yukon Geological Survey, p. 177-191.

## ABSTRACT

Whitehorse Trough is a frontier basin in south-central Yukon that is thought to contain gas and possibly oil. It formed in the early Triassic as an arc-marginal basin between the ancient North American margin to the east and the volcano-plutonic Stikine Terrane to the west. Three stratigraphic units, termed the Lewes River Group (Upper Triassic), the Laberge Group (Lower-Middle Jurassic) and the Tantalus Formation (Upper Jurassic-Lower Cretaceous), are recognized in the Whitehorse Trough. The Laberge Group is informally subdivided into four units, which, from the base upwards includes the Richthofen, Conglomerate, Nordenskiöld and Tanglefoot formations. The Richthofen formation in the Laberge map area (NTS 105E) is characterized by thin- to medium-bedded turbidites, massive sandstone, matrix- and clast-supported conglomerate, scarce ammonites and belemnites, and abundant trace fossils, particularly *Chondrites*. No comprehensive stratigraphic section exists for the Richthofen formation, but it is estimated to be at least 500 m thick and appears to consist of a lower clast-supported conglomerate unit, a middle unit dominated by thin- to-medium bedded turbidites with minor amounts of massive sandstone and clast- and matrix-supported conglomerate, and an upper clast-supported conglomerate unit. The Richthofen formation unconformably overlies the Lewes River Group and was deposited by a southeast-prograding submarine fan (or fans) during the Early Jurassic. It is correlative with the Inklin Formation in northwestern British Columbia. Programmed pyrolysis using Rock-Eval 6 analysis of 63 samples from the Richthofen formation indicates that it is a poor to fair source rock and is gas-prone.

## RÉSUMÉ

La cuvette de Whitehorse est un bassin sous-exploré du centre-sud du Yukon qui pourrait renfermer du gaz et probablement du pétrole. Il s'est formée au cours du Trias précoce sous forme de bassin marginal d'arc entre l'ancienne marge nord-américaine à l'est et le terrane volcano-plutonique de Stikine à l'ouest. On a identifié trois unités stratigraphiques dans le bassin de Whitehorse, désignées comme le Groupe de Lewes River (Trias supérieur), le Groupe de Laberge (Jurassique inférieur à moyen) et la Formation de Tantalus (Jurassique supérieur à Crétacé inférieur). Le Groupe de Laberge se subdivise en quatre unités informelles qui, de la base vers le haut, comprennent les formations de Richthofen, de Conglomerate, de Nordenskiöld et de Tanglefoot. La formation de Richthofen, située dans la région de la carte Laberge (105E), est caractérisée par des turbidites en lits variant de minces à moyens, du grès massif, des conglomérats à texture non jointive et jointive, de rares ammonites et bélemnites, ainsi que d'abondantes empreintes fossiles, particulièrement des chondrites. Bien qu'aucune coupe stratigraphique détaillée n'existe pour la formation de Richthofen, son épaisseur est estimée à au moins 500 m et elle semble se composer d'une unité inférieure de conglomérat à texture jointive, d'une unité médiane dominée par des turbidites en lits minces à moyens avec de petites quantités de grès massif et de conglomérats à texture jointive et non jointive, ainsi que d'une unité supérieure de conglomérat à texture jointive. La formation de Richthofen repose en discordance sur le Groupe de Lewes River et a été déposée sous forme d'un cône (ou de plusieurs cônes) sous-marin progradant vers le sud-est, au Jurassique précoce. Cette formation est en corrélation avec la Formation d'Inklin, au nord-ouest de la Colombie-Britannique. Une pyrolyse programmée, réalisée par analyse Rock-Eval 6 de 63 échantillons de la formation de Richthofen, indique qu'il s'agit d'une roche mère de faible à bonne qualité, susceptible de renfermer du gaz.

<sup>1</sup>grant.lowey@gov.yk.ca



## INTRODUCTION

The Whitehorse Trough is the northernmost of four 'Interior Cordilleran' basins in northwestern Canada (i.e., from south to north: Quesnel, Nechako, Bowser and Whitehorse) that exhibit similar patterns of sedimentary history and tectonic evolution, and have corresponding oil and gas potential (Teitz and Young, 1982). It forms a northward-tapering belt (approximately 70 km wide and 650 km long) of Mesozoic volcanic and sedimentary rocks that extends from northern British Columbia to Carmacks in south-central Yukon (Fig. 1). No petroleum shows have been documented in this 'frontier' basin and no wells have been drilled, but 170 km of deep sounding multi-channel seismic reflection data was acquired in 2004 (White et al., 2004). The National Energy Board (2001) describes the Whitehorse Trough as an 'immature, mainly gas-prone' basin and identified potential source rocks (i.e., Triassic carbonates and Jurassic mudstones), reservoirs (i.e., Triassic carbonates and Jurassic and Cretaceous sandstones), seals (i.e., Jurassic mudstones

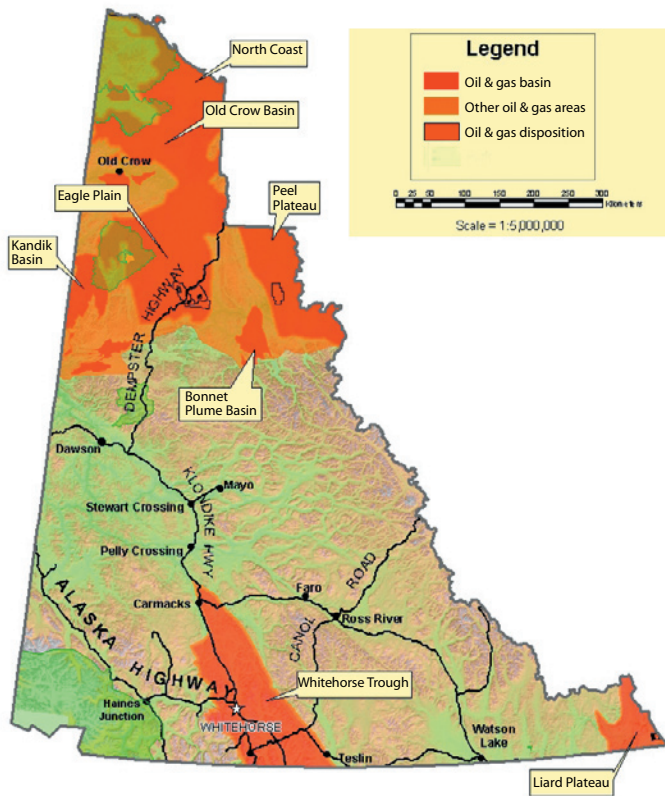


**Figure 1.** Oil and gas basins in the Yukon showing the location of the Whitehorse Trough (Energy, Mines and Resources).

and volcanoclastic rocks) and traps (i.e., anticlines and pinchouts). It is estimated that the expected mean oil content of the basin is  $\sim 15 \times 10^6$  m<sup>3</sup>, and the expected mean gas volume is  $\sim 136 \times 10^6$  m<sup>3</sup> (K. Osadetz, pers. comm., 2004).

Wheeler (1961) introduced the term 'Whitehorse Trough' and recognized three stratigraphic units (i.e., the Lewes River and Laberge groups and the Tantalus Formation). The Lewes River Group (Upper Triassic) is informally subdivided into the lowermost Povoas formation, consisting of basalt, tuff and agglomerate, and interpreted as subaqueous lava flows; and the uppermost Aksala formation, consisting of sandstone, shale, conglomerate and limestone, and interpreted as deep-marine, reef, beach and tidal flat deposits (Tempelman-Kluit, 1978, 1980, 1984). The Laberge Group (Lower-Middle Jurassic) was informally subdivided by Tempelman-Kluit (1984) into four units, which, from the base upwards includes the Richthofen (i.e., thin- to medium-bedded turbidites), Conglomerate (i.e., framework-supported conglomerate), Nordenskiöld (i.e., dacite tuff) and Tanglefoot (i.e., coal-bearing sandstone, shale and conglomerate) formations, which are interpreted as submarine fan, fan delta, subaqueous pyroclastic and delta deposits, respectively (Cairnes, 1910; Lees, 1934; Bostock and Lees, 1938; Lowey, 2004). The Tantalus Formation (Upper Jurassic-Lower Cretaceous) consists of fluvial and paralic sandstone, conglomerate and coal (Lowey and Hills, 1988).

The Whitehorse Trough is interpreted to have originated in Middle to Late Triassic time as either a back-arc or fore-arc basin undergoing oblique convergence, with the ancient North American margin on the east and the volcano-plutonic Stikine Terrane on the west (Tempelman-Kluit, 1978, 1979; Bultman, 1979). Lowey and Hills (1988) demonstrated that sandstone compositions from the Lewes River and Laberge groups and the Tantalus formation indicate sedimentation in two discrete basins: sandstones from the Lewes River and Laberge groups reflect an undissected through to dissected magmatic arc provenance, compatible with a back-arc or fore-arc basin, whereas sandstones from the Tantalus Formation reflect a lithic and transitional orogenic provenance, compatible with an intra-suture embayment basin.

The purpose of this paper is to document the sedimentology and stratigraphy (i.e., lithology, fossils, contacts, distribution, environment of deposition, age and correlation) of the Richthofen formation, primarily in the

Lake Laberge map area (NTS 105E). It is based on examination of outcrops mapped as the Richthofen formation, during which data was recorded on the thickness, type of contact(s), texture, sorting, grading, sedimentary structures, paleoflow direction, colour, clast composition, shape and roundness, and type of lithofacies observed. In addition, samples were collected for thin section microscopy, microfossils, major and trace element whole-rock geochemistry, source rock potential and x-ray diffraction analysis. This report is a preliminary step towards properly formalizing the stratigraphy of the Laberge Group, which is required because of confusion regarding the stratigraphy of the Whitehorse Trough and incorrect descriptions of the strata as ‘time-rock’ units (see discussion in Lowey, 2004). The paper also presents the results of programmed pyrolysis of samples from the Richthofen formation (mostly from the Lake Laberge map area) that was used to evaluate the source rock potential of this unit.

The Lake Laberge map area was previously mapped by Cairnes (1910), Lees (1934), Bostock and Lees (1938) and Tempelman-Kluit (1978, 1980, 1984). Dickie (1989) and Dickie and Hein (1988, 1992, 1995) provide initial descriptions of the sedimentology and stratigraphy of the Richthofen formation, and Lowey (2004) summarizes the lithostratigraphy of the unit.

## SEDIMENTOLOGY AND STRATIGRAPHY

Tempelman-Kluit (1984) proposed the name ‘Richthofen formation’ for ‘recessive, dark brown weathering, thin-bedded, dark brown to greenish, silty shale’ with minor conglomerate exposed in the Lake Laberge (NTS 105E) and Carmacks (NTS 1151) map areas. No formal definition of the Richthofen formation has been published and no type section was identified for this unit, although the west shore of Lake Laberge opposite Richthofen Island was designated as the type area (see Lowey, 2004).

## LITHOLOGY

Eleven stratigraphically repetitive lithofacies types are recognized in the Richthofen formation (Table 1). The most common lithofacies, based on the total thickness of lithofacies in all measured sections, includes thin-bedded sandstone-mudstone couplets (i.e., facies C2.3, using the code for deep-water sediments of Pickering et al., 1989) and disorganized conglomerate (i.e., facies A1.1). Medium-bedded turbidites (i.e., facies C2.2), disorganized muddy conglomerate (i.e., facies A1.2), and coherently folded and contorted strata (i.e., facies F2.1) are common; whereas disorganized pebbly sandstone (i.e., facies A1.4), graded-stratified pebbly sandstone (i.e., facies A2.8), medium- to thick-bedded sandstone (i.e., facies B1.1), parallel-stratified

**Table 1.** Lithofacies types observed in the Richthofen formation, Lake Laberge area (lithofacies classification after Pickering et al., 1989).

Code	Description	Other characteristics
A1.1	disorganized conglomerate	clasts up to 120 cm long
A1.2	disorganized muddy conglomerate	clasts up to 15 m long
A1.4	disorganized pebbly sandstone	clasts up to 2 cm long
A2.8	graded stratified pebbly sandstone	clasts up to 1 cm long, tuffaceous
B1.1	thick/medium-bedded, disorganized sandstone	–
B2.1	parallel-stratified sandstone	locally tuffaceous
B2.2	cross-stratified sandstone	coarse- to very coarse-grained sand
C2.2	medium-bedded sandstone-mudstone couplets	very fine- to medium-grained sand
C2.3	thin-bedded sandstone-mudstone couplets	very fine- to fine-grained sand, calcareous
C2.3/ D2.1	mixed thin-bedded sandstone-mudstone couplets and muddy siltstone	–
D2.1	graded stratified siltstone	–
F2.1	coherent folded and contorted strata	–



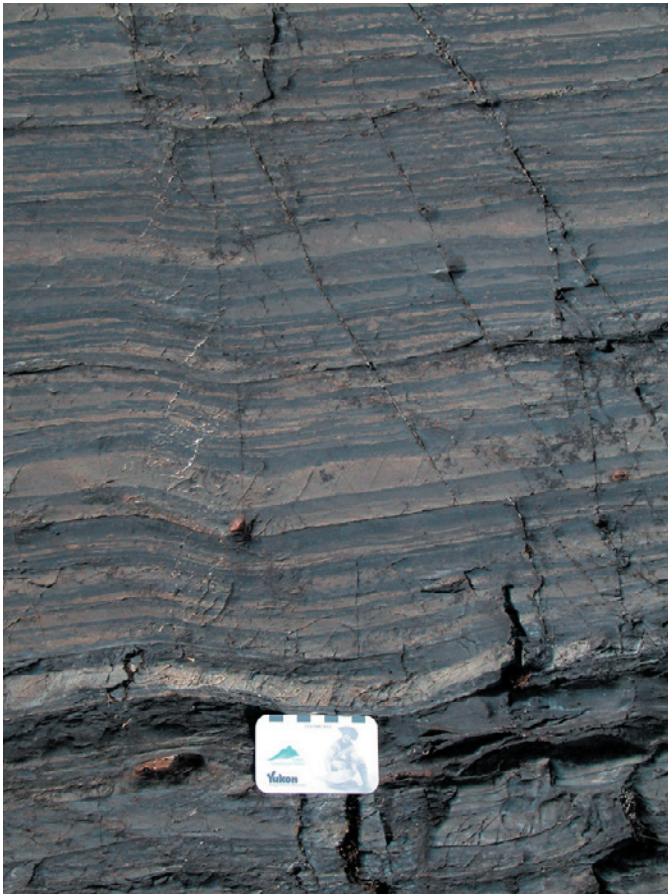


**Figure 2.** Thin-bedded sandstone-mudstone couplets (facies C2.3).

sandstone (i.e., facies B2.1), cross-stratified sandstone (i.e., facies B2.2) and graded-stratified siltstone (i.e., facies D2.1) are rare.

Thin-bedded sandstone-mudstone couplets (C2.3) are less than 10 cm thick, characterized by graded bedding with Bouma Tcde subdivisions (Bouma, 1962), and form sequences at least 40 m thick (Fig. 2). The sandstone is very fine- to fine-grained, and ripple foresets are commonly preserved. These represent 'classical' turbidites and were deposited by turbidity currents (Pickering et al., 1989).

Disorganized conglomerate (A1.1) is clast-supported and characterized by subrounded and spherical plutonic, volcanic and limestone clasts in a sandy to muddy matrix (Fig. 3). Bedding is not apparent and the conglomerate forms sequences at least 85 m thick. It was deposited by confined, noncohesive debris flows (Pickering et al., 1989).

Medium-bedded sandstone-mudstone couplets are 10-30 cm thick (Fig. 4), display graded bedding, contain



**Figure 3.** Clast-supported, disorganized conglomerate (facies A1.1), consisting of subrounded volcanic, plutonic and limestone clasts (Jacob's staff is 1.5 m long).



**Figure 4.** Medium-bedded sandstone-mudstone couplets (facies C2.2).

Bouma Ta(c)de and Tb(c)de subdivisions, and form sequences at least 40 m thick. They were also deposited by turbidity currents (Pickering et al., 1989).

Disorganized muddy conglomerate (A1.2) is matrix-supported and characterized by subangular to subrounded, spherical limestone and volcanic clasts in a muddy matrix (Fig. 5). Limestone clasts are up to 15 m long in exposed outcrop dimension (Fig. 6). The disorganized muddy conglomerate was deposited by unconfined, cohesive debris flows (Pickering et al., 1989), and is commonly associated with coherently folded and contorted strata (F2.1). This lithofacies is composed of folded and contorted thin-bedded sandstone-mudstone





**Figure 5.** Matrix-supported, disorganized conglomerate (facies A1.2), consisting of subangular limestone clasts.



**Figure 7.** Folded and contorted thin-bedded sandstone-mudstone couplets (facies F2.1; card 8 cm long).



**Figure 6.** Limestone megaclast from matrix-supported, disorganized conglomerate.



**Figure 8.** Massive, medium- to thick-bedded sandstone (facies B1.1; Jacob's staff 1.5 m long).

couplets (Fig. 7) that represent underwater slides and slumps (Pickering et al., 1989).

Disorganized pebbly sandstone (A1.4) and graded-stratified pebbly sandstone (A2.8) form beds ranging from 0.4 to 1.4 m thick and represent deposition by high concentration turbidity currents (Pickering et al., 1989) or hyperconcentrated density flows (Mulder and Alexander, 2001).

Medium- to thick-bedded sandstone (B1.1) is massive, fine- to medium-grained, and forms sequences at least 38 m thick (Fig. 8). It was deposited by hyperconcentrated density flows (Mulder and Alexander, 2001). Parallel-stratified sandstone (B2.1) and cross-stratified sandstone

(B2.2) form beds ranging from 0.5-1.0 m thick, are fine- to medium-grained and represent deposition by high-concentration turbidity currents (Pickering et al., 1989) or hyperconcentrated density flows (Mulder and Alexander, 2001). Graded-stratified siltstone (D2.1) forms sequences at least 10 m thick and was deposited by low concentration turbidity currents (Pickering et al., 1989).

## FOSSILS

The Richthofen formation is characterized by a variety of fossils, particularly in the sandstone-mudstone couplets. Pelagic fauna like ammonites are scarce and are preserved as impressions or thin carbonaceous films on bedding planes; belemnites are also scarce, with the



guards occurring as longitudinal or transverse sections in outcrop. Trace fossils are common, and in order of decreasing abundance include *Chondrites*, *Thalassinoides*, *Zoophycos* and *Planolites*. This ichnocoenose (association of trace fossils) shares characteristics of both the Cruziana ichnofacies (i.e., lower shoreface to lower offshore environments) and the *Zoophycos* ichnofacies (i.e., shelf to slope environments; Pemberton et al., 2001).

## THICKNESS

The total thickness of the Richthofen formation is uncertain because no comprehensive stratigraphic section exists. Bostock and Lees (1938) thought that the sandstone-mudstone couplets along the west shore of Lake Laberge formed a sequence at least 300 m thick and possibly more than 1200 m thick. However, examination of the strata reveals that it alternates from right-side-up to overturned and is interbedded with massive sandstone and clast- and matrix-supported conglomerate. Relatively short (~200 m), continuous sedimentologic sections have been measured in the Lake Laberge area, which indicate that the Richthofen formation consists of a lower, clast-supported conglomerate unit at least 200 m thick, a middle unit dominated by thin- to medium-bedded sandstone-mudstone couplets with minor amounts of massive sandstone and clast- and matrix-supported conglomerate at least 100 m thick, and an upper clast-supported conglomerate unit at least 200 m thick.

## CONTACTS

Cairnes (1910) determined that the basal unit of the Laberge Group was conglomerate and that it unconformably overlies limestone of the Lewes River Group. Bostock and Lees (1938) suggested that the Laberge Group appears to overlie the Lewes River Group conformably, but were unable to establish with certainty the relations of the two units. However, they (Bostock and Lees, 1938) noted that conglomerate assigned to the Laberge Group appears to rest directly on the Lewes River Group, indicating that a period of erosion had preceded deposition of the conglomerate. Tempelman-Kluit (1978) proposed that the Lewes River and Laberge groups represent a single, continuous depositional sequence with perhaps many “local, but minor hiatuses”, leading Hills and Tozer (1981) to conclude that it was impractical to separate the Lewes River and Laberge groups. Tempelman-Kluit (1984) later identified two localities where the Lewes River Group-Laberge Group contact is exposed in outcrop: along the east shore of

Lake Laberge opposite Ptarmigan Point (61°16'N, 135°12'W) and on Mount Laurier (61°02'N, 134°02'W). At both of these localities, Tempelman-Kluit (1984) indicates that the Richthofen formation conformably overlies limestone of the Hancock member of the Lewes River Group.

Examination of strata exposed along the east shore of Lake Laberge, opposite Ptarmigan Point, indicates that thin-bedded sandstone-mudstone couplets of the Richthofen formation are overturned and terminate abruptly against massive to thick-bedded limestone belonging to the Hancock member (Fig. 9). This contact is reinterpreted as a steep fault that developed along the south limb of an east-west-trending syncline that is overturned towards the north.

A section measured on the southeast spur of Mount Laurier (Fig. 10) reveals that at least 50 m of fine- to medium-grained, horizontally laminated sandstone and



**Figure 9.** Overturned sandstone-mudstone couplets of the Richthofen formation juxtaposed against massive limestone of the Hancock Member (Lewes River Group).

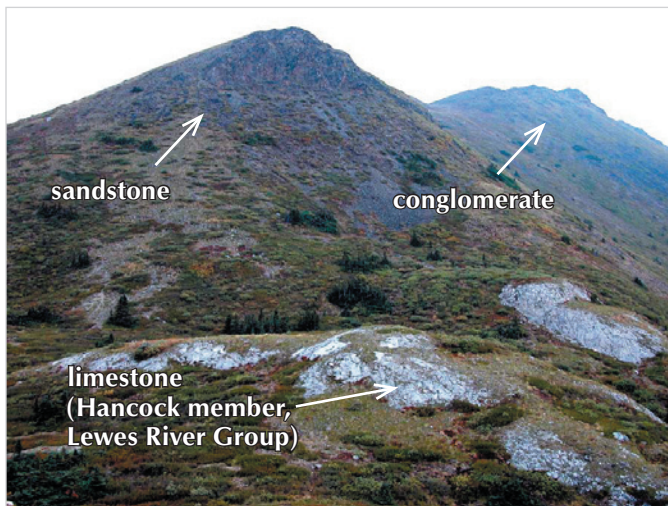


**Figure 10.** Mount Laurier, looking north.

minor amounts of horizontally laminated tuff (Fig. 11), with locally herringbone cross-stratified sandstone, interlaminated mudstone, and rare *Skolithos*, overlies massive to thick-bedded limestone of the Hancock member. Herringbone cross-stratification is commonly associated with tidal deposits (Klein, 1977) and *Skolithos* is commonly associated with shoreline and tidal deposits (Pemberton et al., 2001). This sandstone sequence was mapped by Tempelman-Kluit (1984) as the Richthofen formation, and it is overlain by clast-supported conglomerate with minor amounts of interbedded sandstone that Tempelman-Kluit (1984) mapped as the Conglomerate formation. However, the sandstone sequence is unlike any lithology present in the Richthofen



**Figure 11.** Horizontally laminated sandstone and tuff, Mount Laurier.

formation and more closely resembles the Mandanna member of the Lewes River Group.

The Mandanna member, the uppermost unit of the Lewes River Group, is described by Tempelman-Kluit (1984), and Dickie and Hein (1995) as a sequence of siltstone, sandstone and tuff, with locally abundant *Skolithos*, that was deposited in a tidal environment. In addition, Tempelman-Kluit (1978) describes “cross-bedded, quartzose sandstone” (mapped as the Lewes River Group) that grades into bioclastic limestone of the Hancock member in the vicinity of Lime Peak (i.e., directly north of Mount Laurier). Therefore, the sandstone sequence exposed on Mount Laurier is also interpreted as the Mandanna member.

Although Dickie and Hein (1995) state that the Mandanna member is of questionable affinity and could belong to either the uppermost Lewes River Group or the basal Laberge Group, the overlying conglomerate contains, in addition to rounded volcanic and limestone clasts, rounded siltstone and fine-grained sandstone clasts that resemble the underlying sandstone sequence. According to Lahee (1961) and Compton (1985), one of the criteria used in recognizing an unconformity is the presence of clasts from an underlying unit in the overlying unit. Hence, the contact between the sandstone sequence and the conglomerate is interpreted as an unconformity and the conglomerate is assigned to the Richthofen formation.

This conglomerate is interpreted as a submarine fan channel deposit (see the section on Environment of Deposition), and although most ‘good’ outcrops are ~10 to 100 m wide, submarine fan channels can be ~1 km wide or more (Bouma et al., 1985). Hence, the contact between the Lewes River Group and the overlying Laberge Group may be a disconformity, or even an angular unconformity, and does not support the conclusion of Hills and Tozer (1981) that it is impractical to separate the Lewes River and Laberge groups.

The upper contact of the Richthofen formation is not exposed, but Tempelman-Kluit (1984) indicates that this unit overlaps in age with the Nordenskiöld and Conglomerate formations. He (Tempelman-Kluit, 1984) also shows the Richthofen and Tanglefoot formations juxtaposed in an apparent conformable contact along Fox Lake, whereas Dickie and Hein (1995) present a stratigraphic column showing the Richthofen formation interfingering with both the Conglomerate and Tanglefoot formations. The upper contact of the Richthofen formation is the focus of future research.





**Figure 12.** Lenticular and wavy bedding in very fine-grained sandstone and mudstone in drill core from the Division Mountain area. The core was incorrectly mapped as Richthofen formation and has now been assigned to the Tanglefoot formation.

## DISTRIBUTION

### *Division Mountain area*

Lowey (2004) demonstrated that the Richthofen formation does not occur at Five Finger Rapids north of Carmacks in the Carmacks map area (NTS 115I) as mapped by Tempelman-Kluit (1984); nor does it occur along Joe or Fossil creeks east of the Division Mountain coal deposit in the Laberge map area (NTS 105E) as mapped by Tempelman-Kluit (1984) and Allen (2000). However, Carnes and Gish (1996, p. 38) reported the Richthofen formation in the Division Mountain area, describing it as “brown weathering black mudstone, with wispy siltstone to fine sandstone laminae in the form of low amplitude cross-stratification, (that) alternates with thick (>10 m) intervals of massive brown weathering calcareous sandstone”. In addition, Cash Resources Ltd. (1998) present several cross-sections showing that the Richthofen formation was intersected in drill core beneath the Tanglefoot formation [Note: in both of these reports and in Dickie (1989), the Richthofen formation is misspelled]. Examination of the drill core at Division Mountain (Fig. 12) reveals that the “black mudstone, with wispy siltstone to fine sandstone laminae”, has lenticular to wavy bedding, and not the graded bedded, sandstone-mudstone couplets characteristic of the Richthofen formation. According to Reineck and Singh (1975), lenticular and wavy bedding is common in tidal and delta-

front deposits. Hence, the Richthofen formation does not occur in the Division Mountain area, and strata previously interpreted as this unit is herein assigned to the Tanglefoot formation. This interpretation has important implications regarding the coal reserves in the area, because Cash Resources Ltd. stopped drilling when they intersected what they thought was the Richthofen formation; deeper drilling may reveal additional coal deposits.

### *Lake Laberge area*

Tempelman-Kluit (1984) apparently included all mappable occurrences of conglomerate, including clast- and matrix-supported varieties, in the ‘Conglomerate formation’. However, the matrix-supported conglomerate exposed along Lake Laberge is intrinsically associated with folded and contorted thin-bedded sandstone-mudstone couplets and sandstone-mudstone couplets that are characteristic of the Richthofen formation. In addition, both the matrix-supported and clast-supported conglomerate occurs as stratigraphically repetitive lithofacies which are part of the same depositional system as the sandstone-mudstone couplets. Hence, they should be assigned to the Richthofen formation (perhaps as members), or they should be designated as a new formation(s), because they are not correlative with the Conglomerate formation in the type area at Conglomerate Mountain. The conglomerate at Conglomerate Mountain occurs at a different stratigraphic level and represents a spatially separate deposit than the conglomerate in the Lake Laberge area. In addition, Dickie and Hein (1992) pointed out that the so-called Richthofen and Conglomerate formations in the Whitehorse map area (NTS 105D) are “strongly intercalated” and occur as “laterally equivalent lithozones”. Note that both the North American Stratigraphic Code (North American Commission on Stratigraphic Nomenclature, 1983) and the International Stratigraphic Guide (Salvador, 1994) state that lithocorrelation requires the demonstration of similar lithologic properties and stratigraphic position, which according to Schoch (1989) generally implies that a lithostratigraphic unit was deposited as a continuous body of rock without breaks.

## AGE

According to Tempelman-Kluit (1984), the Richthofen formation ranges from Hettangian to Pliensbachian in age (i.e., earliest to middle Early Jurassic). However, Lowey (2004) proposed that the unit ranges from Hettangian to Toarcian in age (i.e., earliest to latest Early Jurassic), based on re-assigning misidentified strata to other formations. Mihalyuk (1999) concluded that Richthofen formation

correlative strata across the Yukon border in northwestern British Columbia ranges from Sinemurian to Toarcian in age.

## ENVIRONMENT OF DEPOSITION

Paleoflow indicators are sparse in the Richthofen formation, but ripple foresets from thin- and medium-bedded turbidites (i.e., the Bouma Tc division) dip southeast and northwest; groove marks from the base of massive sandstone beds reveal an approximately southeast-northwest to east-west paleoflow direction; and flute marks and current crescent marks from the base of clast-supported conglomerate beds indicate scouring by a southeast-directed paleocurrent (Fig. 13). Flutes and crescents are considered the most reliable paleoflow indicators (i.e., they were deposited by sustained, high-energy flows), and together with the southeast and east direction recorded by the grooves, indicate an overall southeast paleoflow direction. The dip directions of ripple foresets are considered less reliable for recording paleoflow directions because they are difficult to measure (i.e., three-dimensional exposures are generally required) and measured paleocurrent directions may differ by 90° or more from other paleoflow indicators (i.e., thin-bedded turbidites are commonly deposited as overflow sediments on levees adjacent to major channels and in interchannel areas). Dickie (1989) also reports a southeast paleoflow for Richthofen strata from the Lake Laberge area.

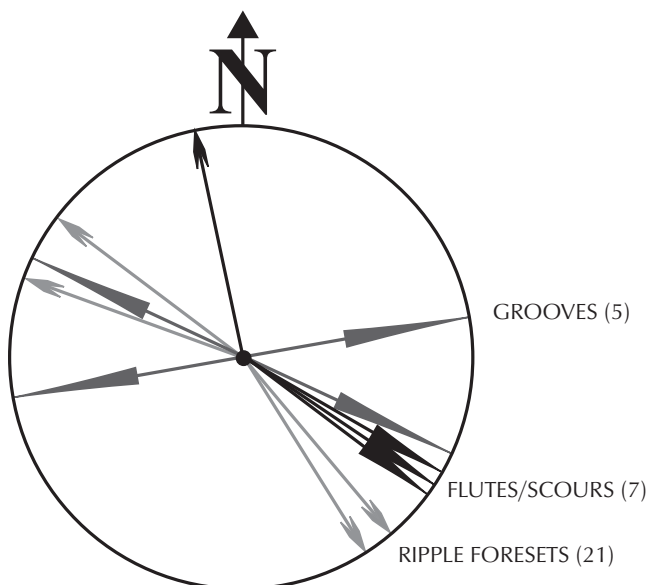


**Figure 13.** Summary of paleocurrent data, Richthofen formation (arrows represent mean paleocurrent directions for the number of measurements indicated).

The various lithofacies observed in the Richthofen formation and their mode of transport (i.e., primarily sediment gravity flows) are compatible with deposition on a submarine fan (or fans), such as the model proposed by Pickering et al. (1989). Hence, clast-supported conglomerate (i.e., lithofacies A) represents inner-fan channel deposits, massive sandstone (i.e., lithofacies B) represents middle-fan lobe deposits, and thin- to medium-bedded sandstone-mudstone couplets (i.e., lithofacies C) represent outer-fan levee and interchannel/interlobe deposits. The Richthofen formation and correlative strata (see the section on Correlation) crop out for a distance of approximately 400 km along the Whitehorse Trough, which is comparable to some modern days fans, such as the Laurentian Fan and the Mississippi Fan (i.e., 500-1500 km long). However, these are passive-margin fans, and active-margin fans are generally smaller (i.e., 40-400 km long). Reading and Richards (1994) present a classification for turbidite systems based on grain size and feeder system, but not enough paleocurrent data has been obtained from the Richthofen formation to determine if it originated as 'point-source' (i.e., submarine fan), 'multiple-source' (i.e., submarine ramp), or 'linear-source' (i.e., submarine slope apron) sedimentation.

## CORRELATION

Souther (1971), working in the Tulsequah map area in northwestern British Columbia, assigned the Inklin and Takwahoni formations of Kerr (1948) to the Laberge Group. The Inklin formation (Lower-Middle Jurassic) consists of approximately 3000 m of interbedded sandstone, sandstone-mudstone couplets, clast- and matrix-supported conglomerate, and minor amounts of limestone interpreted as deep-water marine deposits. The Takwahoni Formation (Lower-Middle Jurassic) consists of approximately 3300 m of clast-supported conglomerate, sandstone and mudstone interpreted as shallow-water marine and fluvial deposits (Souther, 1971). Dickie and Hein (1995) and The National Energy Board (2001) suggested that the Richthofen formation is also correlative, in part, with the Inklin Formation.

## SOURCE ROCK POTENTIAL

The petroleum source-rock potential of the Richthofen formation was evaluated by programmed pyrolysis using Rock-Eval 6 analysis (Peters, 1986). Essentially, this method takes approximately 70 mg of pulverized rock and heats it in a nitrogen atmosphere in a special oven,

measuring, among other things, the amount of free hydrocarbons in the sample (S1), the amount of potential hydrocarbons in the sample (S2, or kerogen that can be pyrolyzed into hydrocarbons), and the total amount of carbon present in the sample (basically a sum of S1, S2 and other parameters; Tissot and Welte, 1984; Waples, 1985). Sixty-three samples were collected from outcrop of the sandstone-mudstone couplets, and the analyses were performed by the Geological Survey of Canada at Calgary, Alberta (Appendix 1). The guidelines published by Peters (1986) were used for evaluating the source rock potential based on the results of programmed pyrolysis (Table 2). Note that Behar et al. (2001), Lafargue et al. (1998) and Peters (1986) all advise that results of programmed pyrolysis from outcrop samples be interpreted with caution (i.e., organic matter may have been oxidized, resulting in low S1 and S2 values) and supported by other analyses (i.e., vitrinite reflectance). In addition, Waples (1985) notes that results of Rock-Eval analyses provide information only on the present-day hydrocarbon generative capacity of kerogen in the rock.

Three main factors are considered in determining the source rock potential: 1) the generative potential, based on the percent of total organic carbon (TOC), the amount of free hydrocarbons (S1) and the amount of pyrolyzed hydrocarbons (S2); 2) the level of thermal maturation, based on the production index [ $PI = S1/(S1+S2)$ ] and the temperature of maximum production of pyrolyzed hydrocarbons ( $T_{max}$ ); and 3) the type of hydrocarbon generated, based on the hydrogen index [ $HI = (S2 \times 100)/TOC$ ] and the ratio of S2/S3 ( $S3 = CO_2$  from organic matter; Peters, 1986).

The thermal maturation of the Richthofen strata is quite favourable, with several samples having a PI within the oil window, or the correct maturation (Fig. 14); similarly, a plot of  $T_{max}$  (Fig. 15) shows several samples within the oil window (i.e., some samples are mature, but some are under-mature and over-mature). Note that Peters (1986) considers  $T_{max}$  obtained from small S2 values (i.e.,  $<0.2$  mg HC/g TOC) unreliable. The generative potential of the rocks is less favourable. A plot of TOC (Fig. 16) shows that most of the samples have only a poor to fair source rock potential due to low amounts of organic carbon. A plot of S1 is even less favourable (Fig. 17), with all samples containing very minor amounts of free hydrocarbons. Similarly, for S2, all samples contain very little organic matter that can be converted to petroleum (Fig. 18). Due to the small values obtained for S2, determining the type of hydrocarbons present is not

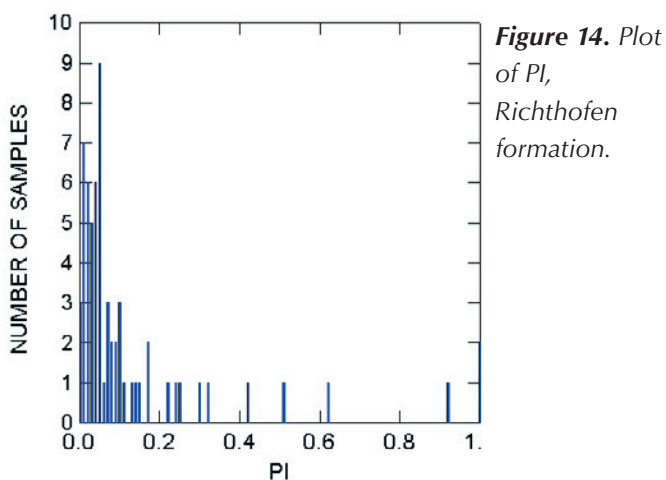


**Figure 14.** Plot of PI, Richthofen formation.

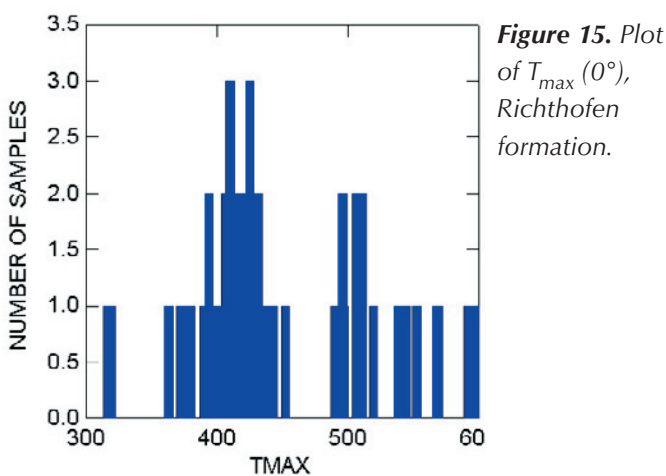


**Figure 15.** Plot of  $T_{max}$  ( $^{\circ}C$ ), Richthofen formation.

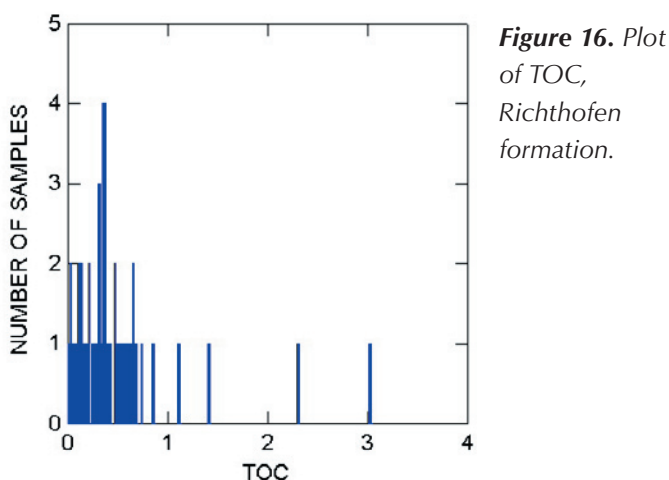


**Figure 16.** Plot of TOC, Richthofen formation.



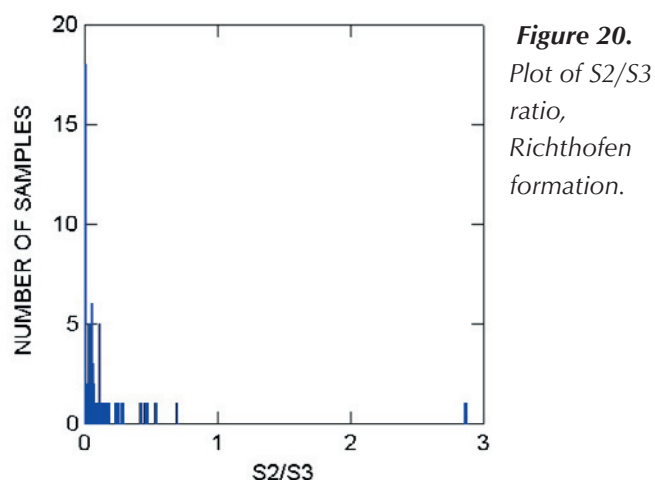
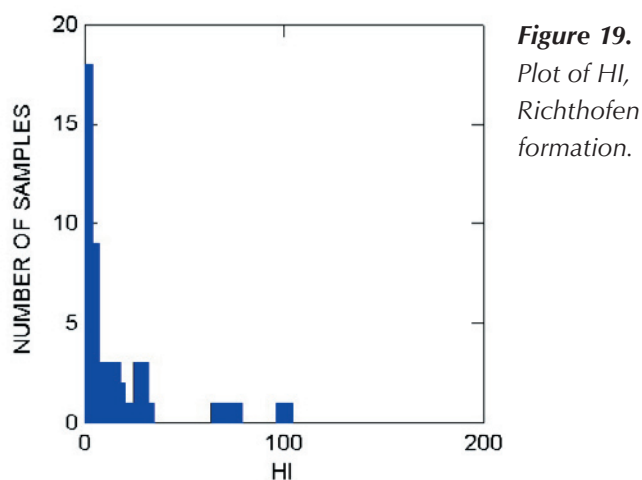
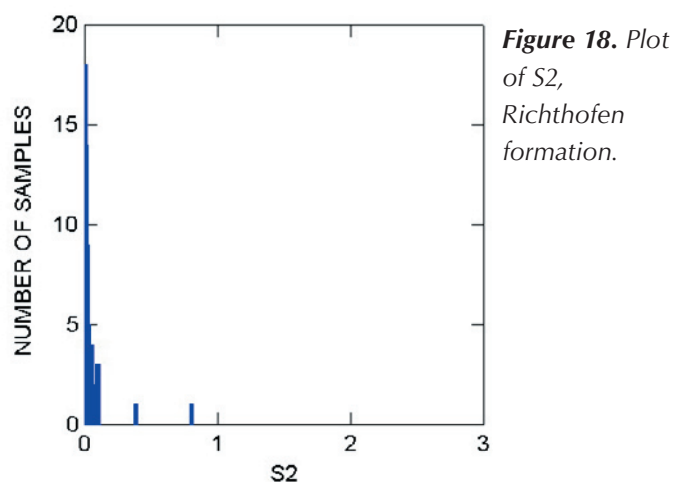
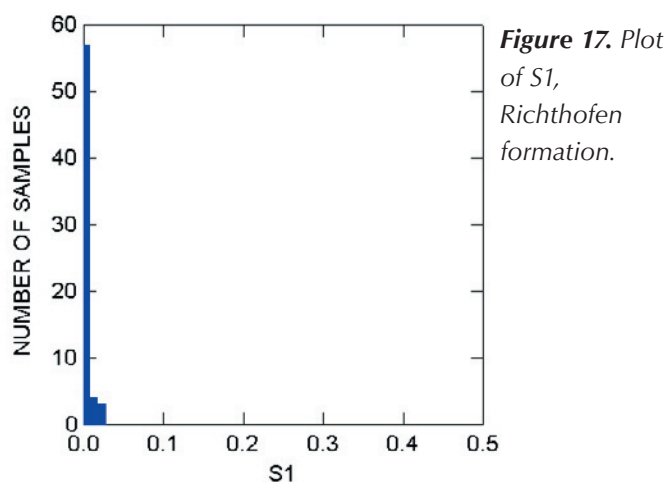


**Table 2.** Programmed pyrolysis guidelines describing level of thermal maturation, generative potential, and type of hydrocarbon generated (from Peters, 1986).

Level of thermal maturation			
Maturation	PI [S1/(S1+S2)]	T <sub>max</sub> (°C)	
top of oil window (birthline)	~0.1	~435 to 445*	
bottom of oil window (deadline)	~0.4	~470	
*depends on the type of organic matter			
Generative potential			
Quantity	TOC (wt. %)	S1 (mg HC/g C <sub>org</sub> )	S2 (mg HC/g C <sub>org</sub> )
poor	<0.5	0 to 0.5	0 to 2.5
fair	0.5 to 1	0.5 to 1	2.5 to 5
good	1 to 2	1 to 2	5 to 10
very good	>2	>2	>10
Type of hydrocarbon generated			
Type	HI (mg HC/g C <sub>org</sub> )	S2/S3	
gas	0 to 150	0 to 3	
gas and oil	150 to 300	3 to 5	
oil	>300	>5	

very accurate, but a plot of HI (Fig. 19) and S2/S3 (Fig. 20) indicates that only gas would have been generated. Similarly, the OI-HI diagram is not considered very reliable because most of the carbon is inert, but again only gas would be expected.

## DISCUSSION

A study in 1985 by Petro-Canada (Gilmore, 1985; Gunther, 1985) found the Richthofen formation to be the most prospective unit within the Whitehorse Trough, with a strong probability of gas, and possibly some oil, being present. A review of their results, however, indicates that it is actually the Tanglefoot formation (i.e., the uppermost unit of the Laberge Group), and not the Richthofen formation, that has the best source rock potential. Gilmore (1985) makes reference to a "coal-bearing" bed in the Richthofen formation and Gunther (1985) reports vitrinite reflectance values of 0.75 and 0.93 (i.e., within the oil window). However, coal occurs in the Tanglefoot formation, but not in the Richthofen formation.

The fact that the Richthofen formation is not a very good source rock for oil or gas is supported by English (2004) who examined the source rock potential of the correlative Inklin Formation in the Whitehorse Trough in northern British Columbia. Although several samples from his study plot within the oil window, most contain very small amounts of free- and potential-hydrocarbons, indicating that the Inklin Formation has only a poor to fair source rock potential and is gas-prone, similar to the Richthofen formation.

## CONCLUSIONS

In conclusion, the Richthofen formation in the Lake Laberge (NTS 105E) map area:

- 1) is characterized by thin-bedded sandstone-mudstone couplets (i.e., turbidites) and clast-supported conglomerate, and to a lesser extent, medium-bedded sandstone-mudstone couplets, massive sandstone and matrix-supported conglomerate;
- 2) unconformably overlies the Lewes River Group;
- 3) does not extend far north or west of Lake Laberge;
- 4) was deposited as a southeast-prograding submarine fan (or fans); and
- 5) is a poor to fair source rock and is gas-prone.

## ACKNOWLEDGEMENTS

I thank Karl Ziehe for his expert helicopter flying and David Gatensby for his help as a summer fieldwork assistant. The Rock-Eval analyses and comments by Martin Fowler are gratefully appreciated. Discussions with Darrel Long, Steve Piercy, Maurice Colpron and Lee Pigage concerning the Whitehorse Trough and Laberge Group stratigraphy were enlightening.

## REFERENCES

- Allen, T., 2000. An evaluation of coal-bearing strata at Division Mountain (115H/8 east-half, 105E/5 west-half), south-central Yukon. *In: Yukon Exploration and Geology 1999*, D.S. Emond and L.H. Weston (eds.), Exploration and Geological Services Division, Yukon Region, Indian and Northern Affairs Canada, p. 177-198.
- Behar, F., Beaumont, V. and Pentead, H.L. De B., 2001. Rock-Eval 6 technology: performances and developments. *Oil & Gas Science and Technology*, vol. 56, p. 111-134.
- Bostock, H.S. and Lees, E.J., 1938. Laberge map-area, Yukon. Geological Survey of Canada, Memoir 217, 32 p.
- Bouma, A.H., 1962. Sedimentology of some flysch deposits. Elsevier, Amsterdam, Netherlands, 168 p.
- Bouma, A.H., Normark, W.R. and Barnes, N.E., 1985. COMFAN: Needs and initial results. *In: Submarine fans and related turbidite systems*, A.H. Bouma, W.R. Normark and N.E. Barnes (eds.), Springer-Verlag, New York, New York, p. 7-11.
- Bultman, T.R., 1979. Geology and tectonic history of the Whitehorse Trough west of Atlin, British Columbia. Unpublished Ph.D. thesis, Yale University, New Haven, Connecticut, 284 p.
- Cairnes, D.D., 1910. Preliminary memoir on the Lewes and Nordenskiöld rivers coal district, Yukon Territory. Geological Survey of Canada, Memoir 5, 70 p.
- Carne, R.C. and Gish, R.F., 1996. Geology of the Division Mountain coal deposit of Cash Resources Ltd. *In: Yukon Exploration and Geology 1995*, Exploration and Geological Services Division, Yukon Region, Indian and Northern Affairs Canada, p. 37-42.
- Cash Resources Ltd., 1998. Division Mountain thermal coal project, Unpublished Report, Cash Resources Ltd., 80 p., available in EMR Library.

- Compton, R.R., 1985. *Geology in the field*. John Wiley and Sons, New York, New York, 398 p.
- Dickie, J.R., 1989. Sedimentary response to arc-continent transpressive tectonics, Laberge conglomerates (Jurassic), Whitehorse Trough, Yukon Territory. Unpublished M.Sc. thesis, Department of Geology, Dalhousie University, Halifax, Nova Scotia, 361 p.
- Dickie, J.R. and Hein, F.J., 1988. Facies and depositional setting of Laberge conglomerates (Jurassic), Whitehorse Trough. *In: Yukon Geology, Volume 2, Exploration and Geological Services Division, Yukon Region, Indian and Northern Affairs Canada*, p. 26-32.
- Dickie, J.R. and Hein, F.J., 1992. Pliensbachian submarine slope and conglomeratic gully-fill succession: Richthofen to Conglomerate formation transition (Laberge Group), Brute Mountain, Yukon. *In: Yukon Geology, Volume 3, Exploration and Geological Services Division, Yukon Region, Indian and Northern Affairs Canada*, p. 71-86.
- Dickie, J.R. and Hein, F.J., 1995. Conglomeratic fan deltas and submarine fans of the Jurassic Laberge Group, Whitehorse Trough, Yukon Territory, Canada: fore-arc sedimentation and unroofing of a volcanic arc complex. *Sedimentary Geology*, vol. 98, p. 263-292.
- English, J.M., 2004. Convergent margin tectonics in the North American Cordillera: implications for continental growth and orogeny. Unpublished Ph.D. thesis, University of Victoria, Victoria, BC, 191 p.
- Gilmore, R.G., 1985. Whitehorse field party. Unpublished report, Petro-Canada, 16 p. (plus photographs), available in Energy, Mines and Resources library.
- Gunther, P.R., 1985. Geochemical evaluation of Whitehorse field party samples. Unpublished Report, Petro-Canada, 19 p. plus appendices.
- Hills, L.V. and Tozer, E.T., 1981. Lewes River Group. *In: Lexicon of Canadian Stratigraphy, Volume 2, Yukon and District of Mackenzie*, L.V. Hills, E.V. Sangster and L.B. Suneby (eds.), Canadian Society of Petroleum Geologists, Calgary, Alberta, p. 105-106.
- Kerr, F.A., 1948. Taku River map area, British Columbia. Geological Survey of Canada, Memoir 248, 45 p.
- Klein, G. deV., 1977. Clastic tidal facies. Continuing Education Publication Company, Champaign, Illinois, 149 p.
- Lafargue, E., Marquis, F. and Pillot, D., 1998. Rock-Eval 6 applications in hydrocarbon exploration, production, and soil contamination studies. *Oil & Gas Science and Technologies*, vol. 53, p. 421-437.
- Lahee, F.H., 1961. *Field geology*. McGraw-Hill Book Company, New York, New York, 926 p.
- Lees, E.J., 1934. Geology of the Laberge area, Yukon. *Transactions of the Royal Canadian Institute*, no. 43, vol. 20, Part 1, 48 p.
- Lowey, G.W. and Hills, L.V., 1988. Lithofacies, petrography and environments of deposition, Tantalus Formation (Lower Cretaceous), Indian River area, west-central Yukon. *Bulletin of Canadian Petroleum Geology*, vol. 36, p. 296-310.
- Lowey, G.W., 2004. Preliminary lithostratigraphy of the Laberge Group (Jurassic), south-central Yukon: implications concerning the petroleum potential of the Whitehorse Trough. *In: Yukon Exploration and Geology 2003*, D.S. Emond and L.L. Lewis (eds.), Yukon Geological Survey, p. 129-142.
- Mihalynuk, M., 1999. Geology and mineral resources of the Tagish Lake area (NTS 104M/8, 9, 10E, 15 and 104N/12W) Northwestern British Columbia. British Columbia Ministry of Energy and Mines, Geological Survey Branch, Bulletin 105, 217 p.
- Mulder, T. and Alexander, J., 2001. The physical character of subaqueous sedimentary density flows and their deposits. *Sedimentology*, vol. 48, p. 269-299.
- National Energy Board, 2001. Petroleum resource assessment of the Whitehorse Trough, Yukon Territory, Canada. Oil and Gas Resource Branch, Department of Economic Development, Government of the Yukon, 59 p.
- North American Commission on Stratigraphic Nomenclature, 1983. North American Stratigraphic Code. *American Association of Petroleum Geologists Bulletin*, vol. 67, p. 841-875.
- Pemberton, S.G., Spila, M., Pulham, A.J., Saunders, T., MacEachern, J.A., Robbins, D. and Sinclair, I.K., 2001. Ichnology and sedimentology of shallow to marginal marine systems: Ben Nevis and Avalon Reservoirs, Jeanne D'Arc Basin. *Geological Association of Canada, Short Course Notes*, vol. 15, 343 p.



- Peters, K.E., 1986. Guidelines for evaluating petroleum source rock using programmed pyrolysis. *The American Association of Petroleum Geologists Bulletin*, vol. 70, p. 318-329.
- Pickering, K.T., Hiscott, R.N. and Hein, F.J., 1989. Deep marine environments. Unwin Hyman, London, 416 p.
- Reineck, H.E. and Singh, I.B., 1975. Depositional sedimentary environments. Springer-Verlag, New York, New York, 439 p.
- Reading, H.G. and Richards, M., 1994. Turbidite systems in deep-water basin margins classified by grain size and feeder system. *The American Association of Petroleum Geologists Bulletin*, vol. 78, p. 792-822.
- Salvador, A. 1994. *International Stratigraphic Guide, Second Edition*. The International Union of Geological Sciences and The Geological Society of America, Inc., 214 p.
- Schoch, R.M., 1989. *Stratigraphy, Principles and Methods*. Van Nostrand Reinhold, New York, New York, 375 p.
- Souther, J.G., 1971. Geology and mineral deposits of Tulsequah map-area, British Columbia (104K). *Geological Survey of Canada, Memoir 362*, 84 p.
- Teitz, H.H. and Young, F.G., 1982. Canadian hydrocarbon resource development up to the year 2000. *Journal of Petroleum Geology*, vol. 4, p. 347-375.
- Tempelman-Kluit, D.J., 1978. Reconnaissance geology, Laberge map-area, Yukon. *In: Current Research, Part A, Geological Survey of Canada, Paper 78-1A*, p. 61-66.
- Tempelman-Kluit, D.J., 1979. Transported cataclastite, ophiolite and granodiorite in Yukon: evidence of arc-continent collision. *Geological Survey of Canada, Paper 79-14*, 27 p.
- Tempelman-Kluit, D.J., 1980. Highlights of field work in Laberge and Carmacks map areas, Yukon Territory. *In: Current Research, Part A, Geological Survey of Canada, Paper 80-1A*, p. 357-362.
- Tempelman-Kluit, D.J., 1984. Geology, Laberge (105E) and Carmacks (115I), Yukon Territory. *Geological Survey of Canada, Open File 1101*, 1:250,000 scale.
- Tissot, B.P. and Welte, D.H., 1984. *Petroleum formation and occurrence*. Springer-Verlag, New York, New York, 699p.
- Waples, D.W., 1985. *Geochemistry in petroleum exploration*. International Hyman Resources Development Corporation, Boston, 232 p.
- Wheeler, J.O., 1961. Whitehorse map-area, Yukon Territory. *Geological Survey of Canada, Memoir 312*, 156 p.
- White, D., Buffet, G., Roberts, B., Colpron, M. and Abbott, G., 2004. Seismic images from an inverted sedimentary basin: The Whitehorse Trough, Yukon, Canada. Abstract submitted to the American Association of Petroleum Geologists Annual Meeting, June, 2004, Calgary, Alberta.

## APPENDIX 1

## RESULTS OF ROCK-EVAL 6 ANALYSIS

Sample	Easting	Northing	Qty	S1	S2	PI	T <sub>max</sub>	TOC	HI
GL03-90A	489245	6772712	69.9	0.00	0.00	1.00	-40	0.85	0
GL03-90B	489245	6772712	70.1	0.00	0.00	0.00	-40	0.37	0
GL104-01A	482978	6802442	70.1	0.00	0.09	0.01	494	0.32	28
GL104-02A	482393	6803720	70.7	0.02	0.38	0.04	497	1.41	28
GL104-03A	482168	6804552	70.5	0.01	0.10	0.06	491	0.37	27
GL104-05A	482623	6799519	70.7	0.00	0.03	0.05	508	0.21	14
GL104-08A	480760	6799644	70.6	0.00	0.10	0.03	496	0.48	21
GL104-08B	480760	6799644	70.4	0.02	0.80	0.02	506	3.02	28
GL104-10A	482916	6796053	70.2	0.00	0.09	0.03	506	0.58	16
GL104-16A	485588	6792821	70.5	0.00	0.04	0.02	511	0.39	10
GL104-16B	485588	6792821	70.7	0.00	0.00	0.09	490	0.09	0
GL104-16C	485588	6792821	70.3	0.00	0.10	0.01	519	1.11	9
GL104-17A	487670	6784498	70.5	0.00	0.04	0.01	414	0.52	8
GL104-18A	487314	6784785	70.0	0.00	0.04	0.04	406	0.74	5
GL104-19A	487296	6785151	70.0	0.00	0.02	0.08	395	0.33	6
GL104-20A	487103	6785663	70.6	0.00	0.01	0.11	419	0.14	7
GL104-22A	486673	6786747	70.7	0.00	0.00	0.10	417	0.16	0
GL104-23A	486360	6788169	70.6	0.00	0.00	0.09	404	0.17	0
GL104-24A	489553	6778917	70.7	0.00	0.00	0.15	427	0.32	0
GL104-26A	489406	6778202	70.6	0.00	0.01	0.08	415	0.35	3
GL104-27A	489383	6779415	70.8	0.01	0.01	0.51	372	0.30	3
GL104-28A	489268	6780112	70.3	0.00	0.00	0.00	390	0.11	0
GL104-29A	489175	6780655	70.1	0.00	0.00	0.01	363	0.03	0
GL104-30A	489037	6781689	70.5	0.00	0.04	0.05	427	0.13	31
GL104-31A	488848	6782553	70.2	0.00	0.01	0.07	425	0.36	3
GL104-32A	488094	6783424	70.3	0.00	0.01	0.01	400	0.15	7
GL104-33A	491444	6771562	70.4	0.00	0.01	0.02	443	0.11	9
GL104-34A	491725	6771506	70.0	0.00	0.01	0.04	412	0.01	100
GL104-36A	492078	6772503	70.9	0.00	0.00	0.32	394	0.51	0
GL104-38A	491169	6775360	70.2	0.00	0.01	0.03	380	0.31	3
GL104-41A	489115	6773985	70.4	0.00	0.00	0.14	410	0.61	0
GL104-42A	489883	6775821	70.2	0.00	0.02	0.10	418	0.03	67

Sample	Easting	Northing	Qty	S1	S2	PI	T <sub>max</sub>	TOC	HI
GL104-43A	490070	6775227	70.5	0.00	0.03	0.02	379	0.04	75
GL104-44A	490421	6773773	70.5	0.00	0.01	0.10	406	0.05	20
GL104-45A	490594	6768588	70.5	0.00	0.05	0.05	425	0.36	14
GL104-47A	488682	6795733	70.7	0.00	0.01	0.02	591	0.67	1
GL104-48A	488298	6794223	70.6	0.00	0.01	0.25	568	0.32	3
GL104-48B	488298	6794223	70.5	0.00	0.02	0.17	538	0.65	3
GL104-48C	488298	6794223	70.1	0.00	0.00	0.42	418	0.37	0
GL104-49A	489163	6793656	70.4	0.00	0.08	0.05	439	0.31	26
GL104-50A	488339	6791663	70.1	0.00	0.00	0.05	544	0.13	0
GL104-52A	489026	6789126	70.2	0.00	0.02	0.04	569	0.37	5
GL104-53A	489319	6788320	70.0	0.00	0.02	0.01	552	0.65	3
GL104-55A	494422	6776779	70.8	0.02	0.05	0.24	493	0.21	24
GL104-56A	495108	6775504	70.9	0.01	0.03	0.13	496	0.19	16
GL104-57A	495525	6774105	70.8	0.01	0.05	0.17	511	0.35	14
GL104-59A	493297	6763660	70.0	0.00	0.09	0.05	417	0.49	18
GL104-59B	493297	6763660	70.6	0.00	0.02	0.05	410	0.31	6
GL104-60A	491993	6766061	70.9	0.00	0.00	0.22	394	0.18	0
GL104-60B	491993	6766061	70.1	0.00	0.03	0.00	425	0.25	12
GL104-61A	491415	6766150	70.3	0.00	0.02	0.04	402	0.26	8
GL104-63A	492320	6765079	70.8	0.00	0.08	0.03	419	2.30	3
GL104-64B	463503	6802692	70.9	0.00	0.00	0.01	407	0.07	0
GL104-65A	474962	6788368	70.9	0.00	0.01	0.07	452	0.40	3
GL104-74A	490495	6760518	70.6	0.00	0.00	0.92	598	0.55	0
GL104-83A	491538	6763490	70.9	0.00	0.02	0.02	431	0.35	6
GL104-85B	491119	6763203	71.2	0.00	0.01	0.03	438	0.28	4
GL104-86A	491441	6763165	71.1	0.00	0.01	0.05	431	0.68	1
GL104-92A	489819	6759345	70.3	0.00	0.02	0.07	416	0.42	5
GL104-92C	489819	6759345	70.0	0.00	0.03	0.05	410	0.35	9
GL104-93A	490232	6759119	70.1	0.00	0.00	0.30	319	0.47	0
GL104-93C	492711	6760581	70.8	0.00	0.00	0.62	316	0.63	0
GL104-94B	492711	6760581	70.4	0.00	0.00	1.00	-40	0.47	0
GL104-95A	492000	6761523	70.0	0.00	0.05	0.04	433	0.29	17





# Landslide processes in discontinuous permafrost, Little Salmon Lake (NTS 105L/1 and 2), south-central Yukon

Ryan R. Lyle<sup>1</sup>, D. Jean Hutchinson<sup>2</sup> and Yana Preston

Queen's University<sup>3</sup>

Lyle, R.R., Hutchinson, D.J. and Preston, Y., 2005. Landslide processes in discontinuous permafrost, Little Salmon Lake (NTS 105L/1 and 2), south-central Yukon. *In: Yukon Exploration and Geology 2004*, D.S. Emond, L.L. Lewis and G.D. Bradshaw (eds.), Yukon Geological Survey, p. 193-204.

## ABSTRACT

With increasing development in areas of discontinuous permafrost, greater emphasis is being placed on slope hazard assessment. The current research project was initiated in response to the occurrence of a large flow-type slide, the Magundy River landslide, with the aim of identifying and characterizing slope hazards in the Little Salmon Lake area of the central Yukon. Terrain evaluation studies identified over 35 areas of past and present landslide activity in the project area. Field work was completed in the summer of 2004 to obtain ground truth for the terrain evaluation and to further characterize the most prominent and active landslides. This paper provides an overview of the research project and summarizes observations on four distinct landslide processes found in the Little Salmon Lake area: debris flow, rock slumping, bimodal flow and multiple retrogressive slumping.

## RÉSUMÉ

Avec la croissance du développement dans les zones de pergélisol discontinu, on met davantage l'accent sur l'évaluation des risques de glissement de terrain. Le projet de recherche actuel a été entrepris en réponse à un grand glissement par liquéfaction, le glissement de la rivière Magundy, afin d'identifier et de caractériser les risques de glissement dans la région du lac Little Salmon dans le centre du Yukon. Des études d'évaluation du terrain ont permis d'identifier plus de 35 zones de glissements passés et contemporains dans la région du présent projet. Des travaux de vérification sur le terrain ont été réalisés au cours de l'été 2004 aux fins de l'évaluation du terrain et d'une meilleure caractérisation des glissements les plus importants et les plus actifs. Le présent article fournit une vue d'ensemble du projet de recherche et résume les observations sur quatre processus distincts de glissement identifiés dans la région du lac Little Salmon, notamment la coulée de débris, l'effondrement de blocs, l'écoulement bi-modal et l'effondrement régressif multiple.

<sup>1</sup>lyle@students.geol.queensu.ca

<sup>2</sup>jhutchin@geol.queensu.ca

<sup>3</sup>Department of Geological Sciences and Geological Engineering, Miller Hall, Queen's University, Kingston, Ontario, Canada K7L 3N6

## INTRODUCTION

This project was initiated following the discovery of a large flow-type landslide in the Magundy River valley of central Yukon (J.D. Bond., pers. comm., 2003). A regional landslide inventory and assessment was proposed based on this slide and other landslides in the area documented by Ward and Jackson (2000). The objective of this project was to investigate landslide processes in discontinuous permafrost from an engineering geology perspective, using the Little Salmon Lake area (NTS 105L/1 and 2) as a case study.

Little Salmon Lake is located halfway between Carmacks and Faro, along the Robert Campbell Highway in central Yukon (Fig. 1). The work is confined to an east-west corridor accessible by the Robert Campbell Highway and by boat/canoe on Little Salmon Lake and the Magundy River. Figure 2 shows the general geographical features of the project area.

This paper is based on initial results of the project and highlights the different landslide processes observed in the Little Salmon Lake area. A discussion of the role of permafrost in the various landslides is also given.

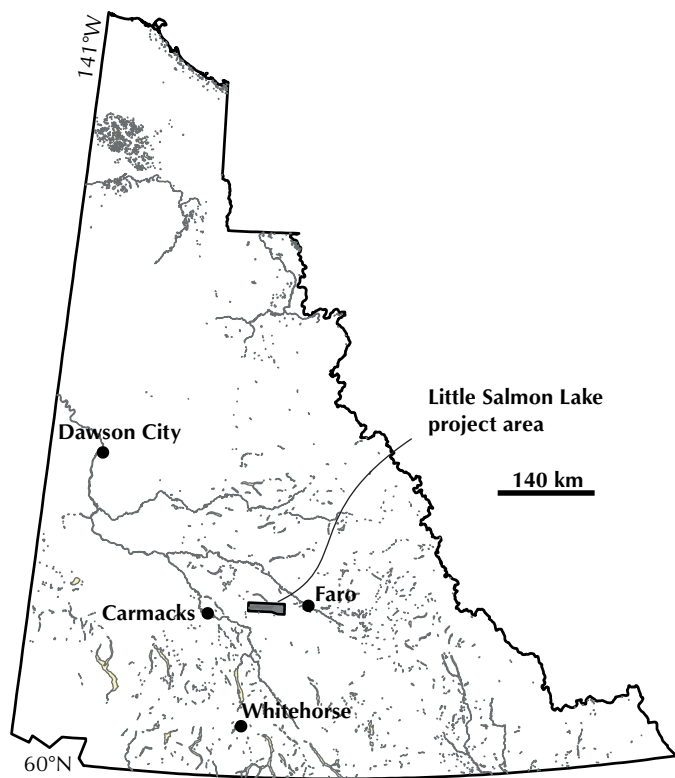


**Figure 1.** Map of the Yukon showing the Little Salmon Lake project area.

## BACKGROUND

### PHYSIOGRAPHY

The Little Salmon Lake valley primarily lies within the physiographic region of the Lewes Plateau, a part of the Yukon Plateaus. The Lewes Plateau region is a broad uplands area consisting of low, rolling hills and some mountain ranges (Ward and Jackson, 2000). The Little Salmon Lake area contains some of the highest peaks within the Lewes Plateau with elevations in the Big and Little Salmon ranges exceeding 1700 m. The northeast portion of the project area is adjacent to the Glenlyon Range, an extension of the Pelly Mountains.

The east-west corridor being studied consists of the Little Salmon Lake valley and the western portion of the Magundy River valley, where the river flows into Little Salmon Lake. The lake level is approximately 600 m above sea level (a.s.l.) and local relief is greater than 1000 m. The lake sits in a glacially scoured and over-deepened U-shaped valley that is approximately 33 km long and 2 km wide. The Magundy River valley consists of an approximately 2-km-wide floodplain bounded by the Glenlyon Range to the north and the Big Salmon Range to the south (Fig. 2).

### CLIMATE AND PERMAFROST

The study area is within the sub-arctic continental climate zone, which is characterized by long, cold winters, short, warm summers, low relative humidity and low to moderate precipitation. Table 1 shows climate data for the nearest meteorological stations in Faro and Carmacks. Climate in the Little Salmon Lake valley may be influenced by cold air drainage into the valley floor in winter as described by Burn (1994) for other Yukon valleys.

The Little Salmon Lake area is within the zone of sporadic discontinuous permafrost (Heginbottom et al., 1995). Primary controls on permafrost distribution include slope aspect, elevation, surficial material type and age, vegetation cover and drainage conditions. Local climatic

**Table 1.** Environment Canada mean climate data for the period 1971 to 2000.

Station	Daily mean air temperature (°C)			Mean precipitation (mm)		
	January	July	Annual	January	July	Annual
Faro	-21.5	15.0	-2.2	14.8	58.8	316
Carmacks	-24.9	15.4	-2.9	---	not available	---

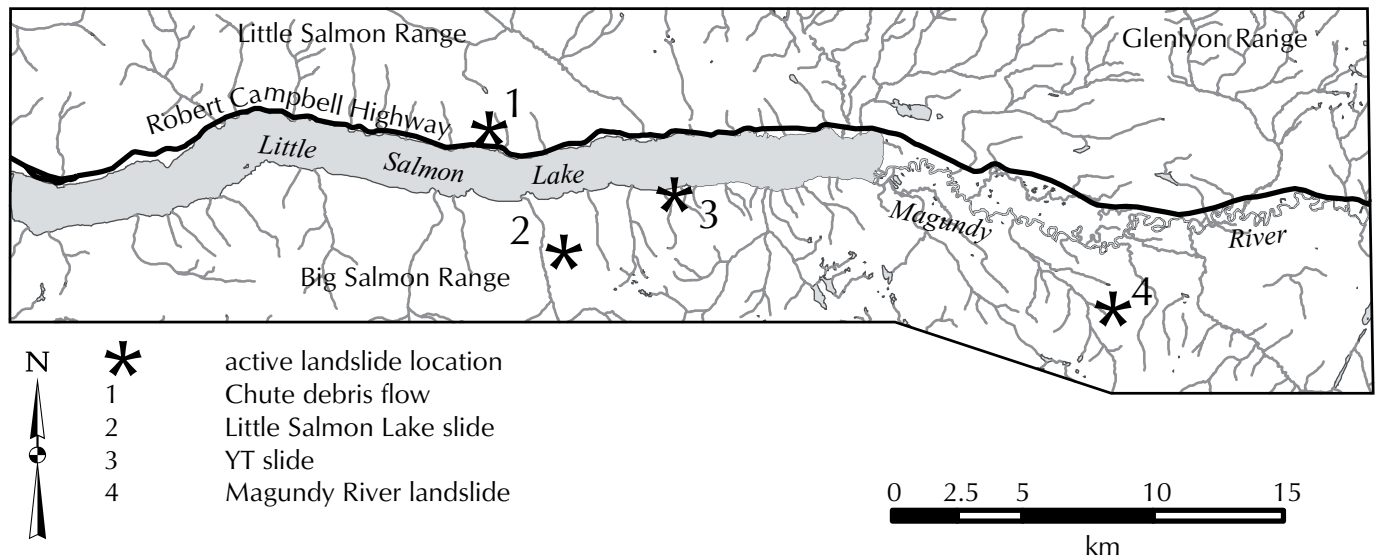


Figure 2. Map of the project area showing key physiographic features and active landslide locations.

effects such as snow depth variation and temperature inversions may also control permafrost distribution. In general, permafrost is thicker and more widespread on north-facing slopes where hill-slope shading, thick vegetative mats and poor drainage conditions exist.

**BEDROCK GEOLOGY**

The bedrock geology in the Little Salmon Lake area is complex, and includes displaced North American strata (Cassiar Terrane), pericratonic terrane (Yukon-Tanana Terrane), accreted terrane (Slide Mountain Terrane) and post-accretion strata. Reconnaissance geology was carried out by Campbell (1967). The area has since been re-interpreted and mapped at a larger scale as summarized by Colpron et al. (2003).

The western half of the project area is underlain by the Snowcap assemblage of the Yukon-Tanana Terrane. It is composed of Carboniferous volcanic arc successions, associated subvolcanic plutonic suites and pre-Mississippian metasedimentary basement rocks. This assemblage has been metamorphosed and intensely deformed. The area east of Little Salmon Lake is underlain by the Cambrian to Devonian Cassiar Terrane. The Cassiar Terrane consists of a lower phyllite-dominated unit and an overlying marble unit. The Slide Mountain Terrane, consisting of an obducted volcanic arc sequence, is present at the east end of Little Salmon Lake between the Cassiar and Yukon-Tanana terranes. Post-accretion strata

include a Cretaceous pluton near Little Salmon Lake’s western margin and the Glenlyon Batholith along the eastern boundary of the project area. Colpron et al. (2003) present details on the bedrock geology.

**SURFICIAL GEOLOGY**

Regional Quaternary mapping studies in the Glenlyon map area (105L) were undertaken by Ward and Jackson (2000). Their study built upon earlier reconnaissance mapping by Campbell (1967).

In the Glenlyon area, there is evidence for at least three glaciations: pre-Reid (Early Pleistocene), Reid (Middle Pleistocene) and McConnell (Late Wisconsinan). Exposures of pre-Reid and Reid glacial deposits are rare or absent in the project area. Sediments and landforms of the McConnell glaciation, which took place 26 000 to 10 000 years BP (Bond and Plouffe, 2003), are well preserved.

The Selwyn lobe of the Cordilleran Ice Sheet covered the Little Salmon Lake area during the McConnell event. This lobe, which originated in the Selwyn Mountains, flowed in a general northwest direction. Topography had a strong influence on controlling ice flow and many nunataks existed. Local alpine glaciers in the study area did not contribute significantly to the regional glaciation. Interpretation of stratigraphy reveals that during glacial advance, there was significant oscillation at the ice front. Glacial retreat was very rapid, with ice sheet down-



wasting and stagnation. Variable thicknesses of glacial till cover the valley sides and plateau summits. Mixed glaciofluvial, till and glaciolacustrine sediments are found in the valley bottoms. Post-glacial lacustrine, fluvial, organic and colluvial deposits of Holocene age are also common in the valley bottom. Ward and Jackson (2000) present further details on surficial geology.

## METHODOLOGY

The methodology being employed for this project is summarized as follows:

- Investigate published background information on permafrost- and non-permafrost-related landslide processes, periglacial processes, regional geology, and landslide assessment techniques;
- Perform a remote analysis of the project area by completing a terrain evaluation;
- Perform field-based ground-truthing in the project area. This includes assessment of the veracity of the results of the terrain evaluation exercise and further characterization of active landslide areas;
- Complete lab tests on soil samples collected during the field season to determine their engineering characteristics; and
- Investigate methods of modeling the natural processes at each landslide.

The terrain analysis was completed in the winter/spring of 2004 and is summarized below. Field work took place throughout the summer of 2004. Traverses by foot, boat and canoe were made to assess the terrain and investigate landslide locations. One day was also spent on a helicopter reconnaissance of the area. Lab testing and the modelling of natural processes are now being undertaken and are briefly described at the end of this paper (see Future Work).

## TERRAIN ANALYSIS

In order to identify the landslide processes in the project area, terrain analyses were undertaken. The evaluation was completed following the Terrain Classification System for British Columbia (Howes and Kenk, 1988).

Numerous sources of background data were used in the evaluation, and a brief discussion of the background data follows. All the background geospatial data was compiled in a geographic information system (GIS) database.

The majority of the project area was covered by recent (1998) airphotos at a 1:50 000 scale. Select 1989 airphotos (1:40 000) and airphotos from the 1940s (~1:40 000) as well as LandSat 7 imagery and digital geospatial data were used. Elevation models, slope models and aspect models were all used in the terrain evaluation.

Geological data at various scales were compiled. Regional reconnaissance mapping by Campbell (1967) produced both bedrock and surficial maps at a scale of 1:250 000. The bedrock geology was refined with 1:50 000-scale maps from a geological compilation for the Glenlyon area (NTS 105L) by Colpron et al. (2003). Ward and Jackson (2000) published a report and maps (1:100 000) of the surficial geology of the Glenlyon map area.

Background information on landslide processes in permafrost is summarized by Tart (1996), Lewkowicz (1988) and Harris (1987). However, there are very few case studies presented in these compilations dealing with slopes in the Yukon. Huscroft et al. (2004) summarize many of the landslide case studies in the southern Yukon. Ward et al. (1992) provide an excellent case study of the Surprise Rapids landslide along the South MacMillan River.

Using the data listed above, a 1:50 000-scale map was produced (R. Lyle, unpublished). The map shows the geographic distribution of terrain polygons and geomorphologic features. Identification of polygons is based on interpreted surficial material, texture, surface expression and geological processes. The evaluation revealed more than 35 areas of active or past landslide activity. The majority of the landslides were recognized based on their morphological signature and are mostly relict.

## ACTIVE LANDSLIDES

Four areas of prominent and active mass wasting were found in the Little Salmon Lake area. These four distinct landslide processes are summarized in this section. Observations include permafrost conditions, geological materials and slope conditions. Figure 2 shows the locations of the four slide areas.

This is possibly the first published report of any of the landslides described below. The names given for the landslides are as used in the field and have not been formally adopted.

## CHUTE DEBRIS FLOW

The Chute is a debris-flow area situated above the Robert Campbell Highway on the north side of Little Salmon Lake. A photo of the overall debris-flow track is presented in Figure 3. There is no evidence for the presence of permafrost in the area of this debris flow. The last major flow event at the Chute likely took place in 1996 (based on discussions with local residents).

Observations from the flow are grouped into initiation, transport and fan zones. The initiation zone headscarp is 1.5 to 2 m high at an angle of 35-45°. The surficial sediment is a polymicton containing angular clasts of local bedrock with sizes ranging from pebble to 25 cm or more. Finer material consists of sand and some silt. The sediments are wet to saturated with a couple of small streams flowing over and through them. One such stream was traced up slope to a spring. The headscarp is located at a slight break in slope with the area above having a gentler slope (15-25°). Morphological evidence from airphoto interpretation shows a relict talus cone in the source area.



**Figure 3.** Chute debris-flow track, looking north. The Robert Campbell Highway is the clearing at bottom of the photo.

The transport zone is an 8- to 15-m-wide track free of vegetation (Fig. 4). A small stream cuts through the middle creating a gully up to 2.5 m deep through the flow mass. The slope is moderately steep (25-35°) in this zone. The transport zone, which extends from the headscarp to the fan, is approximately 450 m long. The sediments, as shown in the stream-cut sections, are nearly identical to those seen in the headscarp. No structure or sediment gradation trends were observed.

The fan zone begins with a slope change to a gentle to moderate slope (10 to 20°). A large pile of woody debris, including logs over 35 cm in diameter, marks this area. Below this, the cleared track disappears and there are few fallen trees. Large amounts of angular clasts of quartzite, marble and schist are found in accumulations on the upslope side of trees. As the flow reached the cleared electrical transmission right-of-way, it downcut a channel up to 2 m deep in the existing sediments. The channel continues until it reaches a highway cut of the Robert Campbell Highway, where the ditch filled with sediment.



**Figure 4.** Chute debris-flow track, looking north.



The soil structure and texture provides evidence that the Chute represents a reoccurring debris-flow track. Trees in the transport and fan zones show multiple phases of damage that support this theory.

### LITTLE SALMON LAKE SLIDE

The Little Salmon Lake (LSL) slide (Fig. 5) sits high above the south shore of the lake. It is a deep-seated rotational/translational slide in psammitic schist and quartzite bedrock. The date of initiation is unknown; however, there has been significant movement in the six years since the last airphoto coverage.

The LSL slide headscarp sits at an elevation of about 1150 m a.s.l. or about 550 m above Little Salmon Lake. The maximum width of rupture surface is approximately 350 m and the total length is estimated to be greater than 800 m. The slide occurs on a moderate slope (15° to 25°). The height of the headscarp varies from 10 to 50 m.

Field time at this slide was limited due to poor accessibility and safety concerns. Numerous small rock falls occurred during inspection of the headscarp.



**Figure 5.** Little Salmon Lake slide, looking south

Dimensions of fallen blocks ranged from a few centimetres to 2 m.

The following key observations were noted. There is an older, relict landslide near the summit of the mountain immediately above the LSL slide. Bedrock in the area consists of the early Mississippian and older (?) Snowcap assemblage (Colpron et al., 2003). Foliated quartzite and psammitic schist were found at the LSL slide. Graphitic layering was found in talus at the base of the headscarp.

### YT SLIDE

The YT slide was discovered during the work carried out on this project. The slide appears to be very similar to the multiple retrogressive slumps described by Morgenstern and McRoberts (1974) and Dyke (2004). However, the soil types and their distribution vary greatly from those described for the Mackenzie Valley. Multiple retrogressive slumps are characterized by 'a series of arcuate, concave-toward-the-toe blocks that step upward toward the headscarp' (Lewkowicz, 1988; Fig. 6).

The landslide is described as being primarily rotational, with a slope that bulges out into the lake. Material at the lake margin is very ice-rich (Fig. 7) and is quickly thermally eroded by the lake water. Undercutting of the ice-rich material that has bulged initiates the toppling of large blocks of frozen sediment into the lake. Melting of ice above lake level also enables sediment to fall or flow into the lake. A large frozen block (estimated to be 1200 m<sup>3</sup>) was seen toppling from the slope in August, 2004. The block remained coherent and rolled out into the lake approximately 40 m before disappearing.

The stratigraphy is well exposed in the numerous scarps and extensional cracks at the YT slide. The entire north-facing slope is underlain by varying thicknesses of permafrost and is covered with up to 0.5 m of organic material, a colluvial veneer, and a thin layer of volcanic ash (White River tephra). The stratigraphy exposed in the scarps is as follows: the top scarp exposes the edge of a very gently sloping till plain (over 12 m thick). This is underlain by a >20-m-thick ice-contact sequence of dense glaciofluvial (apparently unfrozen) (Fig. 8) and frozen glaciolacustrine sediments containing millimetre-scale ice lenses. Underlying the McConnell ice-proximal sequence is a monolithological diamicton interpreted to be a pre-glacial debris flow or colluvial apron dated at >47 000 years BP (Beta-197221). Many massive ice lenses were found in this unit (Fig. 9). Clasts found in the diamicton are composed of poorly sorted, angular





**Figure 6.** YT slide, looking south. Little Salmon Lake is at bottom of photo. The top scarp is 350 m wide.



**Figure 7.** Massive ice exposure in the lower levels of the YT slide.



**Figure 8.** Glaciofluvial sediments in the main scarp of the YT slide.





**Figure 9.** Massive ice in the old colluvial unit, YT slide.

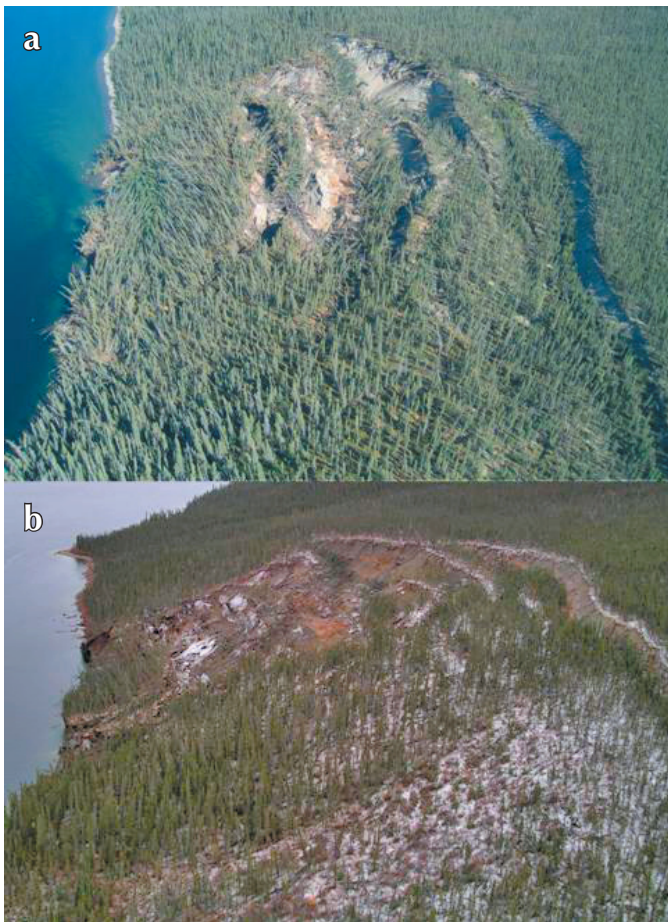


**Figure 10.** Photos showing the movement over nearly a two-month period at the YT slide: (a) August 4, 2004 and (b) September 28, 2004 (photo by Panya Lipovsky).

psammitic schist and/or quartzite (local bedrock). The sediment exposed at the lake margin is a colluvial mass derived from the described stratigraphy. It contains greater than 50% ice by volume, much of which is in massive ice lenses (Fig. 7).

A comparison of photographs taken in late September 2004 (P. Lipovsky, pers. comm., 2004) with others taken in August, 2004 (Fig. 10) shows there has been constant and considerable movement of the lowest sliding block of the YT slide during this time.

### MAGUNDY RIVER LANDSLIDE

The Magundy River landslide (Fig. 11) was first noted by Jeff Bond (pers. comm., 2003) of the Yukon Geological Survey in 1998. Based on discussions with local residents, the slide was probably initiated in 1996. It is a large, complex example of a landslide similar to the bimodal flows described by McRoberts and Morgenstern (1974), and Ward et al. (1992). The term bimodal flow is used as the slide can be divided into two distinct morphological sectors: 1) an upper headscarp, where ablation and erosion release sediment, which slides, flows or falls down into 2) a gently inclined mudflow lobe, where it flows away (Harris, 1987).

The Magundy River landslide is set on a gentle to moderate (10-20°) north-facing slope approximately 10 km east of Little Salmon Lake. Material from a source area (approximately 350 by 400 m) has flowed down the slope. The debris flow has eroded two substantial channels, each having a distinct depositional area (Fig. 11).

There are two main surficial geology units found in the slide area. A colluvial layer of variable thickness overlies a denser glacial diamicton (till). Both units have a similar texture and contain large boulders. The colluvium consists of reworked till, and is very thin or absent in some areas. Multiple organic horizons separated by diamicton layers were found in one active scarp, suggesting previous debris-flow activity. In addition, buried upright tree stumps were found in an upper scarp.

The source area is rimmed by active and inactive scarps. The east-facing inactive scarps primarily sit at the angle of repose of till, and vegetation is slowly taking hold. During the summer of 2004, three areas of active thaw slumping were found. The active areas are located on south- and west-facing slopes. Scarps in these areas are very steep – from 40° to near-vertical – commonly with an overhanging organic mat. The active scarps range from approximately 5 to 10 m in height (Fig. 12). Massive ice





**Figure 11.** Overview of the Magundy River landslide, looking south. The top scarp is approximately 350 m wide.

was found in all of the active areas, and presumably provides the necessary moisture to form the debris flows. Close-up study of the ice structure was hampered by problems associated with thaw and accessibility.

The debris has flowed in two general directions. The first is into a small valley to the northwest. Here a small lake was completely infilled with sediment. The second flow path is to the northeast; this channel opened up between 1998 and 2002, and takes the debris to the Magundy River floodplain, nearly 400 m below the top of the slide. A large fan has developed on the floodplain and a small creek has moved limited amounts of sediment to the Magundy River. Currently, the dominant flow is to the northeast, while the northwest valley is mostly inactive.

The debris flows contain the complete range of grain sizes found in the till and colluvial materials, as well as the organic mat and trees that have fallen to the base of the active scarps. Most of the flow witnessed was very viscous. However, very wet, rapid surging flows were noted one day at a single location. Primary controls on the debris-flow rheology likely include moisture availability, clay content and clay mineralogy. Examples of viscous flow paths are shown in Figure 13. Flow and texture patterns on the most viscous flows were very similar to some lava flows with ropey and popcorn textures.



**Figure 12.** Active scarp, Magundy River landslide, looking northeast.





**Figure 13.** (a) Active and (b) inactive flow paths, Magundy River landslide.

## SUMMARY AND DISCUSSION

Four separate landslide processes at work in the Little Salmon Lake area have been described. Three of these processes involve unconsolidated sediments, with two of these involving the degradation of permafrost. The fourth slide is a deep rotational failure in bedrock. A variety of factors thought to be contributing to instability are summarized below.

The Chute, though dormant, appears to be a reoccurring debris-flow track. It is likely activated by extreme moisture

conditions such as rapid snowmelt and/or intense rainfall. Seismic activity may also play a role in initiating the flow.

The Little Salmon Lake slide is an active rock slide that illustrates the potential of failure in rock slopes at a moderate angle. Factors such as rock structure and melting ground-ice may be important controls. Graphitic layering in the schist was the weakest rock structure found in the brief investigation of this slide.

The active YT and Magundy River slides involve the degradation of permafrost, though each in their own distinctive manner. It is difficult to compare these slides to slides reported elsewhere. Lewkowicz (1988) concludes that field studies of rapid mass movements in permafrost are problematic due to their episodic and spatially discontinuous nature.

Bimodal flows, such as the Magundy River slide, are most commonly associated with fine-grained (lacustrine) sediments and thermokarst terrain in valley bottom settings (Ward et al., 1992). Furthermore, multiple retrogressive slumps are generally associated with lacustrine sediments (Dyke, 2004). No evidence of widespread lacustrine sediments has been found in any exposures at slides studied in this project. It is possible that there are glaciolacustrine clays at depth in the YT slide. Nevertheless, the Little Salmon Lake area shows that landslide processes in permafrost need not include any widespread lacustrine deposits.

The impact of climate change on permafrost slopes is an issue drawing significant attention today (Dyke and Brooks, 2000; Huscroft et al., 2004). Triggering events for many of the landslides noted are likely in response to changing climatic conditions. Huscroft et al. (2004, p. 118) concluded that determining how global atmospheric conditions will impact site-specific slope stability requires “transcendence of multiple levels of uncertainty and complexity” and will therefore be qualitative. However, the impact of changing climate must be looked at when completing any slope stability assessment in warming discontinuous permafrost.

Dynamic loading is widely regarded as an important triggering factor in landslides throughout the world. However, there is very little published research on the impacts of seismicity on slopes containing permafrost. Dynamic loading may be an important factor in the Little Salmon Lake area as numerous small earthquakes have been recorded in the area. As recently as 2002, an earthquake was recorded approximately 70 km west of

the Magundy River slide with a Richter magnitude of 4.6\*. Davis (2001) discusses the spectacular effects of earthquakes in discontinuous permafrost in Alaska including one bimodal flow. However, the seismic loading in the discussed region of Alaska is much higher than at Little Salmon Lake.

This project illustrates the difficulty of locating and predicting landslide risk in areas of discontinuous permafrost. At present, all human activity and infrastructure in the project area avoids north-facing slopes that may be susceptible to permafrost degradation. However, hazards not related to permafrost, such as the Chute slide, are equally as important and must be considered prior to any development in the region.

## FUTURE WORK

The laboratory testing of samples obtained in the summer of 2004 is on-going. Lab testing for the project includes basic soil index testing: grain-size analysis, Atterberg limits and moisture content, as well as clay mineralogy determination using x-ray diffraction.

An investigation of methods of modeling the natural processes at each landslide is underway. One such natural process is climatic triggering events. Daily climate data from Environment Canada will be used to try to correlate climatic conditions with triggering events. As mentioned previously, seismic loading may play a role in the landslide processes and this will be investigated.

## ACKNOWLEDGEMENTS

Results presented in this paper are from field work completed during the summer of 2004. This study is part of an M.Sc.E. thesis of the first author at Queen's University. Funding for the project was provided by the following sources: the Yukon Geological Survey (YGS); Department of Indian Affairs and Northern Development (DIAND) Knowledge and Innovation Fund; a National Science and Engineering Research Council (NSERC) Northern Supplement to R.R. Lyle; a Geomatics for Informed Decisions (GEOIDE) grant to D.J. Hutchinson; and the Northern Scientific Training Program (NSTP).

The field work could not have been completed without the support and assistance of Glenda and Wolfgang Eberlein, the staff at the Drury Creek Highway

Maintenance Camp, Peter Lickes at Salmon Lake Adventures, Jason Berkers and Richard Trimble of EBA Engineering, as well as Monique Raitchey and Maurice Colpron at the YGS. Safe and efficient helicopter travel was courtesy of Brian Parsons at TransNorth Helicopters. Dr. Alan Gorman and Robin Harrap at Queen's University have been helpful throughout the project especially in airphoto interpretation and GIS, respectively. Most importantly, the project has been greatly improved by discussions with Crystal Huscroft (Thompson Rivers University), Panya Lipovsky (YGS) and Jeffrey Bond (YGS). Careful review by Jeffrey Bond has enhanced this manuscript, and his time and efforts are very much appreciated.

## REFERENCES

- Bond, J.D. and Plouffe, A., 2003. Yukon Targeted Geoscience Initiative, Part 2: Glacial history, till geochemistry and new mineral exploration targets in Glenlyon and eastern Carmacks map areas, central Yukon. *In: Yukon Exploration and Geology 2002*, D.S. Emond and L.L. Lewis (eds.), Exploration and Geological Services Division, Yukon Region, Indian and Northern Affairs Canada, p. 109-134.
- Burn, C.R., 1994. Permafrost, tectonics, and past and future regional climate change, Yukon and adjacent Northwest Territories. *Canadian Journal of Earth Sciences*, vol. 31, p. 182-191.
- Campbell, R.B., 1967. Reconnaissance Geology of Glenlyon Map-Area, Yukon Territory. Geological Survey of Canada, Memoir 352, 92 p.
- Colpron, M., Bond, J.D., Lipovsky, P.S., Gladwin, K., Gordey, S.P., Murphy, D.C., Nelson, J.L., Plouffe, A., Roots, C.F. and Abbott, J.G., 2003. Digital compilation of bedrock geology and till geochemistry, Glenlyon (105 L) and eastern Carmacks (115 I) map areas, Yukon Territory. Geological Survey of Canada, Open File 1561; and Exploration and Geological Services Division, Yukon Region, Indian and Northern Affairs Canada, Open File 2003-7D, CD-ROM.
- Davis, N., 2001. Permafrost: A Guide to Frozen Ground in Transition. University of Alaska Press, Anchorage, Alaska, 351 p.

\*<http://www.pgc.nrcan.gc.ca/seismo/recent/eqmaps.html>. Unpublished Geological Survey of Canada data.

- Dyke, L.D., 2004. Stability of Frozen and Thawing Slopes in the Mackenzie Valley, Northwest Territories. *In: Proceedings of the 57th Canadian Geotechnical Conference, Quebec City, Quebec, Session 1G*, p. 31-38.
- Dyke, L.D. and Brooks, G.R. (eds), 2000. The Physical Environment of the Mackenzie Valley, Northwest Territories: A Base Line for the Assessment of Environmental Change. Geological Survey of Canada, Bulletin 547, 212 p.
- Harris, C., 1987, Mechanisms of mass movement in periglacial environments. *In: Slope Stability: Geotechnical Engineering and Geomorphology*, M.G. Anderson and K.S. Richards (eds.), John Wiley and Sons Ltd., Chichester, UK, p. 531-559.
- Heginbottom, J.A., Dubreuil, M.A. and Harker, P.A., 1995. Canada – Permafrost. *In: National Atlas of Canada*, 5th ed., Natural Resources Canada, Ottawa, Plate 2.1: MCR 4177.
- Howes, D. and Kenk E., 1988. Terrain Classification System for British Columbia (revised Edition), British Columbia Ministry of Environment, Manual 10, 90 p.
- Huscroft, C.A., Lipovsky, P. and Bond, J.D., 2004. Permafrost and landslide activity: Case studies from southwestern Yukon Territory. *In: Yukon Exploration and Geology 2003*, D.S. Emond and L.L. Lewis (eds.), Yukon Geological Survey, p. 107-119.
- Lewkowicz, A.G., 1988. Slope Processes. *In: Advances in Periglacial Geomorphology*, M.J. Clark (ed.), John Wiley and Sons Ltd., Chichester, UK, p. 325-360.
- McRoberts, E.C. and Morgenstern, N.R., 1974. Stability of Slopes in Frozen Soil, Mackenzie Valley, N.W.T. *Canadian Geotechnical Journal*, vol. 11, p. 554-573.
- Tart, R.G., 1996. Permafrost. *In: Landslides: Investigation and Mitigation*, A.K. Turner and R.L. Schuster (eds.), Transportation Research Board Special Report 247, p. 620-645.
- Ward, B. and Jackson, L.E. Jr., 2000. Surficial Geology of the Glenlyon Map Area, Yukon Territory. Geological Survey of Canada, Bulletin 559, 60 p.
- Ward, B., Jackson, L.E. Jr. and Savigny, K.W., 1992. Evolution of Surprise Rapids landslide, Yukon Territory. Geological Survey of Canada, Paper 90-18, 25 p.



# Application of placer and lode gold geochemistry to gold exploration in western Yukon

**Jim K. Mortensen**

*Earth and Ocean Sciences, University of British Columbia<sup>1</sup>*

**Rob Chapman**

*School of Earth Sciences, University of Leeds<sup>2</sup>*

**William LeBarge**

*Yukon Geological Survey<sup>3</sup>*

**Lionel Jackson**

*Geological Survey of Canada<sup>4</sup>*

Mortensen, J.K., Chapman, R., LeBarge, W. and Jackson, L., 2005. Application of placer and lode gold geochemistry to gold exploration in western Yukon. *In: Yukon Exploration and Geology 2004*, D.S. Emond, L.L. Lewis and G.D. Bradshaw (eds.), Yukon Geological Survey, p. 205-212.

## ABSTRACT

Placer gold is widely distributed throughout the western Yukon; however, lode sources for most of these deposits remain unknown. Previous studies of gold compositions in this region using scanning electron microscope (SEM) and electron microprobe (EMP) methods showed 1) that there are consistent differences in average composition (although with considerable overlap) between gold from different styles of lode gold mineralization; and 2) the composition(s) of placer gold can be matched with specific lode sources, or the most likely style of lode source can be identified. In the current study we employ SEM and EMP methods together with laser ablation ICP-MS trace element analysis and study of the micro-inclusion suite(s) to more completely characterize the major, minor and trace element composition of the gold as well as the mineralogy of the lode sources themselves. We also report new data for placer and lode gold, mainly from the Klondike District.

## RÉSUMÉ

L'or placérien est largement répandu dans l'ouest du Yukon; les sources filoniennes de la plupart de ces gisements demeurent cependant inconnues. Des études antérieures de l'or de cette région à l'aide des méthodes d'analyse par microscopie électronique à balayage (MEB) et par microsonde électronique ont démontré 1) qu'il existe des différences cohérentes moyennes (malgré des recouvrements considérables) entre l'or de différents styles de minéralisation filonienne et 2) que l'or placérien peut être apparié à des sources filoniennes spécifiques ou que le style le plus probable de la source filonienne peut être identifié. Dans la présente étude, on utilise les méthodes d'analyse par MEB et par microsonde électronique combinées avec l'analyse d'éléments traces par ICP-MS à ablation par laser et avec l'étude de la ou des suites de micro-inclusions, afin de caractériser de manière plus complète la composition en éléments majeurs, mineurs et traces ainsi que la minéralogie des sources filoniennes elles-mêmes. De nouvelles données sur l'or placérien et filonien du district du Klondike sont signalées dans le présent document.

<sup>1</sup>6339 Stores Road, Vancouver, British Columbia, Canada V6T 1Z4, [jmortensen@eos.ubc.ca](mailto:jmortensen@eos.ubc.ca)

<sup>2</sup>United Kingdom

<sup>3</sup>Whitehorse, Yukon, [bill.lebarge@gov.yk.ca](mailto:bill.lebarge@gov.yk.ca)

<sup>4</sup>Vancouver, British Columbia

## INTRODUCTION

Western Yukon hosts very widespread occurrences of placer gold, including the well-known deposits of the Klondike, Sixtymile and lower Fortymile districts. The lode (bedrock) source(s) from which most of these deposits were derived, however, remains largely unknown. This is due to several factors. Most importantly, much of the western Yukon escaped glaciation, and although this undoubtedly played a major role in the development and preservation of the placer deposits, it also resulted in very limited bedrock exposure (<1% in most areas), and consequently, a somewhat fragmentary understanding of the bedrock geology of the region. In addition, the area experienced deep surface weathering during the Paleogene and the geochemical signature of underlying mineralization in soils and silts is commonly relatively subdued on regional geochemical surveys. Exploration has identified a wide range of styles and ages of lode gold mineralization in western Yukon, but very few detailed mineral deposit studies have been carried out thus far.

The western Yukon lies in the central portion of the Tintina Gold Province (TGP; e.g., Hart et al., 2002), and some of the exploration within the TGP over the last decade has focused on this area, in part because of the presence of the placer gold deposits. Gold is widely distributed in soils and silts in the region in addition to the placer deposits themselves. Exploration has been greatly hampered, however, by the lack of detailed bedrock geology maps for the area and an inadequate understanding of what types of lode targets are present. The presence of widely distributed and commonly very

rich deposits of placer gold suggests that the potential for economically important lode sources certainly exists.

One approach to assessing the significance of placer gold deposits in western Yukon, with respect to the potential for economically important lode deposits, is to examine the composition and morphology of the placer gold in various areas and attempt to determine what style(s) of lode source(s) it was derived from. Two studies of this type have previously been carried out in the western Yukon. In this study we expand on the previous work and apply new analytical approaches to a much more comprehensive suite of placer and lode gold samples from throughout the region.

## LODE GOLD MINERALIZATION IN WESTERN YUKON

There is a very broad range of styles and ages of lode mineralization in western Yukon that are known, or inferred, to contain gold of sufficiently coarse grain size to have potentially been concentrated into placer deposits (Table 1). Based on our current knowledge of the regional geology and types of mineral deposits present in western Yukon, however, only some of these deposit types (shown in bold in Table 1) are considered to have any realistic potential of forming a deposit of economic size and grade. From an exploration point of view, it would be very valuable to be able to filter out gold geochemical anomalies (including placer gold deposits) that were derived from deposit types that are less likely to have significant economic potential.

**Table 1.** Styles/ages of lode occurrences and occurrences containing gold in western Yukon. Bold type indicates deposit types that could form an economic deposit in western Yukon.

Deposit/occurrence type	Age	Examples (occurrences and/or areas)
<b>Epithermal vein</b>	<b>Mid-Cretaceous</b>	<b>Mt. Nansen area</b>
<b>Epithermal vein</b>	<b>Late Cretaceous</b>	<b>Sixtymile area, Eureka Dome</b>
Epithermal vein	Early Paleogene	Germaine Creek (Dawson map area)
<b>Intrusion-related vein</b>	<b>Mid-Cretaceous</b>	<b>Moosehorn Range, central Dawson Range</b>
Intrusion-related vein	Late Cretaceous	Mosquito Gulch area (NW Stewart River map area)
Intrusion-related vein	Early Jurassic?	Tenmile Creek area (central Stewart River map area)
Gold-bearing skarn	Late Cretaceous	south side of Sixtymile River
<b>Gold-bearing porphyry</b>	<b>Early Jurassic</b>	<b>Minto, Williams Creek (Carmacks Copper)</b>
<b>Intrusion-related vein</b>	<b>Late Cretaceous</b>	<b>Casino</b>
<b>Metamorphogenic (orogenic) vein</b>	<b>Early or Middle Jurassic</b>	<b>Klondike</b>
"Listwanite-type" veins	Jurassic?	Atlin, Sixtymile?
Gold-enriched VMS	Permian	Lone Star, Bronson, Baldy (in Klondike Schist)

## PREVIOUS GOLD COMPOSITIONAL STUDIES IN WESTERN YUKON

Two previous studies investigated the composition (and morphology) of placer and lode gold in the western Yukon. Knight et al. (1999a,b) carried out a very detailed study of gold from both placer deposits and known gold-bearing metamorphogenic vein occurrences in the Klondike District. They employed scanning electron microscope (SEM) and electron microprobe (EMP) methods to characterize the compositional ranges of gold from various lode occurrences throughout the Klondike District, as well as the compositions of unleached cores and leached rims on placer gold particles from most of the placer streams in the district. Placer gold frequently exhibits a gold-enriched rind or rim, typically 1 to 20 microns in thickness, surrounding a core. Compositional studies relating placer to lode gold typically investigate the core composition, as this has been shown to be faithful to gold grains liberated from the hypogene source (e.g., Herail et al., 1990; Loen, 1994; Lange and Gignoux, 1999). In addition to this compositional data, the shapes of the placer grains were documented and the relationship between grain shape (especially flatness and roundness) vs. inferred transport distance was evaluated. The study by Knight et al. (1999a,b) identified several discrete source areas for compositionally distinct placer gold in the Klondike. Dumula and Mortensen (2002) carried out a regional study which examined the composition of placer gold and potential lode sources from several localities in the central and southern Stewart River map area. The main conclusions that resulted from the Knight et al. (1999a,b) and Dumula and Mortensen (2002) studies include:

- There are consistent and measurable differences in average composition (although with considerable overlap) between gold from different styles of lode gold and from specific occurrences;
- The shape of placer gold grains (flatness, roundness, etc.) changes in a consistent manner with increasing distance traveled;
- In some instances the composition(s) of placer gold can be matched with specific lode source(s), or at least the most likely style of lode source can be identified.

Two limitations of the previous studies are that only major and minor element (i.e., gold, silver, copper and mercury) concentrations could be measured using EMP methods, and there were relatively limited sample suites from a

small number of areas. Importantly, Knight et al. (1999a,b) analysed a large number of grains, and thereby generated data that define the degree of internal variation within alloy composition from a particular source.

## ANALYTICAL APPROACH

Our aim is to employ several different analytical methods to develop as unique a compositional signature as possible for placer and lode samples from western Yukon. We will use four main analytical approaches in this study:

- document the micro-inclusion suite within the placer (and lode) gold grains;
- determine, using electron microprobe (EMP) methods, the major and minor element composition of lode gold itself and unleached cores of placer grains;
- determine, using laser ablation ICP-MS, the trace and ultra-trace element composition of the grains; and
- examine the shape of placer gold grains using scanning electron microscope (SEM) methods to estimate how far the individual grains have traveled from their bedrock source.

Some of the advantages and potential problems with each of these methods are discussed below; however, we believe that this coordinated approach to gold characterization is the most appropriate method for addressing the historically intractable problem of sourcing placer gold in the western Yukon.

## MICRO-INCLUSION SUITES

This approach has not previously been employed to any significant extent in the Yukon, although it has been used to establish a specific “signature” for placer gold in other districts (e.g., Chapman et al., 2000). Micro-inclusions contained within placer gold grains should provide a sampling (albeit not necessarily a complete representation) of the ore and gangue mineralogy of the lode source from which it was derived. In some cases this should provide a unique signature for specific deposit types – e.g., inclusions of enargite might be taken to indicate that the gold was most likely derived from a high-sulphidation epithermal deposit. In other cases, an unusual mineral may be common and hence diagnostic of a specific mineralizing event. For example, argentite inclusions are present in mesothermal gold from Walhalla goldfield, Victoria, Australia. Most common mineral inclusions (e.g., pyrite, galena, sphalerite, arsenopyrite),



however, are not unique to a particular deposit type. Despite this, with a large sample size, the relative proportions of mineral inclusions within gold grains that belong to the specific mineral classes (e.g., sulphides, sulpharsenides, tellurides and sulphosalts) can provide useful information for comparative studies (e.g., Leake et al., 1997; Chapman et al., 2000). Potential problems associated with this approach are that inclusions are not always initially present in the gold, and inclusions tend to become less abundant the farther a placer grain has traveled (likely due to hammering and/or alteration during transport and subsequent residence in the surficial environment).

### MAJOR AND MINOR ELEMENT COMPOSITION

A considerable amount of EMP compositional data exists for gold from many different styles and ages of lode gold from around the world. This provides a template against which to compare compositions of the unleached cores of placer gold grains. Limitations of the technique are: (1) only a relatively small number of elements are commonly present in naturally occurring gold at sufficient concentrations to be measurable by EMP methods (gold, silver, copper and mercury, rarely bismuth and tellurium); (2) the compositional data for gold from different deposit types are generally not unique; and (3) a large sample size is commonly required to adequately characterize the alloy composition of gold from a single mineralizing event. This third limitation is particularly relevant when a population of placer gold grains represents more than one bedrock source.

### TRACE ELEMENT COMPOSITION

Laser ablation ICP-MS (LA-ICP-MS) analyses of samples of lode and placer gold (e.g., J. Youngson, pers. comm., 2004) shows that measurable amounts of many elements (e.g., molybdenum, bismuth, tellurium, antimony, tin, etc.) are present at detectable and highly variable levels in gold from different styles of lode mineralization. This provides a much greater range of elements to use as a geochemical fingerprint for gold than is offered by EMP methods alone. To date, very little LA-ICP-MS compositional data is available for gold, therefore there are limited compositional data with which to compare the initial results from the western Yukon samples.

### GRAIN SHAPE

Knight et al. (1999b) used measured shape data, especially grain flatness and roundness, for placer gold

grains from the Klondike District to generate shape vs. transport distance curves (e.g., Fig. 4 in Knight et al., 1999b). Their data suggested that gold grains transported in streams flatten rapidly within the first 2 to 3 km of transport from source and then flatten at a slower but relatively constant rate with increasing transport distance. There are several considerations that must be kept in mind when constructing such a model curve. First, an estimate of the distance a particular placer grain has been transported assumes that the location of the source is accurately known. Secondly, at least some lode gold grains in the Klondike initially form relatively flat, rather than rough or equant, morphologies. Thirdly, there is undoubtedly some amount of "armouring" of gold particles during transport. The probable source of all or most of the Klondike placer deposits is considered to be gold-bearing quartz veins (Knight et al., 1999a). In this style of mineralization, gold grains commonly occur within grains or grain aggregates of pyrite or as free grains enclosed by quartz, and many such grains may have initially been encapsulated in quartz or pyrite and not liberated from their mineral host until some time after transport began. The flatness vs. transport distance curve developed by Knight et al. (1999b) is based on a very large number of grain measurements, and should be adequate to derive at least a first-order estimate of transport distance for placer gold grains, not only in the Klondike itself, but also in other parts of western Yukon that are unglaciated and shared the same general history of climate and landscape evolution.

Townley et al. (2003) also investigated the relationship between gold grain shape and transport distance in several localities in central Chile and developed several generic criteria indicative of transport distance.

### INITIAL RESULTS

As a starting point for this study, we examined a number of samples of lode and placer gold from the Klondike District. Figure 1 shows locations of the main lode occurrences in the Klondike, and also shows the three main inferred "high fineness" and two inferred "low fineness" source areas as identified by Knight et al. (1999a). Our EMP analyses for the lode gold samples from five of the main lode occurrences are plotted as cumulative percentile plot for silver (Ag) in Figure 2a. Our results generally confirm the compositional ranges described by Knight et al. (1999a). Several features are evident from the data.

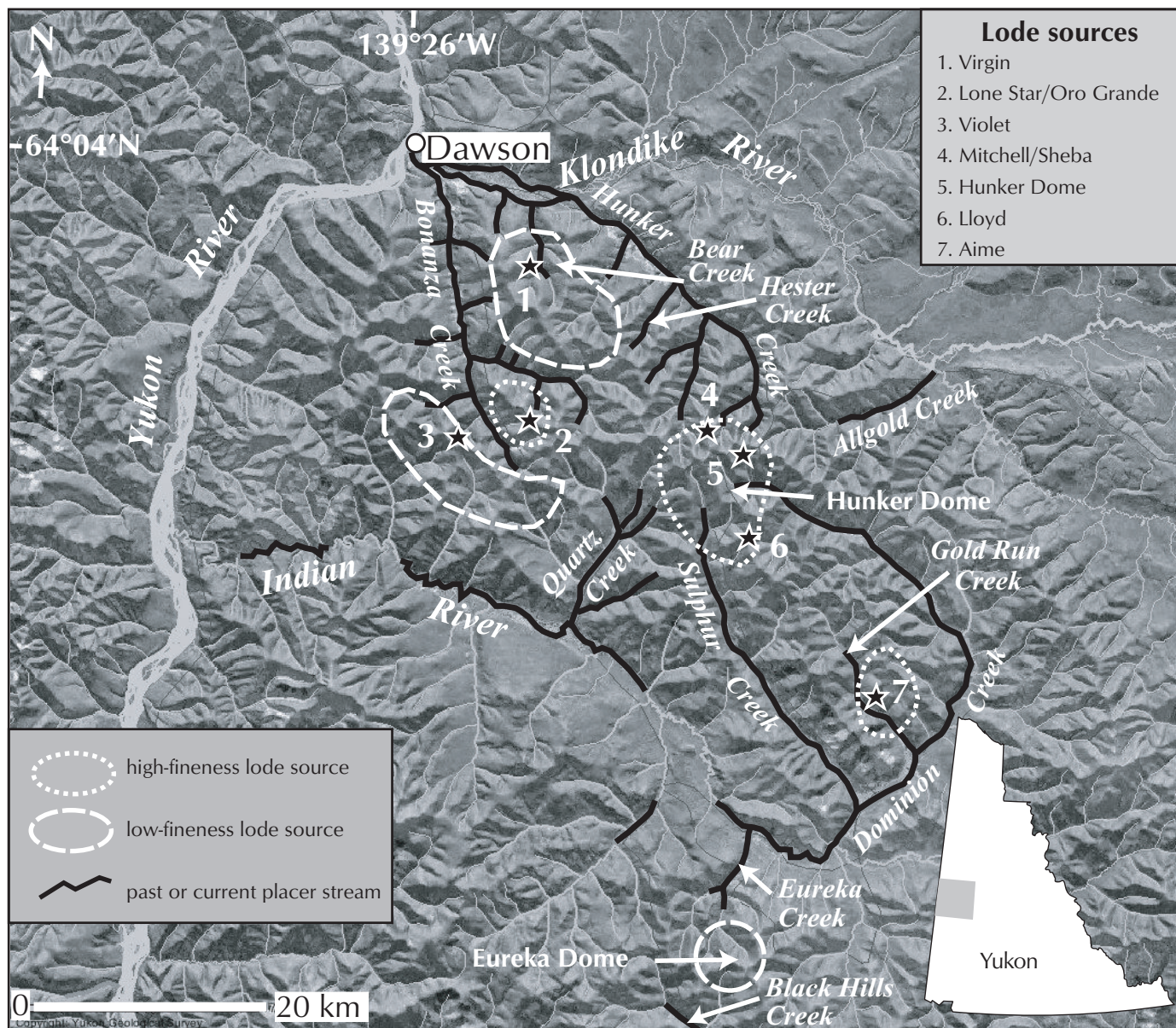


**Figure 1.** Shaded relief map of the Klondike District and surrounding areas showing the main placer streams. Also shown are the main lode gold occurrences as well as inferred low fineness and high fineness gold source areas as determined by Knight et al. (1999a) and Dumula and Mortensen (2002).

First, most of the lode gold samples from throughout the Klondike fall within the same relatively narrow range of silver contents (~13 to 20 wt.% Ag, or roughly 800 to 870 fineness). Gold from the Hunker Dome occurrence consists of two distinct populations in terms of silver content, one at ~14 to 15 wt.% Ag and one at ~17 to 20 wt.% Ag (Fig. 2a). Gold from the Virgin occurrence on Bear Creek (Fig. 1) is distinct by containing much higher silver contents (~28 to 32 wt.% Ag; Fig. 2a). Second, on a cumulative percentile plot for mercury (Hg) content of

Klondike lode gold (Fig. 2b), data from most of the occurrences are similar to those shown for the Hunker Dome lode, with most analyses containing mercury levels below the detection limit of the EMP method, except for a relatively small proportion of grains with up to 0.2 wt.% Hg. This contrasts with gold from the Virgin occurrence, nearly all of which contains detectable amounts of mercury and in some cases up to several weight percent. Finally, gold compositions from the Mitchell vein occurrence are indistinguishable from the



compositions of gold from samples of gold-bearing altered schist wall rocks to the vein. Gold in the wall rocks occurs within narrow (up to 40 cm in width) zones of strong bleaching, sericitization and pyritization (e.g., Mortensen et al., 1992). Gold in this altered schist mainly

occurs within secondary pyrite that replaces original porphyroblasts of magnetite.

In Figure 3, silver and mercury contents of placer gold recovered from middle Bonanza Creek, lower Hunker Creek, Bear Creek and Hester Creek are plotted together with lode gold from the Hunker Dome and Virgin lode

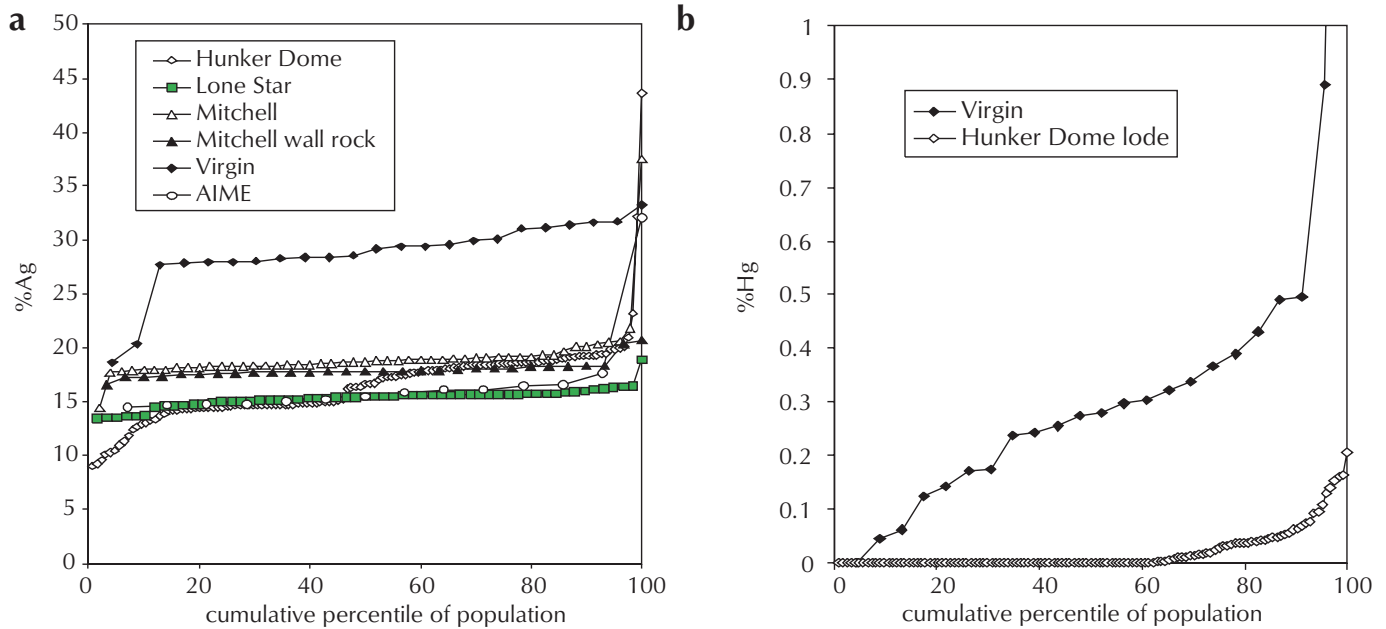


Figure 2. Cumulative percentile plots for silver and mercury contents for gold from lode occurrences in the Klondike District.

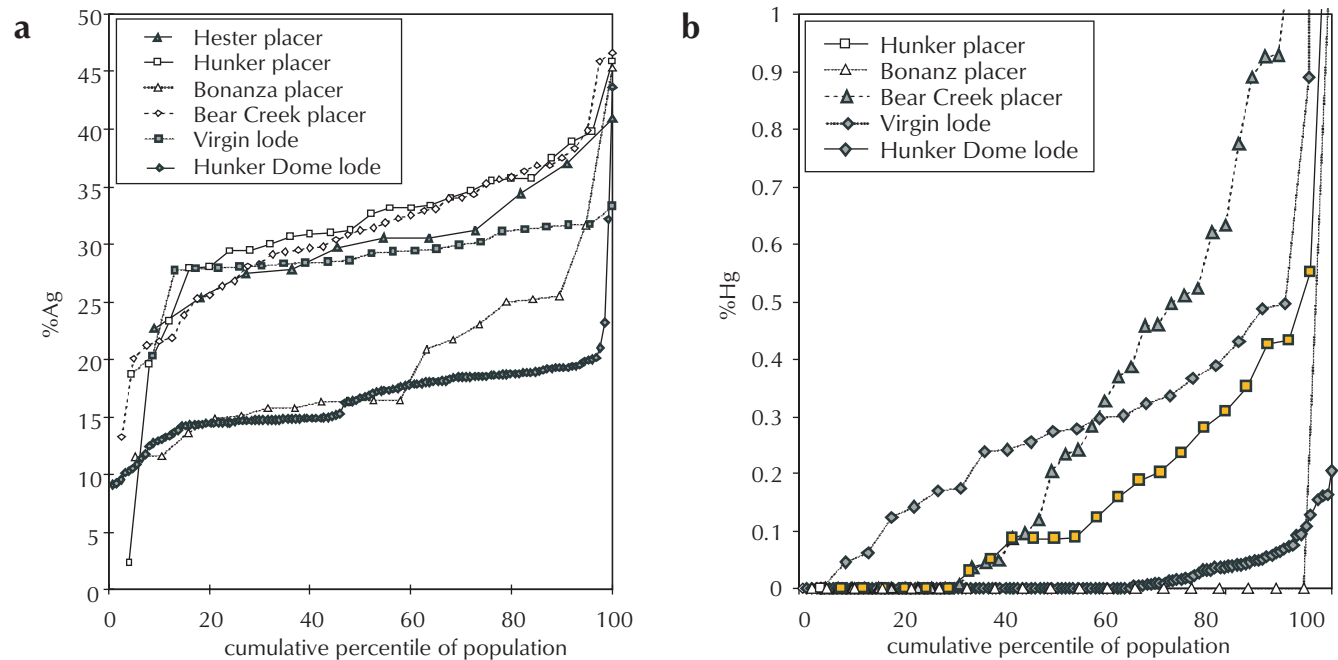
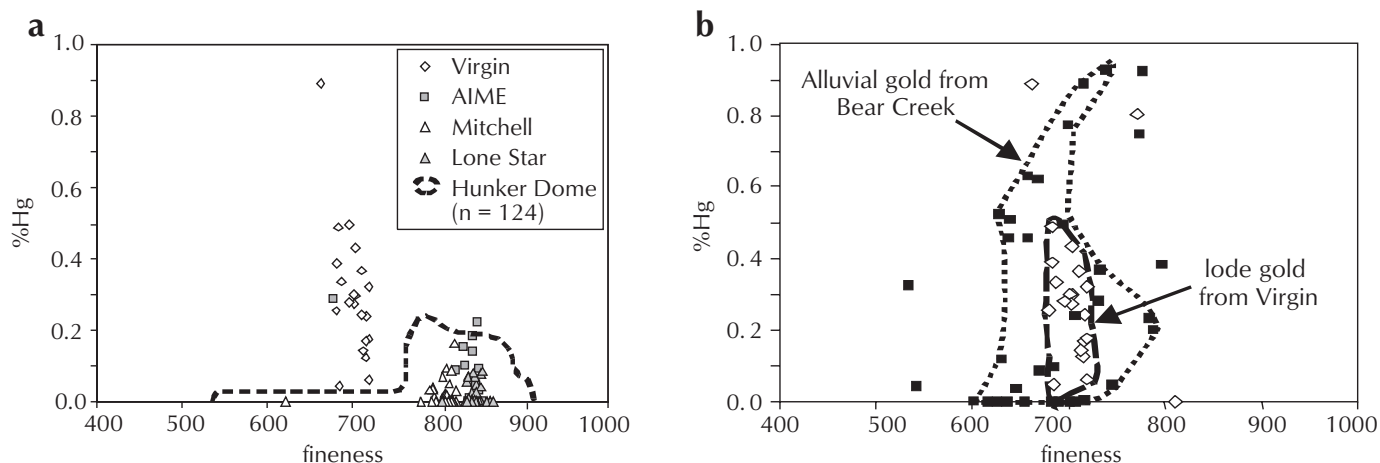


Figure 3. Cumulative percentile plots for silver and mercury contents for gold from various placer deposits and lode occurrences in the Klondike District.





**Figure 4.** (a) Plot of mercury content vs. fineness for gold from various Klondike lode occurrences; (b) detailed comparison between placer gold from Bear Creek and lode gold from the Virgin lode occurrence.

occurrences. Figure 3a shows that placer gold from Bear, Hester and lower Hunker creeks displays similar high wt.% Ag (low fineness) to that from the Virgin lode, and is quite distinct from low wt.% Ag (high fineness) gold from the Hunker Dome lode. Some of the placer gold from the middle part of Bonanza Creek has compositions that are similar to those of high fineness gold from the Hunker Dome occurrence, whereas some of the gold has distinct compositions with more intermediate silver contents. All but one of the placer gold grains analysed from Bonanza Creek do not contain detectable mercury and therefore most resemble the Hunker Dome lode gold (Fig. 3b). Placer gold grains from Bear and lower Hunker creeks contain variable but generally substantial mercury and therefore most closely resemble gold from the Virgin lode.

The lode gold data for the Klondike District is recast in a plot of wt.% Hg vs. fineness (Fig. 4a). This plot highlights the overall similarity in composition of most of the lode gold in the Klondike and the very distinct composition of gold from the Virgin lode. Gold from the Violet lode occurrence (Fig. 1) yields similar low fineness and high mercury compositions (Knight et al., 1999a). A detailed comparison of the compositions of placer gold from Bear Creek and lode gold from the Virgin occurrence (Fig. 4b) shows clearly that the Bear Creek gold was derived from the Virgin lode and/or lodes of similar geochemical character.

## WORK IN PROGRESS

We are currently preparing an extensive suite of placer gold samples from deposits from throughout western Yukon for detailed study. These samples are first examined using binocular microscope and SEM methods to characterize the overall shape characteristics. The grains are then mounted in epoxy 'pucks', ground down to expose the centres of each grain and brought to a high polish. The grains are mounted in an orientation that allows the aspect ratio of each grain (a measure of flattening) to be directly measured on the SEM. The nature and thickness of leached rims is then examined on the SEM using back-scattered electron images, and mineral micro-inclusions are identified and analysed. The major and minor element composition of the cores and in some cases the rims of the grains are determined using EMP methods. Finally, the trace element composition of the gold grains is determined using laser ablation ICP-MS methods. All shape, micro-inclusion and compositional data is then compiled on a sample-by-sample basis. Approximately 50 to 100 individual grains are analysed from each placer sample in order to confidently identify all the main compositional populations.

## ACKNOWLEDGMENTS

We thank the Yukon Geological Survey for providing seed funding for the project, as well as numerous placer miners from western Yukon for contributing samples for study.

Thanks also to many of the lode and placer mining exploration personnel working in the region for guidance and discussions in the field.

## REFERENCES

- Chapman, R.J., Leake, R.C., Moles, N.R., Earls, G., Cooper, C., Harrington, K. and Berzins, R., 2000. The application of microchemical analysis of gold grains to the understanding of complex local and regional gold mineralization: A case study in Ireland and Scotland. *Economic Geology*, vol. 95, p. 1753-1773.
- Chapman, R., Leake, R. and Styles, M., 2002. Microchemical characterization of alluvial gold grains as an exploration tool. *Gold Bulletin*, vol. 35, p. 53-65.
- Dumula, M.R. and Mortensen, J.K., 2002. Composition of placer and lode gold as an exploration tool in the Stewart River map area, western Yukon. *In: Exploration and Geological Services Division, Yukon, Indian and Northern Affairs Canada, 2000, Yukon Exploration and Geology 2001*, D.S. Emond, L.H. Weston and L.L. Lewis (eds.), p. 1-16.
- Hart, C.J.R., McCoy, D.T., Goldfarb, R.J., Smith, M., Roberts, P., Hulstein, R., Bakke, A.A. and Bundtzen, T.K., 2002. Geology, exploration and discovery in the Tintina Gold Province, Alaska and Yukon. *In: Society of Economic Geologists Special Publication 9, Integrated Methods for Discovery: Global Exploration in the 21st Century*, p. 241-274.
- Lange, I.M. and Gignoux, T., 1999. Distribution, characteristics, and genesis of high fineness gold placers, Ninemile Valley, Central-Western Montana. *Economic Geology*, vol. 94, p. 375-386.
- Leake, R.C., Chapman, R.J., Bland, D.J., Stone, P., Cameron D.G. and Styles, M.T., 1998. The origin of alluvial gold in the Leadhills area of Scotland: Evidence from internal chemical characteristics. *Journal of Exploration Geochemistry*, vol. 63, p. 7-36.
- Loen, J.S., 1994. Origin of placer gold nuggets and history of formation of glacial gold placers, Gold Creek, Granite County, Montana. *Economic Geology*, vol. 89, p. 91-104.
- Knight, J.B., Mortensen, J.K. and Morison, S.R., 1999a. Lode and placer gold compositions from the Klondike District, Yukon Territory, Canada: Its implications for the nature and genesis of Klondike placer and lode gold deposits, *Economic Geology*, vol. 94, p. 649-664.
- Knight, J.B., Morison, S.R. and Mortensen, J.K., 1999b. The relationship between placer gold particle shape, rimming and distance of fluvial transport; as exemplified by gold from the Klondike District, Yukon Territory, Canada; *Economic Geology*, vol. 94, p. 635-648.
- Mortensen, J.K., Nesbitt, B.E. and Rushton, R., 1992. Preliminary observations on the geology and geochemistry of quartz veins in the Klondike District, west-central Yukon. *Yukon Geology*, vol. 3, p. 260-270.
- Townley, B.K., Herail, G., MaksaeV, V., Palacios, C., de Parseval, P., Sepulveda, F., Orellana, R., Rivas, P. and Ulloa, C. 2003. Gold grain morphology and composition as an exploration tool: application to gold exploration in covered areas. *Geochemistry, Exploration, Environment, Analysis*, 3, p. 29-38.

# Reconnaissance geological and geochemical studies of the Joe Mountain Formation, Joe Mountain region (NTS 105D/15), Yukon

Stephen J. Piercey<sup>1</sup>

Mineral Exploration Research Centre, Department of Earth Sciences, Laurentian University<sup>2</sup>

Piercey, S.J., 2005. Reconnaissance geological and geochemical studies of the Joe Mountain Formation, Joe Mountain region (NTS 105D/15), Yukon. *In: Yukon Exploration and Geology 2004*, D.S. Emond, L.L. Lewis and G.D. Bradshaw (eds.), Yukon Geological Survey, p. 213-226.

## ABSTRACT

The Joe Mountain area of the Yukon contains Middle Triassic to Upper Triassic volcanic, sedimentary and intrusive rocks of the Stikine Terrane. The Ladinian (~237 to 228 Ma) rocks of the Joe Mountain Formation of Stikinia are divided into four units, including: 1) a lowermost mafic-ultramafic complex (mTJM<sub>4</sub>); 2) a lower basalt-flow-dominated unit (mTJM<sub>3</sub>); 3) a volcanoclastic- and sedimentary-rock-dominated unit; and 4) an uppermost unit of black pillow basalts and volcanoclastic rocks (mTJM<sub>4</sub>). In the Joe Mountain Formation there is a general increase in the abundance of volcanoclastic and sedimentary material, and a decrease in flow material, away from Joe Mountain suggesting that Joe Mountain is a volcanic centre.

Hematite-magnetite iron formation was discovered in 2004 interlayered with unit mTJM<sub>3</sub> basalts. These iron formations have anomalous metal concentrations, but more importantly, have hydrothermal geochemical signatures (e.g., high Fe/Al ratios) similar to volcanogenic massive sulphide-associated iron formations globally.

## RÉSUMÉ

La région du mont Joe, au Yukon, renferme des roches volcaniques, sédimentaires et intrusives du terrane de Stikine, datant du Trias moyen à supérieur. Les roches du Ladinien (~237 à 228 Ma) de la formation de Joe Mountain se divisent en quatre unités, comprenant : 1) à la base un complexe mafique-ultramafique (mTJM<sub>4</sub>); 2) une unité inférieure dominée par une coulée basaltique (mTJM<sub>3</sub>); 3) une unité à prédominance de roches volcanoclastiques et sédimentaires et 4) une unité supérieure formée de basalte noir en coussins et de roches volcanoclastiques (mTJM<sub>4</sub>). De façon générale, l'abondance des matériaux volcanoclastiques et sédimentaires augmente, alors que la quantité de matériaux de coulées volcaniques diminue, à mesure qu'on s'éloigne du mont Joe, indiquant ainsi que ce dernier constituait un centre volcanique.

La formation de fer à hématite et magnétite, découverte en 2004, est interstratifiée de basaltes de l'unité mTJM<sub>3</sub>. Ces formations de fer présentent des concentrations de métal anormales, mais, ce qui est plus important, elles présentent des signatures géochimiques hydrothermales (par ex. des rapports Fe/Al élevés) similaires à celles de formations de fer associées ailleurs dans le monde à des sulfures massifs volcanogènes.

<sup>1</sup>spiercey@laurentian.ca

<sup>2</sup>Ramsey Lake Road, Sudbury, Ontario, Canada P3E 2C6, phone 705-675-1151, ext. 2364, fax 705-675-4898



## INTRODUCTION

The Stikine Terrane in the Whitehorse to Carmacks region of Yukon represents one of the largest accumulations of Mesozoic Stikine Terrane rocks in the Canadian Cordillera (Fig. 1). This accumulation of Stikine Terrane rocks has been termed the Whitehorse Trough (e.g., Wheeler, 1961) and consists of predominantly Mesozoic volcanic, intrusive and sedimentary rocks (Hart, 1997). In 2004, the author initiated a study of the field, tectonic and metallogenic setting of Mesozoic volcanic and volcano-sedimentary rocks of the Whitehorse Trough. This research project is a complement to other ongoing research aimed at assessing the mineral and petroleum potential of the Whitehorse Trough (e.g., Lowey, 2004; Lowey, this volume; Long, this volume; Colpron, this volume; Tizzard, this volume). In this paper, preliminary field and geochemical results of studies of the Middle Triassic (Ladinian) Joe Mountain Formation in the Joe Mountain region of southern Yukon are presented. In particular, this paper provides: 1) geological and facies relationships for volcanic, intrusive and sedimentary rocks of the Joe Mountain Formation; 2) a preliminary assessment of initial results from litho-geochemical studies of rocks from the Joe Mountain Formation; and 3) results from geological and geochemical analyses of hydrothermal iron formations discovered during the 2004

field season. The key initial results of this study are that the Joe Mountain region likely represents a volcanic centre (e.g., Hart, 1997) that formed within an ocean floor setting. Furthermore, the iron formations found during 2004 have hydrothermal signatures and suggest that this area has potential to host volcanogenic massive sulphide (VMS) mineralization.

## GEOLOGICAL RELATIONSHIPS IN THE JOE MOUNTAIN AREA

The Joe Mountain area is approximately 30 km northeast of the city of Whitehorse (Fig. 1). The area consists predominantly of Triassic to Jurassic volcanic, volcano-sedimentary and sedimentary rocks of the Stikine Terrane; Cretaceous volcanic rocks; and Cretaceous intrusive rocks of the Teslin, Whitehorse and Mount McIntyre plutonic suites (Fig. 2; Hart, 1997, and references therein). The Joe Mountain Formation is one of the lowermost units within the Stikine Terrane in the Whitehorse region. It stratigraphically overlies the Mississippian and older Takhini assemblage and underlies the Triassic-Jurassic Lewes River Group (Figs. 1, 2, 3; Tempelman-Kluit, 1984; Hart, 1997).

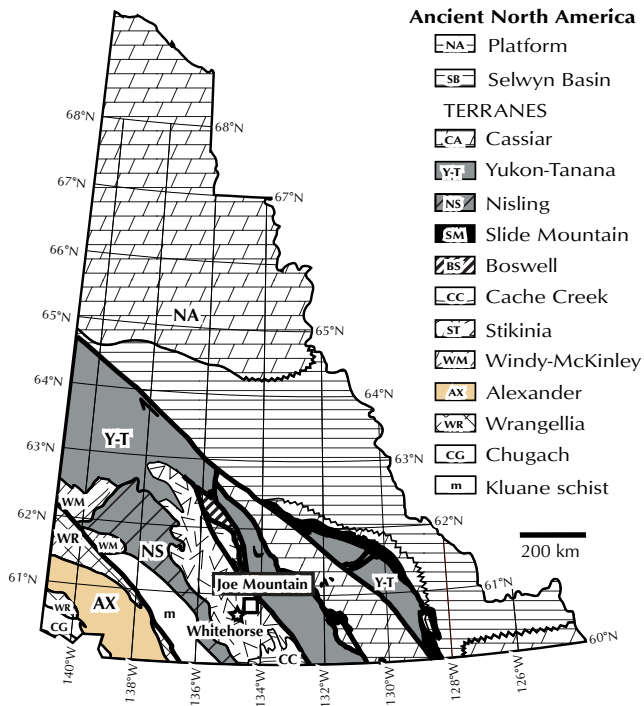


Figure 1. Yukon terrane map, modified from Colpron (this volume).

### Legend, Figure 2 (facing page)

#### Middle Cretaceous

- mKdW:** Cap Creek pluton: medium grey-weathering, medium-grained, equigranular, biotite-hornblende granodiorite
- mKgt:** M'Clintock granodiorite: white- to pale-weathering, recessive, leucocratic, equigranular biotite-hornblende granodiorite

#### Lower to Middle Jurassic

##### Lagerge Group

- JL:** brown- to tan-weathering sedimentary rocks including siltstone, greywacke, interbedded silt and sand couplets; minor conglomerate and limestone
- JR: Richthofen formation:** dark weathering, black, finely laminated turbiditic mudstone and sandstone

#### Middle Triassic

##### Aksala formation

- uTH: Aksala (undivided):** undifferentiated sedimentary rocks with siltstone, shale, sandstone, conglomerate and diamictite; locally limestone.
- uTH: Hancock member:** white-weathering massive to poorly bedded, bioclastic limestone, marble and skarn; some sandy limestone

#### Middle Triassic (Ladinian)

##### Joe Mountain Formation

- mJM<sub>1</sub>:** dark weathering cumulate gabbro, pyroxenite, anorthositic and diorite; locally, some diabase dykes
- mJM<sub>2</sub>:** dark grey weathering pillowed basalts; minor diabase; pillows tubular and locally with radial, concentric and tortoise shell fracturing
- mJM<sub>2</sub>:** chaotic assemblage of volcanoclastic and sedimentary rocks; mostly turbiditic with significant volcanic and carbonate component
- mJM<sub>1</sub> or mJM<sub>2</sub>**
- mTJM<sub>1</sub>:** black- to grey-weathering pillowed basalts; some pyrite-quartz-calcite weathering

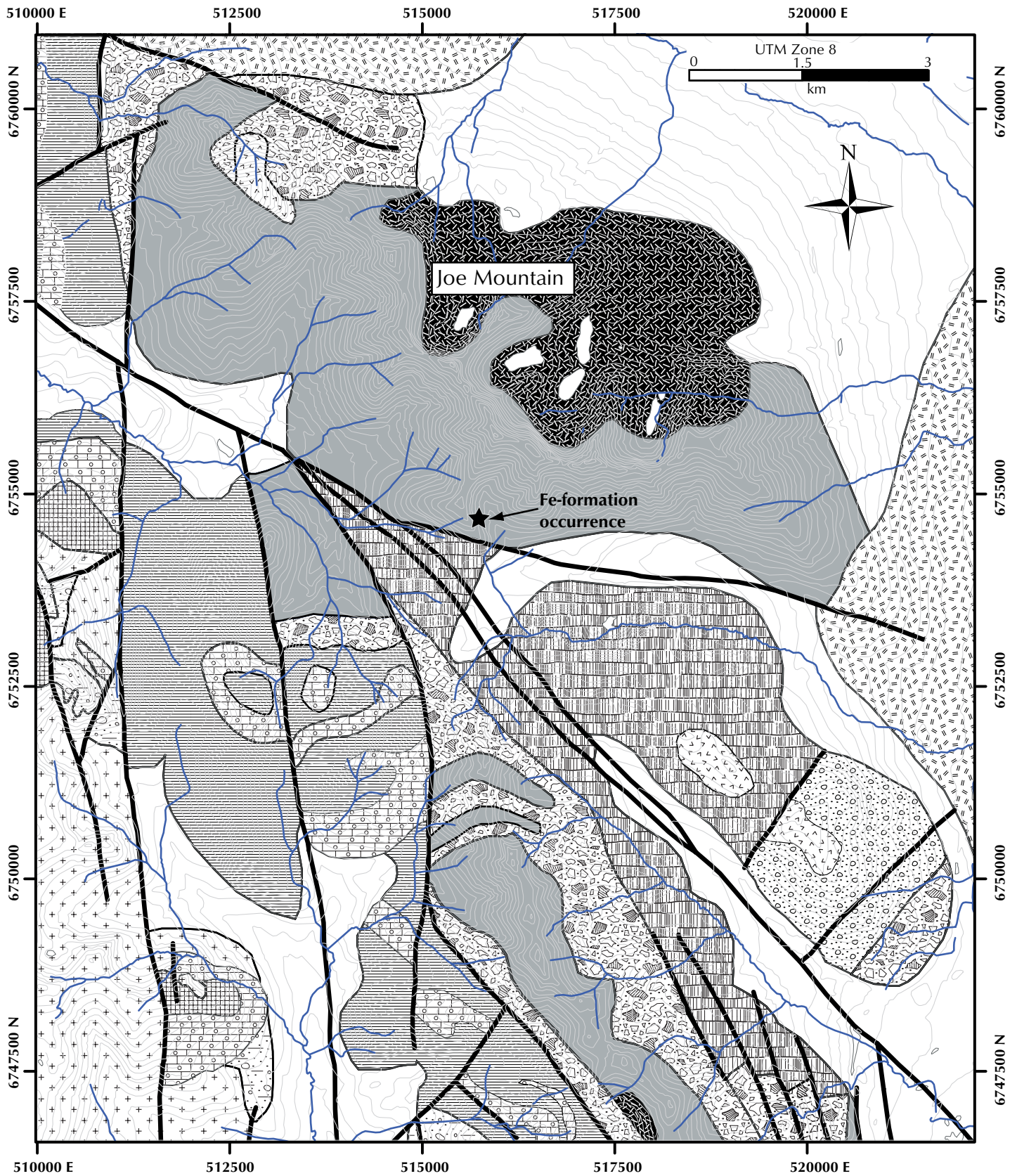
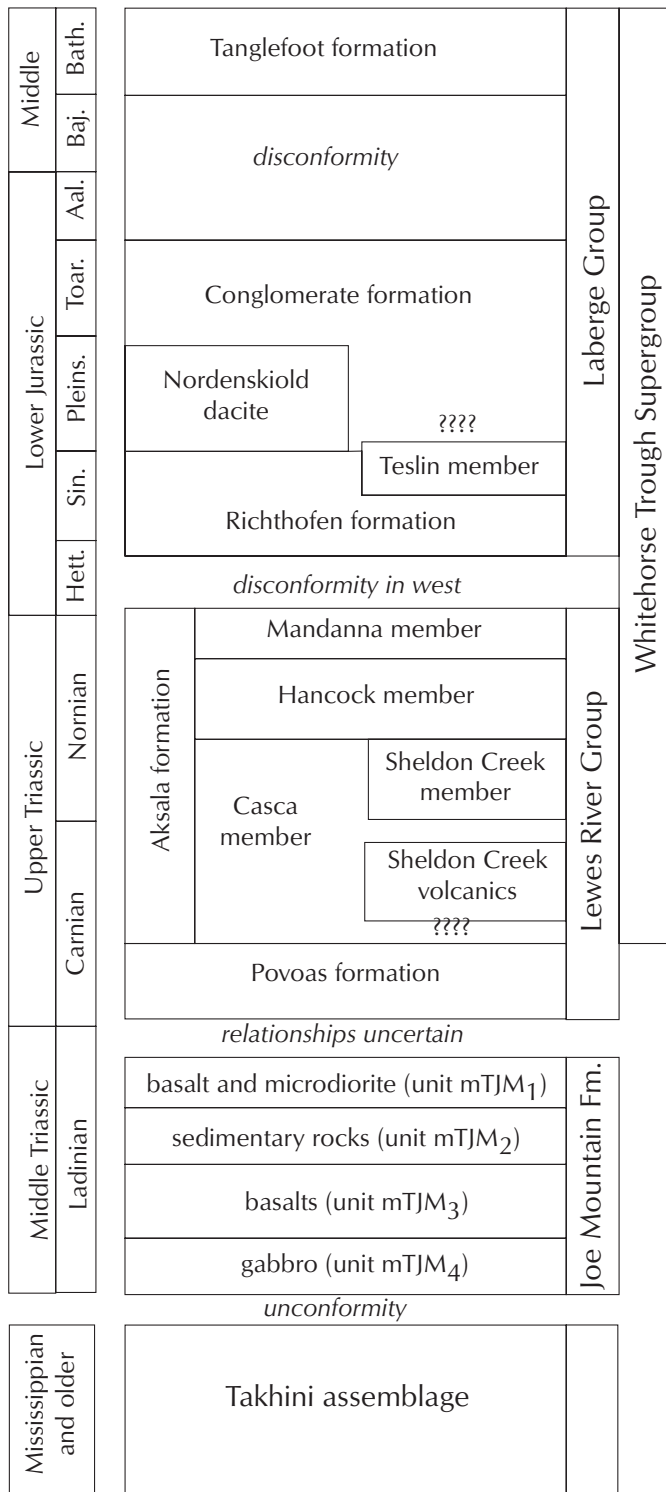


Figure 2. Geological map of the Joe Mountain region. Map modified from Hart and Hunt (1997). Legend on previous page.





**Figure 3.** Stratigraphic relationships of Stikinia within the Whitehorse Trough. Figure modified from Hart (1997). Abbreviations: Hett.=Hettangian, Sin.=Sinemurian, Pleins.=Pleinsbachian, Toar.=Toarcian, Aal.=Aalenian, Baj.=Bajocian, Bath=Bathonian, Fm=Formation.

The Joe Mountain area is the type locality for the Joe Mountain Formation (Hart, 1997). The formation consists of Middle Triassic (Ladinian – 237 to 228 Ma; based on fossil ages in Hart, 1997 and the time scale of Gradstein et al., 2004) mafic volcanic, high-level subvolcanic (diabase/microdiorite), volcano-sedimentary, sedimentary, and mafic-ultramafic intrusive rocks. Hart (1997) erected the formational status of these volcanic and intrusive rocks as a distinctive stratigraphic entity from the younger Povoas Formation of the Lewes River Group (Fig. 3). He further suggested that the Joe Mountain Formation has some similarities to the Cache Creek Terrane, but depositional ties to Stikinia explain its inclusion within the Stikine Terrane.

In the Joe Mountain region, the Joe Mountain Formation is subdivided into four units: mTJM<sub>1</sub> through mTJM<sub>4</sub> (Hart, 1997). The first three units (mTJM<sub>1</sub>-mTJM<sub>3</sub>) consist predominantly of volcanic, volcanoclastic and sedimentary rocks, whereas the fourth (mTJM<sub>4</sub>) is a mafic to ultramafic intrusive unit (Figs. 2 and 3).

**Unit mTJM<sub>4</sub>** intrusive rocks intrude the volcanic assemblages, but are interpreted to be synvolcanic intrusions coeval with the volcanic assemblages (Hart, 1997). This relationship is supported by geochemical relationships (see below). The intrusive rocks of unit mTJM<sub>4</sub> form the core of Joe Mountain (Fig. 2) and consist of gabbro, pyroxenite, leucogabbro and lesser anorthosite; diabase dykes cross-cut the gabbro in places. The bulk of intrusive rocks consist of coarse cumulate gabbro that contain coarse centimetre-scale pyroxene and plagioclase cumulate grains, and locally contain coarse pegmatoidal patches of pyroxene and plagioclase (Fig. 4a). Patches of leucogabbro, anorthosite and pyroxenite are commonly gradational with the cumulate gabbroic rocks. The rocks are fairly fresh and unaltered in places and are observed in thin section to contain very well-preserved intercumulus clinopyroxene and cumulate plagioclase. Most rocks, however, exhibit some degree of alteration and/or metamorphism. For example, most samples contain patches and millimetre- to centimetre-scale veinlets of calcite, epidote and quartz, with many pyroxene grains replaced by chlorite and actinolite, and feldspar grains replaced by minor sericite. Given the excellent textural preservation of these rocks (Fig. 4a,b), it is interpreted that these mineral assemblages represent hydrothermal alteration due to high-temperature seawater-rock interaction (e.g., Gillis and Thompson, 1993; Galley, 1993). Medium-grained, salt- and pepper-textured,





**Figure 4.** Joe Mountain Formation: (a) cumulate gabbro with cumulate pyroxene and plagioclase from unit mTJM<sub>4</sub>; (b) unit mTJM<sub>4</sub> gabbro cross-cut by unit mTJM<sub>4</sub> diabase dyke on Joe Mountain; (c) pillow basalt from unit mTJM<sub>3</sub> with radial cooling fractures; (d) pillow basalt from unit mTJM<sub>3</sub> with tortoise shell fracturing due to seawater-rock interaction.

~045°-trending diabase dykes (Fig. 4b; sheeted dykes?) cross-cut the gabbroic rocks in a few localities. These diabase dykes are straight-walled and likely intruded into partly solidified gabbro. They contain similar hydrothermal alteration assemblages as the gabbro, however, which suggests that they are broadly coeval with the gabbroic rocks of unit mTJM<sub>4</sub>.

**Unit mTJM<sub>3</sub>** is the lowermost volcanic unit within the Joe Mountain Formation and consists of a well preserved sequence of basaltic lava flows with lesser volcano-sedimentary rocks (Figs. 2 and 3). Well preserved pillow basalt flows are the predominant rock type throughout this unit. In general, the flows are greenish to grey-black, and aphyric to weakly plagioclase-phyric. The pillows are

typically 50 to 60 cm in diameter but some are as large as 1.5 m in size and tubular in shape. Most pillows exhibit radial and concentric cooling fractures (Fig. 4c), which indicate rapid cooling in the presence of water, and have thin centimetre-scale rinds composed of calcite and chlorite. In most localities the pillows exhibit a tortoise shell fracturing on their outer surfaces (Fig. 4d) due to rapid quenching of the lavas upon interaction with seawater. In addition, some pillows exhibit pillow tube forms, with one lava tongue extruding through another pillow (Fig. 5a; McPhie et al. 1993). Notably, the pillows are very densely packed on a regional scale and there is very little reworked and resedimented volcanic rock between pillows. Collectively, these features indicate that high effusion rates were prevalent at the time of





**Figure 5.** Joe Mountain Formation: (a) unit mTJM<sub>3</sub> pillow basalts illustrating pillow tubes, with one flow-tube coming out of an original pillowed flow; (b) unit mTJM<sub>2</sub> laminated marble turbidites with recessive carbonate layers and more resistant sandy layers; (c) unit mTJM<sub>2</sub> finely laminated volcanic sandstone turbiditic rocks with very fine ash (?) layers; (d) unit mTJM<sub>2</sub> heterolithic conglomerate.

deposition, and that there was little or no quiescence in between volcanic episodes to allow for abundant hyaloclastite formation or resedimentation (McPhie et al., 1993; Gibson et al., 1999). Where there are volcanoclastic rocks, they consist of monolithic tuff breccias with angular fragments and have limited areal extent (metres to tens of metres). Styles of hydrothermal alteration affecting rocks of this unit include millimetre-scale veinlets of calcite and quartz; minor epidote; and replacement of original glass by minor chlorite, epidote and clays. Despite this minor hydrothermal alteration, these rocks are very well preserved, as illustrated by the results of the geochemistry described below.

**Unit mTJM<sub>2</sub>** consists of mixed sedimentary and volcanoclastic rocks and is very chaotic in nature (e.g., Hart and Hunt, 1997). The unit contains a variety of rock types but is dominated by carbonate (marble) turbidites, volcanic-derived turbidites and associated rocks, and heterolithic conglomerates. Within the formation, marble layers of the unit are conformable with unit mTJM<sub>3</sub>. Marble units within the formation are grey to tan, and are recrystallized with grey recessive bands that alternate with more resistant tan, sandier bands (Fig. 5b). These layers may represent reworked and resedimented carbonate detritus in turbidite layers. Volcanic-derived turbidites are composed of glassy, ash-like material in sandy to silty



black to grey-green sand-silt couplets (Fig. 5c). In some localities, mTJM<sub>3</sub> basalt flows and conglomerate layers of mTJM<sub>2</sub> are interlayered with coarse conglomerates made up of centimetre-scale fragments of marble, siltstone, chert and mudstone within a matrix of granule-sized sandy material. There are also pebble- to cobble-conglomerates in this unit that are matrix-supported and are composed of subrounded clasts of grey quartz porphyry dacite, white rhyolite, grey siltstone and chert (Fig. 5d). These conglomerates are commonly interlayered with granular sandstone that is composed of greenish detrital granules of potentially volcanic origin. Collectively, the rock types and textures in unit mTJM<sub>2</sub> suggest that this package formed from volcanic- and carbonate-rich debris flows.

**Unit mTJM<sub>1</sub>** is a second layer of basalts that are distinguished from those of mTJM<sub>3</sub> by their black weathering and mostly smaller pillow diameters. The pillowed flows are generally densely packed, range from very fine-grained (e.g., glassy) to medium-grained, and in places are recrystallized. Typically the pillows are black to dark grey with bulbous margins and are up to 1.5 m long, but are typically 30 to 80 cm in diameter (Fig. 6a). Most of the pillows have no rinds, but do have radial cooling fractures in places (Fig. 6b), and some are amygdaloidal. In some localities the fractures and amygdules in the pillows are filled with quartz and pyrite. Although not always present, the interpillow regions commonly contain angular hyaloclastite fragments. Interlayered with the

pillows are matrix- to clast-supported pillow breccias that contain 1 to 2 cm rounded to angular basalt clasts. The association between the pillows and pillow breccias is consistent with a lobe and breccia volcanic facies association.

Hart (1997) suggested that Joe Mountain represents a volcanic centre, and results from regional facies relationships support this assertion. For example, in localities away from Joe Mountain, toward the south and southeast, the abundance of volcanoclastic rock and reworked sedimentary rock increases (e.g., unit uTJM<sub>2</sub>) and the amount of flow material decreases. Furthermore, in the region of Joe Mountain, unit uTJM<sub>3</sub> is characterized by very large flows and little hyaloclastite and volcanoclastic rock, which suggests very high eruption rates with very little reworking in between flow events. The latter features are indicative of high effusion rates, which suggest closer proximity to their vent source (Gibson et al., 1999). In addition, the very large pillowed sequence near Joe Mountain is proximal to the mafic-ultramafic intrusive rocks and diabase dykes of unit uTJM<sub>4</sub> (Fig. 2). Combined with the geochemistry below, these relationships suggest that the rocks of unit uTJM<sub>4</sub> are synvolcanic intrusions to the volcanic rocks. The synvolcanic nature of the intrusions implies that the Joe Mountain region represents a volcanic centre or near-vent environment.

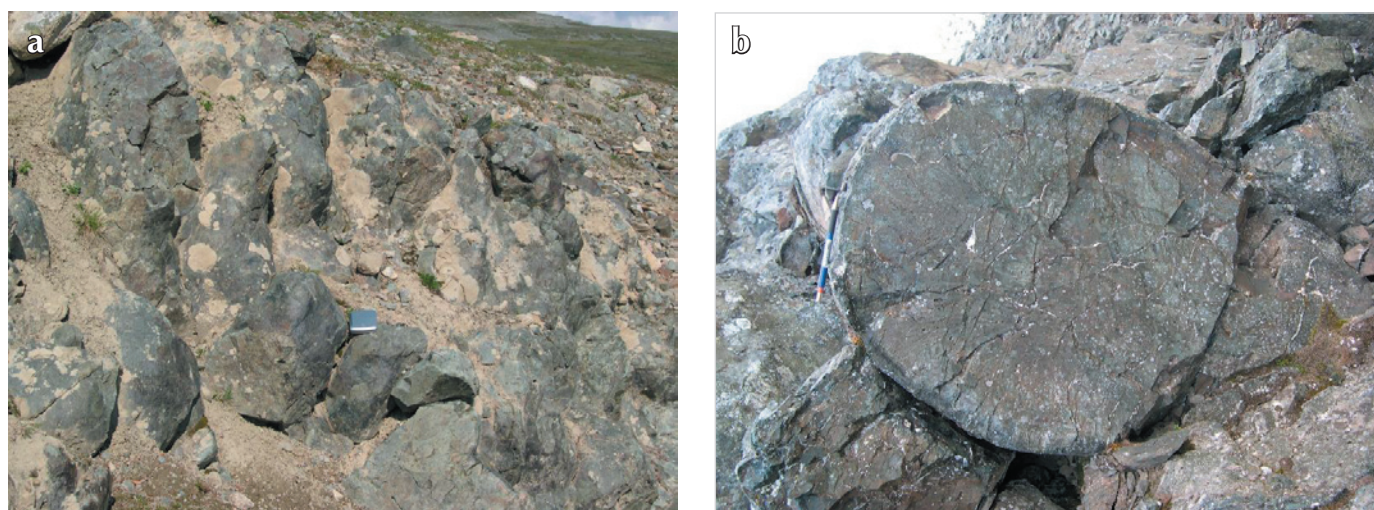


**Figure 6.** Photos of the Joe Mountain Formation: (a) unit mTJM<sub>1</sub>, black-coloured pillow basalts; and (b) unit mTJM<sub>1</sub>, pillow basalt with radial cooling fractures.



## GEOCHEMISTRY: PRELIMINARY RESULTS

Samples from the Joe Mountain Formation were analysed at Activation Laboratories in Ancaster, Ontario. Major elements and material lost on ignition (LOI) were analysed by fused-disc X-ray fluorescence (XRF), whereas the trace elements Ni, Cr, V, Nb, Zr and Y were analysed by pressed-pellet X-ray fluorescence (XRF). During the course of the study, duplicate analysis and reference materials were analysed to test precision and accuracy. Precision for major elements is <5% of the reported values, and for the trace elements it is <10%, with most <7%. Accuracy, as measured from repeat analysis of reference materials, is <5% relative difference for most major elements, and is <10% relative difference for trace elements, with most <7% relative difference.

Preliminary results for the Joe Mountain Formation pillowed and massive volcanic rocks, and gabbro and diabase intrusive rocks are illustrated in Figure 7. Most of the samples from the Joe Mountain Formation have basaltic to andesitic SiO<sub>2</sub> contents (46 to 55%, average=50.5%), which is consistent with field calls for rocks of the formation. The rocks have relatively low Al<sub>2</sub>O<sub>3</sub>/Na<sub>2</sub>O index values (<5.5; Spitz and Darling, 1978), moderate Na<sub>2</sub>O values (Fig. 7a), and relatively low LOI values (average =2.9%), suggesting that the rocks are relatively fresh. Furthermore, on an alteration box plot, the samples have low Hashimoto alteration index (Saeki and Date, 1980) values and low chlorite-carbonate-pyrite index (Large et al., 2001) values, with most samples plotting in the field for least-altered andesites/basalts (Fig. 7b), which further suggests that the rocks are relatively fresh.

The immobile high field strength element (HFSE: Zr, Nb, Y) and transition element (TiO<sub>2</sub>, V) systematics of the Joe Mountain Formation rocks are illustrated on Figure 7c-e. The bulk of the Joe Mountain Formation mafic rocks have sulbalkalic Nb/Y ratios (<0.7) and basaltic Zr/TiO<sub>2</sub> ratios (Fig. 7c), consistent with their SiO<sub>2</sub> content determinations. Most of the samples have Zr/Y ratios <4, indicative of a tholeiitic basaltic affinity (Fig. 7d; e.g., Barrett and MacLean, 1999). The Ti-V systematics of the Joe Mountain Formation basaltic rocks indicate a mid-ocean ridge basalt (MORB) or back-arc basin (BAB) affinity (Fig. 7e), which is also supported by elevated TiO<sub>2</sub> contents (0.52-3.08%, average 1.55%). Further rare-earth element and HFSE geochemical work will be required to further test and refine this tectonic discrimination.

It is also notable that there are no significant variations in the geochemical signatures of the mafic rocks from the different volcanic units of the Joe Mountain Formation (Fig. 7a-e). Furthermore, there is overlap between the trace element systematics of the volcanic rocks and intrusive rocks of the formation, which suggests that they are coeval and were derived from similar mantle source regions (Fig. 7a-e).

## MINERAL OCCURRENCES AND ASSAY RESULTS

Numerous occurrences have been previously described from the Joe Mountain region, with most being gold occurrences (Hart, 1997). In 2004, the author discovered an iron formation occurrence south of Joe Mountain (UTM: 515584E, 6754534N, NAD83 Datum, Zone 8). The occurrence consists of Algoma-style iron formation (Peter, 2003) that occurs in a 2- x 2-m-wide outcrop and is approximately 2 m thick (Fig. 8a). Float from the occurrence trends approximately 1 to 2 km southwest of the occurrence, which suggests that the iron formation may have some lateral extent. The iron formation is reddish, is jasperoidal, and is interlayered with pillow lavas of unit mTJM<sub>3</sub>. The iron formation is composed primarily of hematite with wispy 2- to 3-mm-wide magnetite layers and quartz (Fig. 8a). The unit does not contain significant sulphide minerals but is interpreted to represent a hydrothermal precipitate, based on the lateral extent of the unit, its occurrence as drapings around pillow lavas, and its geochemical characteristics (see below).

Reflected and transmitted light microscopy of the iron formations illustrate that they are made up primarily of hematite, magnetite, quartz, apatite and minor pyrite. Hematite and quartz are the dominant minerals in the iron formation. Quartz occurs as polycrystalline, rounded aggregates that are intergrown with the hematite. Hematite generally occurs in masses that contain ovoidal grains of hematite with deep red internal reflections and commonly contain inclusions of quartz and magnetite (Fig. 8b). Magnetite typically occurs as irregularly shaped, wispy aggregates in between the hematite masses (Fig. 9d). The magnetite is typically euhedral to subhedral, has lamellar twinning in places, and is commonly intergrown with apatite (Fig. 8c,d). Apatite also occurs as inclusions in the magnetite in some places. Pyrite is sparse in the iron formations, but is present as irregular, blebby-shaped inclusions in magnetite (Fig. 8d).

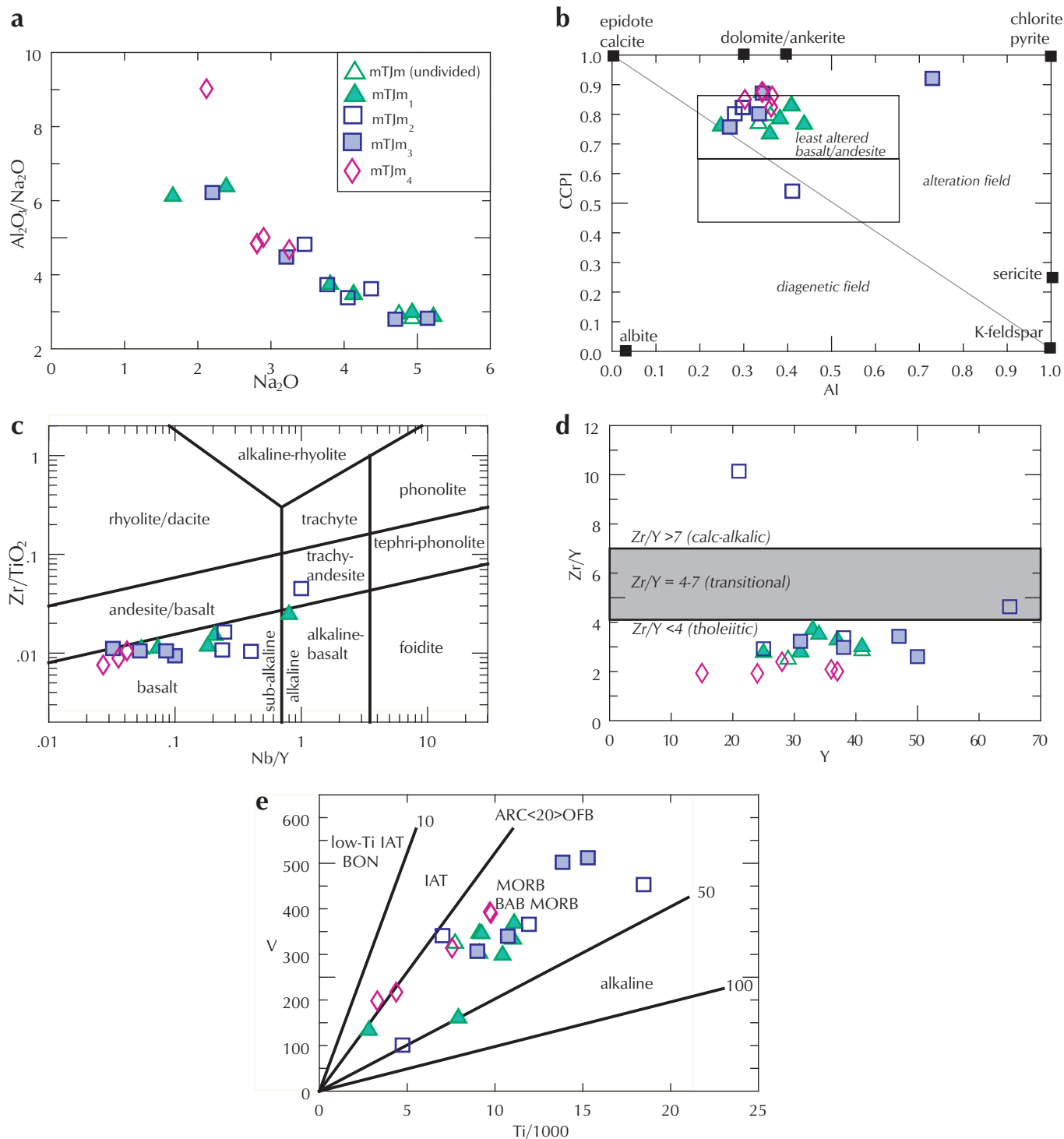


**Figure 7.** Plots of preliminary lithogeochemical data for the Joe Mountain Formation igneous rocks: **(a)**  $Al_2O_3/Na_2O$  (Spitz-Darling index; Spitz and Darling 1978) versus  $Na_2O$  plot; **(b)** alteration box plot with chlorite-carbonate-pyrite index (CCPI) versus alteration index (AI). Modified from Large et al. (2001); **(c)** Pearce (1996) version of the Winchester and Floyd (1977)  $Zr/TiO_2$  versus  $Nb/Y$  diagram; **(d)**  $Zr/Y$  versus  $Y$  diagram outlining tholeiitic versus calc-alkalic affinities, based on the concepts of Barrett and MacLean (1999); and **(e)**  $Ti$  versus  $V$  discrimination diagram of Shervais (1982). All samples from units mTJM (undivided), and mTJM<sub>1</sub> to mTJM<sub>3</sub> are extrusive rocks (e.g., flows, pillow lavas), whereas mTJM<sub>4</sub> is intrusive in nature (e.g., gabbro, diabase). Abbreviations: IAT=island arc tholeiites, BON=boninites; ARC=arc; BAB=back-arc basin; MORB=mid-ocean ridge basalt; OFB=ocean floor basalt.

Two samples were taken from the outcrop and assayed with the Group 1F-MS package at Acme Analytical Laboratories. The samples were digested using an aqua regia digest and subsequently analysed using an inductively coupled plasma mass spectrometer (ICP-MS); the results are presented in Table 1 and Figure 9. There are anomalous metal abundances within the iron formation samples; however, the aqua regia digest likely underestimates the actual total metal content of the samples because it does not totally dissolve the sample, particularly material residing within silicate or oxide phases. Nonetheless, these geochemical results can be used to test whether the iron formations have a

hydrothermal signature, and by association, if there was hydrothermal activity within the basin in which the Joe Mountain Formation and these iron formations were deposited.

Numerous workers have considered Algoma-type iron formations as potential vectors to volcanogenic massive sulphide (VMS) or seafloor vent-style mineralization (e.g., Peter, 2003, and references therein), and have devised chemical means of delineating hydrothermal versus detrital sedimentary signatures in these exhalative rocks. In general, the greater the hydrothermal component in the iron formation, the higher the iron content relative to aluminum and other detrital sedimentary components

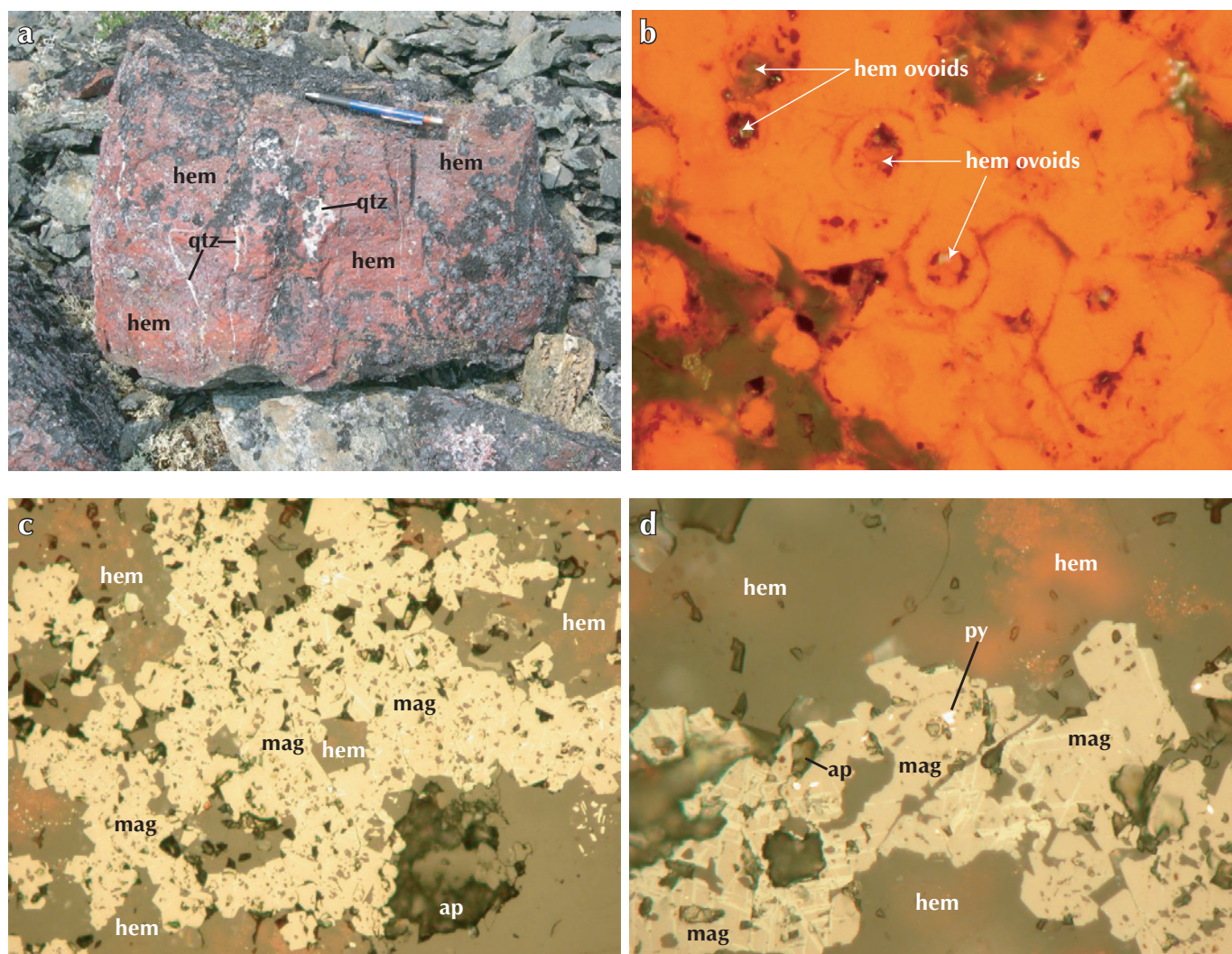


**Figure 8.** (a) Outcrop of the hydrothermal iron formations on Joe Mountain. Photomicrographs of the iron formation: (b) ovoidal grains of hematite with internal reflections (field of view: 1.1 mm, transmitted light, crossed polars); (c) euhedral magnetite intergrown with hematite and apatite (field of view: 0.55 mm, transmitted light, plane light); and (d) intergrown magnetite and hematite with blebby inclusion of pyrite within magnetite (field of view: 0.22 mm). Abbreviations: qtz=quartz, hem=hematite, mag=magnetite, py=pyrite, ap=apatite.



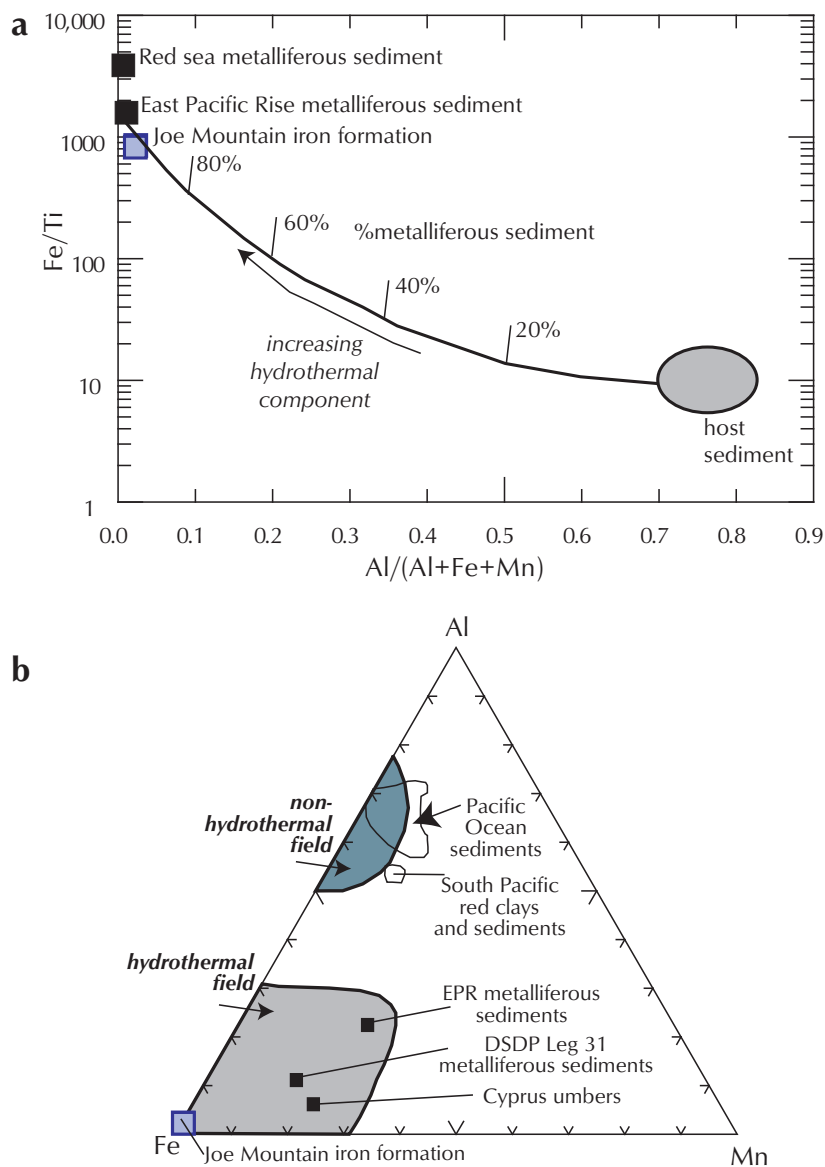


**Figure 9.** Fe/Ti versus Al/(Al+Fe+Mn) plot (a) and Fe versus Al versus Mn plot (b) for iron formations in the Joe Mountain Formation. Note very high Fe/Al ratios that are similar to modern seafloor hydrothermal vent fluids. These data suggest that the Joe Mountain area may have potential to host volcanogenic massive sulphide mineralization. Abbreviations: EPR=East Pacific Rise; DSDP=Deep Sea Drilling Program. Figure modified from Peter (2003), and references therein.

**Table 1.** Assay results for two samples of Joe Mountain Formation iron formation.

Sample	04SJP570-2-2	04SJP570-2-3
Easting	515584	515584
Northing	6754534	6754534
<b>Fe (%)</b>	6.81	7.41
<b>Ca</b>	0.71	0.84
<b>P</b>	0.015	0.017
<b>Mg</b>	0.21	0.21
<b>Ti</b>	0.008	0.009
<b>Al</b>	0.16	0.17
<b>Na</b>	0.003	0.004
<b>K</b>	<.01	<.01
<b>S</b>	0.02	0.02
<b>Mo (ppm)</b>	1.92	1.32
<b>Cu</b>	19.39	14.73
<b>Pb</b>	0.70	0.80
<b>Zn</b>	4.3	5.1
<b>Ni</b>	2.9	3.7
<b>Co</b>	2.0	1.7
<b>Mn</b>	183	219
<b>As</b>	1.5	1.3
<b>U</b>	0.1	0.1
<b>Th</b>	<.1	<.1
<b>Sr</b>	11.8	15.1
<b>Cd</b>	0.07	0.11
<b>Sb</b>	0.49	0.45
<b>Bi</b>	<.02	<.02
<b>V</b>	53	58
<b>La</b>	2.5	2.5
<b>Cr</b>	13.9	12.2
<b>Ba</b>	27.7	31.0
<b>B</b>	<1	1
<b>W</b>	0.3	2
<b>Sc</b>	0.9	1.0
<b>Tl</b>	<.02	<.02
<b>Se</b>	0.2	0.2
<b>Te</b>	<.02	<.02
<b>Ga</b>	1.0	1.0
<b>Au (ppb)</b>	1.3	1.3
<b>Ag</b>	27	23
<b>Hg</b>	<5	<5

such as titanium and manganese. Furthermore, the greater the hydrothermal component, the more proximal the rocks may be to the vent source that generated the hydrothermal fluids (Peter, 2003; Peter and Goodfellow, 1996).

The Joe Mountain iron formations have very high Fe/Al ratios (Fig. 10a-b), and have signatures similar to modern-day hydrothermal sediments associated with seafloor hydrothermal vents. These data suggest that seafloor hydrothermal activity existed within the basin that the Joe Mountain Formation formed in. Further work is required to ascertain whether this venting was of high enough temperature, was sustained for long enough, and if there were sufficient traps to form massive sulphide mineralized rock. Nonetheless, the occurrence of hydrothermal sedimentary rocks with strong hydrothermal signatures hints that there may be potential for VMS mineralization in the Joe Mountain Formation.

## SUMMARY

The following points summarize the results of this preliminary research:

- The Joe Mountain Formation in the Joe Mountain area consists of a sequence of Ladinian (~237 to 228 Ma) volcanic, intrusive and sedimentary rocks that can be divided into four packages (Hart and Hunt, 1997): 1) unit mTJM<sub>4</sub> consists predominantly of cumulate mafic-ultramafic intrusive rocks and is interpreted to be synvolcanic with the overlying mafic volcanic rocks; 2) unit mTJM<sub>3</sub> consists predominantly of pillowed and massive basalt flows, lesser volcanoclastic rocks, and minor iron formation; 3) mTJM<sub>2</sub> consists of mixed sedimentary and volcano-sedimentary rocks that include heterolithic conglomerates, volcanoclastic and tuffaceous rocks, carbonates and marble, and some carbonate-rich turbidites; and 4) unit mTJM<sub>1</sub>, the youngest basalt package, consists predominantly of black-weathering pillow lavas and lesser pillow breccia.
- In the Joe Mountain Formation there is a general increase in the abundance of volcanoclastic and sedimentary rocks, and a decrease in basalt flows with increasing distance from Joe Mountain proper. This regional variation in volcanic facies suggests that Joe Mountain proper may be the location of a volcanic centre (i.e., vent-proximal environment), as was previously suggested by Hart (1997).
- Preliminary litho-geochemical results from the Joe Mountain Formation indicate that these rocks are subalkalic with low Nb/Y (<0.7), moderate to high TiO<sub>2</sub> (0.52 to 3.08%), Ti/V ratios > 20 and tholeiitic Zr/Y ratios (<4). Collectively, these features are consistent with the rocks being subalkaline, tholeiitic rocks that likely formed in an oceanic environment. Whether this environment was a mid-ocean ridge spreading centre (e.g., mid-ocean ridge), an oceanic plateau (e.g., Ontong-Java plateau, Mahoney et al., 1993), or a back-arc basin (e.g., Japan Sea, Poulet et al., 1995) requires further geochemical and isotopic work.
- A hematite-magnetite iron formation was discovered interlayered with basalts of unit mTJM<sub>3</sub> in 2004. This iron formation is ~2 m thick and extends in float for about 1 to 2 km from the occurrence. The iron formation consists of interlayered hematite and quartz, with wispy layers of magnetite, minor pyrite and apatite. Assays from this iron formation yielded anomalous metals, but more importantly, the iron formations have geochemical signatures (e.g., high Fe/Al ratios) consistent with derivation via deposition from hydrothermal fluids. These types of iron formations have been found in association with volcanogenic massive sulphide (VMS) mineralization in numerous massive sulphide camps worldwide (e.g., Cyprus, Bathurst, Finlayson Lake), and this suggests that the Joe Mountain Formation may have potential to host VMS-style mineralization.

## ACKNOWLEDGEMENTS

This research was supported by a grant from the Yukon Geological Survey and a Discovery Grant from the Natural Sciences and Engineering Research Council of Canada (NSERC). Discussions with Maurice Colpron, Craig Hart, Darrel Long and Grant Lowey have been fruitful and informative, and are gratefully acknowledged. Cheerful and capable field assistance was provided by Janis Lloyd. Maurice Colpron is thanked for providing the map for Figure 1. Darrel Long is thanked for a review of a previous draft of this manuscript. Editorial comments by Geoff Bradshaw are also acknowledged.

## REFERENCES

- Barrett, T.J. and MacLean, W.H., 1999. Volcanic sequences, lithogeochemistry, and hydrothermal alteration in some bimodal volcanic-associated massive sulfide systems. *In: Volcanic-Associated Massive Sulfide Deposits: Processes and Examples in Modern and Ancient Environments*, C.T. Barrie and M.D. Hannington (eds.), Society of Economic Geologists, Reviews in Economic Geology, vol. 8, p. 101-131.
- Colpron, M., 2005 (this volume). Preliminary investigation of the bedrock geology of the Livingstone Creek area (NTS 105E/8), south-central Yukon. *In: Yukon Exploration and Geology 2004*, D.S. Emond, L.L. Lewis and G.D. Bradshaw (eds.), Yukon Geological Survey, p. 95-107.
- Galley, A.G., 1993. Characteristics of semi-conformable alteration zones associated with volcanogenic massive sulphide districts. *Journal of Geochemical Exploration*, vol. 48, p. 175-200.
- Gibson, H.L., Morton, R.L. and Hudak, G.J., 1999. Submarine volcanic processes, deposits, and environments favorable for the location of volcanic-associated massive sulfide deposits. *In: Volcanic-Associated Massive Sulfide Deposits: Processes and Examples in Modern and Ancient Environments*, C.T. Barrie and M.D. Hannington (eds.), Reviews in Economic Geology, vol. 8, p. 13-51.
- Gillis, K.M. and Thompson, G., 1993. Metabasalts from the Mid-Atlantic Ridge: New insights into hydrothermal systems in slow-spreading crust. *Contributions to Mineralogy and Petrology*, vol. 113, p. 503-523.
- Gradstein, F.M., Ogg, J.G. and Smith, A.D., 2004. *A Geological Time Scale 2004*. Cambridge University Press, Cambridge, England.
- Hart, C.J.R., 1997. A transect across northern Stikinia: geology of the northern Whitehorse map area, southern Yukon Territory (105D/13-16). Exploration and Geological Services Division, Yukon Region, Indian and Northern Affairs Canada, Bulletin 8, 112 p.
- Hart, C.J.R. and Hunt, J.A., 1997. Geology of Joe Mountain map area, southern Yukon (105D/15). Exploration and Geological Services Division, Yukon Region, Indian and Northern Affairs Canada, Geoscience Map 1997-6, 1:50 000 scale.
- Large, R.R., Gemmell, J.B., Paulick, H. and Huston, D.L., 2001. The alteration box plot: a simple approach to understanding the relationships between alteration mineralogy and lithogeochemistry associated with VHMS deposits. *Economic Geology*, vol. 96, p. 957-971.
- Long, D.G.F., 2005 (this volume). Sedimentology and hydrocarbon potential of fluvial strata in the Tantalus and Aksala Formations, northern Whitehorse Trough, Yukon. *In: Yukon Exploration and Geology 2004*, D.S. Emond, L.L. Lewis and G.D. Bradshaw (eds.), Yukon Geological Survey, p. 167-176.
- Lowey, G. W. 2004. Preliminary lithostratigraphy of the Laberge Group (Jurassic), south-central Yukon: Implications concerning the petroleum potential of the Whitehorse Trough. *In: Yukon Exploration and Geology 2003*, D.S. Emond and L. L. Lewis (eds.), Yukon Geological Survey, p. 129-142.
- Lowey, G.W., 2005 (this volume). Sedimentology, stratigraphy and source rock potential of the Richthofen formation (Jurassic), northern Whitehorse Trough, Yukon. *In: Yukon Exploration and Geology 2004*, D.S. Emond, L.L. Lewis and G.D. Bradshaw (eds.), Yukon Geological Survey, p. 177-191.
- Mahoney, J.J., Neal, C.R., Petterson, M.G., McGrail, B.A., Saunders, A.D. and Babbs, T.L., 1993. Formation of an oceanic plateau: Speculations from field and geophysical observations of the Ontong Java Plateau. *EOS*, vol. 74, p. 552.
- McPhie, J., Doyle, M. and Allen, R.L., 1993. *Volcanic Textures: A guide to the interpretation of textures in volcanic rocks*. Centre for Ore Deposit and Exploration Studies, University of Tasmania, Tasmania, Australia.
- Pearce, J.A., 1996. A user's guide to basalt discrimination diagrams. *In: Trace Element Geochemistry of Volcanic Rocks: Applications for Massive Sulphide Exploration*, D.A. Wyman (ed.), Geological Association of Canada, Short Course Notes, Volume 12, p. 79-113.
- Peter, J.M., 2003. Ancient iron formations: their genesis and use in the exploration for stratiform base metal sulphide deposits, with examples from the Bathurst Mining Camp. *In: Geochemistry of Sediments and Sedimentary Rocks: Secular Evolutionary Considerations to Mineral Deposit-Forming Environments*, D.R. Lentz (ed.), Geological Association of Canada, *GEOtext*, vol. 4, p. 145-176.



- Peter, J.M. and Goodfellow, W.D., 1996. Mineralogy, bulk and rare earth element geochemistry of massive sulphide-associated hydrothermal sediments of the Brunswick horizon, Bathurst mining camp, New Brunswick. *Canadian Journal of Earth Sciences*, vol. 33, p. 252-283.
- Poucllet, A., Lee, J.-S., Vidal, P., Cousens, B.L. and Bellon, H., 1995. Cretaceous to Cenozoic volcanism in South Korea and in the Sea of Japan: Magmatic constraints on the opening of the backarc basin. *In: Volcanism associated with extension at consuming plate margins*, J.L. Smellie (ed.), Geological Society of London Special Publication 81, p. 169-181.
- Saeki, Y. and Date, J., 1980. Computer application to the alteration data of the footwall dacite lava at the Ezuri Kuroko deposits, Akito Prefecture. *Mining Geology*, vol. 30, p. 241-250.
- Shervais, J.W., 1982. Ti-V plots and the petrogenesis of modern and ophiolitic lavas. *Earth and Planetary Science Letters*, vol. 59, p. 101-118.
- Spitz, G. and Darling, R., 1978. Major and minor element lithochemical anomalies surrounding the Louvem copper deposit, Val d'Or, Quebec. *Canadian Journal of Earth Sciences*, vol. 15, p. 1161-1169.
- Tempelman-Kluit, D.J., 1984. Geology, Laberge (105E) and Carmacks (105I), Yukon Territory. Geological Survey of Canada, Open File 1101, 1:250 000 scale.
- Tizzard, A. and Johnston, S., 2005 (this volume). Structural evolution of the Tally Ho shear zone (NTS 105D), southern Yukon. *In: Yukon Exploration and Geology 2004*, D.S. Emond, L.L. Lewis and G.D. Bradshaw (eds.), Yukon Geological Survey, p. 237-246.
- Wheeler, J.O., 1961. Whitehorse map-area, Yukon Territory, 105D. Geological Survey of Canada, Memoir 312, Department of Mines and Technical Surveys, Canada, Ottawa, Ontario.
- Wheeler, J.O. and McFeeley, P., 1991. Tectonic Assemblage Map of the Canadian Cordillera. Geological Survey of Canada, Map 1712A.
- Winchester, J.A. and Floyd, P.A., 1977. Geochemical discrimination of different magma series and their differentiation products using immobile elements. *Chemical Geology*, vol. 20, p. 325-343.

# The isotopic sulphur composition of two barite samples from Rose Mountain area near Faro, Yukon

Lee C. Pigage<sup>1</sup>  
Yukon Geological Survey

Pigage, L.C., 2005. The isotopic sulphur composition of two barite samples from Rose Mountain area near Faro, Yukon. *In: Yukon Exploration and Geology 2004*, D.S. Emond, L.L. Lewis and G.D. Bradshaw (eds.), Yukon Geological Survey, p. 227-236.

## ABSTRACT

The Rose Mountain area northwest of Faro is underlain by a succession of phyllites, cherts, sandstones, chert-pebble conglomerates and basalt belonging to the Slide Mountain Terrane. At least two, laterally extensive, massive barite horizons are interbedded with phyllite, bedded chert, sandstone and chert-pebble conglomerate of the Early Carboniferous Mount Aho formation, the lowermost unit in this succession. Samples from two barite horizons produced  $\delta^{34}\text{S}$  values (‰) of  $+14.3 \pm 0.2$  ( $2\sigma$ ) and  $+13.8 \pm 0.2$  ( $2\sigma$ ), which are consistent with  $\delta^{34}\text{S}$  values for coeval dissolved sulphate in seawater. Ambient seawater is therefore the most probable source of the sulphate in the barite. The results suggest barite precipitated from mixing of sulphate-poor hydrothermal fluids with ambient seawater rather than inversion of anoxic, stagnant, stratified basin waters.

## RÉSUMÉ

La région du mont Rose, au nord-ouest de Faro, repose sur une succession de phyllites, de cherts, de grès, de conglomérats de galets de chert et de basalte appartenant au terrane de Slide Mountain. Une stratification entremêlée de phyllite, de chert lité, de grès et de conglomérat de galets de chert, appartenant à la formation de Mount Aho du Carbonifère précoce, forment les couches lithologiques les plus basses de la succession. De multiples horizons étendus de barytine et de chert phylliteux massifs sont interstratifiés avec ces roches sédimentaires. Des échantillons de deux horizons de barytine ont donné des valeurs (‰) de  $\delta^{34}\text{S}$  de  $+14,3 \pm 0,2$  ( $2\sigma$ ) et de  $+13,8 \pm 0,2$  ( $2\sigma$ ), qui sont cohérentes avec les valeurs de  $\delta^{34}\text{S}$  des sulfates du même âge dissous dans l'eau de mer. Par conséquent, l'eau de mer ambiante représente la source la plus probable de sulfates dans la barytine. Les résultats indiquent que la barytine n'a pas été précipitée par l'inversion des eaux de bassin anoxiques, stagnantes et stratifiées. Cependant, les valeurs de  $\delta^{34}\text{S}$  résultantes permettraient une précipitation de la barytine résultant du mélange de fluides hydrothermaux à faible teneur en sulfates avec l'eau de mer ambiante.

<sup>1</sup>lee.pigage@gov.yk.ca

## INTRODUCTION

The isotopic composition of dissolved sulphate in modern ocean water is constant ( $\delta^{34}\text{S} = +20.0\text{‰}$ ) because of the rapid mixing of oceanic currents relative to the average residence time of sulphate in seawater (Claypool et al., 1980). This ratio has varied between  $+10\text{‰}$  and  $+30\text{‰}$  through geological time (Claypool et al., 1980); the variation results from a multitude of global processes, including climate change, volcanic activity, plate tectonics and ocean water circulation (Kampschulte et al., 2001). In earlier studies, this sulphur isotope variation in seawater sulphate through geologic time was tracked by measuring of isotopic compositions of evaporite calcium-sulphate deposits (gypsum and anhydrite) and barite deposits (Claypool et al., 1980). More recently, isotopic composition of trace sulphate dissolved in fossil shell material and whole-rock carbonate has also been used to refine geologic seawater sulphate compositions (Kampschulte et al., 2001) through geologic time.

Slide Mountain stratigraphy near Rose Mountain (NTS 105K/5 and 6) contains thin, laterally extensive, stratiform barite horizons. Sulphur isotope compositions for two barite samples from different horizons were measured during a regional compilation project of the Anvil District completed by the Yukon Geological Survey. An Early Carboniferous age for both barite horizons was also successfully determined from conodont collections obtained during the same project. This article presents the sulphur isotope data in the context of the fossil control, compares the isotope values to sulphur isotopes of coeval seawater, and briefly discusses how results are consistent with open oceanic circulation during precipitation of the barite.

### SULPHUR ISOTOPE SYSTEMATICS

Sulphur has four stable isotopes  $^{32}\text{S}$  (95.02%),  $^{33}\text{S}$  (0.75%),  $^{34}\text{S}$  (4.21%) and  $^{36}\text{S}$  (0.02%) (Faure and Mensing, 2005). Isotopic sulphur composition is reported as the expression:

$$\delta^{34}\text{S} (\text{‰}) = \left[ \frac{(^{34}\text{S}/^{32}\text{S})_{\text{sa}} - (^{34}\text{S}/^{32}\text{S})_{\text{std}}}{(^{34}\text{S}/^{32}\text{S})_{\text{std}}} \right] * 1000$$

where "sa" represents the sample and "std" represents the standard. The reference sulphur isotope standard for this expression is the isotopic ratio of  $^{34}\text{S}/^{32}\text{S}$  ( $= 0.0450$ ) for the mineral troilite (FeS) in the Canyon Diablo meteorite (CDT). The value for CDT is very similar to the measured values of sulphur isotopes in mafic igneous rocks.

Variations in sulphur isotopic composition are caused by two kinds of processes (Faure and Mensing, 2005):

- 1) reduction of sulphate to hydrogen sulphide by anaerobic bacteria. During the reduction process, hydrogen sulphide is enriched in  $^{32}\text{S}$  and the residual sulphate is enriched in  $^{34}\text{S}$ ;
- 2) isotopic exchange reactions occurring during exchange of sulphur between different ions, molecules and solids. During this process,  $^{34}\text{S}$  is typically slightly enriched in compounds having the highest sulphur oxidation state and/or strongest bond strength.

Biogenic sulphate reduction (process 1 above) is the most important source of sulphur fractionation in nature. In an open system, fractionation is reasonably constant and depends on the physical parameters at the site of deposition. If sulphate availability is restricted (closed system), both remaining dissolved sulphate and reduced hydrogen sulphide have increasing  $\delta^{34}\text{S}$  values with continuing biogenic reduction of sulphate and precipitation of sulphide minerals.

Sulphur isotope fractionation between gypsum mineral and dissolved sulphate in seawater during precipitation of the gypsum in modern sediments ranges from 0 to  $+2.4\text{‰}$  (Strauss, 1997). Calcium sulphate therefore accurately reflects the dissolved sulphate isotopic composition of seawater at the time of precipitation. Recent work on marine barite indicates that barite also may accurately reflect dissolved sulphate compositions of contemporaneous seawater (Cecile et al., 1983; Paytan et al., 1998).

## GEOLOGY FOR ROSE MOUNTAIN SAMPLES

Rose Mountain is located on the southwest flank of the Anvil District in central Yukon (Fig. 1), approximately 200 km northeast of Whitehorse and 14 km northwest of the town of Faro. Outcrop is extensive on ridges above tree line (approximately 1370 m) and is restricted to stream cuts and scattered ridge crests below that. Valley bottoms are typically covered with thin to thick glacial till. Overgrown exploration roads and outfitting trails extend into the area. Access is most readily accomplished by helicopter. Camps during the 1998 field season were placed using contract helicopter service based in Ross River.

The area lies within Tay River map sheet (NTS 105K). Regional geology was mapped by Roddick and Green



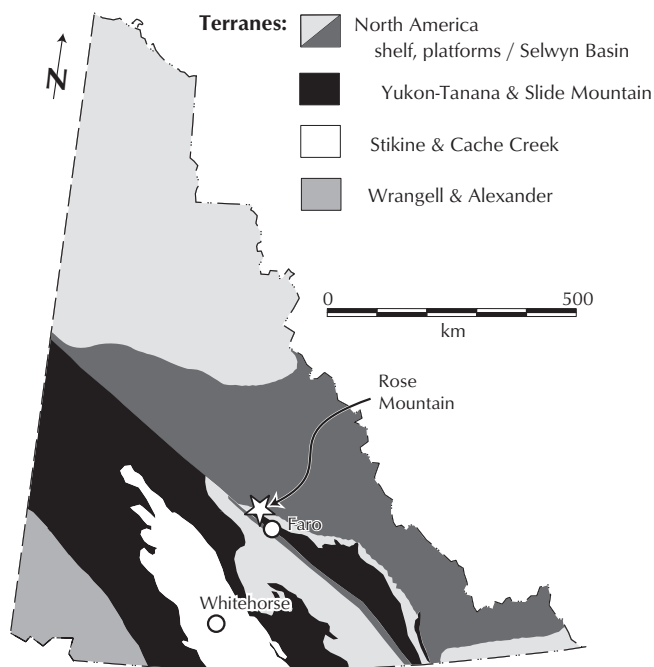


Figure 1. Location of Rose Mountain in Yukon. Modified from Wheeler and McFeely (1991).

(1961), and Gordey and Irwin (1987). More detailed studies by Tempelman-Kluit (1972) and Gordey (1990) were completed in response to exploration interest generated by the discovery of the massive sulphide deposits in the Anvil District. Jennings and Jilson (1986) and Pigage (2004) have also presented regional stratigraphic and structural summaries which have included this area.

Early exploration activity occurred dominantly on the north slopes of Rose Mountain and was focused primarily on lead-zinc targets because of the Anvil District massive sulphide discoveries. The two barite horizons discussed here were staked as the URN Claims by Cyprus Anvil Mining Corporation in 1977. The upper horizon was sampled in several locations in 1977 (Franzen, 1978) and 1981 (Read, 1982) to evaluate its industrial mineral potential. Exploration work on the URN claims is summarized in Yukon MINFILE (105K 106, Deklerk and Traynor, 2004).

Two or more barite horizons (Figs. 2 and 3) are contained within a uniformly southwest-dipping sequence of dark

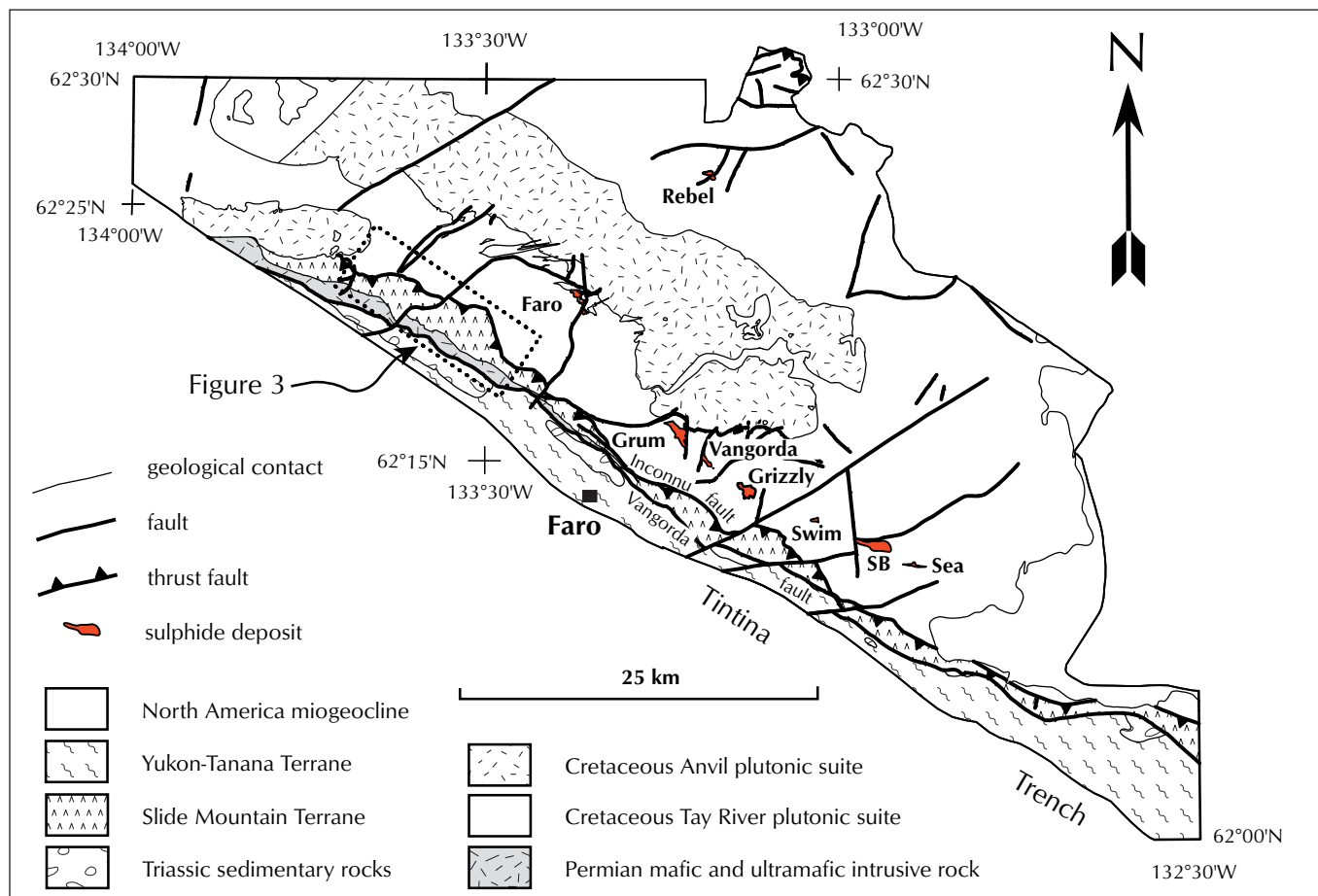


Figure 2. Major tectonic/stratigraphic successions. Modified from Pigage (2004)

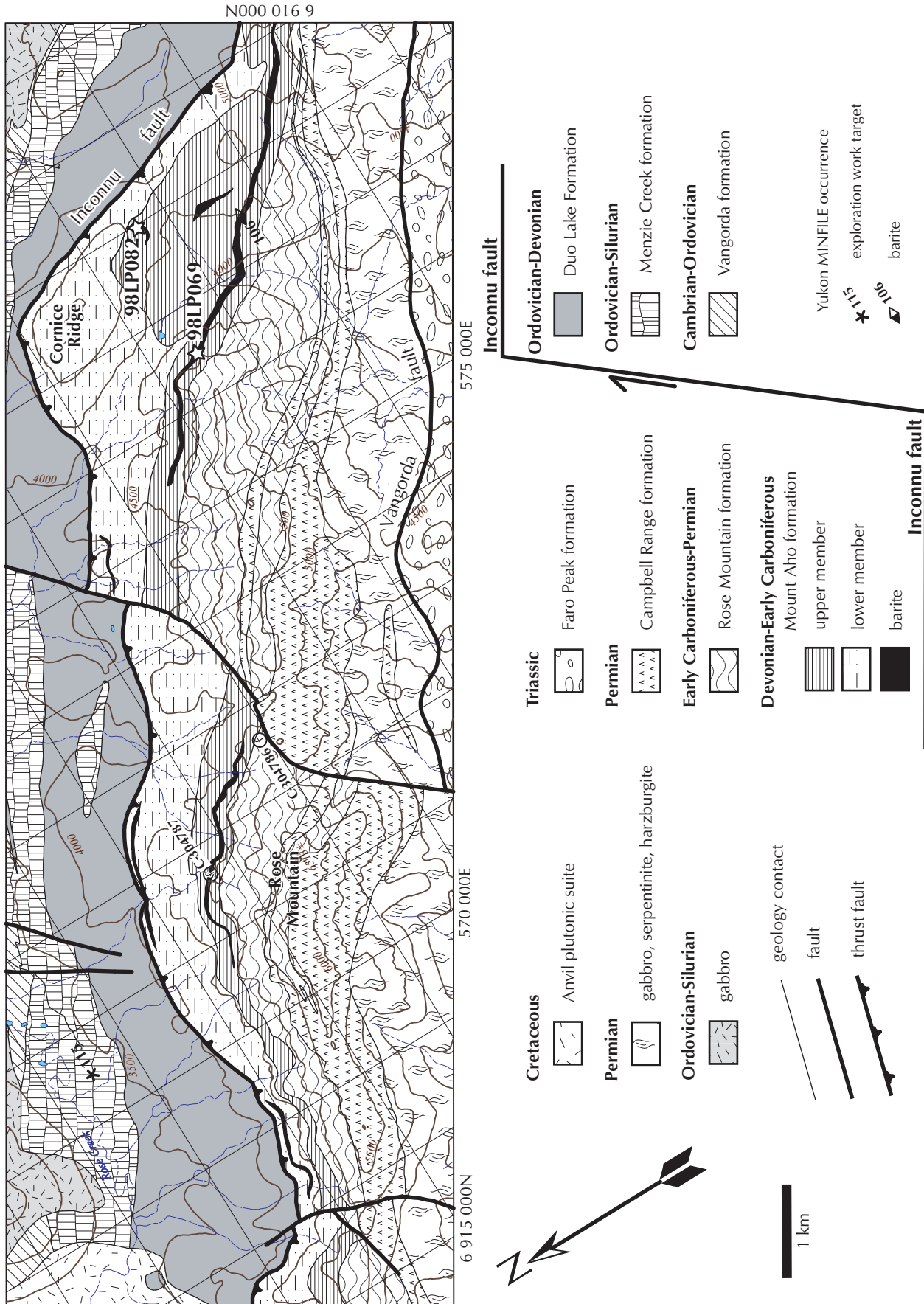


Figure 3. Geology of Rose Mountain. Modified from Pigage (2004).

grey to black, bedded chert, chert-pebble conglomerate, sandstone, and siliceous phyllite and sandstone belonging to the Mount Aho formation (Pigage, 2004). The Mount Aho formation ranges up to 1500 m thick, and has been informally divided into a lower pale green member and an upper dark grey member. Barite horizons occur in both members.

Mount Aho formation is the lowest unit in a continuous succession of three formations. Bedded cherts and phyllites of the Rose Mountain Formation conformably(?) overlies the Mount Aho formation and are in turn capped by basalts of the Campbell Range formation (Pigage, 2004). Tectonic affiliation of this assemblage has been controversial (Jennings and Jilson, 1986; Pigage, 1999 and 2004). Most recently it has been assigned to the Slide Mountain Terrane, an ocean-floor back-arc basin in Carboniferous-Permian time, which was subsequently partially subducted and amalgamated between ancestral North America and Yukon-Tanana Terrane (Tempelman-Kluit, 1979; Creaser et al., 1999; Pigage, 2004). The lower contact of Mount Aho formation is the Inconnu fault, the major northeast-verging thrust fault

placing Slide Mountain Terrane onto ancestral North America.

Both members of the Mount Aho formation contain barite. The immediate host for the barite in both members consists of tan-weathering, pale cream, phyllitic bedded chert and argillite ranging up to 40 m thick. Barite is nodular to massive within bedded chert and argillite. Sulphide minerals are not visibly associated with the barite. Exploration work by Cyprus Anvil Mining Corporation (Franzen, 1978) and recent mapping by Pigage (2004) has confirmed that the barite horizons can be laterally traced along strike for several kilometres. The other major mineral associated with the barite is quartz (Read, 1982).

### SULPHUR ISOTOPES FOR ROSE MOUNTAIN BARITE

Two samples of barite were collected from different barite horizons within the Mount Aho formation, one near the bottom and one near the top of the upper black to grey member. Locations of the samples are indicated in

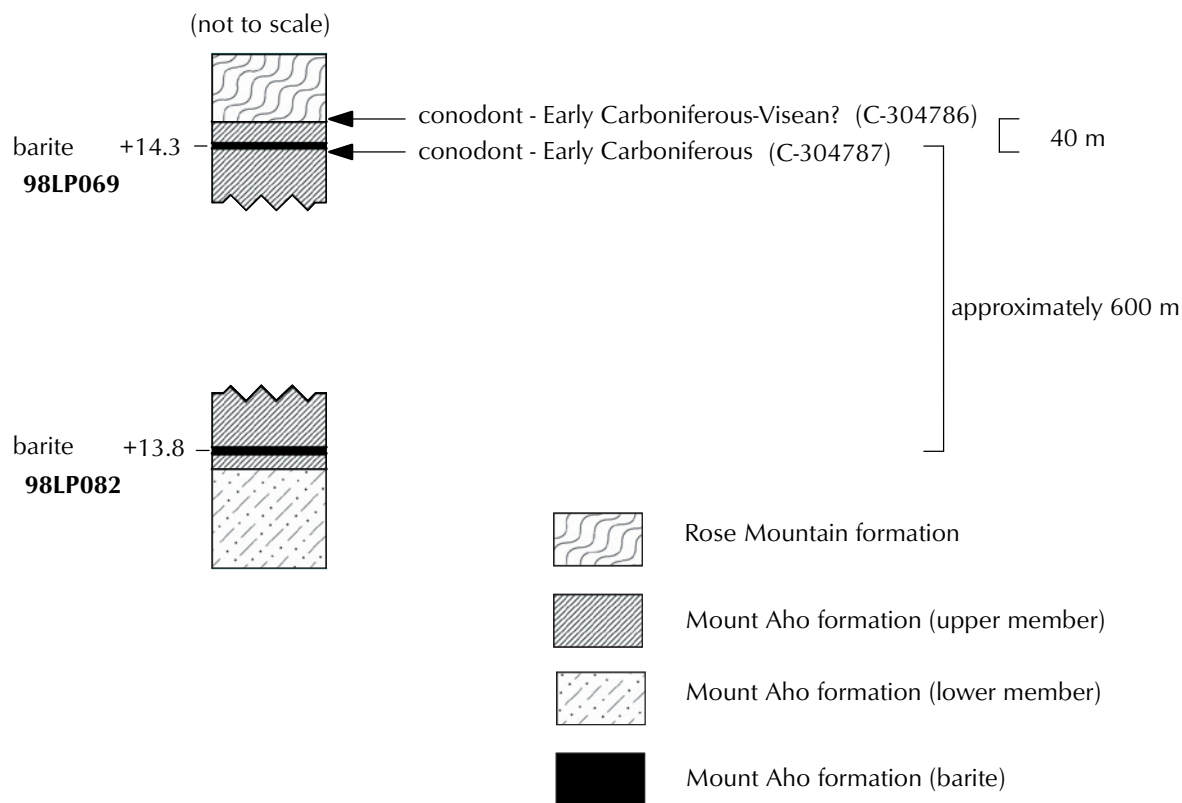


**Figure 4.** Schematic stratigraphic column showing barite horizons with sample locations indicated. Based on geology from Pigage (2004).



**Table 1.** Isotopic sulphur composition of barite samples.

Sample	98LP069	98LP082
Barite horizon	Upper horizon	Lower horizon
UTM East	576 481	578 008
UTM North	6 912 485	6 912 358
UTM Zone	8	8
Datum	NAD83	NAD83
S <sup>34</sup> (‰, CDT)	+14.3	+13.8
2σ precision	±0.20	±0.20

Figure 3; UTM coordinates are presented in Table 1. Figure 4 is a schematic stratigraphic section for the two samples indicating their relative location approximately 600 m apart stratigraphically, assuming a homoclinal southwest-dipping succession. Figure 4 also indicates approximate locations of two productive conodont samples which returned Early Carboniferous ages (Orchard, 2000).

#### SAMPLE 98LP082

Sample 98LP082 was collected from a barite horizon located in the pass at the south end of Cornice Ridge (Fig. 3). Medium crystalline, grey barite forms beds up to 10 cm thick (Fig. 5) within light cream to tan argillite and chert. Exposed surfaces weather to a very rusty brown, and the barite contains a poorly developed slaty cleavage. Overall thickness of the horizon is about 10 m, and bedding dips 20 degrees to the southwest. The barite horizon cannot be traced laterally along strike away from



**Figure 5.** Barite horizon at field station 98LP082. Massive barite occurs in tan chert and argillite. Pencil magnet is 12.5 cm long.

the pass. Metasedimentary rocks on both upper and lower contacts consist of black, siliceous argillite. The barite horizon occurs in the lowermost part of the upper member of the Mount Aho formation; within metres, the black siliceous argillite changes to interbedded maroon and green chert and argillite.

#### SAMPLE 98LP069

Sample 98LP069 was collected from an interbedded sequence of barite and light creamy white weathering chert and siliceous argillite (Fig 3) on a small ridge at the south end of Rose Mountain. Bedding dips 20 degrees to the northwest, and this horizon can be traced laterally, with discontinuous occurrences along strike for up to 5 km. The baritic horizon is at least 10 m thick. It is underlain by a dark grey to black chert-pebble conglomerate with abundant clasts of grey and black chert and overlain by a dark, dull grey, fine siltstone to silty argillite. The horizon is located near the top of the upper member of the Mount Aho formation. Two conodont samples collected within short distances above and below this horizon (Fig. 4) returned Early Carboniferous ages (Orchard, 2000 in Pigage, 2004) with the upper sample being identified as Viséan.

Sulphur isotope analyses were completed at the G.G. Hatch Isotope Laboratories, University of Ottawa, Ottawa, Ontario. The two barite samples were crushed, mixed with a set ratio of copper-oxide and quartz powders, and combusted at 1100°C. The resulting gases produced were cryogenically separated using a -80°C ethanol bath and -200°C liquid nitrogen. The amount of SO<sub>2</sub> generated was measured as it was collected in a breakseal pyrex tube. SO<sub>2</sub> in the tube was analysed on a triple collector VG SIRA 12 mass spectrometer. Two calibrated internal barite standards were run at the same time as the Rose Mountain barite samples. The calibrated standards were used to normalize the Rose Mountain barite data by linear regression. Routine precision of the analyses was ±0.20‰ (2 standard deviations).

Results of the analyses are presented in Table 1. Isotopic compositions are reasonably consistent. Without multiple analyses from each sample location, it would be difficult to delineate the range in δ<sup>34</sup>S for a particular horizon.

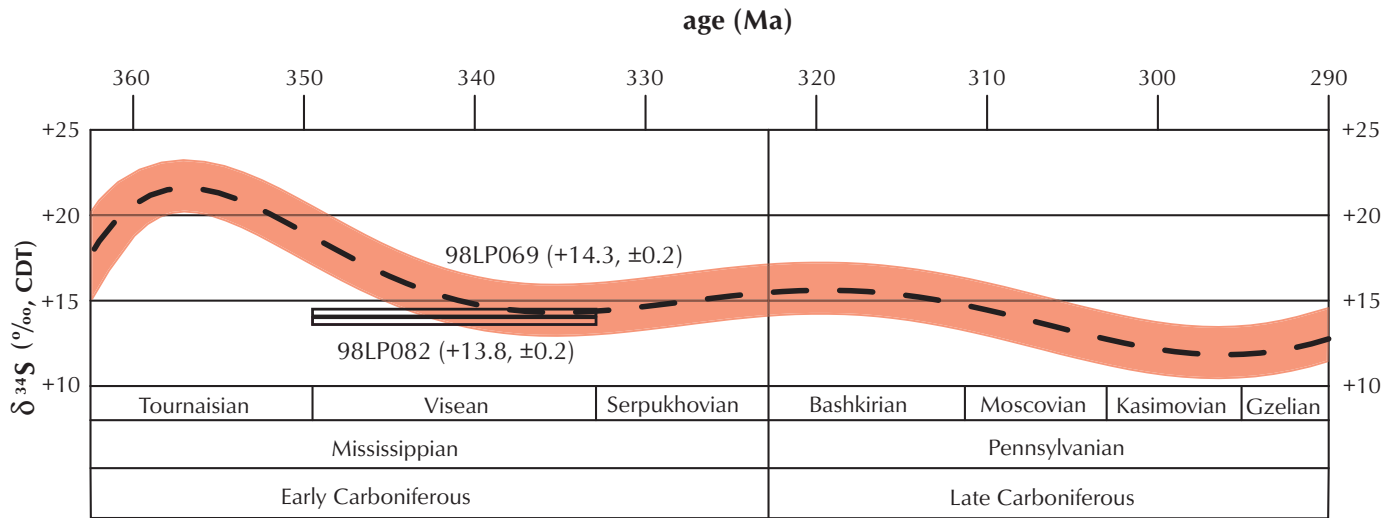


**Figure 6.** Carboniferous isotopic sulphate composition for ambient seawater. Measured sulphate values for barite samples shown assuming Viséan age. Modified from Kampschulte et al. (2001) using geologic time scale from Harland et al. (1990). Black rectangles=Rose Mountain samples with associated error, black dashed line=carboniferous seawater curve; thick, shaded line=error spread on curve.

## DISCUSSION AND CONCLUSION

Kampschulte et al. (2001) recently published a detailed  $\delta^{34}\text{S}$  curve for Carboniferous seawater (Fig. 6). The sulphur isotope variation is based on measured trace sulphate compositions within brachiopod fossils. The time scale of Harland et al. (1990) was used to translate fossil zones to absolute ages for tracking the sulphur isotope variation with time. Kampschulte et al. (2001) do not give an estimated error for their  $\delta^{34}\text{S}$  curve; visual inspection of their data points indicate an estimated spread of  $\pm 1.5\text{‰}$ , which incorporates all of the spread in the sample data points. This “error” spread is indicated in Figure 6 as the shaded area around the calibrated curve.

The measured  $\delta^{34}\text{S}$  values for the Rose Mountain barite samples are also shown in Figure 6. The Rose Mountain barites have  $\delta^{34}\text{S}$  values consistent with the calibrated values of coeval dissolved seawater sulphate during Viséan (and Serpukhovian) time. When combined with the Early Carboniferous (Viséan?) age from the conodont assemblages, these results indicated that ambient, oxygenated seawater is a reasonable source for the sulphate in the barite.

Stratiform massive barite deposits form as chemical sediments, either from hydrothermal fluids or from diagenetic or cold-seep fluids (Paradis et al., 1998; Koski and Hein, 2003). Hydrothermal barite is commonly

associated with sulphide minerals (pyrite, galena, sphalerite), and commonly forms a zoned deposit with sulphide minerals being vent-proximal and barite being distal. Depositional environment is shallow- to deep-water and occurs within intracratonic or continental margin, fault-controlled marine basins. Sulphur isotope composition of barite precipitated at  $21^\circ\text{N}$ , at the East Pacific Rise, is the same as that of ambient seawater sulphate, and indicates the source of sulphur for barite deposition is seawater sulphate (Zierenberg et al., 1984). Lydon et al. (1985) argued from solubilities of barite, calcite, sphalerite, quartz and amorphous silica that Devonian-Mississippian sulphide-absent barite deposits in Selwyn Basin precipitated from lower temperature hydrothermal fluids ( $100^\circ\text{C}$  formational waters) relative to sulphide-bearing barite deposits ( $>200^\circ\text{C}$  formational waters).

Diagenetic or cold-seep barite deposits are thought to result from precipitation of barite at an anoxic-oxygenated seawater interface. An oxygenated-anoxic interface may develop locally in the sub-seafloor or may develop as a result of stratification of a marine basin with reduced waters at the ocean floor in the basin and oxygenated waters occurring higher in the water column. Barium remains in solution in the reduced waters, but precipitates when exposed to overlying or nearby oxygenated waters. Inversion of stratified basin waters would provide a

mechanism for mixing of fluids and formation of extensive barite deposits. Sulphur isotope compositions of barite from these deposits is commonly heavier than contemporaneous seawater sulphate, due to the isotope fractionation associated with bacterial reduction of sulphate in the reduced anoxic seawater. Goodfellow and Jonasson (1986) noted that in Lower Paleozoic Selwyn Basin, barite  $\delta^{34}\text{S}$  values are heavier by +2‰ to +20‰ relative to contemporaneous seawater sulphate. They attributed these heavier values to anoxic, stratified basinal waters which periodically underwent inversion with subsequent rapid deposition of barite. Cecile et al. (1983) noted that barite deposits with heavy  $\delta^{34}\text{S}$  values in the western Canada Cordillera were from thin or nodular barite deposits in organic-rich sediments. They hypothesized a cycling barite precipitation-dissolution-precipitation process in a zone encompassing both reducing and oxidizing conditions. Some of the released sulphate during the dissolution process is bacterially reduced to hydrogen sulphide, thereby fractionating the remaining sulphate to heavier  $\delta^{34}\text{S}$  values.

The preliminary  $\delta^{34}\text{S}$  values of +14.3‰ and +13.8‰ for Rose Mountain barites (2 samples) indicates that ambient seawater is the most probable source of sulphate in the barite. Further, the  $\delta^{34}\text{S}$  values from the barite are not more positive than contemporaneous seawater sulphate, suggesting that the barite did not precipitate as a result of diagenetic oxidation-reduction reactions or inversion of anoxic, stratified basin waters. The measured  $\delta^{34}\text{S}$  values therefore suggest the alternative process of precipitation of barite from mixing of low-temperature, sulphate-poor hydrothermal fluids with ambient seawater.

Physical characteristics of the barite horizons are inconclusive. The 5-km lateral extent for the upper horizon suggests barite precipitation is not occurring at a single vent source, and perhaps is occurring at a basin-wide change in barium solubility. The absence of visible organic material (creamy tan colour) of the immediate host for the barite horizons points to local oxygenated conditions or alteration in a more general reducing basin (black cherts and argillites).

Lydon et al. (1985) suggested that stratiform barite deposits and barite-sulphide deposits within Selwyn Basin both formed from exhalation of hydrothermal fluids at the sea floor, with sulphide-bearing deposits precipitating from higher temperature fluids sourced from deeper levels of the crust. The deposit models for these two

types of stratiform barite have the same processes involved in their genesis. The occurrence of stratiform barite deposits in Selwyn Basin therefore indicates that genetic parameters are also broadly appropriate for the presence of stratiform barite-sulphide deposits in other parts of Selwyn Basin. Similarly, the presence of barite deposits in the Rose Mountain area indicates that the Slide Mountain stratigraphy is a viable exploration target for barite-sulphide deposits, as well as barite deposits.

It must be remembered that these results are preliminary and are based on only two  $\delta^{34}\text{S}$  measurements. For more rigorous determination of depositional environment and possible source areas for barium-rich fluids, barite should be more extensively sampled for sulphur isotope studies to verify continued correspondence to coeval seawater sulphate. Chemical analysis of the barite samples and determination of Sr isotope ratios further help distinguish between different types of barite (Paytan et al., 2002).

## ACKNOWLEDGEMENTS

Jason Adams provided field assistance with the 1998 field work. Helicopter transport was supplied by Trans North Air based out of Ross River. Discussion of Rose Mountain outcrops with Gregg Jilson, Maurice Colpron, Don Murphy and Steve Gordey has been a continuing adventure. This article was reviewed by Grant Abbott.



## REFERENCES

- Cecile, M.P., Shakur, M.A. and Krouse, H.R., 1983. The isotopic composition of western Canadian barites and the possible derivation of oceanic sulphate  $\delta^{34}\text{S}$  and  $\delta^{18}\text{O}$  age curves. *Canadian Journal of Earth Sciences*, vol. 20, p. 1528-1535.
- Claypool, G.E., Holser, W.T., Kaplan, I.R., Sakai, H. and Zak, I., 1980. The age curves of sulphur and oxygen isotopes in marine sulphate and their mutual interpretation. *Chemical Geology*, vol. 28, p. 199-260.
- Creaser, R.A., Goodwin-Bell, J.S. and Erdmer, P., 1999. Geochemical and Nd isotopic constraints for the origin of eclogite protoliths, northern Cordillera: implications for the Paleozoic tectonic evolution of the Yukon-Tanana Terrane. *Canadian Journal of Earth Sciences*, vol. 36, p. 1697-1709.
- Deklerk, R. and Traynor, S., 2004. Yukon MINFILE – A database of mineral occurrences. Yukon Geological Survey, CD-ROM.
- Faure, G. and Mensing, T., 2005. *Isotopes, Principles and Applications*, third edition. John Wiley & Sons, Inc., Hoboken, New Jersey, 897 p.
- Franzen, J.P., 1978. Geological Report, Urn Claim Group. Unpublished assessment report #090345. Energy, Mines and Resources, Yukon government.
- Goodfellow, W.D. and Jonasson, I.R., 1984. Ocean stagnation and ventilation defined by  $\delta^{34}\text{S}$  secular trends in pyrite and barite, Selwyn Basin, Yukon. *Geology*, vol. 12, p. 583-586.
- Gordey, S.P., 1990. Geology of Mount Atherton (105K/4), Rose Mountain (105K/5), and Mount Mye (105K/6) map areas, Yukon Territory. Geological Survey of Canada, Open File 2250 (1:50 000 scale).
- Gordey, S.P. and Irwin, S.E.B., 1987. Geology, Sheldon Lake and Tay River map areas, Yukon Territory. Geological Survey of Canada, Map 19-1987 (3 sheets) (1: 250 000 scale).
- Harland, W.B., Armstrong, R.L., Cox, A.V., Craig, L.E., Smith, A.G. and Smith, D.G., 1990. *A geologic time scale 1989*. Cambridge University Press, Cambridge, United Kingdom, 263 p.
- Jennings, D.S. and Jilson, G.A., 1986. Geology and sulphide deposits of Anvil Range, Yukon. *In: Mineral Deposits of Northern Cordillera*, J.A. Morin (ed.), Canadian Institute of Mining and Metallurgy, Special Volume 37, p. 319-361.
- Kampschulte, A., Bruckschen, P. and Strauss, H., 2001. The sulphur isotopic composition of trace sulphates in Carboniferous brachiopods: implications for coeval seawater, correlation with other geochemical cycles and isotope stratigraphy. *Chemical Geology*, vol. 175, p. 149-173.
- Koski, R.A. and Hein, J.R., 2003. Stratiform barite deposits in the Roberts Mountains allochthon, Nevada: a review of potential analogs in modern sea-floor environments. United States Geological Survey, Bulletin 2209-H, 17 p.
- Lydon, J.W., Goodfellow, W.D. and Jonasson, I.R., 1985. A general genetic model for stratiform baritic deposits of the Selwyn Basin, Yukon Territory and District of Mackenzie. Geological Survey of Canada, Paper 85-1A, p. 651-660.
- Orchard, M.J., 2000. Report on conodonts and other microfossils, Tay River (105K), 12 samples (5 productive) collected by L. Pigage, Yukon Geoscience Office. Geological Survey of Canada, Report MJO-2000-3, 5 p.
- Paradis, S., Simandl, G., MacIntyre, D. and Orris, G.J., 1998. Sedimentary-hosted, stratiform barite. *In: Geological Fieldwork 1997*, British Columbia Ministry of Employment and Investment, Paper 1998-1, p. 24F-1 to 24F-4.
- Paytan, A., Kastner, M., Campbell, D. and Thiemens, M.H., 1998. Sulphur isotopic composition of Cenozoic seawater sulphate. *Science*, vol. 282, p. 1459-1462.
- Paytan, A., Mearon, S., Cobb, K. and Kastner, M., 2002. Origin of marine barite deposits: Sr and S isotope characterization. *Geology*, vol. 30, p. 747-750.
- Pigage, L.C., 1999. Preliminary geology of Rose Mountain, Anvil District, central Yukon (105K/05). *In: Yukon Exploration and Geology 1998*, C.F. Roots and D.S. Emond (eds.), Exploration and Geological Services Division, Yukon Region, Indian and Northern Affairs Canada, p. 91-103.
- Pigage, L.C., 2004. Bedrock geology compilation of the Anvil District (parts of NTS 105K/2, 3, 5, 6, 7 and 11), central Yukon. Yukon Geological Survey, Bulletin 15, 103 p.

- Read, W.S., 1982. Report on URN barite property. Unpublished assessment report #091369. Energy, Mines and Resources, Yukon government.
- Roddick, J.A. and Green, L.H., 1961. Tay River, Yukon Territory. Geological Survey of Canada, Map 13-1961, 1:253 440 scale.
- Strauss, H., 1997. The isotopic composition of sedimentary sulphur through time. *Palaeogeography, Palaeo-climatology, Palaeoecology*, vol. 132, p. 97-118.
- Tempelman-Kluit, D.J., 1972. Geology and origin of the Faro, Vangorda, and Swim concordant zinc-lead deposits, central Yukon Territory. Geological Survey of Canada, Bulletin 208, 1:125 000 scale, 73 p.
- Tempelman-Kluit, D.J., 1979. Transported cataclasite, ophiolite and granodiorite in Yukon: Evidence of arc-continent collision. Geological Survey of Canada, Paper 79-14, 27 p.
- Wheeler, J.O., Brookfield, A.J., Gabrielse, H., Monger, J.W.H., Tipper, H.W. and Woodsworth, G.J., 1991. Terrane Map of the Canadian Cordillera. Geological Survey of Canada, Map 1713A, 1:2 000 000 scale.
- Zierenberg, R.A., Shanks, W.C. III and Bischoff, J.L., 1984. Massive sulfide deposits at 21°N, East Pacific Rise: Chemical composition, stable isotopes, and phase equilibria. *Geological Society of America Bulletin*, vol. 95, p. 922-929.

# Structural evolution of the Tally Ho shear zone (NTS 105D), southern Yukon

*Amy Tizzard and Stephen Johnston<sup>1</sup>*

*University of Victoria*

Tizzard, A. and Johnston, S., 2005. Structural evolution of the Tally Ho shear zone (NTS 105D), southern Yukon. *In: Yukon Exploration and Geology 2004*, D.S. Emond, L.L. Lewis and G.D. Bradshaw (eds.), Yukon Geological Survey, p. 237-246.

## **ABSTRACT**

The Tally Ho shear zone is located along the western boundary of the Whitehorse Trough in southern Yukon, and separates the Stikine Terrane to the east and the Nisling Assemblage to the west. Complex geologic structures, Jurassic and Cretaceous plutonism and abundant Tertiary volcanism obscure the nature of this boundary and its relation to adjacent terranes. Pyroxenite, gabbro, marble, and highly strained volcanoclastic rocks form a 3-km-wide belt that is in intrusive- and fault-contact with megacrystic granite and granodiorite, respectively. Structural relations in the field indicate that the ultramafic rocks in the Tally Ho shear zone are allochthonous, and have been thrust to their present position and subsequently folded in the Early Jurassic. Younger brittle and semi-brittle faulting occurred along the Llewellyn fault in the Late Cretaceous.

## **RÉSUMÉ**

La zone de cisaillement Tally Ho est située le long de la limite ouest du bassin de Whitehorse, au sud du Yukon, et sépare le terrane de Stikine, à l'est, du terrane de Nisling, à l'ouest. Des structures géologiques complexes, un plutonisme du Jurassique et du Crétacé, et un abondant volcanisme du Tertiaire rendent moins évidente la nature de cette limite et sa relation avec les terranes adjacents. De la péridotite, du gabbro, du marbre et des roches volcanoclastiques très déformées forment une ceinture, atteignant 3 km de largeur au contact intrusif et de faille, respectivement avec du granite mégacristallin et de la granodiorite. Les relations structurales sur le terrain indiquent que les roches ultramafiques dans la zone de cisaillement Tally Ho sont allochtones et ont été charriées jusqu'à leur position actuelle et plissées par la suite, au Jurassique précoce. Il y a eu par la suite formation plus récente de failles cassantes et semi-cassantes le long de la faille de Llewellyn, au Crétacé tardif.

<sup>1</sup>stj@uvic.ca



## INTRODUCTION

The Tally Ho shear zone (THSZ) is a 40-km-long zone of highly strained rocks along the western margin of the Whitehorse Trough in southern Yukon, first recognized by Hart and Radloff (1990). The deformed belt of rocks is 3 km wide and separates the Stikine Terrane to the east from Nisling Assemblage rocks of the Yukon-Tanana Terrane to the west (Fig. 1). The Tally Ho shear zone passes through the Wheaton valley area and is accessible via the Annie Lake Road off of the Klondike Highway near Carcross (Fig. 2). Mineral exploration trails provide access

to much of the study area (parts of NTS map sheets 105 D/2, 3, 6 and 7).

The THSZ is well exposed at Tally Ho Mountain where it is characterized by northwest-trending belts of heterogeneously strained volcanic and volcanoclastic rocks, gabbro and pyroxenite, and various massive intrusive bodies (Fig. 3). Hart and Radloff (1990) interpreted the THSZ as having experienced at least two phases of deformation: 1) Late Triassic sinistral ductile shear; and 2) mid-Cretaceous and younger dextral brittle shear. An interesting feature of the shear zone is a small (1700 x 600 m) body of pyroxenite. Wheeler (1961) suggested three possible mechanisms for the origin of the pyroxenite: 1) an intrusion that was folded with the surrounding rocks; 2) an allochthonous sheet that was folded with the surrounding rocks after emplacement; or 3) a syn-kinematic pluton that intruded during mid-Cretaceous folding. This paper presents additional structural relationships in the THSZ to that of Hart and Radloff (1990) and suggests a mechanism for the emplacement of the ultramafic rocks on Tally Ho Mountain.

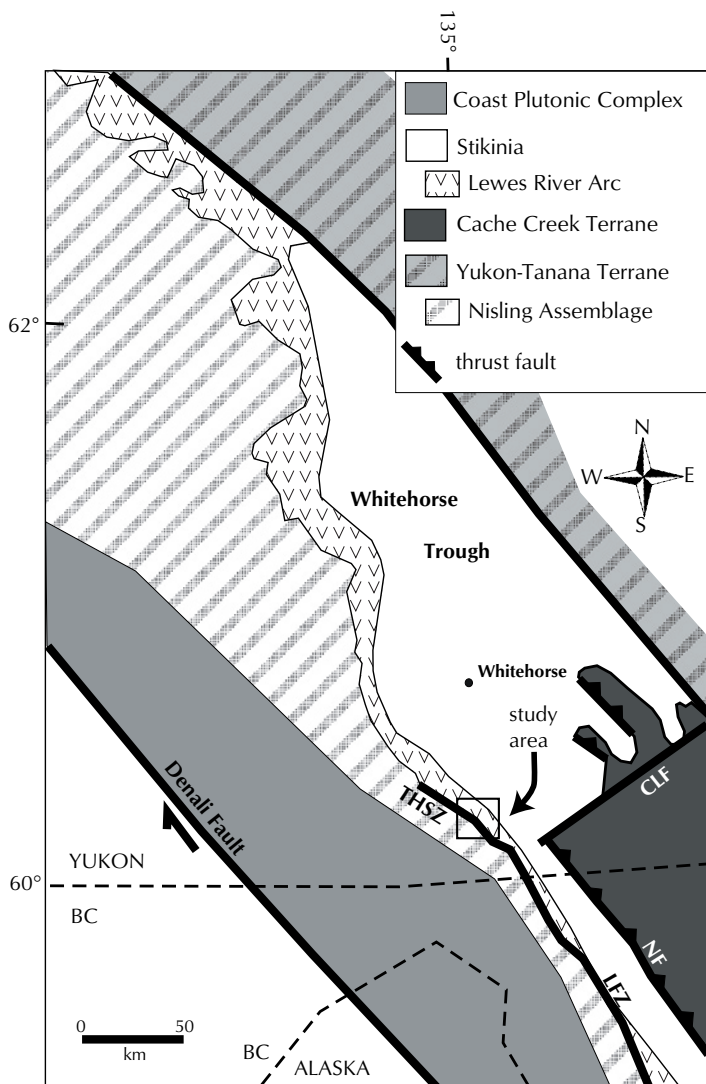


**Figure 1.** Simplified tectonic boundaries of southern Yukon showing location of the Tally Ho shear zone (THSZ) and Llewellyn fault zone (LFZ) and their relation to the Nisling Assemblage (of Yukon-Tanana Terrane), Stikinia and Cache Creek Terrane. CLF = Crag Lake fault; NF = Nahlin fault. Modified after Wheeler and McFeeley (1991).

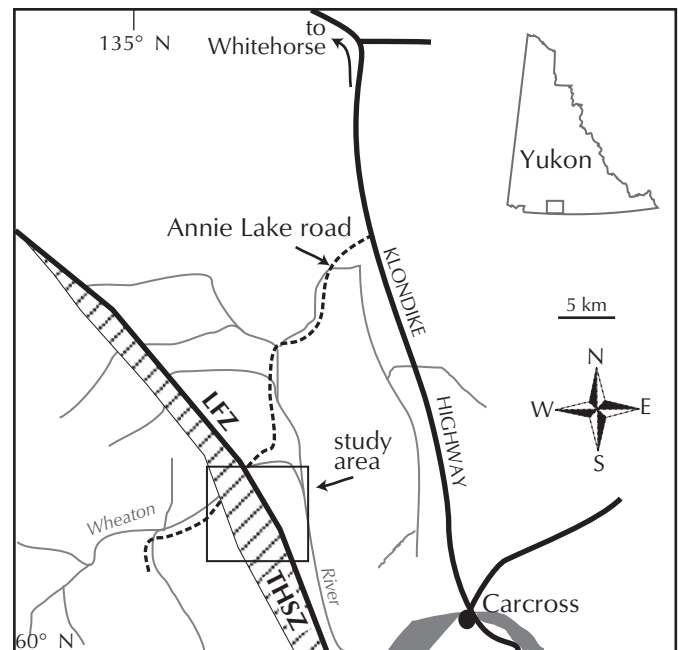


**Figure 2.** Access to the Tally Ho shear zone (THSZ) and Llewellyn fault zone (LFZ) via the Annie Lake Road.

## REGIONAL TECTONIC FRAMEWORK

The THSZ lies within the northern part of the Intermontane Superterrane, an amalgamation of the Stikine, Cache Creek, and Quesnel terranes (Gabrielese et al., 1991; Gordey and Makepeace, 2001). The Whitehorse Trough is part of Stikinia (Fig. 1) and consists, in part, of a Late Triassic to mid-Jurassic onlap assemblage of immature sedimentary rocks derived from middle to Late Triassic volcanic rocks of the Lewes River Group and Joe Mountain volcanics to the east (Hart, 1995). The clastic sedimentary sequence and associated reefal carbonates of the Lewes River Group may host significant oil and gas reserves (Lowey, 2004; English et al., 2005). The Lewes River Group volcanic rocks and the Whitehorse Trough strata underlie much of the THSZ.

Approximately 20 km east of the THSZ, the Cache Creek Terrane is juxtaposed with Stikinia along a number of southwest-vergent thrust faults and normal faults (Fig. 1). The Cache Creek Terrane consists of Lower Carboniferous to Middle Jurassic rocks of oceanic affinity and is interpreted to have been thrust southwestwards over Stikinia by the Middle Jurassic (Monger et al., 1991).

West of Stikinia, the Nisling Assemblage is part of the pericratonic Yukon-Tanana Terrane, and is characterized by Proterozoic to Paleozoic metasedimentary rocks (Johnston et al., 1996). The Stikinia/Yukon-Tanana Terrane boundary in southwest Yukon has been interpreted as the Tally Ho shear zone. Plutons of the Long Lake Suite intruded and pinned together the Yukon-Tanana and Stikine terranes by the Early to Middle Jurassic (Johnston et al., 1996; Hart, 1997). The Llewellyn fault zone (LFZ), a kilometre-wide north-trending zone of semi-brittle fracturing that affects rocks as young as mid-Cretaceous age, overprints and further complicates the Stikinia/Yukon-Tanana boundary. The style of deformation in the THSZ and LFZ is commonly obscured by younger structures, Jurassic and Cretaceous plutons, and Tertiary volcanic rocks.

## MAJOR LITHOLOGICAL UNITS IN THE TALLY HO MOUNTAIN AREA

The THSZ and associated rocks are well exposed on the four mountains that make up the Tally Ho massif: Tally Ho Mountain, Wheaton Mountain, Mt. Stevens and Dickson Hill (Fig. 3). The majority of the study area is composed of heterogeneously strained volcanic and volcanoclastic rocks and several bodies of intrusive rocks.

## LEWES RIVER GROUP

Rocks of the Tally Ho shear zone are mainly part of the Upper Triassic Lewes River Group (Wheeler, 1961; Hart and Radloff, 1990). Regionally, the Lewes River Group consists of dominantly volcanic Povoas formation overlain by sedimentary Aksala formation (Hart, 1997). In the study area, the Lewes River Group is composed of a variably strained tuffaceous and volcanoclastic sequence referred to as the Annie Member, consisting of massive augite-phyric basalt, tuff, marble and associated volcanoclastic rocks. The Annie Member occurs on Dickson Hill and is characterized by dark reddish brown- to green-weathering, medium- to fine-grained, massive tuff. Massive augite-phyric dark grey-weathering basalt exists on Tally Ho Mountain and Dickson Hill and is distinguished by black augite phenocrysts up to one centimetre in diameter. The basalt weathers dark greenish grey and is dark grey on fresh surfaces. Chlorite alteration is common.

Marble and variably strained volcanic and volcanoclastic rocks are intercalated on Tally Ho Mountain. The buff-weathering marble is white on fresh surfaces and exhibits a pervasive flaggy fabric. Highly strained volcanic and volcanoclastic rocks are characterized by a mylonitic to gneissic fabric with distinct, black augite porphyroclasts (Fig. 4) up to one centimetre in diameter. The augite-porphycroclastic schist weathers dark greenish grey and is dark grey on fresh surfaces. Away from the high strain zone, small clasts and relict bedding are visible in lesser strained volcanoclastic rocks. Both the highly strained and



**Figure 4.** Rotated augite porphyroclasts in augite schist on Dickson Hill indicating top-to-the-east displacement.

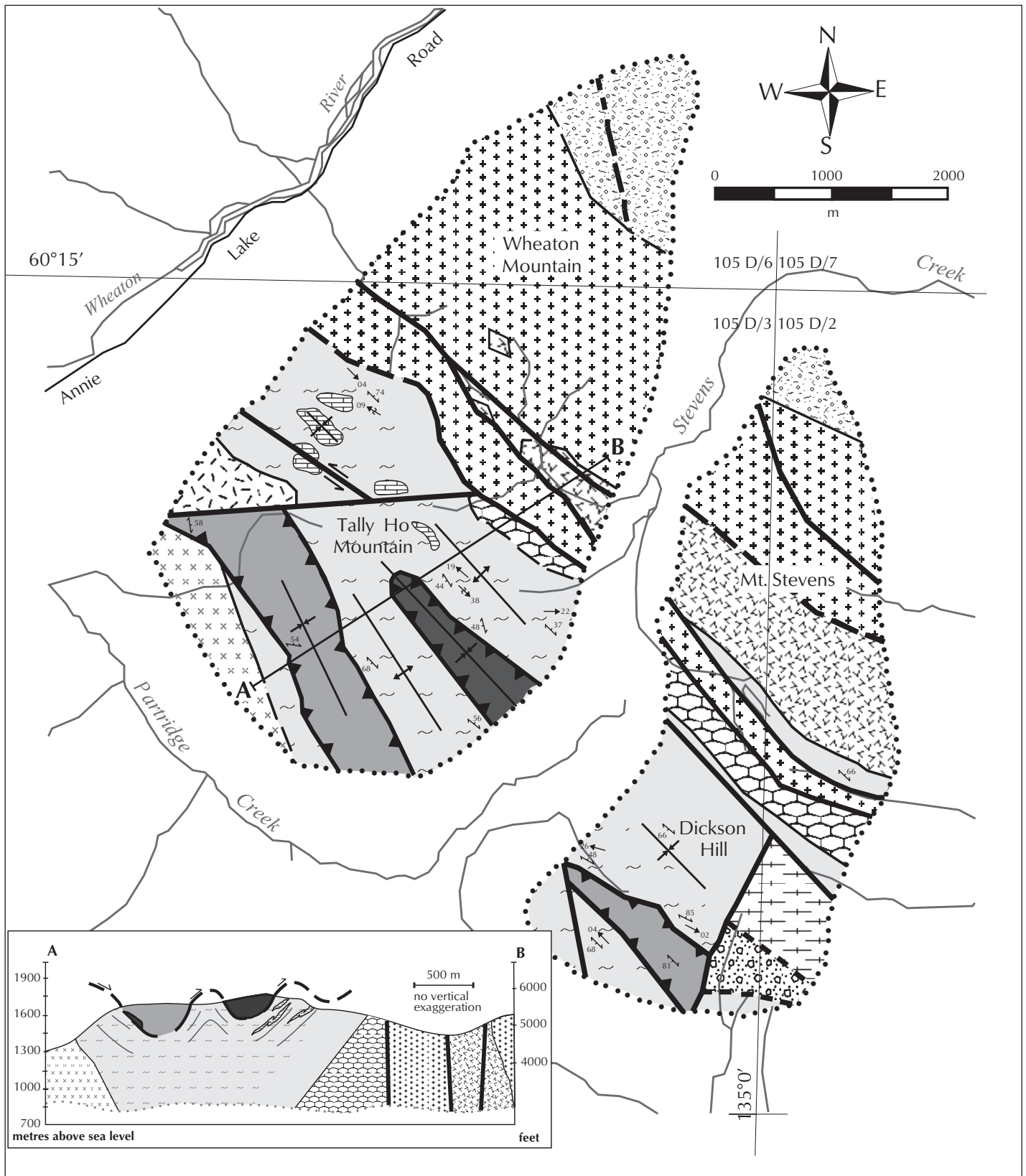


**Figure 3.** Geological map of the Tally Ho Mountain area; geologic cross-section of Tally Ho Mountain, A-B. Legend on facing page. Modified after Hart (1997).



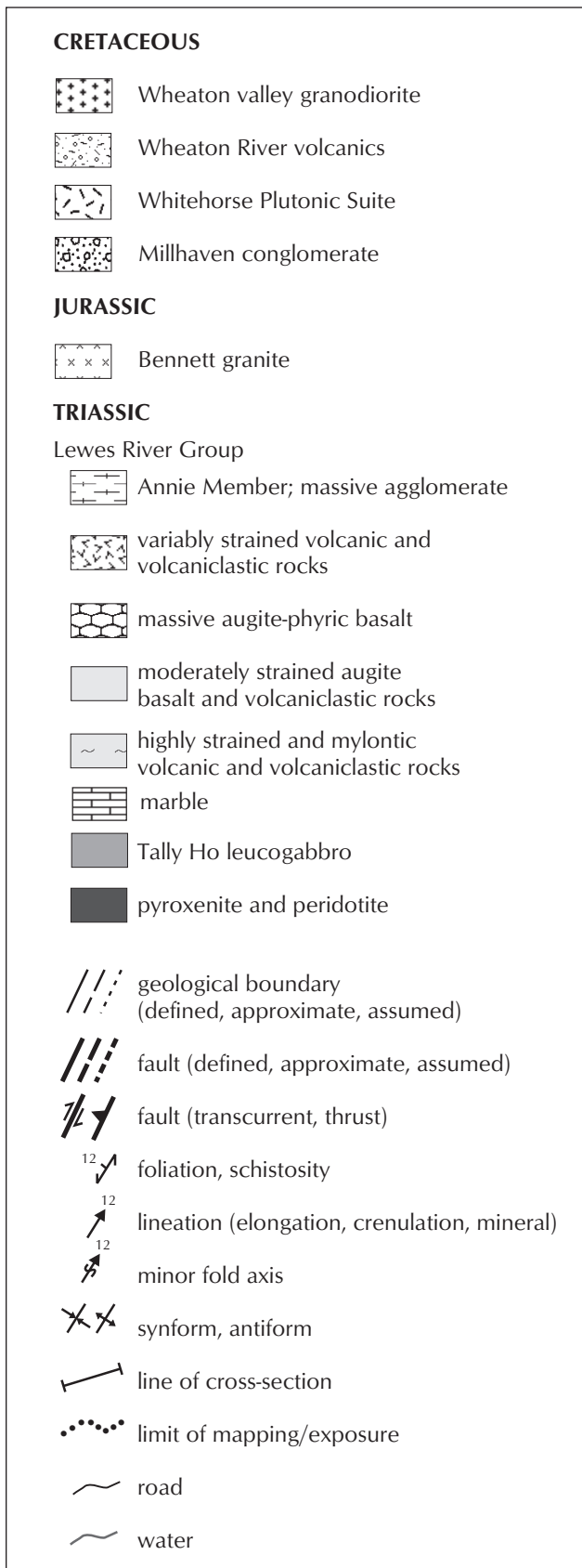


Figure 3. Legend.



Figure 5. Coarse-grained and mottled appearance of the Tally Ho leucogabbro on Tally Ho Mountain.

less strained rocks weather greenish grey and exhibit chlorite alteration in the THSZ.

Gabbro and pyroxenite occur on Tally Ho Mountain and Dickson Hill and, based on a U-Pb age date of  $213.8 \pm 0.6$  Ma on Tally Ho gabbro (Hart, 1995), likely belong to the Lewes River Group. The Tally Ho leucogabbro (Hart and Radloff, 1990) is a mottled dark green, black and white, medium- to very coarse-grained plagioclase-hornblende gabbro that is weakly to moderately well foliated (Fig. 5). The leucogabbro is weakly to moderately well foliated and has been intruded by the Bennett granite. A massive, variably serpentinized body of pyroxenite and peridotite forms a resistant, blocky ridge line on the top of Tally Ho Mountain. The massive to well foliated ultramafic rock weathers dark greyish brown and is medium- to coarse-grained. Chrysotile and magnetite can be found in veinlets within the pyroxenite. The gabbro and pyroxenite are likely part of the same body as suggested by interlaying of gabbro and pyroxenite on the western flank of Tally Ho Mountain. Although the gabbro and pyroxenite are included within the Lewes River Group, this is speculative and future work will examine the origin of these rocks.

## BENNETT GRANITE

The massive coarse-grained and megacrystic Bennett granite occurs in the westernmost part of the map area where it intrudes augite-schist and foliated gabbro (Fig. 6). The light grey-weathering granite is characterized by



**Figure 6.** Intrusive contact between the Bennett granite (BG) and foliated Tally Ho leucogabbro (THL) on Tally Ho Mountain.

potassium-feldspar megacrysts up to 2 cm in length, and contains less than 10% mafic minerals. The Bennett batholith is believed to be Early Jurassic in age, based on U-Pb dates of the felsic phase of the intrusion and age dates of other phases comprising this polyphase batholith (Hart, 1995). The Bennett granite in the study area is likely a phase of this batholith. Future U-Pb zircon geochronological analysis of the granite will provide further constraints on the age of crystallization.

### MILLHAVEN CONGLOMERATE

A dark reddish brown-weathering, massive, polymictic orthoconglomerate outcrops on Dickson Hill. Clasts of quartz, quartzite, schist, granite, chert and volcanic rock (Hart and Radloff, 1990) are up to 6 cm in diameter and are subangular to subrounded. The formation appears to be in fault-contact with all other units in the study area.

### WHEATON RIVER VOLCANICS

The easternmost study area is underlain by pale green to grey massive volcanic and volcanoclastic rocks that are in intrusive-contact with the Wheaton valley granodiorite (Fig. 3). On Wheaton Mountain, the rocks are typically green-grey-weathering and tuffaceous. On Mt. Stevens, the Wheaton River volcanics are represented by dark grey,



**Figure 7.** Mafic xenolith cross-cut by small aplite dyke in the mid-Cretaceous Whitehorse Suite on Tally Ho Mountain.

massive, phenocrystic basalt, andesite and lapilli tuff. A weakly developed planar depositional flow fabric is locally developed in volcanic rocks on Wheaton Mountain.

### WHEATON VALLEY GRANODIORITE

Medium- to coarse-grained xenolithic Wheaton valley granodiorite and diorite make up most of Wheaton Mountain and part of Mt. Stevens (Fig. 3). An intrusive- and fault-contact relationship exists with rocks of the Lewes River Group. The granodiorite is medium-grained, equigranular and locally characterized by a magmatic fabric. Variably chloritized hornblende and biotite account for up to 30% of the rock. A U-Pb zircon age of 78 Ma was obtained (Hart, 1995).

### WHITEHORSE PLUTONIC SUITE

An undeformed, buff-weathering, medium-grained and equigranular granitic stock of the Cretaceous Whitehorse Plutonic Suite is in fault- and intrusive-contact with strained rocks on Tally Ho Mountain (Fig. 3). This rock is characterized by pink-weathering potassium-feldspar crystals, up to 5% mafic minerals and xenoliths. Associated pink aplitic dykes up to 60 cm wide are offset by small north-trending faults (Fig. 7).



## YOUNGER VOLCANISM

Numerous rhyolite, basalt and porphyry intrusions cross-cut the geologic trend of the shear zone throughout the study area. These small intrusions are dominantly undeformed and are believed to be related to the Late Cretaceous to Eocene Mount Skukum Volcanic Complex, Bennett Lake Caldera Complex and the Wheaton River volcanics (Hart and Radloff, 1990).

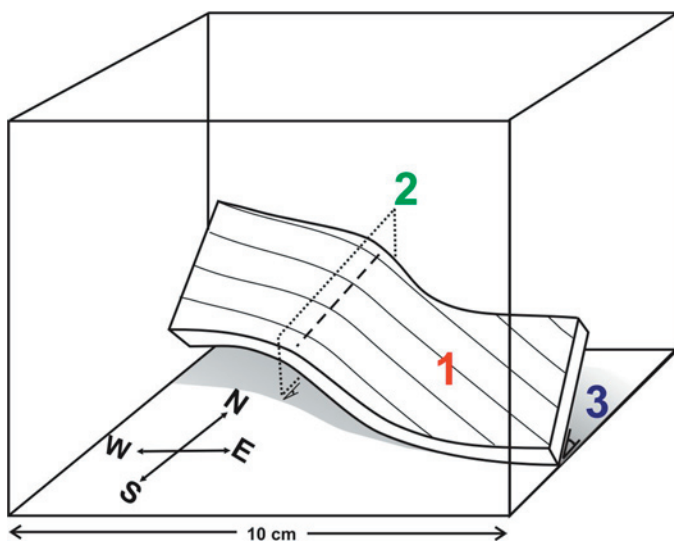


**Figure 8.** Schematic diagram showing the relationship between lineations (1), crenulations (2) and foliation (3) in mylonitic rocks on Tally Ho Mountain.



**Figure 9.** East-vergent crenulations in mylonite on Tally Ho Mountain.

## STRUCTURE

Two structural domains, the THSZ and the LFZ, each characterized by a distinct structural style, are recognized in the study area. The Llewellyn fault is a younger event that overprinted structures of the THSZ, resulting in steep brittle to brittle-ductile deformation in the Late Cretaceous or younger. The THSZ is moderately inclined and decreases in strain beneath and to the east of the highly strained volcanoclastic rocks at the summit of Tally Ho Mountain.

## TALLY HO SHEAR ZONE

The Tally Ho shear zone is a zone of highly strained, northwest-trending gneissic to mylonitic rocks (Fig. 8). Lineations developed on the foliation surface dominantly plunge shallowly to the southeast, however, many also trend shallowly to the northwest. Variations in foliation measurements on Dickson Hill and Tally Ho Mountain indicate that the shear zone fabric is folded. Crenulations of the schistose and mylonitic fabric verge predominantly east (Fig. 9), likely mimicking the larger fold structure. Fold axes on Tally Ho Mountain plunge shallowly to moderately to the southeast. The majority of observed rotated augite porphyroclasts and extensional shears (Fig. 10) indicate a top-to-the-east sense of shear.

On the eastern flank of Tally Ho Mountain, fabric development and strain in volcanic and volcanoclastic rocks decreases easterly from mylonitic to weakly foliated at structurally deeper levels beneath the shear zone. The decrease in strain is interpreted as being a transition from



**Figure 10.** Extensional  $C'$  shears in mylonite on Tally Ho Mountain. The sense of movement indicated by the shears is top-down and to the east. Pencil parallels  $C$  fabric.





**Figure 11.** East-vergent duplex structures repeating marble (m) and mylonite (my) on the north face of Tally Ho Mountain.

the THSZ to less-strained volcanoclastic and volcanic rocks of the Lewes River Group cropping out beneath the shear zone (cross-section in Fig. 3).

A thrust fault on Tally Ho Mountain juxtaposes the Tally Ho leucogabbro and associated ultramafic rocks, which occur within and above the shear zone, against volcanic and volcanoclastic rocks that lie in and below the shear zone. Pyroxenite and leucogabbro are, in general, less strained than the underlying volcanoclastic rocks. Partitioning of strain into the volcanoclastic rocks may have occurred due to their finer grained, more siliceous nature. No evidence of contact metamorphism was found



**Figure 12.** Tension gashes in granodiorite indicating post mid-Cretaceous sinistral brittle deformation on Mt. Wheaton.

in the mylonite to indicate an intrusive origin of the pyroxenite. The lack of any evidence of intrusion of the gabbro or pyroxenite, coupled with the observed high-strain rocks along the contact with the volcanoclastic succession (mylonite), indicates that the pyroxenite and leucogabbro were tectonically emplaced above the volcanoclastic rocks along the THSZ. On the north face of Tally Ho Mountain a series of duplex structures stacking mylonite and marble indicates an apparent eastward vergence (Fig. 11). The duplex structures measure 2 m and greater in cross-section and may reflect the sense of movement of the larger thrust fault on Tally Ho Mountain.

### LLLEWELLYN FAULT ZONE

The Lllewellyn fault zone (LFZ) is characterized by a number of fault splays that isolate and surround less strained fault bound blocks. Fault splays commonly trend northwest and cut all lithological units in the area, and locally appear to have exploited lithological boundaries. For example, the western contact of the Wheaton valley granodiorite with the Tally Ho shear zone is fractured and faulted, as is the intrusive contact between volcanic rocks and the granodiorite between Tally Ho and Wheaton mountains. Displacement along the fault splays is variable, changing from dextral strike-slip to dip-slip, as indicated by movement indicators in the field such as slickensides and slickenlines. Tension gashes and Reidel shears on

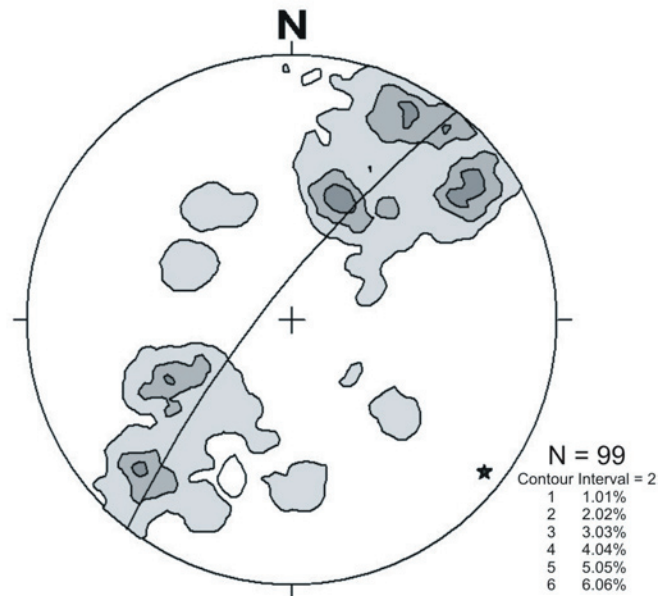


**Figure 13.** Contoured stereoplot of poles to foliation measurements in schistose and mylonitic rocks on Tally Ho Mountain and Dickson Hill. Star = pole to girdle.

Mt. Wheaton and Mt. Stevens imply sinistral strike-slip displacement (Fig. 12). Variable displacement vectors may indicate multiple displacement events along the LFZ.

### STEREOPLOT ANALYSIS

An analysis of fabrics, lineations and fault orientation data using lower hemisphere equal-angle stereoplots was carried out using the methods of Woodcock and Naylor (1983), Lin and Williams (1992), and Ramsay and Huber (1987). Poles to foliation from the strained volcanoclastic and volcanic rocks on Tally Ho Mountain and Dickson Hill define a weak girdle pattern, consistent with folding about a shallowly southeast-plunging fold axis (Fig. 13). Lineations in the same area parallel the fold axis (Fig. 14).

### DISCUSSION AND INTERPRETATION

Ductile deformation that characterizes the THSZ post-dates deposition of the Upper Triassic Lewes River Group (which is highly strained within the shear zone), and pre-dates crystallization of the Early Jurassic Bennett granite since the granite intrudes Lewes River Group augite porphyroclastic schist and foliated leucogabbro. It is likely that folding of the THSZ occurred before the intrusion of the Bennett granite as the granite appears to cross-cut the folded shear zone. Thus the THSZ is probably an Early Jurassic structure. Discrete shears and brittle faults

observable in Cretaceous plutons in the study area constrain the timing of the LFZ to Late Cretaceous or younger. Multiple displacement events along the LFZ may explain the array of movement indicators.

Peridotite and leucogabbro were emplaced over the Lewes River Group volcanoclastic rocks within the THSZ. The thrust fault on Tally Ho Mountain likely carried the pyroxenite and leucogabbro in from the west, based on top-to-the-east vorticity of rotated porphyroclasts, extensional shears and east-trending elongation lineations. Potential sources of the mafic and ultramafic rocks in the THSZ are the Cache Creek Terrane to the east or, more likely, the exhumed roots of the Lewes River arc. Although the Cache Creek Terrane includes a significant volume of ultramafic and mafic rocks, the leucogabbro and pyroxenite are not characteristic of this terrane. Moreover, the timing of Stikinia-Cache Creek interaction post-dates the timing of the THSZ (Mihalnyuk et al., 2004; Ricketts et al., 1992). Alternatively, westerly derived garnet peridotite and ultra-high pressure rocks deposited in the Laberge Group of the Whitehorse Trough (MacKenzie et al., in press) suggests that rapid uplift and erosion of deep-seated rocks occurred during the Early Jurassic, which corresponds to the timing of the THSZ.

### SUMMARY

Ultramafic and gabbroic rocks of the Tally Ho shear zone are allochthonous, having been thrust to their present position and folded by the Early Jurassic. Timing of the THSZ is constrained by the age of crystallization of the Early Jurassic Bennett granite, which cross-cuts the shear zone. Late Cretaceous and younger brittle and semi-brittle faulting occurred along the Lllewellyn fault zone.

### ACKNOWLEDGEMENTS

A multitude of thanks goes to the Yukon Geological Survey for supporting this project and providing me with the necessary resources for the field season and beyond. Additional funding was provided by an NSERC Northern Research Internship and the University of Victoria. Thanks also goes to Craig Hart for valuable discussions and reviewing this paper. I would also like to thank Derek Turner, Fiona Keenan and Peter Green for their excellent assistance and entertainment in the field.

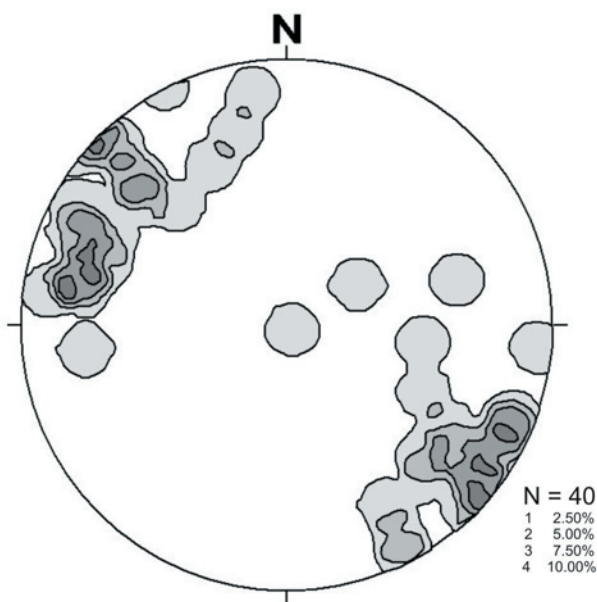


**Figure 14.** Contoured stereoplot of lineation measurements from Tally Ho Mountain and Dickson Hill.

## REFERENCES

- English, J.M., Johannson, G.G., Johnston, S.T., Mihalyuk, M.G., Fowler, M. and Wight, K.L., 2005. Structure, stratigraphy and hydrocarbon potential of the central Whitehorse Trough, northern Canadian Cordillera. *Bulletin of the Canadian Society of Petroleum Geology*, in press.
- Gabrielse, H., Monger, J.W.H., Wheeler, J.O. and Yorath, C.J., 1991. Part A. Morphogeological belts, tectonic assemblages, and terranes. *In: Chapter 2: Geology of the Cordilleran Orogen in Canada*, H. Gabrielse and C.J. Yorath (eds). Geological Survey of Canada, *Geology of Canada*, no. 4, p. 15-28.
- Gordey, S.P. and Makepeace, A.J., 2001. Bedrock geology, Yukon Territory. Geological Survey of Canada, Open File 3754, and Exploration and Geological Services Division, Yukon Region, Indian and Northern Affairs Canada, Open File 2001-1, 1:1 000 000 scale.
- Hart, C.J.R., 1995. Magmatic and tectonic evolution of the Intermontane Superterrane and Coast Plutonic Complex in southern Yukon Territory. Unpublished MSc thesis, University of British Columbia, Vancouver, BC, 196 p.
- Hart, C.J.R., 1997. A Transect Across Northern Stikinia: Geology of the Northern Whitehorse Map Area, Southern Yukon Territory (105D/13-16). Exploration and Geological Services Division, Yukon Region, Indian and Northern Affairs Canada, *Bulletin 8*, 112 p.
- Hart, C.J.R. and Radloff, J.K., 1990. Geology of Whitehorse, Alligator Lake, Fenwick Creek, Carcross and part of Robinson map areas (105D/11, 6, 3, 2 and 7). Exploration and Geological Services Division, Yukon Region, Indian and Northern Affairs Canada, Open File 1990-4, 113 p.
- Johnston, S.T., Mortensen, J.K. and Erdmer, P., 1996. Igneous and metaigneous age constraints for the Aishihik metamorphic suite, southwest Yukon. *Canadian Journal of Earth Science*, vol. 33, p. 1543-1555.
- Lin, S. and Williams, P.F., 1992. The geometrical relationship between the stretching lineation and the movement direction of shear zones. *Journal of Structural Geology*, vol. 14, no. 4, p. 491-497.
- Lowey, G.W., 2004. Preliminary lithostratigraphy of the Laberge Group (Jurassic), south-central Yukon: Implications concerning the petroleum potential of the Whitehorse Trough. *In: Yukon Exploration and Geology 2003*, D.S. Emond and L.L. Lewis (eds.), Yukon Geological Survey, p. 129-142.
- MacKenzie, J.J.M., Canil, D., Johnston, S.T., English, J., Mihalyuk, M.G. and Grant, B., 2005. First evidence for ultrahigh-pressure garnet peridotite in the North American Cordillera. Geological Society of America, in press.
- Mihalyuk, M.G., Edrmer, P., Ghent, E.D., Corery, F., Archibald, D.A., Friedman, R.M. and Johannson, G.G., 2004. Coherent French Range bluechist: Subduction to exhumation in <2.5 m.y.? *Geological Society of America Bulletin*, vol. 116, no. 7, p. 910-922.
- Monger, J.W.H., Wheeler, J.O., Tipper, H.W., Gabrielse, H., Harms, T., Struik, L.C., Campbell, R.B., Dodds, C.J., Gehrels, G.E. and O'Brien, J., 1991. Part B. Cordilleran terranes. *In: Upper Devonian to Middle Jurassic assemblages, Chapter 8: Geology of the Cordilleran Orogen in Canada*, H. Gabrielse and C.J. Yorath (eds.), Geological Survey of Canada, *Geology of Canada*, no. 4, p. 281-327.
- Ramsay, J.G. and Huber, M.I., 1987. The techniques of modern structural geology. Academic Press, New York, 700 p.
- Ricketts, B.D., Evenchick, C.A., Anderson, R.G. and Murphy, D.C., 1992. Bowser basin, northern British Columbia: Constraints on the timing of initial subsidence and Stikinia-North America terrane interactions. *Geology*, vol. 20, p. 1119-1122.
- Wheeler, J.O., 1961. Whitehorse map-area, Yukon Territory (105D). Geological Survey of Canada, *Memoir 312*, 156 p.
- Wheeler, J.O. and McFeeley, P., 1991. Tectonic Assemblage Map of the Canadian Cordillera. Geological Survey of Canada, Map 1712A.
- Woodcock, N.H. and Naylor, M.A., 1983. Randomness testing in three-dimensional orientation data. *Journal of Structural Geology*, vol. 5, no. 5, p. 539-548



# Case study of Donjek debris flow, southwest Yukon

*David P. Van Zeyl<sup>1</sup> and J. Graham Cogley*  
*Department of Geography, Trent University<sup>2</sup>*

Van Zeyl, D.P. and Cogley, J.G., 2005. Case study of Donjek debris flow, southwest Yukon. *In: Yukon Exploration and Geology 2004*, D.S. Emond, L.L. Lewis and G.D. Bradshaw (eds.), Yukon Geological Survey, p. 247-257.

## ABSTRACT

A high-magnitude debris flow occurred in late summer 2000 from tightly folded sedimentary rocks in a steep 2.66 km<sup>2</sup> basin in the remote Donjek River valley of southwest Yukon. The debris flow deposited at least 206 344 m<sup>3</sup> of material, with a peak discharge on the order of 1000 m<sup>3</sup>/s. No evidence of any previous events of this magnitude was found at the site. The headscarp is aligned with the strike of a west-plunging overturned syncline in heavily weathered Upper Paleozoic to Upper Triassic argillite, interbedded siltstone and argillite, and thinly bedded limestone. Tree-ring analysis on two white spruce killed by the debris flow indicate that the debris flow occurred in July to early-mid August 2000. The heaviest monthly total precipitation on record (1967-2003) for August occurred in 2000 and most likely played a role in slope failure. The volume and peak discharge estimated are the largest reported from a debris flow occurring in the last 100 years in the St. Elias Mountains.

## RÉSUMÉ

Une importante coulée de débris s'est produite à la fin de l'été 2000. La coulée s'est produite dans des roches sédimentaires à plis serrés, dans un bassin abrupt de 2,66 km<sup>2</sup> situé dans la vallée de la rivière Donjek, au sud-ouest du Yukon. La coulée de débris a déposé au moins 206 344 m<sup>3</sup> de matériaux, avec un débit de pointe de l'ordre de 1000 m<sup>3</sup>/s. Aucune trace d'événements antérieurs de cette ampleur n'a été trouvée sur le site. L'escarpement est aligné avec l'orientation est-ouest d'un pli synclinal renversé composé d'argillite fortement altérée de siltite et d'argillite interstratifiées, et de calcaire finement stratifié du Paléozoïque supérieur ou du Trias supérieur. L'analyse dendrochronologique de deux épinettes blanches tuées par la coulée de débris révèle que cette dernière s'est produite en juillet ou vers le début ou le milieu d'août 2000. Des précipitations mensuelles record pour la saison (données de 1967 à 2003) en août 2000, et ont très probablement joué un rôle dans le glissement de terrain. Le volume et le débit maximal de ce glissement de terrain sont les plus importants jamais enregistrés pour une coulée de débris depuis au moins un siècle dans les monts St. Elias.

<sup>1</sup>dvanzeyl@trentu.ca

<sup>2</sup>1600 West Bank Drive, Peterborough, Ontario, Canada K9J 7B8

## INTRODUCTION

Mass wasting is extremely active in the St. Elias Mountains (e.g., Huscroft et al., 2004b). There are small frequent debris flows and rockfalls, as well as occasional large debris flows and rockfall avalanches (e.g., Broscoe and Thomson, 1969; Power, 1989; Harris and Gustafson, 1993; Everard, 1994; Harris and McDermid, 1998; Clague, 1981). To date, debris flows have caused millions of dollars in damage to the Alaska Highway (Evans and Clague, 1989). The aim of this paper is to report details of an unusually large debris flow in a remote part of the St. Elias Mountains. This debris flow, termed the Donjek debris flow, occurred recently and has not been reported in the literature. It is important to monitor and report landslides in the St. Elias Mountains because of concerns that have been raised (e.g., Kulkarni and Blais-Stevens, 2004; Huscroft et al., 2004a) with the potential impact of climate change on landslide frequency and the resulting threat to existing and planned infrastructure in the region.

## SETTING

### LOCATION

The Donjek debris flow is located in the southwest Yukon on the southwest slope of the Donjek River valley (Fig. 1). The debris flow was undocumented for a number of years, mainly because of the paucity of human activity and lack of debris-flow monitoring in this part of the St. Elias Mountains. The failure was observed from the air in either 2000 or 2001 and the Yukon Geological Survey was notified in summer 2004.

### PHYSIOGRAPHY

The Donjek debris flow spans two physiographic elements of the St. Elias Mountains (Rampton, 1981): the Icefield Ranges and the Donjek River valley. The debris flow originated from the north-facing headwall of a v-shaped basin, here termed the Donjek basin, with a peak

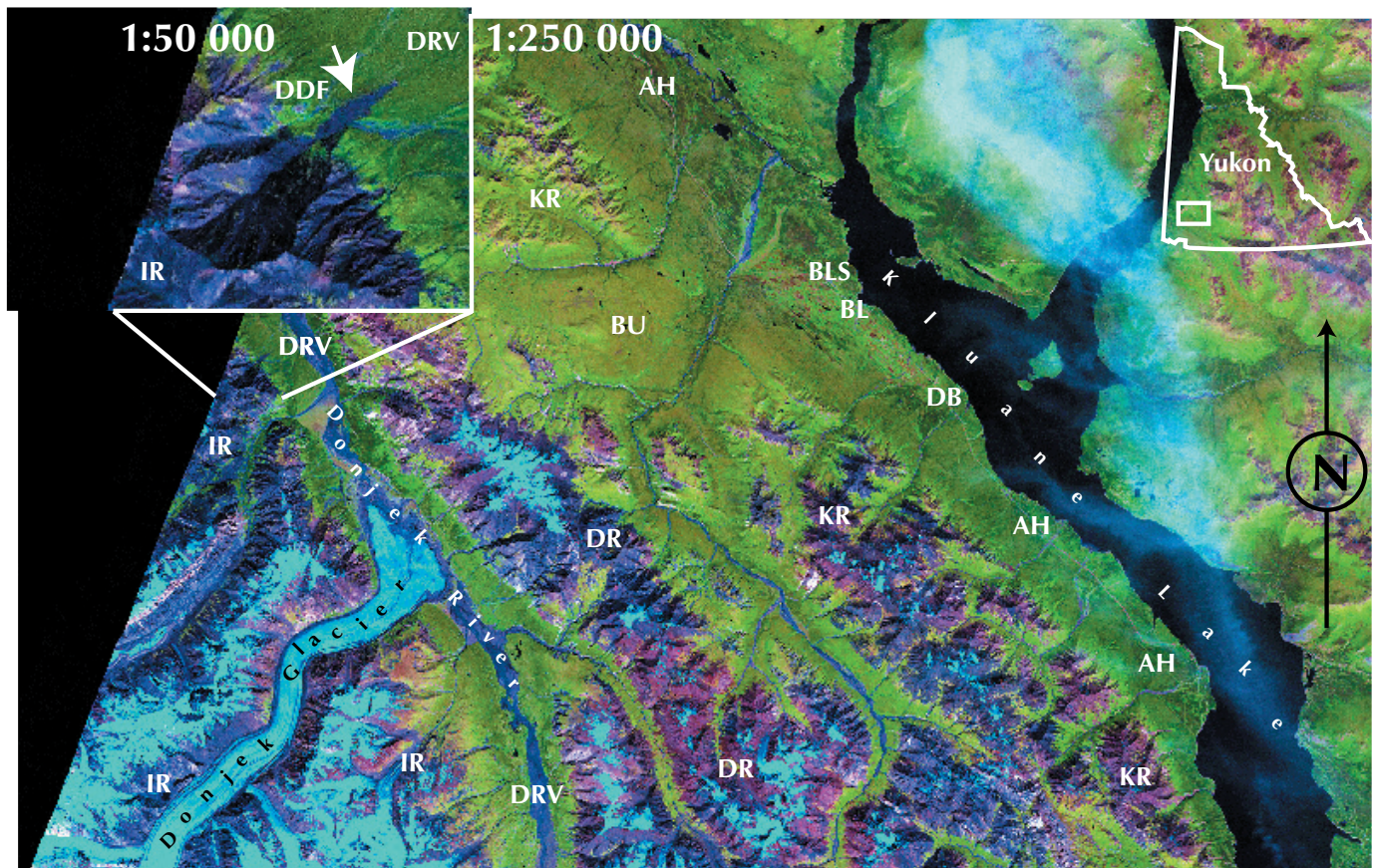


**Figure 1.** Landsat 7 scene (July 19, 2000) of the St. Elias Mountains and Shakwak Valley, southwest Yukon. The Donjek debris flow is shown at 1:50 000 in the inset. BLS=Burwash Landing station; DRV=Donjek River valley; IR=Icefield Ranges; KR=Kluane Ranges; BU=Burwash Uplands; DB=Destruction Bay; DR=Donjek Range; BL=Burwash Landing; AH=Alaska Highway; DDF=Donjek debris flow. The inset map of Yukon shows the location of the 1:250 000 Landsat scene.



elevation of 2363 m above sea level (a.s.l.). The area of this northeast-trending pear-shaped basin is estimated to be 2.66 km<sup>2</sup>. The debris-flow material is deposited on a gentle forested slope a maximum of 1197 m below and 2745 m away from the source scarp.

Ice extends northeast from the interior of the Icefields Ranges to within 300 m of the Donjek debris-flow source basin. The Donjek River valley is one of several major trunk valleys in the St. Elias Mountains (Rampton, 1981). The Donjek River collects meltwater from the Kluane, Donjek, Spring and Steele glaciers.

### GLACIAL HISTORY

There have been a number of glaciations in the St. Elias Mountains since the late Tertiary (Denton and Stuiver, 1967). The most recent glaciation occurred from 29 000 to 12 500 years ago (Rampton, 1981). During the last glaciation, ice reached a maximum elevation of 1520 m a.s.l. (Rampton, 1981) approximately 36 km down the Donjek River from the Donjek debris flow. Ice was therefore at least that deep in Donjek River valley at the location of the debris flow. This is important because valley glaciers over-steepen valley walls (e.g., Johnson, 1984), predisposing them to relaxation through mass wasting. However, no mass wasting deposits are observed on the valley slope in front of the Donjek basin (e.g., Rampton, 1981), and if paraglacial mass wasting occurred at this site, receding valley ice carried the resulting deposits away.

### BEDROCK AND SOILS

The bedrock geology in the Donjek basin was mapped by Dodds and Campbell (1992) and is composed of Upper Paleozoic to Upper Triassic sedimentary rocks. They provided the following descriptions of the bedrock geology and structural features in the basin. A relatively small area at the top of the headscarp consists of light grey massive limestone and thin-bedded dark blue-grey limestone (uPc). Most of the basin, however, is composed of dark argillite, interbedded dark siltstone and argillite, and minor thin-bedded blue-grey limestone (uPpc). The former unit is tightly folded into the axis of a west-southwest-plunging overturned syncline that is oriented parallel to the strike of the headscarp.

Most soil in the basin is poorly consolidated, dark coloured and contains variable amounts of ice (Fig. 2). A veneer of light beige colluvium covers the southeast-facing slope. The soil on the northwest-facing slope is



**Figure 2.** Deeply weathered loose dark and icy soil in the basin amongst vertically bedded limestone units. View looks toward the Donjek River from the north slope of the basin.

likely derived mainly from dark siltstones. The basin more closely resembles a transport-limited than a weathering-limited basin because of the abundance of unconsolidated soil (e.g., Bovis and Jakob, 1999). The v-bottom of the basin contains high-density ice, under which the watercourse flows. Frozen colluvium, derived from dark siltstone in the walls of the gorge, is also indicative of interstitial ice in the basin. The presence of ice is important because retrogressive thaw slumps and other related processes have been responsible for producing unconsolidated sediment that is susceptible to failure by debris-flow processes in other areas of the St. Elias Mountains (Harris and Gustafson, 1988). Therefore, ice in the basin suggests that rising temperatures could contribute material that would be susceptible to mass-wasting processes (e.g., Harris and Gustafson, 1993).

### CLIMATE

Climate in this area has been historically dynamic. A warm interval occurred between 8700 and 2800 years ago (Rampton, 1981). One estimate shows that the warm interval was 2.5°C warmer than present temperatures in the foothills of the Canadian Rockies (Harris, 2002). Subsequent cooling took place during Neoglaciation, which involved glacier advances 2800 years ago, between 1250 and 1050 years ago and during the last 450 years (Rampton, 1981).

Meteorological data have been collected to the east of the Donjek debris flow (Fig. 1) at the Burwash Landing airport (806 m a.s.l.) by Environment Canada since 1967.



The following climate statistics for the period 1971-2000 were collected. The daily average temperature (and standard deviation) for January is -22.0°C (6.6), whereas for July it is 12.8°C (0.8). These two months represent the extremes in temperature magnitude and variability. Average precipitation for January and July are 9.6 mm and 66.2 mm respectively, with the month of July receiving the most rain on average. Typically, snow melts in May and returns by the end of September.

## DONJEK DEBRIS FLOW

### MAGNITUDE

#### Volume

Debris-flow volume is estimated by multiplying the plan area of the debris flow by an estimate of the average thickness. The plan area of the debris flow was calculated by field mapping and a geographic information system (GIS). First, a field map was created using 81 GPS points that were taken at major inflection points around the debris-flow perimeter. Second, the 81 data points were entered into a GIS and converted to a polygon shape file. The shape of the polygon was then improved by using

oblique aerial photographs taken from a helicopter. This detailed map of the debris flow is shown in Figure 3. The area of the debris flow is 206 344 m<sup>2</sup>. This area does not include the levees and the material underlying the fan and gorge.

As pointed out by Jakob and Bovis (1996), debris-flow volume can be difficult to determine because of subsequent fluvial reworking. An inactive channel, incised by a temporarily diverted watercourse, was traced for 1.12 km on the surface of the Donjek debris flow (Figs. 3 and 4). This watercourse deposited variably sorted fluvial material in an elongate series of 'pools' down the centre of the debris flow. The diversion of the watercourse onto the debris flow probably redistributed more material than was added or subtracted. The watercourse regained its original path, however, by eroding through and transporting away the dam-forming debris-flow material. Therefore, some unknown volume of debris-flow material was removed. Furthermore, material continues to be removed since the current streambed is composed of debris-flow material.

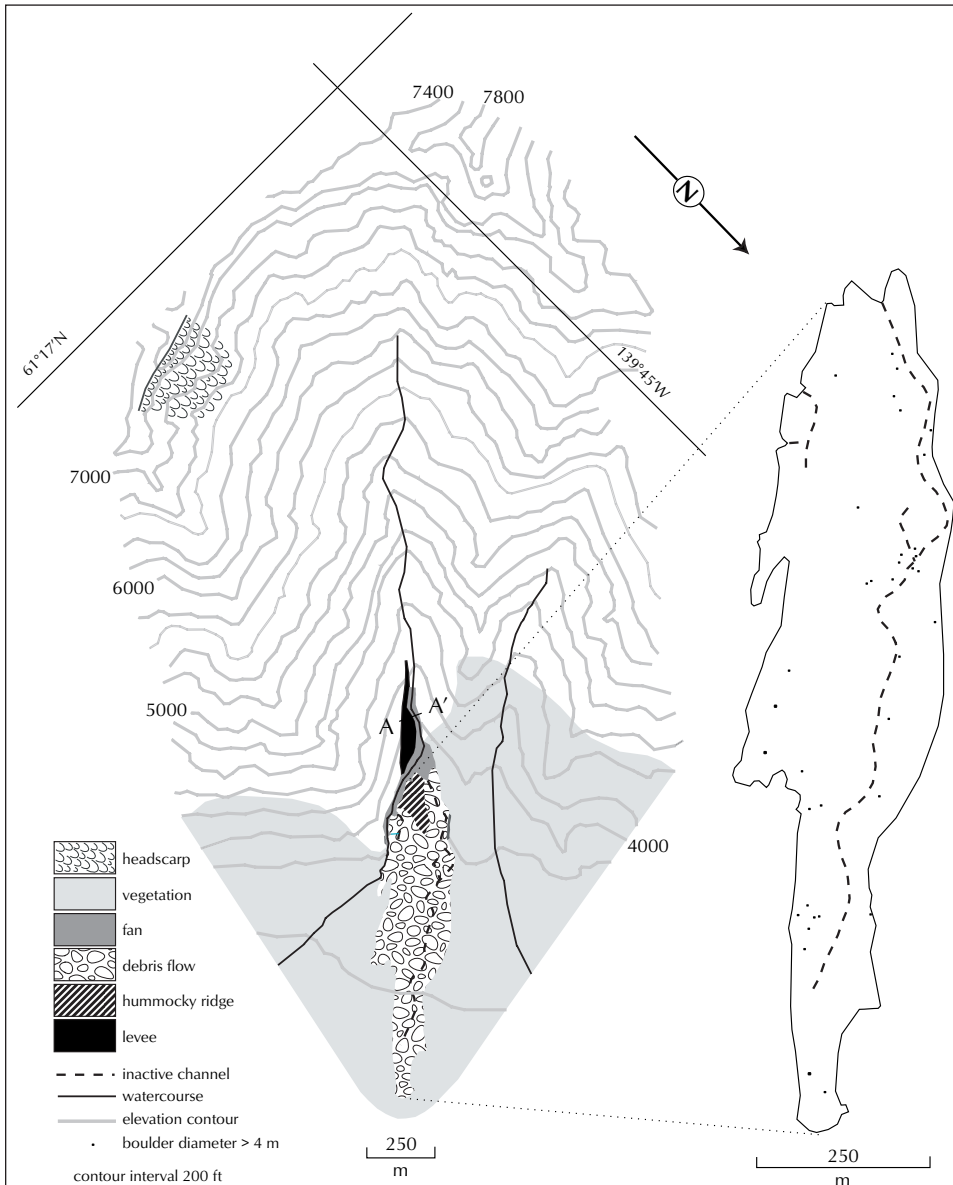
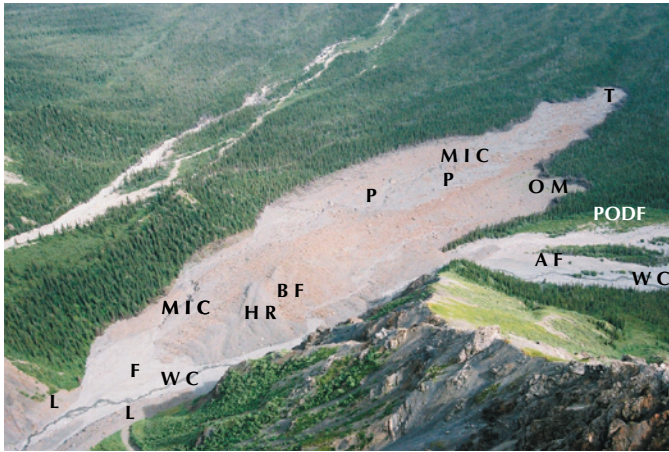


Figure 3. Map of Donjek debris flow.

The thickness of the Donjek debris flow is highly non-uniform. Organic regolith is present at the surface in an area where flow diverged into two streams (Fig. 4). Vegetated ground cover is found beneath nearly 1 m of debris near the toe of the debris flow. A pebbly alluvial fan surface is found beneath 2.33 m of debris where the



**Figure 4.** Oblique aerial photo to the north-northeast of the Donjek debris flow. The hummocky ridge (HR) at the head of the debris flow represents the greatest thickness. MIC=main inactive channel; L=levee; BF=boulder front; OM=an area where organic material is exposed at the surface; AF=alluvial fan; WC=the water course; F=fan; PODF=possible older debris flow; T=the toe of the debris flow where original regolith is found below 1 m of debris flow material; P=the “pools” of sorted fluvial deposits.

watercourse leaves the debris flow. Trees rarely protrude from the debris-flow surface, which implies that the thickness is enough to bury the timber completely. The greatest thickness is at the head of the debris flow (Fig. 4). For instance, debris flow material rises as high as 5.02 m above the channel bed in the largest of the inactive channels created when the watercourse was diverted onto the debris flow. Furthermore, the channel bed in this location is composed of large boulders embedded into the channel bottom, which suggests that the debris flow thickness is more than 5 m at this location. Although there are places on the lower portion of the debris flow where thickness is close to zero, much of the lower area of the deposit is probably more than 1 m thick. The head of the debris flow has a thickness in excess of 5 m in many places, which suggests that an overall 1 m thickness of the debris flow is an underestimate. By multiplying the area by a conservatively estimated average thickness of 1 m, the volume obtained is 206 344 m<sup>3</sup>. This estimate is much greater than any of the reported debris flows that have occurred in the last 100 years in the St. Elias Mountains.

*Peak discharge*

Debris-flow peak discharge is estimated using cross-sectional area and velocity. It is important that the cross-sectional area is calculated at a location in the confined gorge where levees are formed on both walls (Fig. 5). Jakob et al. (2000) note two reasons why calculating peak

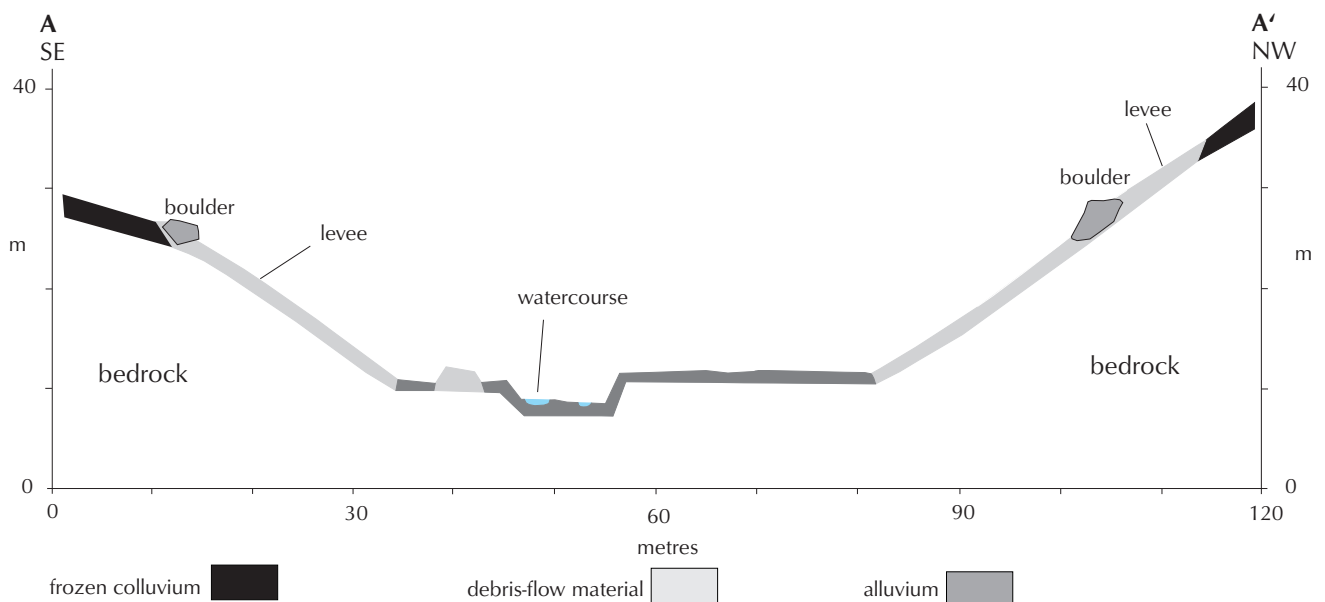


**Figure 5.** Cross-section in the gorge where peak discharge was calculated. The location of this cross-section is shown on Figure 3.

discharge from the product of cross-sectional area and velocity can be problematic. First, the cross-sectional area can be inaccurate because of scour or deposition after the debris flow. Second, cross-sectional area measured at channel bends may be greater than that measured where the channel is straight. In the case of the Donjek debris flow, there is material within the cross-section (Fig. 5) that could be from a subsequent debris flow or snow avalanche. Additionally, as discussed earlier, the watercourse has lowered the channel bed. An attempt was made to determine the original cross-sectional area at this location by estimating the amount of material removed by scour or added by deposition. A conservative estimate of the original cross-sectional area of the debris flow is 80 m<sup>2</sup>. The fact that the location of the cross-section is in a part of the gorge that is straight for approximately 480 m increases the confidence of this area estimate.

The velocity used to estimate the peak discharge of the debris flow was subjectively inferred rather than calculated. The velocities of most debris flows range from 1 to 20 m/s (Hungri et al., 2001), and those classified as extremely rapid are >5 m/s (Cruden and Varnes, 1996). Extremely rapid velocity must have been attained by the Donjek debris flow, because 100-tonne boulders were moved 1.25 km from the mouth of the gorge down a 9° slope to the furthest reach of the debris flow. Therefore, a subjective estimate of the peak velocity of the Donjek debris flow is between 5 to 20 m/s. When this velocity range is applied to the area estimate of the channel cross-section, a peak discharge of 400 to 1600 m<sup>3</sup>/s is obtained. This discharge is far greater than any of the reported peak discharges from debris flows in the St. Elias Mountains to date.

## FREQUENCY

No evidence for an earlier large debris flow was found in the area. A 1979 air photo (#A25288-04) of the area of the Donjek debris flow shows tree density to be the same at the debris flow site as it is on the slopes surrounding the present-day debris flow. No major debris-flow levees were identified in the gorge from the air photo. The course of the pre-debris-flow stream is very similar to its course today. There is a partially forested arm that extends away from the debris flow where the watercourse bends sharply, which may be an old debris-flow fan or a fluvial fan (Fig. 4). The area of this surface, however, is much less than that of the Donjek debris flow. Without high-resolution imagery of the site after 1979 it is difficult

to determine whether the Donjek debris flow was deposited on an older event.

## MATERIALS AND MORPHOLOGY

The materials that comprise the Donjek debris flow are like those expected in debris flows (e.g., Hungri et al., 2001). The texture is highly variable and surficial deposits range from clast to matrix supported. For example, in front of a matrix-supported hummocky ridge at the head of the debris flow there is a clast supported boulder front (Fig. 4). Rough inverse grading is observed where clast-supported surficial material gives way to matrix-supported material below. Materials are unsorted, except where inactive channels on the debris-flow surface give way to sorted fluvial deposits (Fig. 4). Grain size of the debris-flow material ranges from clay to boulders several metres across. Clay content is low overall.

The hummocky and lobate shape of the deposit suggests flow-like movement. For example, the hummocky ridge and boulder front are features produced when longitudinal sorting is facilitated by large flow depth, which is only possible when flow occurs within a confined channel (Hungri et al., 2001). These deposits are located a short distance from the mouth of the gorge, where velocity must have decreased after leaving the confinement of the gorge. The levees are also features that are deposited when velocity decreases as a debris flow reaches the apex of its fan (Hungri et al., 2001). In total, 1.53 km of the 3.29 km Donjek debris-flow path are confined. Furthermore, most of the confined channel is a first order drainage channel where low-magnitude debris flows have probably been a recurrent process. These characteristics suggest that the mass movement should be classified as a debris flow.

## HEADSCARP GEOLOGY

Boulders located on the debris flow provide clues to the pre-failure geology. In total, 36 boulders with diameters >4 m are exposed on the debris-flow surface (Fig. 3). Each of these boulders weighs over 100 tonnes. Invariably, they are composed of dark argillite and interbedded argillite and siltstone. Many smaller dark blue-grey limestone boulders with diameters of <4 m were also identified.

All the boulders are oxidized and weathered to some extent, and the debris flow has a remarkable rusty appearance. This suggests that chemical weathering played a role in predisposing the rock-slope material to failure. A soft, yellow weathered material that has a



sulphurous odour is common on rock surfaces. Small, thinly bedded siltstone boulders are particularly susceptible to this type of weathering, which suggests that this lithology may have formed a weak inner layer in or at the base of the failure volume that succumbed to intense chemical, and probably, physical weathering.

Most of the large boulders are foliated and folded at a small scale. For instance, on one boulder there is a tight fold preserved on a 100-cm<sup>2</sup> surface in argillite. The foliation and tight folding suggests that the source rocks to the debris flow suffered a considerable degree of tectonic stress. Folding could have resulted in reorientation of bedding planes to positions that are unfavourable for slope stability.

A headscarp was identified during helicopter reconnaissance by well-defined scarp edges and the fresh dark appearance of unconsolidated material in a lower wedge-shaped depression (Fig. 6). Further investigation of the source scar revealed upright bedding and foliation that is oriented parallel to scarp slopes. The predominant

headscarp structure dips 65° to the north-northwest (Fig. 7), which is oblique to the valley axis. The sediments in the wedge-shaped depression appear remarkably similar to those found on the debris flow. Furthermore, argillite and siltstone-argillites with minor dark blue-grey limestone bands outcrop in the wedge-shaped depression (Fig. 6). At the scarp, siltstones are the dominant lithology.

The observations at the headscarp further suggest that a siltstone unit may be the failure surface from which a volume of argillite and interbedded siltstone-argillite was ejected. The failure mode was probably a slide, because the dips are 65°, and at this low-angled orientation, the toppling or fall failure mechanisms are mechanically unlikely. Since the boulders were subangular to subrounded, not angular or very angular, it is inferred that the prefailure rock mass was broken into blocks. Geological mapping in the source basin (Dodds and Campbell, 1992) indicated the presence of an overturned syncline oriented parallel to the strike of the headscarp. Careful analysis of the 1979 air photo reveals that a

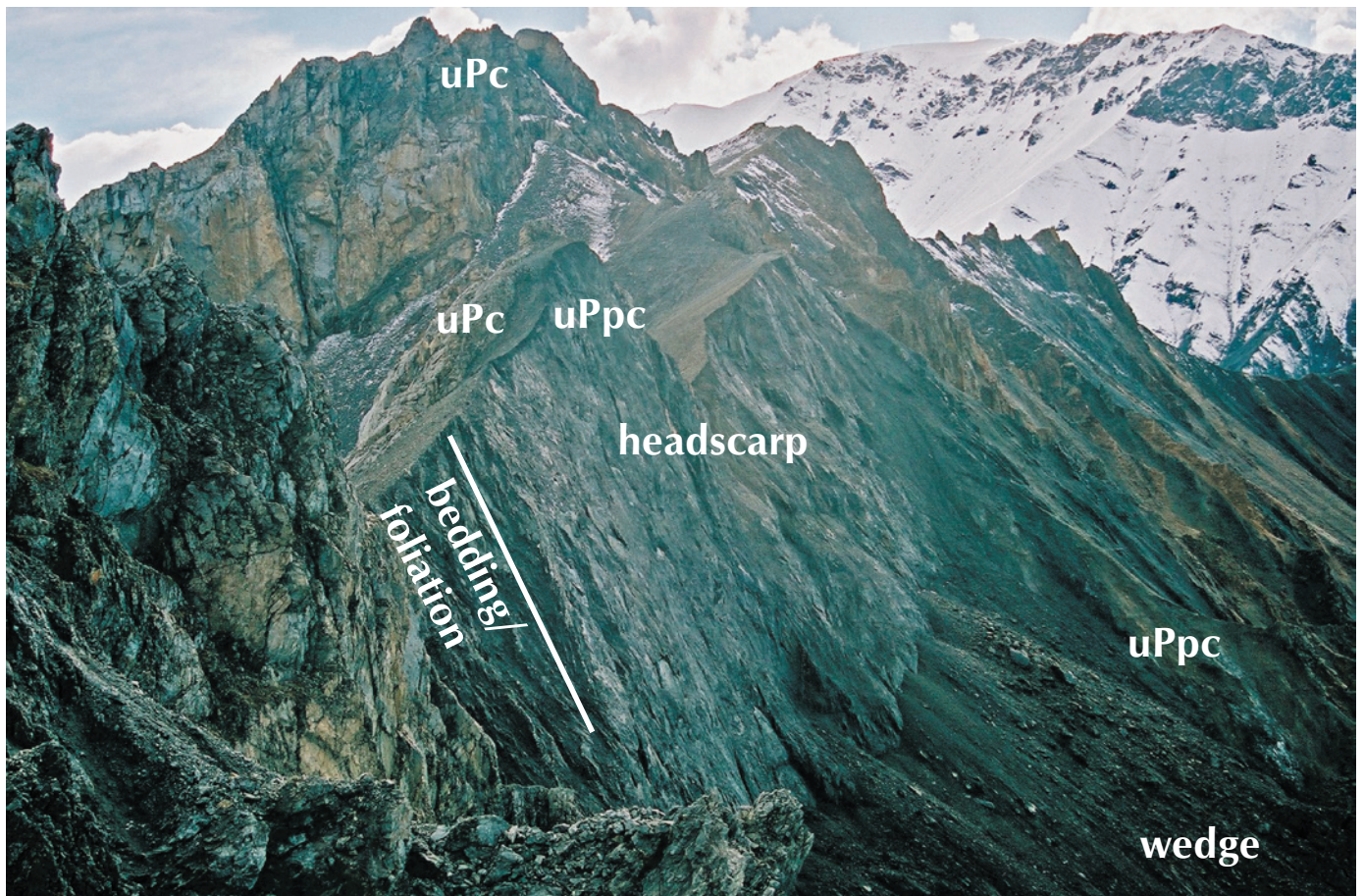


**Figure 6.** Photo of the headscarp showing the fresh scarp edges and the dark sediments below. Units uPc and uPpc are massive limestone, and interbedded argillite and siltstone respectively; from Dodds and Campbell (1992).



volume of material is missing from the location identified initially as the headscarp, which confirms the location of the principle source area. Finally, the description of unit uPpc (Dodds and Campbell, 1992) matches the lithologies described in this study on the deposit in the wedge-shaped depression below the headscarp, as well as those of the boulders.

## DEBRIS-FLOW TIMING

Anecdotal information suggests that the Donjek debris flow occurred in summer 2000 or 2001. Tree-ring cross-

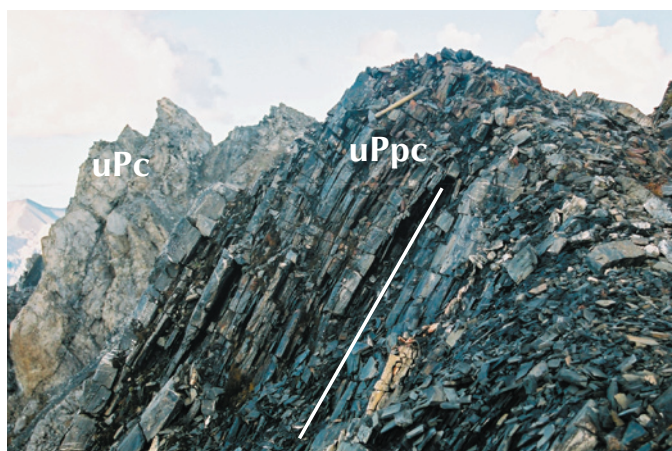


**Figure 7.** Photo of bedding and foliation planes in siltstones and argillites at the headscarp. Rock hammer for scale.

**Table 1.** Results of tree-ring cross-dating between collected specimens and on-site chronology.

Radii	Interval	Years	N. intervals	Flags	Correlation with master
209Da	1848–1999	152	6	2	0.51
209Db	1848–1999	152	6	1	0.49
212Da	1653–1999	347	13	3	0.55
212Db	1653–1999	347	13	0	0.55
203Da	1719–1804	86	4	0	0.50
203Db	1719–1804	86	4	0	0.55
207Aa	1950–2003	54	2	0	0.55
207Ab	1950–2003	54	2	1	0.30
213Aa	1798–2003	206	9	1	0.54
213Ab	1799–2003	205	9	0	0.57

Note: A “D” following the sample number indicates a tree killed by the debris flow; an “A” after the sample number indicates a tree that was living when cut for sampling. Two radius measurements (a and b) were taken for each sample.

dating suggests that the debris flow occurred in late summer 2000. Timber is violently uprooted and accumulated into piles around the landslide perimeter. The trees killed by the debris flow allow for tree-ring cross-dating analysis.

Seven tree-discs were sampled, five from trees that were killed by the landslide and two from trees standing alive outside of the landslide impact zone. Tree-discs were processed at the University of Western Ontario tree-ring lab. Ring widths were measured under a microscope to  $\pm 0.001$  mm on each of the seven specimens on two different radii to ensure dating and measurement consistency.

The ring widths from the living trees were cross-dated initially, then individual dead trees were cross-dated with the living tree chronology. As individual dead trees were successfully dated, the ring width patterns were added to the master chronology for the debris-flow site. These data were then cross-dated against a chronology based on measurements from 15 to 20 trees at the Donjek Bridge (35 km away) to validate the Donjek site cross-dating.

The tree-ring lab was able to establish weak but consistent cross-dates in three of the specimens killed by the landslide (Table 1). The number of flags in Table 1 indicates the number of 50-year ring-width intervals where individual series did not match with a series from the Donjek Bridge chronology or the correlation coefficient was not significant. Four radii (209a, b and 212a, b) showed 1999 as their last complete rings. Tree rings are composed of inner and outer parts. Earlywood is the inner component of a tree ring that is established in the spring. Latewood is the outer portion and is usually thinner than earlywood and is established towards the end of the summer. These specimens showed earlywood (B. Luckman, pers. comm., 2004) but no latewood, which suggests that the landslide occurred before latewood was established. Latewood is established in late August or September in southwest Yukon (B. Luckman, pers. comm, 2004). These results suggest that the landslide occurred sometime in July or early-to-mid August 2000. The third specimen (203a, b) showed 1804 as its final complete ring, which most likely indicates that the tree was already dead when partially buried by the landslide.

## DEBRIS-FLOW INITIATION

### EARTHQUAKES

Evidence outlined below suggests that earthquakes are unlikely to have initiated the Donjek debris flow. Keefer (1984) inventoried 300 earthquakes worldwide with and without associated reports of landslides. Out of 62 earthquakes with seismic-moment magnitude (M) less than 4.0, only one was associated with a landslide report. Therefore, the minimum intensity of earthquakes that are able to cause landslides is considered to be  $M=4.0$  (Keefer, 1984). Also, a more recent study by Malamuda et al. (2004) has found  $M=4.3$  to be the minimum magnitude of earthquake capable of generating slides. Furthermore, Keefer (1984) examined the relationship between earthquake magnitude and the maximum distance of reported slides or falls from earthquake epicentres. He found that for  $M=5.0$ , the maximum distance at which slides or falls were reported was 16 km from the epicentre. Table 2 is the list of recorded seismic events that occurred within 200 km of the Donjek debris flow between 1 July 2000 and 30 September 2000. In this list, all earthquakes are  $M < 5.0$  and all are much further than 16 km from the Donjek debris flow. Therefore, it is unlikely that any of the recorded seismic events caused the initial slide that produced the Donjek debris flow.

### METEOROLOGY

The evidence presented below suggests that the initiation of the Donjek debris flow may have been influenced by excess pore-water pressure associated with abnormally

**Table 2.** Recorded seismic events within 200 km of Donjek debris flow between July 1, 2000 and September 30, 2000.

Date (time) UT	Distance (km)	Magnitude (M)
00 07 01 (14:16:22)	127.6	2.9
00 07 03 (17:24:44)	123.8	4.1
00 07 03 (19:23:00)	137.2	4.1
00 07 03 (19:45:13)	102.9	2.5
00 07 04 (02:21:19)	115.3	3.1
00 07 04 (10:26:48)	99.1	2.5
00 07 13 (21:20:44)	170.3	2.8
00 08 01 (15:36:27)	196.5	3.4
00 08 03 (13:12:59)	187.6	4.5
00 08 03 (13:54:03)	190.7	2.9
00 08 10 (14:34:13)	95.2	2.5
00 08 27 (21:48:04)	193.7	2.8
00 09 03 (14:55:03)	103.0	3.1
00 09 27 (08:16:13)	61.5	2.5

wet conditions in August, 2000. The cumulative monthly total precipitation, tallied from January to June, July and August, for each year in the period 1968-2000 is presented in Figure 8. These data represent the amount of precipitation received at Burwash Landing station from January to June, July and August. The data in Figure 8 do not represent soil moisture at the Donjek debris flow headscarp, since antecedent soil moisture conditions and factors such as snowmelt, evapotranspiration and runoff have not been considered. Thus, the data in Figure 8 may

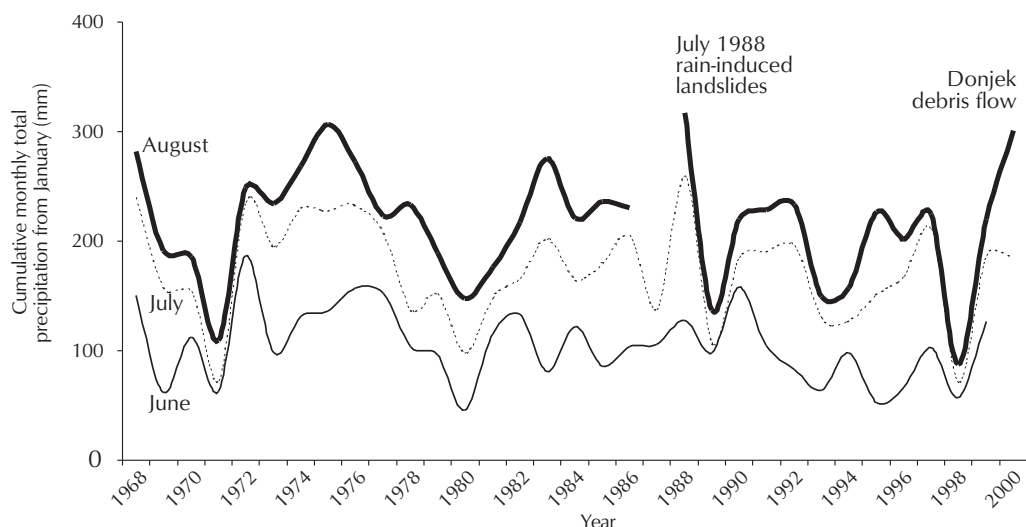


**Figure 8.** Cumulative monthly total precipitation from January to June, July and August at Burwash Landing from 1968 to 2000.



only provide a crude indication of possible soil moisture levels at any location in the area surrounding the Burwash Landing station. Slopes are more susceptible to failure in years with high soil moisture because pore-water pressure increases with increases in soil moisture, thus decreasing the shear strength of slope material. Cumulative monthly total precipitation from January to August, 2000 was abnormally high, primarily because the August, 2000 monthly total precipitation (115.7 mm) was the highest on the 1968-2003 August record. These data suggest that high pore-water pressures likely contributed to instability at the headscarp of the Donjek debris flow.

## DISCUSSION

An unusually large debris flow occurred in the Donjek River valley in mid-to-late summer, 2000. The movement mechanism probably began as a slide and changed to flow shortly after initiation and collapse of the initial source volume. The initial slide movement is inferred from the predominant dip of 65° at the source scarp and the large number of boulders in the debris flow. It is often difficult, however, to distinguish between slide and flow mechanisms in most mass movements (Hungre et al., 2001). Flow movement shortly after initiation is inferred from the flow-like features of the Donjek debris flow. The structural features in the bedrock, associated with an overturned syncline (Dodds and Campbell, 1992), acted to predispose the slope to failure. The failure surface appears to be a bed of relatively highly weathered siltstones in an interbedded siltstone and argillite mass. This mass likely had a higher porosity allowing water to infiltrate more readily, thus setting up an unstable hydro-geologic condition for the initial failure volume. Intensely weathered and oxidized boulders within the debris flow suggest that chemical weathering was involved, and the abundance of residual soil clinging to steep slopes in the basin allowed the initial bedrock failure to entrain a larger volume of material.

Water that infiltrated the slope material is likely a major factor in predisposing the initial slope to failure, as well as facilitating the entrainment of residuum in the debris-flow path. This is inferred from the flow-like form of the debris flow and from the anomalous precipitation from January to the end of August, 2000. Ongoing research aims to date the event more precisely and thereby characterize the daily-scale meteorological conditions leading up to the event. Unfortunately, there are not enough detailed case studies of debris flows in southwest Yukon to fully

understand the relationship between hydrological and mass-wasting processes. The monitoring of debris flows is certainly warranted if future development is intended for southwest Yukon, especially considering the possibility that global climate change could make meteorological extremes more common (e.g., Kulkarni and Blais-Stevens, 2004).

## ACKNOWLEDGEMENTS

I wish to thank Steve Israel and Crystal Huscroft for the logistical and planning support they provided for the fieldwork. Sarah Newmann helped in the field and was a great cook. Kluane National Park provided timely access to the park for the fieldwork. Fes de Scally provided helpful comments at an early stage in the project. Caroline Fric improved the first draft of the manuscript. John Barlow and Stuart Harris provided many helpful comments when they reviewed the manuscript.

## REFERENCES

- Bovis, M.J. and Jakob, M., 1999. The role of debris supply conditions in predicting debris-flow activity. *Earth Surface Processes and Landforms*, vol. 24, p. 1039-1054.
- Broscoe, A.J. and Thomson, S., 1969. Observations on an alpine mudflow, Steele Creek, Yukon. *Canadian Journal of Earth Sciences*, vol. 6, p. 219-229.
- Clague, J.J., 1981. Landslides at the south end of Kluane Lake, Yukon Territory. *Canadian Journal of Earth Sciences*, vol. 18, p. 959-971.
- Cruden, D.M. and Varnes, D.J., 1996. Landslide types and processes. *In: Landslides Investigation and Mitigation: Transportation Research Board, A.K. Turner and R.L. Schuster (eds.), US National Research Council, Special Report 247, Washington, DC, p. 153-171.*
- Denton, G.H. and Stuiver, M., 1967. Late Pleistocene glacial stratigraphy and chronology, Northeastern St. Elias Mountains, Yukon Territory, Canada. *Geological Society of America Bulletin*, vol. 78, p. 485-510.
- Dodds, C.J. and Campbell, R.B., 1992. Geology of SW Kluane Lake Map Area (115G and F [E1/2]), Yukon Territory. *Geological Survey of Canada, Open File 2188, 85 p.*
- Evans, S.G. and Clague, J.J., 1989. Rain-induced landslides in the Canadian Cordillera, July 1988. *Geoscience Canada*, vol. 16, no. 3, p. 193-200.

- Everard, K.A., 1994. Regional characterization of large landslides in southwest Yukon, with emphasis on the role of neotectonics. Unpublished MSc thesis, University of British Columbia, Vancouver, British Columbia.
- Harris, S.A. and Gustafson, C.A., 1988. Retrogressive slumps, debris flows and river valley development in icy, unconsolidated sediments on hills and mountains. *Zeitschrift für Geomorphologie*, vol. 32, no. 4, p. 441-455.
- Harris, S.A. and Gustafson, C.A., 1993. Debris-flow characteristics in an area of continuous permafrost, St. Elias Range, Yukon Territory. *Zeitschrift für Geomorphologie*, vol. 37, no. 1, p. 41-56.
- Harris, S.A. and McDermid, G., 1998. Frequency of debris flows on the Sheep Mountain fan, Kluane Lake, Yukon Territory. *Zeitschrift für Geomorphologie*, vol. 42, no. 2, p. 159-175.
- Harris, S.A., 2002. Biodiversity of the vascular timberline flora in the Rocky Mountains of Alberta, Canada. *In: Mountain Biodiversity*, C. Korner and E.M. Spehn (eds.), Parthenon, New York, New York.
- Hungr, O., Evans, S.G., Bovis, M.J. and Hutchinson, J.N., 2001. A review of the classification of landslides of the flow type. *Environmental and Engineering Geoscience*, vol. 7, no. 3, p. 221-238.
- Huscroft, C.A., Lipovsky, P.S. and Bond, J.D., 2004a. Permafrost and landslide activity: Case studies from southwestern Yukon Territory. *In: Yukon Exploration and Geology 2003*, D.S. Emond and L.L. Lewis (eds.), Yukon Geological Survey, p. 107-119.
- Huscroft, C.A., Lipovsky P.S. and Bond J.D., 2004b. A regional characterization of landslides in the Alaska Highway corridor, Yukon. Yukon Geological Survey, Open File 2004-18, 65 p.
- Jakob, M. and Bovis, M.J., 1996. Morphometric and geotechnical controls of debris-flow activity, southern Coast Mountains, British Columbia, Canada. *Zeitschrift für Geomorphologie, Supplement Band*, vol. 104, p. 13-26.
- Jakob, M., Anderson, D., Fuller, T. Hungr, O. and Aytte, D., 2000. An unusually large debris flow at Hummingbird Creek, Mara Lake, British Columbia. *Canadian Geotechnical Journal*, vol. 37, p. 1109-1125.
- Johnson, P.G., 1984. Paraglacial conditions of instability and mass movement: A discussion. *Zeitschrift für Geomorphologie*, vol. 28, no. 2, p. 235-250.
- Keefer, D.K., 1984. Landslides caused by earthquakes. *Geological Society of America Bulletin*, vol. 95, p. 406-421.
- Kulkarni, T. and Blais-Stevens, A., 2004. Vulnerability of landslide risk to climate change. *Proceedings from C-CIARN Landscape Hazards Workshop 2003*, Geological Survey of Canada, Landscape Hazard Report 04-01, 36 p.
- Malamud, B.D., Turcotte, D.L., Guzzetti, F. and Reichenbach, P., 2004. Landslides, earthquakes, and erosion, *Earth and Planetary Science Letters*, vol. 229, no. 1-2, p. 45-59.
- Power, M.A., 1989. Landsliding at Cement Creek, Kluane Ranges, southwestern Yukon. *In: Yukon Geology, Volume 2, Exploration and Geological Services Division, Yukon Region, Indian and Northern Affairs Canada*, p. 51-60.
- Rampton, V.N., 1981. Surficial materials and landforms of Kluane National Park, Yukon Territory. *Geological Survey of Canada, Paper 79-24*.





## PROPERTY DESCRIPTION

<i>The Tsa da Glisza (Regal Ridge) emerald occurrence, Finlayson Lake district (NTS 105G/7), Yukon: New results and implications for continued regional exploration</i> H.L.D. Neufeld, J.K. Mortensen and L.A. Groat .....	261
<i>Mineralogical and geochemical study of the True Blue aquamarine showing, Shark property, southern Yukon</i> D. Turner, L.A. Groat and W. Wengzynowski .....	275



# The Tsa da Glisza (Regal Ridge) emerald occurrence, Finlayson Lake district (NTS 105G/7), Yukon: New results and implications for continued regional exploration

Heather L.D. Neufeld, James K. Mortensen<sup>1</sup> and Lee A. Groat<sup>2</sup>  
University of British Columbia<sup>3</sup>

Neufeld, H.L.D., Mortensen, J.K. and Groat, L.A., 2005. The Tsa da Glisza (Regal Ridge) emerald occurrence, Finlayson Lake district (NTS 105G/7), Yukon: New results and implications for continued regional exploration. *In*: Yukon Exploration and Geology 2004, D.S. Emond, L.L. Lewis and G.D. Bradshaw (eds.), Yukon Geological Survey, p. 261-273.

## ABSTRACT

Emerald at the Tsa da Glisza property in southeast Yukon is associated with abundant quartz-tourmaline veins within chromium-rich mafic metavolcanic rocks. A genetic model for the emerald mineralization has been formulated: vein fluids were mixtures of fluids from both magmatic and metamorphic sources. Beryllium derived from an adjacent Cretaceous granite pluton travelled as both hydroxide and fluoride complexes within dominantly magmatic fluids. Emerald crystallized during cooling, after the magmatic fluids mixed with hydrothermal fluids that had scavenged chromium from the surrounding mafic schist. Property-scale exploration targets the permeable, high-chromium mafic schists as potential hosts (rather than nearby chromium-rich, but impermeable, serpentized ultramafic rocks). Soil geochemistry, drilling and prospecting are used to locate emerald mineralization. Based on the genetic model, further exploration in the Finlayson Lake region should focus on areas where permeable, high-chromium host rock (schist, rather than serpentized ultramafic) is in close proximity to evolved felsic intrusive rocks.

## RÉSUMÉ

À la propriété Tsa da Glisza au sud-est du Yukon, l'émeraude est associée à d'abondantes veines de quartz avec tourmaline dans des métavolcanites mafiques riches en chrome. On a établi un modèle génétique pour la minéralisation en émeraude : les fluides présents dans les veines étaient des mélanges de fluides provenant de sources magmatiques et météoriques. Le béryllium, dérivé d'un pluton de granite adjacent du Crétacé, s'est déplacé sous forme de complexes avec hydroxydes et fluorures dans des fluides à prédominance magmatique. L'émeraude s'est cristallisée pendant le refroidissement, après que des fluides magmatiques se sont mélangés à des fluides hydrothermaux qui avaient extrait du chrome du schiste mafique environnant. L'exploration à l'échelle de la propriété vise les schistes mafiques perméables à haute teneur en chrome comme roches hôtes possibles (plutôt que les roches ultrabasiqes serpentinisées, riches en chrome mais imperméables, qui se trouvent à proximité). Les levés géochimiques, des forages et la prospection servent à situer les minéralisations en émeraude. S'appuyant sur le modèle génétique, la future exploration dans la région du lac Finlayson devrait se concentrer sur des zones où la roche hôte perméable (schiste plutôt que roche ultrabasiqse serpentinisée), riche en chrome, se trouve à proximité immédiate de roches intrusives felsiques évoluées

<sup>1</sup>jmortens@eos.ubc.ca

<sup>2</sup>lgroat@eos.ubc.ca

<sup>3</sup>6339 Stores Road, Vancouver, British Columbia, Canada V6T 1Z4



## INTRODUCTION

The Tsa da Glisza (previously known as Regal Ridge) emerald occurrence is centered at 61°16.6' N latitude, 133°5.5' W longitude on NTS map sheet 105G/7, in the Finlayson Lake district within the Pelly Mountains of southeastern Yukon (Fig. 1). Emerald is an extremely valuable gemstone and is rare because the required elements beryllium and chromium (with or without vanadium) are geochemically incompatible, and therefore are rarely found together in environments in which beryl is stable. The Tsa da Glisza occurrence hosts the only known chromium-bearing emerald in the Canadian Cordillera. The definition of "emerald" is still under considerable debate (e.g., Schwartz and Schmetzer, 2002). In this paper, emerald is defined as bright green, clear, gem-quality beryl, which is distinct from opaque white to medium green beryl and clear beryl that is less than bright green.

This paper compiles results from both field and laboratory research on the Tsa da Glisza emerald occurrence since 2003, develops a genetic model for the formation of emerald at Tsa da Glisza based on the results of this research, and outlines an updated exploration model to develop targets for emerald mineralization similar to that found at Tsa da Glisza.

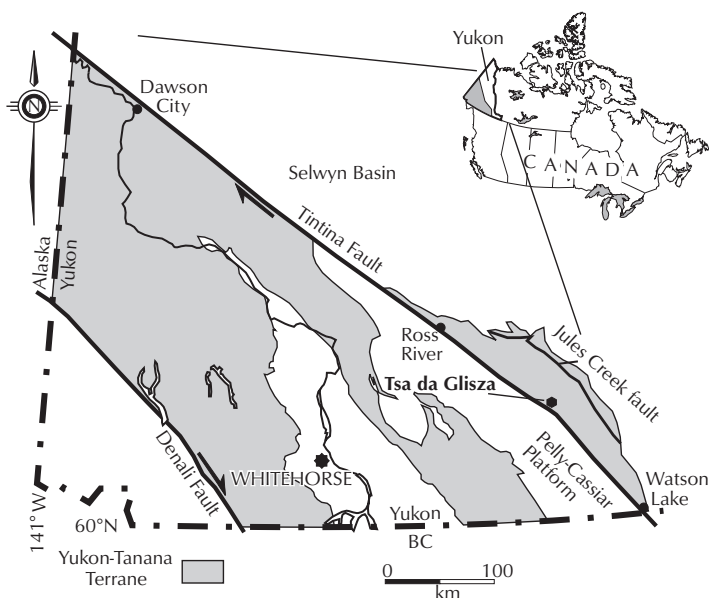


**Figure 1.** Map of southern Yukon showing the Yukon Tanana Terrane and the location of the Tsa da Glisza emerald occurrence.

## REGIONAL GEOLOGY

The Tsa da Glisza study area is located in the Finlayson Lake district of the Yukon. The area was mapped most recently by Murphy (1997), Murphy and Piercey (1999), Murphy et al. (2001) and Murphy et al. (2004). The geologic setting of the region has been described in detail by Murphy (2004) and Murphy et al. (2002). Neufeld et al. (2004) discussed the geological setting of the Tsa da Glisza emerald occurrence in some detail, and in this paper we provide a brief review of the lithologies that are present within the immediate vicinity of the Tsa da Glisza property and highlight recent changes in the geological interpretation.

The Finlayson Lake district consists of rocks of the Yukon-Tanana Terrane (Fig. 1), which is regionally bounded to the west by the Tintina Fault, and to the east by the Jules Creek fault (Murphy, 2004). The structurally deepest rocks are contained within the Big Campbell thrust sheet, which is composed of the Upper Devonian Grass Lakes group, and the Lower Mississippian Wolverine Lake group. The Tsa da Glisza occurrence is hosted within the Grass Lakes group, which consists of mafic and felsic metavolcanic rocks and dark clastic rocks of the Fire Lake, Kudz Ze Kayah and Wind Lake formations. The Fire Lake Formation is a mafic metavolcanic package composed mainly of chloritic phyllite, and is spatially associated with mafic and ultramafic plutonic rocks (Murphy, 2004; Piercey et al., 2004). The Kudz Ze Kayah Formation stratigraphically overlies the Fire Lake Formation and consists of carbonaceous phyllite and schist, felsic metavolcanic rocks and rare quartzofeldspathic metaclastic rocks (Murphy, 2004). The rocks in the Finlayson Lake district are intruded by several ca. 112 to 110 Ma granitic bodies of the Cassiar-Anvil plutonic suite (Mortensen, pers. comm., 2004). The intrusions are syn- to post-kinematic with respect to the main Cretaceous deformation in the area.

A recent structural interpretation of the Finlayson Lake region (Murphy, 2004) suggests that the rocks in the Finlayson Lake district were strongly deformed during the Cretaceous. As the numerous felsic plutons in the region were emplaced, the east-trending North River normal fault moved to accommodate uplift and cooling of rocks in the footwall of the fault. Movement of the hanging wall of the fault was broadly north to south. Rock units in the footwall have mid-Cretaceous Ar-Ar cooling ages, and were ductily deformed prior to and during the emplacement of mid-Cretaceous granite plutons.

Tsa da Glisza occurs within the footwall of this fault, within 10 km of the present-day fault trace. The Tintina Fault lies 14 km southwest of the Tsa da Glisza property (Fig. 1). Early Tertiary volcanic rocks occur adjacent to the Tintina Fault, and faults and porphyritic dykes, likely related to Tertiary movement along the Tintina Fault, occur throughout the Finlayson Lake district (Jackson et al., 1986).

## PROPERTY GEOLOGY

Neufeld et al. (2004) described the geology associated with mineralization at the Summit Zone (Regal Ridge proper). This area is underlain by rocks of the Fire Lake Formation, as well as Cretaceous and Eocene intrusive rocks. A two-week mapping program conducted in July 2004 covered the entire claim block, and resulted in a 1:10 000-scale geologic map (Fig. 2). A brief description of the rock units is given below, along with some new observations. Rock unit nomenclature is from previous mapping (Murphy et al., 2001).

The Tsa da Glisza property is mainly underlain by rocks of the Fire Lake Formation, a suite of Devonian mafic metavolcanic rocks and associated mafic and ultramafic plutonic rocks. The emerald occurrence is mainly hosted within the Fire Lake mafic metavolcanic unit (DF; Fig. 2). This rock unit was studied extensively by Piercey (1999, 2000, 2004; Murphy and Piercey 2000). It occurs as dark to medium green plagioclase-chlorite schist to phyllite, with common biotite and actinolite porphyroblasts. Greenschist facies metamorphism resulted in replacement of most primary mafic minerals with chlorite and actinolite. The finer-grained groundmass consists mainly of quartz, chlorite and actinolite with less abundant muscovite, biotite and rare carbonate. At Tsa da Glisza, the composition of the chlorite schist is equivalent to that of high-calcium boninite, which is geochemically distinct from other mafic metavolcanic rocks within the Fire Lake Formation because of high MgO, intermediate SiO<sub>2</sub>, and anomalous Cr, Ni, Co and Sc (Table 1; Piercey et al., 2004). Chlorite alteration likely occurred prior to the Cretaceous deformation event, during which some of the chlorite schist was altered to jarosite- and mica-rich schist, while scheelite and tourmaline formed close to quartz vein contacts. This altered schist occurs mainly at the top of Regal Ridge.

Red-weathering, moderately serpentized ultramafic rock (unit Dum) and actinolite-plagioclase-biotite leucogabbro to pyroxenite (unit Dmi) occur mainly to the west of the

mineralized areas (Fig. 2). Average geochemical analyses for these ultramafic units are given in Table 1. Quartz-tourmaline veins within these units are very rare, likely due to the extremely competent nature of the rock type and the distance from the granite. Geological mapping of the property suggests that the ultramafic unit is not present at depth between the granite and unit DF (Fig. 2).

Carbonaceous phyllite (unit DKcp) occurs over much of the southeastern part of the property, and makes up the upper part of the stratigraphy in this area. A thin band of rusty quartzite marks the contact between the chlorite schist and carbonaceous phyllite units. The rusty quartzite was included within unit DKcp by Murphy et al. (2001), but was mapped separately in this study as unit DKq. Neither the carbonaceous phyllite nor the quartzite within the Kudze Kayah Formation host quartz-tourmaline or emerald-bearing veins.

A biotite-muscovite granite to muscovite leucogranite, previously called a quartz monzonite by Neufeld et al. (2004), crops out in the valley between the two mineralized ridges (unit Kg; Fig. 2). This  $112.2 \pm 0.5$  Ma pluton (Neufeld, 2004) contains rare garnet, and does not contain miarolitic cavities. The geochemistry of the granite is discussed in Neufeld et al. (2004) and average results from analyses of this rock type are presented in Table 1. A contact aureole extending approximately 500 m from granite contacts is defined by the presence of biotite and tourmaline within the surrounding schist.

Numerous leucogranite and aplite-pegmatite dykes and sills (unit Ka, not mapped separately by Murphy et al., 2001) from 30 cm to ten metres in width are present on the property. The aplite dykes consist of plagioclase, quartz, muscovite, and minor potassium feldspar, tourmaline and garnet. Pegmatite is rare, and has the same mineralogy as aplite, but with increased amounts of muscovite. Both white and green beryl occur in quartz-rich segregations within at least two of the aplite dykes. Some of the aplite and pegmatite dykes are altered, and contain albite, intergrowths of albite and muscovite, and rare interstitial calcite and sulphides. The geochemistry of the aplite dykes is discussed in Neufeld et al. (2004) and average results from analyses of this rock type are presented in Table 1.

Beige-, purple-grey-, and pink-weathering feldspar- and quartz-phyric porphyry dykes and sills (unit Eq) of inferred Eocene age occur throughout the property, and intrude along the same zones of weakness exploited by the Cretaceous aplite and leucogranite dykes and sills, or



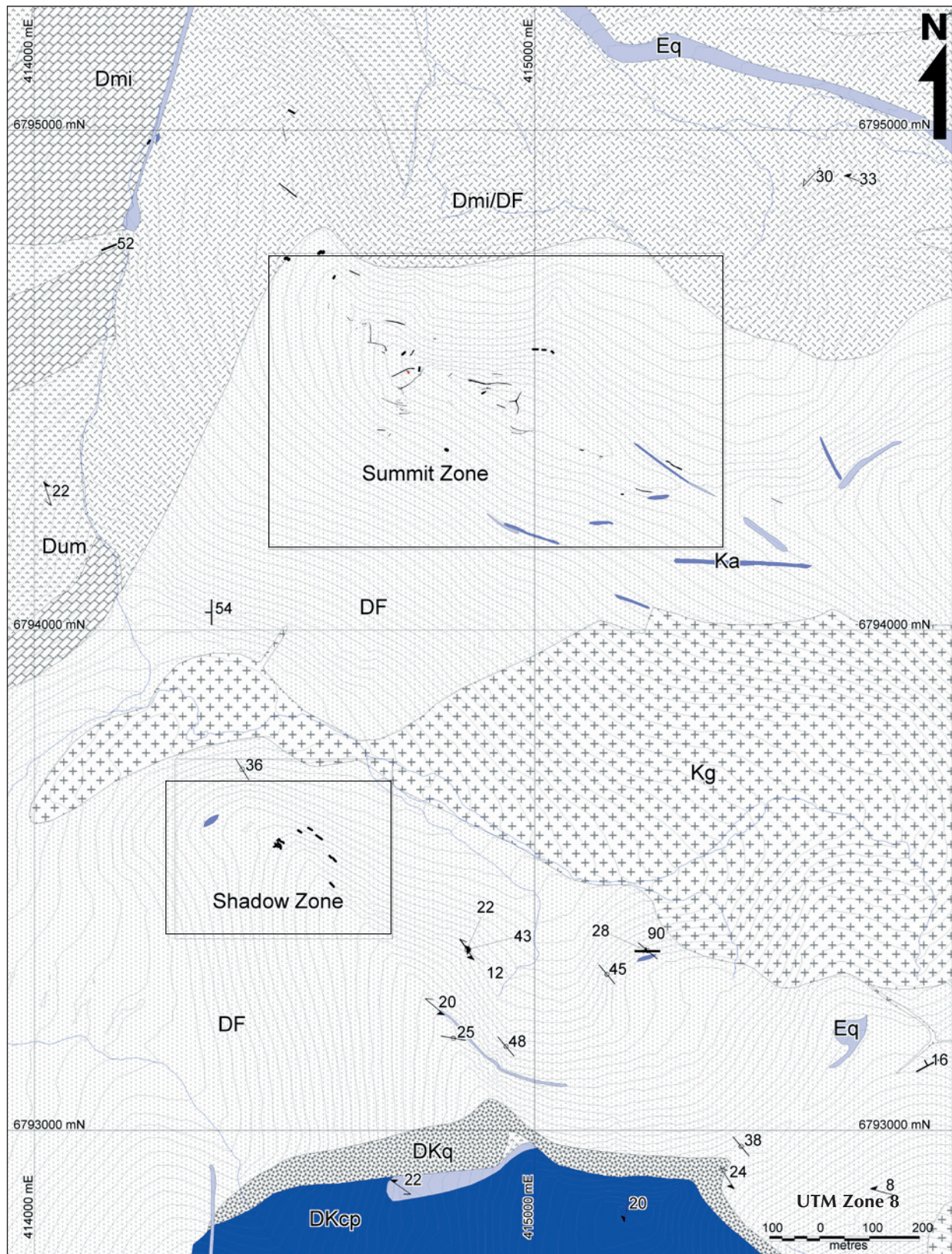


**Figure 2.** Geological map of the Tsa da Glisza property, adapted from Neufeld (2004). The property occurs in NTS map sheet 105G/7. Rock unit nomenclature is mainly from YGS mapping (Murphy et al., 2001).



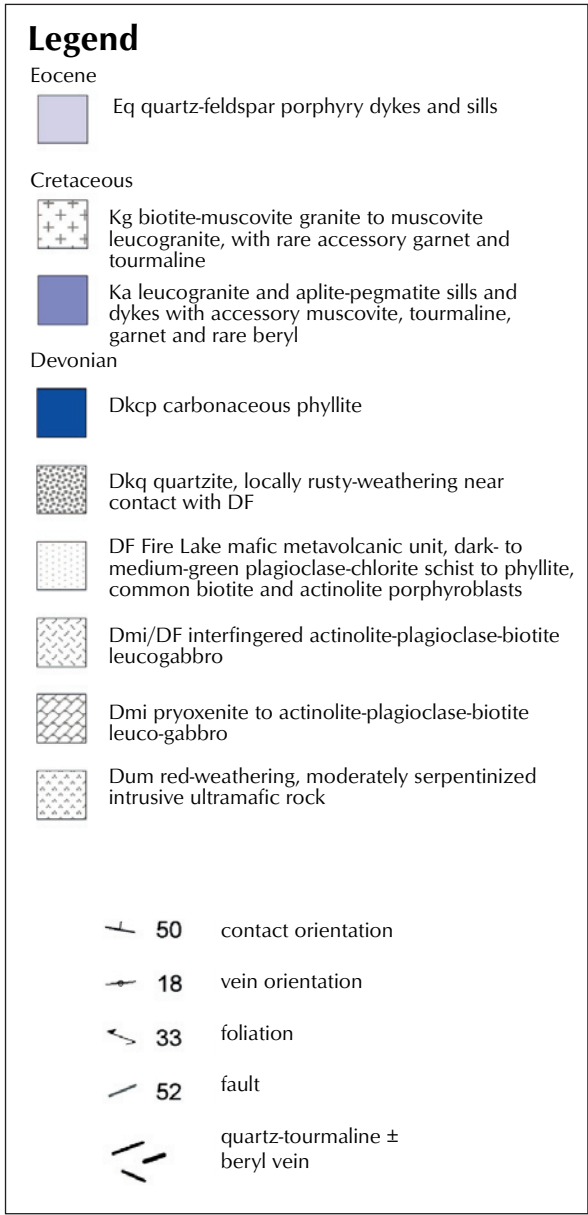
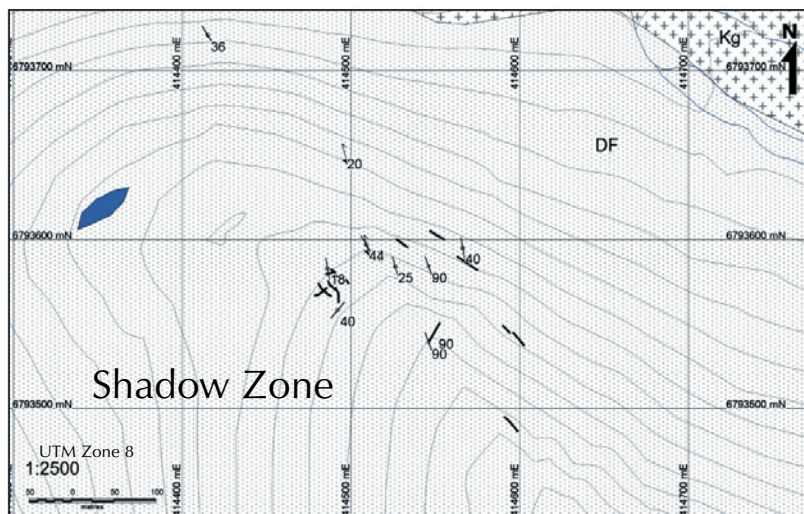
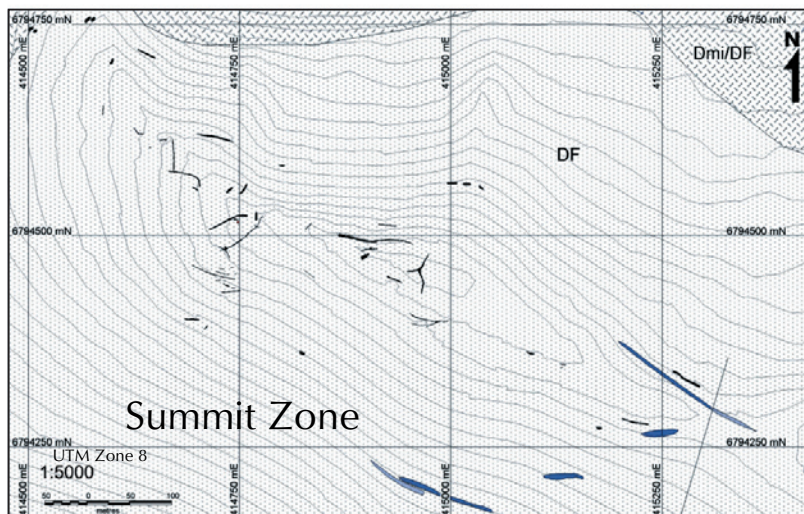


Figure 2. continued. Inset maps of the Summit and Shadow zones.

along geologic contacts. The porphyry intrusions are approximately 5 to 50 m thick, and are commonly intensely altered to brown rounded pebbles. Some late faulting and alteration of host rocks and emerald at Tsa da Glisza are attributed to this Eocene event.

**MINERALIZATION AND ALTERATION**

At Tsa da Glisza, emerald occurs: (1) in the altered selvages of quartz-tourmaline veins; (2) within quartz-tourmaline veins; and (3) in linear zones of highly altered schist, with no quartz-tourmaline veins immediately

adjacent to the emerald. The formation of the quartz veins is interpreted to be syn- to late-tectonic, and coincided with the waning stages of granite emplacement (Neufeld et al., 2004). No distinct preferred orientation of emplacement for the veins is evident, and the degree of deformation is variable; some veins appear relatively linear and tabular, whereas others are extensively boudinaged. Emerald is associated with both extremes of vein type, and the crystals show no preferred growth orientation relative to either the schist foliation or to tourmaline-filled fractures within the quartz veins. Alteration of the quartz-tourmaline vein selvages consists of jarosite, tourmaline,

PROPERTY DESCRIPTION

	ultramafic (Dum)	leuco- amphibolite (Dmi)	chlorite schist (DF)		granite (Kg)		aplite (Ka)		aplite containing qtz-beryl veinlets (Ka)	
			average n=3	std dev	average n=5	std dev	average n=8	std dev	average n=3	std dev
P <sub>2</sub> O <sub>5</sub> (wt.%)	0.01	<0.01	0.02	0.01	0.1	0.02	0.05	0.02	0.02	0.01
SiO <sub>2</sub>	42.02	49.6	51.34	1.85	72.51	1.39	73.98	0.62	74.92	4.46
TiO <sub>2</sub>	0.03	0.1	0.25	0.06	0.23	0.07	0.06	0.03	0.04	0.02
Al <sub>2</sub> O <sub>3</sub>	1.65	2.03	11.42	2.44	14.96	0.55	15.02	0.6	15.04	2.9
Cr <sub>2</sub> O <sub>3</sub>	0.43	0.37	0.13	0.11	0.02	0.01	0.01	0	0.02	0
Fe <sub>2</sub> O <sub>3</sub>	9.75	7.51	9.98	1.49	1.24	0.31	0.59	0.15	0.3	0.11
MgO	35.99	25.03	13.13	3.04	0.41	0.11	0.14	0.1	0.07	0
CaO	0.04	9.51	8.23	1.48	0.98	0.24	0.85	0.37	2.14	1.05
MnO	0.08	0.19	0.18	0.04	0.02	0.01	0.03	0.03	0.06	0.03
FeO	3.6	3.29	7.6	1.13	0.89	0.18	0.36	0.15	0.26	0.04
Na <sub>2</sub> O	0.13	0.07	1.29	0.71	3.22	0.28	3.8	0.44	4.93	1.36
K <sub>2</sub> O	0.03	0.03	0.17	0.11	4.7	0.36	4.05	0.62	0.75	0.64
BaO	<0.01	<0.01	0.01	0	0.04	0.01	0.01	0	0.02	0
SrO	<0.01	0.01	0.02	0.01	0.02	0.01	0.01	0	0.02	0.02
LOI	9.53	4.15	2.73	0.98	1.07	0.19	0.87	0.29	0.88	0.14
<b>Total</b>	<b>99.67</b>	<b>98.62</b>	<b>98.9</b>	<b>0.33</b>	<b>99.61</b>	<b>0.31</b>	<b>99.44</b>	<b>0.37</b>	<b>99.15</b>	<b>0.53</b>
<b>Li (ppm)</b>	7.1	1.4	58.9	21	143.4	43.5	61.6	21.9	14.7	10.5
<b>Be</b>	1.24	0.25	0.29	0.22	11.65	1.36	14.41	3.31	145.05	74.89
<b>B</b>	30	<20	-	-	33	5	42	26	20	0
<b>C</b>	<0.05	0.08	0.08	0.02	-	-	-	-	0.05	0
<b>F</b>	430	<20	69	54	974	268	460	138	83	40
<b>Cl</b>	<50	<50	253	99	-	-	100	0	-	-
<b>Sc</b>	5.7	24.2	44.4	8.8	4.2	0.7	2.4	1	0.3	0.2
<b>V</b>	23	35	237	45	14	6	-	-	-	-
<b>Cr</b>	3080	2460	964	767	102	56	123	14	140	25
<b>Co</b>	120	54.2	49.9	12	7.1	7.7	0.8	0.3	1.1	0.6
<b>Ni</b>	1635	303	284	223	8	2	7	1	7	<1
<b>Cu</b>	18	<5	63	64	17	12	61	29	8	0
<b>Zn</b>	57	33	65	14	54	23	16	5	8	3
<b>Ga</b>	4	2	11	2	30	2	32	37	31	11
<b>Rb</b>	1	0.3	10.3	10.6	397	16.7	340	26.2	134.2	142.5
<b>Sr</b>	2.5	11.2	65.2	57.2	111.8	43.4	25.1	16.3	108.5	106.8
<b>Y</b>	<0.5	2.2	6.2	1.3	10.5	1	16.6	6.7	8.1	5.2
<b>Zr</b>	1.5	2.1	13.2	11.9	195.1	170.2	101.2	107.2	35.2	3.5
<b>Nb</b>	<1	<1	-	-	13	2	9	2	34	33
<b>Mo</b>	3	3	3	1	3	1	4	0	4	0
<b>Ag</b>	<1	<1	-	-	1	0	-	-	-	-
<b>Sn</b>	5	<1	1	0	23	13	27	11	35	31
<b>Cs</b>	4.3	0.1	6.5	8.2	23	6.9	12.9	1.6	12.3	7.9
<b>Ba</b>	2.4	15.4	77	61.8	345.38	140.3	30.3	24.8	88.8	51.3
<b>La</b>	0.6	1	1.5	0.3	34.5	9.2	7.3	4	2.1	0.1
<b>Ce</b>	0.6	0.7	1.8	0.3	73.8	23.1	15.6	8.4	4.2	0.6
<b>Pr</b>	<0.1	0.1	0.2	0.1	8	2.2	1.8	0.9	0.5	0.1
<b>Nd</b>	<0.5	<0.5	1.1	0.2	26.5	7.3	6.6	3.4	1.8	0.4
<b>Sm</b>	<0.1	0.1	0.4	0.1	4.8	1.1	2	0.5	1.1	0.2
<b>Eu</b>	<0.1	0.1	0.2	0.1	0.5	0.2	0.1	0.1	0.1	0
<b>Gd</b>	<0.1	0.2	0.6	0.1	3.6	0.9	1.9	0.4	0.8	0.5
<b>Tb</b>	<0.1	<0.1	0.1	0	0.5	0.1	0.4	0.1	0.4	0.1
<b>Dy</b>	<0.1	0.4	1	0.2	2.1	0.2	2.4	0.7	1.3	0.8
<b>Ho</b>	<0.1	0.1	0.2	0.1	0.4	0	0.5	0.2	0.3	0.1
<b>Er</b>	0.1	0.3	0.8	0.1	1	0.1	1.5	0.7	0.5	0.3
<b>Tm</b>	<0.1	<0.1	0.1	0	0.1	0.1	0.1	0	0.1	0
<b>Yb</b>	<0.1	0.3	0.9	0.2	0.9	0.1	1.6	0.8	0.7	0.5
<b>Lu</b>	<0.1	0.1	0.1	0.1	0.1	0	0.2	0.1	0.1	0
<b>Hf</b>	<1	<1	1	0	5	3	3	2	6	<1
<b>Ta</b>	<0.5	<0.5	-	-	4.2	3.7	1.4	0.3	17.5	14.4
<b>W</b>	31	16	12	4	64	84	6	3	15	9
<b>Tl</b>	<0.5	<0.5	-	-	1.2	0.2	1	0	1	0
<b>Pb</b>	<5	<5	5	0	47	4	31	7	9	3
<b>Th</b>	<1	<1	-	-	21	5	6	3	3	1
<b>U</b>	<0.5	<0.5	-	-	8.7	3.4	11.8	5.9	8.1	3.5
<b>CO<sub>2</sub></b>	<0.2	0.3	0.3	0.1	-	-	-	-	0.2	0
<b>H<sub>2</sub>O-</b>	0.38	0.07	0.14	0.07	0.1	0.03	0.03	0.01	0.06	0.02
<b>H<sub>2</sub>O+</b>	9.61	4.16	3.22	1	0.72	0.1	0.56	0.22	0.45	0.29

Note: Most major elements were analyzed using XRF and most trace elements by ICP-MS or ICP-ES. Li, Be, Cr and Mo were determined by AAS, B and Cl by INAA, FeO by titration, CO<sub>2</sub> and H<sub>2</sub>O by infrared spectroscopy, and F by specific ion potentiometry.

**Table 1.** (facing page) Whole-rock geochemistry of selected rock types present at the Tsa da Glisza emerald occurrence. Analyses represent average values for each rock type and are from samples collected from different locations on the property.

lepidolite (fluorine- and lithium-rich mica), scheelite and fluorite, in order of abundance. Scheelite and fluorite crystals are less than 1 mm in size. Tourmaline and mica are most abundant within 10 cm of the vein-host contact, whereas more distal alteration consists mainly of jarosite within foliation planes of the chlorite schist. Whole-rock geochemistry of samples taken across numerous mineralized veins shows a consistent enrichment of lithium, tin, and fluorine within the vein selvages, and rare enrichment of beryllium, bismuth and tungsten within the vein itself (Fig. 3; Table 2). This is consistent with the abundant lepidolite in vein selvages. Boron is enriched in both the veins and selvages relative to unaltered chlorite schist, likely reflecting the abundant tourmaline in both veins and selvages.

Beryl and rare emerald are found in quartz-rich segregations within two albitized aplite dykes at Tsa da Glisza. Beryl within the aplite dykes may have formed from late-crystallizing fluids trapped within the

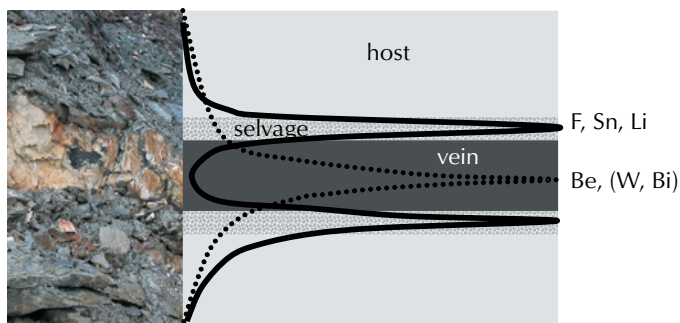


**Figure 3.** Typical geochemical trend across a mineralized quartz vein. Based on data from 94 whole rock geochemical samples, from 11 different mineralized veins. Geochemical data for each of the six elements of interest were normalized to the highest values of that element. Elements consistently partition into the area around the vein (Li, F, Sn), or peak within or in the immediate selvage of the vein (Bi, W, Be). The photo shows a quartz-tourmaline vein approximately 1 m in width.

aplite. These residual fluids are expected to have been rich in Be. Alternately, these occurrences may indicate that some Be was sourced from plagioclase, which, when altered by sodium-rich fluids to a more albitic composition, released the minor amount of Be that was originally incorporated into the plagioclase structure (cf. Charoy, 1999). It is highly unlikely that all of the Be within the mineralizing fluids was sourced from the aplites after they had crystallized, since most mineralized quartz vein selvages are anomalous in several magmatic-associated elements (B, W, Bi, F, Sn, Li) and it is unlikely that all of these were remobilized from aplite during a later metasomatic event.

**Table 2.** Selected element geochemistry from samples taken across a mineralized quartz vein at the Tsa da Glisza emerald occurrence.

Element (ppm)	Bottom					host (DF)	Top host (DF)
	host (DF)	selvage	qtz vn	qtz vn	selvage		
Ag	0.04	0.18	0.02	0	0.06	0.05	0.15
As	0.6	0.2	0.6	0.7	0	0.4	0
Ba	280	370	30	20	30	40	40
Be	6.75	32.4	145.5	65.2	21.2	34.5	19.5
Bi	0.58	9.68	2.37	0.64	1.64	2.17	1.87
Cd	0.1	0.12	0	0	0.1	0.14	0.14
Ce	1.29	1.13	0.22	0.28	1.22	1.27	1.52
Co	53.8	51	4.8	3	30.8	37.4	42.6
Cr	564	574	224	184	243	281	262
Cs	245	211	14.3	15.9	52.2	32.5	22.1
Cu	22.6	188.5	25.6	10.7	77.2	59.4	175.5
F	1140	4450	1480	1190	2340	4390	2250
Ga	8.24	10.9	8.75	6.17	19.2	13.35	17
Ge	0.26	0.28	0.07	0.05	0.24	0.24	0.24
Hf	0.2	0.2	0	0	0.3	0.3	0.3
In	0.031	0.027	0	0	0.058	0.042	0.048
La	0.5	0.5	0	0	0.5	0.5	0.6
Li	177.5	204	25.1	21.7	32.2	57.6	41.7
Mn	1490	1360	160	135	1200	1330	1185
Mo	0.32	1.2	1.72	1.86	0.38	0.67	0.28
Nb	0.5	1.4	0.1	0.1	1.1	1.2	2.2
Ni	321	300	18.4	9.5	76.4	91.3	94.2
P	40	20	10	20	90	70	110
Pb	2.1	1.9	1.4	1.2	3.5	3.1	4.5
Rb	273	371	20.8	29.7	97.8	56.5	35.1
Re	0.003	0.006	0.009	0.003	0.006	0.005	0.005
Sb	0.09	0.05	0	0	0.06	0.07	0.05
Se	0	1	0	0	0	0	1
Sn	14.5	45.2	8.8	6.7	53.1	35	33.1
Sr	31.9	17.3	9.6	7.3	125.5	64.3	115.5
Ta	0.07	0.2	0	0	0.07	0.17	0.11
Te	0	0	0	0	0	0	0
Th	0	0	0	0	0	0	0
Tl	1.91	2.42	0.17	0.16	0.59	0.35	0.21
U	0.1	0.1	0	0	0.2	0.1	0.1
V	227	202	24	15	304	237	258
W	2.8	78.1	233	50.3	111	112.5	69.2
Y	5.7	5.8	1.2	0.7	8.2	7.7	8.7
Zn	87	112	36	34	59	83	64
Zr	2.2	2.7	1.4	0	4.2	3.6	4

Note: Most major elements were analyzed using XRF, and most trace elements by ICP-MS or ICP-ES. Li, Be, Cr and Mo were determined by AAS, and F by specific ion potentiometry.



## GENETIC MODEL

Emerald formation at Tsa da Glisza was associated with the interaction of magmatic and hydrothermal fluids within the actively deforming zone in relatively close proximity to a peraluminous granite (Neufeld et al., in press). The mineralizing event was mainly syn- to late-tectonic, and coincided with the waning stages of granite emplacement and peak metamorphic (upper greenschist) conditions (Neufeld et al., 2004). The Tsa da Glisza deposit best fits a deposit model for beryl proposed by Barton and Young (2002) in which mineralization is related to magmatic-hydrothermal fluids that originate from strongly peraluminous W-Mo (biotite-muscovite) granites. Any genetic model for emerald mineralization must account for the incompatibility of two necessary elements for emerald formation, Be and Cr, which are rarely found together in environments in which beryl is stable.

The genetic model we propose for emerald mineralization at Tsa da Glisza is shown in schematic form in Figure 4 (modified from Neufeld et al., in press). Be, together with other magmatic elements such as B, W, Li, Bi and F, moves out from the granite within highly evolved magmatic fluids. Be is increasingly mobile in fluids containing B and phosphate, and may complex with F, chlorine, and hydroxyl ions. The high F content within mineralized vein selvages suggests that Be most likely travelled as a fluoride or possibly hydroxide complex. Aplite and pegmatite dykes formed with the onset of cooling. Although the dykes locally contain Be concentrations of up to 100 ppm, little Be was incorporated into the aplite-forming minerals, and the beryllium continued to move through the host rocks, within dominantly magmatic fluids (Neufeld, 2004).

A hydrothermal fluid cell was initiated in the host rocks with emplacement of the granite. These fluids percolated through the chlorite schist, and leached Cr from the mafic groundmass. Geochemical transects from unaltered chlorite schist through altered schist, to quartz-tourmaline veins give no indication of how far Cr may have travelled within these fluids (Table 2, Neufeld, 2004). Cr may have been directly sourced from host rock within centimetres of quartz-tourmaline veins through contact metasomatism, or may have travelled some distance along hydrothermal fluid pathways.

The following scenarios could have triggered beryl crystallization: (1) mixing of the Be-rich magmatic fluid with cooler hydrothermal fluids; (2) crystallization of tourmaline, which would have removed boron and

possibly some Li and F and/or lowered the aluminium activity of the Be-rich fluid, thereby reducing the solubility of Be (cf. London and Evensen, 2002); (3) an increase in the Ca content of the fluid due to interaction with the host schist; (4) an increase in host-rock permeability or porosity due to either rock type differences or fracture propagation related to deformation; (5) precipitation of lepidolite within the vein selvage, removing fluorine (ligand) and lithium (buffer) from the fluids; and/or (6) a decrease in pressure and/or temperature. Likely all of these factors played some role in initiating beryl precipitation, particularly where mineralization is contained within highly altered vein selvages. Where emerald occurs solely within the quartz veins, factors (3) and (5) above are probably not involved, and where emerald occurs within linear zones of alteration away from quartz-tourmaline veins, low silica activity may also be a factor in prompting precipitation of beryl (London and Evensen, 2002).

## EXPLORATION MODEL

Emerald exploration in the Yukon has been ongoing since at least 1999, and has resulted in the 2003 discovery of aquamarine at the True Blue occurrence (Deklerk, 2003; Turner, this volume). Emerald mineralization was also discovered one kilometre away from known mineralization at the Tsa da Glisza property in 2004 (Shadow Zone; Fig. 2). Walton (1996) first discussed the possibility of gem mineralization in Yukon, and the various models for emerald formation worldwide as applicable to Yukon exploration are discussed by Walton (2004). In this paper, we discuss an exploration model based solely on the style of emerald mineralization at the Tsa da Glisza occurrence. Such a model may be applicable to much of the Canadian Cordillera, but is specifically aimed at the Finlayson Lake district of the Yukon-Tanana Terrane. Key aspects of the model are discussed below.

## HOST ROCK

### *Geochemistry*

The amount of emerald mineralization within quartz-tourmaline veins is limited by the availability and transport of Cr from the host rock (Laurs et al., 1996). The main host rock for emerald mineralization at Tsa da Glisza is a fine-grained chlorite schist (unit DF) of boninitic composition, with an average Cr content of 800 ppm, which is higher than any other mafic metavolcanic rocks

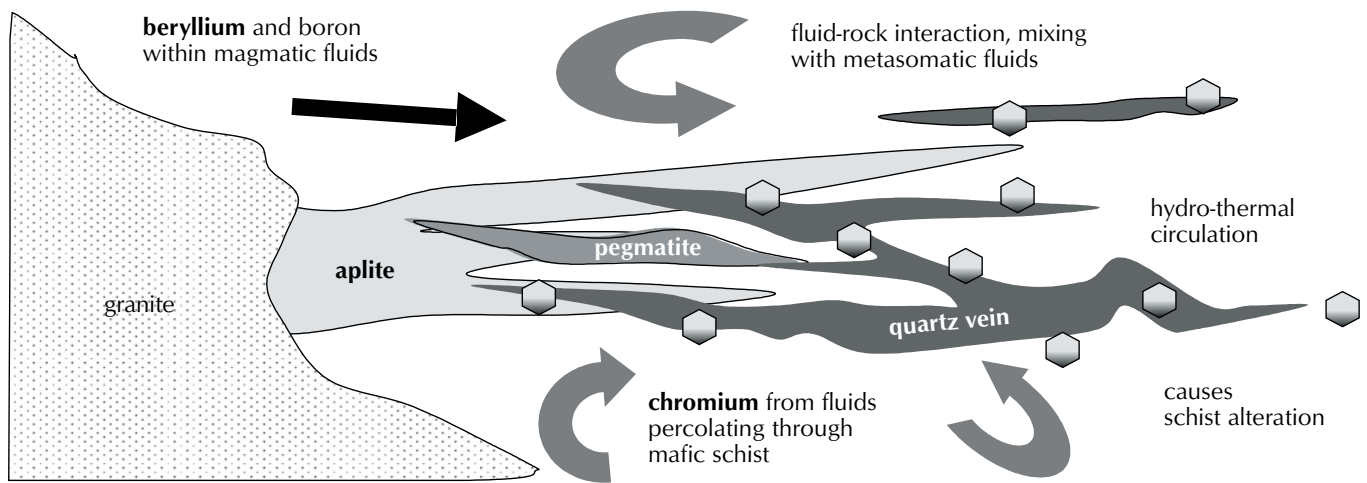


**Figure 4.** Proposed genetic model for emerald mineralization at Tsa da Glisza.

in the Finlayson Lake district, including other rock compositions within unit DF (Table 1; Neufeld et al, 2004; Piercey et al., 2004). This suggests that emerald exploration within the Finlayson Lake district should focus on host rocks of boninitic composition, which are found regionally within unit DF. Although the Cr content of the ultramafic unit is much higher than that of the chlorite schist (Table 1), two factors argue against it being the source of Cr in the mineralizing fluids. Firstly, geological mapping of the property indicates that the ultramafic unit is not present at depth beneath the deposit (i.e. between the granite and the mineralized region; Fig. 2). Secondly, aplite and quartz veins within the ultramafic unit generally display little or no surrounding alteration, suggesting limited interaction between the host and the hydrothermal fluids. The more likely source of the Cr in the Tsa da Glisza occurrence is the chlorite schist, which, due to its schistosity and high mica content, is both highly permeable and reactive. Therefore, exploration should target high-Cr content, permeable mafic schist hosts rather than ultramafic rock. Data available from the Yukon Geological Survey website\* can be used to produce maps that show the locations of intermediate to mafic volcanic and metamorphic rocks in Yukon that may help in targeting appropriate host lithologies.

#### Alteration

Emerald mineralization at Tsa da Glisza is commonly associated with narrow, highly altered vein envelopes and selvages, and zones of less-altered host rock that extend up to several metres away from the quartz veins. This

style of alteration indicates that the host rocks were permeable, and if present, increases the potential for emerald mineralization within a prospective area.

#### RELATED INTRUSIVE ROCKS

Close proximity of an evolved felsic intrusion is obviously implicit in the model for magmatic-hydrothermal emerald deposits. Tsa da Glisza is one of numerous emerald deposits worldwide that are closely associated with peraluminous granite (Guiliani, 1990; Barton and Young, 2002). In addition, the presence of aplite and pegmatite dykes outside of the pluton indicates that not only did the magma produce evolved fluids, but also that at least some of those fluids moved out into the surrounding rocks, rather than cooling and crystallizing within the pluton itself. While beryl is a common component of pegmatites within granitic plutons, emerald will not form unless some amount of mixing of the magmatic fluids with a Cr- or V-bearing source has occurred.

#### Age

At Tsa da Glisza, the  $112.2 \pm 0.6$  Ma biotite-muscovite granite underlying the deposit is part of the Anvil plutonic suite (Mortensen et al., 2000). The Cretaceous age of the related intrusive is not a restrictive factor of the model; however, it is a good “rule of thumb” for emerald exploration within the Yukon, as the Cretaceous Cassiar and Tungsten magmatic suites also contain evolved, felsic granites (L.L. Lewis, pers. comm., 2003).

\*www.geology.gov.yk.ca

### Mineralogy

The mineralogy of a granitic pluton can be used to determine whether Be was likely a component of the evolved magmatic fluids, or was accommodated into the structure of common minerals within the pluton itself. Cordierite, muscovite and plagioclase can all accommodate some Be into their structure during crystallization. Cordierite has by far the highest Be partition coefficient of these three minerals, but plagioclase of composition An<sub>30</sub> (oligoclase-andesine) can also remove substantial amounts of Be from the magmatic fluids. A pluton that contains cordierite or abundant oligoclase-andesine is unlikely to have produced Be-rich residual fluids during crystallization.

The mineralogy of associated aplite dykes provides important information for the exploration model. For example, aplite dykes that contain white beryl reveal that Be moved out of the pluton, but suggest limited mixing of fluids with host rocks. In general, aplite bodies with more albite than potassium feldspar (Laurs et al., 1996) and those that contain tourmaline are increasingly likely to be associated with emerald mineralization.

### Geochemistry

The Be content of the granite at Tsa da Glisza averages 12 ppm (Table 1), which is relatively high compared to crustal values (3 ppm, Wedepohl, 1995) but at the low end of the global average Be-content of granites (1 to 160 ppm, London and Evensen, 2002). Yukon granites with associated beryl tend to have between 12 to 20 ppm Be (L.L. Lewis, pers. comm., 2003). Lithium, fluorine, phosphorous and boron contents are also high in the granite at Tsa da Glisza (Table 1). As discussed previously, high concentrations of these potential ligands and buffers within a fluid increase the mobility of Be within that fluid.

The geochemistry of aplite dykes is unlikely to assist in assessing a target for emerald potential, although high sodium to potassium ratios and Be contents greater than 30 ppm may indicate the presence of Be-F within a sodium-rich fluid during crystallization of the aplite (Neufeld, 2004).

### STRUCTURAL ENVIRONMENT

As discussed above, the Tsa da Glisza occurrence lies in the footwall of the Cretaceous North River fault, within 10 km of the present-day fault trace. This indicates that unloading of the rock units at Tsa da Glisza was relatively late in the local tectonic regime. The structural geology at

Tsa da Glisza is complex and deserves further study; however, the Cretaceous structural setting as discussed by Neufeld et al. (2004) clearly shows a re-orientation of the shear system late in the Cretaceous event. Emerald mineralization was syn-to post-tectonic, and possibly coincided with this environment of rapid unloading, which would have decreased lithostatic pressure and increased the permeability of the host rocks to fluids.

Cretaceous granites within the Finlayson Lake district show a moderate emplacement depth (Mortensen et al., 2000). The quartz-tourmaline veins at Tsa da Glisza were emplaced into greenschist facies rocks near the brittle-ductile transition (Marshall et al., 2003; Neufeld et al., 2004). Be saturation, although dependent on alumina activity, commonly occurs at temperatures of 450 to 550°C (e.g., Barton, 1986). Mineralization has thus far been found within 800 m of outcropping granite, and between 200 and 500 m above granite that is not exposed at the surface.

### GEOCHEMICAL INDICATORS

Preliminary element correlation studies on soil geochemical data from the Tsa da Glisza property highlight a correlation of Be, W, Sn and Bi anomalies near emerald mineralization (Neufeld, 2004). Different analytical methods, however, give drastically varying results for Be concentrations (L.L. Lewis, pers. comm., 2004). New soil geochemical data from the Tsa da Glisza property are pending, and are expected to more clearly delineate element correlations. In general, Be values greater than 10 ppm in soil are considered anomalous. High Be values, however, do not necessarily indicate the presence of beryl. During regional exploration for emerald at various locations throughout the Yukon in 2004, several Be soil geochemistry anomalies were caused by Be-rich mica occurring on pegmatite selvages, or by clay minerals, rather than by the presence of beryl. Conversely, the soil that overlies some mineralized areas at Tsa da Glisza is not anomalous in Be. This is observed in some of the areas where emerald occurs within relatively impermeable quartz veins, rather than on altered selvages where it is more susceptible to weathering and mobilization. Although they don't conform to this model, areas with Be-rich clays might be considered for Colombian-style emerald mineralization, where emerald forms within thrust faults and shear zones. Areas with abundant Be-rich micas are relatively unlikely to contain beryl mineralization, since beryl will typically form prior to mica, and remove Be from the residual fluid. Many of the elements that are strongly correlated



with mineralized quartz veins and selvages (e.g., B, F, Li) in geochemical transects across the veins, are relatively mobile elements and do not correlate well with Be in soil geochemistry.

Regional soil geochemistry can be used to distinguish rock types with high Cr contents. However, as mentioned above, ultramafic rocks, which give the highest regional Cr values, are unlikely to host emerald mineralization similar to Tsa da Glisza. By correlating regional geophysical data with Cr soil geochemistry (e.g., Bond et al., 2002), high-Cr rocks with lower magnetic susceptibilities (therefore not likely to be ultramafic) can be identified. Since regional geochemical coverage may be scarce, this method likely will require some scavenging through old assessment reports for results from property-scale soil geochemistry programs.

## GEOPHYSICAL INDICATORS

The quartz-tourmaline veins associated with emerald at Tsa da Glisza do not produce magnetic anomalies on any scale. They occur within a mafic metavolcanic host rock that is neither a magnetic high nor low on regional geophysical maps (Bond et al., 2002). The associated pluton produces a distinct magnetic low, attesting to its S-type, peraluminous nature (lack of magnetite or hornblende). The nearby ultramafic unit is regionally a strong magnetic high. As mentioned above, a correlation between magnetic highs and high Cr soil geochemistry may help to narrow the target zones, since ultramafic rocks are not a requirement of the exploration model. Areas with a medium magnetic response and medium to high Cr in soil geochemistry are viable targets because mafic metavolcanic rocks can host emerald mineralization, particularly where they occur near a felsic pluton.

## CONCLUSIONS

The coincidence at Tsa da Glisza of the many necessary factors for emerald formation is fortuitous, but it is not necessarily unique. Many of the factors commonly occur together, such as granitic plutons and the deformational environment above and adjacent to them, or mafic host rocks with schistose, and therefore permeable, textures. Emerald typically occurs over small areas that are difficult to find using typical exploration methods such as soil geochemistry and geophysical surveys. Highly prospective targets can be identified using the exploration model outlined above, which constrains host rocks, associated intrusive rocks, structural environments,

and geochemical and geophysical indicators. Detailed prospecting of those specific targets is the most effective method of exploration for emerald.

## ACKNOWLEDGEMENTS

This research, part of work towards H. Neufeld's MSc thesis at the University of British Columbia, was funded by the National Sciences and Engineering Research Council (NSERC) of Canada, True North Gems Inc. (TNGI) and the Yukon Geological Survey. We thank Archer, Cathro and Associates (1981) Ltd. for challenging field experience during regional exploration for emerald in 2003 and 2004, and Greg Davison, Gary Dyck and Twila Skinner of True North Gems Inc. for enlightening discussions while at the Tsa da Glisza property. Bonnie Pemberton (TNGI) patiently drafted the property geology map. This work benefited from a review by James Scoates (UBC), and careful editing by Geoff Bradshaw and Diane Emond (YGS).

## REFERENCES

- Barton, M.D., 1986. Phase equilibria and thermodynamic properties of minerals in the BeO-Al<sub>2</sub>O<sub>3</sub>-SiO<sub>2</sub>-H<sub>2</sub>O (BASH) system, with petrologic applications. *American Mineralogist*, vol. 71, p. 277-300.
- Barton, M.D. and Young, S., 2002. Non-pegmatitic Deposits of Beryllium: Mineralogy, Geology, Phase Equilibria and Origin. *In: Beryllium: Mineralogy, Petrology and Geochemistry*, E.S. Grew (ed.), *Reviews in Mineralogy and Geochemistry*, vol. 50, p. 591-691.
- Bond, J.D., Murphy, D.C., Colpron, M., Gordey, S.P., Plouffe, A., Roots, C.F., Lipovsky, P.S., Stronghill, G. and Abbott, J.G., 2002. Digital compilation of bedrock geology and till geochemistry of northern Finlayson Lake area, southeastern Yukon (105G). Exploration and Geological Services Division, Yukon Region, Indian and Northern Affairs Canada, Open File 2002-7 (D) and Geological Survey of Canada, Open File 4243.
- Breitsprecher, K., Mortensen, J.K. and Villeneuve, M.E. (comps.) 2003. YukonAge 2002, a database of isotopic age determinations for rock units from Yukon Territory. *In: Yukon Digital Geology*, Version 2.0, S.P. Gordey and A.J. Makepeace (comps.); Geological Survey of Canada, Open File 1749 and Yukon Geological Survey, Open File 2003-9(D).

- Charoy, B., 1999. Beryllium speciation in evolved granitic magmas: phosphates versus silicates. *European Journal of Mineralogy*, vol. 11, p. 135-148.
- Deklerk, R. (comp.), 2003. Yukon MINFILE 2002. Exploration and Geological Services Division, Yukon Region, Indian and Northern Affairs Canada.
- Giuliani, G., Silva, L.J.H.D. and Couto, P., 1990. Origin of emerald deposits of Brazil. *Mineralogica Deposita*, vol. 25, p. 57-64.
- Gordey, S.P. and Makepeace, A.J. (comps.), 2003. Yukon Digital Geology, Version 2.0; Geological Survey of Canada, Open File 1749 and Yukon Geological Survey, Open File 2003-9(D).
- Groat, L.A., Marshall, D.D., Giuliani, G., Murphy, D.C., Piercey, S.J., Jambor, J.L., Mortensen, J.K., Ercit, T.S., Gault, R.A., Matthey, D.P., Schwartz, D.P., Maluski, H., Wise, M.A., Wengzynowski, W. and Eaton, W.D., 2002. Mineralogical and geochemical study of the Regal Ridge showing emeralds, southeastern Yukon. *Canadian Mineralogist*, vol. 40, no. 5, p. 1313-1338.
- Jackson, L.E., Gordey, S.P., Armstrong, R.L. and Harakal, J.E., 1986. Bimodal Paleogene volcanics near Tintina Fault, east-central Yukon, and their possible relationship to placer gold. *Yukon Geology, Exploration and Geological Services Division, Yukon Region, Indian and Northern Affairs Canada*, vol. 1, p.139-147.
- Laurs, B.M., Dilles, J.H. and Snee, L.W., 1996. Emerald mineralization and metasomatism of amphibolite, Khaltaro granitic pegmatite-hydrothermal vein system, Haramosh mountains, northern Pakistan. *Canadian Mineralogist*, vol. 34, p. 1253-1286.
- London, D. and Evensen, J.M., 2002. Beryllium in silicic magmas: origin of beryl-bearing pegmatites. *In: Beryllium: Mineralogy, Petrology and Geochemistry*, E.S. Grew (ed.), *Reviews in Mineralogy and Geochemistry*, vol. 50, p. 445-486.
- Lowe, C., Miles, W., Kung, R. and Makepeace, A.J., 2003. Aeromagnetic data over the Yukon Territory. *In: Yukon Digital Geology, Version 2.0*, S.P. Gordey and A.J. Makepeace (comps.); Geological Survey of Canada, Open File 1749 and Yukon Geological Survey, Open File 2003-9(D).
- Marshall, D. D., Groat, L.A., Giuliani, G., Murphy, D.C., Matthey, D., Ercit, T.S., Wise, M.A., Wengzynowski, W. and Eaton, W.D., 2003. Pressure, temperature and fluid conditions during emerald precipitation, Southeastern Yukon: Fluid inclusion and stable isotope evidence. *Chemical Geology*, vol. 194, p. 187-199.
- Mortensen, J.K., Hart, C.J.R., Murphy, D.C. and Heffernan, S., 2000. Temporal evolution of early and mid-Cretaceous magmatism in the Tintina Gold Belt. *In: The Tintina Gold Belt: Concepts, Exploration and Discoveries*, J.L. Jambor (ed.), British Columbia and Yukon Chamber of Mines, special volume 2, p. 49-57.
- Murphy, D.C., 1997. Preliminary geological map of Grass Lakes area, Pelly Mountains, southeastern Yukon (105G/7). Exploration and Geological Services Division, Yukon Region, Indian and Northern Affairs Canada, Open File 1999-4, 1:100 000 scale.
- Murphy, D.C. and Piercey, S.J., 1999. Geological map of parts of Finlayson Lake (105G/7,8 and parts of 1, 2 and 9) and Frances Lake (parts of 105H/5 and 12) areas, southeastern Yukon. Exploration and Geological Services Division, Yukon Region, Indian and Northern Affairs Canada, Open File 1997-3, 1:50 000 scale.
- Murphy, D.C. and Piercey, S.J., 2000. Syn-mineralization faults and their re-activation, Finlayson Lake massive sulphide district, Yukon-Tanana Terrane, southeastern Yukon. *In: Yukon Exploration and Geology 1999*, D.S. Emond and L.H. Weston, (eds.), Exploration and Geological Services Division, Yukon Region, Indian and Northern Affairs Canada (55-66).
- Murphy, D.C., Colpron, M., Gordey, S.P., Roots, C.F., Abbott, J.G. and Lipovsky, P.S., 2001. Preliminary geological map of northern Finlayson Lake area (NTS 105 G), Yukon Territory (1:100 000 scale). Exploration and Geological Services Division, Yukon Region, Indian and Northern Affairs Canada, Open File 2001-33.
- Murphy, D.C., Colpron, M., Roots, C.F., Gordey, S.P. and Abbott, J.G., 2002. Finlayson Lake targeted geoscience initiative (southeastern Yukon), Part 1: Bedrock geology. *In: Yukon Exploration and Geology 2001*, D.S. Emond, L.H. Weston and L.L. Lewis, (eds.), Exploration and Geological Services Division, Yukon Region, Indian and Northern Affairs Canada, p. 189-207.

- Murphy, D.C., 2004. Devonian-Mississippian metavolcanic stratigraphy, massive sulphide potential and structural re-interpretation of Yukon-Tanana Terrane south of the Finlayson Lake massive sulphide district, southeastern Yukon (105G/1, 105H/3,4,5). *In: Yukon Exploration and Geology 2003*, D.S. Emond and L.L. Lewis (eds.), Yukon Geological Survey, p. 157-175.
- Murphy, D.C., Kennedy, R. and Tizzard, A., 2004. Geological map of part of Waters Creek and Fire Lake map areas (NTS 105G/1, part of 105G/2), southeastern Yukon (1:50 000 scale). Yukon Geological Survey, Open File 2004-11.
- Neufeld, H.L.D., Groat, L.A. and Mortensen, J.K., 2003. Preliminary investigations of emerald mineralization in the Regal Ridge area, Finlayson Lake district, southeastern Yukon. *In: Yukon Exploration and Geology 2002*, D.S. Emond and L.L. Lewis (eds.), Exploration and Geological Services Division, Yukon Region, Indian and Northern Affairs Canada, p. 281-284.
- Neufeld, H.L.D., 2004. The Tsa da Glisza emerald occurrence: Descriptive, Genetic, and Exploration Models. Unpublished MSc thesis, University of British Columbia, Canada, 85 p.
- Neufeld, H.L.D., Israel, S., Groat, L.A. and Mortensen, J.K., 2004. Geology and structural setting of the Regal Ridge emerald property, Finlayson Lake district, southeastern Yukon. *In: Yukon Exploration and Geology 2003*, D.S. Emond and L.L. Lewis (eds.), Yukon Geological Survey, p. 281-288.
- Neufeld, H.L.D., Groat, L.A., Mortensen, J.K. and Israel, S., (in press). The Regal Ridge emerald deposit: New mineralogical, geochemical, isotopic, and petrologic results, and inferred genetic model. *Canadian Mineralogist*.
- Piercey, S.J., Hunt, J.A. and Murphy, D.C., 1999. Litho-geochemistry of meta-volcanic rocks from Yukon-Tanana Terrane, Finlayson Lake region: preliminary results. *In: Yukon Exploration and Geology 1998*, C.F. Roots and D.S. Emond (eds.), Exploration and Geological Services Division, Yukon Region, Indian and Northern Affairs Canada, p. 55-66.
- Piercey, S.J., Murphy, D.C., Mortensen, J.K. and Paradis, S.A., 2000. Arc-rifting and ensialic back-arc basin magmatism in the northern Canadian Cordillera: evidence from the Yukon-Tanana Terrane, Finlayson Lake region, Yukon. *Lithoprobe Report*, vol. 72, p. 129-138.
- Piercey, S.J., Murphy, D.C., Mortensen, J.K. and Creaser, R.A., 2004. Mid-Paleozoic initiation of the northern Cordilleran marginal backarc basin: Geologic, geochemical, and neodymium isotope evidence from the oldest mafic magmatic rocks in the Yukon-Tanana terrane, Finlayson Lake district, southeast Yukon, Canada. *Geological Society of America Bulletin*, vol. 116, no. 9, p. 1087-1106.
- Schwartz, D. and Schmetzer, K., 2002. The definition of emerald: the green variety of beryl colored by chromium and/or vanadium. *In: Emeralds of the world, extraLapis English No. 2: the legendary green beryl*. Lapis International, East Hampton, 100 p.
- Turner, D., Groat, L.A. and Wengzynowski, W., 2005 (this volume). Mineralogical and geochemical study of the True Blue aquamarine showing, Shark property, southern Yukon. *In: Yukon Exploration and Geology 2004*, D.S. Emond, L.L. Lewis and G.D. Bradshaw (eds.), Yukon Geological Survey, p. 275-285.
- Wedepohl, K.H., 1995. The composition of the continental crust. *Geochimica et Cosmochimica Acta*, vol. 59, p. 1217-1232.
- Walton, L., 1996. Exploration criteria for gemstone deposits and their application to Yukon geology. Exploration and Geological Services Division, Yukon Region, Indian and Northern Affairs Canada, Open File 1996-2.
- Walton, L., 2004. Exploration Criteria for Coloured Gemstone Deposits in the Yukon. Yukon Geological Survey, Open File 2004-10, 184 p.





# Mineralogical and geochemical study of the True Blue aquamarine showing, Shark property, southern Yukon

*David Turner and Lee A. Groat<sup>1</sup>*

*Department of Earth and Ocean Sciences, University of British Columbia<sup>2</sup>*

*William Wengzynowski*

*Archer, Cathro & Associates (1981) Limited<sup>3</sup>*

Turner, D., Groat, L.A. and Wengzynowski, W., 2005. Mineralogical and geochemical study of the True Blue aquamarine showing, Shark property, southern Yukon. *In: Yukon Exploration and Geology 2004*, D.S. Emond, L.L. Lewis and G.D. Bradshaw (eds.), Yukon Geological Survey, p. 275-285.

## ABSTRACT

The True Blue aquamarine occurrence in the Quiet Lake area of southern Yukon is underlain by Paleozoic Cassiar Platform miogeoclinal clastic and carbonate rocks, a Mississippian syenite stock, Mississippian felsic metavolcanic rocks (Pelly Mountain Volcanic Belt), and a small carbonatite body associated with the syenitic intrusion. Beryl occurs in quartz veins and tension gashes, and is restricted to those that cut the syenite. Accessory minerals in the quartz veins include varying amounts of fluorite, siderite, calcite, allanite and ilmenite. Mineralization has been dated at  $172 \pm 5$  Ma, using the Sm-Nd system on fluorite from several veins. Aquamarine discovered on the property is distinctive because of its deep blue colour and high  $\text{Fe}^{2+}$  concentration, up to 5.79 wt.% FeO. During the 2004 field season, diamond chainsaws were used to extract beryl-bearing vein material from the syenite.

## RÉSUMÉ

Le gisement d'aigue-marine True Blue, situé dans la région du lac Quiet, dans le sud du Yukon, recouvre des roches clastiques et carbonatées miogéoclinales de la plate-forme de Cassiar datant du Paléozoïque, un stock de syénite du Mississippien, des roches métavolcaniques felsiques du Mississippien (ceinture volcanique de Pelly Mountain), ainsi qu'un massif de carbonatite associé à l'intrusion syénitique. Du béryl est présent dans des veines de quartz et des fissures d'extension, et se limite à celles qui ont recoupé la syénite. Les minéraux accessoires dans les veines de quartz comprennent des quantités variables de fluorine, de sidérite, de calcite, d'allanite et d'ilménite. L'âge de la minéralisation a été établi à  $172 \pm 5$  Ma par la méthode Sm-Nd appliquée à la fluorine provenant de plusieurs veines. L'aigue-marine découverte dans la propriété se distingue par sa couleur bleu foncé et par sa concentration élevée de  $\text{Fe}^{2+}$ , la proportion de FeO pouvant atteindre 5,79 % en poids. Au cours des travaux sur le terrain de 2004, on a utilisé des scies à chaîne à tranchants au diamant pour extraire les matériaux de la veine bérylifère de la syénite..

<sup>1</sup>lgroat@eos.ubc.ca

<sup>2</sup>6339 Stores Road, Vancouver, British Columbia, Canada V6T 1Z4

<sup>3</sup>1016-510 West Hastings Street, Vancouver, British Columbia, Canada V6B 1L8

## INTRODUCTION

The True Blue aquamarine occurrence on the Shark claims is situated in the Ketzá-Seagull District in southern Yukon, and is wholly owned by True North Gems Inc. (True North). The contiguous 94-claim block lies within NTS map sheets 105F/8, 9 and 10 with central coordinates of 61°30' latitude north and 132°30' longitude west (Fig. 1).

Dark blue gem beryl mineralization was identified in quartz veins cutting a Mississippian syenite during the 2003 field season and exploration continued into 2004. Recent work on the property consisted of geological

mapping, geochemical soil and silt sampling, specimen extraction, and laboratory investigations following the field seasons. These further investigations make up an MSc thesis by the first author at the University of British Columbia. Mineralogical, geochemical and geochronological studies of the veins and host rock are currently being pursued in order to better understand the geology and mineralogy of the True Blue aquamarine occurrence. These studies will provide essential information for developing a deposit model that will more specifically define exploration parameters for this style of beryl mineralization. In this article we discuss the results of our fieldwork and the most recent findings on the geological setting of this occurrence.

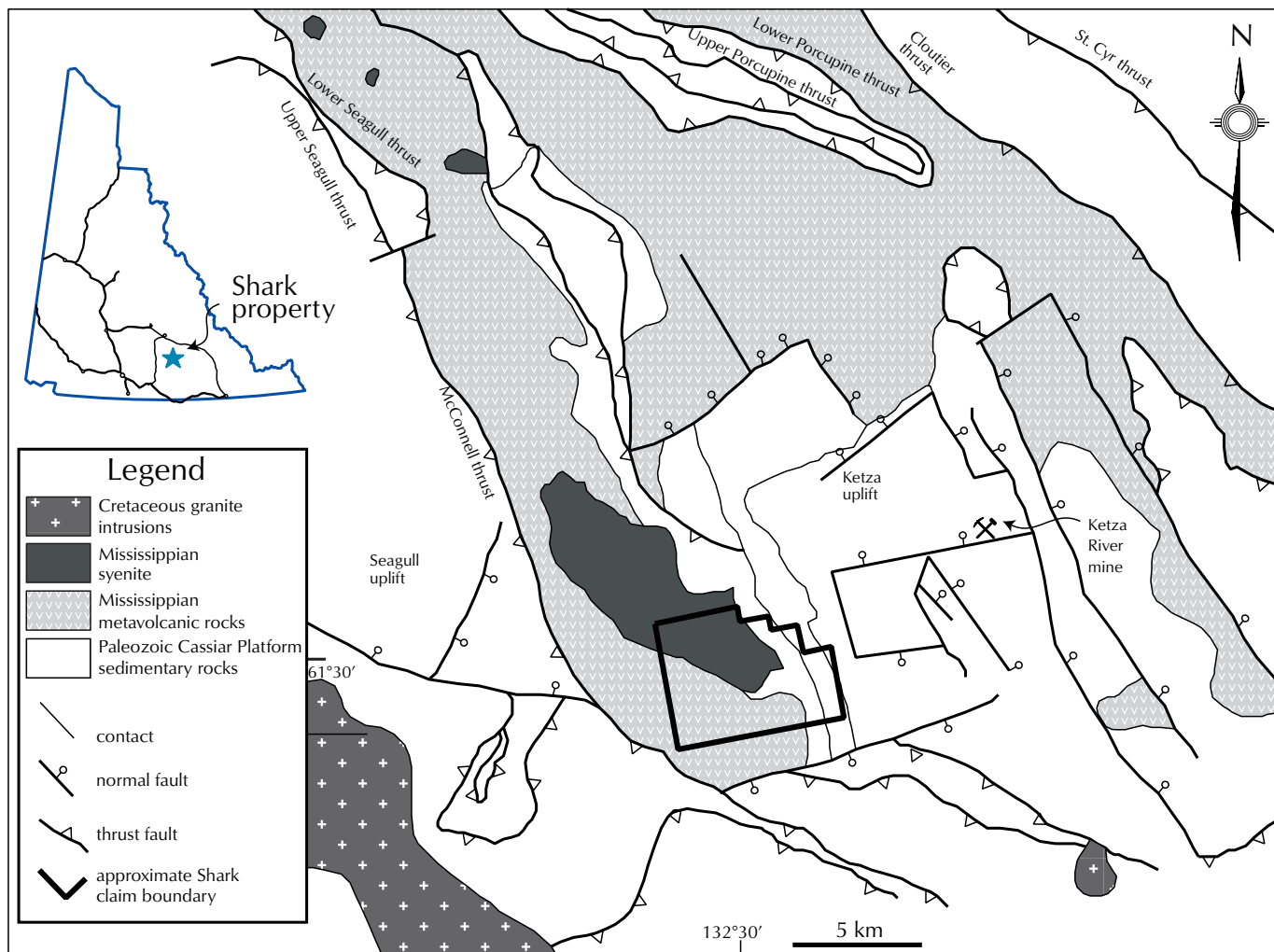


**Figure 1.** True Blue property location and regional geology of the Ketzá-Seagull District, southern Yukon. Modified after Tempelman-Kluit (1977) and Gordey and Makepeace (2003).



## PROPERTY EXPLORATION HISTORY

Since the late 1960s, considerable work has been done in the Ketzia-Seagull District. Exploration has focused on lead-zinc veins, gold-rich vein and manto deposits, uranium-rare earth element prospects, and volcanogenic massive sulphide (VMS) mineralization (Deklerk, 2003).

In 1976, the Guano claims were staked by Ukon Joint Venture (Chevron Minerals Limited and Kerr Addison Mines Limited) to cover the eastern portion of the present Shark property. Those claims were explored for uranium and rare earth elements (REE) associated with skarns and veins developed peripheral to a Mississippian syenite stock (Archer, 1977). In 1979, an Msc thesis that focused on uranium-REE enrichment at the Guano property was completed at the University of British Columbia (Chronic, 1979).

In the late 1980s, the White and PS claims were staked by Mountain Province Mining Inc. to cover a large gold target. Most of those claims were north of the Shark claims but some covered the eastern portion of the current Shark property (Deklerk, 2003).

In 1988, B. Hall staked the Matthew claims, which included what now is the southwestern corner of the Shark property, in order to cover a Kuroko-type VMS target. After a number of option agreements, the Matthew claims expired during the 1990s and were restaked as the Mamu-Bravo-Kulan claims (Deklerk, 2003).

While conducting exploration peripheral to the Guano claims during the 1976 Ukon Joint Venture program, D. Eaton of Archer Cathro discovered an unidentified blue mineral within a quartz vein that cut a syenite boulder. The occurrence was documented in a traverse report but its importance was not appreciated until L. Groat identified the mineral as beryl in fall 2002. In response to the confirmation of beryl, Archer Cathro staked the Shark claims on behalf of True North as part of a regional gem-beryl exploration program.

## 2004 FIELD SEASON WORK

Exploration during the 2004 field season was conducted by Archer Cathro for True North, and focused on Shark Bowl and Guano Ridge (Fig. 2). Shark Bowl is the main area of dark blue gem-beryl mineralization and Guano Ridge has geological characteristics similar to Colombian-type emerald occurrences.

A diamond-disc hand saw had been used to extract material during the 2003 field season; however, this only allowed incisions up to ~12 cm deep. As a result, quartz vein extraction within Shark Bowl during the 2003 field season focused on beryl mineralization on exposed vein surfaces. Although gem-grade material was obtained in 2003, some of the crystals had suffered damage from natural surficial processes such as rock fall. Accordingly, the potential for gem-quality stones was thought to be better in unexposed quartz veins and as such, work during 2004 focused on extracting undamaged quartz veins.

During and following the 2003 field season, hypotheses were developed about the conditions of beryl crystallization and a paragenetic sequence. However, no key minerals were identified within the veins that positively indicated the presence of beryl. Consequently, only those veins that showed beryl mineralization on the surface were examined and sampled in 2004, with particular attention being paid to those crystals with dark blue colouration.

During the 2004 field season, several improvements were made to the extraction process. Two 18-inch (~ 40 cm) diamond chain saws were used to facilitate deeper cuts for removal of larger amounts of intact veins. To cool the saws, three pumps, drill hose and a number of holding drums were flown via helicopter to the head of the Shark Bowl, to prepared sites at approximately 70-m vertical intervals. At each pump and active cutting site, 170-litre drums were used to hold water and supply hydraulic head to the saws via garden hoses. In total, 785 kg of concentrated vein material was extracted from syenite talus and bedrock exposures in Shark Bowl during a two-week period. Following completion of the extraction work in August, the concentrate was moved from the Shark property to Regal Ridge (located 100 km to the east-southeast). Processing of the concentrate is scheduled for early in the 2005 field season.

The geological setting of Guano Ridge is similar to the setting of Colombian-type emerald deposits (Walton, 2004). Furthermore, previous geochemical data showed enrichment of both beryllium and chromium, which are essential components for emerald mineralization. Soil sampling and prospecting was conducted on this portion of the property, but no beryl has been identified thus far.

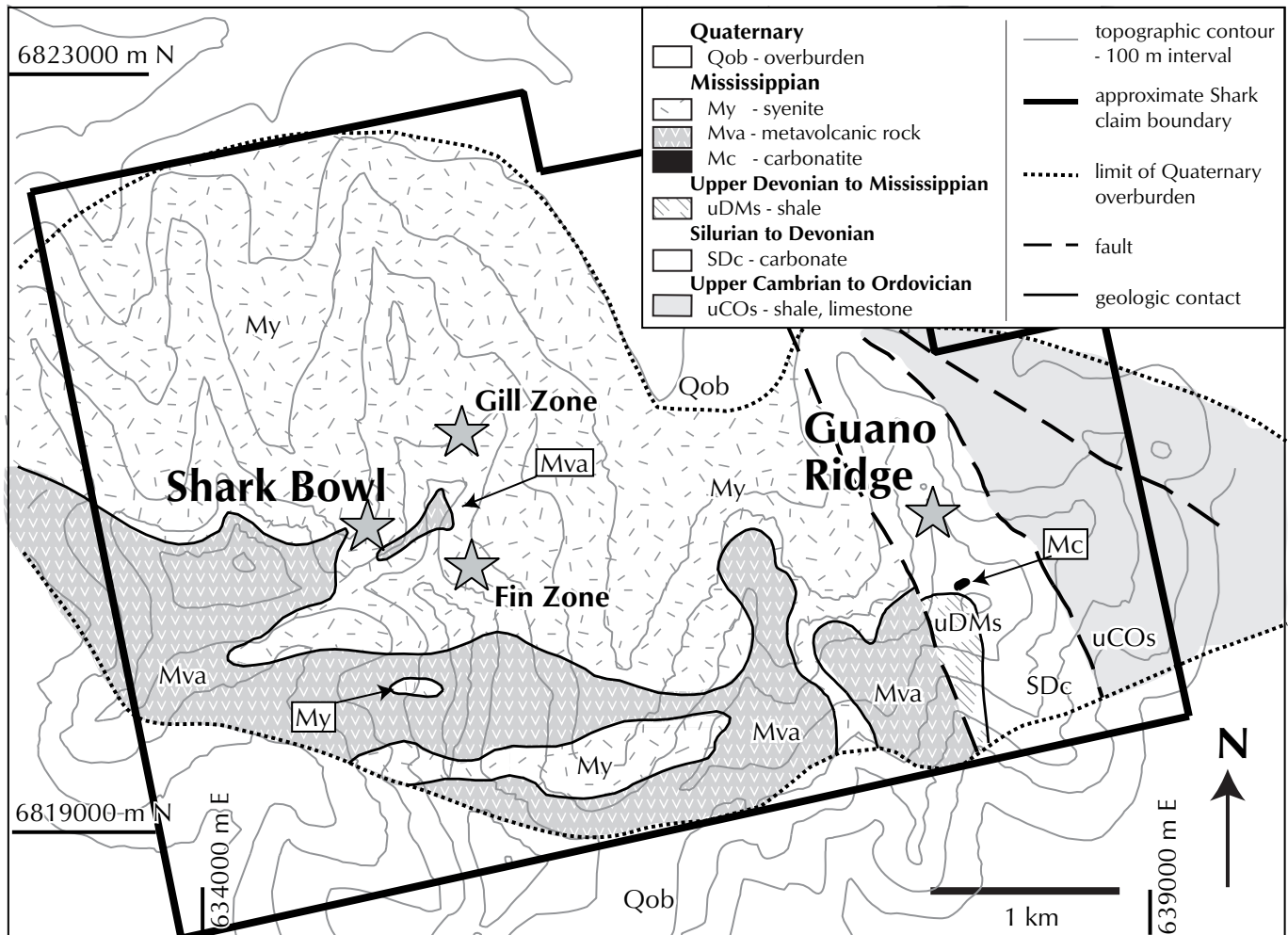


Figure 2. Geology map of the True Blue property. Grid coordinates are UTM zone 8. Labelled stars indicate beryl targets.

## REGIONAL GEOLOGY AND STRUCTURAL SETTING

The Shark property is located within the Cassiar Platform, which is a displaced tectonic element composed of Lower Paleozoic miogeoclinal clastic and carbonate rocks (Fig. 1) that are overlain and interfingered with felsic to mafic metavolcanic rocks of Mississippian age. These volcanic rocks form the arcuate northwest-trending Pelly Mountain Volcanic Belt (Hunt, 1997) and are believed to have been deposited in a continental rift environment (Mortensen, 1982). Roughly coincident with the southwestern edge of the volcanic belt is a 32-km-long string of syenite intrusions, which are thought to be the subvolcanic equivalent of extrusive components of the Pelly Mountains Volcanic Belt. The largest of the syenite

intrusions is partially covered by the Shark claim block (Figs. 1 and 2). This entire package of rocks was subject to several phases of deformation and faulting during arc-continent collision. Early phases of deformation, likely post-Late Triassic in age, are thrust-related events that produced several “southwest-dipping thrust panels and northeasterly verging folds within the region” (Gibson et al., 1999, p. 238). Locally, this deformation event produced foliations that are both parallel and subparallel to bedding in the layered rocks. Late-phase deformation is characterized by normal faults that cross-cut prior structures and are likely related to Cretaceous intrusions of the Cassiar Suite.

In a detailed study of the Ketz River mine area, Fonseca (1997) described two phases of regional ductile deformation, followed by regional thrusting, and finally

local extension. The latter extension was accompanied by influx of hydrothermal fluids, which are thought to have been related to a buried Cretaceous intrusion.

## PROPERTY GEOLOGY

The largest pluton within the suite of Mississippian syenitic intrusions and its extrusive equivalents underlie the bulk of the Shark property (Fig. 2). Older metasedimentary units (uCOs, SDc and uDMs) are intruded and overlain by these Mississippian igneous rocks. The following paragraphs describe each of the units, from oldest to youngest.

**Unit uCOs** is Late Cambrian to Ordovician in age and comprises grey to black, lustrous phyllite and minor black shale. The rocks are typically thinly bedded and moderately deformed. Quartz-calcite veining in the unit is predominantly deformed and bedding parallel.

**Unit SDc** includes thinly to thickly bedded, grey limestone and orange-weathering dolomite with minor quartzite. This Silurian to Devonian unit forms the bulk of Guano Ridge and hosts a subeconomic REE skarn (Chronic, 1979). Minor brecciation and quartz-calcite cementation is present within this unit.

**Unit uDMs** consists of thinly laminated, dark grey to black shale that weathers to blocky cobble- and smaller-sized clasts. Quartz veins in this unit are rare, barren and up to 4 cm in width.

**Unit Mva** is a package of felsic metavolcanic rocks with minor sedimentary interbeds. It includes phyllite, argillite, chert, lapilli tuffs, volcanic breccias, trachytic flows, and sericite and chlorite-talc-altered schist. Metamorphic grades range from lower greenschist to lower amphibolite facies. This unit typically ranges from pale green to grey to maroon in colour, and weathers to form platy to blocky talus. Quartz veins hosted in this unit typically contain siderite and rarely fluorite and sulphide minerals. Vein abundance generally increases with proximity to the syenite.

**Unit My** forms a 12-km-long, 3-km-wide syenite stock, the southeastern half of which is located on the Shark property. It is medium- to fine-grained, equigranular and perthitic. Accessory minerals identified in thin section include magnetite, zircon, apatite, fluorite and pyrite. The colour is variable, ranging from light grey to pink to dark green. The rock is massive and weathers resistantly to form prominent cliffs along ridges. Pockets of Mva,

possibly roof pendants too small to be mapped at a regional scale, are present within this unit. Zircons from unit My have been dated at  $362.7 \pm 3.6$  Ma using U-Pb methods (J.K. Mortensen, pers. comm., 2004). Tension gashes are locally abundant in this unit, comprising up to 30% of the rock and ranging in size from mm- to m-scale.

**Unit Mc**, a light to dark green carbonatite, crops out just outside the margin of Unit My within Unit SDc. Macroscopic minerals include a possible feldspathoid that stands out from the more recessive matrix on weathered surfaces, and a black tourmaline-like mineral with similar habits.

**Unit KqC** comprises quartz monzonite and granite of Cretaceous age that has been assigned to the Cassiar Plutonic Suite, with ages between 100 and 110 Ma (Mortensen et al., 2000). This unit has not been recognized thus far on the Shark property, and the closest outcrop of the unit lies ~10 km to the southwest. However, Cretaceous granite may underlie the map area and thus warrants a description. Locally in the Ketzia-Seagull District, the Cassiar Suite intrusive rocks typically consist of grey-weathering, equigranular, medium- to coarse-grained quartz monzonites.

## PROPERTY-SCALE STRUCTURES

Unit uCOs is separated from units SDc and uDMs by a near-vertical, north-northwest ( $330^\circ$ ) trending fault. A second fault (located ~800 m to the southwest and trending approximately  $335^\circ$ ) separates the carbonate and clastic rocks in the eastern part of the property from the main body of syenite and metavolcanic rocks to the west. Bedding in stratified units across the property strikes roughly northeast and dips moderately to the southeast.

## VEIN MINERALOGY

Beryl mineralization on the True Blue property occurs in quartz veins and tension gashes and is restricted to veins that cut the syenite. Vein mineralogy is currently being investigated using a variety of techniques, including thin section petrography, scanning electron microscopy (SEM) and electron probe micro-analysis (EPMA). Major components of the quartz veins include beryl, siderite, fluorite and allanite, and minor phases include ilmenite, pyrite and calcite. Tourmaline was identified in the field; however, these grains were subsequently identified as allanite by powder X-ray diffraction. Additional samples



are currently being investigated in order to determine if tourmaline is indeed present at the True Blue property.

## BERYL

The beryl ranges in colour from dark blue to light blue, and from yellow-green to green to turquoise. Colour zonation has been noted in several crystals, and is characterized by blue cores surrounded by green rims. Variable amounts of iron in beryl are known to result in blue, green and yellow colours (Sinkankas, 1981). Some of the colour-zoned crystals occur adjacent to allanite, suggesting that iron is partitioning favourably into that phase. Beryl is most commonly observed as externally euhedral crystals in both finely crystallized masses, as well as in larger single crystals or clusters of crystals. Single crystal sizes discovered thus far range from submillimetre to ~2.5 cm in width, and up to several centimetres in length, whereas clusters of crystals have been found to measure up to 9 cm x 8 cm. The clarity of the beryl ranges from opaque to transparent. Poor clarity is commonly due to fractures perpendicular to the c-axis and, less commonly, mineral inclusions.

Euhedral to anhedral cores (single and multiple) and complex internal zoning are present in many crystals when observed in back-scatter electron (BSE) mode in the SEM (Fig. 3). Mineral inclusions observed in the beryl include siderite, calcite, quartz, and a calcium-REE phase. A total of 142 analyses of major and minor elements from numerous beryl specimens have been acquired via EMPA. Weight % FeO values average around 2.5 and range up to 5.79, which are the highest FeO contents ever described in scientific literature for beryl. Significant amounts of Na, Ca and Mg have also been detected. Figure 4 shows octahedral Al-site substitution by cations  $\text{Fe}^{2+}$  and  $\text{Fe}^{3+}$ ,  $\text{Mg}^{2+}$ ,  $\text{Mn}^{2+}$ ,  $\text{Cr}^{3+}$ ,  $\text{V}^{3+}$  and  $\text{Sc}^{3+}$ . Specimens with lower total FeO content show typical patterns of octahedral substitution, while those with higher FeO content exhibit higher over-substitution at the Al site. This deviation from normal behaviour may be due to iron residing in the channel sites within the beryl crystal, and is likely the cause of the dark blue colour of the high-FeO-content beryl. This phenomenon is being investigated further with single crystal neutron diffraction and Mössbauer spectroscopic techniques.

Dark blue beryl is very rare, having been recognized only in United States (Lone Pine), Madagascar (Ambositra), Pakistan (Gilgit), and a small number of localities in Brazil (e.g., Marambaia and Paraiba). Unfortunately, none of these sites have received detailed investigations and none

of these sites have consistently produced gem-quality material. Since there is no steady supply of dark blue beryl in today's market, valuation of the True Blue beryl is difficult.

## CARBONATES

Siderite is the dominant carbonate mineral present in the veins, and forms euhedral crystals up to several centimetres in width with a purplish metallic lustre, as well as more typical euhedral crystals with brownish submetallic lustre. Much of the siderite has been heavily weathered

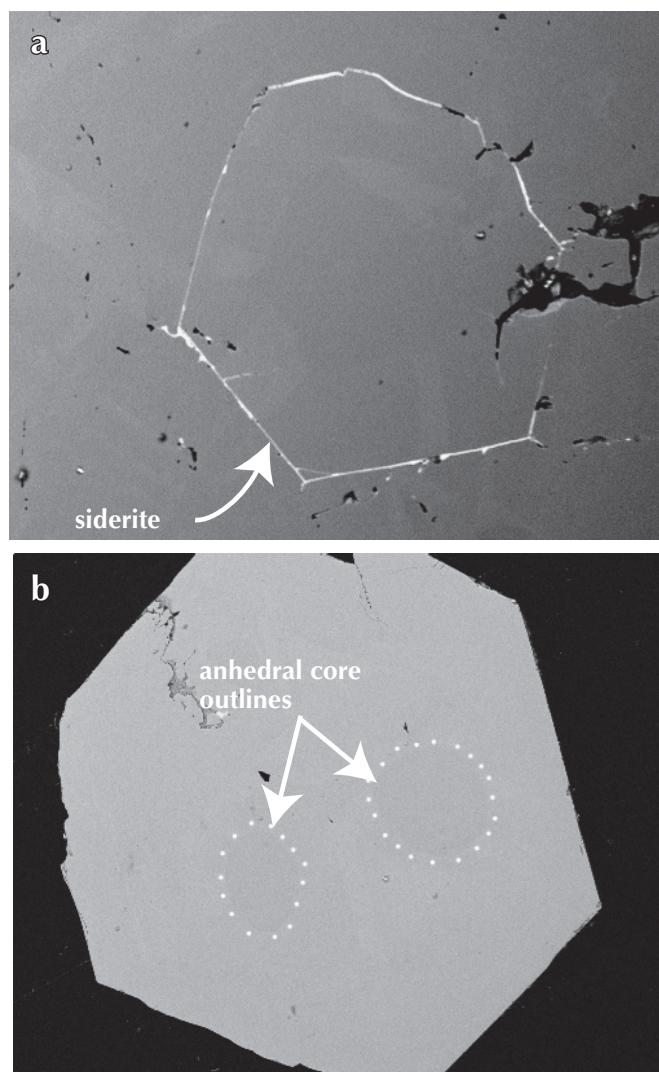


**Figure 3.** SEM photomicrographs (BSE mode) of beryl from True Blue. (a) A euhedral core surrounded by siderite inclusions (light tone); (b) an example of beryl with multiple anhedral cores and complex compositional zonation. Field of view is ~800 µm for each image.

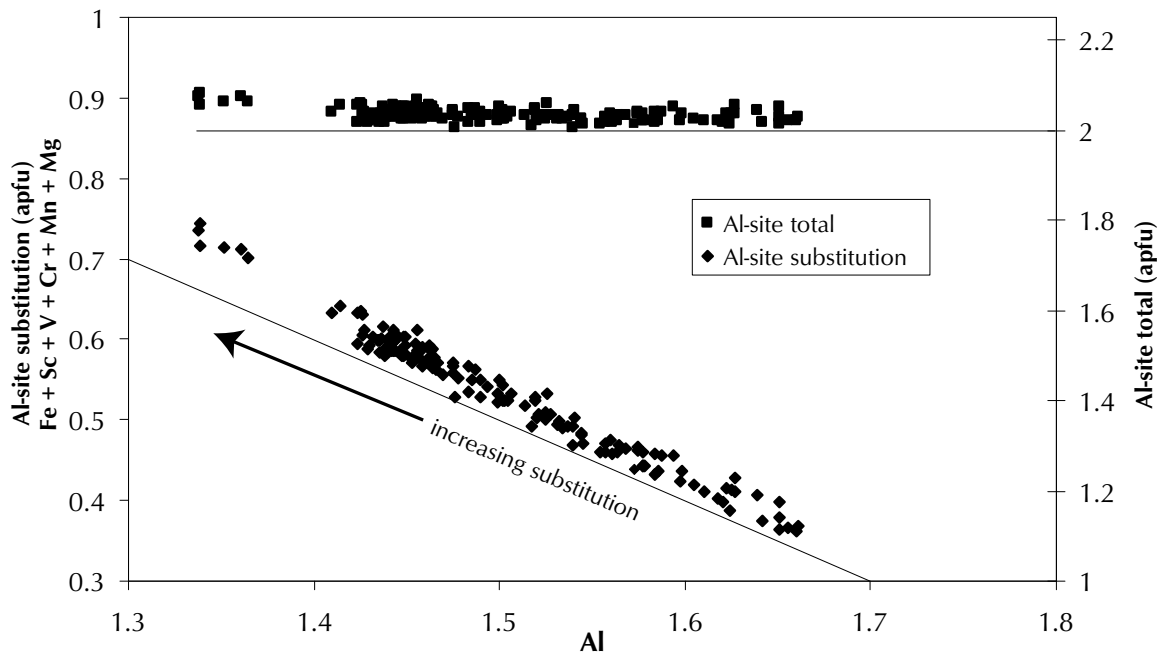


**Figure 4.** Transition metal substitution for Al and total occupation of the octahedral Al-site within beryl (ideal formula =  $Be_3Al_2Si_6O_{18}$ ) from the True Blue occurrence. The outlying set of data with low Al contains the highest FeO contents and shows the deepest blue colouration. APFU=atoms per formula unit.

and carbonate-pitting in exposed veins is common. Minor magnesium-calcium-carbonate has also been observed in the veins, and trace amounts of what is most likely a REE-carbonate have been observed with the SEM. Carbonates are the next abundant phase after quartz in the tension gashes.

### FLUORITE

Clear and light to dark purple fluorite are common components of quartz veins. Fluorite commonly makes up the entire width of individual veins, forming clots up to 10 cm across as opposed to euhedral crystals. Figure 5 shows REE compositions of fluorite collected during geochronological studies. REE concentrations are moderately elevated and show a prominent negative Eu anomaly when compared to chondritic values (McDonough and Sun, 1995). The variability of light rare earth elements (LREE) is likely due to the presence or absence of proximal allanite, which preferentially incorporates LREE over HREE (Giere and Sorensen, 2004).

### ALLANITE

Allanite was positively identified using X-ray powder diffraction techniques after unusual textures and X-ray patterns were observed from what was initially thought to be tourmaline. Crystals form individually up to several centimetres in length and as radiating masses up to several centimetres in length and width. A total of 39 EPMA analyses have been carried out on allanite crystals, which display up to 29 wt.%  $REE_2O_3$ , classifying the allanite as the cerium-dominant variety (Ercit, 2002). Figure 6 (Petrik et al., 1995) confirms this classification in the epidote mineral group and also estimates a  $Fe^{3+}/Fe_{total}$  value of ~0.25. Unusual zoning and REE-carbonate inclusions are apparent with the SEM in BSE mode.

### ILMENITE AND PYRITE

Trace amounts of pyrite and ilmenite have been found within the quartz veins. It is unlikely that either of these minerals is critically involved in beryl precipitation; however, their systematics will be used to constrain fluid conditions. Ilmenite forms platy euhedral crystals up to 1 cm in diameter and 3 mm thickness, whereas the pyrite occurs as fine-grained masses.

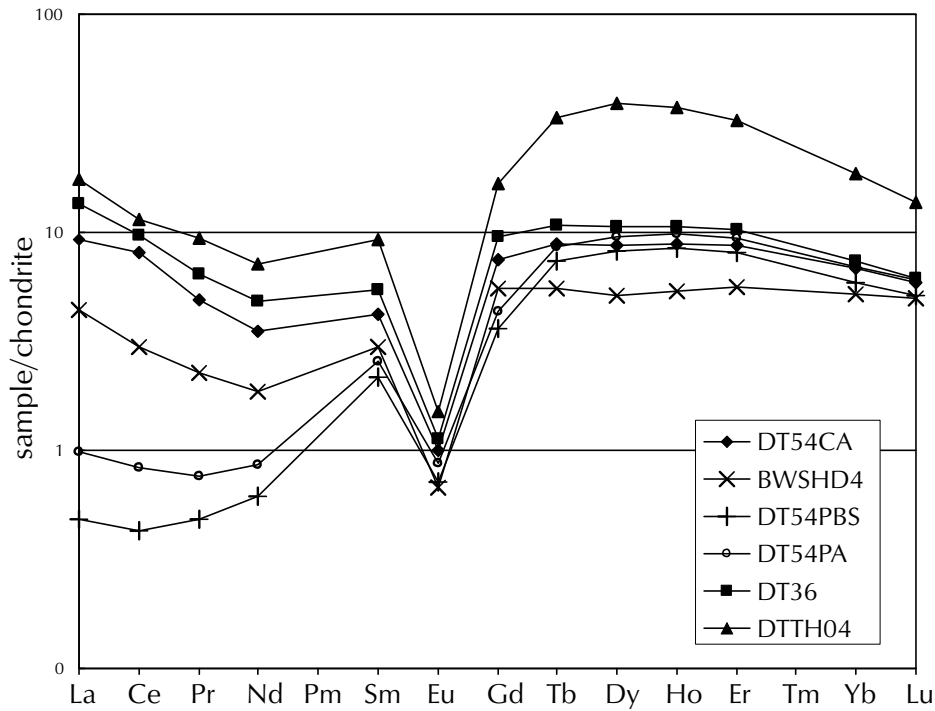


Figure 5. Chondrite-normalized REE profiles of fluorite from tension gashes cutting syenite within Shark Bowl. Note the variable LREE concentrations and pronounced negative europium anomalies.

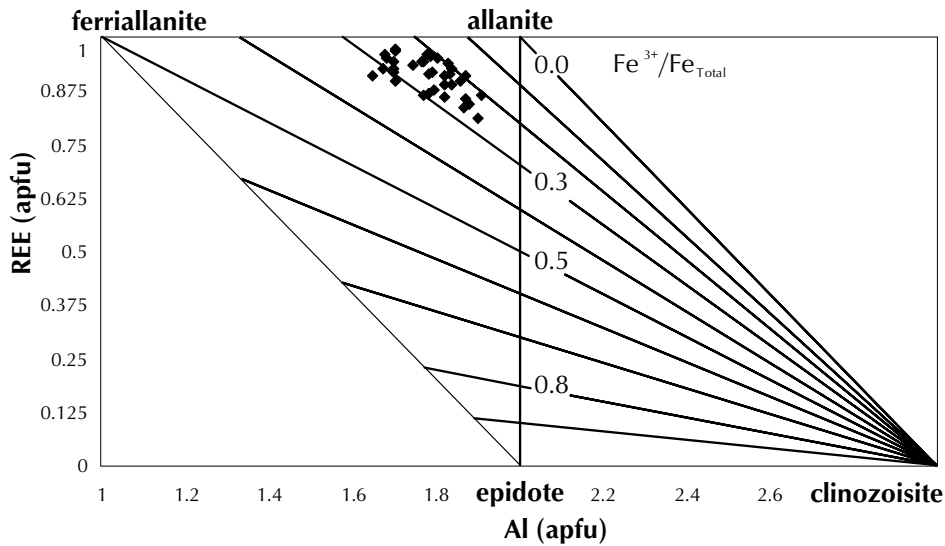


Figure 6. Discrimination diagram between four members of the epidote group. Lines of constant  $Fe^{3+}/Fe_{total}$  value originate from clinozoisite and allow an estimation of this value (after Petrik et al., 1995).



## PARAGENETIC SEQUENCE OF VEIN MINERALS

A full paragenetic sequence for vein components is currently being developed, although the relative timing of some individual mineral phases remains unclear. However, a few general statements about system conditions and mineral relationships may be inferred:

- Siderite is present in virtually all tension gashes, both within the syenite host and outside within the metavolcanic wall rocks.
- Siderite crystallized both before and after beryl, and between beryl growth periods as inclusions around beryl cores.
- Ubiquitous fluorite suggests that beryllium and REEs were being complexed by fluoride anions, which is supported by examples of beryl and allanite that crystallized adjacent to one another.
- Large variations in LREE concentrations within fluorite suggest co-precipitation of the fluorite and LREE-enriched allanite.
- Ilmenite crystallized both before and after beryl and allanite.
- Resorbed cores in beryl indicate periods of fluid conditions out of equilibrium with previously crystallized minerals.

Initial investigations suggest that multiple disequilibrium and re-equilibration events occurred as fluid conditions changed through vein mineral crystallization and wall-rock alteration. Pressure-temperature changes and fluid mixing are also potential mechanisms for mineral crystallization, and are being investigated.

## GEOCHRONOLOGY

A sample from the northern end of the syenite stock was dated at  $362.7 \pm 3.6$  Ma by Mortensen (J.K. Mortensen, pers. comm., 2004) using U-Pb techniques, and skarn related to the syenite to the south yielded a three-point Rb-Sr isochron of  $333 \pm 10$  Ma (Chronic, 1979). Granitic magmatism of the Cassiar Suite has been dated as Cretaceous (~110 Ma; Mortensen et al., 2000), and gold mineralization at the nearby Ketz River mine has also been dated as Cretaceous (~108 Ma; Fonseca, 1998).

The exact timing of vein emplacement on the Shark property is unclear; however, constraining this event is

necessary to understand the origin of the beryl. Fluorite in the veins has been dated as mid-Jurassic ( $172 \pm 5$  Ma) using Sm-Nd techniques (D. Weis and B. Keiffer, pers. comm., 2004). This date does not correspond to known igneous events in the area; consequently additional dating techniques (e.g., U-Pb on allanite) will be used to attempt to verify this age.

## DEPOSIT MODELS

Beryllium enrichment in the form of beryl is typically associated with late-stage fluids derived from a highly differentiated intrusion, commonly of granitic or less commonly syenitic composition (Barton and Young, 2002). Consequently, in order to understand occurrences and develop exploration parameters for this style of mineralization, a source of beryllium (Be) must first be defined. At the True Blue aquamarine occurrence there are four possible Be sources:

1. late-stage fluids related to the Early Mississippian syenite;
2. late-stage fluids related to unrecognized or buried Cretaceous granite;
3. beryllium leached from syenite; or
4. beryllium leached from unidentified source rocks.

If the mid-Jurassic age from the fluorite is disregarded, the two simplest explanations for beryl formation involve late-stage igneous fluids. If mineralization occurred during the waning stages of syenite intrusion, late deformation could produce tension gashes and a place for Be-rich fluids to escape. Since whole-rock geochemical values for the syenite show enrichment in REE and Be, this would allow for a simple system.

If mineralization were attributed to Cretaceous magmatic fluids, a buried granitic intrusion would have to be invoked and a mechanism for restricting beryl crystallization to the syenite host would also be needed. In addition, the high REE and low tungsten, tin, molybdenum and boron concentrations in the veins would have to be explained. Since both of these hypotheses do not correspond with a mid-Jurassic age (~172 Ma), they would require that the age from the fluorite be dismissed and an indisputable age of ~100 Ma or ~360 Ma be determined from another phase in the vein.

If mid-Jurassic (~172 Ma) is the true age of mineralization, then a regional metamorphic fluid was likely the medium

from which the veins crystallized. In this scenario, the most probable source for Be was through leaching of the syenite, although other unidentified Be sources cannot be discounted at this time. Thrust-faulting in the region occurred during the Jurassic, and thrust-related deformation could explain the presence of tension gashes as well as a regional metamorphic fluid. If this fluid were out of equilibrium with the host rocks (syenite), alteration along the vein selvages would likely occur. If the altered phases contained minor amounts of Be or REE, that could explain the presence of beryl and allanite, as well as their restriction to the limits of the intrusion. Furthermore, a reduced oxidation state within the silica-saturated quartz veins is expressed through a number of minerals with ferrous ( $\text{Fe}^{2+}$ ) iron such as siderite, allanite, ilmenite and beryl. This contrasts with the magnetite-bearing ( $\text{Fe}^{3+}$ ) silica-undersaturated syenite, thus supporting the hypothesis of a later regional fluid in disequilibrium with the host syenite.

## CONCLUSION AND FUTURE WORK

The True Blue aquamarine occurrence contains gem-beryl with exceptionally dark blue colour, which is likely due to high ferrous ( $\text{Fe}^{2+}$ ) iron content. A handful of other dark blue beryl occurrences exist elsewhere in the world; however, all of these are poorly characterized, and beryl examined from these sites exhibits a lighter colour. Currently, the True Blue occurrence of gem beryl appears to be markedly different from other beryl occurrences in Yukon.

Future work at the University of British Columbia will constrain the conditions of mineralization and the source of beryllium and rare earth elements. This will be accomplished using geochemical, mineralogical and petrographic investigations of all phases within the veins, host syenite, and possible alteration zones associated with the veins. Further in-depth mineralogical studies of the beryl will be carried out with a focus on understanding element substitutions and their effect on colour. A deposit model will then be created to help develop guidelines and parameters for further exploration, with an emphasis on Yukon targets.

## ACKNOWLEDGMENTS

This work comprises part of an MSc study funded by True North Gems Inc. and the National Sciences and Engineering Research Council of Canada at the University of British Columbia. The Yukon Geological Survey and Archer, Cathro & Associates (1981) Ltd. are also thanked for their support. D. Weis and B. Kieffer are thanked for their contributions, and J. Mortensen and H. Neufeld are thanked for their helpful reviews of the manuscript.

## REFERENCES

- Abbott, J.G., 1986. Epigenetic mineral deposits of the Ketzsa-Seagull district, Yukon. *In: Yukon Geology*, Volume 1, Exploration and Geological Services Division, Yukon Region, Indian and Northern Affairs Canada, p. 55-56.
- Barton, M. and Young, S., 2002. Non-pegmatitic deposits of beryllium: Mineralogy, geology, phase equilibria and origin. *In: Reviews in Mineralogy and Geochemistry*, E.S. Grew (ed.), vol. 52, p. 591-691.
- Breitsprecher, K., Mortensen, J.K. and Villeneuve, M.E., 2003. YukonAge, an Isotopic Database for the Yukon Territory. *In: Yukon Digital Geology*, version 2.0, S.P. Gordey and A.J. Makepeace (comps.); Geological Survey of Canada Open File 1749, and Yukon Geological Survey Open File 2003-9(D), 2 CD-ROMs.
- Chronic, F., 1979. Geology of the Guano-Guayes rare earth element bearing skarn property, Pelly Mountains, Yukon Territory. Unpublished M.Sc. thesis, University of British Columbia, Vancouver, British Columbia, 122 p.
- Deklerk, R., 2003 (compiler). Yukon MINFILE 2003 – A database of mineral occurrences. Quiet Lake-105 G. Yukon Geological Survey, CD-ROM.
- Ercit, T.S., 2002. The mess that is "allanite." *Canadian Mineralogist*, vol. 40, p. 1411-1419.
- Fonseca, A., 1998. Origin of carbonate hosted gold rich replacement deposits and related mineralization styles in the Ketzsa River deposit, Yukon Territory. Unpublished M.Sc. thesis, University of British Columbia, Vancouver, B.C., 173 p.
- Giere, R. and Sorensen, S.S., 2004. Allanite and Other REE-Rich Epidote-Group Minerals. *In: Epidotes. Reviews in Mineralogy and Geochemistry*, A. Liebscher and G. Franz (eds.), vol. 56, p. 431-493.

- Gibson, A.M., Holbek, P.M. and Wilson, R.G., 1999. The Wolf property – 1998 update: Volcanogenic massive sulphides hosted by rift-related, alkaline, felsic volcanic rocks, Pelly Mountains, Yukon. *In: Yukon Exploration and Geology 1998*, C.F. Roots and D.S. Emond (eds.), Exploration and Geological Services Division, Yukon Region, Indian and Northern Affairs Canada, p. 237-242.
- Hunt, J.A., 1997. Massive sulphide deposits in the Yukon-Tanana and adjacent terranes. *In: Yukon Exploration and Geology 1996*, Exploration and Geological Services Division, Yukon Region, Indian and Northern Affairs Canada, p. 35-45.
- Mortensen J.K., 1982. Geological setting and tectonic significance of Mississippian felsic metavolcanic rocks in the Pelly Mountains, southeastern Yukon Territory. *Canadian Journal of Earth Sciences*, vol. 19, p. 8-22.
- Mortensen, J.K., Hart, C.J.R, Murphy, D.C. and Heffernan, S., 2000. Temporal Evolution of Early and Mid-Cretaceous Magmatism in the Tintina Gold Belt. *In: Concepts Exploration and Discoveries, Special Volume 2*, Terry L. Tucker and Moira T. Smith (eds.), British Columbia and Yukon Chamber of Mines, Cordilleran Roundup, p. 49-57.
- Petrik, I., Broska, I., Lipka, J. and Siman, P., 1995. Granitoid allanite-(Ce): substitution relations, redox conditions and REE distributions (on an example of I-type granitoids, western Carpathis, Slovakia). *Geologica Carpathica*, vol. 46, p. 79-94.
- McDonough, W.F. and Sun, S.-S., 1995. Composition of the Earth. *Chemical Geology*, vol. 120, p. 223-253.
- Sinkankas, J., 1981. Emerald and other beryls. *Geoscience Press, Tucson, Arizona*, p. 665.
- Tempelman-Kluit, D.J., 1977. Geology of Quiet Lake (NTS 105F) and Finlayson Lake (NTS 105G), Yukon Territory. *Geological Survey of Canada Open File 486*, 1:250 000 scale.



